

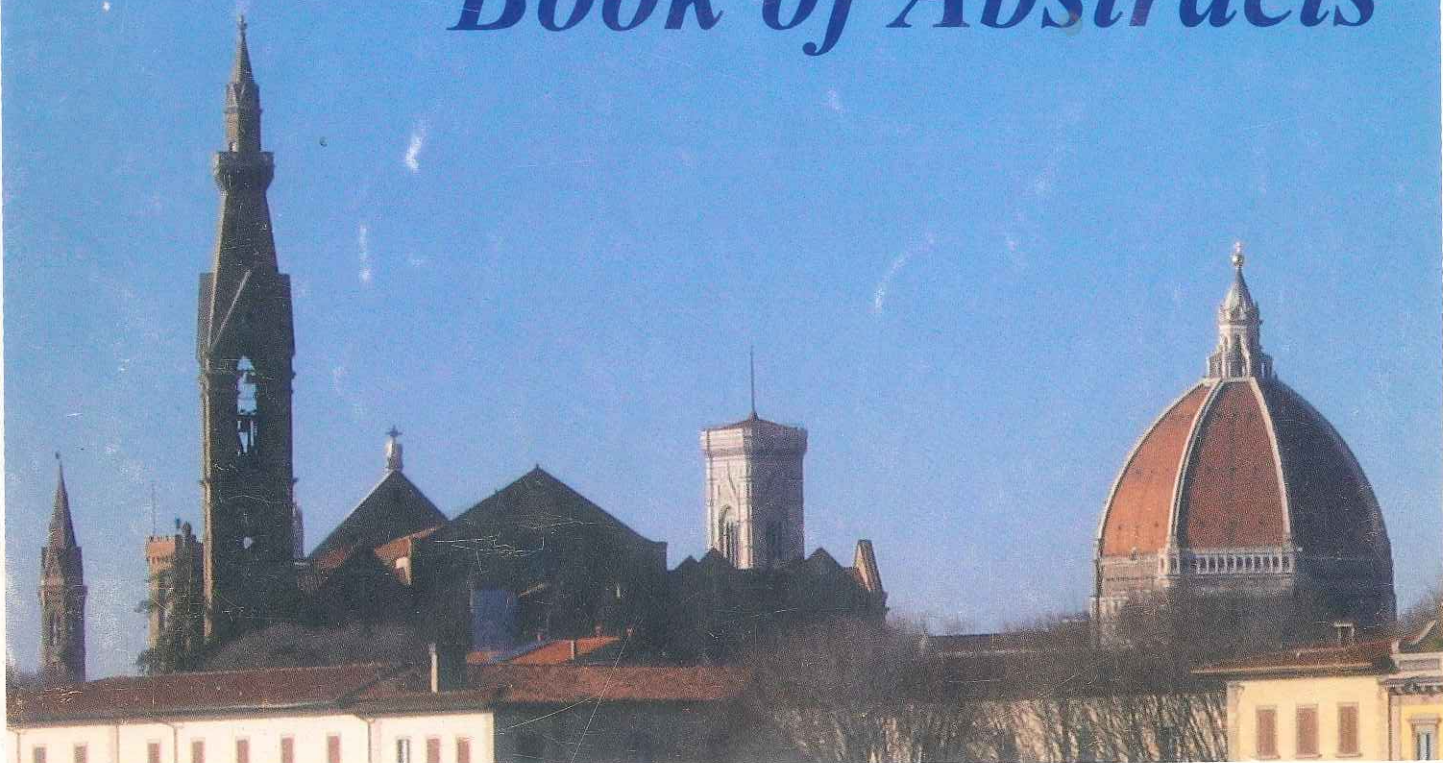
# EUCMOS 2010

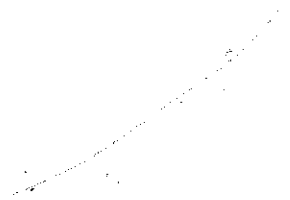
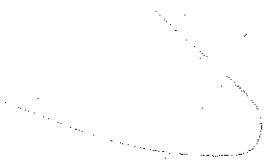


30<sup>th</sup> European Congress on Molecular Spectroscopy  
with GISR 2010



*Book of Abstracts*





**EUCMOS 2010**

**30<sup>th</sup> European Congress  
on Molecular Spectroscopy**

**Florence (I), 29 August - 3 September 2010**

**Edited by:**

**Maurizio Becucci**

**Cristina Gellini**

**Vincenzo Schettino**



**INTERNATIONAL COMMITTEE**

W. J. Orville Thomas (UK)  
 Honorary Life President  
 A. J. Barnes (UK)  
 President  
 R. Fausto (Portugal)  
 Vice-President  
 H. Ratajczak (Poland)  
 Vice-President

S. Akyüz (Turkey)  
 J. Bellanato (Spain)  
 J. R. Durig (USA)  
 T. A. Ford (S.Africa)  
 K. Furić (Croatia)  
 H. Hamaguchi (Japan)  
 H.M. Heise (Germany)  
 J. Laane (USA)  
 H. H. Mantsch (Canada)  
 S. Musić (Croatia)  
 S. Turrell (France)  
 V. Schettino (Italy)  
 G. Zerbi (Italy)

**SCIENTIFIC PROGRAM COMMITTEE**

V. Schettino - Chairman  
 S. Akyüz (Turkey)  
 A. J. Barnes (UK)  
 J. Bellanato (Spain)  
 F. J. Berry (UK)  
 E. De Grave (Belgium)  
 J. R. Durig (USA)  
 H. G. M. Edwards (UK)  
 R. Fausto (Portugal)  
 T. A. Ford (South Africa)  
 H. Hamaguchi (Japan)  
 H.M. Heise (Germany)  
 Z. Homonnay (Hungary)  
 L. Klasinc (Croatia)  
 J. Laane (USA)  
 A. Loewenschuss (Israel)  
 Z. Maksić (Croatia)  
 H.H. Mantsch (Canada)  
 Z. Meić (Croatia)  
 M.I. Oshtrakh (Russia)  
 H. Ratajczak (Poland)  
 V. Schettino (Italy)  
 S. Turrell (France)  
 G. Zerbi (Italy)



**LOCAL SCIENTIFIC COMMITTEE**

M. Becucci  
R. Bini  
S. Califano  
G. Cardini  
E.M. Castellucci  
R. Chelli  
A. Feis  
C. Gellini  
M. Marzocchi  
M. Muniz-Miranda  
G. Pietraperzia  
P. Procacci  
R. Righini  
P.R. Salvi  
V. Schettino  
G. Smulevich

**LOCAL ORGANIZING COMMITTEE**

S. Califano - Honorary Chairman  
V. Schettino - Chairman  
M. Becucci - Conference Secretary  
R. Bini  
G. Cardini  
E.M. Castellucci  
M. Ceppatelli  
R. Chelli  
M. Citroni  
E. Droghetti  
A. Feis  
C. Gellini  
A. Lapini  
M. Lima  
G. Lorenzetti  
A. Marcelli  
M. Marzocchi  
F. Muniz-Miranda  
M. Muniz-Miranda  
M. Pagliai  
M. Pasquini  
G. Piani  
G. Pietraperzia  
P. Procacci  
R. Righini  
P.R. Salvi  
G. Schettino  
G. Smulevich



**GISR**

Workgroup on Raman Spectroscopy and Non-Linear Optical Effects  
of the Italian Chemical Society organized by the Physical Chemistry and  
Analytical Chemistry Divisions of the Italian Chemical Society

organizes as a satellite meeting of EUCMOS 2010

**GISR 2010**

**1<sup>st</sup> Italian Meeting on Raman Spectroscopy  
and Non-Linear Optical Effects**

**M. Becucci**

Chairman

**C. Gellini**

Secretary

**NATIONAL SCIENTIFIC  
COMMITTEE:**

G. Compagnini, Catania - President  
R. Bozio, Padua  
G. Spoto, Catania  
M. Becucci, Florence  
M. Tommasini, Milano  
S. Bruni, Milano

**LOCAL SCIENTIFIC AND  
ORGANIZATIVE COMMITTEE:**

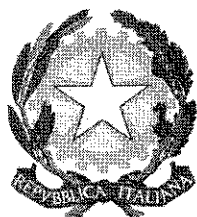
M. Becucci  
R. Bini  
S. Califano  
G. Cardini  
E. Castellucci  
R. Chelli  
A. Feis  
C. Gellini  
M. Marzocchi  
M. Muniz-Miranda  
G. Pietrapperia  
P. Procacci  
R. Righini  
P. R. Salvi  
V. Schettino  
G. Smulevich  
R. Udisti



## EUCMOS 2010 Organization

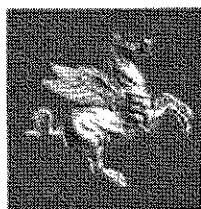
EUCMOS 2010 is organized by the University of Florence and the European Laboratory for Non-Linear Spectroscopy - LENS,

under the High Patronage of:

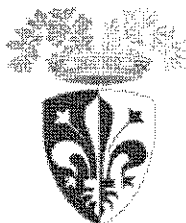


Presidente della Repubblica Italiana

and the Patronage of:



Regione Toscana



Provincia di Firenze



Comune di Firenze



Comune di Vinci



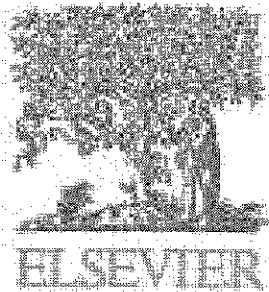
Università degli Studi di Firenze



Società Chimica Italiana



# EUCMOS 2010 Sponsorships





# LIST OF ABSTRACTS

## INVITED LECTURES

**T. W. Haensch**

Spectroscopy with laser frequency combs

**M. Schmitt**

Eigenstate resolved spectroscopy in the gas-phase: towards larger systems and higher energies

**D. Anglos**

Laser spectroscopies for cultural heritage

**D. Bicanic**

On a few interesting applications of photothermal science in the characterization of foods

**J. M. Thomas**

The confluence of spectroscopy, microscopy and tomography

**M. Zanni**

Watching proteins aggregates and electron transfer with 2D-IR spectroscopy

**P. Hildebrandt**

Raman and IR spectroscopic approaches for studying protein structure and dynamics

**J. V. Garcia Ramos**

New approaches in metal enhanced spectroscopy (SERS and SEF) in solution: Detection of insoluble compounds and pharmaceutical drugs

**R. J. Hemley**

Molecules under pressure

**M. Parrinello**

Title

**V. Balzani**

Photochemically controlled molecular devices and machines

## PLENARY LECTURES

**M. Zharnikov**

Characterization of self-assembled monomolecular films by advanced spectroscopic techniques

**H. Abramczyk**

Ultrafast primary events in photostable systems: H-bond, excess electron, biological photoreceptors

**H. H. Mantsch**

The renaissance of far infrared spectroscopy, better known as terahertz spectroscopy

**C. Castiglioni**

Raman evidences of unusual electronic and molecular structures

**M.S. Pshenichnikov**

2D IR spectroscopy of water dynamics near hydrophobes

**S. Astilean**

EUCMOS 2012 presentation



## ORAL and POSTER Contributions

### Applied Spectroscopy (cultural heritage, environment, ...)

#### Oral

##### Monday

- 15.10 - 15.30 **B. Zimmermann**  
Pollen analysis by transmittance FT-IR spectroscopy
- 15.30 - 15.50 **P. Matejka, J. Weissova, Z. Cieslarova, L. Mrnka, M. Clupek, K. Matejkova**  
Vibrational spectroscopy as a tool for analysis of tree leaves
- 15.50 - 16.10 **S. Osmanoglu, I. Y. Dicle**  
Effect of radiation in single crystal of L-glutamine
- 16.10 - 16.30 **M. Rudbeck, M. Blomberg, A. Barth**  
Environmental effects on phosphorylated amino acids

##### Tuesday

- 11.30 - 11.50 **B. Doherty, C. Miliani, B. G. Brunetti, A. Sgamellotti**  
A detachable SERS active polymer film: a minimally invasive approach to the study of painting lakes
- 11.50 - 12.10 **M.I. Oshtrakh, M.Yu. Larionov, V.I. Grokhovsky, V.A. Semionkin**  
An analysis of Fe and Ni distribution in M1, M2 and M3 sites of iron nickel phosphides extracted from Sikhote-Alin meteorite using Mössbauer spectroscopy with a high velocity resolution
- 12.10 - 12.30 **S. Ilieva, D. Cheshmedzhieva, D. Tasheva**  
Diastereoselectivity in the Michael addition reaction of CH-acidic Schiff base to  $\alpha,\beta$ -unsaturated ketones
- 12.30 - 12.50 **M. Volny, M. Strohalm, V. Vidova, K. Lemr, J. Pol, M. Hajduch, V. Havlicek**  
Mass imaging as a viable 2D alternative for molecular spectroscopists
- 15.10 - 15.30 **I. Osticioli, A. Nevin, M. Pagliai, D. Comelli, A. Gallone, G. Valentini, V. Schettino, E.M. Castellucci, R. Cubeddu**  
Micro-Raman spectroscopy for the non-destructive molecular characterization of red organic pigments in cross-sections of paintings by Leonardo, Masolino Veronese and Tintoretto
- 15.30 - 15.50 **D.K. Breitinger, G. Brehm, L. Steguweit**  
Characterization by vibrational spectrometries of neolithic axe-heads from the Lake Constance region and Northern Switzerland
- 15.50 - 16.10 **M. Mattarelli, S. Mengon, N. Boschiero, L. Benedetti, F. Deflorian**  
Emilio Vedova's paintings: materials and conservation issues
- 16.10 - 16.30 **T. K. N. Nguyen, K. Bourhis, S. Blanc, E. Péré, C. Vieillescazes**  
Solid state complexation of natural organic dyes with Al(III): Electronic and vibrational spectroscopies
- 16.30 - 16.50 **A. Amat, L. Cartechini, C. Miliani, A. Sgamellotti, S. Fantacci**  
Computational spectroscopy in cultural heritage



## Friday

11.45 - 12.00

S. Astilean, M. Baia, D. Maniu, C. Farcau, M. Iosin, V. Canpean, S. Boca, M. Potara, A. M. Gabudean

New approaches to develop multifunctional plasmonic nanosensors for bioanalytical applications

## Poster

- PS1-1 G. Lorenzetti, J. Striova, A. Zoppi, E. M. Castellucci  
Confocal Raman microscopy for in depth analysis in the field of cultural heritage
- PS1-2 S. Dallongeville, M.C. Dhameincourt, G. Di Lonardo, B. Hernandez, S. Turrell  
Spectroscopic studies of pigment-binder interactions in wall paintings
- PS1-3 O. Cristini, C. Kinowski, S. Turrell  
Micro-Raman spectroscopic study of frescoes from the antiquity period
- PS1-4 N. Stamatovska, P. Makreski, L. Pejov, G. Jovanovski  
Minerals from Macedonia. XXVII. Theoretical and experimental study of the vibrational spectra of Nežilovite
- PS1-5 M. Praisler, D. Domnisoru, S. Gosav  
Multivariate analysis of ancient *Cucuteni* Ceramics from Romanian cultural heritage
- PS1-6 W. Mozgawa, M. Król, T. Bajda  
Application of IR spectra in the studies of anion sorption on natural sorbents
- PS1-7 L. Szabó, L.F. Leopold, N. Leopold, I.B. Cozar, V. Chiş  
Zn (II) determination in contaminated soil by SERS spectroscopy
- PS1-8 S. Salami, E. Péré, G. Lespes  
Aqueous complexation of humic acid with organostannic compounds by IR spectroscopy and FFF
- PS1-9 M. Sitarz, M. Łodziński, A. Pieczka  
Microprobe analysis and spectroscopic (mir, raman and nmr) studies of various members of tourmaline group minerals from sudety mts, sw Poland
- PS1-10 C. F. Dascalu, B. C. Zelinschi, D. O. Dorohoi  
Main refractive indices of some carpathian crystals
- PS1-11 M. Bartoszek, J. Polak, W. Kapica, W.W. Sułkowski  
The use of UV/Vis spectroscopy for the estimation of humic acids maturity
- PS1-12 G. Trojsi, F. Marazzi, P. Baraldi  
San Vincenzo al Volturmo (Italy) and the identification of blues.
- PS1-13 J. Polak, M. Bartoszek, M. Żądło, W.W. Sułkowski  
The EPR study of humic acid extracted from sediment collected at various seasons
- PS1-14 P. Leyton, C. Paipa, A. Zárate, S. Fuentes, R. Sánchez, Y. Leyton  
Thermal synthesis of Gly-Gln Polymer on Rutile. A vibrational study.
- PS1-15 M. Žic, M. Ristić and S. Musić  
Monitoring of hydrothermal precipitation of  $\gamma\text{-Fe}_2\text{O}_3$  from concentrated  $\text{Fe}(\text{NO}_3)_3$  solutions partially neutralized with NaOH
- PS1-16 A. Adamczyk, W. Mozgawa  
The influence of different type precursors of  $\text{Al}_2\text{O}_3$  and  $\text{SiO}_2$  on structure and microstructure of mullite-like gels and coatings
- PS1-17 M. Ritz, L. Vaculíková, E. Plevová  
Identification of clay minerals by infrared spectroscopy and discriminant analysis
- PS1-18 M. Ristić, I. Czakó-Nagy, S. Musić, A. Vértés  
Spectroscopic characterization of chrysotile asbestos from different regions



- PS1-19 **J. Wąs-Gubała, J. Zięba Palus, B. Trzcińska**  
Microspectrophotometry in visible range as important part of the analysis of coloured forensic traces
- PS1-20 **J. Zięba Palus, J. Wąs-Gubała**  
An investigation into the use of micro-Raman spectroscopy for the analysis of car paints and single textile fibres
- PS1-21 **J. Zięba-Palus, A. Michalska, A. Weselucha-Birczyńska**  
Characterisation of paint samples by infrared and Raman spectroscopy for criminalistic purposes
- PS1-22 **M. Iliut, M. Iosin, S. Astilean**  
Temperature and light-induced effects on milk monitored by fluorescence spectroscopy
- PS1-23 **L. Bonoldi, C. Flego, L. Montanari**  
The origin of yellowness in Fischer Tropsch waxes studied by molecular spectroscopies.
- PS1-24 **A. Iordache, E. Horj, M. Culea, O. Cozar**  
Determination of amino acids, fatty acids and selenium in fish plasma by mass spectrometry
- PS1-25 **Ş. Osmanoğlu, Y. Dicle**  
Spectroscopic features of radical induced in gamma irradiated Gabapentin: an EPR Study
- PS1-26 **P. Mojzeš, J. Palacký, J. Bok**  
SVD-based method for intensity normalization, solvent subtraction and background correction of extensive Raman datasets
- PS1-27 **B. Zimmermann, G. Baranović**  
Baseline analysis: a simple FT-IR method for obtaining phase transition temperatures
- PS1-28 **S. Gosav, M. Praisler**  
Optimization of the performances of a hybrid expert system designed for the elucidation of molecular structures
- PS1-29 **E. Droghetti, C. Focardi, M. Nocentini, G. Smulevich**  
Development of a spectrophotometric method to detect the amount of carbon monoxide in fraudulently treated beef meat
- PS1-30 **F. Longo, G. Barone, V. Crupi, D. Majolino, P. Mazzoleni, V. Venuti**  
Characterization of archaeological pottery: the case of "Ionic Cups"
- PS1-31 **V. Venuti, G. Barone, V. Crupi, F. Longo, D. Majolino, P. Mazzoleni, D. Tanasi**  
FTIR spectroscopic analysis to study the firing processes of prehistoric ceramics
- PS1-32 **P. Taddei, G. Freddi, M. Tsukada**  
Vibrational study on the modifications induced by chemical and grafting agents in silk and wool fibres
- PS1-33 **L. Brambilla, P. Baraldi, L. Toniolo, M.C. Gamberini, S. Goidanich, C. Baraldi**  
Spectroscopic techniques applied to the study of Roman atramenta
- PS1-34 **M. Pagliai, M. Muniz-Miranda, G. Cardini, V. Schettino**  
Infrared and Raman spectra of minerals from *ab initio* molecular dynamics simulations
- PS1-35 **G. Perna, M. Lasalvia, P. D'Antonio, G. Quartucci, N. L'Abbate, V. Capozzi**  
Characterization of human cells exposed to deltamethrin by means of Raman microspectroscopy and Atomic Force Microscopy
- PS1-36 **G. Schettino, P. Cancio Pastor, C. Baffa, E. Giani, M. Inguscio, E. Oliva, A. Tozzi**  
Optical Frequency Comb as the calibration source for the GIANO spectrograph



- PS1-37 M. Sitarz, M. Łodziński, M. Kozanecki  
Spectroscopic and chemical characterization of cavansite and pentagonite from Wagholi, Poonah district, Maharashtra state, India

## Biological and Medical Applications

### Oral

#### Monday

- 11.00 - 11.20 V. Mohaček Grošev, J. Grdadolnik  
Preferred conformations of dipeptides: crystals vs. solutions
- 11.20 - 11.40 A. Bebu, L. Szabó, N. Leopold, C. Berindean, V. Chiş, L. David  
IR, Raman, SERS and DFT study of amoxicillin
- 11.40 - 12.00 M. Pučetaitė, V. Hendrixson, A. Želvys, F. Jankevičius, J. Čeponkus, V. Šablinskas  
Highly resolved morphological analysis of renal stones found in mammals using Infrared spectroscopical imaging technique
- 12.00 - 12.20 A. Torreggiani, Z. Jurasekova, C. Ferreri, C. Chatgililoglu  
Effects of radical stress on sulfur-containing proteins: desulfurisation reactions associated with the formation of trans lipids in model membrane
- 12.20 - 12.40 V. Profant, P. Bouř, V. Baumruk  
Formation of PPII helical conformation studied by Raman optical activity
- 12.40 - 13.00 A. P. Mendham, B. Z. Chowdhry, T. J. Dines  
Experimental and theoretical studies of cyclic di-amino acid peptides in the solid state

#### Tuesday

- 11.30 - 11.50 S. S. Stavrov  
Carbon monoxide infrared absorption band of carboxyheme proteins as a probe of the protein collective motions.
- 11.50 - 12.10 A. Mezzetti, M. Malferrari, F. Francia, A. Idrissi, G. Venturoli, W. Leibl  
Time-resolved FTIR investigation on light-induced proton-coupled electron transfer reactions in photosynthetic reaction centers
- 12.10 - 12.30 E. Nemtseva, D. Gulnov, M. Gerasimova, V. Kratasyuk  
Fluorescence spectroscopy of the components of the bacterial bioluminescent reaction in viscous media
- 12.30 - 12.50 N. Belogurova, N. Kudryasheva  
Fluorescence features of photoprotein obelin
- 15.10 - 15.30 H. M. Heise, U. Damm, V. R. Kondepoti, R. Kuckuk, J. K. Mader, F. Feichtner, M. Ellmerer  
Infrared spectroscopy in clinical chemistry - from laboratory to continuous patient monitoring
- 15.30 - 15.50 G. Steiner, A. Stelling, K. Geiger, E. Koch, R. Salzer, G. Schackert, M. Kirsch  
Vibrational Spectroscopy: Towards Neurosurgical Applications
- 15.50 - 16.10 E. Horj, S. Cîntă Pînzaru, C. Soica, C. Dehelean, L. David  
Vibrational spectroscopy characterization of a new pharmaceutical complex of chlorthalidone
- 16.10 - 16.30 M. Larraona-Puy, A. Ghita, A. Zoladek, W. Perkins, S. Varma, I. H. Leach, A. A. Koloydenko, H. Williams, I. Notingher  
Raman micro-spectroscopy as a diagnostics tool for skin cancer detection



16.30 - 16.50 F.C. Pascut, I. Notingher  
Label-free time-course imaging of live cells by confocal Raman micro-spectroscopy

**Wednesday**

11.40 - 12.00 O.F. Nielsen, T.M. Greve, A. Engdahl  
FTIR-synchrotron and NIR-FT-Raman studies of water in animal and human skin

12.00 - 12.20 T. Pazderka, V. Kopecký Jr., K. Hofbauerová, V. Baumruk  
Two-dimensional Raman and Raman optical activity correlation and factor analysis of lysozyme fibrillation

12.20 - 12.40 M. Talu, E. Uzluk  
Synthesis and characterization of antibacterial Poly(N-vinylimidazole-co-maleic anhydride)/Sodium Bentonite composites

12.40 - 13.00 K. Hauser, C. Krejtschi, O. Ridderbusch, R. Huang, L. Wu, T. A. Keiderling  
Folding dynamics of hairpin peptides studied by temperature-jump infrared-spectroscopy and isotopic editing

**Poster**

- PS2-1 E. Droghetti, M. Zamocky, P.G. Furtmüller, C. Obinger, G. Smulevich  
Resonance Raman spectroscopy of catalase-peroxidase from the phytopathogenic rice blast fungus *Magnaporthe grisea*
- PS2-2 M.I. Oshtrakh, I.V. Alenkina, S.M. Dubiel, V.A. Semionkin  
Structural variations of the iron cores in human liver ferritin and its pharmaceutically important models: a comparative study using Mössbauer spectroscopy with a high velocity resolution
- PS2-3 M.I. Oshtrakh, A. Kumar, S. Kundu, A.L. Berkovsky, V.A. Semionkin  
Study of human, rabbit and pig oxyhemoglobins using high velocity resolution Mössbauer spectroscopy in relation to its structural and functional variations
- PS2-4 V. Šablinskas, V. Urbonienė, E. Kaveckaitė, F. Jankevičius, G. Steiner, L. Kintys  
Infrared spectral microscopy of cancerous kidney tissues
- PS2-5 H. Abramczyk, B. Brożek-Płuska, J. Surmacki, J. Jabłońska, R. Kordek  
The label-free Raman imaging of human breast cancer
- PS2-6 T. Yasui, T. Araki  
Visualization of collagen molecule orientation in wrinkled skin using a polarization-resolved second-harmonic-generation microscope
- PS2-7 M. Sefa Ozel, A. E. Ozel, S. Akyuz, T. Akyuz  
Combined micro-Raman and EDXRF study of characterization of mineralized tissue of human bone of osteoporosis patients
- PS2-8 C. Paluszkiwicz, E. Stodolak, J.W.M. Kwiatek, P. Jeleń  
Bioactivity of montmorillonite - chitosane nanocomposite materials for regenerative medicine
- PS2-9 L. Bednářová, P. Maloň, H. Dlouhá, M. Kubáňová, P. Mojžeš, E. Kočíšová, K. Hofbauerová, V. Kopecký Jr.  
Antibacterial peptides in interaction with model membranes studied by various spectroscopic methods
- PS2-10 A. Falamas, S. Cinta Pinzaru, C. Dehelean, A. Bebu  
Spectroscopic investigations of newly formed guest-host type complexes as potential



- anti skin cancer candidates
- PS2-11 **J. Równicka-Zubik, A. Sułkowska, E. Kurek, M. Maciążek-Jurczyk, B. Bojko, W. W. Sułkowski**  
The comparison of the binding properties of native and destabilized serum albumins
- PS2-12 **M. Maciążek-Jurczyk, A. Sułkowska, B. Bojko, J. Równicka-Zubik, W. W. Sułkowski**  
Polypharmacotherapy in rheumatology. <sup>1</sup>HNMR analysis of binding of phenylbutazone and methotrexate to serum albumin
- PS2-13 **M. Di Foggia, E. Benassi, S. Bonora, S. Ottani**  
Vibrational (Raman and SERS) and electronic UV study on triazine herbicides
- PS2-14 **I. B. Cozar, L. Szabó, O. Cozar, N. Leopold, V. Chiş, L. David**  
IR, SERS and DFT Study of Pindolol and Verapamil Drugs
- PS2-15 **B. Brycki, I. Kowalczyk, A. Szulc**  
Spectroscopic analysis of gemini alkylammonium salts with the antimicrobial activity
- PS2-16 **A. Hense, A-K. Mossberg, C. Svanborg, A. Barth**  
Infrared spectroscopic study of HAMLET, a tumor-killing variant of  $\alpha$ -lactalbumin
- PS2-17 **P. Maloň, L. Bednářová, M. Kubáňová, M. Flegel, J. Hlaváček, V. Baumruk**  
Vibrational and electronic optical activity of amide and disulfide groups in neurohypophyseal hormones and their models
- PS2-18 **N. Mironova-Ulmane, M. Polakovs, A. Pavlenko, N. Kurjane, E. Reinholds, M. Grube**  
Spectroscopic study of blood after irradiation
- PS2-19 **P. Praus, E. Kočíšová, P. Mojzeš, J. Štěpánek, F. Sureau, P.-Y. Turpin**  
Cellular uptake of modified oligonucleotides enhanced by zinc porphyrins studied by time-resolved micro-spectrofluorimetry and fluorescence imaging techniques
- PS2-20 **S. Boca, D. Rugina, A. Pinteá, L.-B. Tudoran, S. Astilean**  
Synthesis and characterization of flower-shaped gold nanoparticles for applications as SERS-active tags in cellular spectral imaging
- PS2-21 **S. Akyuz, A. E. Ozel, K. Balci, T. Akyuz, A. Coker, E. D. Arisan, N. Palavan-Unsal, A. Ozalpan**  
Micro Raman spectroscopic investigation of the interaction of cultured HCT116 colon cancer cells with alpha-difluoromethylornithine (DFMO), an irreversible inhibitor of ornithine decarboxylase
- PS2-22 **L. Andronie, S. C. Pînzaru, O. Cozar**  
Surface-enhanced Raman scattering of DL-tryptophan
- PS2-23 **A. Torreggiani, M. Di Foggia, A. Tinti**  
Investigations on metallothioneins: An help from Raman spectroscopy
- PS2-24 **J. Kaminsky, J. Kubelka, P. Bour**  
Theoretical models for better understanding of IR and CD spectra of proteins
- PS2-25 **M. Śmiechowski, E. Gojto, J. Stangret**  
Hydration of simple carboxylic acids from infrared spectroscopy of HDO
- PS2-26 **M. Grube, M. Gavare, R. Rutkis, U. Kalnenieks, N. Mironova-Ulmane**  
Use of FT-IR spectroscopy data for systems analysis of *Zymomonas mobilis* metabolism
- PS2-27 **P. Ottová, B. Řezáčová, J. Vachoušek, J. Štěpánek**  
Structural stability and complexation with aptamers of RNA hairpins in HIV-1 genome
- PS2-28 **F. Torrens, G. Castellano**  
Binding of proteins to vesicles: Asymmetry and cooperativity



- PS2-29 G. Petruševski, S. Ugarkovic, P. Makreski  
Solid-state transformation of the pseudopolymorphic forms of codeine phosphate hemihydrate and codeine phosphate sesquihydrate monitored by FTIR spectroscopy and TGA/DSC
- PS2-30 R. Świsłocka, M. Kalinowska, W. Ferenc, J. Sarzyński, W. Lewandowski  
Spectroscopic and magnetic properties of Cu(II) complexes with selected biologically important ligands
- PS2-31 M. Kalinowska, J. Piekut, W. Lewandowski  
Relationship between chemical structure and biological activity of alkali metal *o*-, *m*- and *p*-anisates. FT-IR and microbiological studies
- PS2-32 M. Potara, S. Astilean  
Solution-phase, dual LSPR-SERS plasmonic sensors of high sensitivity and stability based on chitosan-coated anisotropic silver nanoparticles
- PS2-33 M. Kubáňová, L. Bednářová, P. Maloň, V. Baumruk  
Raman optical activity of amide and disulfide group in peptides and proteins
- PS2-34 A. Tinti, G. Navarra, M. Leone, V. Militello, A. Torreggiani  
Influence of metal ions on thermal aggregation processes of globular proteins
- PS2-35 A. Wesetucha-Birczyńska, B. Borzęcka-Prokop  
Compound formation assistance by Raman spectroscopy and PXRD method
- PS2-36 P.T.C. Freire, R.O. Holanda, C. Luz-Lima, J. Mendes Filho, F.E.A. Melo  
Raman spectroscopy of L-glutamine under high pressure conditions
- PS2-37 A. Pallagi, P. Sebők, P. Sipos, I. Pálinkó  
Structure-reactivity relationship of Ca<sup>2+</sup>-carbohydrate solution complexes studied by H, <sup>13</sup>C and <sup>43</sup>Ca NMR spectroscopy
- PS2-38 K. Balci, Y. Akkaya, S. Akyuz, N. Palavan-Unsal  
An IR and Raman spectroscopic investigation on  $\alpha$ -difluoromethyl-ornithine (DFMO), a potential target as chemotherapeutic agent
- PS2-39 A. K. Przybył, Z. Nowakowska  
A comparative study of EI-MS and NMR in analysis of the new derivatives of cytosine with aminoacids
- PS2-40 C. M. Muntean, R. Misselwitz and H. Welfle  
A Raman spectroscopic study on the DNA structure at reduced pH values, in the presence of Mn<sup>2+</sup> ions
- PS2-41 B. Jasiewicz, K. Skrycki  
New methyl sparteine derivatives as potential hypoglycemic agents
- PS2-42 P. Bruździak, J. Stangret  
Characterization of changes in structure and stability of lysozyme caused by glycine and its methyl derivatives
- PS2-43 P. Rakowska, M. Olszewski, J. Stangret, J. Kur  
The use of FT-IR spectra in examination of structure and stability changes of TaqSSB protein and its complex with ssDNA
- PS2-44 A. Panuszko, D. Wyrzykowski, J. Stangret  
Spectroscopic, calorimetric and ab initio study of water interactions with stabilizing and denaturing osmolytes
- PS2-45 S. Celik, A. E. Ozel, S. Akyuz, S. Kecel and G. Agaeva  
Conformational preferences, experiment and theoretical vibrational spectra of cyclo(Gly-Val) dipetide
- PS2-46 T. Pazderka, V. Kopecký Jr., K. Hofbauerová, V. Baumruk  
Raman and infrared spectroscopy of amino acids and its implication for improvement of the protein secondary structure determination





- PS2-47 S. Kecel, A. E. Ozel, S. Akyuz, S. Celik, G. Agaeva  
Structural and spectroscopic elucidation of L-proline tyrosine (L-pro-tyr) dipeptide
- PS2-48 E. Kočiřová, M. Procházka, J. Štěpánek  
DCDR spectroscopy as efficient tool for study of liposome interaction with biomolecular complexes
- PS2-49 E.-L. Karjalainen, A. Barth  
Calculations of infrared spectra of the amide I band of proteins - method development and application to SR Ca<sup>2+</sup>-ATPase
- PS2-50 A. Dijanošić, S. Miljanić, Z. Meić, I. Piantanida, M. T. Albelda, A. Sornosa-Ten, E. García-España  
Surface-enhanced Raman study of the interactions between cationic polyamines and polynucleotides
- PS2-51 Y. Akkaya, K. Balci, S. Akyuz  
Studies on Valine-Tyrosine, antihypertensive dipeptide in Aqueous Solution by Raman Spectroscopy
- PS2-52 G. Uraz, B. Çelik  
Evaluation of existence of biofilm in the isolates of Pseudomonas with spectrophotometer
- PS2-53 O. Cozar, L. Szabó, I. B. Cozar, N. Leopold, V. Chiş, L. David  
Vibrational and DFT Study of some cardiovascular drugs and their copper complexes
- PS2-54 P. Taddei, E. Modena, A. Tinti, F. Siboni, C. Prati, M.G. Gandolfi  
Vibrational investigation on the *in vitro* bioactivity of commercial and experimental calcium-silicate cements for root-end endodontic therapy
- PS2-55 I. Iriepa, J. Bellanato, E. Gálvez  
Synthesis, conformational and pharmacological study of some carbamates derived from endo-8-methyl-8-azabicyclo[3.2.1]octan-3a-ol hydrochlorides
- PS2-56 V. Venuti, V. Crupi, D. Majolino, A. Mazzaglia, A. Paciaroni, R. Stancanelli  
Chiral recognition and complexation behaviour of  $\beta$ -CyDs vs. L-, D- and DL-serine by FTIR-ATR spectroscopy.
- PS2-57 J. Hudecová, J. Kapitán, V. Baumruk, P. Bouř  
Flexibility of a Model Cyclic Hexapeptide Studied by the Raman and Raman Optical Activity
- PS2-58 S. Osmanoglu, Y. Dicle  
Free radicals in gamma irradiated neurological drug topimarate: an EPR study

## Materials and Surfaces

### Oral

#### Monday

- 11.00 - 11.20 J. Habinshuti, S. Turrell, C. Kinowski, D. Stievenard, B. Grandidier, T. Xu, O. Cristini  
Development of semi-conductor nanoparticle systems for Si-nanowire solar cells
- 11.20 - 11.40 S. Krawczyk, A. Zdyb, A. Nawrocka  
Localized vs charge-transfer excited states of photosensitizers on TiO<sub>2</sub> nanoparticles. Stark effect spectroscopy
- 11.40 - 12.00 A.M. Yaremko, V.O. Yukhymchuk, V.M. Dzhagan  
Spectroscopy study of exciton-phonon interaction in organic and semiconductor quantum dots
- 12.00 - 12.20 A. Wesełucha-Birczyńska, A. Frączek-Szczypta, S. Błażewicz  
PAN-based carbon fibers modified with carbon nanotubes



- 12.20 - 12.40 O. Dammer, B. Vlckova, J. Pflieger, M. Prochazka, M. Slouf  
Specific aspects of SERS and SERRS of Ag nanoparticles-polymer nanocomposites
- 12.40 - 13.00 P. Wilhelm, B. Chernev, H. Plank, M. Sezen, M. Dienstleder, T. Haber, F. Hofer  
Raman microprobe imaging of submicron structures and interdisciplinary characterization of beam damage
- 17.00 - 17.20 A. Gajović, R. Krsmanović, J. Macan, D. S. Su, H. Ivanković  
Raman spectroscopy and luminescence of mesoporous ZrTiO<sub>4</sub> ceramics
- 17.20 - 17.40 A. Rogojanu, C. F. Dascalu, B. C. Zelinschi, D. O. Dorohoi  
Electronic absorption spectra of some phtalazinium ylids used to characterize the local ordering processes in liquid and solid solutions
- 17.40 - 18.00 T. Ishii, H. Kanazawa, S. Kojima  
Micro-Brillouin scattering study of orthorhombic HEWL crystals in glycerol

**Tuesday**

- 11.30 - 11.50 D. Srankó, M. Sipiczki, É.G. Bajnóczi, M. Darányi, Á. Kukovecz, Z. Kónya, S.E. Canton, K. Norén, P. Sipos, I. Pálinkó  
A SEM, EDX and XAS characterization of Ba(II)Fe(III) layered double hydroxides
- 11.50 - 12.10 M. Handke, M. Gajewicz, A. Kowalewska  
Spectroscopy studies of mesotextured cross-linked octahydrodoctasilsesquioxanes materials
- 12.10 - 12.30 Kh. M. Al-Khamis, Z. Al-Othman, N. M. Al-Andis, R. M. Mahfouz  
Kinetic studies for isothermal decomposition of un-irradiated and  $\gamma$ -irradiated gallium acetylacetonate new route for synthesis of gallium oxide nanoparticles
- 12.30 - 12.50 M. Modreanu  
Infrared and Raman spectroscopy investigation of high-k metal oxide thin films: chemical stability, interfacial properties and solid state crystallization

**Wednesday**

- 11.40 - 12.00 K. Csankó, M. Darányi, G. Kozma, Á. Kukovecz, Z. Kónya, I. Pálinkó  
Self-assembling of Z- $\alpha$ -pyridylcinnamic acid dimers over polycrystalline Ag and Au surfaces followed by FT-IR and atomic force microscopies
- 12.00 - 12.20 R. Stiufiuc, B. Grandidier, G. Stiufiuc, C. M. Lucaciu  
STM/STS characterization of PTCDI/melamine self assembly on Si(111)  $\sqrt{3} \times \sqrt{3}$  Ag surface
- 12.20 - 12.40 W. Pohle, D.R. Gauger, V. Andrushchenko, P. Bouř, F. Billes  
A spectroscopic method to estimate the binding potency of amphiphile assemblies
- 12.40 - 13.00 Do Thi Minh, K. Volka  
Vibrational spectroscopy in the study of self-assembled monolayers of thiols on gold. An example of 4-mercaptobenzoic acid

**Poster**

- PS1-38 M. Kawashima, S. Aramomi, Y. Matsuda, S. Kojima  
Temperature dependence of elastic properties in alkali borate binary glasses
- PS1-39 A. Rogojanu, R. Stanculescu, D. Dorohoi  
Dichroic polymer foils analysed by spectral means



- PS1-40 **E. Filip, M. Dulcescu, D. Dorohoi**  
Intermolecular interactions in pyridinium ylid ternary protic solutions. theoretical and spectral study
- PS1-41 **D. Dorohoi**  
Solvent influence on the zwitterionic solutes studied by electron spectroscopy
- PS1-42 **J. Pisarska, W.A. Pisarski**  
Optical spectroscopy of  $Dy^{3+}$  ions in heavy metal lead-based glasses and glass-ceramics
- PS1-43 **A. Gajović, J. Vukajlović, K. Žagar, M. Plodinec, M. Čeh**  
Structural phase transitions of  $BaTiO_3$  nanorods investigated by Raman spectroscopy *in situ* at different temperatures
- PS1-44 **C. Bayrak, M.T. Aytakin Aydın**  
Vibrational Spectroscopic Studies on the  $T_d$ -type Clathrates:  $Cd(2,5$ -dimethylpyrazine) $M(CN)_4 \cdot 2C_6H_6$  ( $M= Cd$  or  $Hg$ )
- PS1-45 **Ö. Bağlayan, M.T. Aytakin Aydın, M. Şenyel**  
Vibrational Spectroscopic Studies on the Hofmann-type Clathrates:  $M(C_4H_7NH_2)_2Pd(CN)_4 \cdot 2C_6H_6$  ( $M=Ni, Cd$  or  $Co$ ;  $G=benzene$ )
- PS1-46 **N. Vedeanu, D. A. Magdas, O. Cozar**  
IR and 2D correlation spectroscopic investigation of  $CuO-V_2O_5-P_2O_5-CaF_2$  glass system
- PS1-47 **R. Dēdic, V. Vyklický, A. Svoboda, J. Hála**  
Singlet Oxygen Photosensitization in Polymer Films
- PS1-48 **R. Dēdic, V. Vyklický, J. Hála**  
Dependence of singlet Oxygen kinetics on photosensitizer concentration in lipid films
- PS1-49 **M. Alloisio, A. Demartini, S. Loporatti, A. Rindi, C. Cuniberti, G. Dellepiane, G. Margheri, E. Giorgetti, M. Muniz-Miranda**  
Spectroscopic investigation on noble metal-organic nanohybrids with controlled shapes and properties
- PS1-50 **T. V. Tran, S. Turrell, C. Kinowski, O. Cristini, B. Capoen, M. Bouazaoui, P. Roussel, S. Berneschi, G. Righini, M. Ferrari, S.N. B. Bhaktha**  
Kinetics of crystallization of  $SnO_2$  nanoparticles in sol-gel -based glass ceramics: comparison of thin films and bulk systems
- PS1-51 **C. Zimmerer, G. Steiner, V. Sablinskas, G. Heinrich**  
Nanoparticle enhanced FTIR Spectroscopy of Polymer Interfaces
- PS1-52 **O. Ryazanova, I. Voloshin, V. Zozulya**  
Spectroscopic study of tetracationic porphyrin H-aggregation on polyanionic matrix
- PS1-53 **S. Rada, V. Dan, M. Rada, M. Culea, T. Rusu, M. Bosca, L. Pop, E. Culea**  
FTIR, UV-VIS spectroscopy and DFT calculations on the structure of the gadolinium-lead-germanate glasses
- PS1-54 **R. Chelcea, S. Rada, E. Culea**  
FTIR, UV-VIS and EPR spectroscopy investigations of the copper-lead-germanate glasses
- PS1-55 **S. Rada, R. Chelcea, A. Dehelean, P. Pascuta, T. Ristoiu, I. Coroiu, M. Barlea, E. Culea**  
FTIR, UV-VIS and EPR investigations of the gadolinium-lead-tellurate unconventional glasses
- PS1-56 **A. Dehelean, S. Rada, E. Culea**  
Redox processes in iron-lead-tellurate glasses
- PS1-57 **M. Rada, V. Maties, S. Rada, I. V. Simiti, E. Culea**  
Novel photochromic properties of the tungsten-lead-borate glasses



- PS1-58 M. Gotić, S. Musić  
Hydrothermal synthesis of iron oxide nanorings by Mn-doping
- PS1-59 M. Vyskovska, V. Prokopec, M. Clupek, A. Kokaislova, J. Cejkova, P. Matejka  
Development of copper nanostructured materials for surface-enhanced Raman scattering spectroscopy
- PS1-60 D. Bauman, N. Bielejewska  
Molecular aggregation of naphthalimide dyes in Langmuir-Blodgett films
- PS1-61 R. Stanescu, N. Vedeanu, S. Filip, O. Cozar  
EPR and IR structural investigation of  $V_2O_5 - P_2O_5 - BaO$  glass system with opto-electronic potential
- PS1-62 P. Angelova, N. Kuchukova, G. Dobrikov, I. Petkova, E. Giorgetti, I. Timtcheva, K. Kostova, E. Vauthey  
Preparation and photophysical study of fluorophore modified Gold nanoparticles
- PS1-63 M. Plodinec, D. Iveković, D. Su, A. Gajović.  
*In situ* high temperature Raman spectroscopy of modified titanate nanotubes
- PS1-64 M. Handke, M. Sitarz, E. Długóń  
FT-IR and MAS-NMR spectra of  $SiC_xO_y$  glass materials
- PS1-65 L. Mikac, M. Ivanda, G. Štefanić, S. Musić, K. Furić  
Spherical vibrational modes of amorphous and crystalline  $ZrO_2 - CuO$  nanoparticles
- PS1-66 M. Ivanda, M. Balarin, O. Gamulin, V. Đerek, D. Ristić, S. Musić, M. Ristić, K. Furić  
Porous silicon prepared by electrochemical etching of silicon epitaxial layer
- PS1-67 D. A. Magdas, N. Vedeanu, O. Cozar  
Spectroscopic studies of  $Mo-Cu-Pb-P_2O_5$  glass system
- PS1-68 D. Mikociak, C. Paluszkiwicz, S. Błażewicz  
FTIR spectroscopy analysis of oxidation process of coal tar pitches
- PS1-69 D. Rusu, A. R. Tomsa, M. H. Dickman, U. Kortz, O. Baban, M. Rusu  
Synthesis and characterization of the novel heteropolyoxotungstates based on  $[BiW_9O_{33}]^{9-}$  units
- PS1-70 Z. Csendes, N. Földi, N. Varga, J.T. Kiss, I. Labádi, I. Pálinkó  
Covalently grafted, silica gel supported mixed amino acid iron complexes – syntheses, structural characterization and catalytic testing
- PS1-71 M. Balarin, O. Gamulin, M. Ivanda, M. Kosović, D. Ristić, M. Ristić, S. Musić, K. Furić  
Optical properties of porous silicon on an insulator layer
- PS1-72 I. Bryndał, E. Kucharska, K. Hermanowicz, M. Mączka, M. Wandas, J. Hanuza  
The crystal and molecular structure of new hybrid material: 2-amino-4-methyl-3-nitropyridinium hydrogen oxalate
- PS1-73 D. Ristić, V. Holy, M. Ivanda, M. Marciuš, M. Buljan, O. Gamulin, K. Furić, M. Ristić, S. Musić, M. Mazzola, A. Chiasera, M. Ferrari, G.C. Righini  
Surface characterisation of thin silicon rich oxide thin films
- PS1-74 A. Šarić, S. Musić, M. Ivanda  
Varying the microstructural properties of ZnO particles using different synthesis routes
- PS1-75 M. Maczka, M. Ptak, W. Paraguassu, P.T.C. Freire, A.G. Souza Filho, J. Mendes Filho, J. Hanuza  
Lattice dynamics and high-pressure Raman scattering studies of cation-deficient Aurivillius compounds
- PS1-76 W. Paraguassu, M. Maczka, K. Pereira da Silva, A. G. Souza Filho, P.T.C. Freire, J. Mendes Filho, and J. Hanuza



- Vibrational properties of hexagonal bronze systems: High pressure and polarized Raman spectra
- PS1-77 W. Makulski  
Reconsideration of the  $^{13}\text{C}$  absolute nuclear magnetic shielding scale from NMR measurements of CO/He and CH<sub>4</sub>/He gas phase mixtures
- PS1-78 M. Ziabka, C. Paluszkiwicz, J. Chlopek  
FTIR study of PGLA modified with nanoadditives
- PS1-79 W. Pohle, D.R. Gauger, E. Mrazkova, P. Hobza  
Headgroup hydrocarbon groups are involved in water binding as revealed by isotope IR spectroscopy
- PS1-80 A. Nyczyk, C. Paluszkiwicz, M. Hasik  
Polysiloxane networks formation studied by FTIR spectroscopy
- PS1-81 C. Paluszkiwicz, E. Sołtysiak, M. Blazewicz  
Characterization of ceramic/poly-ε-caprolactone nanocomposite materials by FTIR spectroscopy
- PS1-82 M. Piccardo, M. Ottonelli, D. Duce, S. Thea, G. Dellepiane  
Tuning the photophysical properties of pyrene-based systems: a theoretical study
- PS1-83 A. Rindi, G. Margheri, M. Muniz-Miranda, G. Dellepiane, M. Alloisio  
Metal-organic platforms for photonic applications based on poly-10,12 dicosadiynedioic acid (PDCDA)
- PS2-59 S. Krehula, S. Musić  
The influence of platinum(IV) ions on the formation of iron oxides in a highly alkaline medium
- PS2-60 M. Samsonowicz, E. Regulska, W. Lewandowski  
Influence of alkaline earth metals on molecular structure of 3-nitrobenzoic acid in comparison with alkali metals effect.
- PS2-61 E. Regulska, M. Kalinowska, W. Lewandowski  
Experimental and theoretical study of molecular structure of alkali metal para substituted benzoates.
- PS2-62 S. Kumar, A. Barth  
Phosphoenolpyruvate and Mg<sup>2+</sup> binding to pyruvate kinase monitored by infrared spectroscopy
- PS2-63 C. Rémazeilles, P. Refait  
FTIR-ATR analysis of synthetic iron(II-III) hydroxysalts green rusts
- PS2-64 E. Akalin, S. Akyuz  
Experimental and theoretical vibrational spectroscopic investigation of Zn(II) halide complexes of pyridine derivatives
- PS2-65 O. Cozar, I. Bratu, L. Szabo, I. B. Cozar, M. Culea, L. David  
IR and EPR study of copper(II) complexes with <sup>15</sup>N-labelled lysine and ornithine
- PS2-66 A. Bebu, A. Kozma, E. Forizs, M. Toderas, L. David  
Spectral and ESR study of Cu(II), Co(II) and Ni(II) theophyllinato complexes containing propanolamine ligands
- PS2-67 A. Stanila, S. Stanila, L. Leopold  
Spectroscopic investigations of some transitional metals complexes with methionine as ligand
- PS2-68 A. Baran, E. Mrozek, M. Baranska  
FT-Raman analysis of luteolin and its complexes with Al (III)
- PS2-69 I. Georgieva, N. Trendafilova, I. Kostova, Tz. Mihaylov  
FTIR, Raman, NMR and theoretical studies of lanthanide complexes with coumarin-3-carboxylic acid



- PS2-70 **M. Kalinowska, R. Świśtocka, W. Lewandowski**  
Zn(II), Cd(II) and Hg(I) complexes of biologically important ligands: FT-IR, FT-Raman,  $^1\text{H}$  and  $^{13}\text{C}$  NMR studies
- PS2-71 **R. Świśtocka, M. Kowczyk, M. Kalinowska, W. Lewandowski**  
Molecular structure of alkali metal salts of *p*-coumaric acid: Spectroscopic (FT-IR, FT-Raman,  $^1\text{H}$  and  $^{13}\text{C}$  NMR) and theoretical (in B3LYP/6-311++G\*\* level) studies
- PS2-72 **P. Matejka, M. Vyskovska, A. Kokaislova, V. Prokopec, J. Cejkova, M. Clupek**  
Surface-enhanced spectroscopic methods on metal nano-surfaces: What is the role of oxidation reduction cycles?
- PS2-73 **J.L. Castro, J.F. Arenas, M.R. López-Ramírez, J.C. Otero**  
Surface-Enhanced Raman Scattering of aromatic amides
- PS2-74 **M. Kokoskova, M. Prochazka, B. Vlckova**  
SERS/SERRS spectra and excitation profiles of Ru (II) bis(2,2-bipyridine)(4,4-dicarboxybipyridine) complex in systems with Ag nanoparticles: chemisorption versus electrostatic bonding
- PS2-75 **M. Giloan, S. Astilean**  
Computation of electromagnetic properties of plasmonic metamaterials with relevance in SERS by using S-parameter retrieval approach
- PS2-76 **A.M. Gabudean, S. Astilean**  
A pH-dependent SERS study of 4-aminothiophenol adsorbed on gold nanorods
- PS2-77 **J.L. Castro, M.R. López-Ramírez, J.F. Arenas, J.C. Otero**  
SERS of benzenesulfonamide adsorbed on silver nanoclusters
- PS2-78 **P. Šimáková, M. Procházka**  
SERRS microspectroscopy of porphyrins on Ag immobilized nanoparticles
- PS2-79 **N. Mircescu, L. Szabo, N. Leopold, O. Cozar, V. Chi**  
Surface-enhanced Raman and DFT study on melamine
- PS2-80 **I. López-Tocón, J.C. Otero, J.F. Arenas, J.V. Garcia-Ramos, S. Sanchez-Cortes**  
Trace-detection of triphenylene by SERS spectroscopy using functionalized silver nanoparticles with bis-acridinium lucigenine

## Spectroscopy and Dynamics: Gas Phase and Matrices

### Oral

#### Monday

- 11.00 - 11.20 **E. J. Ocola, A.A. Al-Saadi, J. Laane**  
Spectroscopic and theoretical investigation of intramolecular  $\pi$ -type hydrogen bonding in 3-Cyclopentenol and related molecules
- 11.20 - 11.40 **L. Rubio-Lago, A. García-Vela, A. Arregui, G. A. Amaral, J. Rodríguez, M. González, L. Bañares**  
The photodissociation of  $\text{CH}_3\text{I}$  in the edges of the A-band: Comparison between slice imaging experiments and multisurface wave packet calculations
- 11.40 - 12.00 **R. Flammini, E. Fainelli, L. Avaldi, M. Satta**  
Dissociation of the ethyne dication: the case of  $\text{C}^+ - \text{H}^+ - \text{CH}$  channel
- 12.00 - 12.20 **G. Pianj, L. Poisson, B. Soep, J.-M. Mestdagh**  
Micro-solvation effects in ultrafast relaxation. Application to photochromic molecules
- 12.20 - 12.40 **G. B. Poparić, M. M. Ristić, D. S. Belić**  
Forward-to-backward differential-cross-section ratio in electron-impact vibrational excitation via the  $^2\Sigma_u^+$  resonance of  $\text{H}_2$



- 12.40 - 13.00 A. Loewenschuss, M. Rozenberg, C. J. Nielsen  
Hydrogen bonding in solid Xenon. A matrix isolation study
- 15.10 - 15.30 M. Coreno, K. Prince  
Molecular photoionization spectroscopy with synchrotron radiation
- 15.30 - 15.50 C. Puzzarini, G. Cazzoli, J. Gauss  
Hyperfine structure of rotational spectra: interplay of experiment and theory
- 15.50 - 16.10 S. Melandri, A. Maris, B.M. Giuliano, L.B. Favero, A. Merloni, W. Caminati  
The shape of biomolecules and their weakly bound molecular complexes reviewed by microwave spectroscopy.
- 16.10 - 16.30 P. R. Joshi, L. Krim  
The vibration structure of OH radical and OH-H<sub>2</sub>O complex: A Matrix Isolation Study
- 17.00 - 17.20 J. R. Durig, A. Ganguly, S. S. Panikar, I. D. Darkhalil,  
T. Iwata  
Conformational stability of some organoamines by utilizing variable temperature infrared spectra of rare gas solutions
- 17.20 - 17.40 M. Nedić, T. N. Wassermann, R. W. Larsen, M. A. Suhm  
Small water/alcohol clusters: a combined Raman- and FTIR-jet study
- 17.40 - 18.00 S. X. Zhou, J. R. Durig  
Conformational stability, structural parameters and vibrational assignment from variable temperature infrared spectra of krypton solution of ethylisocyanate

## Ultrafast spectroscopy and computational methods

### Oral

#### Thursday

- 15.00 - 15.20 A.A. Bakulin, J.C. Hummelen, P.H.M. van Loosdrecht, M.S. Pshenichnikov  
30-fs Hole-transfer dynamics in Polymer/PCBM bulk heterojunction
- 15.20 - 15.40 T. Mančal, F. Šanda, N. Christensson, V. Butkus, J. Olšina, V. Balevicius Jr., L. Valkunas  
Two-dimensional coherent electronic spectroscopy of electron-phonon coupling
- 15.40 - 16.00 S.V. Krasnoshchekov, E.V. Isayeva, N.F. Stepanov  
Mixed numerical/analytic solution of the anharmonic vibrational problem for a polyatomic molecule using high orders of canonical perturbation theory
- 16.00 - 16.20 M.J. Wójcik, Ł. Boda, M. Boczar  
Theoretical study of proton tunneling in the excited state of tropolone
- 16.50 - 17.10 K. Itoh  
DFT Calculation of Low Frequency Vibrational Modes of Polypeptides Consisting of L- and D-Alanine Residues
- 17.10 - 17.30 T. Burova, A. Anashkin  
Quantum-mechanical analysis of intensity distribution in resonance hyper Raman spectra of polyatomic molecules
- 17.30 - 17.50 A. Milani, C. Castiglioni  
Atomic charges and charge fluxes derived from IR intensities
- 17.50 - 18.10 V.H. Rusu, M.N. Ramos, R.L. Longo  
CCFOM and CCFDF models to interpret infrared intensities: A Comparative Study



**Poster**

- PS2-81 **F. Muniz Miranda, M. Pagliai, G. Cardini, V. Schettino**  
Spectroscopic properties of hydrogen-bonded systems by wavelet analysis
- PS2-82 **C. Araujo-Andrade, S. Lopes, R. Fausto, A. Gómez-Zavaglia**  
Conformational study of arbutin by quantum chemical calculations and multivariate analysis
- PS3-83 **M. Ristova, J. Petreska, Lj. Pejov, B. Šoptrajanov**  
Conformational equilibria and intramolecular proton transfer in Hydrogenmalonate anion: Influence of the crystalline environment. A combined vibrational spectroscopic and quantum chemical study
- PS2-84 **H. Yurtseven, B. Raşitoğlu**  
Vibrational frequencies studies as a function of pressure near the I-II phase transition in solid benzene
- PS2-85 **H. Yurtseven**  
Critical behavior of the order parameter from birefringence and Raman intensity data close to the  $\lambda$ -transition in  $\text{NH}_4\text{Br}$
- PS2-86 **N. Trendafilova, I. Georgieva, B.S. Creaven**  
Structure and spectroscopic properties of Ni(II), Co(II) and Zn(II) complexes with coumarin derivative predicted by DFT calculations
- PS2-87 **C. D. Contreras, A. E. Ledesma, J. Zinzuk, S. A. Brandán**  
Structural and vibrational study of 2-benzyl-4,5-dihydro-1H-imidazole
- PS2-88 **E. C. Aguiar, J. B. P. da Silva, M. N. Ramos**  
A theoretical interpretation of the Infrared intensities of Maleimide
- PS2-89 **G. Keresztury, T. Sundius, M. Rogojerov, Cs. Németh**  
Performance of polarized continuum solvation models in DFT prediction of IR band polarization properties for anisotropic LC solutions
- PS2-90 **A. Padilla, J. Pérez**  
A simulation study of the far-infrared absorption spectra of HCl diluted in liquid Ar
- PS2-91 **A. Milani, F. Innocenti, C. Castiglioni**  
Raman spectra of polyyenes and cumulenes: a computational investigation
- PS2-92 **L. C. Bichara, E. G. Ferrer, H. E. Lanús, C. G. Nieto, S. A. Brandán**  
Theoretical and experimental vibrational study of anhydrous Citric Acid as monomer and dimer
- PS2-93 **T. Teslaru, A. Sebi, R. Stanculescu, D.-O. Dorohoi**  
Spectral and quantum-chemical characterization of some carbanion monosubstituted cycloimmonium Ylids
- PS2-94 **R. E. Stanculescu, V. Sunel, D.-O. Dorohoi**  
Electro-optical parameters of some thiosemicarbazides studies by spectral and computational means
- PS2-95 **N. F.C. Mendes, P. Ribeiro-Claro**  
Crystal polymorphism: a combined approach using vibrational spectroscopy and ab initio calculations
- PS2-96 **O.V. Postlyakov**  
Transformation of spectral radiance by inelastic and elastic scattering in the gaseous atmosphere
- PS2-97 **M. Avadanei, Virgil Barboiu, Mihaela Dulcescu, Lenuta Profire, Dana-Ortansa Dorohoi**  
7-[2-Hydroxy-3-(4-Acetyl-Amino)-Phenoxy-Propyl]-1,3 Dimethylxantine derivatives characterized by hyperchem 8.0.6 and spectral means





- PS2-98 **R.M. Mahfouz, N.S. Al-Hokbany, S.M. Akriche, M. Rzaigui**  
Structural and Theoretical Studies of 2-amino-3-nitropyridine
- PS2-99 **C. Gellini, M. Muniz-Miranda, P. R. Salvi, M. Alloisio, G. Dellepiane**  
Structural and vibrational properties of photochromic polydiacetylenes
- PS2-100 **D. Duce, M. Ottonelli, M. Piccardo, G. Dellepiane**  
A theoretical study on the spectroscopical effects of rhodamine b and noble metals nanoparticles interactions
- PS2-101 **M. Pagliai, F. Muniz Miranda, G. Cardini, R. Righini, V. Schettino**  
Hydrogen bond dynamics of methyl acetate in methanol
- PS2-102 **T. A. Ford**  
*Ab initio* studies of the homodimers of methane and silane, and of methyl and silyl fluoride and chloride
- PS2-103 **G. Świdorski, S. Wojtulewski, M. Kalinowska, R. Świśtocka, W. Lewandowski**  
Effect of alkali metal ions on the pyrrole and pyridine  $\pi$ -electron systems in pyrrole-2-carboxylate and pyridine-2-carboxylate molecules: FT-IR, FT-Raman, NMR and theoretical studies
- PS2-104 **M. J. Wójcik, J. Kwiendacz, M. Boczar, Ł. Boda, Y. Ozaki**  
Theoretical and spectroscopic study of hydrogen bond vibrations in imidazole and its deuterated derivative
- PS2-105 **G. Mile, M. Oltean, V. Chis**  
Potential energy curves for PTCDI and PTCD A dimers obtained by MP2 and DFT methods with dispersion correction
- PS2-106 **M. Candelaresi, L. Bussotti, M. Paolantoni, P. Foggi**  
Methanol under moderate pressures: a dynamical study by femtosecond transient spectroscopy
- PS2-107 **E. Collini, F. Todescato, C. Ferrante, R. Bozio**  
Energy Transfer across metal films mediated by Surface Plasmon Polaritons: a time-resolved fluorescence study
- PS2-108 **B. Brożek-Płuska, P. Ciąćka and H. Abramczyk**  
Vibrational dynamics at the phospholipid - water interface
- PS2-109 **T. Atsbeha, L. Bussotti, A. Marcelli, P. Foggi, S. Cicchi, G. Ghini, P. Fabbri**  
Photophysical characterization of low molecular weight organogels for energy transfer and light harvesting
- PS2-110 **A. Lapini, P. Tourón Touceda, S. Mosquera Vazquez, M. Lima, A. Dei, P. Foggi, R. Righini**  
Characterization of a cobalt-dioxolene complex by Transient Infrared Spectroscopy
- PS2-111 **S. Mosquera Vazquez, P. Foggi, A. Lapini, P. Tourón Touceda, A. Abbotto, F. De Angelis, M. Lobello**  
Transient absorption spectroscopy of Heteroaromatic Donor-Acceptor  $\pi$ -conjugated 2,2'-Bipyridines
- PS1-112 **M. Lima, A. Lapini, P. Tourón Touceda, S. Mosquera Vazquez**  
Cross Phase modulation in visible-pump/infrared-probe spectroscopy



## Vibrational and Electronic Spectroscopy

### Oral

#### Thursday

- 15.00 - 15.20 **V. Aleksa, J. Kausteklis, Z. Gdaniec, V. Balevicius**  
2D Raman correlation and NMR spectroscopy study of liquid crystalline ionogel phase formation in ionic liquid/H<sub>2</sub>O mixtures
- 15.20 - 15.40 **S. Cîntă Pînzaru, A. Falamas, N. Leopold, C. Dehelean, C. Lehene**  
Challenging SERS from biomolecules to tissue
- 15.40 - 16.00 **J. Grdadolnik**  
Backbone structures of 19 dipeptides in Aqueous Solution
- 16.00 - 16.20 **Horiba Jobin-Yvon**  
Advances in Raman spectroscopy
- 16.50 - 17.10 **V.A. Karachevtsev, A.M. Plokhotnichenko, M.V. Karachevtsev and V. S. Leontiev**  
Noncovalent interaction of carbon nanotubes with DNA and polynucleotides: UV absorption spectroscopy and molecular dynamic simulation
- 17.10 - 17.30 **M. Kozanecki, P. Zawadzka, R. Kisiel, M. Pastorczak**  
Intermolecular interactions in water-aliphatic halogen systems - vibrational spectroscopy studies
- 17.30 - 17.50 **B. Řezáčová, Ch. Zentz, P-Y Turpin, J. Štěpánek**  
Spectroscopic study of MADS box and its interaction with DNA
- 17.50 - 18.10 **V. Kopecký Jr., K. Hofbauerová, J. Kohoutová, J. Štěpánek, R. Etrich**  
Can drop coating deposition Raman spectroscopy distinguish shortcomings or inaccuracies in protein crystals?

### Poster

- PS1-84 **S. A. Brandán, E. Eroğlu, A. E. Ledesma, O. Oltulu, O. B. Yalçinkaya**  
DFT molecular force field of acetazolamide compound
- PS1-85 **Z. Dega-Szafran, A. Katrusiak, M. Szafran, P. Barczyński**  
Spectroscopic and structural studies of 2-(quinuclidinium)-butyric acid bromide hydrate
- PS1-86 **N. Eremina, A. Barth**  
Infrared spectroscopic studies of Ca<sup>2+</sup> ATPase phosphoenzyme
- PS1-87 **M. Samsonowicz, E. Regulska, R. Świsłocka, W. Lewandowski**  
Experimental and theoretical study of molecular structure of magnesium, calcium, strontium and barium 4-nitrobenzoates
- PS1-88 **A. Gatjal, H. Juhásová, M. Gróf, J. Kožíšek, V. Milata, N. Prónayová, P. Matějka**  
Isomerizational and conformational study of methyl-2-cyano-3-methoxyacrylate (MCMA) and methyl-2-cyano-3-aminoacrylate (MCAA) and its N-methyl derivatives
- PS1-89 **V. Sablinskas, I. Doroshenko, V. Pogorelov, V. Balevicius**  
Propanol in argon matrix: 2D FTIR correlation spectroscopy
- PS1-90 **A. Şengül, E. Eroğlu**  
Vibrational and structural study of 6,6'-diacetyl-2,2'-bipyridine dioxime using FT-IR Raman and quantum chemical calculations
- PS1-91 **N. Vedeanu, A. Pîrnău, B. I. Cozar, O. Oniga, C. Moldovan, C. M. Lucaciu**  
NMR, IR and Raman investigation of 3-[2-(4-Methyl-2-phenyl-thiazol-5-yl)-2-oxo-ethyl]-thiazolidine-2,4-dione compound with antimicrobial potential
- PS1-92 **M.M. Szostak, K. Piela, H. Chojnacki, E. Bidzińska, K. Dyrek**



- Paramagnetic species generated by near IR as possible intermediates in molecular mechanism of optical nonlinearity in 1,3-dinitrobenzene crystal. NIR, EPR, CD and quantum chemical studies
- PS1-93 F. Kollipost, S. Hesse, J. J. Lee, M. A. Suhm  
Dimers of cyclic carbonates: Chirality recognition in battery solvents
- PS1-94 M. Citroni, R. Bini, M. Pagliai, G. Cardini, V. Schettino  
The reactivity of nitromethane under high static pressure
- PS1-95 A. Maris, S. Melandri, W. Caminati, L. B. Favero  
Rotational spectrum of glycolamide-water and glycolamide-ammonia molecular complexes.
- PS1-96 A. Mayer, M. Sipiczki, Gy. Szöllösi, J.T. Kiss, I. Pálkó  
Synthesis, structural characterization and some applications of immobilized organocatalysts
- PS1-97 I.B. Cozar, L. Szabó, N. Leopold, D. Mare, V. Chiş, L. David  
Vibrational spectroscopic and DFT study of paroxetine
- PS1-98 M. Kurt, H. Yurtseven  
Analysis of the frequency shift and the linewidth as a function of temperature in solid nitrogen
- PS1-99 C. Ivascu, L. Daraban, O. Cozar, I. Ardelean  
FT-IR and Raman studies on the  $P_2O_5$ -BaO-Li<sub>2</sub>O glass system
- PS1-100 S. Demirci, S. Kınalı, Z. Çalışır, M. Kurt, A. Ataç  
DFT, FT-Raman, FT-IR and NMR studies of 4-(substituted phenylazo)-3,5-diacetamido-1H-pyrazoles
- PS1-101** G. Ogruc-Ildiz  
Theoretical and experimental vibrational analysis of Hydantion
- PS1-102 M. Nedić, M. Albrecht, B. Dittrich, M. A. Suhm  
Methyl Mandelate - From Dimers to Crystals
- PS1-103 N. O. B. Lüttschwager, T. N. Wassermann, S. Coussan, M. A. Suhm  
Environmental and vibrational influence on the proton transfer in malonaldehyde
- PS1-104 A. Bebu, A. Kozma, E. Forizs, M. Toderas, L. David  
Spectral and ESR study of Cu(II), Co(II) and Ni(II) theophyllinato complexes containing propanolamine ligands
- PS1-105 S. Akyuz T. Akyuz  
Adsorption of 2- and 3-Chloropyridine on Sepiolite and Loughlinite: An Infrared Spectroscopic Study
- PS1-106 E. L. Terpugov, O. V. Degtyareva  
Mid-infrared stimulated emission spectroscopy and its applications
- PS1-107 I. Kowalczyk, M. Szafran  
Aminopyridine betaines and their hydrohalides studied by FTIR and NMR spectroscopy and DFT calculations
- PS1-108 M. E. Defonsi Lestard, L. A. Ramos, M.E. Tuttolomondo, S. E. Ulic, A. Ben Altabef  
Synthesis, spectroscopic and structural properties of trichoromethyl trifluoromethanesulphonate,  $CF_3SO_2OCCl_3$
- PS1-109 A. Pîrnău, M. Bogdan, M. Palage, L. Szabo, N. Leopold, R. A. Varga, O. Cozar, V. Chiş  
Experimental and theoretical investigation of 2-phenyl-thiazole-4-yl-methyl-quinolinium iodine
- PS1-110 M. Ptak, M. Maczka, J. Hanuza, A. A. Kaminskii, P. Becker, L. Bohaty  
Raman and IR studies of melilite-type crystals  $Ca_2MgSi_2O_7$ ,  $Ca_2ZnSi_2O_7$  and



- PS1-111** Sr<sub>2</sub>MgSi<sub>2</sub>O<sub>7</sub>  
J. Lorenc  
Effect of methyl group and N-H...N hydrogen bond on IR and Raman spectra of 2-(N-ethylamino)-3(or 5)-methyl-4-nitropyridine
- PS1-112** L. Illés, K. Felföldi, J.T. Kiss, I. Pálkó  
C-H...S hydrogen bonds as the organizing force in 2,3-thienyl- and phenyl- or 2,3-dithienyl-substituted propenoic acid aggregates studied by the combination of FT-IR spectroscopy and computations
- PS1-113** A. A. Yakubov  
Hydrogen bonds and mesomorphism of cholesteryl formiate
- PS1-114** V. M. Petruševski, D. Sazdov, B. Šoptrojanov  
The O-D/HDO stretchings in the Li<sub>2</sub>(S,Se)O<sub>4</sub>(H,D)<sub>2</sub>O system: employing the double isolation method
- PS1-115** T. Jednačák, P. Novak, A. Kišić, T. Hrenar, S. Miljanić, G. Verbanec  
Reaction monitoring of entacapone synthesis by in-line Raman spectroscopy and principal component analysis
- PS1-116** N.P.C. Westwood, J. Wang  
Cyanogen isocyanate, NCNCO; the infrared conundrum
- PS1-117** N.F.L. Machado, L.A.E. Batista de Carvalho, M.P.M. Marques  
Antioxidant chromones - A conformational study
- PS1-118** O. Gamulin, M. Ivanda, V. Mitsa, M. Balarin, and M. Kosović  
Monitoring of structural phase transition of (Ge<sub>2</sub>S<sub>3</sub>)<sub>x</sub>(As<sub>2</sub>S<sub>3</sub>)<sub>1-x</sub> chalcogenide glass with Raman spectroscopy
- PS1-119** A. Lucotti, M. Tommasini, W.A. Chalifoux, D. Fazzi, G. Zerbi, R.R. Tykwinski  
Bent polyynes: Ring strain studied by Raman and Infrared spectroscopies
- PS1-120** R.M. Lees, Li-Hong Xu, B.E. Billingham  
Weeding the Cosmos - FTIR synchrotron spectroscopy of Methanol isotopologues at the Canadian light source
- PS1-121** A. Wesetucha-Birczyńska, T. Toboła  
Raman microspectroscopy of inclusions in bituminous salts
- PS1-122** G. Štefanić, I. I. Štefanić, S. Musić and M. Ivanda  
Structural and microstructural changes in the zirconium-indium mixed oxide system during thermal treatment
- PS1-123** P. Barczyński, M. Szafran  
Structure of 3,4-dicarboxy-1-methylpyridinium betaine studied by X-ray diffraction, DFT calculations, NMR and FTIR spectra
- PS1-124** A. Esme, S. Sagdinc  
The studies of molecular structures and vibrational spectra of Sudan Orange G and Sudan Red G
- PS1-125** K. Chruszcz-Lipska, A. Kaczor  
Structural behavior of selected ionones upon thermal stress conditions
- PS1-126** B. M. Giuliano, I. Reva, R. Fausto, S. Melandri  
Infrared spectroscopy and photochemistry of 2-phenylethylamine and its derivatives isolated in noble gas matrices.
- PS1-127** C. M. Nunes, I. Reva, R. Fausto, T. M.V.D. Pinho e Melo  
Flash Vacuum Pyrolysis of Isoxazole. A low temperature matrix isolation Infrared spectroscopy study.
- PS1-128** A. Sharma, N. Kuş, I. Reva, L. Lapinski, R. Fausto  
Infrared spectra of matrix-isolated 4-methoxybenzaldehyde (*p*-anisaldehyde) conformers



- PS1-129 **I. Doroshenko, V. Pogorelov, P. Uvdal, V. Balevicius, V. Sablinskas**  
Temperature controlled kinetics of growing and relaxation of alcohol clusters in Argon matrix
- PS1-130 **I. Reva, L. Lapinski, R. Fausto**  
Spectral indicators of structural flexibility of matrix isolated methyl isocyanate
- PS1-131 **M. Rozenberg, A. Loewenschuss**  
The matrix isolation infrared spectrum of the Sulfuric Acid-monohydrate complex: New assignments and resolution of "missing H-bonded  $\nu(\text{OH})$  band" issue.
- PS1-132 **N. Kuş, I. Reva, R. Fausto**  
Infrared spectrum and photochemistry of matrix-isolated 3-Furaldehyde
- PS1-133 **J. Dobrowolski, M. H. Jamróz, R. K., J. E. Rode, M. K. Cyrański, J. Sadlej**  
IR low-temperature matrix, X-ray and ab initio study on L-Isoserine conformations
- PS1-134 **M. Ceppatelli, S. Fanetti, M. Citroni, R. Bini**  
Photoinduced reactivity of liquid ethanol at high pressure
- PS2-113 **R. M. Pinto, A. A. Dias, M. L. Costa**  
Study of tetrazole derivatives by UV photoelectron spectroscopy and outer-valence Green's function methods.
- PS2-114 **R. M. Pinto, G. Copeland, A. A. Dias, M. L. Costa, J. M. Dyke**  
Thermal decomposition of benzyl azide and its methyl derivatives studied by UV photoelectron spectroscopy and theoretical calculations.
- PS2-115 **W. Szaśiadek, E. Kucharska, I. Bryndal, M. Wandas, J. Hanuza**  
Excited electronic states, crystal structure and DFT quantum chemical calculations of 2-amino-4-methyl-3-nitropyridine.
- PS2-116 **D. O. Dorohoi, A. Airinei, R. I. Tigoianu**  
Revisiting the electronic spectra of anthracene.
- PS2-117 **M. Scholz, R. Džedić, A. Svoboda, J. Hála**  
TPP and singlet Oxygen quenching by carotene in solution.
- PS2-118 **J. Polak, M. Bartoszek, M. Żądło, W.W. Sułkowski**  
The EPR study of humic acid extracted from sediment collected at various seasons.
- PS2-119 **T. Iwata, Y. Mizutani**  
Comparison of a Pulsed-Excitation and a Phase-Modulation method for estimating fluorescence lifetimes using a convolved-Autoregressive Model and a high-gain PMT.
- PS2-120 **A. Mezzetti, S. Protti, J.-P. Cornard, C. Lapouge, A. Idrissi, M. Fagnoni, A. Albini**  
Solvent effects on 3-hydroxyflavone photophysics / photochemistry. Relevance to its application in optical devices and its use as a (bio-)sensor.
- PS2-121 **A. Mezzetti, S. Protti, S. Lazzaroni, A. Barras, N. Montfillette-Dupont, C. Lapouge, J.P. Cornard**  
Spectroscopic investigation of flavonoids of biomedical relevance in solution and inside lipid nanocapsules.
- PS2-122 **D. Cheshmedzhieva, B. Hadjieva, S. Ilieva, D. Nalbantova, B. Galabov.**  
Reactivity of carbamates in the alkaline hydrolysis reaction.
- PS2-123 **L. Grisanti, C. Sissa, F. Terenziani, A. Painelli**  
CT chromophores and complexes: Spectra and models.
- PS2-124 **G. Piani, M. Pasquini, G. Pietraperzia, E. M. Castellucci, M. Becucci**  
Different methods for ionization threshold determination.
- PS2-125 **M. Scotoni, A. Mazzalai**  
Velocity dependence of  $\text{C}_2\text{H}_2$  rotational temperature in a supersonic expansion.



- PS2-126 M. Becucci, G. Ferrari, M. Prevedelli, I. Boscolo, F. Castelli, S. Cialdi, F. Villa, M.G. Giammarchi  
A laser system for efficient excitation of positronium towards Rydberg levels.
- PS2-127 B. M. Giuliano, V. Feyer, K.C. Prince, M. Coreno, L. Evangelisti, S. Melandri, W. Caminati  
Tautomerism in pyrimidine derivatives investigated with core level spectroscopy techniques
- PS2-128 S. Abbruzzetti, A. Bonamore, A. Boffi, A. Feis, P. Foggi, C. Gellini, A. Marcelli, P.R. Salvi, C. Viappiani  
Time-resolved spectroscopy of native and mutated *Thermobifida fusca* hemoglobins
- PS2-129 M. Ceppatelli, R. Bini, V. Schettino  
High pressure photoinduced reactivity in clathrate hydrates
- PS2-130 G. Das, M.L. Coluccio, A. Nicastrì, F. Gentile, F. De Angelis, E. Di Fabrizio, G. Cuda  
Raman spectroscopy for the evaluation of structural changes of peptides

## Young Scientists

### Oral

#### Thursday

- 15.00 - 15.20 C. F. Dascalu, B. C. Zelinschi, D. O. Dorohoi  
Main refractive indices of some carpathian crystals
- 15.20 - 15.40 M. Vyskovska, V. Prokopec, M. Clupek, A. Kokaislova, J. Cejkova, P. Matejka  
Development of copper nanostructured materials for surface-enhanced Raman scattering spectroscopy
- 15.40 - 16.00 R. E. Stanculescu, V. Sunel, D. O. Dorohoi  
electro-optical parameters of some thio-semicarbazides studied by spectral and computational means
- 16.00 - 16.20 F. Palombo, P. Sassi, M. Paolantoni, A. Morresi, M. G. Giorgini  
Raman spectroscopic study of the effects of ion solvation on liquid phase structure and dynamics of LiI-acetone solutions
- 16.50 - 17.10 S. Kumar, A. Barth  
Phosphoenolpyruvate and Mg<sup>2+</sup> binding to pyruvate kinase monitored by infrared spectroscopy
- 17.10 - 17.30 V. Andrushchenko, H. Wieser, M. Straka, P. Bouř  
Combination of circular dichroism spectroscopy with theoretical spectra simulations as a tool for structural studies of macromolecules
- 17.30 - 17.50 N. O. B. Lüttschwager, T. N. Wassermann, S. Coussan, M. A. Suhm  
Environmental and vibrational influence on the proton transfer in malonaldehyde

## GISR

### Oral

#### Wednesday

- 11.40 - 12.00 E. Collini, G.D.Scholes  
Coherent dynamics in energy migration at room temperature: Evidence for subtle quantum-mechanical strategies for energy transfer optimization
- 12.00 - 12.20 E. Garbin, E. Lubian, S. Kovalenko, N. Ernstring, T. Carofiglio, C. Ferrante



- Energy transfer processes in homo and hetero dimers of porphyrins  
 12.20 - 12.40 H. Torii, M. G. Giorgini, M. Musso  
 One- and two-mode behavior of the  $\nu(\text{C}=\text{O})$  band in N,N-dimethylformamide isotopic mixtures: DMF/DMF- $\text{d}_6$  and DMF/DMF- $^{13}\text{C}$ O
- 12.40 - 13.00 A. Lapini, P. Tourón Touceda, S. Mosquera Vazquez, M. Lima, A. Dei, P. Foggi, R. Righini  
 Transient Infrared Spectroscopy: A new approach to investigate Valence Tautomeric Interconversion
- 14.30 - 14.50 C. Lofrumento, Ph. Sciau, Y. Leon, E. M. Castellucci  
 A semi-quantitative LIBS analysis on *Terra Sigillata* wares
- 14.50 - 15.10 G. Das, M.L. Coluccio, A. Nicastrì, F. Gentile, F. De Angelis, E. Di Fabrizio, G. Cuda  
 Raman spectroscopy for the evaluation of structural changes of peptides
- 15.10 - 15.30 M. Ceppatelli, R. Bini, V. Schettino  
 High pressure photoinduced reactivity in clathrate hydrates
- 15.30 - 15.50 S. Abbruzzetti, A. Bonamore, A. Boffi, A. Feis, P. Foggi, C. Gellini, A. Marcelli, P.R. Salvi, C. Viappiani  
 Time-resolved spectroscopy of native and mutated *Thermobifida fusca* hemoglobins
- 15.50 - 16.10 B. M. Giuliano, V. Feyer, K.C. Prince, M. Coreno, L. Evangelisti, S. Melandri, W. Caminati  
 Tautomerism in pyrimidine derivatives investigated with core level spectroscopy techniques
- 16.40 - 17.00 M. Biczysko  
 Computational spectroscopy as a tool to interpret experimental results: from small molecules in the gas phase to large systems in condensed phases.
- 17.00 - 17.20 V. Amendola, G. Marcolongo, G. Fracasso, M. Colombatti and M. Meneghetti  
 SERS active gold nanostructures for selective and ultrabright biolabelling: synthesis and quantitative study
- 17.20 - 17.40 P. Taddei, E. Modena, A. Tinti, F. Siboni, C. Prati, M.G. Gandolfi  
 Vibrational investigation on the in vitro bioactivity of commercial and experimental calcium-silicate cements for root-end endodontic therapy

#### Thursday

- 15.00 - 15.20 B. Rossi, G. Cazzolli, G. Vilianni, C. M.C. Gambi, S. Marchetti  
 Molecular aggregation processes in self-assembled micellar systems investigated by Raman scattering and numerical simulation
- 15.20 - 15.40 E. Fazio, F. Neri, S. Trusso  
 Surface-enhanced Raman scattering (SERS) from  $\text{SnO}_2$  material
- 15.40 - 16.00 G. D'Avino, A. Girlando, M. Masino, A. Painelli  
 Electron-phonon entanglement near a ferroelectric phase transition: evidences from low-frequency Raman scattering
- 16.00 - 16.20 M.A. Ferrara, L. Sirleto, I. Rendina, S.N. Basu, J. Warga, R. Li, L. Dal Negro  
 Enhanced stimulated Raman scattering in silicon nanocrystals embedded in silicon-rich nitride/silicon superlattice structures



- 16.50 - 17.10 M. Paolantoni, L. Comez, D. Fioretto, M. E. Gallina, L. Lupi, A. Morresi, S. Perticaroli, P. Sassi, F. Scarponi  
The dynamics of water in aqueous solutions of biological molecules assessed by broadband depolarized light scattering experiments
- 17.10 - 17.30 B.D. Howes, D. Giordano, L. Boechi, M. Fittipaldi, D.A. Estrin, M. Coletta, G. Di Prisco, C. Verde, G. Smulevich  
The pronounced structural flexibility of the 2/2 hemoglobin of the antarctic cold-adapted *Pseudoalteromonas haloplanktis* TAC125
- 17.30 - 17.50 M. Tommasini, A. Lucotti, G. Zerbi  
A Raman study of Schiff base protonation in bacteriorhodopsin and related molecular models
- 17.50 - 18.10 P. Sassi, G. Onori, A. Giugliarelli, M. Paolantoni, S. Cinelli, A. Morresi  
The thermal unfolding of lysozyme in solution: the role of the solvent

**Poster**

- PS2-131 G. Compagnini, G. Forte, F. Giannazzo, V. Raineri, A. La Magna, I. Deretzis  
Ion beam induced defects in graphene: Raman spectroscopy and DFT calculations
- PS2-132 C. Lofrumento, M. Ricci, L. Bachechi, D. De Feo, E. M. Castellucci  
Spectroscopic analyses on rock art paintings from east central Ethiopia.
- PS2-133 M. P. Marzocchi, A. Belshi  
Combined analysis of structural and spectral observables for heme proteins.
- PS2-134 F.P. Nicoletti, E. Droghetti, A. Feis, A. Boffi, G. Smulevich  
Resonance Raman and UV-vis absorption spectra of *Thermobifida fusca* truncated hemoglobin in its ferric state.
- PS2-135 F. Palombo, P. Sassi, M. Paolantoni, A. Morresi, M. G. Giorgini  
Raman spectroscopic study of the effects of ion solvation on liquid phase structure and dynamics of LiI-acetone solutions.
- PS2-136 G. Piani, L. Rubio Lago, M. Becucci  
Photoelectron imaging on Iodine atoms produced by CF<sub>3</sub>I photodissociation.
- PS2-137 M. Biczysko  
Computational spectroscopy as a tool to interpret experimental results: from small molecules in the gas phase to large systems in condensed phases
- PS2-138 A. Weselucha-Birczyńska, L. Natkaniec-Nowak  
Raman microspectroscopic study of organic inclusions in „watermelon” tourmaline from the Paprok mine (Nuristan, Afganistan)
- PS2-139 C. Paluszkiwicz, A. Weselucha-Birczyńska, E. Stodolak  
Raman Spectroscopy Investigations of a Chitosan-Clay Nanocomposite





## **Spectroscopy with laser frequency combs**

T. W. Haensch

*Max Plank Institut für Quantenoptik, Garching, Germany*

### **Eigenstate resolved spectroscopy in the gas-phase: towards larger systems and higher energies**

M. Schmitt

*Heinrich-Heine-Universität Düsseldorf*

Here the body of your abstract. The abstracts must be max. 1 page with the format used here. Please underline the name of the presenting author. You can insert black and white figures only. Intrinsic properties of large isolated molecules can be investigated by eigenstate resolving electronic spectroscopy in molecular beams. The rotationally resolved spectra even of medium sized molecules are generally quite congested due to the existence of various conformers, which often spectrally overlap. Nevertheless, the spectral discrimination of conformers due to their different centre frequency because of their different zero-point energies or electronic effects is one of the most important benefits of this method compared to other, higher resolving techniques like microwave spectroscopy. Direct evaluation of the molecular parameters which can be used to determine the structure using line position assigned fits are in most cases difficult or even impossible. Automated fits without the need for manual line position assignments using a Genetic Algorithm (GA) [1,2] or Evolutionary Algorithm (EA) approach have been shown to be very successful in these cases. Information about vibronic coupling between higher vibronic states is contained in the intensities of individual rovibronic transitions and can be used for a more thorough understanding of photophysical processes at high vibronic energies. The limitations and prospects of the method will be discussed.

- [1] W. L. Meerts and M. Schmitt, *Algorithms Phys. Scripta* 73 (2005) C47
- [2] W. L. Meerts and M. Schmitt, *Rev. Phys. Chem.* 25 (2006) 353



### Laser spectroscopies for cultural heritage

D. Anglos,<sup>1,2</sup> and C. Fotakis,<sup>1,3</sup>

<sup>1</sup>*Institute of Electronic Structure and Laser, Foundation for Research and Technology-Hellas, P.O.Box 1385, 711 10 Heraklion, Crete, Greece*

<sup>2</sup>*Department of Chemistry, University of Crete, Heraklion, Crete, Greece*

<sup>3</sup>*Department of Physics, University of Crete, Heraklion, Crete, Greece*

The study and preservation or restoration of objects of cultural heritage is an issue of enormous importance to history and civilization. From the scientific standpoint this, primarily, relies on our capabilities to determine the composition of complex materials, understand ageing processes and apply efficient conservation treatments. And as it turns out, it is a highly challenging task, considering the inherently complex, multi-component nature of materials in such objects, which calls for elaborate and quite often case-specific analysis and conservation procedures. Furthermore, given the value and sensitivity of works of art, analysis needs to be carried out in as non-invasive a manner as possible, often directly on the object itself or, in certain cases, on increasingly small samples.

In recent years laser based techniques have been shown as capable to illuminate complex diagnostic and restoration problems. In fact a number of laser material processing and spectroscopic methods has been specifically adapted with exceptional success to the requirements of a wide range of demanding conservation applications. By tuning the wavelength of the laser source and/or by controlling the flux of photons it is possible to realize many different types of light-matter interactions and therefore probe the composition of materials from different perspectives or even exploit laser cleaning. Linear and non-linear spectroscopies, remote sensing methods and laser-assisted sampling-excitation schemes evidence the versatility offered by lasers. In parallel, with advances in laser and detector technology, compact, mobile instrumentation is becoming available permitting field use of such laser-based techniques for analysis of materials in works of art and archaeological findings.

Illustrative examples related to laser cleaning will be given and the prospects and limitations of laser technology in sculpture and painting restoration applications will be discussed on the basis of the underlying fundamental processes. Also the prospects of employing laser analytical techniques in art conservation and archaeometry will be presented in view of recent advances on compact, portable instrumentation.

[1] "Photons in the service of our past: Lasers in the preservation of cultural heritage" S. Georgiou, D. Anglos, C. Fotakis, *Contemporary Physics* **49**, 1-27 (2008).

[2] "Lasers in the analysis of cultural heritage materials" D. Anglos, S. Georgiou, C. Fotakis, *Journal of Nano Research* **8**, 47-60 (2009).



### On a few interesting applications of photothermal science in the characterization of foods

D. Bicanic

*Laboratory of Biophysics, Department of Agrotechnology and Food Sciences, Wageningen University and Research Center, Driejenlaan 3-Transitorium, 6703 HD Wageningen, The Netherlands*

Carotenoids are notable for their widespread distribution, structural variety and various functions. Within the class of carotenoids only a few compounds are encountered in foods. They were demonstrated to have the health promoting effects; which has been associated with the potential of carotenoids to react with the free radicals. The composition of carotenoids in food varies greatly. Although the absolute concentrations differ considerably relative proportions of specific carotenoids are rather constant [1]. Carotenoids of primary interest are beta-carotene (the most potent provitamin A) lycopene and the yellow pigment lutein.

The traditional approaches to analysis of carotenoids are known for their inherent complexity; they are tedious and also error prone. It is therefore of practical interest, in particular for the population in certain regions of the world, to investigate the potential of alternative methods for the rapid, sensitive and the low cost detection of carotenoids in some foods.

In the recent years one has developed interest to explore possibilities offered by what is generally known as the photothermal (PT) science. This latter encompasses a wide range of PT techniques that all rely upon the conversion of absorbed optical energy into heat. Carotenoids in the liquid and semi-liquid foods, as well as in pasty and powdered specimens have received particular attention. Lycopene (because of the effect it has on the human health) has drawn considerable interest. The performance of the proposed PT methods as a new means for probing the matter has been compared to well that of the adapted techniques such as HPLC, spectrophotometry, Raman spectroscopy and colorimetry.

In addition, there is a perpetual demand for the reliable measurements of basic thermal properties of the vast range of foods. The two such examples are the heat penetration coefficient (thermal effusivity) and the thermal diffusivity: both can be accurately and directly determined by PT techniques.

- [1] Rodriguez-Amaya D.B. and Kimura M.; HarvestPlus Handbook for Carotenoid Analysis, HarvestPlus Technical Monograph Series 2, Washington DC and Cali: International Food Policy Research Institute (IFPRI) and International Centre for Tropical Agriculture (CIAT), 2004.



## The confluence of spectroscopy, microscopy and tomography

J. M. Thomas

*Department of Materials Science and Metallurgy, University of Cambridge,  
Pembroke Street, Cambridge, CB2 3QZ, UK*

High-energy electron-energy-loss spectroscopy (HEEELS) is a powerful analytical tool for probing the nature and properties of nanostructured materials in the solid state. Chemical composition, atomically-resolved structure, oxidation states, plasmonic behaviour and the momentum density of electrons in all solid materials in extremely minute amounts (sub attogram  $10^{-18}$ g or less) may be routinely investigated using this technique. Traditionally, static HEEELS has been carried out using either transmission or scanning transmission electron microscopes (TEM or STEM) fitted with the appropriate electron spectrometer and/or electron filtering device. A special advantages accrue by using high-angle, annular dark-field, scanning transmission electron microscopy (HAADF-STEM), principally because element specific (*i.e.* Z-contrast) images may be readily recorded in this way<sup>[1]</sup> Dark-field electron tomography is superior to the bright-field variety, partly because of its incoherent nature.<sup>[2,3]</sup>

By combining electron tomography (ET) with HEEELS,<sup>[4]</sup> a four-dimensional picture of solid specimens (both inorganic and biological) can be obtained *i.e.* 3D microscopic images with the added dimension of electron energy-loss signals. In this was a kind of “volume spectroscopy” is achieved, in which chemical composition of sub-attogram amounts of specimen may be determined non-destructively.

In the last five years, 4D electron microscopy of another kind (time-resolved), involving imaging in space and time, with picometer spatial and femtosecond timescales, retrospectively, has come of age.<sup>[5-8]</sup> The essence of this approach, in which the electrons are generated by photo-emission, along with some of its achievements, promise and future potential will be highlighted. The key feature of this 4D electron microscopy is that images are obtained stroboscopically with single-electron coherent packets. Under such conditions, electron repulsion is absent, thereby permitting highly-resolved real-space imaging, Fourier-space diffraction and energy-space electron spectroscopy with high spatio-temporal resolution.

- [1] JM Thomas in “*Physical Biology: From Atoms to Medicine*” (ed AH Zewail) Imperial College Press, (2008), p51
- [2] JM Thomas, PA Midgley, TJV Yates, JS Barnard, R Raja, I Arslan and M Weyland, *Angew. Chemie Intl. Ed.*, (2004) 43, 3735
- [3] PA Midgley, EPW Ward, AB Hugi and JM Thomas, *Chem. Soc. Rev.*, (2007), 36, 1477.
- [4] MH Grass, KK Koziol, AH Windle and PA Midgley, *Nano Letters*, (2006), 6, 376
- [5] AH Zewail, *Annu. Rev. Phys. Chem.* (2006), 57, 65
- [6] AH Zewail and JM Thomas “*4D Electron Microscopy: Imaging in Space and Time*”, Imperial College Press, (2010)
- [7] JM Thomas *Angew. Chemie. Intl. Ed.*, (2009) 48, 8824
- [8] AH Zewail, *Science*, (2010) in press.



## Watching proteins aggregate and electrons transfer with transient 2D IR spectroscopy

M. Zanni

*University of Wisconsin, Madison, USA*

Dynamics are a central and perplexing issue in structural biology and the energy sciences. Among the tools available to structural biologists and material scientists, 2D IR spectroscopy has a unique combination of structure and time-resolution. With this technique, it is possible to probe structural changes with bond-specificity and femtosecond accuracy. This talk will present recent results on applying the technique to study the aggregation of the amyloid polypeptide implicated in type 2 diabetes. In conjunction with isotope labeling, transient 2D IR spectra have been collected that reveals a detailed pathway of the peptide backbone as it forms toxic oligomers and fibrils. Experiments will also be presented in applying the technology to monitor the kinetics of electron transfer in dye-sensitized solar cells. In the latter experiments, it will be shown that 2D IR spectroscopy is an excellent probe of the electron dynamics, because the free-electron signal, which often overwhelms molecular features in linear spectroscopy, is not present in the 2D IR spectra, thereby permitting a thorough investigation of the dynamics.



## **Raman and IR spectroscopic approaches for studying protein structure and dynamics**

P. Hildebrandt<sup>1</sup>, D. H. Murgida<sup>2</sup>, M. A. Mroginski<sup>1</sup>, U. Kuhlmann<sup>1</sup>, I. Weidinger<sup>1</sup>, I. Zegber<sup>1</sup>

<sup>1</sup>*Technische Universität Berlin, Institut f. Chemie, Sekr. PC14, Straße des 17. Juni 136, D-10623 Berlin, Germany*

<sup>2</sup>*Departamento de Química Inorgánica, Analítica y Química Física / INQUIMAE-CONICET, Facultad de Ciencias Exactas y Naturales, Universidad de Buenos Aires, Ciudad Universitaria Pab. 2, piso 1, C1428EHA-Buenos Aires, Argentina*

Due to the substantial progress of structural biology made in the past years, detailed three-dimensional structure data are now available for a large number of proteins which is a prerequisite for understanding protein function on a molecular level. However, important information cannot be provided by X-ray crystallography since this technique fails to locate hydrogen atoms and protons which are essential determinants for controlling active site structures and reaction mechanism of proteins and enzymes. Furthermore, X-ray radiation may cause damages specifically of cofactors and thus may lead to structural models that are not sufficiently accurate in this specific part of the protein. In addition, only in rare cases X-ray crystallography can be extended to (short-lived) intermediate states of the protein's reaction cascade. Finally, this technique probes the protein in an artificial environment (i.e., the crystalline state) that does not correspond to the natural reaction conditions (e.g., membrane-bound proteins). Thus, crystallographic structure constitutes the indispensable starting point but not the end point for a comprehensive structure-dynamics-function analysis of proteins. In this respect, tailored vibrational spectroscopic techniques can contribute to overcome the inherent limitations of X-ray crystallography and may provide complementary information about (i) the cofactor site structure in proteins and (ii) elementary molecular processes of proteins in complex environments.

(i) On the basis of the photoreceptor phytochrome and its reaction cycle it will be shown how the combination of resonance Raman (RR) spectroscopy and modern theoretical methods may complement X-ray crystallographic data [1]. This approach offers the possibility for refining existing structural models of cofactor sites and may even allow for generating preliminary structural models of protein states not directly accessible by X-ray crystallography. The principles of this approach as well as its potential and current limitations will be illustrated.

(ii) Stationary and time-resolved surface enhanced RR (SERR) and surface enhanced infrared absorption (SEIRA) spectroscopic techniques can be adapted to conditions that mimic natural environments of proteins, i.e., proteins at membrane/solution interfaces. Here, recent achievements will be presented to demonstrate that complex interfacial processes of redox proteins can be disentangled in terms of electron tunneling, protein re-orientation, as well as protein and cofactor structure changes [2,3]. The results obtained from such biomimetic systems provide important insight into the parameters controlling protein processes under physiological conditions.

[1] M. A. Mroginski, D. von Stetten; F. Velazquez Escobar, H. M. Strauss, S. Kaminski, P. Scheerer, M. Günther, D. H. Murgida, P. Schmieder, C. Bongards, W. Gärtner, J. Maillet, J. Hughes, L. O. Essen, P. Hildebrandt, *Biophys. J.* 96 (2009) 4153-4163.

[2] D. H. Murgida, P. Hildebrandt, *Chem. Soc. Rev.* 37 (2008) 937-945.

[3] D. H. Murgida, P. Hildebrandt, *Phys.Chem. Chem. Phys.* 7 (2005) 3773-3784.



**New approaches in Metal Enhanced Spectroscopy (SERS and SEF)  
in solution:  
Detection of insoluble compounds and pharmaceutical drugs**

J.V. García-Ramos, P. Sevilla, E. del Puerto, R. de Llanos, I. Izquierdo, S. Sánchez-Cortés,  
C. Domingo

*Instituto de Estructura de la Materia, CSIC, Serrano 121, 28006 Madrid, Spain*

Fields so different as forensic (where unambiguous detection of paint and ink materials is a key point), medicine (use of “drug delivery on silver magic bullets”) or high level competitive sport (detection of prohibited doping agents) can benefit from the advantages and high sensitivity of Metal Enhanced Spectroscopy in any of its more widespread forms, either Surface Enhanced Raman Scattering (SERS) and/or Surface Enhanced Fluorescence (SEF). We will present new approaches recently developed in our group to apply such techniques in solution to the detection of highly insoluble pigments, as well as to the characterization of pharmaceutical drugs.

Synthetic organic pigments have presently many applications not only in modern art but also in printing inks, and as “high performance” automotive paintings. A new strategy for getting SERS spectra of totally insoluble - in water and organic solvents - compounds, employing calixarenes as dispersive cavitands, has been successfully applied to the SERS detection of Quinacridone Quinone (CI 73920), one of the most relevant synthetic organic pigments.

On the other side, fluorescence emission can be altered by the presence of metallic nanoparticles through changes in the radiative and non-radiative decay rates. At a certain distance between the metal surface and the fluorophore the interaction between donor molecules and nanoparticle plasmon resonance causes an increase on the effective quantum yield of the donor because of enhanced radiative decay rate. These effects are commonly known as surface enhanced fluorescence (SEF). A spacer molecule has been generally used to establish the optimum distance to achieve maximum enhanced fluorescence. Although metal nanoparticles in suspension are considered useful and simple methods to produce high SERS enhancement, this is not the case in SEF because of the difficulty in the control of the fluorophore-metal distance. Nevertheless, we have succeeded in obtaining enhanced fluorescence emission of emodin, an anticancer drug, at pH=6 and pH=2 using the aggregation properties of emodin at these conditions: the aggregated forms of the molecule permits the fluorophore to be placed at the adequate SEF distance. Besides, in order to understand how nanomaterials interact with biological molecules we have focused our study not only on the enhancement of the spectroscopic signals but also in the influence that metal plasmon resonances have on the structure and function of molecules adsorbed. In this sense, we have studied the effects on the binding of the emodin to bovine serum albumin adsorbed on silver nanoparticles

Preliminary results on the SERS detection of some of the World Anti-Doping Agency's list of prohibited drugs for Olympic athletes ( $\beta$ -agonists clenbuterol, salbutamol y terbutaline) will be also reported.

*Ministerio de Ciencia e Innovación* of Spain (Projects FIS2007-63065 and CONSOLIDER CSD2007-0058) and *Comunidad de Madrid* (S2009/TIC-1476 MICROSERES II) are gratefully acknowledged for financial support. EdP and II acknowledge CSIC and FSE 2007-2013 for JAE-CSIC predoctoral grants. RdLI acknowledges MICINN for a predoctoral grant.





**Molecules under pressure**

R. J. Hemley

*Geophysical Laboratory, Carnegie Institution of Washington, 5251 Broad Branch Road, NW  
Washington, DC 20015*



**Titolo**

M. Parrinello

*Department of Chemistry and Applied Biosciences, ETH Zurich, CH*



# Photochemically Controlled Molecular Devices and Machines

V. Balzani

*"G. Ciamician" Department of Chemistry, University of Bologna, Bologna, Italy*

Generally speaking, devices and machines are assemblies of components designed to achieve a specific function. Each component of the assembly performs a simple act, while the entire assembly performs a more complex, useful function, characteristic of that particular device or machine. Any kind of device or machine requires a substrate, energy, and information signals. If we wish to operate at the nanometer scale, we must use molecules as substrate. The macroscopic concepts of a device and a machine can indeed be extended to the molecular level. A *molecular device* can be defined as an assembly of a discrete number of molecular components designed to achieve a specific function. Each molecular component performs a single act, while the entire supramolecular assembly performs a more complex function, which results from the cooperation of the various components. A *molecular machine* is a particular type of device in which the (molecular) component parts can display changes in their relative positions as a result of some external stimulus. Molecular-level devices and machines operate via electronic and/or nuclear rearrangements and, like macroscopic devices and machines, they need energy to operate and signals to communicate with the operator. The extension of the concepts of a device and a machine to the molecular level is of interest not only for basic research, but also for the growth of nanoscience and the development of nanotechnology.

The operation of a molecular device or machine relies on cause/effect relationships between energy inputs and kind of process obtained. Molecular devices and machines are characterized by (i) the type of energy input supplied to make them work, (ii) the way in which their operation can be controlled, (iii) the possibility to establish a cyclic process, (iv) the time scale needed to complete a cycle, and (v) the function performed.

If a molecular device or machine has to work by inputs of chemical energy, it will need addition of fresh reactants ("fuel") at any step of its working cycle, with the concomitant formation of waste products that compromise the operation. Chemical fuel, however, is not the only means by which energy can be supplied. Currently there is an increasing interest in the use of light to power molecular devices and machines and of spectroscopy to understand their operational behavior.

The lecture will illustrate examples of recent achievements [1,2,3], which include molecular wires, switches, plug-socket systems, extension cables, antennas, and light powered nanomotors.

[1] V. Balzani, A. Credi, M. Venturi, *Chem. Soc. Rev.*, 38 (2009)1542.

[2] V. Balzani, A. Credi, M. Venturi, *Molecular Devices and Machines. Concepts and Perspectives for the Nanoworld*, Wiley-VCH, 2008.

[3] V. Balzani, A. Credi, M. Venturi, *Nanotoday*, 2, (2007) 18.



## Characterization of self-assembled monomolecular films by advanced spectroscopic techniques

M. Zharnikov

*Angewandte Physikalische Chemie, Universität Heidelberg, Im Neuenheimer Feld 253, 69120 Heidelberg, Germany*

Frontier areas of modern technology rely on the possibility to tailor surface properties such as wetting, adhesion, lubrication, corrosion, and biocompatibility on both microscopic and macroscopic scales. To a large extent, these options are provided by self-assembled monolayers (SAMs), which are 2D polycrystalline films of semi-rigid molecules that are chemically anchored to a substrate by a suitable headgroup and carrying, at the other end of the molecular chain, a specific tail group, which determines the chemical and physical properties of the entire system (see Figure 1). In addition, such layers represent a general platform for the arrangement of future molecular electronics devices, framework for Chemical Lithography, and a model system for macromolecular and biological assemblies. Advanced spectroscopic techniques represent a powerful tool box for the characterization of SAMs, which is a prerequisite for their design and applications. A basic information on the chemical identity, integrity, molecular conformation and orientation in these films can be obtained by a combination of X-ray photoelectron spectroscopy (XPS), X-ray absorption spectroscopy, and infrared reflection absorption spectroscopy. More specific questions, such as, e.g., bonding configuration of the anchor group or dynamics of the charge transfer along the molecular backbone require special experimental tools such as high-resolution XPS and resonant Auger electron spectroscopy, respectively. Using several model and specially designed systems, we will illustrate application of the above techniques for the characterization of SAMs. In addition, we will show that SAMs can be used as prototypes of highly organized biological systems and provide important implications for cryogenic approaches in advanced electron and x-ray spectroscopy and microscopy of biological macromolecules and cells.

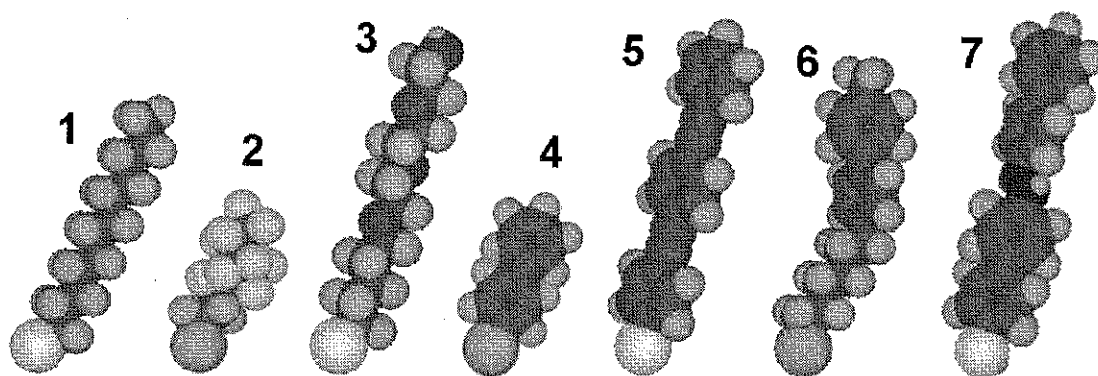


Figure 1. Representative molecular constituents for frequently used SAM systems (the thiol and selenol headgroups are taken as an example): 1 - aliphatic backbone; 2 - partly fluorinated aliphatic backbone; 3 - a combination of aliphatic and oligo(ethylene glycol) chains; 4 - aromatic (oligophenyl) backbone; 5 - oligo(phenylene ethynylene) backbone; 6 - hybrid aliphatic–aromatic backbone; 7 - backbone with azobenzene unit. Different tail groups can be attached to the molecular chain at the SAM–ambient side. Different functional groups can also be imbedded into the chain (see 7).

## Ultrafast primary events in photostable systems: H-bond, excess electron, biological photoreceptors

H. Abramczyk

*Technical University of Lodz, Chemistry Department, Laboratory of Laser Molecular Spectroscopy, 93-590 Lodz, Wroblewskiego 15 str Poland, Max-Born-Institut for Nonlinear Optics and Ultrashort Pulses, Max-Born-Str. 2 A, 12489 Berlin, Germany*

Ultrafast spectroscopies have played an important role in the study of a number of biological processes and have provided unique information about primary events and the role of different type of interactions. Biological activity of molecules are frequently initiated by elementary chemical reactions such as energy and electron transfer, cis-trans isomerizations, and proton transfer. The nature of these reactions generally makes them very fast and efficient, occurring on picosecond and femtosecond timescales. This contribution reviews the current status and recent progress of understanding of light-energy collection and the primary light-initiated reactions of the biological photoreceptors originating from third order nonlinear methods of Raman scattering (CARS) and pump-probe absorption spectroscopies and theoretical methods of nonlinear spectroscopy. We expect that the understanding the mechanisms of energy dissipation will reveal mechanisms that mediate light-induced signal transduction as well as the role of photoreceptors in the photostability protection and repair mechanisms in the biological systems. We discuss the mechanisms of energy dissipation in H-bonded systems, solvation of an excess electron and primary photochemical events in bacteriorhodopsin [1-5].

- [1] Abramczyk, H., Chem. Phys. **1990**, *144*, 305-318.
- [2] Abramczyk, H., Chem. Phys. **1990**, *144*, 319-326.
- [3] Abramczyk, H., J. Phys. Chem. **1991**, *95*, 6149-6155.
- [4] Abramczyk, H.; Kroh, J., J. Phys. Chem. **1992**, *96*, 3653-3658.
- [5] Abramczyk, H., J. Chem.Phys. **2004**, *120*, 11120-11132.
- [6] Terentis, A.; Uji, L.; Abramczyk, H.; Atkinson, G. H., Chem. Phys. **2005**, *313*, 51-62.



**The renaissance of far infrared spectroscopy,  
better known as terahertz spectroscopy**

H. H. Mantsch

*Institute of Biomedical Diagnostics, National Research Council, Winnipeg, Canada*

This presentation is an attempt to raise the awareness of those molecular spectroscopists who may not yet have considered the emerging opportunities offered by this window in the electromagnetic spectrum as a tool for the investigation of molecular structures

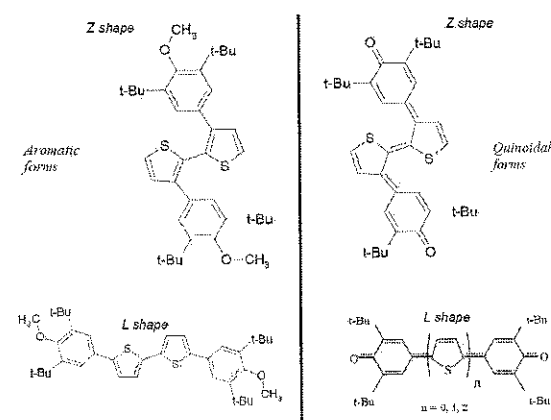


## Raman evidences of unusual electronic and molecular structures.

C. Castiglioni<sup>1,2</sup>, D. Fazzi<sup>2</sup>, A. Milani<sup>1</sup>, E.V. Canesi<sup>2</sup>, C. Bertarelli<sup>1,2</sup>, E. Di Donato<sup>3</sup>, F. Negri<sup>3</sup><sup>1</sup>Dipartimento di Chimica Materiali e Ing. Chimica "G. Natta", Politecnico di Milano, p.zza Leonardo da Vinci 20133 Milano and INSTM UdR Milano PoliMi<sup>2</sup>Center for NanoScience and Technology CNST via Pascoli 70/3, 20133 Milano<sup>3</sup>Dip. di Chimica "G. Ciamician", Univ. di Bologna, via F. Selmi 2 40126 Bologna and INSTM UdR Bologna

This contribution is intended to elucidate the role of vibrational spectroscopy as a unique tool to prove the existence of peculiar molecular and electronic structures, driven by electrons confinement and/or strong electron-vibration interactions. Two different classes of molecules will be discussed, namely linear carbon chains and oligothiophenes with phenyl end groups. For both cases, first principles calculations of molecular structure and Raman response are shown to hold a key role for the interpretation of the experimental findings.

The Raman features of polyynes of different lengths, characterized by a sequence of alternated single and triple CC bonds have been thoroughly interpreted [1,2] in the past. However, it is still debated whether linear carbon chains showing cumulenic structures could exist and also be observed by Raman spectroscopy. A systematic investigation of short linear C<sub>n</sub> chains and of vinyl-capped chains carried out with DFT calculations, showed that they present very small bond length alternation (BLA) values and low CC stretching frequencies ( $\nu < 2000 \text{ cm}^{-1}$ ) vibrational modes, whose Raman cross sections is large enough to be observed. These findings give support to the use of Raman spectroscopy for the detection of cumulenic chains in linear carbon based materials, e.g. amorphous carbon films.



As second case we present a wide spectroscopic (IR/Raman and UV-Vis) study carried out on oligothiophenes, recently used as active organic material for resistive non volatile memories [3] and/or near IR photodetectors [4]. By means of quantum chemical simulations (DFT) we predict Raman and IR spectra for both aromatic (A) and quinoidal (Q) species, assigning all the experimental vibrational features [5] and identifying spectroscopic markers associated to the different stable conformers possibly occurring in solution as well as in crystalline and amorphous solid phases.

This study is important in order to explore the structural order (*short range* – single molecule and *long range* – supramolecular organization) which rules their electronic properties (i.e. charge mobility). Moreover, in the case of Q species the analysis of the Raman spectrum provides unique and unquestionable evidence of the stabilization of a singlet biradical configuration, already for the molecule with a bithiophene core. Excited state simulations (TDDFT and CIS) carried out in order to interpret the UV-vis absorption spectra, will be also presented and discussed.

[1] A. Milani, M. Tommasini, G. Zerbi, J. Chem. Phys. 128 (2008) 064501.

[2] M. Tommasini, D. Fazzi, A. Milani, M. Del Zoppo, C. Castiglioni, G. Zerbi, J. Phys. Chem. A, 111 (2007) 11645.

[3] M. Caironi, et al., App. Phys. Letters 89 (2006) 243519

[4] T. Agostinelli, et al., J. Appl. Phys. 104 (2008) 114508.

[5] D. Fazzi, et al., J. Raman Spect. 41(2010) 406.

## 2D IR spectroscopy of water dynamics near hydrophobes

A. A. Bakulin<sup>1</sup>, C. Petersen<sup>2</sup>, H. J. Bakker<sup>2</sup>, M. S. Pshenichnikov<sup>1</sup><sup>1</sup> *Zernike Institute for Advanced Materials, University of Groningen, Nijenborgh 4, 9747 AG Groningen, The Netherlands*<sup>2</sup> *FOM-institute for Atomic and Molecular Physics, Kruislaan 407, 1098 SJ Amsterdam, The Netherlands*

The attractive interaction of hydrophobic (= water fearing) molecular groups in aqueous environments plays an essential role in the structuring and chemical reaction dynamics of biological systems. Examples are the folding of proteins, the formation of bilipid membranes, and the interactions between enzymes and substrates. The hydrophobic interaction is closely related to the effects of hydrophobic solutes on the structure and dynamics of liquid water. However, neutron scattering studies showed that hydrophobic molecular groups have in fact very little effect on the hydrogen-bonded *structure* of the surrounding water [1]. In contrast, the *dynamics* of the water molecules does appear to be strongly affected, as was found with NMR [2], dielectric relaxation [3], and femtosecond mid-infrared studies [4,5].

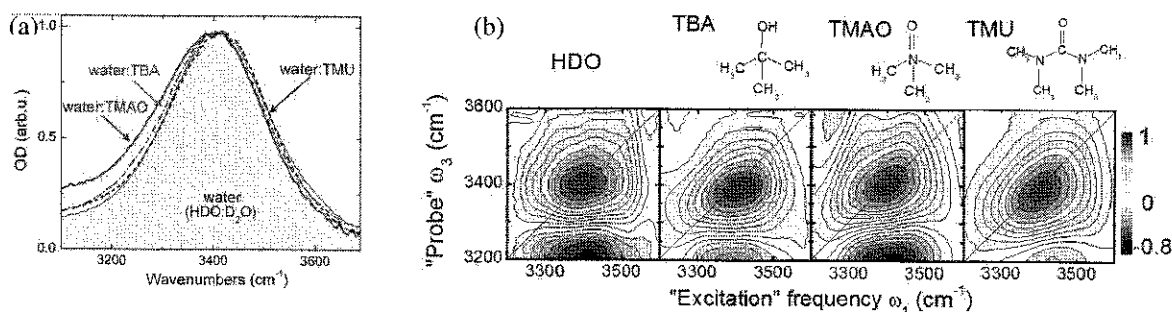


Fig. 1. 1D (a) and 2D (b) correlation spectra (4 out of ~80 in total) of pure HDO:D<sub>2</sub>O and HDO:D<sub>2</sub>O solutions of TMU, TMAO, and TBA at room temperature. For all solutions there are 10 water molecules per solute molecule. The waiting time in (b) is set at  $T=1$  ps. The strong slowing down of the water dynamics of the solutions is represented by the elongation of the 2D spectra along the diagonal direction.

Here we use 2D IR and polarization-resolved pump-probe spectroscopy to study the ultrafast hydrogen-bond dynamics of water molecules interacting with three amphiphilic solutes: tetra-butyl alcohol (TBA), trimethyl-amine-oxide (TMAO), and tetramethylurea (TMU). These solutes have 3 or 4 hydrophobic methyl groups and one hydrophilic group arranged in a similar geometry while the hydrophilic group is quite different. Linear absorption spectra of the OH band of pure HDO:D<sub>2</sub>O (1:20) and solutions of the three solutes look very similar (Fig.1a). However, 2D IR spectra (Fig.2b) show the substantial slowing down of the spectral diffusion due to effect of hydrophobic molecules on the hydrogen-bond dynamics of water.

[1] A. K. Soper, J. L. Finney, Phys. Rev. Lett. 71 (1993) 4346

[2] J. Qvist, B. J. Halle, JACS 130 (2008) 10345

[3] T. Sato, R. Buchner, J. Chem. Phys. 119 (2003) 10789

[4] Y. L. A. Rezus, H. J. Bakker, Phys. Rev. Lett. 99 (2007) 1487301

[5] A. A. Bakulin, C. Liang, Th. I. C. Jansen, D. A. Wiersma, H. J. Bakker, M. S. Pshenichnikov, Acc. Chem. Res. 42 (2009) 1229





## Pollen analysis by transmittance FT-IR spectroscopy

B. Zimmermann

Department of Organic Chemistry and Biochemistry, Ruđer Bošković Institute,  
Bijenička 54, 10002 Zagreb, Croatia

Pollen analysis is almost exclusively based on visual identification of pollen grains under microscope by a qualified specialist. Palynological studies, like aeroallergens monitoring, would greatly benefit if such tedious and time-consuming measurement could be replaced by an automated black-box approach. Vibrational spectroscopy is emerging in recent years as a promising tool for objective pollen identification and a viable alternative to microscopy [1, 2].

The present study describes a method for pollen analysis based on chemical characterization by transmittance FT-IR spectroscopy, one of the oldest and most extensively used spectroscopic techniques. The measurements on pollen samples belonging to 113 plant species clearly show value of FT-IR spectroscopy for biological classification and identification of pollen. Furthermore, the applicability of the method for environmental monitoring was demonstrated by implementing sizeable spectral library with 40 pollen taxa for successful quantitative and qualitative analysis of binary pollen mixtures. Mentioned results imply that FT-IR spectroscopy can be easy and bias-free alternative to optical microscopy in pollen analysis. The method itself is simple, rapid and inexpensive, necessary know-how and instrumentation is rudimentary, and therefore it can be immediately tested, adapted and implemented worldwide in environmental and healthcare studies.

Lastly, a detailed vibrational study of 39 pollen samples belonging to *Pinales* order was conducted using transmittance FT-IR, single reflection ATR FT-IR, and FT-Raman (laser source 1064 nm) spectroscopy. The results of these measurements once again indicate that identification methods based on spectral search can offer rapid taxonomic classification in various environmental studies.

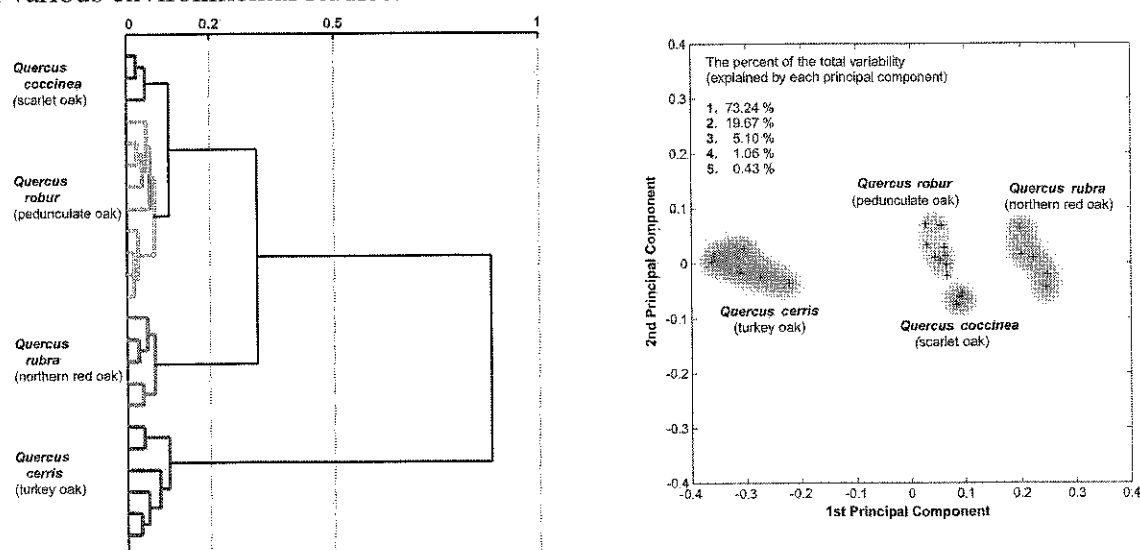


Figure 1. The hierarchical cluster analysis (left) and the principal cluster analysis (right) of IR spectra of the four oak pollen taxa.

[1] F. Schulte, J. Lingott, U. Panne, J. Kneipp, *Anal. Chem.* 80 (2008) 9551-9556.

[2] R. Dell'Anna, P. Lazzeri, M. Frisanco, F. Monti, F. Malvezzi Campaggi, E. Gottardini, M. Bersani, *Anal. Bioanal. Chem.* 394 (2009) 1443-1452.



## Vibrational spectroscopy as a tool for analysis of tree leaves

P. Matejka<sup>1</sup>, J. Weissova<sup>1</sup>, Z. Cieslarova<sup>1</sup>, L. Mrnka<sup>2</sup>, M. Clupek<sup>1</sup>, K. Matejkova<sup>1</sup>

<sup>1</sup>*Dept. of Analytical Chemistry, Institute of Chemical Technology, Technicka 5, 166 28 Prague 6 -Dejvice, Czech Republic*

<sup>2</sup>*Dept. of Mycorrhizal Symbioses, Institute of Botany ASCR, Zamek 1, 252 43 Pruhonic, Czech Republic*

Different techniques of vibrational spectroscopy can be used for non-destructive analysis of many biological samples. Previously, we demonstrated the potential of FT Raman and ATR spectroscopy for monitoring of Norway spruce needles [1 – 3]. In this study we develop a methodology of fresh plant leaves analysis using attenuated total reflection (ATR) FT-IR, FT-Raman scattering and FT-NIR transmission spectroscopy for several common trees in the Czech Republic and in central Europe. The freshly taken leaves were stored at the most several days with water supply, packed in PE bags in brash-ice. Spectral data of leaves taken in different points of vegetation period from spring to early winter were compared and evaluated using of various multivariate statistical methods.

ATR technique provides us with information on the surface layers of the leaves, allows to distinguish both sides of the leaves and to study cuticular waxes and surface humidity. Various classification methods (e.g. cluster analysis, linear discriminant analysis - LDA, and soft independent modeling of class analogy - SIMCA) enable to classify groups of spectra considering various experimental parameters (e.g. group of trees, ageing of leaves, and sampled side of leaves). The spectral parts contributing to such classification can be found out and they are tentatively assigned to characteristic bands of several leaf constituents, e.g. humidity, long-chain alcohols and aliphatic esters.

FT-NIR transmission spectra are dominated by characteristic bands of water. Based on the results of multivariate data analysis, no effect of the sides of the leaves is observed. The overall leaf humidity can be monitored, some other components (e.g. polysaccharides) are identified using principal component analysis, inspecting the loadings graphs of second and third principal components, and comparing the experimental spectra and their derivatives calculated for leaves in early stage of vegetation period and at senescence.

FT Raman spectra exhibit characteristic features of plant (photosynthetic) pigments, predominantly carotenoids. The shape of the background is related evidently to the leaf humidity. The Raman spectral data can be classified mainly with respect to age of leaves. To elucidate the other key factors affecting spectral data the principal component analysis and several classification methods were applied.

Summarily, the group of molecular spectroscopic methods provides us with a complex set of information on physiological state of leaves during vegetation period and at senescence. Several detailed physiological effects (e.g. soil composition and presence of soil filamentous fungi, irradiation conditions, nutrients) can be correlated with spectral data.

[1] L. Mrnka, H. Tokarova, M. Vosatka, P. Matejka, *Trees-Struct. Funct.* 23 (2009) 887

[2] P. Matejka, H. Tokarova, T. Pekarek, K. Volka, *J. Mol. Struct.* 661/662 (2003) 333-345

[3] L. Pleserova, G. Budinova, K. Havirova, P. Matejka, F. Skacel, K. Volka, *J. Mol. Struct.* 565/566 (2001) 311-315



## Effect of radiation in single crystal of L-glutamine

S. Osmanoğlu<sup>1</sup>, I. Dicle<sup>2</sup>

<sup>1</sup>Faculty of Education, Siirt University Güres Street, Siirt, 56100, TURKEY

<sup>2</sup>Faculty of Education, Dicle University, Campus, Diyarbakır, 21280, TURKEY

The solid-state radiation induced free radical formation in simple amino acids like L-glutamine has been the subject of investigation by EPR spectroscopy. EPR spectra of gamma irradiated single crystals of L-Glutamine are obtained and observed at room temperature. The anisotropic hyperfine splittings and g-factors indicate that the radical is oriented in the paramagnetic center. The change of hyperfine splittings of the quintet from 32,6 G to 11 G in motional state is due to the motional averaging of angular dependences of the  $\beta$  hydrogens relative top orbital of the radical carbon atom. The two methylene protons in the radical are equivalent and their hyperfine interactions are nearly isotropic, and the range 22,82-33,10 G.

An analysis of the electron spin resonance of gamma irradiated single crystals of L-Glutamine shows that: the paramagnetic species produced by the radiation damage is  $\text{CH}_2\dot{\text{C}}\text{HCOOH}$ . It was formed by abstraction of the H atom from L-Glutamine spectra resulting from an equal interaction of the unpaired electron with the protons of the two methylen atoms and one  $\alpha$  proton consist of five main components. A description of this radical is given, and overview of the solid-state radiation chemistry of the simple amino acids is present, based on a review of the literature combined with these experimental result.



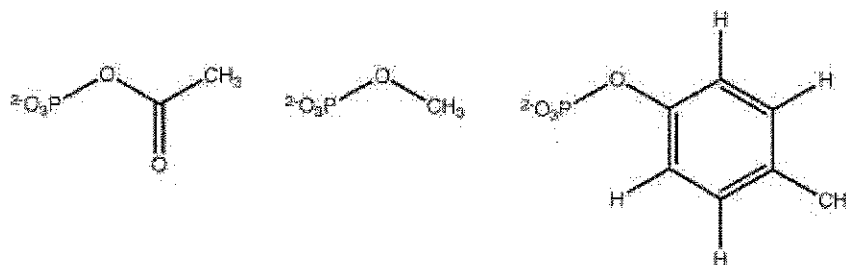
## Environmental effects on phosphorylated amino acids

M. Rudbeck<sup>1</sup>, M. Blomberg<sup>2</sup> and A. Barth<sup>1</sup>

<sup>1</sup>Department of Biochemistry and Biophysics, The Arrhenius Laboratories for Natural Sciences, Stockholm University, SE-106 91 Stockholm, Sweden

<sup>2</sup>Department of Physics, Albanova, The Arrhenius Laboratories for Natural Sciences, Stockholm University, SE-106 91 Stockholm, Sweden

Acetyl phosphate, *p*-tolyl phosphate and methyl phosphate, phosphorylated amino acid model molecules, were studied using density functional theory. In our simulations, the oxygen atoms and the phosphorus atom of the model compounds interacted with hydrogen fluoride at several different distances, simulating individual interactions that may occur in a protein environment. The effects of the interactions on phosphate vibrational frequencies, bond length of the scissile P-O bond, molecular energy and negative hyperconjugation are presented. A correlation was established between the average asymmetric  $\text{PO}_3^{2-}$  stretching vibration and the scissile P-O bond length and used to evaluate previous infrared spectroscopic data regarding the E2P aspartyl phosphate intermediate of the sarcoplasmic reticulum  $\text{Ca}^{2+}$ -ATPase [1]. In this intermediate, the scissile P-O bond is 0.16 Å longer than in the model compound acetylphosphate in aqueous solution. This indicates that the enzyme weakens the aspartyl phosphate in the ground state before the dephosphorylation reaction and prepares it for a transition state with considerable dissociative character.



[1] A. Barth, N. Bezlyepkina (2004), J. Biol. Chem. 279, 51888-51896

## A detachable SERS active polymer film: a minimally invasive approach to the study of painting lakes.

B. Doherty<sup>1</sup>, C. Miliani<sup>2,1</sup>, B. G. Brunetti<sup>1,2</sup>, A. Sgamellotti<sup>1,2</sup>

<sup>1</sup>CNR-ISTM, c/o Dipartimento di Chimica, Via Elce di Sotto, 8 06123 Perugia,

<sup>2</sup>SMAArt, Dipartimento di Chimica, Via Elce di Sotto, 8 06123 Perugia

Analytical examinations in the field of cultural heritage are increasingly progressing towards minimally invasive measurements for the identification of constituent organic dye components in precious and often immovable artworks. The most advanced successful techniques operated for the characterization and identification of lowly concentrated painting lakes in complex matrices remain still micro-destructive. In recent years, however, surface enhanced Raman spectroscopy (SERS) has been introduced into this discipline where procedures for active substrate production and minimum application have been seen to be successfully modulated to combine extractionless non hydrolysis methods with measurements effectuated directly on the sample [1].

This contribution details the synthesis of a neutral pH SERS film fabricated specifically to be removable from the surface of an artwork under study following effective SERS measurements. It is shown that silver nanoparticles prepared by green chemical reduction can be effectively doped into a methylcellulose matrix for the formation of a gel that can be applied to a minute area (circa 2mm) of an artwork to be studied. Studies have been aimed to optimize the film's chemical and physical characteristics and have included the observation of a homogeneous distribution of silver nanoparticles (AgNPs) within the resulting film (figure 1), an attainable shelf-life stability as well as high viscosity and transparency for ease of application and measurement feasibility respectively.



Figure 1: SEM micrograph(magnification 3200x, BSE) detailing the distribution of AgNPs within the methylcellulose film.

Importantly, results have lead to reproducible enhancements through studies effectuated on standard laboratory dye components and unvarnished mock-paintings. Techniques including optical and scanning electron microscopy have been utilized to monitor the drying of the film, its resulting morphology and mapping the silver nanoparticles within so as to account for any visual modification to the underlying surface upon film removal. Portable reflectance fibre-optic infrared has been adopted to investigate the interaction of the film with painting lakes considering that for effective SERS enhancements to occur the substrates necessitate as close an interaction as possible. This data is part of an ongoing process of collection for a SERS database of insoluble painting lakes that can be retained useful for SERS diagnostic purposes with the future aim for concrete on-site routine analyses.

[1] C.L. Brosseau, A. Gambardella, F. Casadio, C. M. Grzywacz, J. Wouters and R. P. Van Duyne, *Anal. Chem.*, 2009, 81 (8), pp 3056–3062.

## An analysis of Fe and Ni distribution in M1, M2 and M3 sites of iron nickel phosphides extracted from Sikhote-Alin meteorite using Mössbauer spectroscopy with a high velocity resolution

M.I. Oshtrakh<sup>1</sup>, M.Yu. Larionov<sup>1</sup>, V.I. Grokhovsky<sup>1</sup>, V.A. Semionkin<sup>1,2</sup>

<sup>1</sup>Faculty of Physical Techniques and Devices for Quality Control, Ural State Technical University – UPI, 620002, Ekaterinburg, Russian Federation

<sup>2</sup>Faculty of Experimental Physics, Ural State Technical University – UPI, 620002, Ekaterinburg, Russian Federation

Iron nickel phosphides (Fe, Ni)<sub>3</sub>P were found in iron meteorites in two forms: schreibersite and rhabdite. Schreibersite is macro inclusions while rhabdite is microcrystals in kamacite matrix. The crystal structure of schreibersite and rhabdite was similar with tetragonal space group *I4*, three crystallographic sites for metal atoms denoted as M1, M2 and M3 and the unit cell with 8 atoms in the each site. These sites were occupied by Fe and Ni atoms in different way for schreibersite and rhabdite extracted from various meteorites. Therefore, in this work a distribution of Fe and Ni atoms in M1, M2 and M3 sites was evaluated using Mössbauer spectroscopy, chemical analysis and (Fe, Ni)<sub>3</sub>P modeling.

Iron nickel phosphides were extracted from Sikhote-Alin iron meteorite. Mössbauer spectra of phosphides samples were measured at temperatures from 295 down to 90 K using automated precision Mössbauer spectrometric system with a high velocity resolution (in 4096 channels) [1, 2]. Then spectra were presented in 1024 channels by consequent summation of 4 neighboring channels. Spectra of rhabdite measured below the room temperature were fitted using 6 magnetic sextets and 1 paramagnetic doublet which were related to <sup>57</sup>Fe nuclei in the M1, M2 and M3 sites by analogy with [3]. In this case the parts of Fe in these sites were evaluated as ~44 %, ~28 % and ~28 %, respectively. Chemical analysis demonstrated average parts of Fe and Ni atoms as 52 % and 48 %, respectively. Thus, it was evaluated that the M1 sites were occupied by 5.5 Fe and 2.5 Ni atoms, the M2 and M3 sites were occupied by 3.5 Fe and 4.5 Ni atoms. In contrast Mössbauer spectrum of schreibersite was more complicated. This spectrum measured at 295 K was also fitted using 6 magnetic sextets and 1 paramagnetic doublet as rough fit. Sextets were related to <sup>57</sup>Fe nuclei in the M1, M2 and M3 sites. The parts of Fe in these sites were evaluated as ~52 %, ~25% and ~19 %, respectively. Chemical analysis demonstrated average parts of Fe and Ni atoms as 64 % and 36 %, respectively. Therefore, it was evaluated that the M1 sites were occupied by 8 Fe atoms, the M2 sites were occupied by 3.8 Fe and 4.2 Ni atoms, and M3 sites were occupied by 2.9 Fe and 5.1 Ni atoms. Modeling of (Fe, Ni)<sub>3</sub>P showed different local environment for the M1, M2 and M3 sites in the unit cell of both rhabdite and schreibersite.

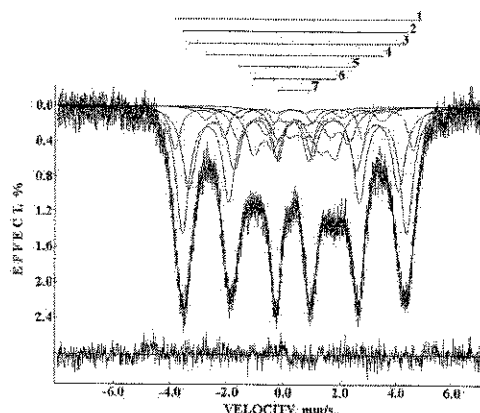


Fig. 1. Mössbauer spectrum of rhabdite presented in 1024 channels. T=150 K.

- [1] M.I. Oshtrakh, V.A. Semionkin, O.B. Milder, E.G. Novikov. J. Radioanal. Nucl. Chem. 281 (2009) 63–67.
- [2] V.A. Semionkin, M.I. Oshtrakh, O.B. Milder, E.G. Novikov. Bull. Rus. Acad. Sci.: Physics, 74 (2010) 416–420.
- [3] E.J. Lisher, C. Wilkinson, T. Ericsson, L. Haggstrom, L. Lundgren, R. Wappling. J. Phys. C: Solid State Phys. 7 (1974) 1344–1352.

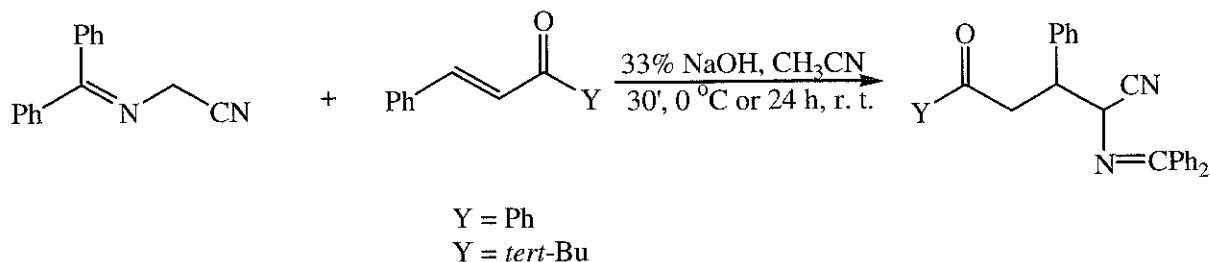


## Diastereoselectivity in the Michael addition reaction of CH-acidic Schiff base to $\alpha,\beta$ -unsaturated ketones

S. Ilieva, D. Cheshmedzhieva, D. Tasheva

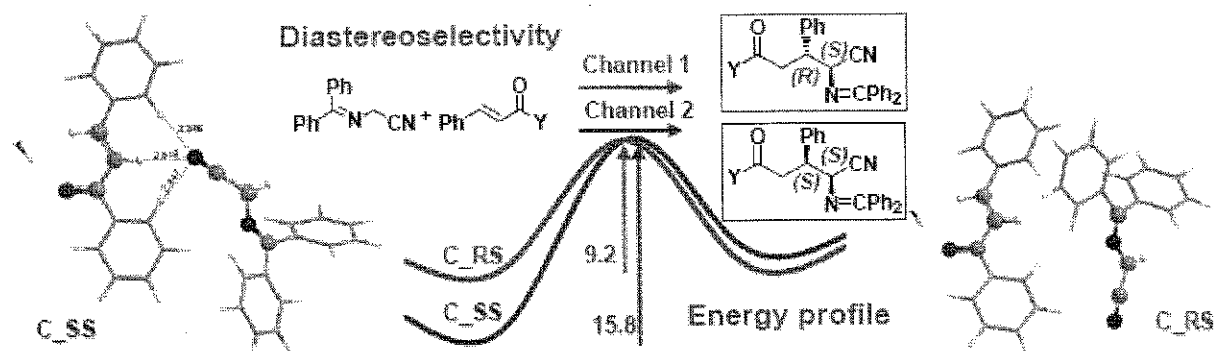
Department of Chemistry, University of Sofia, Sofia 1164, Bulgaria

The Michael reaction of [(diphenylmethylene)amino]acetonitrile (CH-acidic Schiff base) with enones was carried out in aqueous conditions (33% NaOH, CH<sub>3</sub>CN, 0°C). The mechanism of Michael addition of the CH-acidic Schiff base to two types of substrates is studied: (1) diaryl  $\alpha,\beta$ -unsaturated ketone (benzylideneacetophenone, chalcone) and (2) alkyl containing  $\alpha,\beta$ -unsaturated ketone (4,4-dimethyl-1-phenyl-1-pentene-3-one). With benzylideneacetophenone and substituted arylmethyleneacetophenones (chalcones) the reaction proceeds with high diastereoselectivity - the diastereoisomeric ratio 99:1 (<sup>1</sup>H NMR spectroscopy) was observed for the crude products.



Theoretical quantum chemical computations were applied in answering a question set from the experiment: why the Michael addition to chalcones is a highly diastereoselective process? Density functional theory methods were used to examine the mechanistic pathways of the reaction. It was of interest to compare the energy profiles of the Michael addition of [(diphenylmethylene)amino]acetonitrile to  $\alpha,\beta$ -unsaturated ketones (enones) of two types: 1) benzylideneacetophenone (chalcone); 2)  $\alpha,\beta$ -unsaturated ketone containing *tert*-Bu and Ph groups - 4,4-dimethyl-1-phenyl-1-pentene-3-one. In this way it was possible to assess the influence of the substitution at both sides of the enone system on the energy characteristics and diastereoselectivity of the addition reaction.

Transition state structures, prereactive complexes and reaction path energetics for different channels of the reaction were determined. The theoretical predictions reveal that the difference in the stabilization of the prereactive complex explains adequately the experimental findings for diastereoselectivity of the addition to benzylideneacetophenone (chalcone), compared to the nonselective process in the case of 4,4-dimethyl-1-phenyl-1-pentene-3-one.



## Mass imaging as a viable 2D alternative for molecular spectroscopists

M. Volny<sup>1</sup>, M. Strohaln<sup>1</sup>, V. Vidova<sup>1</sup>, K. Lemr<sup>1,2</sup>, J. Pol<sup>1</sup>, M. Hajduch<sup>3</sup>, V. Havlicek<sup>1,2</sup>

<sup>1</sup>*Institute of Microbiology, Videnska 1083, 142 20 Prague 4, Czech Republic*

<sup>2</sup>*Palacky University, Tr. 17.listopadu 12, 771 46 Olomouc, Czech Republic*

<sup>3</sup>*Palacky University, Puskinova 6, 775 50 Olomouc, Czech Republic*

Mass spectrometry imaging will be presented as an attractive and modern tool for spectroscopists interested in 2D sample visualization. In addition to morphology information at about 50  $\mu\text{m}$  spatial resolution mass spectrometry imaging offers the direct access to very detailed structure information. Very often organic components ranging from low molecular weight compounds to large biomolecules can be characterized even in extremely complex sample matrices like human or animal tissues, plants, etc.

We have recently introduced a lab made automated atmospheric pressure mass spectrometry imaging platform coupled to FTICR spectrometer, which allows for the analysis of surfaces in the ambient environment [1]. This platform has been used both in desorption electrospray and atmospheric pressure photoionization modes, with which the fungal infection on a plant leaf was documented [2]. Biomarker discovery thus represents one of the important applications of mass spectrometry imaging.

In this presentation we also will introduce a new approach - imaging of tissue-lipids by matrix-free laser desorption from commercially available nanostructured surfaces (NALDI) where the original lipid distribution was transferred from tissue sections by a simple lithographic procedure without disrupting the original image [3]. On a real kidney sample, NALDI technique was better capable to distinguish adrenal gland from kidney tissue. Detailed comparison of standard MALDI-MS based imaging with the new NALDI-MS matrix free approach was performed using two mouse kidney sections that were cut as two immediately consecutive tissue slices. NALDI-MS identified 40 phospholipids (33 were glycerophospholipids and 7 were sphingolipids). MALDI-MS identified 36 phospholipids (29 were glycerophospholipids and 7 were sphingolipids). The overlap of identified phospholipids was 72%. NALDI spectra were much less complex due to the absence of matrix clusters and alkali-metal adduct ions. This makes identification based on  $m/z$  measurement much more suitable (especially on time-of-flight instruments). Moreover, structural identification by metastable ions fragmentation (PSD) is more unambiguous in NALDI-MS compared to the standard MALDI-MS.

### Acknowledgement

The authors thank Ministry of Education, Youth and Sports of the Czech Republic (LC7017, MSM6198959216) and Czech Science Foundation (H-084) for financing.

### References

- [1] Z. Takats, V. Koblíha, K. Sevcik, P. Novak, G. Kruppa, K. Lemr, V. Havlicek, *J. Mass Spectrom.* 43 (2008) 196-203
- [2] J. Pol, V. Vidova, G. Kruppa, V. Koblíha, P. Novak, K. Lemr, T. Kotiaho, R. Kostianen, V. Havlicek, M. Volny, *Anal. Chem.* 81 (2009) 8479-8487
- [3] V. Vidova, P. Novak, M. Strohaln, J. Pol, V. Havlicek, M. Volny, *Angew. Chem. Int. Ed. Eng.*, submitted.





## Micro-Raman spectroscopy for the non-destructive molecular characterization of red organic pigments in cross-sections of paintings by Leonardo, Masolino Veronese and Tintoretto

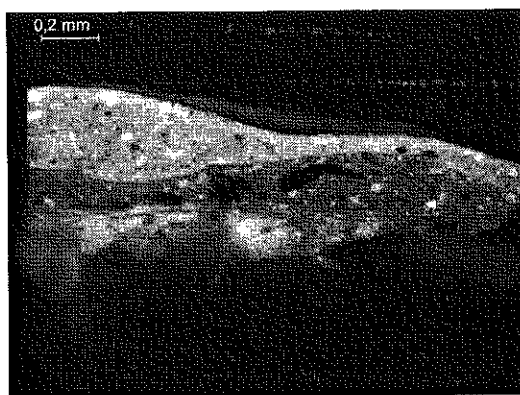
I. Osticioli<sup>1</sup>, A. Nevin<sup>1</sup>, M. Pagliai<sup>2</sup>, D. Comelli<sup>1</sup>, A. Gallone<sup>1</sup>, G. Valentini<sup>1</sup>, V. Schettino<sup>2,3</sup>, E.M. Castellucci<sup>2,3</sup>, R. Cubeddu<sup>4</sup>

<sup>1</sup>Dipartimento di Fisica, Politecnico di Milano, Piazza Leonardo da Vinci 32, 20133, Milano, Italy

<sup>2</sup>Dipartimento di Chimica "Ugo Schiff", Università di Firenze, Via della Lastruccia 3, 50019, Sesto Fiorentino (Fi), Italy

<sup>3</sup>European Laboratory for Non-Linear Spectroscopy (LENS), Via Nello Carrara 1, 50019, Sesto Fiorentino (Fi), Italy

<sup>4</sup>INFN-CNR, Dipartimento di Fisica, Politecnico di Milano, Piazza Leonardo da Vinci 32, 20133, Milano, Italy



An ongoing challenge in the analysis of paint cross-sections is the identification of organic pigments<sup>1</sup>; the focus of this work is the application of micro-Raman spectroscopy for the characterization of organic red pigments<sup>2</sup> in historical paint cross-sections of important 15<sup>th</sup> and 16<sup>th</sup> century paintings by Leonardo, Masolino, Veronese and Tintoretto.

Micro-Raman spectroscopy is a well established technique for the analysis of paint samples where studies have focused on the identification of a large variety of inorganic (and to lesser extent, organic) pigments and, in some case, binding media<sup>3</sup>. Most studies employing micro-Raman spectroscopy have considered the analysis of fragments or micro samples, with few exploring the analysis of organic materials in cross-sections of paint samples. An ongoing challenge in the application of vibration spectroscopy for the analysis of organic pigments<sup>4,5,6</sup> in historical samples is the small size of organic pigments relative to surrounding particles and the strong fluorescence of organic pigment particles.

This work emphasizes novel applications of micro-Raman spectroscopy coupled with Subtracted Shift Raman Spectroscopy (SSRS) for the subtraction of fluorescence on cross-sections. Micro Raman analysis has been performed using 514.5 nm (Argon ion) and 785 nm (Diode) lasers, both providing sufficiently well-defined spectra for the identification of original materials. The non-destructive analysis of organic historical cross-sections has highlighted the presence of anthraquinone-based organic red dyes bound to an Aluminum-based mordant. Spectral differences suggest significant chemical and structural variations within samples. The spectroscopic characterization of the anthraquinone-based pigments has been performed in conjunction with *ab initio* calculations, while the Raman analysis has been complemented by Scanning Electron Microscopy – Energy Dispersive Spectroscopy for elemental analysis of the studied cross-sections. The results will be presented and the advantages and limitations of the new method for the analysis of cross-sections will be discussed.

[1] Anal Bioanal. Chem., 392, (2008) (entire volume)

[2] B.H. Berrie, PNAS 106 (2009) 15095–15096

[3] A. Nevin, I. Osticioli, D. Anglos, A. Burnstock, S. Cather, E. Castellucci, J. Raman Spectrosc. 39 (2008) 993–1000

[4] M.V. Canamares, J.V. Garcia-Ramos, C. Domingo, S. Sanchez-Cortes, Vib. Spectrosc. 40 (2006) 161–167

[5] M. Leona, J. Stenger, E. Ferloni, J. Raman Spectrosc. 37 (2006) 981–992

[6] A. V. Whitney, R. P. Van Duyne, F. Casadio, J. Raman Spectrosc. 37, (2006) 993–1002



## Characterization by vibrational spectrometries of neolithic axe-heads from the Lake Constance region and Northern Switzerland

D.K. Breiting<sup>1</sup>, G. Brehm<sup>2</sup>, L. Steguweit<sup>3</sup>

<sup>1</sup>*Institute of Inorganic Chemistry, Egerlandstr. 1, D-91058 Erlangen, Germany*

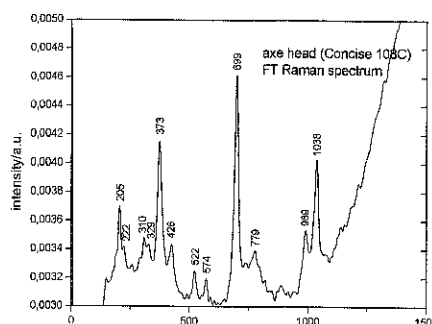
<sup>2</sup>*Institute of Physical Chemistry, Egerlandstr. 3, D-91058 Erlangen, Germany*

<sup>3</sup>*Institute of Proto- and Prehistory, Kochstr. 4, D-91054 Erlangen, Germany*

Investigations by vibrational spectrometries of axe-heads from several neolithic sites on the shores of Lake Constance, southern Germany, and Lake Neuchatel, northern Switzerland, have been started. These studies are aimed at identification of the materials the axes are made of, and eventually at their possible origin.

FT-Raman, dispersive micro-Raman, FT-IR, and micro-ATR spectrometries are applied to collect the spectral data for this purpose.

Thus, FT-Raman spectra showed two small, green axe-heads, polished at the cutting edge, from Concise (Cc), Lake Neuchatel, to consist of jadeite (ideal formula  $\text{NaAlSi}_2\text{O}_6$ ). The agreement with reference spectra of jadeites of various provenances worldwide [1-3] is remarkably good. Therefore, minor differences in the Raman spectra alone are not sufficient to lead to the source of these Cc axes.



However, a thorough study, also applying DRIFT spectrometry, indicates that a lot of jadeite artefacts, widespread in neolithic western Europe, have their origin in early mining at Monte Viso (MV), Piemonte, Italy [4]. So, since Cc is not that far from this mine, MV is a possible source. Radiocarbon dates for charcoal in debris deposits in the quarries of MV indicate a maximum of exploitation of jadeite (and eclogite) around 5000 BC, with subsequent decline and end around 4000 BC [4]. But MV jadeite objects (possibly reshaped) are still found in settlements of the second half of the 4<sup>th</sup> millennium BC, mainly assigned to the Horgen culture in south-western Germany and northern Switzerland, and contemporary cultures in eastern France.

In order to get more pieces of evidence for the origin of these jadeite objects, and thus for possible trade ways, further studies with non-destructive spectrometries, such as X-ray fluorescence, are intended.

[1] D.C. Smith, F. Gendron, J. Raman Spectrosc. 28(1997)731-738

[2] [www.ens-lyon.fr/LST/Raman/spectrum.php?nom=jadeite](http://www.ens-lyon.fr/LST/Raman/spectrum.php?nom=jadeite)

[3] <http://rruff.info/jadeite/names/asc/R050220>

[4] P. Petrequin, M. Errera, A.-M. Petrequin, P. Allard, European J. Archeol. 9(2006)7-30.



## Emilio Vedova's paintings: materials and conservation issues

M. Mattarelli<sup>1</sup>, S. Mengon<sup>1,3</sup>, N. Boschiero<sup>2</sup>, L. Benedetti<sup>3</sup>, F. Deflorian<sup>3</sup>

<sup>1</sup> *Dipartimento di Fisica, Università di Trento, I-38123 Povo (TN), Italy.*

<sup>2</sup> *Mart Museo di Arte moderna e contemporanea di Trento e Rovereto, I-38068 Rovereto (TN), Italy.*

<sup>3</sup> *Dipartimento di Ingegneria dei Materiali e Tecnologie Industriali, Università di Trento, Mesiano, I-38100 Trento, Italy.*

Many materials used in contemporary art, especially those based on synthetic polymers, may present short degradation times. This requires a continuous monitoring of the state of conservation of art objects in order to study different preservation strategies or, as soon as needed, to schedule restoration actions. In this respect, the works by Emilio Vedova (1919-2006) represent an emblematic example. During his career, the artist experimented many techniques, changing support (paper, canvas, wooden board) and binders (oil, acrylics, tempera). In some cases, the works show the presence of an ongoing deterioration process, with painting layers getting brittle and losing adhesion.

Between the various analytical techniques, those based on optical spectroscopy have the advantage of a minimal invasiveness and are therefore particularly suitable for the inspection of art objects. Here we present a thorough characterization (Raman, FTIR, FORS, UV-Vis excitation spectroscopy, EDXS) of the paint used by Vedova in several works made during a limited time span (1953-1962). The works belong to the period of artistic transition from the initial Vedova's production with futurist influences to the more personal style which will make him famous.

Also in this limited choice from the artist production it is possible to realize the variability of techniques and media used by the artist. The Raman measurements allowed identifying the pigments, which range from traditional ones, but still common like carbon black and ultramarine blue, to modern synthetic azo pigments. The binders, identified by FTIR, are egg based tempera, oil or acrylic and they are present together also in the same painting. Moreover, the analysis also showed that the artist chose to use also common material such as sand, papers and coal in his works.

The relevance for the conservation of the use of different binders and of artistic and common materials in the same work will be discussed.



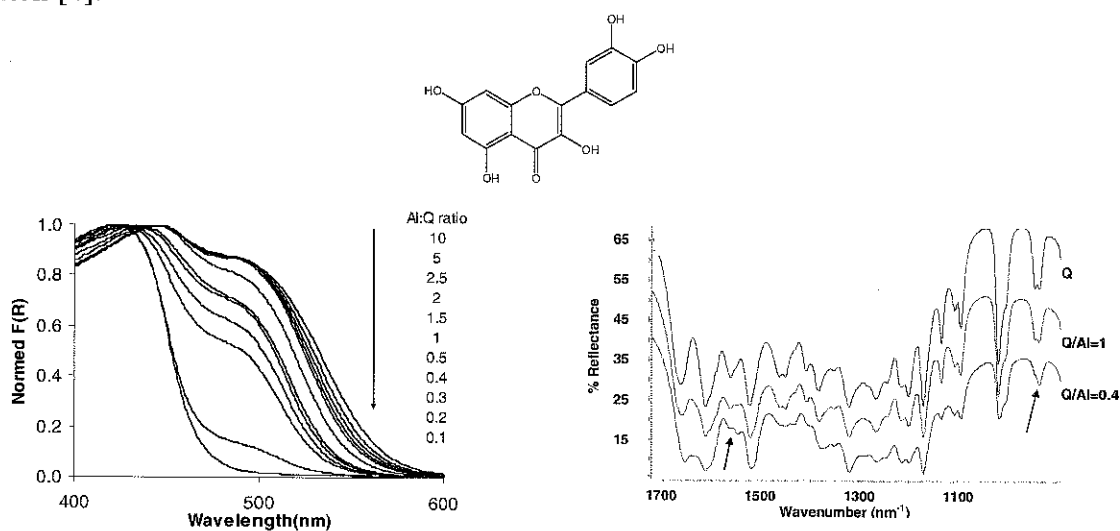
## Solid state complexation of natural organic dyes with Al(III): Electronic and vibrational spectroscopies

T. K. N. Nguyen,<sup>1</sup> K. Bourhis,<sup>1</sup> S. Blanc,<sup>1</sup> E. Péré,<sup>1</sup> C. Vieillescazes<sup>2</sup>

<sup>1</sup>Université de Pau et des Pays de l'Adour - UMR CNRS 5254  
Institut Pluridisciplinaire de Recherche sur l'Environnement et les Matériaux  
2 Avenue du Président Pierre Angot 64053 Pau, France  
Université d'Avignon et des Pays du Vaucluse - UFR Sciences  
LCBOSMV- Equipe Chimie Appliquée à l'Art et à l'Archéologie,  
33 rue Louis Pasteur 84000 Avignon, France

Used in antiquity as pigments in painting, lakes are coloured organic-inorganic hybrid materials [1]. They were prepared by addition of natural organic dyes to a white mineral substrate involving a complexation of colouring molecules with a metallic cation such as Al(III). Knowledge of correlations between the organic and inorganic constituents is required to control the colour and the stability of the pigment.

This work concerns the solid state complexation of aluminium with quercetin. This chromophore is used as a model for the phenolic compounds extracted from immature fruits of *Rhamnus catharticus* L. employed for Stil de grain lake or "jaune d'Avignon" [2,3]. The characterization of the synthesised powder materials was performed by UV-Visible, IR and Raman spectroscopy which makes it possible to correlate the experimental parameters of lake preparation with the physicochemical properties of corresponding aluminium complexes in solution [4].



UV-Visible and IR reflectance spectra as a function of quercetin:Al ratio

Lastly, the comparison of quercetin with historic model lake shows that they are composed of an aluminium complex encapsulated into an amorphous matrix of aluminium hydroxide. For all the lakes the intensity color comes from the dilution of the different complex into the inorganic support.

- [1] D. Cardon Natural dyes: sources, tradition, technology and science. In Archetypes publications, London, 2007.  
[2] K. Bourhis, S. Blanc, C. Mathe, J.-C. Dupin, C. Vieillescazes. Submitted to Dyes and Pigments  
[3] A. Romani, C. Zuccaccia, C. Clementi. 71(2006) 218-223.  
[4] JP Cornard, JC Merlin Journal of Inorganic Biochemistry 92(2002) 19-27.



## Computational spectroscopy in cultural heritage

A. Amat<sup>1</sup>, L. Cartechini<sup>2</sup>, C. Miliani<sup>2</sup>, A. Sgamellotti<sup>1,2</sup>, S. Fantacci<sup>2</sup>

<sup>1</sup>Dipartimento di Chimica, Università degli Studi di Perugia, via Elce di Sotto 8, I-06123 Perugia, Italy

<sup>2</sup>Istituto CNR di Scienze e Tecnologie Molecolari (CNR-ISTM), c/o Dipartimento di Chimica, Università degli Studi di Perugia, via Elce di Sotto 8, I-06123 Perugia, Italy

In the last years computational chemistry has gained a great consideration in many branches of materials science, nevertheless only very recently this tool has been applied to the cultural heritage field, mainly due to the inherent complexity of art materials.

We present the results of a recent research devoted to the simulation of prototypical dyes and pigments relevant in cultural heritage, i.e. indigo, weld and weld lake, minium, and green copper-based pigments, thus providing insight into the assignment of the material composition and degradation processes. The investigated properties range from structural and acid-base properties, to IR/Raman vibrational spectra and UV-vis absorption/emission spectra, including excited state deactivation pathways.

Indigo, responsible for the colour of the Maya Blue pigment, has been widely studied. DFT calculations allow to quantitatively simulate its vibrational spectra, while by TD-DFT we compute its absorption spectrum, relating the appearance of a low-energy absorption band at high solution concentrations to the formation of hydrogen-bonded aggregates.[1]

Weld, extracted from *Reseda Lutelola* L., has been reported as one of the oldest natural dyes known in Europe. By complexating weld with metal salts, a highly prized yellow lake was prepared. Absorption and emission processes, including spectral changes depending on the solution pH, of apigenin and luteolin, the main components of weld, have been investigated by means of DFT and TD-DFT.[2] Moreover, their complexation with Al(III) has been investigated. The comparison between the computed absorption spectra of all the considered Al-apigenin/luteolin complexes and the experimental spectra at various limit  $[Al^{3+}]$  concentrations has been used to discriminate among the possible complexation modes and stoichiometry ratios, thus providing insights into the weld lake composition.[1,3]

Minium ( $Pb_3O_4$ ), also known as red lead, was chosen for modeling inorganic pigments, whose identification is often performed through Raman spectroscopy. Its structural properties and vibrational spectra have been computed and the Raman spectrum compared to the experimental data allowing the assignment of the experimental bands.[1]

Finally, computational chemistry has been used to study a real case of degradation observed in many paintings. In particular, the blackening of copper-based pigments has been rationalized by means of DFT and TD-DFT calculations.

We particularly highlight how computational chemistry application in cultural heritage can complement the experimental investigations in establishing and/or rationalizing structure-property relations of the fundamental artwork components. The results of the discussed applications illustrate the potentialities that computational chemistry offers to the cultural heritage field.

[1] S. Fantacci, A. Amat, A. Sgamellotti, Accounts of Chemical Research, in press.

[2] A. Amat, C. Clementi, F. De Angelis, A. Sgamellotti, S. Fantacci, J. Phys. Chem. A. 113 (2009) 151118-15126

[3] A. Amat, C. Clementi, C. Miliani, A. Romani, A. Sgamellotti, S. Fantacci, PCCP, in press.



## New Approaches to Develop Multifunctional Plasmonic Nanosensors for Bioanalytical Applications

S. Astilean, M. Baia, D. Maniu, C. Farcau, M. Iosin, V. Canpean, S. Boca, M. Potara, and A. M. Gabudean

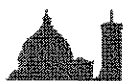
*Babes-Bolyai University, Faculty of Physics, Institute for Interdisciplinary Research in Bioanoscience, Nanobiophotonics Center, T. Laurian 42, 400271 Cluj-Napoca, Romania*

Surface plasmon resonances are collective oscillations of free electrons induced by light in noble-metal nanostructures. In recent years, surface plasmon resonances have gained considerable interest for biosensing via multiple optical methods as surface-enhanced Raman spectroscopy (SERS), surface-enhanced IR absorption (SEIRA), metal-enhanced fluorescence (MEF) and localized surface plasmon resonances (LSPR) spectroscopy. There is a need to design highly sensitive, multifunctional plasmonic sensors which impart good biocompatibility and molecular specificity to detect low levels of chemical species in biological media [1].

In this presentation we report our recent results on the fabrication of plasmonic nanostructures by combining many inexpensive methods ranging from colloidal lithography to controlled chemical synthesis [2]. As for example, we employ self-assembled nanospheres as lithographic masks to deposit metal and generate periodic arrays of nanoparticles or, alternatively, we use biopolymer, protein and cell-assisted synthesis procedures to generate a large variety of biocompatible gold nanoparticles. To characterize and correlate the plasmonic response of as fabricated nanoparticles with their nanometer-scale morphology and topography we combine experimental methods (scanning and transmission electron microscopy, atomic force microscopy, optical measurements) with computational methods (FDTD, DDA). We have recently developed biocompatible SERS substrates for the detection of low-concentration amino-acids and studied the direct interaction between gold nanoparticles (rods, prisms, stars-shaped) and some representative biomolecules by combining LSPR, MEF and SERS measurements. The as fabricated substrates were exploited not only in SERS but also in SEIRA and both FT-SERS and SEIRA spectra of p-aminothiophenol were successfully recorded from the same metallic substrate [3]. We have demonstrated the applicability of metallic films perforated with periodic arrays of subwavelength nanoholes as dual molecular plasmonic sensors based on LSPR and SERS [4]. Finally we were able to register temporal series of SERS spectra at these specific "hot-spot" locations on regular arrays of nanoparticles and observed specific behaviors (fluctuating peak intensities and positions) which can be assigned to the signature of single-molecule SERS signal. The fabricated SERS and SEIRA-active substrates complemented with LSPR and MEF measurements can hold a significant potential for novel biomedical sensing and imaging methods.

**Acknowledgments.** This work was supported by CNCSIS in the frame of PN-II research program under the projects PCE-2007 No. ID 477/2007 and PCCE-2008 No 129/2009.

- [1] Monica Baia, Simion Astilean, and Traian Iliescu, Raman and SERS investigations of pharmaceuticals, Ed. Springer, (2008).
- [2] M. Potara, D. Maniu, S. Astilean, Nanotechnology 20 (2009) 315602-315608
- [3] Monica Baia, Felicia Toderas, Lucian Baia, Dana Maniu and Simion Astilean, ChemPhysChem 10, 7, (2009) 1106 – 1111.
- [4] V. Canpean, S. Astilean, Lab Chip 9 (2009) 3574-3579.



## Confocal Raman microscopy for in depth analysis in the field of cultural heritage.

G. Lorenzetti<sup>1</sup>, J. Striova<sup>2</sup>, A. Zoppi<sup>1</sup>, E. M. Castellucci<sup>1</sup>

<sup>1</sup> Dipartimento di Chimica, Università degli Studi di Firenze, Via della Lastruccia 3, 50019, Sesto F.no (Fi), Italy.

<sup>2</sup> Istituto per la Conservazione e Valorizzazione dei Beni Culturali CNR, via Cozzi 53, 20125, Milano, Italy

Confocal Raman microscopy with metallurgical objectives was tested for the in-depth study of thin samples that are of interest in the field of cultural heritage. The sensitivity of the instrumentation was first evaluated by analyzing single layers of polyethylene terephthalate (PET) films having a thickness of 12, 25 and 50  $\mu\text{m}$  respectively.

Subsequently, the technique was applied to the analysis of historical cotton yarns, dyed with indigo and woad, in order to investigate the penetration degree of the dye inside the fibres. This was done by acquiring the depth profiles of the indigoid dye main Raman band at 1582  $\text{cm}^{-1}$ . A better discrimination of the fibres' signals was also shown by the confocal configurations, making an easier identification of the fibres nature in textiles.

Furthermore, Raman spectroscopy in confocal configuration was also exploited in the evaluation of cleaning efficiency in a project of laser-assisted cleaning of mural painting specimens. These specimens were treated with acrylic resin (Paraloid B72) so as to simulate past restoration intervention. Confocal Raman experiments were performed before and after laser cleaning (at different conditions) in order to monitor presence and the approximate thickness of the polymer film. Raman spectroscopy proved a valid comparative tool in assessment of cleaning efficiencies, especially where other analytical means such as colorimetric measurements were not sufficient due to the colourless of acrylic layers.



## Spectroscopic studies of pigment-binder interactions in wall paintings

S. Dallongeville<sup>a</sup>, M. C. Dhamelincourt<sup>a</sup>, G. Di Lonardo<sup>b</sup>, B. Hernandez<sup>c</sup>, S. Turrell<sup>a</sup>

<sup>a</sup>LASIR (UMR 8516, CNRS), Bât C5, Université de Lille 1, 59650 Villeneuve d'Ascq cedex (France)

<sup>b</sup>Dipartimento di Chimica Fisica e Inorganica, University of Bologna, I-40136 Bologna (Italy)

<sup>c</sup>Groupe de Biophysique Moléculaire, Université Paris 13-UFR SMBH, 93017 Bobigny cedex (France)

The physico-chemical analysis of materials and objects of archeological interest is essential for the structural comprehension, for the conservation and for the restoration of ancient works. The identification of the different materials which compose a work of art makes it possible for the historian to have a better understanding of an artistic period or technique. At the museum level, it is necessary to find the best conditions for conservation of art works and consequently it is essential to understand chemical mechanisms which might be involved in degradation processes. In a similar way, the restorer, if he is to avoid catastrophes, must have a good knowledge of the compounds used in the original work so as to be able to know what to propose for the restoration.

Our interest concerns predominantly paintings of the Middle Ages. At that period, a painting consisted of at least two elements: the pigment to give the color and the binder to provide a medium with adhesive properties into which the pigment could be mixed in suspension. It was this binder that enabled the final "paint" to fix to a support. The binders used at that period were easy-to-find natural products like egg, milk or animal glues. For restoration purposes, however, it is essential to identify the binders used so as to understand aging processes which might have occurred and also so as to know how to proceed with repairs.

The present work concerns the determination of the types of interactions that can occur between proteins and pigments when combined in a paint. Our model studies involve two different pigments (lead white and garance, an organic pigment of vegetal origin) and an egg white binder. However, in order to simplify the studies, the complex-structured egg white was replaced by lysozyme and ovalbumine.

Spectroscopic measurements were carried out for the characterization of the pigments and the two proteins at varying concentrations and different values of pH. Following the descriptions supplied in ancient texts, a recipe was devised for the "paint" using various pigment/protein mixtures. Infrared and Raman spectroscopies were then used, as well as UV absorption spectroscopy, to follow structural evolutions resulting with the mixtures. The results will be discussed in terms of how the apparent molecular interactions can aid in adhesion of the pictorial layer to the support.





## Micro-Raman spectroscopic study of frescoes from the antiquity period

O. Cristini<sup>a</sup>, C. Kinowski<sup>a</sup>, and S. Turrell<sup>b</sup>

<sup>a</sup>PhLAM (UMR 8523, CNRS), Bât P5, Université de Lille 1, 59650 Villeneuve d'Ascq cedex (France)

<sup>b</sup>LASIR (UMR 8516, CNRS), Bât C5, Université de Lille 1, 59650 Villeneuve d'Ascq cedex (France)

Raman spectroscopy is now a well-established method for the identification of crystalline and amorphous phases constituting ancient artifacts, including pigments [1]. Using micro-Raman techniques, samples like archeological frescoes can be examined nondestructively and noninvasively [2]. Moreover this technique provides *in situ* analysis at a micrometric scale. The scientific examination of the pigments used in archeological or art contexts, such as wall paintings, is important in revealing information for the characterization, restoration and preservation of the items. Furthermore, information that is important for the evaluation of cultural and economic features of earlier civilizations can be employed to build up an overview of the artist's materials and the methods employed.

The present work deals with the characterization of the plaster and pictorial layers of frescoes issue from excavations in different locations in Europe (France, Italy and Greece). The samples from France and Italy were found in soil excavations while those from Greece are were uncovered in caves with openings towards the sea.

Raman spectra of the preparation layers and of the pictorial layers were recorded in the wavenumber region of 200 to 1800  $\text{cm}^{-1}$ . Spectra were identified by comparison with various data banks [3]. The analyses of the different samples concerned both the preparation layers and the pigments.

Spectral analyses, with a characteristic vibration band centered at 1085  $\text{cm}^{-1}$ , showed that for most of the samples, calcite ( $\text{CaCO}_3$ ) acted as a binder in the preparation layer. In a few of the Greek samples, however, a sharp band observed at 1007  $\text{cm}^{-1}$  can be attributed to gypsum. Gypsum could be a degradation product; as the interaction between atmospheric sulfur dioxide and calcite can yield the formation of gypsum [4].

Several pigments were identified in the different samples: carbon black, green earth, Egyptian blue, red ochre, minium, and vermilion. All of these pigments are consistent with the antiquity period. Finally, attention will be paid to the serious alteration which is observed in the Greek samples.

[1] P. Vandenabeele, H. G. M. Edwards, L. Moens, *Chem. Review*, 107 (2007) 675-686

[2] P. Dhamelincourt, F. Wallart, M. Leclercq, A. T. Nguyen, D. O Landon *Anal. Chem.*, 51 (1979) A414-A419

[3] R. J. H. Clark, *C.R. Chimie*, 5 (2002) 7-20

[4] H. G. M. Edwards, D. Farwell, *J. Raman Spectros.*, 39 (2008) 972-984



## Minerals from Macedonia. XXVII. Theoretical and experimental study of the vibrational spectra of Nežilovite

N. Stamatovska<sup>1</sup>, P. Makreski<sup>1</sup>, L. Pejov<sup>1</sup>, G. Jovanovski<sup>1,2</sup>

<sup>1</sup>*Institute of Chemistry, Faculty of Science, SS. Cyril and Methodius University, Arhimedova 5, 1000 Skopje, Republic of Macedonia*

<sup>2</sup>*Macedonian Academy of Sciences and Arts, Bul. Krste Misirkov 2, 1000 Skopje, Republic of Macedonia*

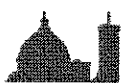
Continuing the process of systematic spectra-structural investigation on the non-silicate minerals originating from Macedonia [1–3], an extremely-rare occurring mineral from the magnetoplumbite group – nežilovite,  $\text{Pb}(\text{Zn,Fe})_2(\text{Fe,Mn,Al,Ti,Sb,Mg})_{10}\text{O}_{19}$ , was studied by vibrational spectroscopy. The mineral is a representative from the Zn-rich variety and is found near the village of Nežilovo, located in the central part of the Pelagonian Massif. The authenticity of the mineral was confirmed by its chemical composition and by X-ray powder diffraction.

To provide a theoretical basis for interpretation and band assignments of the experimental vibrational spectra, a pseudopotential plane-wave density functional theory (PW-DFT) of the title system was performed as well. Within the PW-DFT formalism, several combinations of exchange and correlation functionals were implemented. The geometry of the 3D-periodic system was first optimized by the conjugate gradient methods, and subsequently numerical computation of the second derivatives was carried out for the located stationary points. Harmonic vibrational frequencies were further computed by diagonalization of the mass-weighted Hessian matrices. In order to provide a theoretical basis for the empirical assignments, and also to test the reliability of various levels of the PW-DFT formalism, the theoretical results were compared to the experimental ones.

[1] P. Makreski, G. Jovanovski, B. Kaitner, T. Stafilov, B. Boev, D. Cibrev, *Neues Jahrb. Mineral. Abh.* 180 (2004) 215-243

[2] P. Makreski, G. Jovanovski, S. Dimitrovska, *Vib. Spectrosc.* 39 (2005) 229-239

[3] P. Naumov, P. Makreski, G. Jovanovski, *Inorg. Chem.* 46 (2007) 10624-10631



## Multivariate Analysis of Ancient Cucuteni Ceramics from Romanian Cultural Heritage

M. Praisler, D. Domnisoru, S. Gosav

*Physics Department, Faculty of Sciences, University Dunarea de Jos of Galati, 800201 Domneasca St Galati, Romania, stelagosav@yahoo.com*

Ancient ceramics artifacts from the Cucuteni-Trypillian culture were characterized by using diffuse reflection infrared (IR) spectroscopy in order to build an expert system aiming to the automatic recognition of true and false artifacts. The extent to which IR can be used as a diagnostic analytical method was first analyzed by using a multivariate approach, i.e. Principal Component Analysis. The results which may lead to forensic applications and expertise are discussed. Their spectroscopic meaning yields a useful analytical tool for archeometricians.

*Keywords:* IR spectroscopy, Principal Component Analysis, ceramics artifacts, Cucuteni culture.



## Application of IR spectra in the studies of anion sorption on natural sorbents

W. Mozgawa<sup>1</sup>, M. Król<sup>1</sup>, T. Bajda<sup>2</sup>

<sup>1</sup>*Faculty of Materials Science and Ceramic, AGH University of Science and Technology,*

<sup>2</sup>*Faculty of Geology, Geophysics and Environment Protection, AGH University of Science and Technology*

*Al. Mickiewicza 30, 30-059 Kraków, POLAND*

*mozgawa@agh.edu.pl*

This work presents the results of FT-IR spectroscopic studies of anions - chromate, phosphate and arsenate - sorbed from aqueous solutions (different concentrations of anions) on natural sorbents. The sorption has been conducted on zeolite (clinoptilolite) and smectite (mixtures of clay minerals containing mainly smectite, montmorillonite and kaolinite) which have been separated from natural Polish deposit. The Na-forms of sorbents were exchanged with hexadecyltrimethylammonium cations (HDTMA<sup>+</sup>) and HDTMA-clinoptilolite and HDTMA-smectite were obtained. Cation exchange capacities (CEC) of clinoptilolite and smectite were measured. Their values are 23 mmol./100 g and 41 mmol/100 g respectively. The used initial inputs of HDTMA correspond to 100 and 200% CEC of the minerals. Organo-modified sorbents were subsequently used to immobilization mentioned anions.

It was proven those anions' sorption causes changes in IR spectra of the HDTMA-zeolite and smectite. These alterations are dependent on the kind of anions that were sorbed. In both cases, variations are due to bands corresponding to the characteristic Si-O(Si,Al) vibrations (occurring in alumino- and silicoxygen tetrahedra building spatial framework of zeolite or layer structure of smectite), OH group vibrations and alkylammonium surfactant vibrations have been observed. Systematic changes in the spectra connected with the anion concentration in the initial solution have been revealed.

The amounts of sorbed CrO<sub>4</sub><sup>2-</sup>, AsO<sub>4</sub><sup>3-</sup>, and PO<sub>4</sub><sup>3-</sup> ions were calculated from the difference between their concentrations in solutions before (initial concentration) and after (equilibrium concentration) sorption experiments. Concentrations of chromates were determined by colorimetry using the biphenylcarbazine method. For phosphates and arsenates molybdenum blue method was used.



## Zn (II) Determination in Contaminated Soil by SERS Spectroscopy

L. Szabó<sup>1</sup>, L.F. Leopold<sup>2</sup>, N. Leopold<sup>1</sup>, I.B. Cozar<sup>1</sup>, V. Chiş<sup>1</sup>

<sup>1</sup>Faculty of Physics, Babeş-Bolyai University, Kogălniceanu 1, 400084 Cluj-Napoca, Romania

<sup>2</sup>Department of Chemistry and Biochemistry, University of Agricultural Sciences and Veterinary Medicine, Calea Mănăştur 3-5, 400372 Cluj-Napoca, Romania

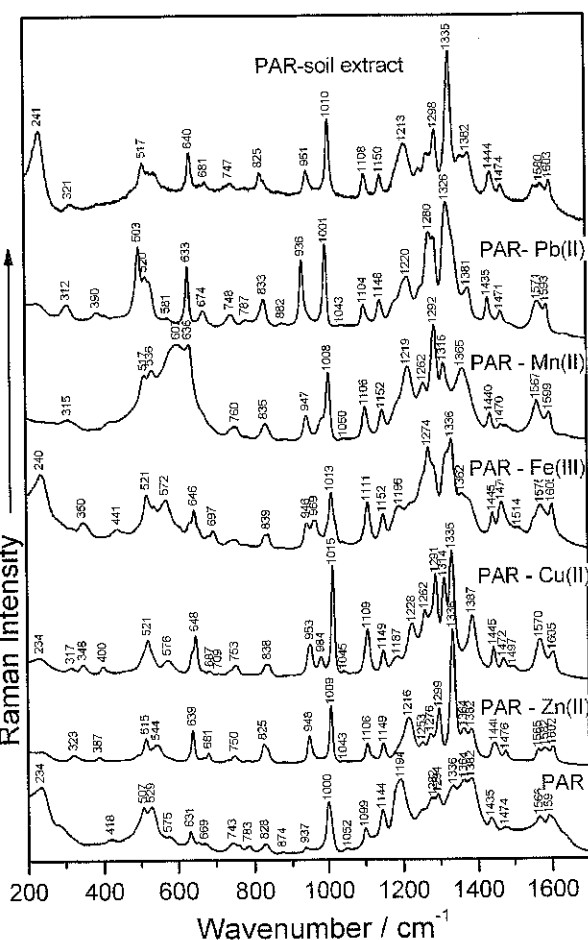
Soil contamination by metals is a common problem encountered in many industrialized countries. Intensive industrial activity has resulted in the accumulation of high concentrations of heavy metals and toxic elements in the soil environment causing serious socio-economic problems.

In this work we present a new approach for heavy metals determination by using surface-enhanced Raman scattering (SERS) spectroscopy. By this method, Zn(II) could be clearly evidenced in contaminated soil from an industrial region.

The extraction from the soil probe was performed with deionized water and after filtration, 1 ml water extract was mixed with 100  $\mu$ l  $10^{-3}$ M 4-(2-pyridylazo)resorcinol (PAR) solution. The mixture turned to a red color, evidencing the formation of PAR-metal ion complexes.

Although this change in the absorption feature seems to be rather important, qualitative determination by UV-VIS spectroscopy is often unreliable. Thus, a new approach based on SERS spectroscopy that offers a much higher molecular selectivity and sensitivity is presented.

The SERS spectra of PAR, of its metal chelates and of the soil extract-PAR mixture (top of figure) were recorded using a hydroxylamine reduced silver colloid [2]. The differentiation between PAR- Zn(II), Cu(II), Fe(III), Mn(II) and Pb(II) chelates is demonstrated on the basis of the SERS characteristic spectral features of each complex [1]. Density functional theory (DFT) based calculations were also performed in order of SERS spectra assignment.



SERS spectra of PAR molecule and its complexes with Zn(II), Cu(II), Fe(III), Mn(II), Pb(II) and SERS spectrum of the PAR-soil extract.

An excellent match of the PAR-soil extract SERS spectrum to the PAR-Zn(II) SERS spectrum can be observed, evidencing the Zn(II) contamination of the soil probe.

[1] N. Leopold, L. Szabó, A. Pîrnău, M. Aluaş, L.F. Leopold, V. Chiş, O. Cozar, J. Mol. Struct. 919 (2009) 94-99

[2] N. Leopold, B. Lendl, J. Phys. Chem. B 107 (2003) 5723



## Aqueous complexation of humic acid with organostannic compounds by IR spectroscopy and FFF

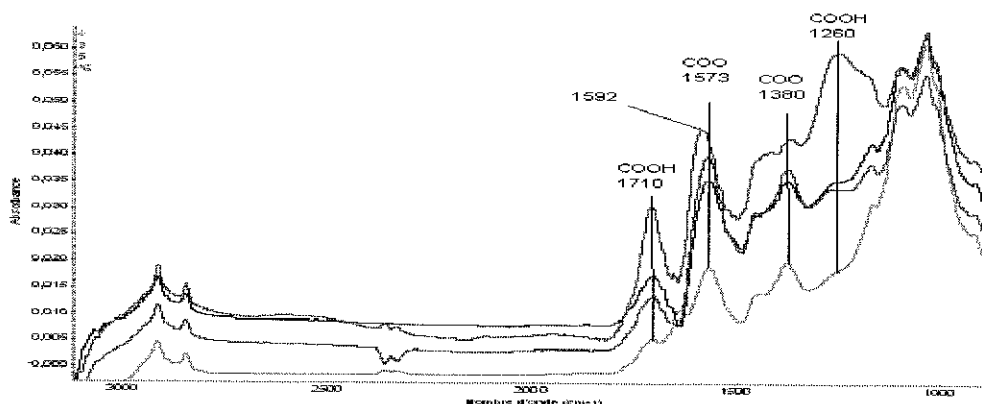
S. Salami, E. Péré, G. Lespes

*Université de Pau et des Pays de l'Adour - UMR CNRS 5254  
Institut Pluridisciplinaire de Recherche sur l'Environnement et les Matériaux  
2 Avenue du Président Pierre Angot 64053 Pau, France*

The fate of chemical elements in the environment is a matter of concern considering their potential toxicity and impact on living organisms. The evaluation of their environmental impact remains an actual challenge, especially with regard to the methodology and approach chosen to acquire elements of knowledge. This choice is all the more critical because of the complexity and variability of the media as well as the numerous chemical compounds involved in a wide range of concentration and molar mass. Among these compounds, natural organic matter (NOM) is recognized as playing a crucial role in the fate of chemical elements i.e. their speciation, mobility and bioavailability [1].

However, the development of new tools able to work at molecular as well as nanometric scale is needed to access the mechanisms involved in the environmental TM fate including transfer to living organisms.

So, we propose to evaluate the potentiality of vibrational spectroscopy combined to online fractionation- multi-detection in order to characterise humic substances – metals - biological matter interactions. This work concerned Sn, metal of environmental interest, and its association with humic acids (HA) commercially available (typically from soil) [2,3]. Molecular and spectroscopic characterisation is performed as a function of pH, ionic strength and cation concentration by Infra-Red ATR spectroscopy associated to Field-Flow Fractionation (FFF) coupled to Ultra-Violet (UV) and Atomic Mass (ICPMS) Spectrometry.



*ATR spectra of aqueous Humic acid as a function of pH*

- [1] J.P. Cornard, L. Dangleterre, *Journal of Physics and Chemistry* 109 (2005) 10044
- [2] P. MacCarty, *Humic substances in soil and crop sciences: Selected readings*. Madison, Wisconsin, Soil Science Society of America, 1990
- [3] M.A. Baalousha, *Thèse de Doctorat de l'Université de Bordeaux* 1.2006



## Microprobe Analysis And Spectroscopic (Mir, Raman And Nmr) Studies Of Various Members Of Tourmaline Group Minerals From Sudety Mts, Sw Poland.

M. Sitarz<sup>1</sup>, M. Łodziński<sup>2</sup>, A. Pieczka<sup>3</sup>

<sup>1</sup> AGH Univ. Science and Technology, Faculty of Materials Science and Ceramics, al. Mickiewicza 30, 30-059 Kraków, Poland

<sup>2</sup> AGH Univ. Science and Technology, Faculty of Geology, Geophysics and Environment Protection, Department of General Geology, Environment Protection and Geotourism, al. Mickiewicza 30, 30-059 Kraków, Poland

<sup>3</sup> AGH Univ. Science and Technology, Faculty of Geology, Geophysics and Environment Protection, Department of Mineralogy, Petrography and Geochemistry, al. Mickiewicza 30, 30-059 Kraków, Poland

The tourmaline group is a group of borosilicate minerals with a general formula  $XY_3Z_6(T_6O_{18})(BO_3)_3V_3W$ , where the <sup>[9]</sup>X site is filled by Na<sup>+</sup>, K<sup>+</sup>, Ca<sup>2+</sup> or vacancy, the <sup>[6]</sup>Y site is occupied by Li<sup>+</sup>, Mg<sup>2+</sup>, Fe<sup>2+</sup>, Mn<sup>2+</sup>, Al<sup>3+</sup>, Cr<sup>3+</sup>, V<sup>3+</sup>, Fe<sup>3+</sup> and Ti<sup>4+</sup>, the <sup>[6]</sup>Z site mainly by Al<sup>3+</sup>, and rarer by Mg<sup>2+</sup>, Fe<sup>3+</sup>, Cr<sup>3+</sup> and V<sup>3+</sup>, the <sup>[4]</sup>T site mainly by Si<sup>4+</sup> and occasionally by Al<sup>3+</sup> and an excess of B<sup>3+</sup>, while the V site by OH<sup>-</sup> and O<sup>2-</sup>, whereas the W site by OH<sup>-</sup>, F<sup>-</sup> and O<sup>2-</sup>.

Various tourmaline specimens were collected from different geological units in the Sudety Mts in Lower Silesia, southwestern Poland. They represent Mg-dominant tourmaline – dravite, NaMg<sub>3</sub>Al<sub>6</sub>(BO<sub>3</sub>)<sub>3</sub>Si<sub>6</sub>O<sub>18</sub>(OH)<sub>4</sub>, Al-Li-tourmaline representing elbaite, Na(Al,Li)<sub>3</sub>Al<sub>6</sub>(BO<sub>3</sub>)<sub>3</sub>Si<sub>6</sub>O<sub>18</sub>(OH)<sub>4</sub>, and Fe<sup>2+</sup>-dominant tourmaline corresponding to schorl, NaFe<sup>2+</sup><sub>3</sub>Al<sub>6</sub>(BO<sub>3</sub>)<sub>3</sub>Si<sub>6</sub>O<sub>18</sub>(OH)<sub>4</sub>.

Dravite has been found in a quartz vein within leucogranite in Wołowa Góra Mt. near Kowary, localized in the eastern envelope of Karkonosze granite, and in a pegmatite vein within gneisses of the Sowie Góry gneissic block at Rzecznka. Elbaite has been found in a pegmatite vein, crossed amphibolite and migmatite at Piława Grn. quarry near Dzierżoniów, also in the Sowie Góry gneissic block, whereas schorl has been collected in a pegmatite vein within granitogneisses of Bystrzyckie and Orlickie Mts metamorphic massif at the Jawornica schist quarry.

The tourmalines form light-brown (dravite), dark-green (elbaite) and black (schorl) prismatic crystals of various sizes from less than 1mm to some centimeters in length. Some of them show typical variations in chemical composition from the core to the rim. The crystallization of selected specimens is connected with pneumatolitic and hydrothermal stages.

The samples of tourmaline were analysed in microarea using electron-microprobe and Raman spectroscopy. Powdered samples were used to IR-spectroscopic measurements.

Literature data concerning tourmalines allowed the precise assignation of bands to the corresponding vibration type on the MIR and Raman spectra. The influence of non-tetrahedral cations from the X, Y and Z sites on the shape of the spectra, and the positions of bands has been analysed and the crystalline field splitting effect has been discussed.

Based on <sup>11</sup>B MAS NMR spectra we tried to establish the common location of boron in the <sup>[3]</sup>B site and an excess of B<sup>3+</sup> in the tetrahedral T sites.

The main aim of this work is linking the chemical composition derived from microprobe analysis with structural results derived from spectroscopic methods.

**Acknowledgement:** The following research was supported by the AGH University of Science and Technology grants No. DS 11.11.140.447 and BW 10.10.140.677.



## Main refractive indices of some carpathian crystals

C. F. Dascalu, B. C. Zelinschi, D. O. Dorohoi

*Alexandru Ioan Cuza University, Faculty of Physics, 11 Carol I Blv., Iasi, RO-700506, Romania*

Some Carpathian crystals were characterized from the point of view of their visible birefringence by using optical methods based on compensation of the optical way or by using interferometric devices. For the uniax crystals the previously described methods were applied and the main refractive indices and birefringence were estimated.

The obtained results were compared by those obtained by a new method based on polarizing microscope.

For the biaxals crystals a new method based on the inclined propagation of light was implemented. Two indices of refraction were estimated for propagation directions different to the normal incidence by solving the equation of the refractive indices ellipsoid. The other two were determined for the normal incidence on the crystalline plate cut parallel to one of main crystalline plane. The two pairs of refractive indices have a common value. The determined values were used to characterize the crystal from the point of view of optical axes orientation.

The obtained results were analyzed in correlation with the chemical composition of the Carpathian crystals. They can be used in Optics of anisotropic substances for projecting and obtaining devices working in polarized light.





## The use of UV/Vis spectroscopy for the estimation of humic acids maturity

M. Bartoszek, J. Polak, W. Kapica, W.W. Sułkowski

*Department of Environmental Chemistry and Technology, Institute of Chemistry, University of Silesia  
Szkolna 9, 40-006 Katowice, Poland*

UV/Vis spectroscopy was used for the characterization of humic acids extracted from bottom sediment and from sewage sludge. The sediment samples were collected at eight points from an artificial water reservoir at various seasons. The sludge samples were taken from four points of material sampling during the sewage treatment process.

The spectra of humic substances show an increasing absorption with decreasing wavelength without characteristic features. However, monitoring the absorption at a specific wavelength or the absorption ratio at two wavelengths allowed us to estimate the maturity and stability of the humic acids.

Analysis of the obtained spectra shows that UV/Vis spectroscopy is a proper tool for the monitoring humification processes. The properties of humic acids extracted from various points of the reservoir at different depths of the lake and at various distance from the shore were compared. The maturity of humic acids extracted from bottom sediment and from sewage sludge were also compared.

**Acknowledgements:** This work was supported by the Ministry of Science and Higher Education (MNiSW Poland) under Project No. N N204 1932 33.



## San Vincenzo al Volturmo (Italy) and the identification of blues.

G. Trojsi<sup>1</sup>, F. Marazzi<sup>1</sup>, P. Baraldi<sup>2</sup>

<sup>1</sup>*Università degli Studi "Suor Orsola Benincasa", Naples,*

<sup>2</sup>*Department of Chemistry, University of Modena and Reggio Emilia (Italy)*

In the main basilica of the Abbey of S. Vincenzo al Volturmo (Italy) the crypt of abbot Joshua, built in the apse is a typical example of a fair annular crypt dating to the Carolingian times.

The Chronicon Vulturense (beginning of the XII century) tells the events of the monastery of San Vincenzo from its foundation till to the end of the XI century, and situates the consecration of the basilica to the year 808. The pictorial decorations of the crypt, widely preserved, represents perhaps the richest repertoire of all European high Middle ages paintings with abstract and geometrical patterns.

Due to their chronology, these painting can be an interesting subject for research for the reconstruction of the history of use of painting materials and of their techniques.

A deep examination of the elements of the Abbey in its latest years lead archaeologists to identify different pictorial surfaces and to ascertain that different building and revision works were carried out in the past. The identification of some surfaces concerning the IX and X centuries brought to investigate the pigment palette used through times. In this respect, the problem of the end of use of Egyptian blue and of the beginning of use of other blue materials is very attractive.

For the research Raman microscopy and FI-IR spectroscopy were considered, analyses were carried out on small fragments recovered during the archaeological inspections, or sampled properly and pertaining to different walls of the Abbey. In some cases also XRD and XRF techniques were used and some cross sections were properly prepared and carefully examined in order to support the data obtained with the Raman technique.

The spectroscopic data obtained show the continuity of use till the IX century of Egyptian blue in this building and the almost simultaneous use of ultramarine. Some data on the compounds identified in the research are shown and some considerations on the history of the materials are put forward.

F. Marazzi, The second phase of the excavation project in San Vincenzo al Volturmo and its land" (with R.Hodges e P.Foster), in "Scavi Medievali in Italia", di S.Patitucci Uggeri, Roma 1995, pp. 63 - 84.

F. Marazzi, San Vincenzo al Volturmo à l'âge carolingienne: l'invention d'une cité monastique et son arrière-plan politique et économique in "Le christianisme occidental du début du VIIe siècle au milieu du Xie siècle. Textes et documents", a c. di F.Bougard, Condé-sur-Noireau, 1997, pp.187-202



## The EPR study of humic acid extracted from sediment collected at various seasons

J. Polak, M. Bartoszek, M. Żądło, W.W. Sułkowski

*Department of Environmental Chemistry and Technology, Institute of Chemistry, University of Silesia  
Szkolna 9, 40-006 Katowice, Poland*

Goczałkowice Reservoir is the biggest reservoir in the south of Poland. The main task of this dam reservoir is to supply water to the inhabitants of the Upper Silesia agglomeration.

Bottom sediment for studies were collected according to Polish standards at various seasons from eight places of the Goczałkowice Reservoir.

Humic acids (HA) were extracted by conventional procedures. The EPR spectroscopy was applied for both quantitative (free radical concentration) and qualitative (g factor) analysis of humic substances.

EPR spectra of the extracted humic substances exhibit broad lines from the paramagnetic metal ions (eg.  $\text{Fe}^{3+}$ ,  $\text{Mn}^{2+}$ ,  $\text{Cu}^{2+}$ ) and narrow lines from free radicals (Fig 1).

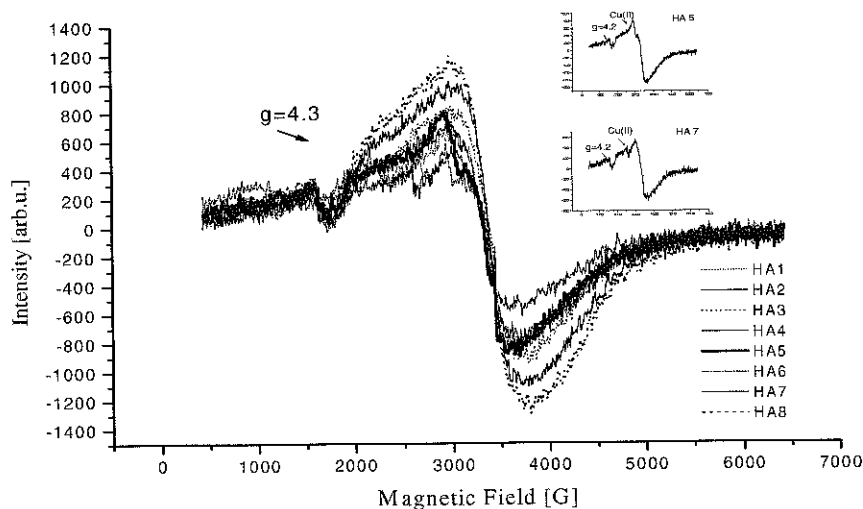


Fig. 1 The EPR spectra of humic acid (HA) extracted from bottom sediment taken at 8 points of the Goczałkowice Reservoir

The values of free radical concentration obtained for humic acids amount to  $1.14\text{-}13.6 \cdot 10^{16}$  spin/g depending on the season and the point of sample collection. These values are comparable with those obtained for aquatic HA ( $\sim 10^{16}$  spin/g) and for HA extracted from sewage sludge ( $\sim 10^{16}\text{-}10^{17}$  spin/g). The values of the g factor obtained for HA equals 2.0027 - 2.0035.

The EPR studies show that HA extracted from the bottom sediment collected at various points of the Goczałkowice Reservoir have similar physico-chemical properties. The influence of the reservoir depth on the content of oxygen functional groups and free radical concentration in humic and fulvic acids was noticed.

**Acknowledgements:** This work was supported by the Ministry of Science and Higher Education (MNiSW Poland) under Project No. N N204 1932 33.



## Thermal Synthesis of Gly-Gln Polymer on Rutile. A Vibrational Study.

P. Leyton<sup>1</sup>, C. Paipa<sup>1</sup>, A. Zárate<sup>2</sup>, S. Fuentes<sup>2</sup>, R. Sánchez<sup>3</sup>, Y. Leyton<sup>3</sup>

<sup>1</sup> Departamento de Ciencias Químicas, Facultad de Ecología y Recursos Naturales, Universidad Andrés Bello (UNAB), Los Fresnos 52, Viña del Mar, Chile.

<sup>2</sup> Departamento de Física, Facultad de Ciencias, Universidad Católica del Norte, Casilla 1280, Antofagasta, Chile.

<sup>3</sup> Instituto de Química, Facultad de Ciencias, Laboratorio de Fotofísica y Espectroscopia Molecular, Pontificia Universidad Católica de Valparaíso, Avenida Brasil 2950, Valparaíso, Chile.

Nearly 50 years ago, Bernal and Goldschmidt independently proposed that clay minerals could play an important role in both the prebiotic chemistry and the origin of life. Most of the non-catalytic prebiotic studied syntheses use simple molecules such as HCN, HCHO, CO, H<sub>2</sub>S and NH<sub>3</sub> as starting materials. Thus, prebiotic reactions proceeding in the absence of catalytic surfaces yield a random mixture of organic compounds as happened in the classic Miller-Urey experiment [1, 2]. A new situation occurs when a molecule establishes an adsorbate-substrate interaction with a surface. In this context, mineral surfaces could establish selectivity over the reactive compounds to form the complex biomolecules and biopolymers that originated life.

The formation of simple polypeptides and short oligomers from amino acids does not proceed readily even under mild conditions. Therefore, the prebiotic polymer formation involves both the use of condensation agents or catalysts and other different conditions, such as high pressure and temperature [3, 4] and melting processes [5]. Thus, prebiotic catalysts must selectively act as microreactors giving favorable environments in the interlamellar spaces of the structure but they should also induce preliminary organization of the molecules on the surface to allow interactions similar to those occurring in solution.

In this work, a vibrational analysis for the Glycine (Gly) and Glutamine (Gln) aminoacids, and the dipeptides (Gly-Gln, Gln-Gly, Gly-Gly) was made and the role of rutile (titanium dioxide) on the thermal synthesis of the glycine – glutamine (Gly-Gln) polymer and its influence on the sequence is described from a vibrational spectroscopy point of view.

The thermal synthesis was carried out in the absence and presence of the oxide. In both cases, the vibrational spectra showed characteristic group frequencies corresponding predominantly to a Gly-Gln polymeric structure with  $\alpha$  form. However, the SEM-EDX characterization of the solid phase involved in the thermal synthesis showed that rutile could participate as a site for nucleation and growth of the polymer, explaining the increase of 15-22% efficiency in the presence of catalyst. The ATR-IR spectra of the water soluble polypeptide fraction obtained shows a random structure, which coincides with circular dichroism data. The reaction conditions used in the synthesis permit speculation on the production of a variety of polypeptides relating to the origins of the Earth.

This research has been financially supported by project N° 1085124 from FONDECYT.

[1] S. L. Miller, J. Am. Chem. Soc. 77 (1955) 2351-2361

[2] M. Martinez-Meeler, N. Aljinovic, D. Swain, J. Chem. Ed. 80 (2003) 665-667

[3] C. E. Fouche Jr, D. L. Rohlfing, Biosystems 8 (1976) 57-65

[4] B. R.T. Simoneit, Advances in Space Research 33 (2004) 88-94

[5] K. Harada, S. W. Fox, J. Am. Chem. Soc. 80 (1958) 2694-2697



## Monitoring of hydrothermal precipitation of $\alpha$ -Fe<sub>2</sub>O<sub>3</sub> from concentrated Fe(NO<sub>3</sub>)<sub>3</sub> solutions partially neutralized with NaOH

M. Žic, M. Ristić and S. Musić

*Division of Materials Chemistry, Ruđer Bošković Institute, P. O. Box 180, Bijenička cesta 54, HR-10002 Zagreb, Croatia*

The phase and microstructural properties of iron oxides precipitated from Fe(III)-salts in aqueous media depend greatly on the experimental factors during their synthesis. Nature and concentration of Fe(III) salt, pH, temperature, time of ageing, the presence of “foreign” cations and anions, organic molecules or surface-active substances are some of these important experimental factors. In our previous investigations the precipitation processes of iron oxides from concentrated FeCl<sub>3</sub> solutions partially neutralized by concentrated NaOH in hydrothermal conditions were studied [1, 2].  $\alpha$ -Fe<sub>2</sub>O<sub>3</sub> particles in the form of double sphere with ring were formed by autoclaving dense  $\beta$ -FeOOH suspensions at 160°C for up to 1 or 3 days. When ammonium amidosulfonate was added to the precipitation system the  $\alpha$ -Fe<sub>2</sub>O<sub>3</sub> particles in the form of double cupola interconnected with the neck were precipitated. In the present work the kinetics of hematite crystallization from concentrated Fe(NO<sub>3</sub>)<sub>3</sub> solutions partially neutralized (90 %) by a concentrated NaOH solution were investigated using <sup>57</sup>Fe Mössbauer and FT-IR spectroscopies, XRD and FE SEM analyses. In addition to that, the influence of ammonium amidosulfonate (AAS) on the microstructure of precipitated  $\alpha$ -Fe<sub>2</sub>O<sub>3</sub> particles was studied.  $\alpha$ -Fe<sub>2</sub>O<sub>3</sub> particles in the form of pseudocubes varying in size from 60-150 nm were precipitated after 2 h of autoclaving at 160°C. An increase in the autoclaving time up to 3 days had no significant effect on the particle morphology and size. Ellipsoidal and hollow  $\alpha$ -Fe<sub>2</sub>O<sub>3</sub> particles with substructure were obtained in the presence of AAS. Preferential adsorption of sulfonate/sulfate groups was responsible for the elongation of  $\alpha$ -Fe<sub>2</sub>O<sub>3</sub> particles.

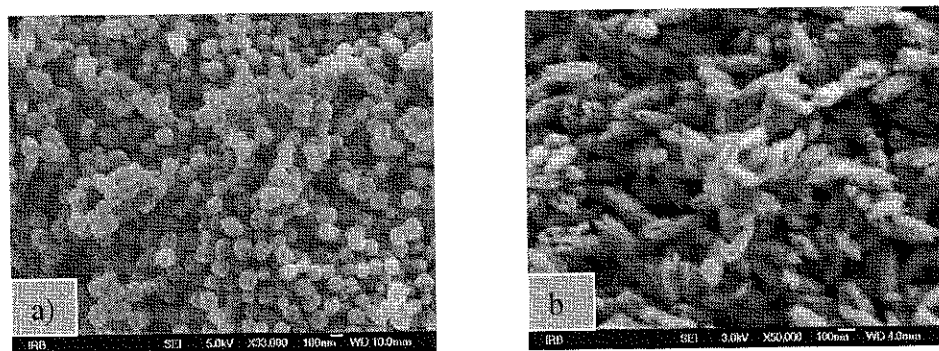


Fig. 1 (a) referent  $\alpha$ -Fe<sub>2</sub>O<sub>3</sub> particles and (b) hollow  $\alpha$ -Fe<sub>2</sub>O<sub>3</sub> particles obtained in the presence of AAS

[1] M. Žic, M. Ristić, S. Musić, *J. Alloys Comp.* 466 (2008) 498-506.

[2] M. Žic, M. Ristić, S. Musić, *J. Mol. Struct.* 924-926 (2009) 235-242.



## The influence of different type precursors of $\text{Al}_2\text{O}_3$ and $\text{SiO}_2$ on structure and microstructure of mullite-like gels and coatings

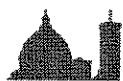
A. Adamczyk, W. Mozgawa

*AGH University of Science and Technology, Faculty of Materials Science and Ceramics,  
Al. Mickiewicza 30, 30-059 Kraków, Poland*

The alumina-silica materials of mullite composition were obtained by sol-gel method, using different  $\text{Al}_2\text{O}_3$  and  $\text{SiO}_2$  precursors in order to prepare proper sols based on water and organic solvents. As  $\text{SiO}_2$  precursors, Aerosil 200<sup>TM</sup> and tetraethoxysilan (TEOS) were chosen, while Disperal<sup>TM</sup> and aluminium secondary butoxide were used for  $\text{Al}_2\text{O}_3$  ones. Such sols allowed to obtain bulk samples by heating gels in air at 500°C, 850°C and at 1150°C and also to synthesize coatings of mullite composition on carbon, steel and alundum (representing porous ceramics) substrates. Samples obtained in form of thin films were then annealed in air (steel and alundum) and in argon (carbon) at different temperatures, depending on a substrate type.

The annealed bulk samples structure was studied by the FTIR spectroscopy and the XRD diffraction. The coatings were also studied by the FTIR spectroscopy (after final annealing) and by the XRD diffraction using GID configuration, and additionally by the electron microscopy (SEM) together with the EDS microanalysis.

The analysis of the FTIR spectra and the X-ray diffraction patterns of bulk samples enables to observe the presence of  $\gamma\text{-Al}_2\text{O}_3$  and  $\delta\text{-Al}_2\text{O}_3$ , together with the small amounts of  $\text{SiO}_2$  in case of some samples. It is confirmed by the vibrations characteristic for bonds occurring in these phases structure, in the range of 400-900  $\text{cm}^{-1}$ , ascribed to the different Al-O bond vibrations - especially bands at about 570  $\text{cm}^{-1}$  and 835  $\text{cm}^{-1}$ . The same phases ( $\gamma\text{-Al}_2\text{O}_3$  and  $\delta\text{-Al}_2\text{O}_3$ ) are observed in coatings, but the presence of particular ones strongly depends on type of  $\text{Al}_2\text{O}_3$  and  $\text{SiO}_2$  precursor and on the temperature of the heating. All thin films contain considerable amounts of an amorphous phase.



## Identification of clay minerals by infrared spectroscopy and discriminant analysis

M. Ritz<sup>1</sup>, L. Vaculíková<sup>2</sup>, E. Plevová<sup>2</sup>

<sup>1</sup> VŠB-Technical University Ostrava, 17. Listopadu 15, 708 33 Ostrava-Poruba, Czech Republic

<sup>2</sup> Institute of Geonics of the AS CR, Studentská 1768, 708 00 Ostrava-Poruba, Czech Republic

A new way of identification of clay minerals was suggested. The identification was based on chemometric analysis of measured IR spectra of clay minerals. IR spectra were collected using diffuse reflectance technique. The discriminant analysis and principal component analysis were used as chemometric methods. Five statistical models were created for separation and identification of clay minerals. Up to 60 samples of various mineral standards (clay minerals, feldspars, carbonates, sulphates and quartz) from different localities were used for the creation of statistical models. The results of this study confirm that the discriminant analysis of IR spectra of clay minerals could provide a powerful tool for identification of clay minerals. Even differentiation of muscovite from illite and identification of mixed structures of illite-smectite were achieved.



## Spectroscopic characterization of chrysotile asbestos from different regions

M. Ristić<sup>1</sup>, I. Czakó-Nagy<sup>2</sup>, S. Musić<sup>1</sup>, and A. Vértes<sup>2</sup>

<sup>1</sup>Department of Materials Chemistry, Ruđer Bošković Institute, P.O. Box 180, HR-10002 Zagreb, Croatia

<sup>2</sup>Department of Nuclear Chemistry, Loránd Eötvös University, H-1518 Budapest, Hungary.

In the past chrysotile asbestos were extensively exploited for different applications in industry and civil engineering. However, at present the use of chrysotile asbestos is prohibited due to their high toxicity to humans. The researchers are searching for the methods of inactivation of chrysotile asbestos, for example by transforming them to glass state. In the present work we are focused to the investigation of chrysotile asbestos with <sup>57</sup>Fe Mössbauer and FT-IR spectroscopies and FE-SEM. Quantitative chemical analyses of all chrysotile asbestos investigated are given. The central part of Mössbauer spectra at RT showed the superposition of subspectra corresponding to Fe<sup>2+</sup> and Fe<sup>3+</sup> ions. It is suggested that Fe<sup>2+</sup> and Fe<sup>3+</sup> ions occupy only the octahedral positions in the chrysotile crystal structure. The ratio of Fe(II)/Fe(III) in chrysotile crystal structure can give an information about the reduction/oxidation conditions during the formation of chrysotile in the Earth's history. In all samples magnetite was found as associated mineral with varying stoichiometry (Fe<sub>3-x</sub>O<sub>4</sub>). FT-IR spectra of chrysotile asbestos from different regions will be also discussed. Morphology of chrysotile asbestos was inspected with FE-SEM.

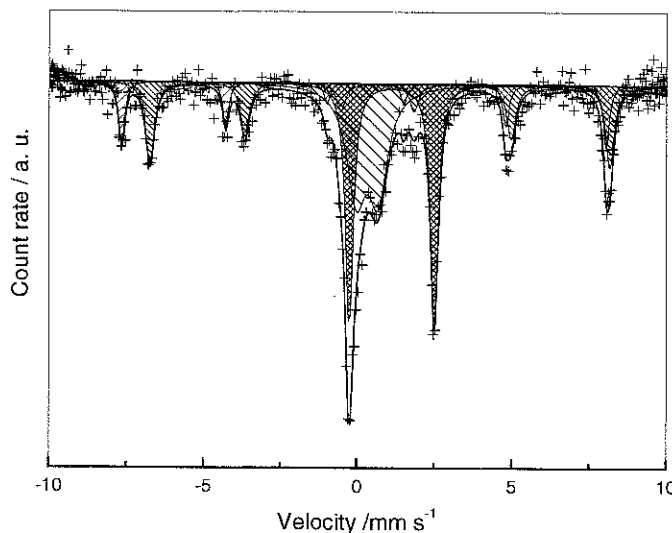


Figure 1. <sup>57</sup>Fe Mössbauer spectrum at RT of chrysotile from Canada (code: BC-110-4D).



## Microspectrophotometry in visible range as important part of the analysis of coloured forensic traces

J. Waś-Gubała<sup>1,2</sup>, J. Zieba-Palus<sup>1</sup>, B. Trzcńska<sup>1</sup>

<sup>1</sup> *Institute of Forensic Research, Westerplatte 9, 31-033 Krakow, Poland*

<sup>2</sup> *Jagiellonian University, Department of Analytical Chemistry, Ingardena 3, 30-060 Krakow, Poland*

Microspectrophotometry is applied in forensic laboratories in examination of such traces like single fibres, paint chips and inks. The microspectrophotometer, being coupling of an optical microscope and a spectrometer for the visible range, allows one to obtain spectra of the investigated samples and compare their colour and also to examine the morphology of very little objects. Moreover, it makes possible establishing of colour of the investigated samples by the assignment of its definite numerical value according to the CIELAB theory. In the paper advantages and disadvantages of the application of the method in colour comparison of forensic traces will be presented.

J&M TIDAS microspectrometer combined with a C. Zeiss Axioplan 2 microscope was used to perform measurements in both reflectance and transmittance mode in the spectral range 380-780 nm.

The analysis of colour similarities and differences for single fibres originating from the original blue, red and grey/black textiles (made of cotton, wool, acrylic and polyester) and the same textiles that undergone the influence of various, home laundry detergents solutions was performed [1]. It was observed that the most significant differences in fibre colour - regardless of the type of the detergent used - were achieved in the case of those of natural origin: wool and cotton. It was also found that the type of dye has an important impact on the observed changes.

The VIS microspectrophotometry method can be used with very good results to estimate similarity of colour of all examined samples. An attempt was made to identify main dyes in inks on the base of VIS spectra. The discriminating power of VIS microspectrophotometry use to be high, but the assessment of the chemical identity of dyes by micro-Raman spectroscopy or TLC is advisable.

The research was partially carried out with a financial support of the Polish Ministry of Science and Higher Education - project number O N204 115036.

[1] J. Waś-Gubała, E. Grzesiak, *Science and Justice* 50 (2010) 55-58.



## An investigation into the use of micro-Raman spectroscopy for the analysis of car paints and single textile fibres

J. Zięba-Palus<sup>1</sup>, J. Waś-Gubała<sup>1, 2</sup>

<sup>1</sup>*Institute of Forensic Research, Westerplatte 9, 31-033 Krakow, Poland*

<sup>2</sup>*Jagiellonian University, Department of Analytical Chemistry, Ingardena 3, 30-060 Krakow, Poland*

Forensic traces like small particles of unknown paint and single fibre need fast, non-destructive, selective and sensitive examination methods. Micro-Raman spectroscopy proved to be a promising technique in the area of forensic examination, where optical microscopy, micro-infrared spectroscopy and microspectrophotometry in the visible and UV range used to be applied for identification and differentiation between traces [1,2]. Often no dyes are detected using these methods because their content in a trace is usually too low. Modern industry fabricates huge number of dyes, their mixtures and pigments being suitable for colouring of textile products and paints, and by that reason dye composition is very characteristic feature of forensic traces.

The aim of this paper was to evaluate if micro-Raman spectroscopy can supply information about the dyes present in a micro paint chip and a single fibre. The study was conducted to determine the degree of discrimination between fibres coloured by definite chemical dye classes.

Raman spectra were measured by the use of an InVia spectrometer (Renishaw, USA) using three excitation lasers: 514, 633 and 785 nm. Thirty samples of green and blue car paint chips and thirty samples of multicoloured natural and synthetic fibres were examined.

It was found that the majority of the obtained Raman spectra provides information about the main dyes present in the sample (about 90% of paint spectra). However, in some cases fluorescence of the samples (dye or matrix) made the dye identification impossible. Spectral libraries for examined paint samples and single fibres has been created in order to quick recognize of similar forensic trace using this analytical method.

The research was financially supported by the Polish Ministry of Science and Higher Education – project number O N204 115036.

[1] J. Zięba-Palus, R. Borusiewicz, *J. Mol. Struct.* 792-793C (2006) 286-292.

[2] G. Massonnet et al., *J. Forensic Sci.* 50 (2005) 1028-38.



## Characterisation of paint samples by infrared and Raman spectroscopy for criminalistic purposes

J. Zięba-Palus<sup>1</sup>, A. Michalska<sup>1</sup>, A. Weselucha-Birczyńska<sup>2</sup>

<sup>1</sup>*Institute of Forensic Research, Westerplatte 9, 31-033 Krakow, Poland*

<sup>2</sup>*Jagiellonian University, Department of Chemistry, Ingardena 3, 30-060 Krakow, Poland*

Car paint as a physical evidence is probably one of the most commonly examined material in forensic laboratories. Chips of paint coat or paint smears are very often transferred to the clothing of victims of hit-and-run road accidents. The forensic examination of car paint samples includes establishing of their chemical content in order to compare samples collected from the road or the victim clothing and samples originated from the suspected car. Application of infrared spectrometry enables one to identify polymer binder, some of the main fillers and inorganic pigments. Raman spectroscopy [1,2] is often use to supplement these investigations providing information about organic pigments and dyes. The aim of this work was to evaluate the usefulness of microinfrared and microRaman spectrometry for characterisation of paint coating for criminalistic purposes and so their differentiation.

Fourty samples of multilayered paint chips were examined directly on their cross-section (layer by layer) by the use of both methods. For measurements the spectrometer FTS 40 Pro with UMA 500 (Difilab, USA) was used. Raman spectra were measured by the use of an InVia spectrometer (Renishaw, USA) using three excitation lasers: 514, 633 and 785 nm. The obtained spectra will be discussed in details.

It was found that application of FTIR and Raman spectroscopy proved to be a good tool for forensic identification of the samples and complemented each other. Because no sample preparation is required both methods provide an exelent means to rapidly screen reference panels for the presence of certain pigments.

The research was partially supported by the Polish Ministry of Science and Higher Education – project number O N204 115036.

[1] EM. Suzuki, M. Carrabba, J. Forensic Sci. 46 (2001) 1053-1069

[2] J. Zieba-Palus, R. Borusiewicz, J.Mol. Struct. 792-793 (2006) 286-292



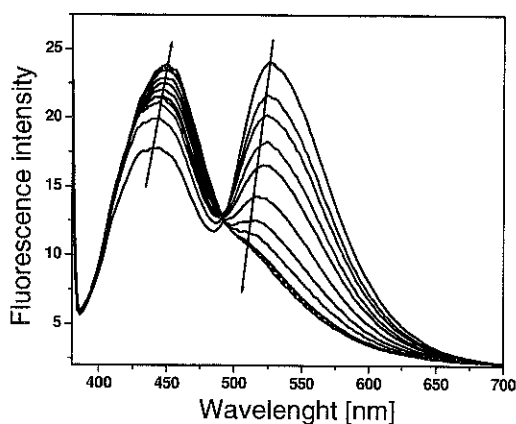
## Temperature and light-induced effects on milk monitorized by fluorescence spectroscopy

M. Iliut, M. Iosin, S. Astilean

*Babes-Bolyai University, Nanobiophotonics Laboratory, Institute for Interdisciplinary Experimental Research, Treboniu Laurian 42, 400271, Cluj-Napoca, Romania*

The understanding of the effects of various external factors, such as light and temperature variations, on dairy products is of outmost importance for food safety. In this context fluorescence spectroscopy is an ideal, rapid and non-destructive method, which provides valuable information on the chemical and physical properties, and induced structural changes of different food products. While the degree of photo-oxidation in food is indicated by the fluorescence emission of Riboflavin, the main photosensitizer in dairy products, the degradation of proteins is evidenced by tryptophan fluorescence [1].

In this work, we studied the effects of heat treatment (between 22 and 100 °C) and light exposure on milk, by monitoring the Riboflavin and Tryptophan fluorescence emission spectra.



Temperature dependences of fluorescence emission spectra of Riboflavin in milk. The arrows depict the variation of the corresponding band intensity with increasing temperature.

The results demonstrated that these external factors lead to the generation of lumichrome and lumiflavin (with characteristic fluorescence emission bands in the 440-480 nm spectral region), two photo breakdown products of Riboflavin (with characteristic fluorescence emission band at 530 nm), assessing the photo-oxidation of the milk. Moreover, the emission intensity of tryptophan residues in milk, occurring at 340 nm, was found to decrease with increasing heat treatment, demonstrating the effect of temperature on the native  $\beta$ -lactoglobulin content of milk.

Subsequently, due to its sensitivity to changes in local environment, we successfully used the fluorescence emission of Tryptophan as an indicator of protein conformation, and Riboflavin as an indicator for oxidation of milk. These results exhibit potential applicability in the monitorization of dairy products, with great importance in food safety.

Acknowledgment: This work was supported by The National University Research Council in the frame of the PN-II program (Project No. IDEI-477/2007).

[1] C.M. Andersen, *J. Agric. Food Chem.* 2008, 56, 720–729



## The origin of yellowness in Fischer Tropsch waxes studied by molecular spectroscopies.

L. Bonoldi, C. Flego, L. Montanari

*eni r&m – CR SDM – Via Maritano 26, 20097 S. Donato Milanese – Italy*

*e-mail: [luciano.montanari@eni.com](mailto:luciano.montanari@eni.com)*

Wax samples produced by Fischer-Tropsch reaction are usually white, but sometimes they appear coloured varying from yellow to hazel brown.

The origin of the colour was investigated by IR (InfraRed) and two electronic spectroscopies, UV-VIS (UltraViolet-Visible) absorption and fluorescence.

From IR analysis the formation of functional groups related to the presence of oxygenated species is monitored, together with that of other potential dyes, as nitro- or azo-group.

UV-VIS absorption spectra are characterized by intense signals in the 190-230 nm range, due to isolated double bond absorption, and in the 230-700 nm range, attributed to traces of unsaturated species at increasing conjugation.

The fluorescence spectra were acquired in synchronous scanning with a fixed wavelength difference ( $\Delta\lambda$ ) of 23 nm between excitation and emission. This synchronous technique offers several advantages, including narrowing of spectral bands, an enhancement in selectivity by spectral simplification. Moreover, in these samples only aromatic molecules can fluoresce and the wavelengths are shifted towards higher values in species with increasing number of fused rings. Fluorescence spectra show the occurrence of large core species (number of fused rings  $\geq 3-4$ ) present only in coloured samples.

These observations corroborate the hypothesis that the colour in waxes could be due to light absorption of extended aromatic species sometimes conjugated to carbonylic groups, that have absorption queues at  $\lambda > 400$  nm, yielding a yellowish colour.

Some colour values (X, Y, Z, W and YI) were determined by a handy colorimeter: XYZ express colours in colour stimulus values, W expresses “whiteness” and YI “Yellowness Index”.

Colour plots versus absorbance and emission intensities are shown revealing some correlations between colours and aromatic nature of species in the waxes.



## Determination of amino acids, fatty acids and selenium in fish plasma by mass spectrometry

A. Iordache<sup>1</sup>, E. Horj<sup>2</sup>, M. Culea<sup>2</sup>, O. Cozar<sup>2</sup>

<sup>1</sup>"National R&D Institute of Cryogenics and Isotopic Technologies – ICSI Rm. Valcea", 4 Uzinei St., 240050, Rm. Valcea, Romania

<sup>2</sup>Babes-Bolyai" University, I. M. Kogalniceanu St, 400084, Cluj-Napoca, Romania

Selenium is a very potent antioxidant protecting the body from damage due to oxidation by free radicals. It is used in fish food as Se-methionine supplements. An isotopic dilution gas chromatography - mass spectrometric (ID-GC/MS) techniques was used to evaluate effects in quantitative amino acids and fatty acids in fish plasma after Se addition in food in comparison with control. The stable isotope internal standard used was <sup>15</sup>N-methionine. A Trace DSQ ThermoFinnigan quadrupole mass spectrometer coupled with a Trace GC was used. Amino acids were separated on a Rtx-5MS capillary column, 30 m x 0.25 mm, 0.25µm film thickness, using a temperature program from 50°C, 1 min, 6°C/min at 100°C, 4°C/min at 200°C, 20°C/min at 300°C, (3min). The transfer line temperature was 250 °C, the injector temperature 200 °C and ion source temperature 250 °C; splitter: 10:1. Electron energy was 70eV and emission current, 100µA. The amino acids were purified on a Dowex 50W-W8 exchange resin and were derivatized in a procedure following two steps to obtain trifluoroacetyl butyl esters. The identification of amino acids was obtained by using NIST library but also by using amino acid standards [1]. Concentrations of majority of amino acids as methionine glutamic acid, aspartic acid, lysine, phenylalanine increased with Se supplementation

Eicosapentaenoic acid (EPA) and docosapentaenoic acid (DHA) are the major fatty acids found in fish. These fatty acids are produced by unicellular algae and phytoplankton which are consumed and then accumulate in fish. The fatty acids in fish plasma, after Se addition (0.03mg/kg) in food, in comparison with control were measured by using an extraction procedure, a derivatization method and separation in a temperature program. The extraction of the fatty acids was performed by mixing plasma and chloroform:methanol (2:1) during 30 seconds, at room temperature. Fatty acids were separated on a Rtx-5MS capillary column, 30 m x 0.25 mm, 0.25µm film thickness, using a suitable temperature program. The fatty acids were derivatized to obtain methyl esters. The identification of fatty acids was obtained by comparison of fatty acids methyl esters (FAME) mass spectra with the mass spectra of FAME kits and of NIST library [2]. Concentrations of majority of unsaturated fatty acids increased with Se supplementation.

An ICP-MS method was developed for measurements of Se in plasma samples. Application of the method for the comparison of control and carps following a Se-methionine diet is presented.

A marked increase in plasma free amino acids and fatty acids occurred at a dietary Se-methionine level of 0.03 mg/kg. Se was also increased in fish plasma samples fed with Se-methionine compared with control.

[1] M. Culea, A. Iordache, C. Mesaros, *Chemické listy Journal*, 102 (2008) s636-368.

[2] A. Iordache, R. Minea, M. Culea, C. Lehene, *Chemické listy Journal*, 102 (2008)s663-664.



## Spectroscopic Features of Radical Induced in Gamma Irradiated Gabapentin: an EPR Study

Ş. Osmanoğlu<sup>1</sup>, Y. Dicle<sup>2</sup>

<sup>1</sup>Faculty of Education, Siirt University, Siirt, Turkey

<sup>2</sup>Faculty of Education, Dicle University, Diyarbakir, Turkey

Using high energy ionising radiation both for sterilization of pharmaceuticals and medical device or for improvement of the hygienic quality of foods is now a well established technology. The aim of this study is to investigate the spectroscopic and kinetic features of the species having unpaired electrons induced gamma irradiated gabapentin at room and different temperatures in dose range 5-50 kGy using EPR spectroscopy. EPR measurements proved that gabapentin contained stable paramagnetic species after irradiation and relative yielding of free radicals depends on the absorbed dose radical species responsible from observed EPR lines are investigated at room and different temperatures. The Gabapentin drug present no EPR signals before irradiation, the irradiated gabapentin exhibited an EPR spectrum with double peak. The storage period of the gabapentin which it conserved its identity was determined. The limits of detection of free radicals after irradiation at 25kGy are 12 months for Gabapentin. This permitted to discriminate irradiated gabapentin from unirradiated one. Some spectroscopic properties and suggestions concerning possible structure of the radicals are discussed in this study.



## SVD-based method for intensity normalization, solvent subtraction and background correction of extensive Raman datasets

P. Mojzeš, J. Palacký, J. Bok

*Charles University in Prague, Faculty of Mathematics and Physics, Ke Karlovu 3, CZ-121 16, Prague 2, Czech Republic*

Introduction of multivariate statistical methods [1] in treatment of Raman spectra influenced experimental approaches, methodologies and requirements on specific parameters and quality of the spectral data. Instead of looking for and presenting obvious spectral differences between few selected Raman spectra taken under particular conditions, more complex and less apparent spectral changes can be discerned, studied and interpreted as a function of a particular physico-chemical parameter gradually varied over selected range. Laborious visual inspection and manual identification of spectral changes, completely unfeasible in the case of extensive Raman datasets, was replaced by routine analysis by multivariate statistical methods (SVD – singular value decomposition, FA - factor analysis, PCA – principal component analysis). However, besides the signal from the analyte, raw Raman spectra include also solvent contribution and non-Raman background, both often evolving with the parameters varied. In addition, absolute intensity of the Raman signal and the non-Raman background present in the real-world spectra can fluctuate in their own way, hindering proper use of multivariate methods for quantitative analysis. Hence, correct quantitative analysis of the analyte spectral changes requires preprocessing of raw Raman datasets, notably intensity normalization, subtraction of the solvent signal and correction for the non-Raman background.

A SVD-based semi-automated method combining intensity normalization with effective elimination of the solvent signal and non-Raman background is presented here for Raman spectra of biochemical and biological analytes in aqueous solutions. The method is particularly suitable for rapid and effortless preprocessing of extensive datasets taken as a function of gradually varied physico-chemical parameters (analyte and/or ligand concentration, temperature, pH, pressure, ionic strength, time evolution). For intensity normalization, Raman OH stretching bands of water in the range of 2700 - 3900  $\text{cm}^{-1}$  recorded together with the analyte spectrum in the fingerprint region below 1800  $\text{cm}^{-1}$ , are employed as internal intensity standard. Concomitant dependences of the solvent spectra are taken into account and, in some cases, turned into advantage. Once Raman spectra of the solvent are acquired for a particular range of parameters varied, it is possible to subtract correctly its contribution from any analyte spectrum taken under the same conditions within this range. The procedure presented here can be efficiently applicable only for the analytes having own Raman signal in the range of OH stretching vibrations much weaker than that of the solvent. However, this is the case for great number of biochemical and biological samples. Accuracy, reliability and robustness of the method was tested for non-absorbing and absorbing analytes under the conditions of spontaneous and resonance Raman scattering, respectively. Serviceability of the method will be demonstrated by several real-world examples including SERS studies on colloids.

[1] E. R. Malinowski, *Factor Analysis in Chemistry*, Wiley, New York 2002





## Baseline analysis: a simple FT-IR method for obtaining phase transition temperatures

B. Zimmermann, G. Baranović

Department of Organic Chemistry and Biochemistry, Ruđer Bošković Institute,  
Bijenička 54, 10002 Zagreb, Croatia, [bzimmer@irb.hr](mailto:bzimmer@irb.hr)

The baseline analysis designates an analysis of the absolute baseline variations obtained from the temperature-dependent transmittance mid-IR spectra at an arbitrarily chosen wavenumber assumed to be free of sample absorption (most often at around  $2000\text{ cm}^{-1}$ ). A simple plot showing transmittance (absorbance) at a given wavenumber versus temperature is found to be sufficient for obtaining phase transition temperatures. If some structural transformation is determined within the available temperature range, more thorough IR search for structural information can be made by applying two-dimensional correlation methods (2D-IR). The analysis is rapid, inexpensive and completely free of any personal bias. The method efficiency was corroborated by measuring various phase phenomena, including polymorphism (different ways of molecular packing in the solid state) and mesomorphism (liquid crystals) (Figure 1.), as well as chemical reactions [1].

The baseline analysis is of particular importance to pharmaceutical industry since the solid state of active pharmaceutical ingredient (API) can drastically alter the bioavailability of the drug. The wide-ranging potential of the baseline analysis for simple and reliable routine screening studies of API polymorphism is established on the model drug paracetamol.

An additional prospect of the method as an economical way of establishing critical temperature regions is demonstrated on determination of glass transition of polymers (polystyrene, polyvinyl chloride, poly(methyl methacrylate), polyethylene terephthalate and polycarbonate).

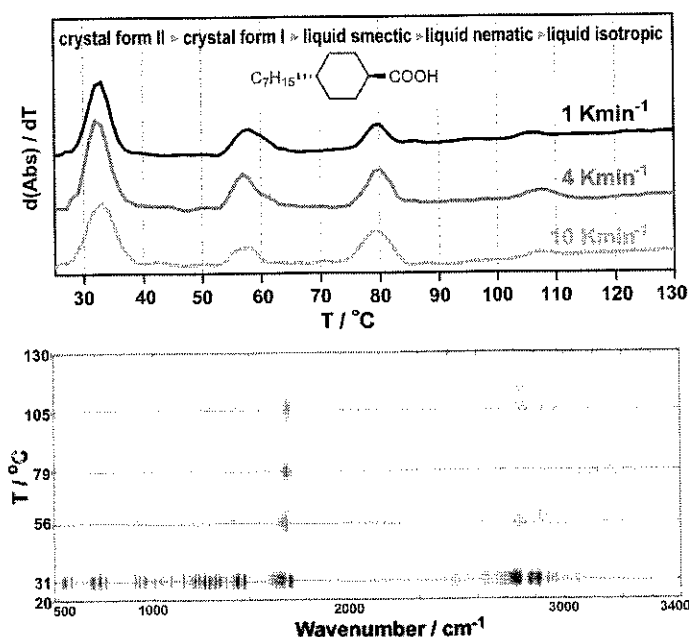


Figure 1. First derivatives of baseline variations and moving window 2D-IR correlation analysis of trans-4-heptylcyclohexanecarboxylic acid

[1] Zimmermann, B.; Baranović, G. *Appl. Spectrosc.*, 63 (2009) 1152-1161



## Optimization of the performances of a hybrid expert system designed for the elucidation of molecular structures

S. Gosay, M. Praisler

*Department of Physics, "Dunărea de Jos" University, 800201 Domneasca St., Galați, Romania,  
stelagosav@yahoo.com*

In this paper we are presenting an expert system built for the identification of small molecular structures by using a hybrid spectral database, formed by concatenating the GC-FTIR (gas chromatography-Fourier transform infrared spectrometry) and GC-MS (gas chromatography-mass spectrometry) spectra of three classes of compounds. The expert system was built using Artificial Neural Networks (ANN) and is dedicated to predict the class identity of the modeled compounds. The advantages and limitations of using a hybrid GC-FTIR - GC-MS spectral database are discussed by analyzing the performances of the expert system (IR-MS-ANN network) together with those obtained for the ANN systems built with homogenous databases (IR-ANN and MS-ANN networks) characterizing the same compounds, i.e a GC-FTIR – based expert system and a GC-MS – based expert system.

We are also applying two selection criteria, i.e. the importance and the sensitivity of the input variables (spectral concatenated database) in order to optimize the sample/variable ratio. The process of optimization also leads to an enhancement of the data-processing speed and improves the efficiency of the class identity assignment by eliminating the redundant information from the spectral concatenated database and maintaining into the system the spectral information needed to obtain a good modeling power. A spectroscopic analysis in order to evaluate the relevance of each type of input variable (absorption and abundance) is presented.

*Keywords:* GC-FTIR; GC-MS; Concatenated database, Amphetamines; Neural networks.



## Development of a spectrophotometric method to detect the amount of carbon monoxide in fraudulently treated beef meat

E. Droghetti<sup>1</sup>, C. Focardi<sup>2</sup>, M. Nocentini<sup>2</sup>, G. Smulevich<sup>1</sup>

<sup>1</sup> Dipartimento di Chimica "Ugo Schiff", Università di Firenze, Via della Lastruccia 3, I-50019, Sesto Fiorentino (FI), Italy

<sup>2</sup> Istituto Zooprofilattico Sperimentale delle Regioni Lazio e Toscana, Sezione di Firenze, Via di Castelpulci 41, I-50010 San Martino alla Palma (FI), Italy

In the United States and in the Netherlands meat products are commonly treated at industrial level with carbon monoxide (CO) [1]. However, CO-treatment is not admitted in the European Community. The aim of this work is to develop a rapid spectrophotometric method to establish the fraudulent treatment of meat with CO, since recently in Italy horse and beef meat have been found to be treated with CO [2,3].

CO forms with ferrous myoglobin (Mb) of the meat tissue a very stable complex, MbCO, that impairs a cherry-like colour to the meat. MbCO is more stable towards oxidation compared to MbO<sub>2</sub> (oxy-Mb) complex. The treatment with CO partially prevents the oxidation of oxy-Mb (Fe<sup>2+</sup>) to met-Mb (Fe<sup>3+</sup>). Therefore, it may mask spoilage, because the CO-complex can be stable beyond the microbiological shelf life of the meat and can mislead the consumer about the preservation state of the product.

Recently, we have developed a rapid spectrophotometric method to detect the presence of MbCO in CO-treated tuna fish [4]. This procedure is based on the combined analysis of electronic absorption spectra (UV-Vis) in their normal and second derivative modes. The different forms of Mb can be distinguished by their peak wavelengths and relative intensities, since the wavelength maxima vary according to the oxidation, spin, and coordination states of the heme iron.

The present proposed method allows us the quantitative determination of CO in the meat drip of beef. It consists of: i) preparations of CO standard solutions titrated against horse heart Mb primary standard solutions; ii) determination of calibration curves to measure CO concentration in treated and untreated samples.

The calibration curves will be presented together with the results obtained on different treated and untreated samples of meat drip of beef.

[1] L. Martínez, D. Djenane, I. Cilla, J. A. Beltrán, P. Roncalés, *Meat Sci.*, 71 (2005) 563-570

[2] S. Soncin, L.M. Chiesa, L. Sironi, M. Caligara, I. Angeli, P. A. Biondi, C. Cantoni, *Boll. Chim. Igien.* 55 (2004) 251-253

[3] M. Squarzoni, S. Limbo, L. Piergiovanni, *Industrie Alimentari* 43(436) (2004) 503-508

[4] G. Smulevich, E. Droghetti, C. Focardi, M. Coletta, C. Ciaccio, M. Nocentini, *Food Chem.*, 101(3) (2007) 1071-1077



## Characterization of archaeological pottery: the case of "Ionic Cups"

F. Longo<sup>1</sup>, G. Barone<sup>2</sup>, V. Crupi<sup>1</sup>, D. Majolino<sup>1</sup>, P. Mazzoleni<sup>2</sup>, V. Venuti<sup>1</sup>

<sup>1</sup>*Department of Physics, University of Messina, C.da Papardo, S.ta Sperone 31, 98166, Messina, Italia*

<sup>2</sup>*Department of Geological Science, University of Catania, Corso Italia 55, 95129, Catania, Italia*

The aim of this study is to establish a possible methodological protocol of joined employment of micro-destructive and non-destructive techniques for the microscopic and mesoscopic characterization of archaeological pottery findings addressed to the identification of the production sites and firing techniques of ceramic objects [1, 2].

Here, we report a study performed on "Ionic Cups", coming from different archaeological sites in eastern Sicily. These cups represent a ceramic typology widely diffused in the Mediterranean Area in archaic age (VI-V century b. C.). The identification of the production sites of these materials, originally manufactured in Greek-Eastern Area and then largely diffused in the West, is still an open question. The employment of various techniques allowed us a description of bulk properties of these findings in terms of a hierarchy of structures of growing size, going from the elements, to the mineral phases, the aggregates and the texture pattern.

In particular, X-Ray Fluorescence (XRF), using a portable energy-dispersive XRF analyser, allowed us to collect major and minor elemental constituents. The microscopic structural characterization was obtained by X-Ray Diffraction (XRD) and Infrared Fourier transform absorption (FT-IR) measurements, which permitted us to determine the mineralogical phases present in the artefacts. Small Angle Neutron Scattering (SANS) measurements permitted the characterization of the size distribution and surface characteristics of the mesoscopic aggregates formed by the minerals. Finally, coulometric measurements of the humidity amount within the pottery findings were performed to select a proper procedure for conservation and/or restoration and to better interpret the spectroscopic data in the peculiar region of water.

[1] D. Barilaro, V. Crupi, S. Interdonato, F. Longo, G. Maisano, D. Majolino, V. Venuti, G. Barone, P. Mazzoleni, G. Tigano, S. Imberti, W. Kockelmann, *Nuovo Cimento C* 31 (2008) 371-388

[2] G. Barone, V. Crupi, D. Majolino, P. Mazzoleni, J. Teixeira, V. Venuti, *J. Appl. Phys.* 106 (2009) 054904



## FTIR spectroscopic analysis to study the firing processes of prehistoric ceramics

V. Venuti<sup>1</sup>, G. Barone<sup>2</sup>, V. Crupi<sup>1</sup>, F. Longo<sup>1</sup>, D. Majolino<sup>1</sup>, P. Mazzoleni<sup>2</sup>, D. Tanasi<sup>3</sup>

<sup>1</sup>*Department of Physics, University of Messina, C.da Papardo, S.ta Sperone 31, 98166, Messina, Italy*

<sup>2</sup>*Department of Geological Science, University of Catania, Corso Italia 55, 95129, Catania, Italy*

<sup>3</sup>*Department of Antropological, Archaeological and Historical-Territorial Science, University of Turin, Via G. Giolitti 21/E, 10123 Turin, Italy*

In this work, we present a spectroscopic study on prehistoric ceramics with the aim of characterizing the phase transformations that occur during the cooking processes, through an FTIR absorbance investigation. It is well known, in fact, that in the firing of clayey sediments reactions, the formations of new phases and the reorganisation of the structure frequently occur without reaching the thermodynamic equilibrium. The formation of new-formed minerals depends on the firing temperature and the composition of the raw material. Therefore, the identification of these phases permits to evaluate the technological knowledge of the primitive populations. The measurements were performed on several potteries of the Middle Bronze Age excavated in the Catania hinterland (Sicily, South Italy). The samples are either coarse and fine but all heterogeneous in the structure and composition [1]. The analysis were carried out through two different sampling preparation methodologies: i) on pellets of powder dispersed in CsI; ii) on powder and on pottery chips.

Furthermore, on some selected specimens, we also performed FTIR measurements by a micro-sampling. This protocol showed the change of mineralogical composition on sub-millimetre scale. The results were compared with the data obtained by means of X-ray diffraction (XRD) and with the qualitative observations of the optical activity of the groundmass by optical microscopy. The whole set of the data showed a firing temperature in the range 800-900°C. The simultaneous presence of calcite and clayey minerals and of new-formed Ca-silicates could be indicative of an inhomogeneous distribution of the temperature on the pottery during the firing process and/or a strong heterogeneity of the paste as suggested also by other authors.

[1] G. Barone, P. Mazzoleni, A. Patanè, D. Tanasi. "Petrographic and geochemical analyse on pre-historical ceramics of the Middle Bronze Age (XV-XIII century B.C.)". AIAR Conference 2010 (Pavia, Italy).



## Vibrational study on the modifications induced by chemical and grafting agents in silk and wool fibres

P. Taddei<sup>1</sup>, G. Freddi<sup>2</sup>, M. Tsukada<sup>3</sup>

<sup>1</sup>Dipartimento di Biochimica "G. Moruzzi", Sez. di Chimica e Prop. Biochimica, Via Belmeloro 8/2, University of Bologna, 40126 Bologna, Italy

<sup>2</sup>Stazione Sperimentale per la Seta, Via G. Colombo 83, 20133 Milano 20133, Italy

<sup>3</sup>Division of Applied Biology, Faculty of Textile Science and Technology, Shinshu University, 3-15-1, Tokida, Ueda, Nagano 386-8567, Japan

Wool keratin and silk fibroin are excellent biopolymers with outstanding properties that make them extremely valuable for biomedical and biotechnological applications. As proteins, fibroin and wool can be chemically modified at side chain groups of constituent amino acids, thus improving their properties according to the desired function.

Among the chemical modifications techniques, graft copolymerization of vinyl monomers onto silk fibres has been considered a powerful method to substantially improve some intrinsic fibre properties. Grafted fibres represent an interesting model for studying the possible structural changes induced by grafting and the interactions between the fibre matrix and the grafted polymer chains.

On the other hand, the reaction of selected chemical agents with fibres is a particularly attractive system that can be used to obtain effective and specific modifications of the fibrous substrate. Significant changes in the physical and chemical properties of the fibres can be obtained, avoiding some of the drawbacks that arise from graft-copolymerization of vinyl monomers and from the loading of the fibre with large amounts of polymer, which is often needed to obtain the desired effects.

In the present study, IR and Raman spectroscopy has been used to comparatively analyse the reactivity of vinyl monomers (styrene, methacrylamide) and anhydrides (succinic and glutaric anhydrides) towards *Bombyx mori* and *Antheraea pernyi* silk fibroin, and wool.

Several spectroscopic ratios were identified as markers of the extent of grafting/chemical modification, due to their rough proportionality to the fibre weight gain.

Vibrational techniques have been widely recognized as valid tools for studying the secondary structure of polypeptides and proteins. The positions and relative intensities of the Amide I, II and III modes were evaluated to probe the possible occurrence of conformational rearrangements upon reaction.

In wool, the Raman  $\nu_{SS}$  stretching region was investigated to gain insight into the conformational changes of the  $C_{\alpha}C_{\beta}$ -S-S- $C_{\beta}C_{\alpha}$  system. In silk fibroin the  $I_{850}/I_{830}$  Raman intensity ratio between the two Tyr bands at 850-830  $\text{cm}^{-1}$  gave information on Tyr environment.

Vibrational spectroscopy proved suitable for evaluating the reactivity of the analysed fibres towards the different agents; the observed differences can be explained in terms of the different composition of the fibres and accessibility of the amino acids potentially involvable in the reactions.



## Spectroscopic techniques applied to the study of Roman atramenta

L. Brambilla<sup>1</sup>, P. Baraldi<sup>2</sup>, L. Toniolo<sup>1</sup>, M.C. Gamberini<sup>3</sup>, S. Goidanich<sup>1</sup>, C. Baraldi<sup>3</sup>

<sup>1</sup> Dipartimento di Chimica, Politecnico di Milano, via Mancinelli, 7, 20131 Milano

<sup>2</sup> Dipartimento di Scienze Farmaceutiche, Università di Modena e Reggio Emilia, via G. Campi, 183, 41115 Modena

<sup>3</sup> Dipartimento di Chimica, Università di Modena e Reggio Emilia, via G. Campi, 183, 41115 Modena

Many vessels from the archaeological sites of Pompeii and Herculaneum have been sampled and analysed by means of microRaman and FT-IR spectroscopy. The aim of the study was to identify the survived materials and those possibly coming from the original ones; then to trace their technology of preparation, and to verify the function and uses of the products. The powdered black samples were collected inside the vessel (sometimes, but not always, classified as atramentaria) where they were preserved. After the analyses a comparison was made with known literature data and some considerations carried out for the understanding of the whole data.

The analyses showed that samples are complex mixtures of inorganic nature, made of gypsum, silicates, and other minor compounds. Only traces of organic substances were found. Carbon black was frequently identified as the main component, while no traces of iron gall ink were found. It was concluded that the materials were inks. Metal residues, mainly bronze, and copper minerals such as malachite and azurite, were found in several samples. Other compounds can be considered as part of their technology or due to degradation products. A comparison with known sources is made.

It is not always clear whether they were intentionally added to the mixture or not; this issue will be carefully examined. In some other cases the black powder could have been eyeliners.

The research was carried out with a financial support of the Italian Ministry, Project PRIN 2007 "CiBA" coordinated by M.P. Colombini (University of Pisa).



## Infrared and Raman spectra of minerals from *ab initio* molecular dynamics simulations

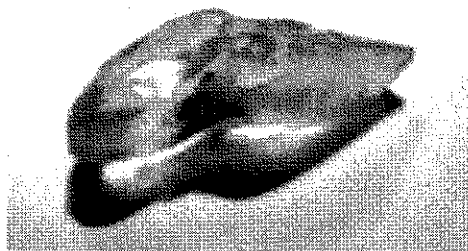
M. Pagliai<sup>1</sup>, M. Muniz-Miranda<sup>1,2</sup>, G. Cardini<sup>1,2</sup>, V. Schettino<sup>1,2</sup>

<sup>1</sup>Dipartimento di Chimica, Università di Firenze, Via della Lastruccia 3, 50019, Sesto Fiorentino, Italy

<sup>2</sup>European Laboratory for Non-Linear Spectroscopy (LENS), Via Nello Carrara 1, 50019, Sesto Fiorentino, Italy

Spodumene is a member of pyroxenes group of minerals with chemical formula  $\text{LiAlSi}_2\text{O}_6$ , that at the ordinary condition of temperature and pressure presents a monoclinic crystal structure. A phase transition occurs increasing the pressure at  $\sim 3.2$  Gpa, accompanied by a symmetry reduction from the  $C2/c$  to  $P2_1/c$  space group, with a consequent change in the spectral features. The phase transition can be monitored by Raman spectroscopy with diamond anvil cell experiments [1].

In order to obtain a detailed description of the mechanism related to the atomic rearrangement due to the phase transition, *ab initio* molecular dynamics simulations with the Car-Parrinello method have been performed. These simulations allow to describe the structural and spectroscopic properties of minerals at the same thermodynamic conditions adopted during the experimental measurement and to calculate accurate anharmonic Raman and infrared spectra [2]. The generalization of the algorithm to compute the polarizability tensor and the polarization to crystals of arbitrary shape allows to interpret the experimental infrared and Raman spectra of minerals and represents a valuable help in their complete characterization.



*A crystal of spodumene*

[1] C. J. S. Pommier, M. B. Denton, R. T. Downs, J. Raman Spectrosc. 34 (2003) 769-775

[2] M. Pagliai, C. Cavazzoni, G. Cardini, G. Erbacci, M. Parrinello, V. Schettino, J. Chem. Phys. 128 (2008) 224514



## Characterization of human cells exposed to deltamethrin by means of Raman microspectroscopy and Atomic Force Microscopy

G. Perna<sup>1</sup>, M. Lasalvia<sup>2</sup>, P. D'Antonio<sup>1</sup>, G. Quartucci<sup>1</sup>, N. L'Abbate<sup>2</sup>, V. Capozzi<sup>1</sup>

<sup>1</sup> *Dipartimento di Scienze Biomediche, Università di Foggia, Viale Pinto, I-71100 Foggia*

<sup>2</sup> *Dipartimento di Scienze Mediche e del Lavoro, Università di Foggia, Viale Pinto, I-71100 Foggia*

Raman microspectroscopy and Atomic Force Microscopy (AFM) have been used to detect biochemical and structural damages in cultured human cells as a consequence of deltamethrin exposure. Deltamethrin is a pyrethroid compound widely used for synthesizing pesticide products for agriculture and household environment disinfection. Although deltamethrin is very effective in damaging the central nervous system of pests, it presents lower poisoning risks in humans with respect to other pesticide compounds, as organophosphates and carbamates. Since of widespread employment of deltamethrin, the study of the effects of exposure, at the concentration provided for the utilization and lowers as well, is important for the safety of those people employed in the manufacturing and utilization activities and consumers. In particular, investigation of exposed cultured cells are essential to evaluate the eventual biochemical modifications caused by the pesticide at cellular level.

Cultured human keratinocyte cells have been exposed at increasing concentrations of deltamethrin from  $10^{-3}$  M to  $10^{-6}$  M for 24 h. A viability test, performed by means of the Trypan blue assay, indicated that exposure at  $2.5 \cdot 10^{-4}$  M of deltamethrin for 24 h can be considered a cytotoxic dose. The compared analysis of Raman microspectroscopy spectra and AFM images allows to state that a strong damage occurs in the plasmatic membrane and it is already detectable after exposure of keratinocytes at the lowest investigated deltamethrin concentration ( $10^{-6}$  M). The most important modifications are related to the breakdown of lipidic chains and to the structure of single aminoacids, whereas proteineous linkages between aminoacids are less involved in the deltamethrin action. In addition, the structure of nucleic acids is damaged as well. On the whole, cellular damage starts after exposure to deltamethrin doses well below that established as cytotoxic.



## Optical Frequency Comb as the calibration source for the GIANO spectrograph.

G. Schettino<sup>1,2</sup>, P. Cancio Pastor<sup>3,4</sup>, C. Baffa<sup>2</sup>, E. Giani<sup>2</sup>, M. Inguscio<sup>1,4</sup>, E. Oliva<sup>2</sup>, A. Tozzi<sup>2</sup>

<sup>1</sup> Dipartimento di Fisica e Astronomia, Via Sansone 1, 50019 Sesto Fiorentino (Fi), Italy

<sup>2</sup> INAF-Osservatorio Astrofisico di Arcetri, Largo Fermi 5, 50125 Firenze, Italy

<sup>3</sup> Istituto nazionale di Ottica-CNR, Largo Fermi 6, 50125 Firenze, Italy

<sup>4</sup> European Laboratory for Non-linear Spectroscopy, Via Carrara 1, 50019 Sesto Fiorentino (Fi), Italy

GIANO is a cross-dispersed echelle spectrograph designed to achieve a high spectral resolution (up to 50000 Resolving Power) in most the full near-IR spectral range (0.9-2.5  $\mu\text{m}$ ) and to maintain long-term stability. One of the GIANO's main goals is the detection of extra-solar rocky planets in Earth-like systems. To this end, a velocity sensitivity less than 1 m/s is required and hence an equally capable calibration source is necessary. The ideal source might consist of a spectrum of uniformly spaced and of almost equal strength lines. They must be unresolved by the astronomical spectrograph and their spectral linewidth has to be narrower than the spectrometer resolution. Moreover, their frequencies must be well known and stable over long time scales. The Optical Frequency Comb (OFC) source fits all these requirements but one, the desired comb spacing.

In the case of GIANO, considering the highest Resolving Power obtainable with the spectrograph, the optimal line spacing for the calibration spectrum lies around 18 GHz, while typical values of near-IR OFC repetition rates ( $f_r$ ) are 100-250 MHz. For our experimental set-up we use an Er-doped fiber laser comb with  $f_r=100$  MHz, so we need to filter out unwanted modes to obtain a 18 GHz line spacing. This could be done using one or more Fabry-Perot (F-P) cavities in series. We decided to use two F-P cavities, the first to filter up to 1.5 GHz, the second to obtain a final 15 GHz spacing.

Fabry-Perot optical filtering in a large spectral range (1-2  $\mu\text{m}$ ) is challenging due to the cavity mirrors dispersion. Our solution has been to work in a limited spectral range, from 1500 nm to 1650 nm. So to obtain the calibration spectrum to be sent to the spectrograph, we plan to broaden successively the already filtered spectrum from 1000 nm to 2000 nm by using a non linear fiber.



## Spectroscopic and chemical characterization of cavansite and pentagonite from Wagholi, Poonah district, Maharashtra state, India.

M. Sitarz<sup>1</sup>, M. Łodziński<sup>2</sup>, M. Kozanecki<sup>3</sup>

<sup>1</sup> AGH University of Science and Technology, Faculty of Materials Science and Ceramics, al. Mickiewicza 30, 30-059 Kraków, Poland

<sup>2</sup> AGH University of Science and Technology, Faculty of Geology, Geophysics and Environment Protection, Dept. General Geology, Environment Protection and Geotourism, al. Mickiewicza 30, 30-059 Kraków, Poland

<sup>3</sup> Technical University of Lodz, Department of Molecular Physics, Zeromskiego street 116, 90-924 Lodz, Poland

Cavansite and pentagonite are two minerals, which belong to Vanadium phyllosilicates. They form dimorphic series [1-3] with identical and nearly stable chemical composition. Their chemical formula is  $\text{Ca}(\text{VO})\text{Si}_4\text{O}_{10} \cdot 4\text{H}_2\text{O}$ . Light blue color and prismatic or spherulitic rosettes are typical for both of them. All optical and physical properties are very similar. It is a hard to discern these minerals by observation under microscope in polarized light and using electron microprobe. But spectroscopic (infrared and microRaman) characterization allow identifying such phases.

Hand specimens were found in Wagholi quarry, Pune District (Poonah District), Maharashtra State, India [4,5]. They occur in volcanic rocks (basalts) and volcano-sedimentary rocks (tuffs), which belong to the so called Deccan Traps. Both cavansite and less common pentagonite crystallized as ones of the latest phases in basalts during hydrothermal stage. Origin of studied minerals is connected with thermal alternation of basalts. They fill empty fractures and geodes together with different zeolite minerals and sometimes with quartz.

Samples were studied using scanning electron microscope with back-scattered electron mode. Content of main elements in studied samples is on average from 12.20 to 12.50 wt% CaO, from 53.20 to 54.50 wt%  $\text{SiO}_2$  and is stable from core to rims of prismatic crystals. But in some parts of cavansite is visible low differentiation of V and Ca. Vanadium content decrease from core to border of prisms from 20.20 to 18.50 wt%  $\text{V}_2\text{O}_5$  and Ca content subtle increase.

Infrared and Raman spectra were registered for cavansite and pentagonite. Precise assignation of bands to the corresponding vibration type was done. Infrared spectra differ distinctly between both phases, mostly in a range between  $3700\text{-}3200\text{ cm}^{-1}$ ,  $1700\text{-}1550\text{ cm}^{-1}$  and  $1400\text{-}1250\text{ cm}^{-1}$ , what is connected with various crystal structure. Point group of cavansite is  $2/m\ 2/m\ 2/m$  and pentagonite is  $mm2$ . Spectroscopic methods are very useful, easy and non-destructive to determine macroscopically and chemically similar cavansite form pentagonite.

**Acknowledgement:** The following research was supported by the AGH University of Science and Technology grant No. DS 11.11.140.447.

[1] Evans, H.T., Jr. *Amer. Mineral.*, 58 (1973) 412

[2] Staples, L.W., Evans, H.T., Lindsay, J.R. *American Mineralogist*, 58 (1973) 405

[3] Ishida, N., Kimata, M., Nishida, N., Hatta, T., Shimizu, M., Akasaka, T. *J. Mineral. Petrol. Sc.*, 104 (2009) 241

[4] Makki, M.F., *The Mineralogical Record*, 36 (2005) 507

[5] Praszkiel, T., *Mineralien-Welt* 20 (2009) 16



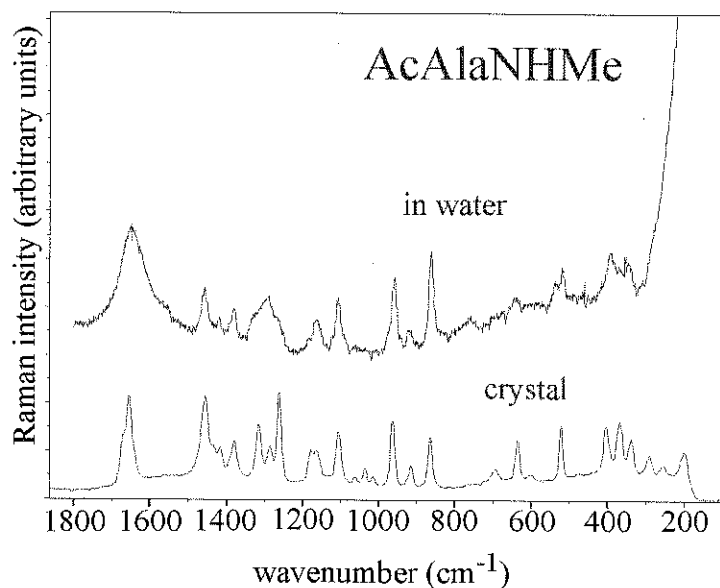
## Preferred conformations of dipeptides: crystals vs. solutions

V. Mohaček Grošev<sup>1</sup>, J. Grdadolnik<sup>2</sup>

<sup>1</sup>Ruder Bošković Institute, Bijenička 54, POB 180, 10002 Zagreb, Croatia,

<sup>2</sup>National Institute of Chemistry, Hajdrihova 19, 1000 Ljubljana, Slovenia

Dipeptides in the form of N-acetyl-aminoacid-NH-methyl have been used as model systems for inspection of the preferred conformations of the  $\Phi$  and  $\Psi$  torsional angles [1]. Often, there exist several conformers in water solution, and the task of determination of their relative populations was undertaken by NMR, infrared spectroscopy, and more recently by Raman spectroscopy [2]. To facilitate the assignment of bands in solution, we have performed vibrational analysis of N-acetyl-X-N'-Methylamide (X = Ala, Val, Leu, His, Tyr) in polycrystalline state and compared the most important bands in the fingerprint region with those of solution. Three bands falling between 1200 and 1300  $\text{cm}^{-1}$  were calculated for different conformers of AcAlaNHMe as combinations of  $\delta(\text{C}_\alpha\text{-H})$ ,  $\delta(\text{N-H})$  and  $\nu(\text{C-N})$  internal coordinates [3]. Their positions and intensities vary with conformation and make this interval particularly sensitive to  $\Phi$  and  $\Psi$  torsional angles. However, the three bands that appear in the Raman spectrum of AcAlaNHMe crystal are well resolved. In order to assess the effects of intermolecular hydrogen bonding which cause further shifting of  $\delta(\text{N-H})$  in particular, crystal structures of these powders are indispensable.



- [1] F. Avbelj, S. Golič Grdadolnik, J. Grdadolnik, L. R. Baldwin, Proc. Natl. Acad. Sci. U.S.A. 103 (2006) 1272-1277
- [2] T. Takekiyo, T. Imai, M. Kato, Y. Taniguchi, Biopolymers 73 (2004) 283-290
- [3] Z. Deng, P. L. Polavarapu, S. J. Ford, L. Hecht, L. D. Barron, C. S. Ewig, K. Jalkanen, J. Phys. Chem. 100 (1996) 2025-2034



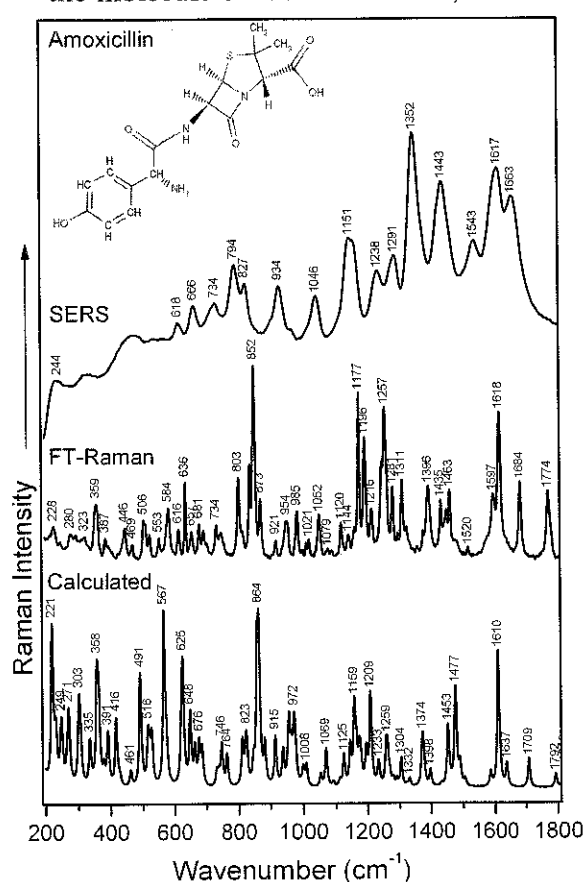
## IR, Raman, SERS and DFT study of amoxicillin

A. Bebu, L. Szabó, N. Leopold, C. Berindean, V. Chiş, L. David

Faculty of Physics, Babeş-Bolyai University Kogălniceanu 1, 400084 Cluj-Napoca, Romania

Amoxicillin is a moderate-spectrum, bacteriolytic,  $\beta$ -lactam antibiotic used to treat bacterial infections caused by susceptible microorganisms. It acts by inhibiting the synthesis of bacterial cell wall. It inhibits cross-linkage between the linear peptidoglycan polymer chains that make up a major component of the cell walls of both Gram-positive and Gram-negative bacteria.

The molecular vibrations of amoxicillin were investigated by FT-IR, FT-Raman and SERS spectroscopies. In parallel, quantum chemical calculations based on density functional theory (DFT) are used to determine the geometrical, energetic and vibrational characteristics of the molecule with particular emphasis put on the interaction and adsorption geometry of the molecule on a silver colloid, at different pH values [1].



The inserted figure shows the experimental and simulated Raman spectra and of the investigated compound. SERS spectrum of amoxicillin was also recorded using a 532 nm laser line and hydroxylamine reduced silver colloid as SERS substrate.

IR and Raman spectra of amoxicillin were assigned based on DFT calculations with the hybrid B3LYP exchange-correlation functional, coupled with the standard 6-31G(d) basis set. The calculated molecular electrostatic potential was used in conjunction with SERS data to predict the adsorption geometry of the molecule on Ag colloid. As seen in the figure, the shifting of the most SERS bands is accompanied by an important change in their relative intensities.

The stretching vibration of the C=O group connecting the hydroxyphenyl ring with the beta-lactam and thiazolidine rings at  $1684\text{ cm}^{-1}$  in the FT-Raman spectrum, appears shifted and enhanced at  $1663\text{ cm}^{-1}$  in the SERS spectrum, most probably, due to the interaction of the oxygen with the silver surface. In contrast, the C=O stretching vibration of the carboxyl group, as well as of the carbonyl group of the four membered ring, both shown at  $1774\text{ cm}^{-1}$  in the FT-Raman spectrum, are absent in the SERS spectrum, being thus not involved in the adsorption to the silver surface.

[1] A. Pîrnău, V. Chiş, O. Oniga, N. Leopold, L. Szabo, M. Baias, O. Cozar, *Vib. Spectrosc.*, 48 (2008) 289–296



## Highly resolved morphological analysis of renal stones found in mammals using infrared spectroscopical imaging technique

M. Pučetaitė<sup>1</sup>, V. Hendrixson<sup>2</sup>, A. Želvys<sup>3</sup>, F. Jankevičius<sup>3</sup>, J. Čeponkus<sup>1</sup> and V. Šablinskas<sup>1</sup>

<sup>1</sup>Faculty of Physics, Vilnius University, Saulėtekio av. 9, 10222, Vilnius, Lithuania

<sup>2</sup>Faculty of Medicine, Vilnius University, M.K. Čiurlionio str. 21, 03101, Vilnius, Lithuania

<sup>3</sup>Vilnius University Hosp. Santariskių klinikos, Vilnius University, Santariškių str. 2, 08661, Vilnius, Lithuania

The composition and structure of renal stones is complex and depend on a variety of factors which include diet, sex, environment, metabolism, etc. The identification of the components and structure of the stone enables to find out the underlying cause of the disease, prescribe treatment and prevent recurrences.

The qualitative and quantitative analysis of urinary calculi is challenging because of their usually small size, fragility, heterogeneous composition. Fourier transform infrared spectroscopy (FTIR) is easy and rapid method to obtain quantitative and qualitative information about chemical composition of the stones even from small amount of the substance. Microspectroscopic surface reflectance imaging is an informative method for analyzing morphology of the cross-sectioned stones [1]. The imaging is performed in specularly reflected infrared light. Specular reflection exhibits absorptions resembling the first-derivative of a conventional absorption spectrum. Intensity of these *reststrahlen* bands is proportional to concentration of particular chemical constituent of the stones. Scanning the infrared beam along the surface of cross-sectioned stone allows to obtain the information about its composition and the distribution of the components in it.

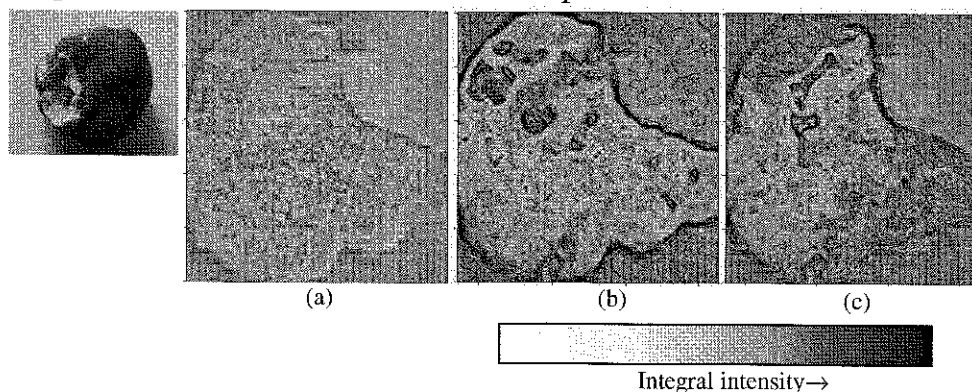


**Fig.** Optical (a) and false-color infrared images of the stone constituted from calcium oxalate (b) and brushite (c). Integral intensities of  $\nu_{as}(\text{C-O})$  band at  $1318\text{ cm}^{-1}$  for calcium oxalate and  $\nu_{as}(\text{P=O})$  at  $1120\text{ cm}^{-1}$  for brushite are used for the false-color images. Dark grey color represents areas with high concentration of the chemical component and light grey color – areas with low concentration or absence of the corresponding component.

In this work for the first time we have found that there are two types of mixed calcium oxalate and calcium phosphate stones. The stones of the first type do not have any domain structure, while the stones of the second type have one domain of calcium phosphate located close to the edge of the stone surrounded by calcium oxalate (Fig.). This finding brings us to conclusion, that the stones with calcium oxalate as a main component can be formed in two ways: (I) loose calcium oxalate stone grows in urinary system from oversaturated salt solution without fixation to the walls of the system; (II) calcium oxalate stone, which was initiated on the walls. In this case the grow starts from formation of calcium phosphate crystal on the wall of the system. Later this crystal is covered by calcium oxalate.

[1] J.C.Anderson et al, Analysis of urinary calculi using an infrared microspectroscopic surface reflectance imaging technique, *Urol. Res.* 35 (2007) 41-48

## Effects of radical stress on sulfur-containing proteins: desulfurisation reactions associated with the formation of trans lipids in model membrane

A. Torreggiani, Z. Jurasekova, C. Ferreri, C. Chatgililoglu

ISOF-CNR, P. Gobetti 101, 4012 Bologna, Italy

Effects of radical stress in the biological environment is a very active field of research connecting various disciplines in life science. Exposure of proteins to free radicals may cause structural and functional changes. In particular, a single radical event that leads to an initial damage involving sulfur-containing amino acid residues could produce a reactive species able to damage another cell compartment such as lipid domains. In this context, damages to some sulfur-containing proteins (i.e. ribonuclease, metallothioneines, human serum albumin, substance P) were considered to elucidate the effects of radical stress exposure on the overall protein structure. Experiments were carried out in both aqueous solutions and vesicle suspensions. Free radical generation, mimicking an endogenous radical stress, was obtained by gamma-irradiation of aqueous solutions. By changing the appropriate conditions of irradiation, a selection of the reacting radical species was carried out.

The protein degradation due to radical exposure was evaluated by Raman spectroscopy [1]. In fact, Raman spectrum can provide valuable information on both amino acid side chains (i.e. S-S, Tyr, Trp, Cys-Metal) and conformational changes in the protein secondary structure. Protein structure and amino acid content resulted to play an important role in blocking the ready access of free radicals both to the sulfur-containing residues and the active site, so strongly affect both the radio-sensitivity of proteins.

Using a biomimetic model based on unsaturated lipid vesicle suspensions the occurrence of tandem protein/lipid damage was shown. In fact, protein degradation is accompanied by structural alteration of unsaturated lipids forming liposome vesicles, which changed the naturally occurring *cis* geometry to the *trans* configuration. In fact, the reactions of reductive reactive species with methionine residues and/or sulfur-containing ligands afford diffusible sulfur-centered radicals, which migrate from the aqueous phase to the lipid bilayer and act as isomerising species of the double bonds.

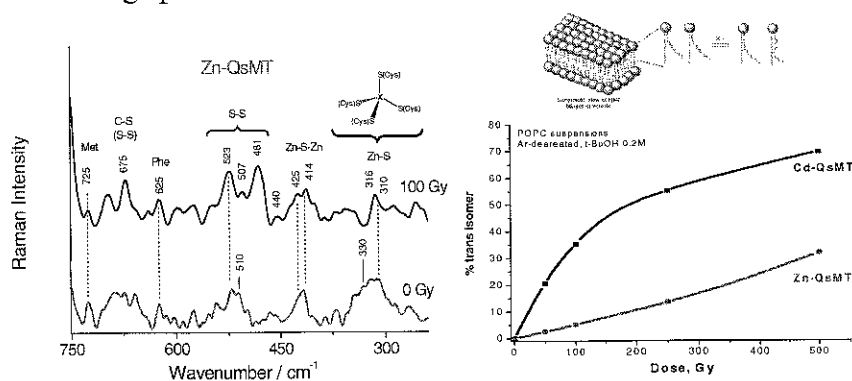


**Figure 1.** Raman spectra of a plant Zn-Metallothionein before and after irradiation (Left); formation of *trans* isomer from irradiation of POPC vesicles (Right).

[1] A. Torreggiani, J Domènech, R.Orihuela, C.Ferreri, S. Atrian, M. Capdevila, C. Chatgililoglu  
*Chem. Eur. J.* 15 (2009) 6015 – 6024.



## Formation of PPII helical conformation studied by Raman optical activity

V. Profant<sup>1</sup>, P. Bouř<sup>2</sup>, V. Baumruk<sup>1</sup>

<sup>1</sup>Charles University in Prague, Faculty of Mathematics and Physics, Institute of Physics, Ke Karlovu 5, 121 16 Prague, Czech Republic

<sup>2</sup>Academy of Sciences, Institute of Organic Chemistry and Biochemistry, Flemingovo nám. 2, 166 10, Prague, Czech Republic

Polyproline-II helical conformation (PPII) represents a less common protein secondary structure. Its structure is rather specific because there are no internal stabilizing hydrogen bonds in it. The rigidity of the helix is caused only by sterical reasons and the interaction with surrounding solvent molecules. Number of recently discovered evidence [1] has lead to a presupposition that the PPII helix is the main element of the random-coil protein structure. This information provides a new reason to study PPII conformation and specifically problematic of its formation, which has not been thoroughly studied yet.

In our experiment we measured Raman and Raman optical activity (ROA) spectra of several oligo- and poly-L-proline samples in a wide frequency range between 120 cm<sup>-1</sup> and 1800 cm<sup>-1</sup> and analyzed them with respect to the length of the proline chain. The relatively new technique of ROA [2,3], which is based on a different interaction of a specimen with the right- and left-handed circularly polarized laser light, represented an ideal methodology for this type of observation due to its high sensitivity to the conformational stability and rigidity of peptide chain backbone. There is also a strong link to previous experiments [4] which were focused on the characterization of proline side chain conformation and its interaction with solvent.

So far, we were able to determine the characteristic spectral peaks associated with formation of stable PPII helical conformation in studied systems. The most relevant peaks are located at 405, 535 and 945 cm<sup>-1</sup>. Moreover, based on our experimental data analysis we were able to determine the minimal length of (L-proline)<sub>N</sub> chain necessary for creation of the stable PPII conformation as N=6 [5].

The stress is laid on the interconnection between experimental and theoretical approach. For that purpose we perform *ab initio* calculations of ROA spectral bands and their intensities for all measured samples in order to obtain more accurate interpretation of recorded spectra and observed phenomena.

[1] Z. Shi, R. W. Woody, N. R. Kallenbach, Adv. Prot. Chem. 62 (2002) 163-240

[2] P. W. Atkins, L. D. Barron, Mol. Phys. 16 (1969) 453-466

[3] L. D. Barron, M. P. Boggard, A. D. Buckingham, Nature 241 (1973) 113-114

[4] J. Kapitán, V. Baumruk, P. Bouř, J. Am. Chem. Soc. 128 (2006) 2438-2443

[5] V. Profant, M. Šafařík, P. Bouř, V. Baumruk, Spectroscopy - Biomed. App., submitted





## Experimental and theoretical studies of cyclic di-amino acid peptides in the solid state

A. P. Mendham<sup>1</sup>, B. Z. Chowdhry<sup>1</sup>, T. J. Dines<sup>2</sup>

<sup>1</sup>University of Greenwich at Medway, School of Science, Chatham Maritime, Kent, ME4 4TB, UK

<sup>2</sup>University of Dundee, Division of Electronic Engineering & Physics, Dundee, DD1 4HN, UK

Cyclic di-amino acid peptides (CDAPs) i.e. diketopiperazine (DKP) derivatives have been of long-standing interdisciplinary scientific interest, particularly as potential anti-cancer and anti-microbial agents [1, 2]. Single crystal x-ray studies of different derivatives have indicated that the six membered DKP ring adopts either a planar (cyclo(Gly-Gly), cyclo(L-Ser-L-Ser)) or boat conformation (cyclo(L-Ala-L-Ala) cyclo(L-Asp-L-Asp), cyclo(L-Glu-L-Glu)), in the solid state [3]. In addition, due to steric constraints, both amide bonds always adopt a *cis* conformation. Unfortunately, the inability to grow crystals of suitable diffraction quality makes it necessary to use other methods for determining solid state structures. In this study a selection of different CDAPs, have been investigated by experimental techniques such as Raman, infra-red spectroscopy and solid state NMR spectroscopy in order to relate structural and conformational relationships with theoretically calculated data. Theoretical gas phase structures have been calculated using DFT calculations (Gaussian03 molecular modeling package), utilizing the B3-LYP/cc-pVDZ basis set. Solid state DFT calculations have also been undertaken, using the pseudopotential-plane-wave CASTEP program.

The minimum energy conformation (gas phase) for cyclo(Gly-Gly), cyclo(L-Ala-Gly), cyclo(L-Ala-L-Ala), cyclo(L-Ser-L-Ser), cyclo(L-Asp-L-Asp) and cyclo(L-Glu-L-Glu) indicates that the DKP ring preferentially adopts a boat conformation. When the DKP ring is constrained to adopt a planar conformation a higher energy structure is produced. In the case of cyclo(GlyGly) the planar conformation is higher in energy by only 0.945 kJ mol<sup>-1</sup>. Simulated theoretical Raman spectra for both planar and boat conformations of cyclo(Gly-Gly) have indicated significant conformational shifts for both the CH<sub>2</sub> stretching vibrations and the *cis* amide II mode. The *cis* amide II mode is, predominantly, an out of phase C<sup>α</sup>-C-N stretch with a lower degree of contribution from the N-H in plane bend than in the *trans* amide II mode. The *cis* amide II mode appears as quite a strong signal in the Raman spectra, but is not observed in the FT-IR spectra [3].

The theoretical calculations are in good agreement with the experimental Raman results, which indicate a potential link with respect to the conformation of the DKP ring, in that a boat conformation has a *cis* amide II mode at a lower wavenumber than that with a planar/near planar DKP ring conformation. For example, the amide II vibrations for the planar/near planar conformations in cyclo(Gly-Gly), cyclo(D-Ala-L-Ala) and cyclo(L-Ala-Gly) are observed at wavenumbers of 1517, 1523, and 1522 cm<sup>-1</sup>, respectively, whereas the amide II modes for the boat conformations of cyclo(L-Glu-L-Glu), cyclo(L-Asp-L-Asp) and cyclo(L-Met-L-Met) are located at 1493, 1489, and 1493 cm<sup>-1</sup>, respectively [3]. The results indicate the significant potential for structural and conformational analysis using a combination of molecular modeling and experimental spectroscopic results.

[1] S. C. Braun, P. Milne, R. Naude, M. Van de Venter, *Anticancer Res.* 24 (2004) 1713

[2] P. J. Milne, A. L. Hunt, K. Rostoll, J. J. Van der Walt, C.J.M. Graz, *J. Pharm. Pharmacol.* 50 (1998) 1331

[3] A. P. Mendham, R. A. Palmer, B. S. Potter, T. J. Dines, M. J. Snowden, R. Withnall, B. Z. Chowdhry, *J. Raman Spectrosc.* 41 3 (2010) 288, and references therein.



## Carbon monoxide infrared absorption band of carboxyheme proteins as a probe of the protein collective motions.

S. S. Stavrov

*Department of Human Molecular Genetics and Biochemistry, Sackler Faculty of Medicine, Tel Aviv University, Ramat Aviv, 69978, Tel Aviv, Israel*

Heme proteins are intensively used to study chemistry and physics of proteins, because they can be studied by virtually any spectroscopic technique. Carboxyheme proteins manifest very strong infrared absorption band in the region of 1900 – 2000  $\text{cm}^{-1}$ , which corresponds to the valence vibration of the heme-coordinated CO molecule. Position of this band was shown to be affected by the protein environment [1, 2] and was used to study the structure and dynamics of heme proteins [1, 2]). Modern infrared spectroscopy allows obtaining high resolution spectra of this band with high signal-noise ratio. Therefore not only position, but also shape of the band is used to obtain information about the protein structure and dynamics [3-5]. In this study we analyze general properties of shape of the CO band.

It was shown earlier [6] that decay weakly contributes to the band width ( $\sim 0.2 \text{ cm}^{-1}$  at room temperature), whereas the band's full width at half maximum is  $\sim 10 \text{ cm}^{-1}$ . Therefore, the main contribution to the CO band broadening stems from interaction of the CO vibration with motion of its environment, whereas the natural width of the band is negligibly small. If this environment moves harmonically, the band shape can be described in terms of theory of multi-phonon optical absorption band [6].

Using this theory we show that (a) the CO band is broadened by the environment motions, which are slower than  $\sim 50 \text{ ps}$ ; (b) most probably these motions correspond to large-scale relative motions of the protein helices bounding heme and distal polar or charged amino acids (in case of hemoglobin and myoglobin, these are E and F helices, respectively [8, 9]); (c) the temperature dependence of the second moment of the band has to be linear in any temperature interval at  $T > 20 \text{ K}$ . Deviation from the linearity points at anharmonic character of motion of the environment; (d) if at any temperature the spectrum is symmetric, it must be Gaussian. Experimental observation of another symmetric bandshape (for example, Voigtian) implies that motion of the environment is anharmonic, and the band is a superposition of Gaussians, each of which corresponds to a conformational substate of the protein. These results explain the experimentally observed temperature dependence of the CO band [5] and, in particular, bring one to a conclusion that even in dry trehalose motions of the heme environment occur.

- [1] S. S. Stavrov, "The FeCO unit vibrations as a probe of the structure and dynamics of the active site of heme proteins: combined quantum chemical, vibronic and spectroscopic study", in *Biopolymer Research Trends*, edited by R. B. Hamil, Nova Publishers, 119 (2008).
- [2] T. G. Spiro, I. H. Wasbotten, *J. Inorg. Biochem.* 99 (2005) 34-44
- [3] J. D. Muller, B. H. McMahon, E. Y. T. Chien, S. G. Sligar, G. U. Nienhaus, *Biophys. J.* 77 (1999) 1036-1051
- [4] A. Cupane, M. Leone, V. Militello, *Biophys. Chem.* 104 (2003) 335-344.
- [5] A. D. Kaposi, J. M. Vanderkooi, S. S. Stavrov, *Biophys. J.* 91 (2006) 4191-4200.
- [6] K. A. Merchant, D. E. Thompson, Q. H. Xu, R. B. Williams, R. F. Loring, M. D. Fayer, *Biophys. J.* 82 (2002) 3277-3288.
- [7] Y. E. Perlin, *Sov. Phys. Uspekhi* 80 (1964) 553-595.
- [8] M. Laberge and T. Yonetani, *Biophys. J.* 94 (2008) 2737-2751.
- [9] G. Schiro, M. Cammarata, M. Levantino and A. Cupane, *Biophys. Chem.* 114 (2005) 27-33



## Time-resolved FTIR investigation on light-induced proton-coupled electron transfer reactions in photosynthetic reaction centers

A. Mezzetti<sup>1,2</sup>, M. Malferrari<sup>3</sup>, F. Francia<sup>3</sup>, A. Idrissi<sup>2</sup>, G. Venturoli<sup>3</sup>, W. Leibl<sup>1</sup>

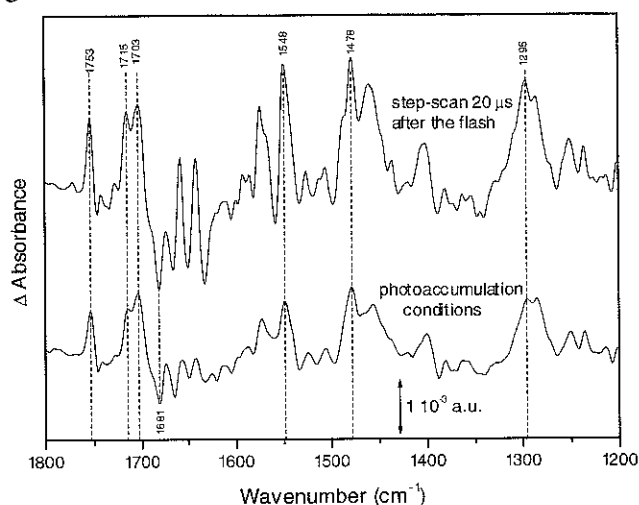
<sup>1</sup>SB2SM,,URA 2096, IbiTec-S, Bat 532, CEA-Saclay, 91191 Gif-sur-Yvette cedex, France

<sup>2</sup>LASIR UMR 8516, Bat C5, Université Lille 1, 59655 Villeneuve d'Ascq, France

<sup>3</sup> Dipartimento di Biologie Evoluzionistica Sperimentale, Univ.Bologna, Via Imerio 42, 40126 Bologna, Italy

Time-resolved difference FTIR is a powerful technique in biochemistry. We studied bacterial photosynthetic reaction centers (RCs) where light induces electron transfer (ET) reactions which are coupled to other processes ( $H^+$  transfer, protein/solvent rearrangement, cofactor displacement). As time-res. FTIR records absorbance changes in a wide spectral range, we could follow simultaneously different events (most of which not accessible by other techniques) and to get information on their coupling (e.g. between ET and  $H^+$  transfer) [1-4 & refs. therein]. We used step-scan FTIR (t. res. 10  $\mu$ s) to study the charge separation process  $PQ_A \rightarrow P^+Q_A^-$  between the primary donor P and the primary quinone acceptor  $Q_A$ . Rapid-scan FTIR (t. res. 25 ms) was used to follow the  $H^+$ -coupled ET reactions leading to the formation/release of ubiquinol  $QH_2$ , a topic recently object of controversy [5,6].

A particular attention has been paid to the effect of the matrix in which the RC is placed. Strong dehydration of RC films or RC inclusion into dehydrated trehalose glasses has been shown to block ET from  $Q_A$  to the secondary quinone  $Q_B$ , as well as to destabilize the  $P^+Q_A^-$  state, mimicking at 298 K effects observed at cryogenic temperatures [7,8]. The effects are reversibly modulated by the content of residual water. Time-res. FTIR monitored light-induced changes attributed to quinones and weakly-bound water molecules; information on conformational changes which follow the event of primary charge separation was obtained.



Step-scan/rapid-scan FTIR difference spectra of photosynthetic RCs. (+) bands:  $P^+Q_A^-$  state (-) bands:  $PQ_A$  state

[1] L. Blanchet, C. Ruckebusch, A. Mezzetti, J.P. Huvenne, A. de Juan, J. Phys Chem. B 113 (2009) 6031-6040.

[2] L. Blanchet, A. Mezzetti, C. Ruckebusch, J.P. Huvenne, A. de Juan, Anal. Bioanal. Chem, 387 (2007) 1863-1874.

[3] A. Mezzetti, W. Leibl, Eur. Biophys. J., 34 (2005) 921-936.

[4] A. Mezzetti, W. Leibl, J. Breton, E. Navedryk, FEBS Letters 537 (2003) 161-165

[5] A. Remy, K. Gerwert, Nat. Struct. Biol. 10, (2003) 637.

[6] J. Breton, Biochemistry 46, (2007) 4459-65

[7] G. Palazzo, A. Mallardi, A.Hochkoeppler, L.Cordone, G.Venturoli, Biophys. J. 82 (2002) 558-568

[8] F.Francia, G.Palazzo, A.Mallardi, L. Cordone, G. Venturoli, Biophys. J. 85 (2002) 2760-2775



## Fluorescence spectroscopy of the components of the bacterial bioluminescent reaction in viscous media

E. Nemtseva<sup>1,2</sup>, D. Gulnov<sup>1</sup>, M. Gerasimova<sup>1</sup>, V. Kratasyuk<sup>1,2</sup>

<sup>1</sup>Siberian Federal University, 79 Svobodny Prospect, 660041, Krasnoyarsk, Russia

<sup>2</sup>Institute of Biophysics SB RAS, 50/50 Akademgorodok, 660036, Krasnoyarsk, Russia

Bacterial bioluminescent reaction is both biochemical and optical phenomenon: during enzymatic oxidation of reduced flavin mononucleotide (FMN) and aliphatic aldehyde a quantum of blue-green light is produced. This process is catalyzed by coupled enzymes – bacterial luciferase (L) and NAD(P)H:FMN-oxidoreductase (R). Earlier viscous media was used to imitate *in vivo* conditions for bacterial bioluminescent reaction [1]. Bioluminescence intensity variation obtained can be the result of the conformational changes of the components and specific effects of media. We used fluorescence spectroscopy techniques to verify these factors. Emission, excitation spectra and anisotropy of fluorescence for FMN, L and R molecules were analyzed in four viscous media containing glycerol (10-70%), sucrose (10-50%), potato starch (0,5-5%) and gelatin (0,1-1%).

Blue shifts of about 5 nm for emission spectra of both L and R were obtained in concentrated solutions of glycerol and sucrose. It can be result of the conformational changes of enzymes followed by closing of some tryptophans to apolar amino acid residues. Low value of steady-state fluorescent anisotropy was registered for enzymes even in very viscous solutions. Spectra and the fluorescence lifetimes obtained for FMN show small changes in emissive and non-radiative decay rates of fluorophore and no effect on the energy of excited state. Fluorescent anisotropy of FMN was found to depend on not only the viscosity value, but the nature of cosolvent (fig. 1). Some interaction between phosphate group of flavin and sucrose molecules was concluded.

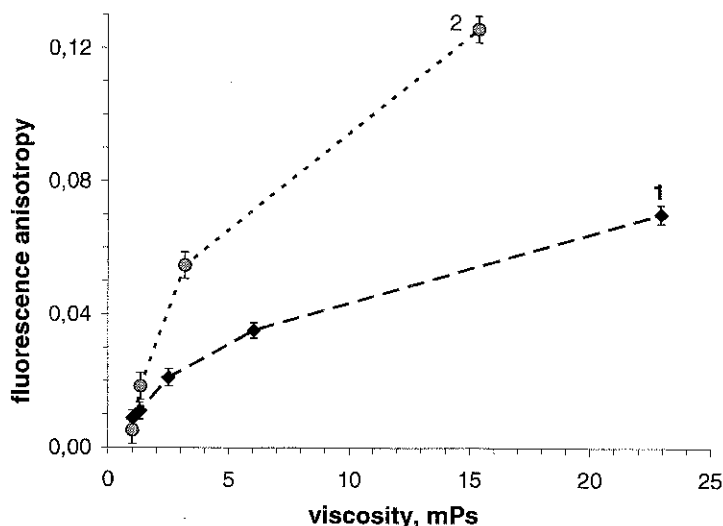


Fig 1. Steady-state fluorescence anisotropy of FMN in viscous solutions containing glycerol (1) and sucrose (2), excitation at 450 nm, 20°C.

Thus the results of this study confirm that in viscous solutions containing glycerol and sucrose conformational changes of bacterial luciferase and NAD(P)H:FMN-oxidoreductase can be responsible for bioluminescence intensity decrease.

[1] I.E. Sukovataya, E.V. Kaykova, N.S. Buka, L. Zadorozhnaya Luminescence 23 (2008) 93.



## Fluorescence features of photoprotein obelin

N. Belogurova<sup>1</sup>, N. Kudryasheva<sup>1,2</sup>

<sup>1</sup>*Institute of Biophysics SB RAS, Akademgorodok, 660036, Krasnoyarsk, Russia*

<sup>2</sup>*Siberian Federal University, Svobodny, 660043, Krasnoyarsk, Russia*

Photoprotein obelin is responsible for bioluminescence of hydroid *Obelia* [1]. The photoprotein is a stable enzyme-substrate complex consisting of a single polypeptide chain and an oxygen “pre-activated” substrate, 2-hydroperoxycoelenterazine, which is tightly but non-covalently bound within a hydrophobic cavity inside the protein [1]. Addition of  $\text{Ca}^{2+}$  to obelin initiates bioluminescent reaction. The bioluminescence intensity of obelin depends on  $\text{Ca}^{2+}$  concentration [2]. This is the factor accounting for application of photoprotein bioluminescence to monitor  $\text{Ca}^{2+}$  concentration. Product of the bioluminescent reaction, discharged obelin, is highly fluorescent. Therefore it can be used as fluorescent marker to visualize intracellular processes and as calcium nano-indicator for monitoring  $\text{Ca}^{2+}$  concentration in different media. From this point of view, dependence of fluorescent intensity of discharged obelin on  $\text{Ca}^{2+}$  concentration is of high interest. In addition the obelin spectra are known to be complex and variable [3]. The aim of the work was to study the way different  $\text{Ca}^{2+}$  concentration, emission and excitation wavelengths affect the fluorescence spectra of discharged obelin.

The recombinant obelin was obtained from Photobiology laboratory of Institute of Biophysics (Krasnoyarsk, Russia) [2]. Fluorescence of discharged obelin is measured when bioluminescent reaction had been over. Concentrations of free  $\text{Ca}^{2+}$  varied from  $10^{-7}$  M to  $10^{-3}$  M. In excitation spectra, emission wavelength varied from 400 to 520 nm in 10-nm step. In emission spectra, excitation wavelength varied from 260 to 420 nm in 10-nm step.

Increase of  $\text{Ca}^{2+}$  concentration elevated the fluorescent intensity of discharged obelin, both in excitation and emission spectra. The dependences can be considered as linear in the double logarithmic coordinates in the  $\text{Ca}^{2+}$  concentration range  $10^{-7}$ – $10^{-6}$  M, both in excitation and emission spectra. Hence, fluorescence of discharged obelin, along with bioluminescence, might be applied as quantitative assay method for monitoring  $\text{Ca}^{2+}$ -related processes *in vitro* and *in vivo*.

It was found that intensity and form of excitation and emission spectra depend on emission and excitation wavelength respectively. The differences in the spectra result from variation of peak components contributions. The spectra were divided into peak components. It was found that excitation spectra are superposition of 3 or 4 components (depending on emission wavelength), and emission spectra - of 4 components. Maxima of corresponding components are close and do not depend on emission or excitation wavelength, while the components contributions do. This dependence is due to the complex mechanism of the spectra formation marked by two interdependent peculiarities: multicomponent character of spectra and various efficiencies of proton transfer in fluorescent state of emitters.

[1] Z. Liu, E. S. Vysotski, C. J. Chen, J. Rose, B. C. Wang, J. Lee. *Protein Sci.* 9 (2000) 2085-2093.

[2] B. A. Illarionov, L. A. Frank, V. A. Illarionova, V. S. Bondar, E. S. Vysotski, J. R. Blinks, J. Methods in Enzymol. 277 (2000) 223-249.

[3] N. V. Belogurova, N. S. Kudryasheva, R. R. Alieva, A. G. Sizykh. *J Photochem Photobiol B.* 92 (2008) 117-122.



## Infrared Spectroscopy in Clinical Chemistry – From Laboratory to Continuous Patient Monitoring

H.M. Heise<sup>1</sup>, U. Damm<sup>1</sup>, V.R. Kondepoti<sup>1</sup>, R. Kuckuk<sup>1</sup>, J.K. Mader<sup>2</sup>, F. Feichtner<sup>3</sup> and M. Ellmerer<sup>2</sup>

<sup>1</sup> ISAS – Institute for Analytical Sciences at Dortmund University of Technology, Bunsen-Kirchhoff-Str. 11, D-44139 Dortmund, Germany, E-Mail: heise@isas.de

<sup>2</sup> Department of Internal Medicine, Division of Endocrinology and Nuclear Medicine, Medical University Graz, Auenbruggerplatz 15, A-8036 Graz, Austria.

<sup>3</sup> Joanneum Research Forschungsgesellschaft mbH, Institute of Medical Technologies and Health Management, Elisabethstr. 11A, A-8010 Graz, Austria

Infrared spectroscopy is a versatile method for the study of various biomedical tissues or biofluid samples.<sup>1</sup> The analysis takes advantage of the fact that a multitude of analytes can be quantified simultaneously without the need for reagents. An automated, drift-free bed-side infrared spectrometric device has been developed by us recently for the continuous monitoring of blood glucose with application for Intensive Care Unit (ICU) patients.

Whole blood continuous measurements show the needs for improving the biocompatibility of micro-cuvette materials to avoid the adsorption of blood immune cells. However, without any complications the system can be reliably applied for patient monitoring using dialysates harvested by means of a subcutaneously implanted micro-dialysis catheter<sup>2</sup> or by an external vascular body interface that includes a micro-dialysis preparation step.<sup>3</sup> The simultaneous assessment of dialysis recovery rates allows for the reliable quantification of interstitial and whole blood concentrations. High correlation of the values to the reference venous blood measurements was achieved and the results are reported using Clarke-Error grid and Bland-Altman graphs. The method also makes the simultaneous determination of metabolites such as urea, lactate and others possible. The performance of the system was tested in several clinical measurement campaigns using the sensor also in combination with a programmed insulin pump for achieving normal blood glucose concentrations in type 1 diabetic subjects.

Infrared spectroscopy in combination with micro-fluidic technology can be used for reliable blood glucose monitoring in the ICU. Prospects for device miniaturisation are promising and will enable even for wearable devices applicable for patient self-monitoring of blood glucose replacing electrochemical enzymatic biosensors.

Financial support from the European Commission with the CLINICIP project (contract no. 506965, 6th Framework Programme) is gratefully acknowledged.

[1] H.M. Heise, Biomedical vibrational spectroscopy – Technical Advances, in: Biomedical Vibrational Spectroscopy, P. Lasc, J. Kneipp (Eds.), Wiley: Hoboken, 9-37 (2008).

[2] H.M. Heise, U. Damm, M. Bodenlenz, V.R. Kondepoti, G. Koehler, M. Ellmerer, J. Biomed. Optics **12**, 024004, (2007).

[3] H.M. Heise, V.R. Kondepoti, U. Damm, M. Licht, F. Feichtner, J.K. Mader, M. Ellmerer, SPIE Proc. **6863**, 686308, (2008).



## Vibrational Spectroscopy: Towards Neurosurgical Applications

G. Steiner<sup>1</sup>, A. Stelling<sup>2</sup>, K. Geiger<sup>3</sup>, E. Koch<sup>1</sup>, R. Salzer<sup>2</sup>, G. Schackert<sup>4</sup>, M. Kirsch<sup>4</sup>

<sup>1</sup> Dresden University of Technology, Medical Faculty Carl Gustav Carus, Clinical Sensing and Monitoring, 01307 Dresden, Germany

<sup>2</sup> Dresden University of Technology, Faculty of Science and Mathematics, Department of Chemistry, 01062 Dresden, Germany

<sup>3</sup> Dresden University of Technology, University Hospital, Institute for Pathology, 01307 Dresden, Germany

<sup>4</sup> Dresden University of Technology, University Hospital, Department of Neurosurgery, 01307 Dresden, Germany

Rapid and reliable discrimination of cell types and tissue is a crucial task in clinical medicine. In current methods, different types of cells, e.g. tumor cells, are classified using the goldstandard histochemical labelling. However histological methods require a preparation of thin tissue sections and do not permit in-situ monitoring. Vibrational spectroscopy (e.g. Raman and infrared spectroscopy) has the potential to characterize thin tissue sections [1] and to monitor cells under in-situ conditions [2].

On the example of different types of human brain tumors, we demonstrate the ability of infrared and Raman spectroscopy to identify tumor cells. In a first series of experiments human brain tumor cells of different cell lines [3] and cells from normal tissue were classified by infrared spectroscopy. Significant spectral features occurred in the wavenumber range between 1000 and 1200  $\text{cm}^{-1}$ , which is associated with vibration modes of phosphate groups, and glycolipids. Next we have extended vibrational spectroscopy to animal models and live surgery. Spectroscopic measurements were carried out on fresh tissue samples. Infrared spectroscopic imaging was applied on thin sections in order to identify borderline tissue. Principal component analysis and linear discriminant analysis were performed on the spectroscopic data sets to distinguish different types of tissue. Differences in the spectroscopic signature were found in the range of RNA and DNA absorption bands as well as in the profile of the amide I and amide II bands. Raman spectroscopy gave similar information to FT-IR spectroscopy.

As the results demonstrate, the potential of vibrational spectroscopic methods such as Raman and infrared spectroscopy to assess the overall molecular composition of cells in a non-destructive manner opens the possibility to characterize tissue in short time without labels or sample preparation.

[1] C. Krafft, G. Steiner, C. Beleites, R. Salzer, J. Biophotonics, 2 (2009) 13-28.

[2] M. K. Kuimova, K. L. A. Chan, and S. G. Kazarian, Appl. Spectr., 63 (2009) 164-171.

[3] G. Steiner, S. Küchler, A. Hermann, E. Koch, R. Salzer, G. Schackert, M. Kirsch, Cytometry A, 37A (2008) 1158-1164.



## Vibrational spectroscopy characterization of a new pharmaceutical complex of chlorthalidone

E. Horj<sup>1</sup>, S. Cîntă Pînzaru<sup>1</sup>, C. Soica<sup>2</sup>, C. Dehelean<sup>2</sup>, L. David<sup>1</sup>

<sup>1</sup>Faculty of Physics, Babes-Bolyai University, Kogalniceanu 1, RO-400084 Cluj-Napoca, Romania

<sup>2</sup>Victor Babes University of Medicine and Pharmacy, Eftimie Murgu Square 2, RO-30004 Timisoara, Romania

Chlorthalidone (2-chloro-5-[(1*S*)-1-hydroxy-3-oxo-2,3-dihydro-1*H*-isoindol-1-yl] benzenesulphonamide, CLT) is an effective diuretic, used for the treatment of edema and hypertension. Because of its low solubility in water, the possibility of inclusion into hydroxypropyl- $\beta$ -cyclodextrin (HPBCD) has been investigated using FT-IR and FT-Raman spectroscopic methods. The CLT:HPBCD kneading product with the molar ratio 1:2 was used in order to obtain the optimal complex formulation based on the previous solubility tests [1] and H-NMR analysis [2].

Molecular geometry optimization and vibrational frequencies calculation were performed by density functional theory (DFT) computations and two possible conformers of chlorthalidone have been identified. The first complete vibrational characterization of chlorthalidone is given here.

The geometry of the 1:2 inclusion complex is proposed based on the vibrational analysis (Fig. 1), highlighting the unique ability of the Raman spectroscopy in rapid identification of the inclusion compounds.

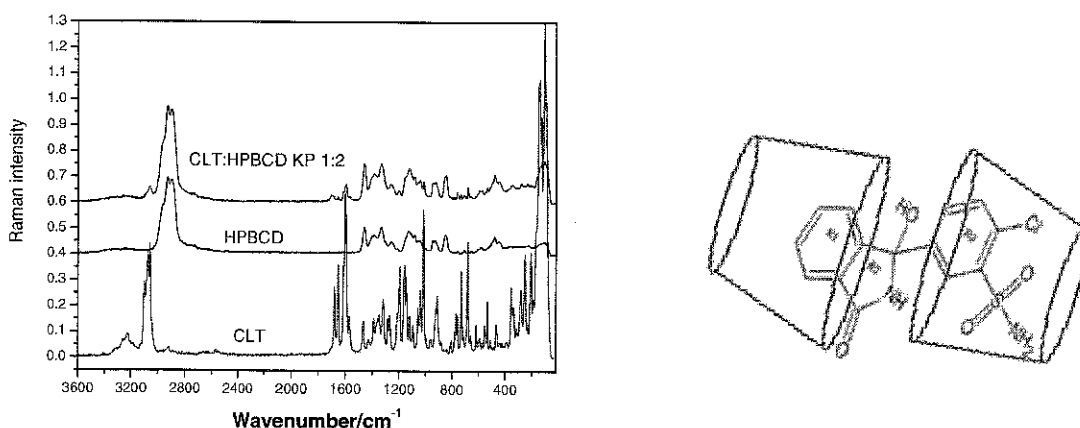


Fig. 1. FT-Raman spectra of CLT, HPBCD and their 1:2 inclusion complex (left) and the proposed geometry of the complex (right).

[1] C. Soica, Á Gyeresi, Z. Aigner, M. Kata, C. Dehelean, *Rev. Chim.*, 57, 4, (2006), 392-397.

[2]. Codruta Soica, A. Gyeresi, B. Frentiu, C. Dehelean, M. Aluas, *Rev. Chim.*, 58, 7, (2007), 606-611.



## Raman micro-spectroscopy as a diagnostics tool for skin cancer detection

M. Larraona-Puy<sup>1</sup>, A. Ghita<sup>1</sup>, A. Zoladek<sup>1</sup>, W. Perkins<sup>2</sup>, S. Varma<sup>2</sup>, I. H. Leach<sup>3</sup>, A. A. Koloydenko<sup>4</sup>, H. Williams<sup>5</sup> and I. Notinger<sup>1\*</sup>.

<sup>1</sup> School of Physics and Astronomy, University of Nottingham, University Park, NG7 2RD, Nottingham, U.K

<sup>2</sup> Dermatology Department, Nottingham University Hospital NHS Trust, QMC Campus, Derby Road, NG7 2UH, Nottingham, U.K.

<sup>3</sup> Histopathology Department, Nottingham University Hospital NHS Trust, QMC Campus, Derby Road, NG7 2UH, Nottingham, U.K.

<sup>4</sup> Mathematics Department, Royal Holloway, University of London, Egham, TW20 0EX, U.K.

<sup>5</sup> Centre of Evidence-Based Dermatology, C Floor South Block, Nottingham University Hospital NHS Trust, QMC Campus, Derby Road, NG7 2UH, Nottingham, U.K.

An automated method for the imaging and diagnosis of the most common skin cancer, basal cell carcinoma (BCC), with Raman micro-spectroscopy (RMS) has been developed. RMS is a powerful technique which has been used for imaging BCC in sections [1] and for diagnosis of BCC *in vivo* [2]. In this study, skin tissue sections obtained during BCC surgery were analysed by RMS and compared to gold-standard of histopathology. A classification model was built using selected Raman bands responsible for the largest spectral differences between BCC and normal skin regions and linear discriminant analysis (LDA) [3]. The model discriminates BCC from healthy tissue with  $90\pm 9\%$  sensitivity and  $85\pm 9\%$  specificity in a 70% to 30% split cross-validation algorithm. The supervised multivariate model was then applied to tissue sections obtained from new patients to produce biochemical images and provide diagnosis of BCC. Histopathology examination and the corresponding hematoxylin and eosin (H&E) images were compared with the Raman maps, achieving excellent agreement. Our model was tested in samples with nodular and morpheic BCC as well as in healthy tissue without tumor presence.

The introduction of the proposed technique into a real clinical scenario will help accurate location of tumors and may improve the feasibility and efficiency of current *state of the art* treatment for BCC.

**Acknowledgments:** The authors would like to acknowledge the financial support. The authors would like to acknowledge the financial support of the UK National Institute for Health Research (NEAT FSG004), the University of Nottingham Hospitals Charity and the Engineering and Physical Sciences Research Council (Bridging the Gaps grant EP/E018580/1).

[1] A. Nijssen, T. C. B. Schut, F. Heule, P. J. Caspers, D. P. Hayes, M. H. Neumann, and G. J. Puppels, *J. Invest. Dermatol.* 119 (2002) 64–69

[2] Lieber CA, Majumder SK, Ellis DJ, Billheimer DD, Mahadevan-Jansen A., *Laser Surg Med.* 40 (2008) 461–467

[3] M. Larraona-Puy, A. Ghita, A. Zoladek, W. Perkins, S. Varma, I. Leach, H. Williams, A. A. Koloydenko and I. Notinger, *J. Biomedical Optics*, 14 (2009) 054031 1-10



## Label-free time-course imaging of live cells by confocal Raman micro-spectroscopy

F.C. Pascut, I. Notingher

*School of Physics and Astronomy, University of Nottingham, Nottingham NG7 2RD, UK*

All biochemical processes underlying the biological activity of cells are time dependent. Understanding such molecular processes in individual cells require imaging methods able to advance our understanding of cell biochemistry. However, non-invasive time-course imaging raises new challenges for currently available microscopy methods. Most of these advance techniques can provide only single snap-shots because of the invasive procedures they require. Conventional label-free imaging microscopy techniques provide morphological information about cells over extended periods of time but lack chemical specificity. Infrared spectroscopy has limited spatial resolution and difficulties caused by the strong absorption of water.

Confocal Raman micro-spectroscopy (CRMS) combines the high chemical specificity of non-resonant Raman spectroscopy with the high-spatial resolution of confocal optical microscopes to produce spectral images corresponding to specific molecules in cells. Since water has weak Raman cross-section compared to most biomolecules, CRMS has been used for high-spatial resolution imaging of fixed and live cells in aqueous solutions. However, most studies imaging live cell, the cells were not maintained under physiological conditions [1,2].

We will report the latest instrumental developments for non-resonant CRMS for imaging live cells. The features required for obtaining time-course images will be highlighted. The effect of excitation laser wavelength on the quality of spectral images and cell viability will be discussed. These optimizations allow full exploitation of the unique features of Raman spectroscopy for molecular imaging of individual live cells. We will include recent results on using CRMS for three applications: time-course imaging of apoptotic cells, polarization of actin in dendritic cells and differentiation of pluripotent stem cells.

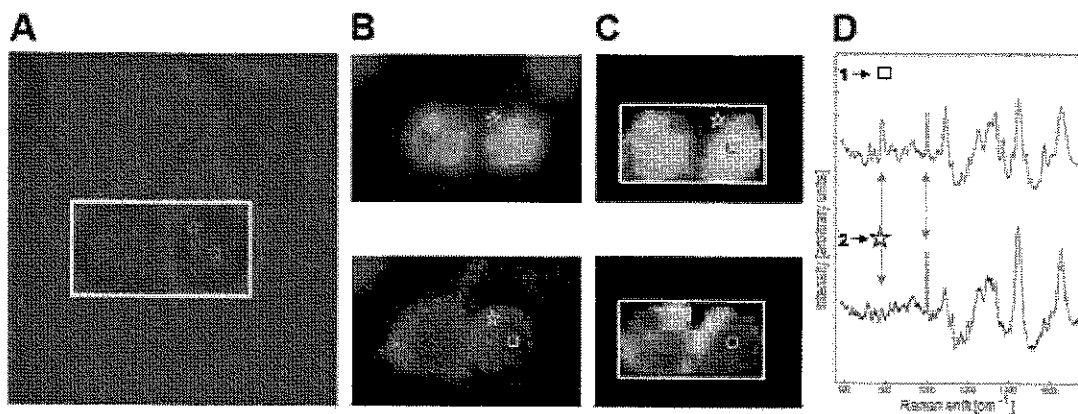


**Figure 1.** Example of label-free imaging of T-cells: A) bright field images, B) fluorescence staining of nucleus (top) and actin (bottom), C) Raman spectral images of DNA (top) and proteins (bottom), D) typical bottom-fluorescence staining, C) typical Raman spectra of at position in the nucleus and cytoplasm.

[1] K. Hamada, K. Fujita, N.I. Smith, M. Kobayashi, Y. Inouye, S. Kawata, *J. Biomed. Opt.* 13 (2008) 044027

[2] Y.S Huang, T. Karashima, M. Yamamoto, H. Hamaguchi, *Biochemistry* 44 (2005), 10009

## FTIR-synchrotron and NIR-FT-Raman studies of water in animal and human skin

O.F. Nielsen<sup>1</sup>, T. M. Greve<sup>1,2</sup>, A. Engdahl<sup>3</sup>

<sup>1</sup>Department of Chemistry, University of Copenhagen, 5 Universitetsparken, DK-2100, Copenhagen, Denmark

<sup>2</sup>Department of Spectroscopy and Physical Chemistry, LEO-Pharma, 55 Industriparken, Ballerup, DK-2750, Denmark

<sup>3</sup>MAX-lab, Lund University, 1 Ole Römers väg, Lund, SE-22363, Sweden

FTIR-spectra were recorded on a Bruker Hyperion 3000 microscope coupled to a Bruker IFS66 FT spectrometer. Radiation from a conventional global or synchrotron radiation from beamline 73 at MAX-lab, Lund was used. FTIR-imaging recordings were obtained from slices cryosectionized perpendicular to the surface of pig ear skin. Raman spectra were recorded on Bruker RFS100 or Bruker RFS100/S FT Raman spectrometers with excitation at 1064 nm. The low-wavenumber part of the Raman spectrum was transformed to the  $R(\bar{\nu})$ -representation in order to get rid of the broad, intense Rayleigh line.

Water is important for the dynamics and function of bio-molecules. In living systems some water molecules are directly hydrogen bonded to ions or bio-molecules while some water molecules may retain a hydrogen bonded structure like that in bulk, liquid water. The OH-stretching region in IR and Raman spectra are indicative of the total amount of water, because the OH-stretching bands are only slightly perturbed by changes in hydrogen bonding. A band in the low-wavenumber region at  $180\text{ cm}^{-1}$  is significant for the presence of water with a local structure as in bulk, liquid water [1,2].

The water content and structure in malignant and benign human tumors were investigated by Raman spectroscopy. The malignant tumors (malignant melanoma and basal cell carcinoma) showed a higher water content of water with a bulk-like structure than skin with benign diseases (seborrheic keratosis and pigmented nevi) [2]. Intensities of the OH-stretching bands in the Raman spectrum showed that skin from humans, pigs and Guinea pigs showed higher water contents than skin from mice. The low-wavenumber Raman spectrum revealed that the mouse skin contained less bulk-like water [2]. The difference in water content of human and animal skin is very important for choosing the most suited animal skin for skin penetration studies of pharmaceuticals in laboratory studies. In this context the low-wavenumber Raman spectrum was used to follow the binding of water to an enhancer in the epidermal tissue of a pig ear [3]. The water band at  $180\text{ cm}^{-1}$  is relatively more intense in the Far-IR spectrum than in the low-wavenumber Raman spectrum. ATR-Far-FTIR was used to study the outer part of a pig ear, the stratum corneum, to a depth of 2-17  $\mu\text{m}$ . The amount of bulk-like water was small, but recognizable [4]. The distribution across the skin of water and biomolecules like proteins and lipids is also an important aspect. FTIR imaging of slices through pig ear skin showed that water and proteins are very similarly distributed across the skin.

- [1] O.F. Nielsen in "Handbook of Raman Spectroscopy", eds. I.R. Lewis and H.G.M. Edwards, Marcel Dekker, Inc, New York, 2001, pp. 593-615
- [2] T.M. Greve, N. R. Andersen, K. B. Andersen, M. Gniadecka, H.C. Wulf and O. F. Nielsen in "New Approaches in Biomedical Spectroscopy", eds K. Kneipp, R. Aroca, H. Kneipp and E. Wenstrup-Byrne, ACS Symposium Series 963 (2007) 30-40
- [3] T.M. Greve, K.B. Andersen and O.F. Nielsen, Spectroscopy 22 (2008) 405-417
- [4] T.M. Greve, K.B. Andersen, O.F. Nielsen and A. Engdahl, Spectroscopy (in press)



## Two-dimensional Raman and Raman optical activity correlation and factor analysis of lysozyme fibrillation

T. Pazderka<sup>1</sup>, V. Kopecký Jr.<sup>1</sup>, K. Hofbauerová<sup>1,2</sup>, V. Baumruk<sup>1</sup>

<sup>1</sup>*Institute of Physics, Faculty of Mathematics and Physics, Charles University in Prague, Ke Karlovu 5, Prague 2, CZ-121 16, Czech Republic; kopecky@karlov.mff.cuni.cz*

<sup>2</sup>*Institute of Microbiology, Academy of Sciences CR, Vídeňská 1083, Prague 4, CZ-142 20, Czech Republic*

Understanding of processes of amyloid fibrils formation is one of the key tasks in searching for proteins structural origin of human neurodegenerative diseases. Therefore, hen egg white lysozyme (HEWL) can serve as a good model of amyloid fibril formation. Furthermore, this protein is homologous to human lysozyme, which is one of the proteins that cause amyloid diseases [1]. Despite the intense scientific research, studying mechanisms in homologous proteins to lysozyme, the detailed mechanism of fibril formation is still far from complete understanding. Nevertheless, Raman optical activity (ROA) and Raman spectroscopy are very powerful techniques for studies of unfolded proteins [2].

Here we present Raman and ROA study using 2D correlation spectroscopy (2DCoS) [3]. Firstly, we model changes of ROA band shapes and positions and investigate characteristic patterns in 2DCoS because the origin of 2D patterns for spectra with positive and negative bands has not been investigated yet. Subsequently, temporal and thermal (from 20 °C to 60 °C) spectral changes in ROA and Raman spectra of HEWL were analyzed by means of factor analysis and 2DCoS. It gave us an opportunity to study delicate details of HEWL fibrillation and denaturation, i.e. sequence of the secondary structure changes upon fibrils formation. Moreover, application of heterospectral 2DCoS enabled to transfer band assignment from Raman spectroscopy to ROA and spectral changes in conformation of S-S bridges were identified in protein ROA spectra for the first time.

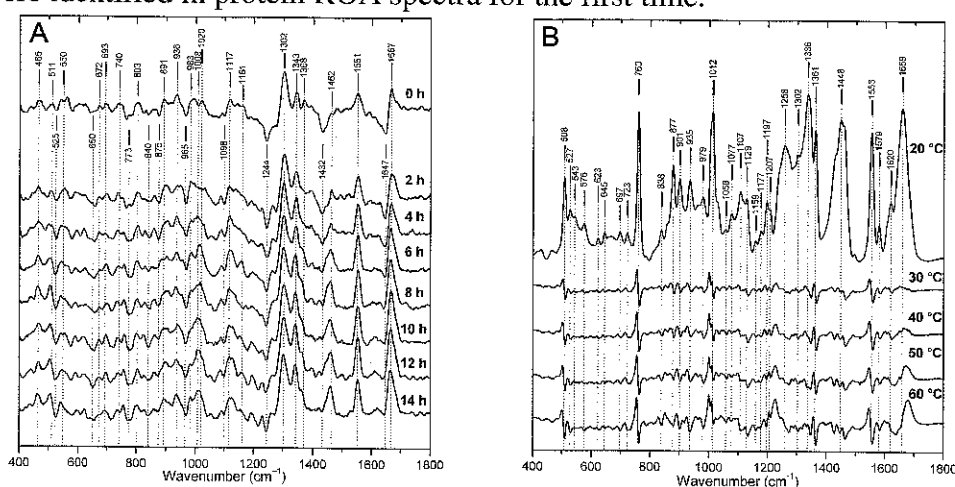
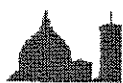


Fig. 1 – A) ROA time dependency of hen egg white lysozyme (400 mg/mL, pH 3.7) fibrillation, B) lysozyme thermal denaturation monitored by Raman spectroscopy

**Acknowledgements:** The Grant Agency of the Czech Republic is acknowledged (Nos. 305/09/0457 and P205/10/1276).

- [1] D. R. Booth, M. Sunde, V. Bellotti et al., *Nature* 385 (1997) 787–793
- [2] E. W. Blanch, L. A. Morozova-Roche, D. A. E. Cochran et al., *J. Mol. Biol.* 301 (2000) 553–563
- [3] I. Noda & Y. Ozaki, *Two dimensional correlation spectroscopy: applications in vibrational and optical spectroscopy*, (Chichester: Wiley), 2004.



## Synthesis and Characterization of Antibacterial Poly(*N*-vinylimidazole-co-maleic anhydride)/Sodium Bentonite Composites

M. Talu, E. Uzluk

Gazi University, Faculty of Science and Arts, Department of Chemistry, Teknikokullar, 06500, Ankara, Turkey

Polymers with high carboxylate content, especially maleic anhydride (MA) copolymers have been found to have biological activity including antitumor, antiviral, antibacterial, antifungal, and antiinflammatory activities [1]. *N*-Vinylimidazole (NVIM) is another interesting monomer which contains the imidazole ring that is present in most of the proteins and is partly responsible for their catalytic activity. It is an electron-rich monomer and therefore is expected to form a charge transfer complex with MA to give bifunctional alternating copolymers [1,2].

In this study, Poly(*N*-vinylimidazole-co-maleic anhydride)/Sodium-bentonite [Poly(NVIM-co-MA)/Na-bentonite] composites were synthesized by free radicalic polymerization of *N*-vinylimidazole and maleic anhydride containing dispersed Na-bentonite. By changing solvents, reaction temperature and the concentration of monomer and clay several copolymer-clay composites were prepared. Poly(NVIM-co-MA) copolymers were synthesized from 1,4-dioxane, methanol and toluene at 65, 70 and 80 °C. Figure 1 schematically illustrates the process the chemical polymerization Poly(NVIM-co-MA)/Na-bentonite. Structure of composites was characterized using FTIR, <sup>1</sup>H NMR, <sup>13</sup>C NMR spectroscopy, X-ray diffraction (XRD), scanning electron microscopy (SEM), thermogravimetric analysis (TGA and DTA) and DSC. Composite composition was determined by elemental analysis. Adsorptive properties were also investigated. In addition, the effect of monomer concentration on the physical properties of nanocomposites such as adsorptive, moisture regain and water uptake were investigated.

Interlayer distance of Na-bentonite increased with *N*-vinylimidazole and maleic anhydride content. The thermogravimetric analysis results revealed that the degradation temperatures of composites were higher than that of pure copolymer and the thermal degradation rates decreased. As seen from adsorptive properties, for higher loading of Poly(NVIM-co-MA), the specific surface area and micromesopore volumes of composites notably decreased. This result could be explained in terms of covering or filling of the pores by Poly(NVIM-co-MA).

The antimicrobial activities of copolymers and composites were investigated against various pathogene Gram-positive and Gram-negative bacteria [3]. The results showed that the clay-containing composites were more effective than copolymers.

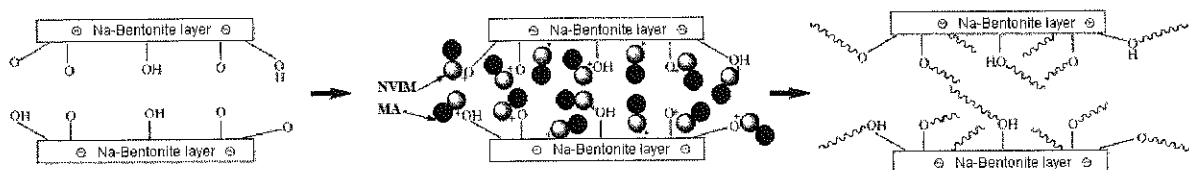


Fig. 1. Schematic representation of chemical polymerization Poly(NVIM-co-MA)/Na-bentonite.

[1] C. Göksel, B. Hacıoğlu, U. Akbulut, *J. Polym. Sci. Pol. Chem.* 35 (1997) 3735-3743

[2] V. Konsulov, Y. Piruleva, *Dokl. Bulg. Akad. Nauk.* 33 (1980) 807

[3] M. Talu, E. Uzluk, B. Yüksel, *Drug. Future* 32A (2007) 99



## Folding dynamics of hairpin peptides studied by temperature-jump infrared-spectroscopy and isotopic editing

K. Hauser<sup>1,2</sup>, C. Krejtschi<sup>2</sup>, O. Ridderbusch<sup>2</sup>, R. Huang<sup>3</sup>, L. Wu<sup>3</sup>, T. A. Keiderling<sup>3</sup>

<sup>1</sup>University of Konstanz, Universitätsstr.10, 78457 Konstanz, Germany

<sup>2</sup>University of Frankfurt, Max-von-Laue-Str.1, 40438 Frankfurt, Germany

<sup>3</sup>University of Illinois at Chicago, 845 W. Taylor St. Chicago, Illinois 60607- 7061, USA

Peptides with well-defined secondary structure are ideally suited to study protein folding mechanisms. We analyze ns-to- $\mu$ s peptide folding dynamics by time-resolved infrared spectroscopy and laser-excited temperature jumps ( $\sim 10^\circ\text{C}$ ). The spectral response is monitored as a function of time following rapid heating of the solvent by a Raman shifted Nd:YAG laser pulse that excites an overtone vibration of  $^2\text{H}_2\text{O}$  at 1909 nm. Lead salt laser diodes are used as a tunable IR source in the amide I' region between  $1600\text{ cm}^{-1}$  to  $1700\text{ cm}^{-1}$ . The amide I' region, mainly consisting of the coupled C=O stretching vibrations of the polypeptide backbone, is a sensitive marker for secondary structure and structural changes. We obtain site-specific dynamics by isotopic labeling of individual  $^{13}\text{C}=\text{O}$  groups.

Site-specific dynamics have been monitored for a set of isotopically labeled beta-hairpin peptides, variants of a 12-mer tryptophan zipper whose conformation is stabilized by a hydrophobic core formed from the interaction of four tryptophan residues. Various single and cross-strand coupled  $^{13}\text{C}=\text{O}$  labeled variants have been analyzed by probing the relaxation kinetics via separate partially resolved  $^{13}\text{C}=\text{O}$  amide I' bands. Differences in the kinetic behavior have been found for the loss of beta-strand and the gain of disordered structure. The isotope-edited kinetics show variations in local structural stability of the hairpin backbone. Our data support a multistate dynamic behavior that prevents a clear determination of folding and unfolding time constants. Nonetheless, the site-specific kinetics are consistent with a hydrophobic collapse hypothesis for hairpin folding [2].

Although the single labels lack intensity enhancement of the double labelled hairpins, their dynamic behaviour in terms of relaxation time and activation energy is similar if they are placed in the beta-strand portion of the hairpin between the tryptophan residues. Single labeled residues on the terminal positions of the hairpin have a different behaviour and are less able to be discriminated from the  $^{12}\text{C}=\text{O}$  components, but, by contrast, studies with double labels are possible due to coupling [3].

The contribution of the hydrophobic core to the hairpin stability has additionally been analyzed with mutants of this sequence whose tryptophan residues have been selectively substituted by valines.

[1] C. Krejtschi, R. Huang, T.A. Keiderling, K. Hauser, *Vibr. Spec.* 48 (2008) 1-7

[2] K. Hauser, C. Krejtschi, R. Huang, L. Wu, T.A. Keiderling, *J. Am. Chem. Soc.* 130 (2008) 2984-2992

[3] K. Hauser, O. Ridderbusch, C. Krejtschi, A. Hellerbach, R. Huang, L. Wu, T.A. Keiderling, manuscript in preparation



## Resonance Raman spectroscopy of catalase-peroxidase from the phytopathogenic rice blast fungus *Magnaporthe grisea*

E. Droghetti<sup>1</sup>, M. Zamocky<sup>2</sup>, P. G. Furtmüller<sup>2</sup>, C. Obinger<sup>2</sup>, G. Smulevich<sup>1</sup>

<sup>1</sup> Dipartimento di Chimica, Università di Firenze, Via della Lastruccia 3, I-50019, Sesto Fiorentino (FI), Italy

<sup>2</sup> Department of Chemistry, BOKU - University of Natural Resources and Applied Life Sciences, Muthgasse 18, A-1190 Vienna, Austria

Catalase-peroxidases (KatGs) are bifunctional heme peroxidases with an overwhelming catalase activity. About 40% of all sequenced prokaryotes possess *katG* gene(s). Comprehensive functional and structural investigations performed with eubacterial and archaeobacterial KatGs revealed the presence of peroxidase-typical proximal and distal heme residues together with features unique to KatG. Functional, structural and mutational studies on prokaryotic KatGs gave similar results irrespective of the origin of the heme protein [1,2].

In the present study, the first detailed spectroscopic analysis of an eukaryotic KatG is reported. In detail, recombinant KatG from the rice blast fungus *Magnaporthe grisea* [3] has been studied by UV-Vis and resonance Raman (RR) spectroscopy. The spectral signatures of the ferric protein indicate the presence of a five-coordinated (5c) high-spin (HS) heme coexisting with six-coordinated (6c) HS and low-spin (LS) species. Polarized RR spectra allowed us to identify a polarized band at 1624 cm<sup>-1</sup>, assigned to two coincident  $\nu(\text{C}=\text{C})$  stretching modes of the vinyl groups in position 2 and 4 of the heme group. This result is consistent with a torsion angle of the vinyl double bond with respect to the heme plane which is identical for both substituents, as a consequence of steric interactions with the protein matrix [4].

RR and UV-Vis spectra of ferrous KatG from *M. grisea* indicate the presence of both 6cLS and 5cHS hemes. The RR spectra of 5cHS ferrous heme proteins and model compounds have been extensively studied [5]. In the region between 200-250 cm<sup>-1</sup> the RR spectra are characterized by the presence of a strong band assigned to  $\nu(\text{Fe}-\text{Im})$  stretching mode between the Fe atom and the proximal ligand. A change of its frequency derives from a change in the status of the proton on the bound imidazole. In particular, in KatGs, this frequency furnishes important information on the strength of the conserved hydrogen bond between the N<sub>δ</sub> atom of the imidazole ring of the proximal histidine and the oxygen atom of the nearby aspartate carboxylate group. This hydrogen bond strengthens the bond between the iron atom and the histidine, causing an upshift of the  $\nu(\text{Fe}-\text{Im})$  stretch. In KatG from *M. grisea* this vibration is observed at 245 cm<sup>-1</sup> confirming the presence of a strong hydrogen bond inferring an imidazolate character to the proximal histidine.

These results will be compared with data available for prokaryotic KatGs.

- [1] S. Yu, S. Giroto, X. Zhao, R. S. Magliozzo, J. Biol. Chem. 278 (2003) 44121-44127
- [2] G. Smulevich, C. Jakopitsch, E. Droghetti, C. Obinger, J. Inorg. Biochem. 100 (2006) 568-586
- [3] M. Zamocky, P. G. Furtmüller, M. Bellei, G. Battistuzzi, J. Stadlmann, J. Vlasits, C. Obinger, Biochem. J. 418 (2009) 443-451
- [4] M. P. Marzocchi, G. Smulevich, J. Raman Spectroscopy 34 (2003) 725-736
- [5] P. Stein, T. G. Spiro, J. Am. Chem. Soc. 102 (1980) 7795-7797



## Structural variations of the iron cores in human liver ferritin and its pharmaceutically important models: a comparative study using Mössbauer spectroscopy with a high velocity resolution

M.I. Oshtrakh<sup>1</sup>, I.V. Alenkina<sup>1,2</sup>, S.M. Dubiel<sup>3</sup>, V.A. Semionkin<sup>1,2</sup>

<sup>1</sup>Faculty of Physical Techniques and Devices for Quality Control, Ural State Technical University – UPI, 620002, Ekaterinburg, Russian Federation

<sup>2</sup>Faculty of Experimental Physics, Ural State Technical University – UPI, 620002, Ekaterinburg, Russian Federation

<sup>3</sup>Faculty of Physics & Computer Science, AGH University of Science & Technology, PL-30-059 Kraków, Poland

Ferritin is an iron-storage protein which consists of nanosized iron core in the form of ferrihydrite with 24 protein subunits shell. A number of ferritin models appeared to be useful for treatment of iron deficiency anemia. These models consist of nanosized iron core in the form of  $\beta$ -FeOOH surrounded with a polysaccharide shell. The iron cores may vary in various ferritins and its pharmaceutically important models. To get a better insight into the issue, we used Mössbauer spectroscopy with a high velocity resolution for a comparative study of human liver ferritin and commercial medicines like: Imferon (iron-dextran complex), Maltofer® and FerrumLek (iron-polymaltose complexes).

<sup>57</sup>Fe Mössbauer spectra of ferritin and its models were measured at 295 and 90 K using an automated precision Mössbauer spectrometric system with the high velocity resolution (4096 channels) [1, 2]. The Mössbauer spectra were represented in 4096 or 2048 channels in the fitting procedure, using two models: (1) homogeneous iron core (one quadrupole doublet fit) and (2) heterogeneous iron core (fit with superposition of several quadrupole doublets). Differences in Mössbauer hyperfine parameters obtained from the homogeneous iron core model were revealed at both 295 and 90 K (see Fig. 1). However, this model may be considered as a rough approximation due to a non-Lorentzian line shape of the spectra. Better fits were obtained applying the heterogeneous model. However, it was found in this case that the number of the quadrupole doublets needed to obtain the best-fit was different for different samples. For instance, using model (2) 3 doublets for Imferon, 4 doublets for ferritin and 5 doublets for Maltofer® and FerrumLek were necessary for the spectra measured at 295 K. These differences may be related to structural and/or size variations in the iron cores of the studied materials. It was also interesting to observe at 90 K a six-line subspectrum of Imferon which may be a result of an aggregation of iron-dextran complexes and/or an increase of the iron core size due to Imferon aging.

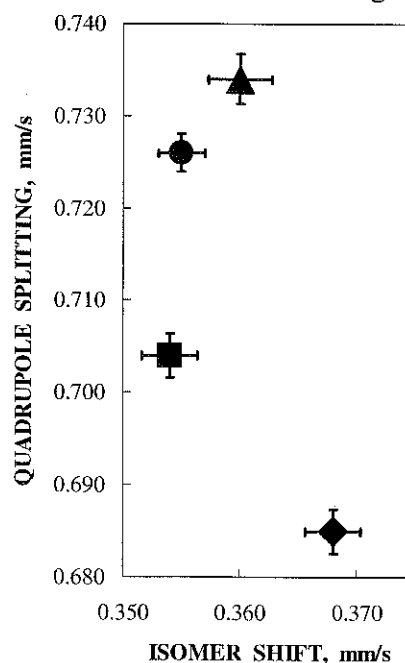


**Fig. 1.** Differences in Mössbauer hyperfine parameters at 295 K obtained from a one quadrupole doublet fit: human liver ferritin (◆), Imferon (■), FerrumLek (●) and Maltofer® (▲).

[1] M.I. Oshtrakh, V.A. Semionkin, O.B. Milder, E.G. Novikov. *J. Radioanal. Nucl. Chem.* 281 (2009) 63–67.

[2] V.A. Semionkin, M.I. Oshtrakh, O.B. Milder, E.G. Novikov. *Bull. Rus. Acad. Sci.: Physics*, 74 (2010) 416–420.





## Study of human, rabbit and pig oxyhemoglobins using high velocity resolution Mössbauer spectroscopy in relation to its structural and functional variations

M.I. Oshtrakh<sup>1</sup>, A. Kumar<sup>2</sup>, S. Kundu<sup>2</sup>, A.L. Berkovsky<sup>3</sup>, V.A. Semionkin<sup>1,4</sup>

<sup>1</sup>Faculty of Physical Techniques and Devices for Quality Control, Ural State Technical University – UPI, 620002, Ekaterinburg, Russian Federation

<sup>2</sup>Department of Biochemistry, University Delhi South Campus, Benito Juarez Road, New Delhi - 110021, India

<sup>3</sup>Hematological Research Center of the Russian Academy of Medical Sciences, 125167, Moscow, Russian Federation

<sup>4</sup>Faculty of Experimental Physics, Ural State Technical University – UPI, 620002, Ekaterinburg, Russian Federation

Mössbauer spectroscopy is an indispensable tool to study iron electronic structure in biological molecules. Hemoglobin is being studied using Mössbauer spectroscopy for about fifty years now. However, there are several open questions that demand attention. For instance, it is interesting to investigate the relationship of the heme iron electronic structure, stereochemistry and functional properties in various hemoglobins. Recently new possibilities of Mössbauer spectroscopy with a high velocity resolution in revealing small variations of Mössbauer hyperfine parameters and the iron electronic structure were demonstrated in [1]. Therefore, in this work we present for the first time results of comparative study of three different mammalian oxyhemoglobins using Mössbauer spectroscopy with a high velocity resolution in relation to its structures and functions.

Mössbauer spectra of human, rabbit and pig oxyhemoglobins were measured at 90 K using automated precision Mössbauer spectrometric system with a high velocity resolution (in 4096 channels) [2]. Then spectra were presented in 1024 channels by consequent summation of 4 neighboring channels. Spectra were fitted in two ways using one quadrupole doublet (model of equivalent iron electronic structure in  $\alpha$ - and  $\beta$ -subunits of hemoglobins) and superposition of two quadrupole doublets (model of non-equivalent iron electronic structure in  $\alpha$ - and  $\beta$ -subunits of hemoglobins). Mössbauer hyperfine parameters of oxyhemoglobins obtained within the first model demonstrated small variations which correlated with known values of oxygen affinity ( $P_{50}$ ) (see Fig. 1). These results as well as differences of Mössbauer hyperfine parameters obtained within the second model were analyzed in relation to  $P_{50}$  values and structural variations of human, rabbit and pig oxyhemoglobins. These results may also be useful in further analysis of patient's hemoglobins.

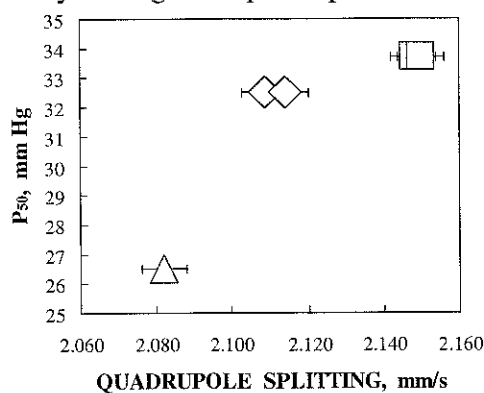


**Fig. 1.** Correlation of quadrupole splitting at 90 K and oxygen affinity for human ( $\Delta$ ), rabbit ( $\diamond$ ) and pig ( $\square$ ) oxyhemoglobins.

This work was supported in part by the Russian Foundation for Basic Research (grant # 09-02-00055-a).

- [1] M.I. Oshtrakh, V.A. Semionkin, O.B. Milder, E.G. Novikov. *J. Mol. Struct.* 924–926 (2009) 20–26.  
 [2] V.A. Semionkin, M.I. Oshtrakh, O.B. Milder, E.G. Novikov. *Bull. Rus. Acad. Sci.: Physics*, 74 (2010) 416–420.



## Infrared spectral microscopy of cancerous kidney tissues

V. Šablinskas<sup>1</sup>, V. Urbonienė<sup>1</sup>, E. Kaveckaitė<sup>1</sup>, F. Jankevičius<sup>2</sup>, G. Steiner<sup>3</sup> and L. Kimtys<sup>1</sup>

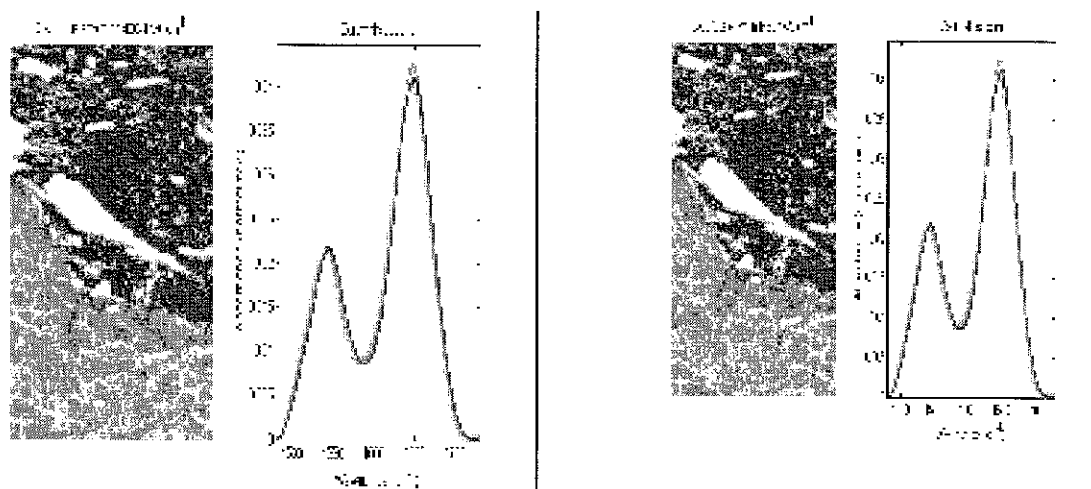
<sup>1</sup>Faculty of Physics, Vilnius University, Saulėtekio av. 9, 10222, Vilnius, Lithuania

<sup>2</sup>Vilnius University Hosp. Santariskių klinikos, Vilnius University, Santariškių str. 2, 08661, Vilnius, Lithuania

<sup>3</sup>Faculty of Medicine, Dresden University of Technology, Fiedlerstraße 42, D-01307 Dresden, Germany

Modern infrared spectroscopy combined with infrared microscopy allows to investigate features of the samples in the micrometric scale. Just recently this method was started to be applied for the studies of biological tissues [1-2]. Determination of the spatial distribution of different chemical components in the biological tissues is possible by using this method because of high sensitivity what enables to identify tumors even in very early stage of this disease.

Early diagnosis of the tumour is very important for its prevention or successful curing of the patient. Biochemical changes in various tumors usually are very different [1]. Chemical information obtained by means of the infrared spectroscopical microscopy is information of the molecular level taken from volume of the sample sized to micrometric scale.



In this work we used the ratio of Amide 1 and Amide 2 infrared absorption bands for distinguishing of cancerous tissue of kidney from the normal one (Fig 1 (a)). The changes in this ratio are small, but various statistical methods applied to large amount of the infrared spectra captured during the imaging allow to define border between the cancerous and healthy tissue (Fig 1 (b)) with higher precision than it is done using standard histopathological methods.

[1] M. Romeo et al, Infrared and Raman Micro-spectroscopic Studies of Individual Human Cells. In: Vibrational Spectroscopy in Medical Diagnosis, M. Diem, P.R. Griffith, J. Chalmers (eds.), 2008.

[1] G. Steiner, Identification and classification of human neural stem cells by infrared spectroscopic imaging, Proceedings of SPIE (7169-31), 2009.



## The label-free Raman imaging of human breast cancer

H. Abramczyk,<sup>1,2\*</sup> B. Brożek-Płuska,<sup>1</sup> J. Surmacki,<sup>1</sup> J. Jabłońska<sup>3</sup> and R. Kordek<sup>3</sup>

*1*Technical University of Lodz, Institute of Applied Radiation Chemistry, Laboratory of Laser Molecular Spectroscopy, Wroblewskiego 15, 93-590 Lodz, Poland.

*2*Max Born Institute, Max-Born Strasse 2A, D 12489 Berlin, Germany.

*3*Medical University of Lodz, Department of Pathology, Chair of Oncology, Paderewskiego 4, 93-509 Lodz, Poland.

Here we report the Raman ‘optical biopsy’ images of the normal and malignant human breast tissue of the same patient that has a potential to replace a conventional biopsy. The results demonstrate the ability of label-free Raman spectroscopy (RS) to accurately characterize cancer tissue and distinguish between normal, and malignant types. The results provide evidence that the composition of carotenoids and lipids of cancerous breast tissues differs significantly from that of the surrounding normal tissue and may be related to key factors responsible for mechanisms of carcinogenesis. We have found that the fatty acid composition of cancerous human breast tissue was greatly different from that of the corresponding normal tissue, with the concentration of unsaturated fatty acids higher in the normal tissue. In contrast, the concentration of saturated fatty acids is higher in the cancerous tissue. Up to date the present study is the most statistically reliable Raman analysis in the world based on data for 145 patients [1-4].

[1] H. Abramczyk, J. Surmacki, B. Brożek-Płuska, Z. Morawiec, M. Tazbir, *J. Mol. Struct.* **2009**, 924-926, 175-182.

[2] H. Abramczyk, I. Placek, B. Brożek-Płuska, K. Kurczewski, Z. Morawiec, M. Tazbir, *Spectroscopy* **2008**, 22, 113-121.

[3] B. Brożek-Płuska, I. Placek, K. Kurczewski, Z. Morawiec, M. Tazbir, H. Abramczyk, *J. Mol. Liq.* **2008**, 141, 145-148.

[4] H. Abramczyk, I. Placek, B. Brożek-Płuska, K. Kurczewski, Z. Morawiec, M. Tazbir, *ISRAPS Bulletin* **2008**, 20, no.1.



## Visualization of collagen molecule orientation in wrinkled skin using a polarization-resolved second-harmonic-generation microscope

T. Yasui, T. Araki

Graduate School of Engineering Science, Osaka University, 1-3 Machikaneyama-cho, Toyonaka, Osaka 560-8531, Japan

Non-invasive methods for in vivo inspection of dermal collagen molecule are necessary in the fields such as dermatology and skin cosmetic development. Among the various probes, we are focusing on an optical probe to investigate the relation between wrinkle direction and collagen orientation in photo-aged mouse skin. For that purpose, we have developed a new microscope that detects orientation of the collagen molecule based on second-harmonic-generation (SHG) light.

Figure 1 shows the polarization-resolved SHG microscope. A mode-locked Cr:Forsterite laser (center wavelength 1250nm, pulse width 90fs, repetition rate 73MHz) is employed to generate SHG signal in the sample. The laser beam is scanned in two dimensions by a pair of galvano mirrors and focused in the sample. The focus portion is also scanned in Z direction by a PZT stage, resulting in construction of optical 3D sectioning images of SHG light. For the polarization measurement of the SHS light, a half waveplate for 1250 nm is inserted in the optical path and used for polarization control of the laser light. As a model of photo-aging sample, UVB-exposed albino hairless mice were used. Winkles were induced by repetitive low-dose of UVB irradiation to the back of the mice according to Kligman [1].

To investigate the collagen orientation quantitatively, polarization anisotropy ( $\alpha$  value),  $\alpha = (IV-IH)/(IV+IH)$ , was used [2], where IV and IH are SHG intensities when the incident light is vertically and horizontally polarized, respectively. Collagen orientation is uniaxial for  $\alpha = \pm 1$  and random or biaxial for  $\alpha = 0$ .

The UVB treatment for 10 weeks resulted in the generation of deep wrinkles perpendicular to the meridian line of the body. Figure 2 shows typical images of the control and photo-aging mouse skin, where the reflection images are shown together with ordinary SHG and polarization anisotropic image ( $\alpha$  image).

The color scale indicates the direction of collagen orientation, with the vertical direction indicated by blue, horizontal by red and neutral by white. There are significant differences in  $\alpha$  images between the control and photo-aging skin, although the differences are ambiguous in the reflection and ordinary SHG images. The  $\alpha$  image indicates that the orientation of dermal collagen fibers is parallel to wrinkle direction in photo-aged skin. This also indicates that the polarization-resolved SHG microscope becomes a powerful tool for inspection of dermal collagen.

This work was supported by Grants-in-Aid for Scientific Research No. 20240044 from Japan Society for the Promotion of Science (JSPS).

[1] L. H. Kligman, *J. Am. Acad. Dermatol.* 21 (1989) 623.

[2] T. Yasui, Y. Tohno, and T. Araki, *Appl Opt* 43 (2004) 2861.

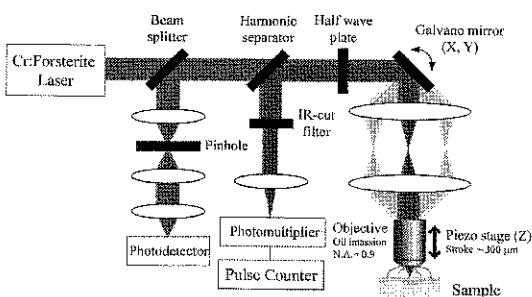


Fig. 1. Polarization-resolved SHG

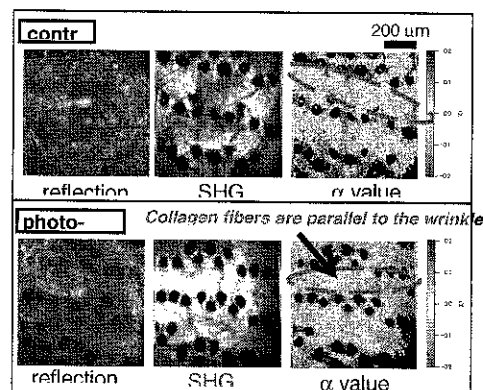


Fig. 2. Reflection, ordinary SHG and  $\alpha$  images at depth of 150 $\mu$ m from the skin surface of control and UVB-exposed mouse of 16 weeks old



## Combined micro-Raman and EDXRF study of characterization of mineralized tissue of human bone of osteoporosis patients

M. S. Ozel<sup>1</sup>, A. E. Ozel<sup>2</sup>, S. Akyuz<sup>3</sup> and T. Akyuz<sup>3</sup>

<sup>1</sup>Haydarpasa Numune Education and Research Hospital, 34860, Istanbul, Turkey

<sup>2</sup>Istanbul University, Faculty of Science, Department of Physics, Vezneciler, 34134, Istanbul, Turkey,

<sup>3</sup>Kultur University, Faculty of Science and Letters, Department of Physics, Atakoy Campus, 34156 Istanbul, Turkey

Osteoporosis is a disease of bone that leads to enhanced bone fragility and a consequent increase in fracture risk. In osteoporosis the bone mineral density is reduced, bone micro-architecture is deteriorated and the amount and variety of proteins in bone is altered [1]. Hip fractures are the most frequent fractures of elderly people, and its frequency tends to be increase. These injuries which cause hip fracture in elderly people are low-energy type and mostly detected after simple fall-down at home. In osteoporosis, the bone mass decrease have been demonstrated with radiologic techniques indirectly according to its radiolucens which was depends on the amount of calcium. In this study, patients with hip fractures were evaluated and all patients had same history like simple fell-down at home, had comorbidities, and had not used any medical treatment for osteoporosis.

In this study combined micro Raman and EDXRF spectroscopy techniques have been used to characterize developmental changes in bone and other mineralized tissues. Raman spectroscopy provides information about the molecular structure of the sample to be investigated. Alterations in cell behavior which involve changes in the biochemistry of the cells are reflected in the Raman spectra. EDXRF analysis of the samples provides us information about elemental concentrations, and to evaluate Ca/P ratios. For this aim, human femoral bone of 10 patients (6 male and 4 female) that have severe osteoporosis, in the age range of 53-85, have been investigated. These patients have not experienced any other disease, and did not have any medical cure for osteoporosis. Femoral heads which had been excised previous hip arthroplasty, were cut in two pieces with an osteotom in the line of coronal plane under sterile condition. Specimens were taken at the mid-point between center of the femoral head and subchondral bone and have homogen trabecular structure. Raman spectroscopic results indicate alterations in amide (I and III) and collagen bands together with those arising from phosphate and carbonate vibrations, depending on the bone mineral density alterations. Combined Raman and EDXRF study is found to be useful to shed in light for elemental and structural features in osteoporosis bone.

**Acknowledgement:** This study was supported by the Research fund of Istanbul University (Project number ONAP-2423).

[1] M. A. Krieg, R. Barkmann, S. Gonnelli, A. Stewart, D. C. Bauer, L. Del Rio Barquero, J. J. Kaufman, R. Lorenc, P. D. Miller, W. P. Olszynski, C. Poiana, A.-M. Schott, E. M. Lewiecki, and D. Hans, *J. Clin. Densitom. Assess. Skelet. Health*, 11 (2008)163.



## Bioactivity of montmorillonite - chitosane nanocomposite materials for regenerative medicine

C. Paluszkiwicz<sup>1</sup>, E. Stodolak<sup>1</sup>, J.W.M. Kwiatek<sup>2</sup>, P. Jeleń<sup>1</sup>

<sup>1</sup>AGH – University of Science and Technology, Faculty of Materials Science and Ceramics, Al. Mickiewicza 30, 30-059 Krakow, Poland

<sup>2</sup>Institute of Nuclear Physics PAN, ul. Radzikowskiego 152, 31-342 Kraków, Poland

The search of materials fulfilling requirements of the regenerative medicine is a still actual issue in biomaterials engineering. Novel materials for regenerative medicine are usually composites or nanocomposites. Their main task is to stimulate damaged tissue for faster regeneration caused by enhanced activity of cells prone to intense proliferation within the defect area. One of the main demands of such materials is bioactivity, which accelerates fixation between the material and surrounding tissue.

Biomaterials basing on natural polysaccharides, i.e. hyaluronic acid, alginate, chitosane are an alternative for already applied bioresorbable synthetic materials basing on synthetic polyhydroxyacids such as polylactide (PLA) or polycaprolacton (PCL). Their main advantages are good accessibility, low cost, easy forming and high biocompatibility. Additionally, they are a perfect matrix for bioactive nanoparticles i.e. hydroxyapatite (HAp) and SiO<sub>2</sub>.

The work presents results of research on bioactivity of a composite consisting of chitosane matrix (CS) modified with a nanofiller, which was natural montmorillonite (MMT). Nanocomposite foils were produced by the casting method. In order to induce better biocompatibility, the surface of the CS/MMT composite was neutralized. The nanocomposite foils were subjected to a bioactivity test by incubation in SBF at 37°C for 7 days. It was observed that the CS/MMT material surface showed a local supersaturation, which was a result of hydroxyapatite nucleation. The CS/MMT nanocomposites were investigated using FT-IR (Fourier Transform Infrared Spectroscopy) and PIXE (Proton Induced X-ray Emission) techniques.

The FTIR microscopy spectra were collected using Bio-Rad Excalibur with microscope UMA500 equipped with MCT detector. FTIR measurements of the samples were carried out on the transmission and reflection modes. Spectra were measured at 4 cm<sup>-1</sup> resolution in the region from 4000 cm<sup>-1</sup> to 700 cm<sup>-1</sup>.

The PIXE analysis were obtained with 2 MeV proton beam from the van de Graaff accelerator was directed to the sample for a multi-trace element analysis. All the spectra were detected with the energy resolution of 190 eV for the 5,9 keV X-ray. The normalization were realized on the basis of detected back-scattered protons. Both the X-ray and back-scattered protons were registered with CAMAC system.

Both techniques were used to determine structural changes of the polymer matrix caused by the presence of MMT, and to characterize the effect of neutralization of the nanocomposite surface. The last step of investigation was a study the nanocomposite surface and their interaction with simulated body fluid (SBF). Both techniques confirmed the presence of groups characteristic for apatite on the nanocomposite surface.

This work was supported by The Ministry of Science and Higher Education, grant No. N N507 370735



## Antibacterial peptides in interaction with model membranes studied by various spectroscopic methods

L. Bednářová<sup>1</sup>, P. Maloň<sup>1</sup>, H. Dlouhá<sup>1</sup>, M. Kubáňová<sup>1,2</sup>, P. Mojžeš<sup>2</sup>, E. Kočišová<sup>2</sup>,  
K. Hofbauerová<sup>2,3</sup>, V. Kopecký Jr.<sup>2</sup>

<sup>1</sup>Institute of Organic Chemistry and Biochemistry, Academy of Sciences of the Czech Republic, Flemingovo náměstí 2, Prague 6, 166 10, Czech Republic; bednarova@uochb.cas.cz

<sup>2</sup>Institute of Physics, Faculty of Mathematics and Physics, Charles University in Prague, Ke Karlovu 5, Prague 2, 121 16, Czech Republic

<sup>3</sup>Institute of Microbiology AS CR, Vídeňská 1083, Prague 4, 142 20, Czech Republic

Naturally occurring antimicrobial peptides (AMPs) represent one successful form of chemical defense of eukaryotic cells against bacteria, protozoa, fungi, and viruses [1]. Many of them have been already isolated, thousands of their synthetic analogs were synthesized and a broad spectrum of their antimicrobial, anticancer and antiviral activities was proven [2, 3]. In spite of large number of known AMPs and their therapeutic potential, exact mechanism of their action remains a matter of controversy. There is a consensus that these peptides selectively disrupt cell membranes and it is believed that their amphiphatic structure plays an important role in this process.

Interaction of peptides with membranes or their models leads to changes of their secondary structure, which could be detected using various spectroscopic methods. Here we present spectroscopic studies of novel AMPs isolated from the venom of cleptoparasitic bee *Melecta albifrons* (melectin) [4], eusocial bees *Lasioglossum laticeps* (lasioglossins) [5] and *Halictus sexcinctus* (halictines) [6] and solitary bee *Macropis fulvipes* (macropin) [7]. All these peptides exhibited potent antimicrobial activity against Gram-positive and Gram-negative bacteria. On the other hand their hemolytic activities are different. Our aim is to study these peptides in interaction with model phospholipids membranes using spectroscopic methods as circular dichroism, infrared and Raman spectroscopy, and in that way contribute to clarification of these differences.

**Acknowledgement:** The Grant Agency of the Czech Republic is acknowledged (No. P208/10/0376).

- [1] M. Zasloff, Nature 415 (2002) 389–395
- [2] R. E. Hancock, G. Diamond, Trends Microbiol. 9 (2000) 402–410
- [3] R. E. Hancock, M. G. Scott, Proc. Natl. Acad. Sci. U.S.A. 97 (2000) 8856–8861
- [4] V. Cerovsky, O. Hovorka, J. Cvacka, Z. Voburka, L. Bednářová, L. Borovickova, J. Slaninova, V. Fucik, ChemBioChem 9 (2008) 2815–21
- [5] V. Cerovsky, M. Budesinsky, O. Hovorka, J. Cvacka, Z. Voburka, J. Slaninova, L. Borovickova, V. Fucik, L. Bednarova, I. Votruba, J. Straka, ChemBioChem 10 (2009) 2089–99
- [6] L. Monincova, M. Budesinsky, J. Slaninova, O. Hovorka, J. Cvacka, J. Voburka, J. Fucik, L. Borovickova, L. Bednarova, J. Straka, V. Cerovsky, AminoAcids (2010) accepted
- [7] L. Monincova, J. Slaninova, Z. Voburka, Biologically Active Peptides XI, 2009, Book of Abstracts, p 49



## Spectroscopic investigations of newly formed guest-host type complexes as potential anti skin cancer candidates

A. Falamas<sup>1</sup>, S. Cîntă Pînzaru<sup>1</sup>, C. Dehelean<sup>2</sup>, A. Bebu<sup>1</sup>

<sup>1</sup>Faculty of Physics, Babes-Bolyai University, Kogalniceanu 1, RO-400084 Cluj-Napoca, Romania

<sup>2</sup>Victor Babes University of Medicine and Pharmacy, Eftimie Murgu Square 2, RO-30004 Timisoara, Romania

This study is intended to investigate the recently formed guest-host type compounds based on betulin (lup-20(29)-ene-3 $\beta$ ,28-diol), main pentacyclic triterpene found in the outer bark of the birch tree [1] and hidroxy-propyl-gamma-cyclodextrin (HPGCD). These inclusion complexes are meant for creating pharmaceutical compounds to be tested on skin malignancies, including melanoma and skin cancer, since betulin has proved to have benefic effects in skin treatments and closed inhibitory activity on proliferation of tumour cells [2, 3].

Pentacyclic triterpenes have a low hidrosolubility that can be resolved by molecular encapsulation in cyclodextrins. Upon creating pharmaceutical compounds using these species, a detailed vibrational investigation is needed. This could help us gain a better insight on the interaction mode of the two molecules, which can be of great importance in pharmaceutical formulation that may heal different skin malignancies or even cancer. This analysis is based on DFT calculations, FT-Raman and FT-IR investigations of betulin and cyclodextrin and of the 1:1 and 1:2 molecular ratios kneading products.

Upon the analysis of the spectra, we have concluded that the kneading products show characteristic features to both betulin and pure cyclodextrins, suggesting the formation of new supramolecular assembly.

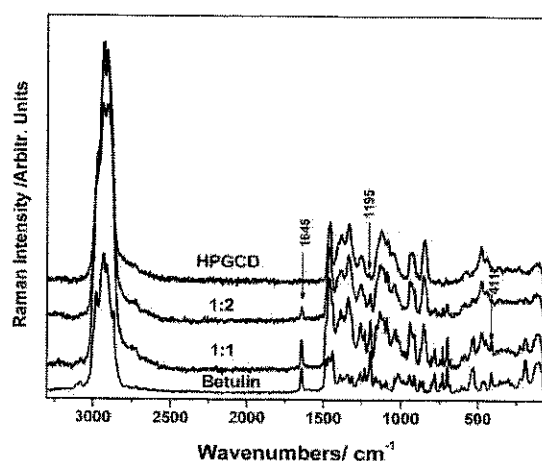


Fig.1. FT-Raman spectra of betulin, HPGCD and their kneading products (1:1 and 1:2 molecular ratios, respectively).

**Acknowledgement:** This study was financially supported by the PN II- ID\_2284, nr.538/2008 grant from CNCSIS, Romania.

[1] S. Cîntă Pînzaru, N. Leopold, W. Kiefer, *Talanta*, 57, (2002), 652-631.

[2] C. M. Soica, C. A. Dehelean, C. I. Peev, G. Coneac, A. T. Gruia, *Farmacia*, 56, 2, (2008), 182.

[3] C. Dehelean, I. Zupko, B. Réthy, C. Soica, G. Coneac, C. Peev and B. Bumbacila, *Toxicology Letters*, 180, 1, (2008), S100.





## The comparison of the binding properties of native and destabilized serum albumins

J.Równicka-Zubik <sup>1</sup>, A.Sułkowska <sup>1</sup>, E.Kurek <sup>1</sup>, M.Maciażek-Jurczyk <sup>1</sup>, B. Bojko <sup>1</sup>, W.W. Sułkowski <sup>2</sup>

<sup>1</sup> Department of Physical Pharmacy, Faculty of Pharmacy, Medical University of Silesia, Jagiellońska 4, 41-200 Sosnowiec, Poland

<sup>2</sup> Department of Environmental Chemistry and Technology, Institute of Chemistry, University of Silesia, Szkolna 9, 40-006 Katowice, Poland

Sulindac (SDK) - {(1Z)-5-fluoro-2-methyl-1-[4-(methylsulfinyl) benzylidene]-1H-indene-3-yl} acetic acid is one of the NSAID (non-steroidal anti-inflammatory drug), useful in the treatment of chronic and acute inflammatory conditions. Binding of sulindac (SDK) to human (HSA) and bovine serum albumin (BSA) were studied by fluorescence spectroscopy and results were compared with those obtained with HSA and BSA after chemical destabilization. To destabilize of tertiary structure of albumins urea (U) and guanidine hydrochloride (Gu.HCl) at concentration from 1.0 to 7.2M were used. Binding ( $K_B$ ) and quenching ( $K_Q$ ) constants for analyzed complexes (BSA-SDK, BSA(U)-SDK, BSA(Gu.HCl)-SDK, HSA-SDK, HSA(U)-SDK, HSA(Gu.HCl)-SDK), were calculated on the basis of Scatchard and Stern-Volmer method, respectively. The most intensive interaction was observed in the complex BSA-SDK (for excitation 295 nm). Then the values of  $K_B$  and  $K_Q$  were  $45.18 \cdot 10^3 [M^{-1}]$  and  $95.24 \cdot 10^3 [M^{-1}]$ , respectively. In the presence of 1.0M urea ( $K_B$ ) was  $52.76 \cdot 10^3 [M^{-1}]$  and ( $K_Q$ ) was  $25.98 \cdot 10^3 [M^{-1}]$ . An addition of 1.0 M Gu.HCl to the complex BSA-SDK caused then change of the value of calculated constants: ( $K_B$ ) was  $38.75 \cdot 10^3 [M^{-1}]$  and ( $K_Q$ ) –  $17.65 \cdot 10^3 [M^{-1}]$ . Sulindac has the tendency to interact with SA within the hydrophobic subdomain IIA (for the systems with HSA) and/or IB (for the systems with BSA). Only one class of binding sites was observed in binding SDK with both native and destabilized by chemical factors albumins (HSA and BSA). The analyze of the binding and quenching constants allow us to assume that the studied albumins preserve their binding capacity in the presence of destabilizing/denaturing agents. An evaluation of the binding ability of SA is important for a safe and effective therapy specially in uremic and diabetic patients whose albumin undergo the structural disorders due to chronic and lives diseases.

**Acknowledgements:** This work was supported by the grants of Medical University of Silesia: KNW -1-.008/09 and KNW-2- 201/09.



## Polypharmacotherapy in rheumatology. $^1\text{H-NMR}$ analysis of binding of phenylbutazone and methotrexate to serum albumin

M. Maciążek-Jurczyk<sup>1</sup>, A. Sułkowska<sup>1</sup>, B. Bojko<sup>1</sup>, J. Równicka-Zubik<sup>1</sup>, W. W. Sułkowski<sup>2</sup>

<sup>1</sup>Department of Physical Pharmacy, Medical University of Silesia, Jagiellońska 4, 41-200 Sosnowiec, POLAND,

<sup>2</sup>Department of Environmental Chemistry and Technology, Institute of Chemistry, University of Silesia, Szkolna 9, 40-006 Katowice, POLAND

In the present studies we investigated the influence of phenylbutazone (Phe) and methotrexate (MTX) on MTX and Phe binding to human (HSA) and bovine (BSA) serum albumin in its low affinity binding sites. Using  $^1\text{HNMR}$  spectroscopy we found the strength and kind of interactions between serum albumin and drugs used in combination therapy in the low affinity. The results showed an important impact of another drug (MTX or Phe) on the affinity of SA towards Phe and MTX in the low affinity binding sites. This alteration should be taken into account in multi-drug therapy due to the possible increase of the uncontrolled toxic effects of drugs.

This work is a subsequent part of the spectroscopic study on Phe-MTX-SA interactions [M. Maciążek-Jurczyk et al., J. Mol. Struct. 924-926 (2009) 378-384].

**Acknowledgements:** This work was supported by the grants of Medical University of Silesia KNW -1-.008/09 and KNW-2- 163/09.



## Vibrational (Raman and SERS) and electronic UV study on triazine herbicides

M. Di Foggia<sup>1</sup>, E. Benassi<sup>2</sup>, S. Bonora<sup>1</sup>, S. Ottani<sup>3</sup>

<sup>1</sup>Department of Biochemistry, University of Bologna, via Belmeloro 8/2, 40126, Bologna, Italy

<sup>2</sup>S3 Center, INFN-CNR, via Campi 213, 41125, Modena, Italy

<sup>3</sup>ISOF-CNR, via Gobetti 101, 40129, Bologna, Italy

The triazine group is a well known class of herbicides and has been widely used for more than 40 years. Atrazine, and the later introduced simetryn and prometryn are the most used triazine herbicides. These chemicals inhibit photosynthesis in plants by blocking the electron transfer at the reducing site of chloroplast photosystem II.

In this paper we studied the SERS spectra of the herbicides on silver colloidal suspension, resulting from the controlled hydroxylamine reduction of silver nitrate. Also Raman and UV spectra were recorded for the three herbicides in the solid and in solution. We performed extensive computations by *ab initio*, molecular mechanics and dynamics methods on the three herbicides alone and in solution.

The vibrational and electronic spectra obtained by the computational methods provided substantial support in the interpretation of the binding mechanism of herbicides to metal.

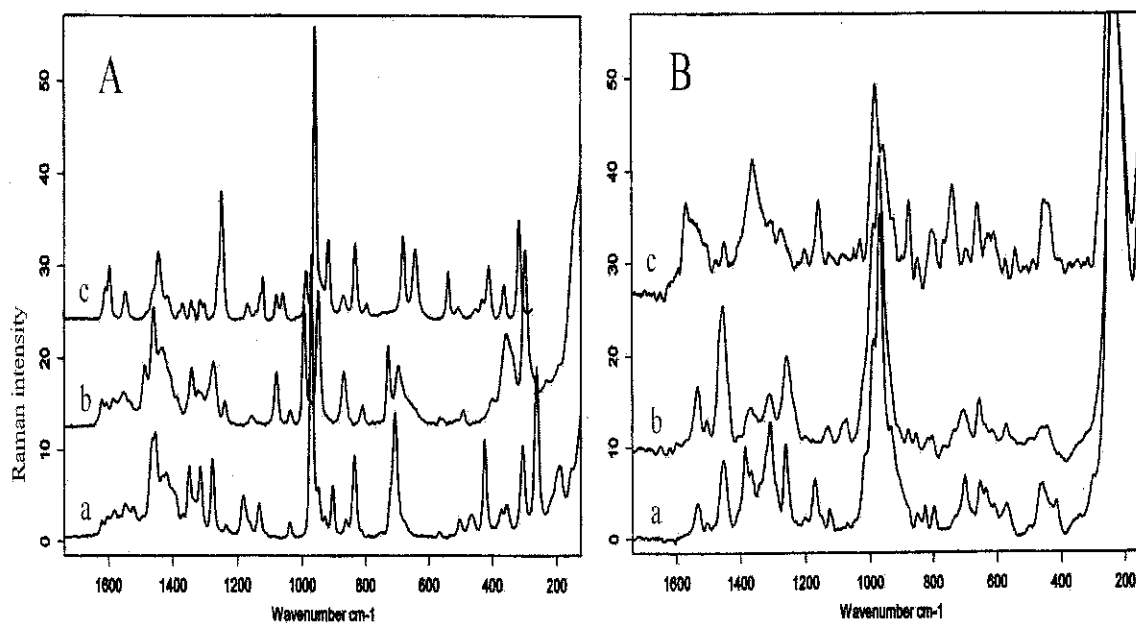


**Figure 1.** 150 – 1100  $\text{cm}^{-1}$  spectral region of: A): Raman spectra of solid prometryn (a); simetryn (b) and atrazine (c); B) SERS spectra (200 ppm in water) of: prometryn (a); simetryn (b) and atrazine (c).

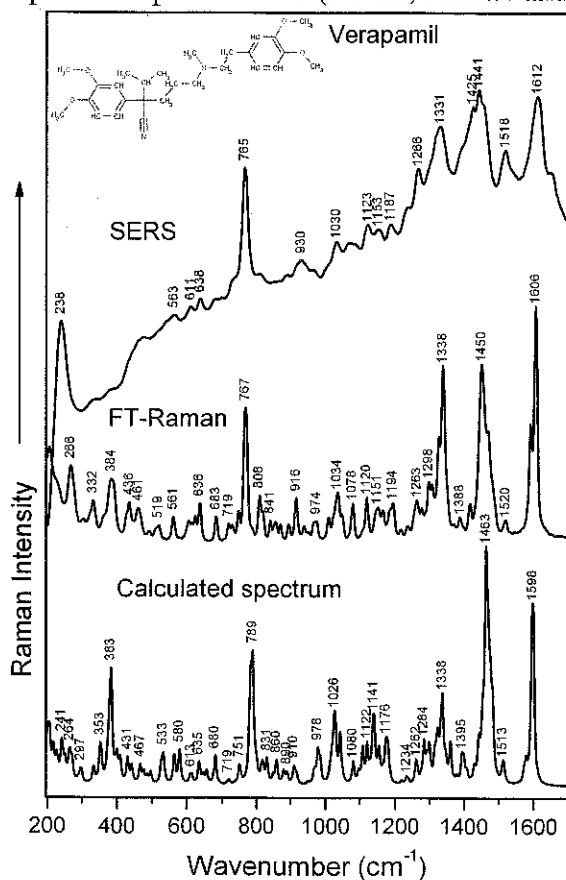
## IR, SERS and DFT Study of Pindolol and Verapamil Drugs

I. B. Cozar, L. Szabó, O. Cozar, N. Leopold, V. Chiş, L. David

Babeş-Bolyai University, Faculty of Physics, Kogălniceanu 1, 400084 Cluj-Napoca, Romania

Pindolol (PIN) and verapamil (VER) are most frequently used drugs in the treatment of cardiovascular diseases. They are selective beta receptor blockers used for various indications, but particularly for the management of cardiac arrhythmias, cardio protection after myocardial infarction (heart attack), and hypertension. These drugs block chemicals, such as adrenaline, and prevent thus from increasing heart rate, blood pressure, and oxygen use [1].

For a better understanding of their activity, structural investigation by different spectroscopic methods (FT-IR, Raman and SERS) was performed.



Density Functional Theory (DFT) methods are increasingly applied to representative pharmacological compounds aiming to elucidate their molecular structures and electronic properties and to describe the influence of electronic and structural factors on the reactions in which these compounds are involved. These studies contribute to the understanding of the structure-activity relationships and the behavior of the investigated system [2, 3].

The molecular vibrations of PIN and VER were investigated by FT-IR/ATR, FT-Raman and SERS spectroscopies. The inserted figure shows the Raman and SERS spectra of verapamil recorded using a 532 nm laser line. In parallel, quantum chemical calculations based on DFT are used to determine the geometrical, energetic and vibrational characteristics of the molecule.

The vibrational spectra of the PIN and VER molecules were assigned based on DFT calculations at B3LYP level of theory using the standard 6-31G(d) basis set. The experimental vibrational bands of both compounds were assigned to the calculated normal modes and a very good correlation was achieved between the experimental and theoretical data. The molecular electrostatic potential of the molecules was calculated and used for predicting site candidates of electrophilic attack.

The enhancement in the SERS spectra of the ring stretching vibration at  $1612\text{ cm}^{-1}$  and the ring breathing vibration at  $785\text{ cm}^{-1}$  indicate a perpendicular adsorption of the aromatic rings to the silver surface.

[1] K. Kneipp, H. Kneipp, I. Itzkan, R.R. Dasari, M.S. Feld. *Chem. Rev.*, 99, 2957(1999)

[2] V. Chiş, S. Filip, V. Miclăuş, A. Pîrnău, C. Tănăselia, V. Almăşan, M. Vasilescu, *J. Mol. Struct.*, 363, 744 (2005)

[3] L. Szabó, V. Chiş, A. Pîrnău, N. Leopold, O. Cozar, Sz. Orosz, *J. Mol. Struct.*, 924–926, 361–370 (2009)

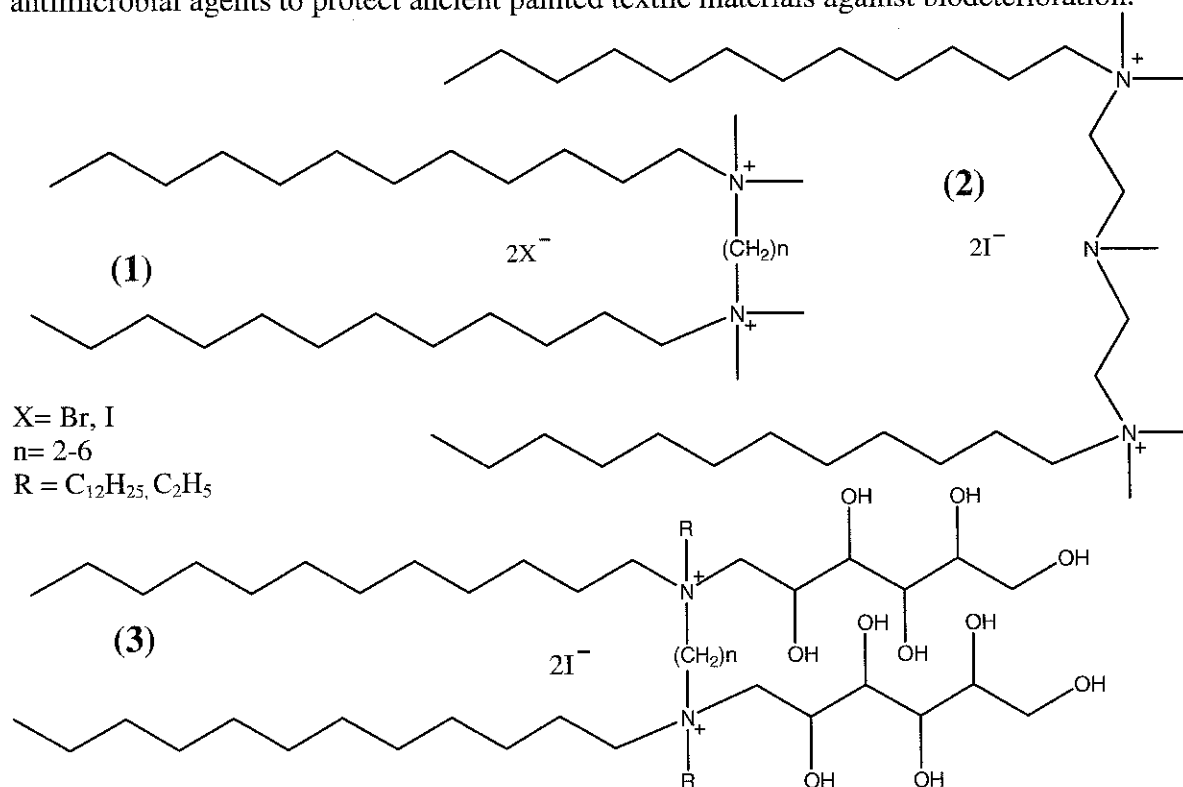


## Spectroscopic analysis of gemini alkylammonium salts with the antimicrobial activity

B. Brycki, I. Kowalczyk, A. Szulc

Laboratory of Microbiobiocides Chemistry, Faculty of Chemistry, A. Mickiewicz University,  
60780 Poznań, Poland

Gemini surfactants - nonionic, anionic and cationic - show unique surface properties concerning lower critical micelle concentration and surface tension, as well as better solubilization in comparison to monomeric surfactants. Moreover, gemini quaternary ammonium salts exhibit an excellent antimicrobial activity. The minimal biocidal concentrations, in many cases, are even hundreds times lower than  $MBC_t$  values for monomeric alkylammonium salts. The purpose of our study was to obtain gemini alkylammonium salts, with variable HLB and the lowest  $MBC_t$  values to use them as antimicrobial agents to protect ancient painted textile materials against biodeterioration.



Three series of gemini alkylammonium bromides and iodides (**1-3**), with different hydrophilic and hydrophobic substituents and spacers, have been synthesized. The detailed spectroscopy analysis (FTIR, ESIMS,  $^1\text{H}$  NMR,  $^{13}\text{C}$  NMR, 2D NMR) has been carried out. The obtained compounds have low CMC values and possess very good antimicrobial and antifungal activity.

- [1] G. Manivannan (ed) 2008. *Disinfection and Decontamination; Principles, Applications and Related Issues*, CRC Press Taylor & Francis Group, Boca Raton USA
- [2] W. Paulus (ed) 2005. *Directory of Microbiocides for the Protection of Materials. A. Handbook*, Springer, Dordrecht, The Netherlands
- [3] R. Zana, J. Xia, (eds), 2003, *Gemini Surfactants: Synthesis, Interfacial and Solution-Phase Behavior, and Applications*, Marcel Dekker, Basel, Switzerland



## Infrared spectroscopic study of HAMLET, a tumor-killing variant of $\alpha$ -lactalbumin

A. Hense<sup>1</sup>, A-K. Mossberg<sup>2</sup>, C. Svanborg<sup>2</sup>, A. Barth<sup>1</sup>

<sup>1</sup>*Department of Biochemistry and Biophysics, Stockholm University, Arrhenius Laboratories, 10691 Stockholm, Sweden*

<sup>2</sup>*Department of Biophysical Chemistry, Lund University, P.O. Box 124, 22100 Lund, Sweden*

Multifunctionality is an intriguing property of many proteins. The milk protein  $\alpha$ -lactalbumin provides a fascinating example: it is a component of the lactose synthase complex but can also be converted into a cytotoxic form - named HAMLET - under conditions which resemble those in the human stomach [1,2]. HAMLET kills cancer cells of different origins and may accordingly reduce the incidents of cancer in breast-fed children. In contrast, it is harmless to most differentiated cells. In spite of HAMLET being a promising tumouricidal agent, essential features of its structure are still not known. We have studied  $\alpha$ -lactalbumin and Hamlet with infrared spectroscopy. Absorption spectra were taken and the second derivative spectrum analysed.

The most obvious difference between HAMLET and  $\alpha$ -lactalbumin are two bands observed only for the latter at 1742 and 1726  $\text{cm}^{-1}$  which are characteristic of protonated carboxyl groups. These are not expected from the atomic structure of  $\alpha$ -lactalbumin where the carboxyl groups are on the surface of the protein. Therefore they are interpreted as resulting from aggregation which buries these groups in the interface between different protein units and protects them from bulk water. Observation of these bands only for  $\alpha$ -lactalbumin indicates that this protein has a stronger tendency to aggregate than HAMLET.

Spectra between HAMLET and  $\alpha$ -lactalbumin were similar but not identical in the amide I region of infrared absorption, which reflects protein secondary structure. This indicates a similar secondary structure of the two protein variants and in particular that the 3-stranded  $\beta$ -sheet is intact in HAMLET. H/D exchange was monitored over 6 days and revealed that this  $\beta$ -sheet is more flexible in HAMLET than in  $\alpha$ -lactalbumin in line with previous results on a shorter time scale [3]. Furthermore, all  $\alpha$ -helices in HAMLET are somewhat flexible, whereas this is true only for a subset of helices in  $\alpha$ -lactalbumin. The turns of HLA become more HAMLET-like upon heating HLA to 50°C. In the absorption region of C-H stretching vibrations, a higher mobility of aliphatic groups was detected for HAMLET, which was little affected by heating to 50°C. In contrast, the mobility increased for  $\alpha$ -lactalbumin.

[1] A. Håkansson, B. Zhivotovsky, S Orrenius, H. Sabharwal, C. Svanborg, Proc. Natl. Acad. Sci. USA 92 (1995) 8064-8068

[2] K. H. Mok, J. Pettersson, S. Orrenius, C. Svanborg, Biochem. Biophys. Res. Commun. 354 (2007) 1-7

[3] A. Casbarra, L. Birolo, G. Infusini, F. Dal Piaz, M. Svensson, P. Pucci, C. Svanborg, G. Marino, Prot. Sci. 13 (2004) 1322-1330



## Vibrational and electronic optical activity of amide and disulfide groups in neurohypophyseal hormones and their models

P. Maloň<sup>1</sup>, L. Bednárová<sup>1</sup>, M. Kubáňová<sup>1,2</sup>, M. Flegel<sup>1</sup>, J. Hlaváček<sup>1</sup>, V. Baumruk<sup>2</sup>

<sup>1</sup>*Institute of Organic Chemistry and Biochemistry, Academy of Sciences of the Czech Republic, Flemingovo nám. 2, 166 10, Prague 6, Czech Republic*

<sup>2</sup>*Institute of Physics, Faculty of Mathematics and Physics, Charles University in Prague, Ke Karlovu 5, Prague 2, 121 16, Czech Republic*

Vibrational and electronic circular dichroism spectra of neurohypophyseal hormones oxytocin, lysine-vasopressin, arginine-vasopressin, several of their analogs and structural models were measured in order to isolate chiroptical manifestation of their peptide backbone from the signals of aromatic chains of tyrosine and phenylalanine chromophores. We have also observed electronic disulfide-related ECD in the long wavelength spectral region and identified features in the spectra of Raman optical activity (ROA) which are associated with the S-S and C-S stretching vibrations. These allow us to infer the sense of disulfide twist in the particular compounds when signs of ROA features are compared to ROA calculations on simple model disulfides [1] and verified by a comparison with spectra of disulfide-bridged cyclodextrins.[2]

The results indicate that (a) there is a remarkable similarity and consistent spectral behavior of the whole family of neurohypophyseal hormones; (b) vibrational optical activity allows to observe chiroptical manifestation of neurohypophyseal hormone backbone without the harmful interference of aromatic groups; (c) vibrational optical activity indicates that the prevailing solution conformation of neurohypophyseal hormones is a short segment of left handed helix. This is in accord with analogous ECD result, however interference with the bands due to side chains of Tyr and Phe makes this observation less discernible;(d) the ROA signals in the S-S and C-S stretching vibration regions are observable also with neurohypophyseal hormones and their sign can be used to deduce the sense of disulfide twist.

**Acknowledgement:** The Grant Agency of the Czech Republic is acknowledged (No. P205/10/1276).

[1] L. Bednárová, P. Bouř, P. Maloň, *Chirality*, in press (2010).

[2] P. Maloň, L. Bednárová, M. Straka, L. Krejčí, L. Kumprecht, T. Kraus, M. Kubáňová, V. Baumruk, *Chirality*, accepted (2010).



## Spectroscopic study of blood after irradiation

N. Mironova-Ulmane<sup>1</sup>, M. Polakovs<sup>1</sup>, A. Pavlenko<sup>1</sup>, N. Kurjane<sup>2</sup>, E. Reinholds<sup>3</sup>, M. Grube<sup>4</sup>

<sup>1</sup>*Institute of Solid State Physics, University of Latvia, Riga, Latvia*

<sup>2</sup>*Centre of Radiol. Medicine of P.Stradins Clinical University Hospital, Latvia*

<sup>3</sup>*Nuclear Medicine Dep. P.Stradins Clinical University Hospital, Riga, Latvia*

<sup>4</sup>*Institute of Microbiology and Biotechnology, University of Latvia, Riga, Latvia*

In the present work we report results of measurements EPR, optical absorption spectra and FT-IR spectroscopy of blood of patients examined by radio-isotopes diagnosis ( $Tc_{99m}$ ).

Venous blood was donated by consenting patients before and after radio-isotopes diagnosis and collected under air in glass tubes containing a small amount of heparin used as an anticoagulant.

The EPR spectra were recorded using an EMX-6/1 spectrometer (BRUKER) working at X-band frequency with 100 kHz modulation. Magnetic field varied between 100 and 7000 Gauss. The g-factors of EPR signals were determined by reference to the external magnetic field. The EPR signal intensities in blood were measured against fixed standard signals using the standard crystal MgO - Cr<sup>3+</sup> placed in resonant cavity.

It is shown that in blood the ion Fe<sup>3+</sup> of methemoglobin is in low-spin state with  $g = 2.3$  and in the high spin state with  $g = 6$ . The EPR signal  $g = 4.3$  is assigned to transferrin Fe(III) ions. These data show that the blood of patients after radio-diagnosis has methemoglobin higher. Radiation of blood leads to the transition from hemoglobin (Fe<sup>2+</sup>) to methemoglobin (Fe<sup>3+</sup>).

This study could be continued applying priorities of infrared micro spectroscopy that hopefully can speed up the evaluation of influence of irradiation and other environmental effects on single erythrocyte cells. Results showed that the combined application of resonance Raman scattering and FT-IR spectroscopy a fruitful tool for determining structural modification hemoglobin by ionizing.





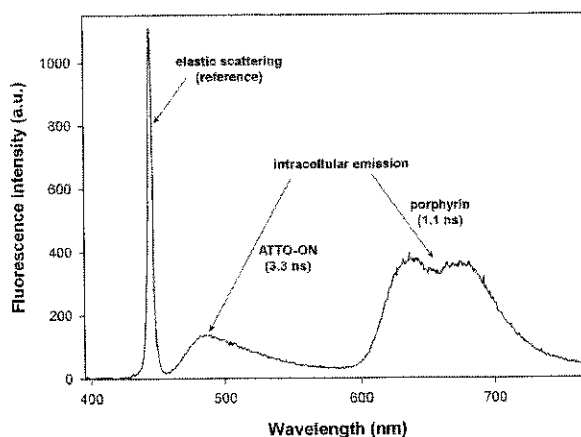
## Cellular uptake of modified oligonucleotides enhanced by zinc porphyrins studied by time-resolved microspectrofluorimetry and fluorescence imaging techniques

P. Praus<sup>1</sup>, E. Kočiřová<sup>1</sup>, P. Mojzeř<sup>1</sup>, J. Štěpánek<sup>1</sup>, F. Sureau<sup>2</sup>, P. Y. Turpin<sup>2</sup>

<sup>1</sup> Charles University in Prague, Faculty of Mathematics and Physics, Ke Karlovu 3, Prague 2, CZ-121 16, Czech Republic

<sup>2</sup> ANBioPhy (Acides Nucleiques & Biophotonique) – UPMC/CNRS FRE 3207 GENOPOLE Campus 1, 5, rue Henri Desbrières 91030 EVRY Cedex, France

Confocal microspectrofluorimeter has been adapted for time-resolved fluorescence measurements by using a phase-modulation principle and homodyne data acquisition method. This approach was employed to acquire intracellular spectra (see figure), which enabled us to determine lifetimes from selected intracellular sites. Modified oligonucleotides (ON) as sequences of chemically prepared deoxyribo- or ribonucleotides are able to regulate the gene expression [1]. Efficient cellular uptake is a key condition to fulfill its biological activity. Synthetic cationic derivatives of porphyrins seem to be one of the promising candidates as effective delivery enhancers. Zinc 5,10,15,20-tetrakis (1-methyl-4-pyridyl) porphyrin (ZnTMPyP4) assisted delivery system is now studied to be used for ON intracellular transport. Time-resolved fluorescence spectra of ATTO labeled ON and porphyrin can reveal interactions with present biomolecules [2]. Moreover, ZnTMPyP4 posses its own fluorescence that can be used to monitor after-delivery fate of both components of the complex. Fluorescence confocal microimaging has been complementarily employed to visualize penetration of the ON and porphyrin through the membrane and their distribution inside the cell.



**Acknowledgements:** The financial support from the Ministry of Education of the Czech Republic (No. MSM 00021620835) is gratefully acknowledged.

[1] J. Goodchild, *Curr. Opin. Mol. Ther.* 6 (2004) 120-8

[2] P. Praus et.al., *Ann. N.Y. Acad. Sci.* 1130 (2008) 117-121



## Synthesis and characterization of flower-shaped gold nanoparticles for applications as SERS-active tags in cellular spectral imaging

S. Boca<sup>1</sup>, D. Rugina<sup>2</sup>, A. Pinte<sup>2</sup>, L. B. Tudoran<sup>3</sup>, S. Astilean<sup>1</sup>

<sup>1</sup>Nanobiophotonics Center, Institute for Interdisciplinary Experimental Research in Nanobioscience, Faculty of Physics, Babes-Bolyai University, T. Laurian 42, 400271, Cluj-Napoca, Romania

<sup>2</sup>Department of Biochemistry, University of Agricultural Sciences and Veterinary Medicine, Manastur 3-5, 400372, Cluj-Napoca, Romania

<sup>3</sup>Electron Microscopy Center, Faculty of Biology and Geology, Babes-Bolyai University, Clinicilor 5-7, 400006, Cluj-Napoca, Romania

Gold nanoparticles are attractive for biological and biomedical applications because of their optical properties, chemical stability, and biocompatibility. Flower-like or star-shaped gold nanoparticles have recently drawn the attention due to their specific anisotropic shape which gives plasmon resonances within the near-infrared optical window (700–900 nm), transparent for biological tissue [1]. Moreover, the tips they present can efficiently amplify the electromagnetic field around them, enabling gold nanoflowers to be successfully used as surface enhanced Raman scattering (SERS) substrates for applications such as spectral diagnosis and imaging inside living organisms [2].

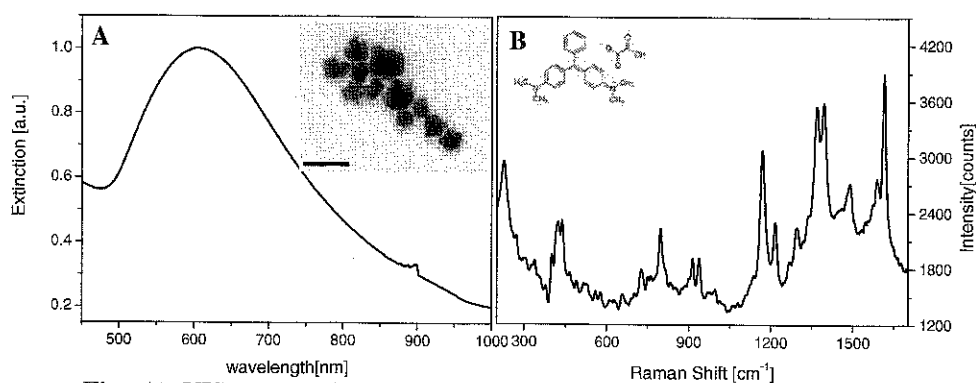


**Fig. A)** VIS-NIR Extinction spectrum of flower-like gold nanoparticles. Inset: TEM image of 20-40 nm gold nanoflowers. **B)** SERS spectrum of MGO adsorbed on gold nanoflowers. Inset: MGO molecular structure.

This work presents the synthesis and characterization of flower-like gold nanoparticles as seen in the inset TEM image in figure A, and demonstrates their applicability as SERS-active tags for cellular spectral imaging. The particles were synthesized by a facile, rapid new route that uses ascorbic acid as a reducing agent of gold salt. Malachite green oxalate (MGO) and basic fuchsin (BF) were used as Raman active molecules and the polymer mPEG-SH as capping material to enhance nanoparticle biocompatibility. As prepared SERS-active nanoparticles were found to be highly stable, to be detectable down to nanomolar particle concentrations under 633 and 785 nm laser excitation and to present low cytotoxicity *in vitro* as tested on a human retinal pigment epithelial cell line. Our studies highlight the potential of such Raman-active nanoparticles to serve as sensitive medical imaging tools.

**Acknowledgements.** This work was supported by CNCSIS under the project No. ID\_477/2007 in the frame of program PN-II-ID-PCE-2007-1

[1] C. L. Nehl, H. Liao, J. H. Hafner, *Nano Lett.* 6 (2006) 683-688

[2] J. Xie, Q. Zhang, J.Y. Lee, D. I. C. Wang, *ACS Nano* 2 (2008) 2473-2480



## Micro Raman spectroscopic investigation of the interaction of cultured HCT116 colon cancer cells with alpha- difluoromethylornithine (DFMO), an irreversible inhibitor of ornithine decarboxylase

S. Akyuz<sup>1</sup>, A. E. Ozel<sup>2</sup>, K. Balci<sup>2</sup>, T. Akyuz<sup>1</sup>, A. Coker<sup>3</sup>, E. D. Arisan<sup>3</sup>, N. Palavan-Unsal<sup>3</sup>, A. Ozalpan<sup>3</sup>

<sup>1</sup>Istanbul Kultur University, Department of Physics, Atakoy Campus, 34156 Bakirkoy, Istanbul, Turkey

<sup>2</sup>Istanbul University, Department of Physics, Vezneciler 34134, Istanbul, Turkey

<sup>3</sup>Istanbul Kultur University, Department of Molecular Biology and Genetics, Atakoy Campus, 34156 Bakirkoy, Istanbul, Turkey

The  $\alpha$ -difluoromethylornithine (DFMO) is an irreversible inhibitor of ornithine decarboxylase, the first enzyme in polyamine synthesis, would be effective as a chemotherapy for hyperproliferative diseases, like cancer and/or infectious processes. Recent clinical cancer chemoprevention studies indicate that DFMO can be given over long periods of time at low doses that suppress polyamine contents in gastrointestinal and other epithelial tissues. Current clinical chemoprevention trials are investigating the efficiency of DFMO to suppress surrogate end point biomarkers (e.g., colon polyp recurrence) of carcinogenesis in patient populations at elevated risk for the development of specific epithelial cancers, including colon, esophageal, breast, cutaneous, and prostate malignancies.

Raman spectroscopy has been widely used for characterizing living cells [1] and for investigation of drug induced effects on the living cells [2]. In this study concentration dependent interaction of cultured colon cancer cells with DFMO has been investigated for the first time using micro-Raman spectroscopy. The aim of this study is to investigate DFMO induced alterations in the cells.

Raman spectra were recorded on a Jasco NRS-3100 micro-Raman spectrometer. 532 nm line of diode laser with 1800 l/mm grating was used for excitation. The laser power during signal acquisition was 4.5 mW. Spectral manipulations such as smoothing, baseline correction, second derivative calculations and band fitting were performed using GRAMS/AI 7.02 (Thermo Electron Corporation) software package. A band fitting procedure was used to fit the band components, which numbers and starting frequencies were determined with the second derivative.

The cultured colon cancer cells containing different DFMO concentrations (0, 1, 2.5, 5 and 7.5 mM) are investigated. Concentration dependent spectral changes were observed at the intensities of characteristic protein and DNA bands indicated DFMO induced apoptosis.

[1] I. Notingher, *Sensors*, 7 (2007)1343-1358.

[2] J. Guo, W. Cai, B. Du, M. Qian and Z. Sun, *Biophysical Chem.* 140 (2009) 57-61.



## Surface-enhanced Raman scattering of DL-tryptophan

L.Andronie<sup>1</sup>, S. C. Pînzaru<sup>2</sup>, O. Cozar<sup>1</sup>

<sup>1</sup>Babes-Bolyai University, Biomedical Phys. Dept., Kogalniceanu 1, Cluj-Napoca, Romania

<sup>2</sup>Babes-Bolyai University, Molecular Spectroscopy Dept., Kogalniceanu 1, Cluj-Napoca, Romania

Amino acids are the molecular basis of proteins and enzymes. Tryptophan is probably the most widely distributed indole derivative in nature and can be converted into many compounds of biological significance [1]. SERS substrate provide an innovative and powerful approach to protein and amino acids [2]. The Surface-enhanced Raman scattering of aromatic acid (DL-tryptophan) adsorbed on Ag colloidal particles have been obtained using citrate-reduces silver colloids at  $10^{-4}$  mol $l^{-1}$  concentration and the vibrational bands have been investigated in the spectral range of 170-1700 nm. SERS of D-tryptophan has also been reported [3] and it was found as the tryptophan molecule interact with the surface trough both the carboxyl and amino groups (fig.1). Different adsorption geometries of the species on the Ag colloidal nanoparticles are discussed.

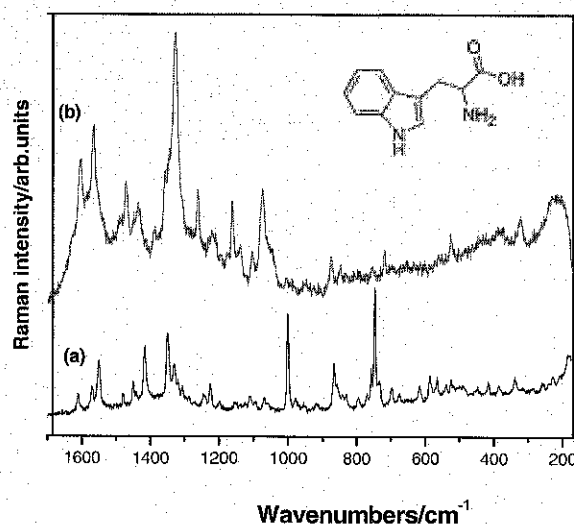


Fig.1. Raman (a) and SERS (b) spectra of DL-Tryptophan, Excitation: 632,8 nm.

- [1] Chi-HungChuang, Yit-TsongChena, Published online in Wiley Interscience: 29 September 2008  
 [2] P.Leyton, P.A.Lizama Vergara, M.M.CamposVallette, M.I.Becker, E.Clavijo, I.Cordova Reyes, M.Vera, C.A.Jerez, J.Chil.Chem.Soc.2005, 50,725  
 [3] A.E.Aliaga, I.Osorio-Roman, P.Leyton, C.Garrido, J.Carcamo, C.Caniulef, F.Celis, G.Díaz F., E.Clavijo, J.S.Gomez-Jeria, M.M.Campos-Vallette, Published online in Wiley Interscience :19 September 2009

## Investigations on Metallothioneins: An help from Raman Spectroscopy

A. Torreggiani<sup>1</sup>, M. Di Foggia<sup>2</sup>, A. Tinti<sup>2</sup>

<sup>1</sup>ISOF-CNR, P. Gobetti 101, 4012 Bologna, Italy

<sup>2</sup>Dept. Biochemistry "G. Moruzzi", University of Bologna, Via Belmeloro 8/2, Bologna, I-40126, Italy

MTs are low molecular weight metalloproteins (6-7 kDa) characterized by a high content in Cys. They are ubiquitously distributed among all living organisms and have an outstanding heavy-metal binding capacity. Overall, the general structural properties that characterize all MTs are the formation of metal-thiolate clusters involving terminal and bridging cysteinyl thiolate groups. Recently, it has been shown that also exogenous ligands such as inorganic ions (i.e. sulfide or chloride ions) can participate in the coordination sphere of metals in MTs [1].

Some Zn- and Cd-complexed MTs, representative of different MT families, enclosing the well-known vertebrate and echinoderm, and the poorly understood nematode, diptera, molluscan, protozoa and plant MTs, have been analysed by Raman Spectroscopy [2,3]. In fact, despite the well-known potentialities of this technique, to our knowledge it has been scarcely used in MT structural studies until now.

Raman spectroscopy has resulted to be very useful in shedding light on the secondary structures eventually present in MTs and the ligands involved in metal coordination. The oxidation state of Cys residues and their participation in the metal chelation can be clearly defined (Figure 1), as well as the eventual involvement of His residues.

As regards exogenous metal ligands such as sulfide anions, their presence can be identified by some marker bands whose intensity is linearly correlated with sulfide/metal molar ratio. Finally, Raman can be also an useful tool for providing information on the favourite sites of the radical attack and radical-induced modification in protein folding.

In conclusion, Raman spectroscopy, in coupling with analytical techniques, can be one of the most promising experimental strategies in the research on new hints on MTs.

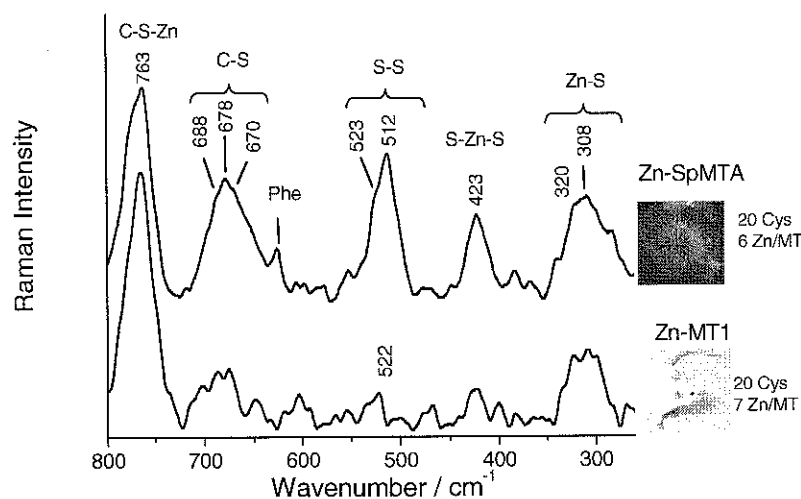


**Figure 1.** Raman spectra of two Zn-MT complexes from vertebrate and echinoderm families.

- [1] M. Capdevila, J. Domenech, A. Pagani, L. Tio, L. Villarreal, S. Atrian, *Angew Chem Int Ed*, 44 (2005) 4618-4622  
 [2] A. Torreggiani, A. Tinti, *Metallomics* (2010) DOI: 10.1039/B922526A.  
 [3] A. Torreggiani, J. Domenech, S. Atrian, M. Capdevila, A. Tinti *Biopolymers* **89** (2008) 1114-1124.



## Theoretical models for better understanding of IR and CD spectra of proteins

J. Kaminsky<sup>1</sup>, J. Kubelka<sup>2</sup>, P. Bouř<sup>1</sup>

<sup>1</sup>Institute of Organic Chemistry and Biochemistry, Flemingovo nam. 2, 166 10 Prague, Czech Republic,  
<sup>2</sup>University of Wyoming, 1000E Univ. Avenue, Laramie, WY 82071, USA.

Protein folding remains one of the top unsolved problems and challenges for modern science. We have focused on small and structurally simple proteins, such as helix-turn-helix motifs, which are excellent models for obtaining new important insights into the secondary and tertiary structure formation in protein folding.[1] Detailed understanding of the folding mechanism of these simple motifs is a crucial step toward solving the protein folding problem in general.

Spectroscopy is an important tool for investigations of protein structural changes during folding or unfolding. The main interest is often turned to infrared spectroscopy (IR), as well as circular dichroism (CD). In parallel to protein folding studies, it is necessary to constantly try to obtain better understanding of complex IR and CD spectra of proteins. In this work we tried to investigate the temperature-dependent amide I frequency shifts complicated by nonstructural effects, which are not related to the thermal unfolding of the peptide or protein structure [2]. The second part was focused on the simulation of CD spectra of  $\alpha$ -helical peptides with a view to the influence of different chain length. The effect of another peptide in the proximity of the helix was also studied. We have used a combination of experimental studies on model compounds, such as N-methylacetamide (NMA) and small oligopeptides, with theoretical simulations of the spectra, predominantly based on density functional theory (DFT) coupled with Molecular dynamic simulations (MD).

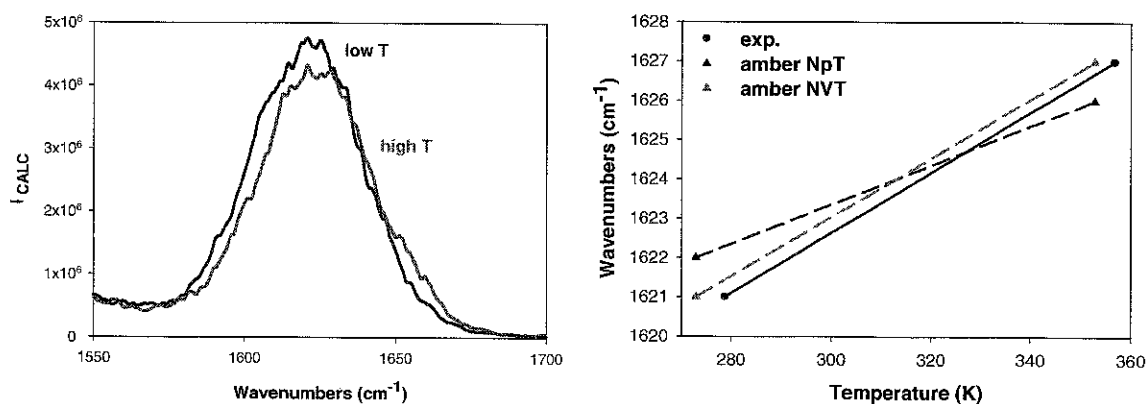


Figure. Simulated temperature dependence of amide I band (left-spectrum, right-frequencies). The BPW91/6-311++G\*\* vacuum values were corrected by the empirical correction obtained from 1ns MD simulations performed with the AMBER99 force fields and two temperatures (~273K and ~353K).

[1] K. E. Amunson, L. Ackels, J. Kubelka, *J. Am. Chem. Soc.* 130 (2008), 8146-8147.

[2] K. E. Amunson, J. Kubelka, *J. Phys. Chem. B* 111 (2007), 9993-9998.



## Hydration of simple carboxylic acids from infrared spectroscopy of HDO

M. Śmiechowski, E. Gojło, J. Stangret

*Department of Physical Chemistry, Chemical Faculty, Gdańsk University of Technology,  
Narutowicza 11/12, 80-233 Gdańsk, Poland*

Carboxylic acids form an important class of biomolecules. Their hydration in dilute aqueous solutions has important implications for our understanding of their functioning in the biochemical context. Owing to the presence of alkyl chains in carboxylic acids, coupled with a hydrophilic  $-\text{COOH}$  head group, they often experience a mixed type of hydration, i.e., the hydrophobic hydration of the alkyl chain combined with the hydrophilic hydration of the head group. The cooperative effects of both types of hydration are supposed to determine the overall interaction of the molecule with the surrounding aqueous medium [1]. For carboxylic acids, the hydrophilic part of the molecule is additionally expected to show specific hydration effects in water, connected with the presence of both proton-donating and accepting groups in close proximity.

Recently, we characterized the hydration of carboxylate anions finding that in an aqueous solution a solvent-induced symmetry breaking of the negative charge of the anion gives rise to an observed splitting of the carboxylate ion-affected HDO band, unique for these solutes [2]. A cooperative system, formed by water molecules interacting with the anion, contributes to this phenomenon. A similar cooperativity of solute-water H-bonding interactions is thought to be equally important in the hydration of carboxylic acids.

Here we apply vibrational spectra of HDO isotopically diluted in  $\text{H}_2\text{O}$  to study the above-mentioned phenomena, using the difference spectra method, originating from our laboratory, for analysis and interpretation of the results [3]. The spectra of HDO affected by formic, acetic and propionic acid display characteristic component bands, significantly red-shifted from the bulk HDO band position ( $\approx 2510 \text{ cm}^{-1}$ ). However, these component bands do not extend beyond  $2000 \text{ cm}^{-1}$ , differentiating carboxylic acids from strong acids, for which a component band at as low as  $1700 \text{ cm}^{-1}$  was found [4]. Similarly to carboxylate anions [2], the number of moles of water affected by one mole of the solute is low for the studied solutes ( $N \approx 4$ ). The appearance of red-shifted component bands is linked with isotopic substitution on the carboxylic acid molecule, which forms a short and strong hydrogen bond with a water molecule. This type of interaction seems to be universal for weak and medium-strength acids, as was already evidenced in our study of phosphoric(V) acid and its anions [5].

The proposed assignments of component bands in the HDO spectra were confirmed by calculating equilibrium structures of small aqueous clusters of the studied acids utilising Density Functional Theory (DFT) with hybrid B3LYP functional and triple-zeta basis set.

**Acknowledgments.** This work was supported from the Republic of Poland scientific funds as a research project, within grant no. N N204 3799 33. Calculations were carried out at the Academic Computer Centre in Gdańsk (TASK).

- [1] E. Gojło, M. Śmiechowski, J. Stangret, *J. Mol. Struct.* 744-747 (2005) 809-814
- [2] E. Gojło, M. Śmiechowski, A. Panuszko, J. Stangret, *J. Phys. Chem. B* 113 (2009) 8128-8136
- [3] J. Stangret, T. Gampe, *J. Phys. Chem. B* 103 (1999) 3778-3783
- [4] M. Śmiechowski, J. Stangret, *J. Chem. Phys.* 125 (2006) 204508
- [5] M. Śmiechowski, E. Gojło, J. Stangret, *J. Phys. Chem. B* 113 (2009) 7650-7661



## Use of FT-IR spectroscopy data for systems analysis of *Zymomonas mobilis* metabolism

M. Grube<sup>1</sup>, M. Gavare<sup>1</sup>, R. Rutkis<sup>1</sup>, U. Kalnenieks<sup>1</sup>, N. Mironova-Ulmane<sup>2</sup>

<sup>1</sup>Institute of Microbiology and Biotechnology, University of Latvia, 4 Kronvalda Blvd., LV 1586, Riga, Latvia

<sup>2</sup>Institute of Solid State Physics, University of Latvia, Kengaraga street 8, LV-1063 Riga, Latvia

Respiratory metabolism and oxidative stress responses of the ethanol-producing bacterium *Zymomonas mobilis* were studied. *Z. mobilis* ATCC 21919 (Zm6) and its knock-out mutant derivatives *ndh*- (strain with disrupted gene of the type II electron transport NADH dehydrogenase), *bc<sub>1</sub>*- (disrupted gene of the cytochrome b subunit of the *bc<sub>1</sub>*- complex) and *cat*- (disrupted catalase gene) were cultivated in a chemostat at 0.2 h<sup>-1</sup> feed rate under anaerobic and aerobic conditions. FT-IR spectra of films formed by drop-drying were recorded on a micro plate reader HTS-XT (Bruker, Germany) over a wavelength range 4000-600 cm<sup>-1</sup>.

It is known that the concentration of principal microbial/bacterial cell components – carbohydrates, proteins, lipids and nucleic acids, may vary in a broad range among strains and can be changed by the growth conditions [1]. FT-IR spectroscopy was shown to be a sufficiently accurate and sensitive method to determine acute changes in erythrocytes during oxidative stress [2]. Our studies of biomass and culture liquids of *Z. mobilis* ATCC 21919 and its mutant derivatives were based on FT-IR qualitative, quantitative and cluster analyses. Samples were collected at different fermentation/growth phases thus following the changes of macromolecular composition.

[1] M. Grube, M. Bekers, D. Upite, E. Kaminska, *Vibrat. Spectrosc.* 28 (2002) 277-285

[2] C. Petibois, G. Deleris, *Analyst* 129 (2004) 912-916





## Structural stability and complexation with aptamers of RNA hairpins in HIV-1 genome

P. Ottová, B. Řezáčová, J. Vachoušek, J. Štěpánek

*Charles University in Prague, Faculty of Mathematics and Physics  
Ke Karlovu 3, CZ-121 16 Prague 2, Czech Republic*

The hairpin, the most common motif in the secondary structure of single-stranded RNA, provides a rich potential for both intra- and intermolecular interactions via nucleotides in its apical loop [1]. We have focused our attention to the RNA hairpins of the trans-activation response (TAR) element and the dimerization initiation site (DIS) inside the genome of Human Immunodeficiency Virus type 1 (HIV-1). These hairpins play a key role in the viral replication cycle and belong among targets of antisense therapy due to their evolutionary conservativeness. The aim is to block the binding site on the hairpin with loop-loop interaction with an aptamer.

TAR element involves the first 59 nucleotides of the viral genome. It forms an imperfect hairpin with a three-nucleotide bulge and a six-base loop, which serve as a scaffold for a specific complex of viral and cellular proteins. This protein complex hyperphosphorylates RNA polymerase II and thus causes a dramatic increase of the HIV-1 transcription efficiency [2]. RNA aptamer R06, found by SELEX technique, forms a kissing complex with the six-base loop and inhibits efficiently the protein binding [3, 4].

DIS hairpin is formed by 35 nucleotides and contains a self-complementary sequence in its loop. Two DIS hairpins can interact via loop-loop interaction forming a kissing complex. The pseudodiploid genome of HIV-1 consists of two homologous copies of the positive sense single-stranded RNA and the dimerization via DIS-DIS complex is essential for encapsidation [5].

In our study we used techniques of UV absorption and Raman scattering to obtain temperature dependent spectra in a wide temperature range. The spectral series were analyzed by means of factor analysis. We also used differential scanning microcalorimetry to obtain thermo-dynamic characterization of temperature induced structural transitions. Besides the high-temperature transition, which was interpreted as a disintegration of the stem and the hairpin opening, a second, low-temperature transition was discovered. Spectral changes connected with the latter transition indicate partial disordering of the A-type duplex geometry of the stem, opening of intraloop hydrogen bonds and weakened conformational regularity of the loop [6].

Our studies of kissing complexes formed in 1:1 mixtures of pertinent RNA hairpins revealed that the kissing complex melts nearly at the same temperature as the less stable hairpin. The results also indicate certain stabilization effect of the kissing complex formation on the hairpin structure in the temperature region of the low-temperature structural transition.

**Acknowledgement:** This work is supported by the Czech Science Foundation (project 202/09/0193) and the Czech Ministry of Education (project MSM 0021620835).

- [1] P. C. Bevilacqua, J. M. Blose, *Annu. Rev. Phys. Chem.* 59 (2008) 79-103
- [2] M. Barboric, B. M. Peterlin, *PLoS Biology* 3(2):e76 (2005) 200-203
- [3] F. Ducongé, J. J. Toulmé, *RNA* 5 (1999) 1605-1614
- [4] F. Darfeuille, D. Sekkai, E. Dausse, G. Kolb, L. Yurchenko, C. Boiziau, J. J. Toulmé, *Combinatorial Chemistry* 5 (2002) 313-325
- [5] M. D. Moore, W. S. Hu, *AIDS Rev.* 11 (2009) 91-102
- [6] J. Vachousek, J. Stepanek, *Spectroscopy* 22 (2008) 267-277



## Binding of proteins to vesicles: Asymmetry and cooperativity

F. Torrens<sup>1</sup>, G. Castellano<sup>2</sup>

<sup>1</sup>Institut Universitari de Ciència Molecular, Universitat de València, Edifici d'Instituts de Paterna, P. O. Box 22085, 46071, València, Spain

<sup>2</sup>Instituto Universitario de Medio Ambiente y Ciencias Marinas, Universidad Católica de Valencia San Vicente Mártir, Guillem de Castro-94, 46003, València, Spain

The role of electrostatics is studied in cationic protein adsorption to zwitterionic phosphatidylcholine (PC) and anionic mixed PC/phosphatidylglycerol (PG) small unilamellar vesicles (SUVs) [1]. Protein interaction is monitored vs. PG content at low ionic strength [2]. The adsorption of lysozyme–myoglobin–bovine serum albumin (BSA) (isoelectric point,  $pI$  5–11) is investigated in SUVs, along with changes of the fluorescence emission spectra of the proteins, *via* their adsorption on SUVs (Fig. 1) [3]. As there is an extensive literature on the structure of zwitterionic SUVs, the objective of this report is to extend the studies to anionic lipid bilayers, given the involvement of negatively charged headgroups in cell activity [4]. The partition coefficients and cooperativity parameters are calculated [5]. At  $pI$  the amount of binding obtains the maximum, while at lower and higher  $pH$ s the binding is significantly decreased [6]. In Gouy–Chapman formalism activity coefficient goes with square charge number [7]. Deviations from ideal model indicate the asymmetric location of anionic phospholipid in bilayer inner leaflet, in mixed zwitterionic/anionic SUVs for both lysozyme– and myoglobin–PC/PG systems, in agreement with experiments–molecular dynamics simulations. SUVs bind myoglobin anti-cooperatively while lysozyme–BSA cooperatively. Apparently the structures of the attached lysozyme–BSA layer on protein–SUVs play a significant role. A model for both proteins, which composes two protein sub-layers with different structures–properties, is proposed. Hill coefficient reflects subunit cooperativity of bi/tridomain proteins. Further protein binding is difficult because the repulsion of like charges becomes dominant. In terms of conventional binding mechanisms this would correspond to a negative cooperativity. Lysozyme–albumin binding to SUVs follow a model of positive cooperativity, representing the interaction between the protein considered as a dipole moment and the anionic phospholipid headgroups.

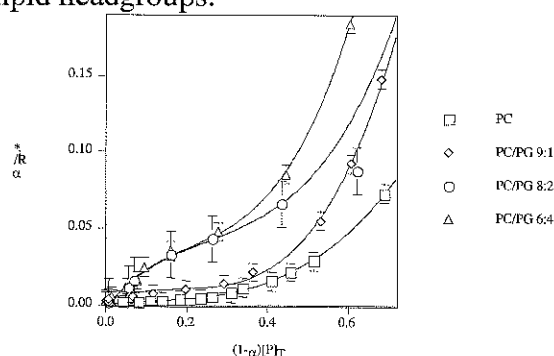


Fig. 1. Effect of vesicle charge on lysozyme–PC/PG ( $pH$  7.0).

- [1] F. Torrens, A. Campos, C. Abad, *Cell. Mol. Biol.* 49 (2003) 991
- [2] F. Torrens, C. Abad, A. Codoñer, R. García-Lopera, A. Campos, *Eur. Polym. J.* 41 (2005) 1439
- [3] F. Torrens, G. Castellano, A. Campos, C. Abad, *J. Mol. Struct.* 834-836 (2007) 216
- [4] F. Torrens, G. Castellano, *SAR QSAR Environ. Res.* 19 (2008) 643
- [5] F. Torrens, G. Castellano, A. Campos, C. Abad, *J. Mol. Struct.* 924-926 (2009) 274
- [6] F. Torrens, G. Castellano, *Anal. Chim. Acta* 654 (2009) 2
- [7] F. Torrens, G. Castellano, *Curr. Proteomics* 6 (2009) 204



## Solid-state transformation of the pseudopolymorphic forms of codeine phosphate hemihydrate and codeine phosphate sesquihydrate monitored by FTIR spectroscopy and TGA/DSC

G. Petruševski<sup>1</sup>, S. Ugarkovic<sup>1</sup>, P. Makreski<sup>2</sup>

<sup>1</sup>Reserch & Development Institute, ALKALOID AD, Aleksandar Makedonski 12,  
1000 Skopje, Republic of Macedonia

<sup>2</sup>Institute of Chemistry, Faculty of Science, SS. Cyril and Methodius University, Arhimedova 5,  
1000 Skopje, Republic of Macedonia

Codeine phosphate (7,8-didehydro-4,5 $\alpha$ -epoxy-3-methoxy-17-methylmorphinan-6 $\alpha$ -ol phosphate) has a long history of medical usage as painkiller active pharmaceutical ingredient (API) in treatment of different indications (cough, diarrhea, mild to moderate pain and irritable bowel syndrome). It is mainly marketed in combination with different analgesics (paracetamol, aspirin), other painkillers and muscle relaxers (phenacetin, indomethacin, diclofenac), or in very complex solid dosage mixtures with paracetamol, caffeine and propyphenazone. It was proved, over the several decades of experience, that the combined formulations have advantageous pharmacological properties over the pure, codeine based products.

Two pseudopolymorphs (described in European Pharmacopoeia, 2009 edition) of codeine phosphate, regularly used for preparation of different pharmaceutical formulations, are the corresponding hemihydrate and sesquihydrate salts. Having in mind their pharmaceutical importance and their behavior during the prolonged exposure of the compounds at ambient conditions, a research was undertaken to describe the IR spectra variations and obtain information about the relative stability of both forms by the use of TG degradation profiles and DSC curves. In addition, the observed spontaneous affinity for solid-solid phase transition from codeine phosphate hemihydrate to codeine phosphate sesquihydrate, upon exposure to open atmosphere was also discussed. The reverse process is also possible but requires higher activation energy (temperature in the range of 65-85 °C). It was observed that the sesquihydrate form has lower potential for water sorption, when being exposed at moderate moisture levels.

To the best of our knowledge, the IR spectra of the both compounds have not been previously published and single thermal characterization study on the codeine and codeine phosphate were only presented [1]. It is worth mentioning that the hemihydrate form has recently attracted the scientific attention and its crystal structure was solved [2].

[1] L. Yang, H. Yin, W. Zhu, S. Niu, J. Therm. Anal. 45 (1995) 207-210

[2] C. Langes, T. Gelbrich, U.J. Griesser, V. Kahlenberg, Acta Cryst. C65 (2009) 419-422



## Spectroscopic and magnetic properties of Cu(II) complexes with selected biologically important ligands

R. Świsłocka<sup>1</sup>, M. Kalinowska<sup>1</sup>, W. Ferenc<sup>2</sup>, J. Sarzyński<sup>3</sup>, W. Lewandowski<sup>1</sup>

<sup>1</sup>*Department of Chemistry, Białystok Technical University, Zamenhofa 29,  
15-435 Białystok, Poland*

<sup>2</sup>*Department of General and Coordination Chemistry, Maria Curie-Skłodowska  
University, Pl. Marii Curie-Skłodowskiej 2, 20-031 Lublin, Poland*

<sup>3</sup>*Institute of Physics, Maria Curie-Skłodowska University, Pl. Marii  
Curie-Skłodowskiej 1, 20-031 Lublin, Poland*

Carboxylic complexes with copper(II) ion are of great importance due to their antimicrobial properties. The antimicrobial uses of copper include production of fungicides, pesticides, antifouling paints, antimicrobial medicines, oral hygiene products, hygienic medical devices, antiseptics and a host of other useful applications.

The aim of this work was to study spectroscopic and magnetic properties of copper (II) *o*-, *m*-, *p*-aminobenzoates and *o*-, *m*-, *p*-methoxybenzoates. The complexes were synthesized, the composition of these complexes was evaluated by elementary analyses, the infrared spectra for Cu(II) aminobenzoates and methoxybenzoates was registered and assigned. The obtained data was compared with previously published for aminobenzoic and methoxybenzoic acids and their sodium salts. The structure of Cu(II) *o*-, *m*-, *p*-aminobenzoates and *o*-, *m*-, *p*-methoxybenzoates as well as the change of electronic charge distribution caused by Cu(II) complex formation was discussed.

This work was supported by grant no. N N305 267534



## Relationship between chemical structure and biological activity of alkali metal *o*-, *m*- and *p*-anisates. FT-IR and microbiological studies

M. Kalinowska, J. Piekut, W. Lewandowski

*Department of Chemistry, Białystok Technical University, Zamenhofa 29,  
15-435 Białystok, Poland, w-lewando@wp.pl*

In this work we investigated the relationship between molecular structure of alkali metal *o*-, *m*-, *p*-anisate molecules and their antimicrobial activity. With this end in view FT-IR spectra for lithium, sodium, potassium, rubidium and caesium anisates in solid state and solution were registered, assigned and analyzed. Microbial activity of studied compounds was tested against *Escherichia coli*, *Pseudomonas aeruginosa*, *Staphylococcus aureus*, *Proteus vulgaris*. In order to evaluate the dependence between chemical structure and biological activity of alkali metal anisates the statistical analysis (multidimensional regression and principal component) was performed for selected wavenumbers from FT-IR spectra and parameters described microbial activity of anisates. The obtained statistical equation show the existence between molecular structure of anisates and their biological properties.

This work was supported by grant no. N N305 267534.



## Solution-phase, dual LSPR-SERS plasmonic sensors of high sensitivity and stability based on chitosan-coated anisotropic silver nanoparticles

M. Potara<sup>1</sup>, S. Astilean<sup>1</sup>

<sup>1</sup>*Babes-Bolyai University, Faculty of Physics, Institute for Interdisciplinary Research in Bionanoscience, Nanobiophotonics Center, T. Laurian 42, 400271 Cluj-Napoca, Romania*

There is a need to design highly sensitive multifunctional plasmonic sensors which impart good biocompatibility and molecular specificity to detect low levels of chemical or biological species in biological media. The approach of combining the sensitivity of localized surface plasmon resonance (LSPR) to local changes in the optical environment of noble-metal nanoparticles with the ability to identify the adsorbed species through surface-enhanced Raman spectroscopy (SERS) represents a promising route toward such multifunctional plasmonic sensors [1,2]. For sensing with plasmonic nanostructures in physiological solutions as for example cell culture medium, the most natural approach toward their stabilizing and biofunctionalization is to coat the surface of plasmonic nanostructures with a biopolymer nanoshell [3].

In this work, with the aim of implementing such solution-phase, dual LSPR-SERS sensing substrates we develop a two-steps approach to prepare anisotropic silver nanoparticles enveloped in a shell of chitosan biopolymer. The method involves the reduction of silver nitrate with ascorbic acid in the presence of trisodium citrate and chitosan through a seed-mediated growth approach. Our results show that the shape of silver particles can be readily tailored from spherical to triangular by synergistic action of chitosan and two reducing and stabilizing agents, ascorbic acid and citrate, respectively. Actually, chitosan plays a multiple role here, ranging from the control of particle size and shape to provide stability through steric hindrance, thereby preventing aggregation and introduce functionality to the particle surface. The flexibility in manipulating the size and morphology of silver nanoparticles combined with the remarkable stability of chitosan-protected nanoparticles allows us to integrate onto the same substrate two highly sensitive methods of molecular detection based on plasmonic properties, specifically LSPR and SERS. The versatility of silver-chitosan nanocomposites to operate as unique substrate for combined LSPR-SERS detection was clearly demonstrated by using *para*-Aminothiophenol (*p*-ATP) as molecular analyte. We measured plasmon resonance shifts of 10 nm due to adsorption of single molecular layer of *p*-ATP onto the metal surface and, subsequently we identified the probe molecule by SERS with three excitation laser lines from visible to near-infrared (NIR). The feasibility of using solution-phase silver nanocomposites as LSPR-enabled SERS sensors makes them ideal platform for *in vivo* quantification of biological processes.

**Acknowledgments:** This work was supported by CNCSIS in the frame of the PN-II research programs under the project PCCE No 129/2009.

- [1] V. Canpean, S. Astilean, *Lab Chip* 9 (2009) 3574-3579
- [2] D. E. Charles, D. Aherne, M. Gara, D. M. Ledwith, Y. K. Gun'ko, J. M. Kelly, W. J. Blau, M. Brennan-Fournet, *ACS Nano* 4 (2010) 55-64
- [3] M. Potara, D. Maniu, S. Astilean, *Nanotechnology* 20 (2009) 315602-315608



## Raman optical activity of amide and disulfide group in peptides and proteins

M. Kubáňová<sup>1,2</sup>, L. Bednářová<sup>2</sup>, P. Maloň<sup>2</sup>, V. Baumruk<sup>1</sup>

<sup>1</sup> Institute of Physics, Faculty of Mathematics and Physics, Charles University in Prague, Ke Karlovu 5, Prague 2, CZ-121 16, Czech Republic

<sup>2</sup> Institute of Organic Chemistry and Biochemistry, Academy of Sciences, Flemingovo nám 2, 166 10, Prague, Czech Republic

The Raman optical activity (ROA) spectroscopy which measures the difference in the intensity of Raman scattering from chiral molecules in the right- and left-circularly polarized incident light [1] has been used to investigate structurally important groups in peptides and proteins. We concentrated on the relationship between three-dimensional structure of peptides/proteins and their Raman optical activity. We investigated vibrations of the disulfide group at 500–700 cm<sup>-1</sup> and deformation vibrations at 900–1200 cm<sup>-1</sup> reflecting the peptide chain. ROA spectra of hinge peptide were measured and interpreted on the basis of [2] and the characteristic polyproline II (left-handed 3<sub>1</sub>-helix) band patterns were investigated in poly(Pro-Gly-Pro).

We also focused our attention to extension of ROA measurements to the C-H stretching region (2500–3200 cm<sup>-1</sup>). Although knowledge of the ROA signal in this region is very important and useful for testing the reliability of theoretical methods considering anharmonic corrections for the vibrational spectra (C-H stretching vibrations are strongly anharmonic), this subject has yet to be further investigated. On model compounds for which both enantiomers were available ((1*S*)-(+)-fenchone, (1*R*)-(-)-fenchone) we successfully demonstrated that the measurement in this region is possible and that we can obtain reliable experimental data.

Supported by Grant Agency of the Czech Republic, project no. P205-10-1276

[1] L.D. Barron, L. Hecht, in: N. Berova, K. Nakanishi, R.W. Woody, *Circular Dichroism, Principles and Applications*, second ed., Wiley, New York, 2000, p. 667

[2] P. Maloň, L. Bednářová, M. Straka, L. Krejčí, L. Kumprecht, T. Kraus, M. Kubáňová, V. Baumruk, *Chirality*, (2010) accepted 2010



## Influence of metal ions on thermal aggregation processes of globular proteins

A. Tinti<sup>1</sup>, G. Navarra<sup>2</sup>, M. Leone<sup>2</sup>, V. Militello<sup>2</sup>, A. Torreggiani<sup>3</sup>

<sup>1</sup>*Dip. Biochimica, Univ. Bologna, Via Belmeloro 8/2, 40126 Bologna, Italy.*

<sup>2</sup>*Dip. Scienze Fisiche ed Astronomiche, Univ. Palermo and CNISM, via Archirafi 36, 90123 Palermo, Italy.*

<sup>3</sup>*ISOF-CNR, P. Gobetti 101, 4012 Bologna, Italy*

Metal ions are implicated in protein aggregation processes of several neurodegenerative pathologies, where the protein deposition occurs. The idea arises from the finding that increased metal concentrations (mainly copper, iron and zinc) are present in the brains of Alzheimer's disease patients both in the amyloid plaques and in the cortical tissue.  $\text{Cu}^{2+}$  and  $\text{Zn}^{2+}$  metals ions have a different physiological role and it has been observed that, in vitro, both promote (zinc more than copper) aggregation in amyloid fibrils and/or in amorphous aggregates. In addition, studying aggregation protein process can be of interest also in the field of biotechnologies like the food technology, since most processes in manufacturing of foods are based on thermal treatments. Knowing the structures of the proteins during and after these treatments is extremely important also for allergenic problems.

The effects of  $\text{Cu(II)}$  and  $\text{Zn(II)}$  ions on heat-induced structural modifications of bovine serum albumin (BSA) and beta-lactoglobulin (BLG) were studied, with the aim of delineating the role of these ions in the early stages of proteins aggregation kinetics. A joint application of different techniques was used. The aggregate growth was followed by Dynamic Light Scattering measurements, whereas the conformational changes occurring in the protein structure were monitored by Raman and IR spectroscopy [1]. Both in absence and in presence of metal ions, heating treatment gave rise to  $\beta$ -structures to the detriment of  $\alpha$ -helix conformation of the proteins (Figure 1). Different efficacy of the  $\text{Cu(II)}$  and  $\text{Zn(II)}$  ions in promoting the protein aggregation were highlighted by Raman measurements, assessing the role of His residues in metal binding. A distinct polypeptide folding of the two metal-protein systems takes place, since the predominant mode of metal binding depends on metal.

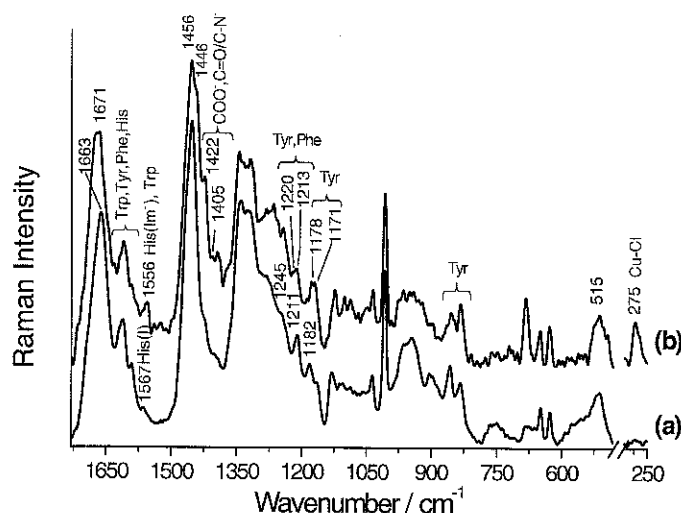


**Figure 1.** Raman spectra of Cu-BSA systems, before (a) and after thermal treatment (b).

[1] G.Navarra, A. Tinti, M. Leone, V. Militello, A. Torreggiani, *J. Inorg. Biochem.* 103 (2009) 1729-1738.



## Compound formation assistance by Raman spectroscopy and PXRD method

A. Weselucha-Birczyńska, B. Borzęcka-Prokop

*Faculty of Chemistry, Jagiellonian University, Ingardena 3, 30-060 Kraków, Poland*

Cinchonine (C<sub>19</sub>H<sub>22</sub>N<sub>2</sub>O) belongs to main *Cinchona* alkaloids exhibiting antimalarial activity. However, the molecular mechanism of action continues to be debated. Biological membranes seem to be the crucial point in these considerations. On the way to the food vacuole of parasite the drug passes three such biological borders. Raman spectroscopy provides valuable insight to trace the interactions of model phospholipids with alkaloids.

In the present study there was undertaken investigation of adducts of the cinchonine with *l*-serine working with several crystallisation settings. There were examined spectral changes in the Raman spectra, of the investigated compound and *l*-serine. X-ray diffraction patterns, obtained on the solid state powder phases, differ from those characterising substrates. These facts indicate that obtained crystalline phase is newly compounds. The observed features are discussed.

**Acknowledgements:** This work has been supported by the Polish Ministry of Science and Higher Education, Statutory Research.

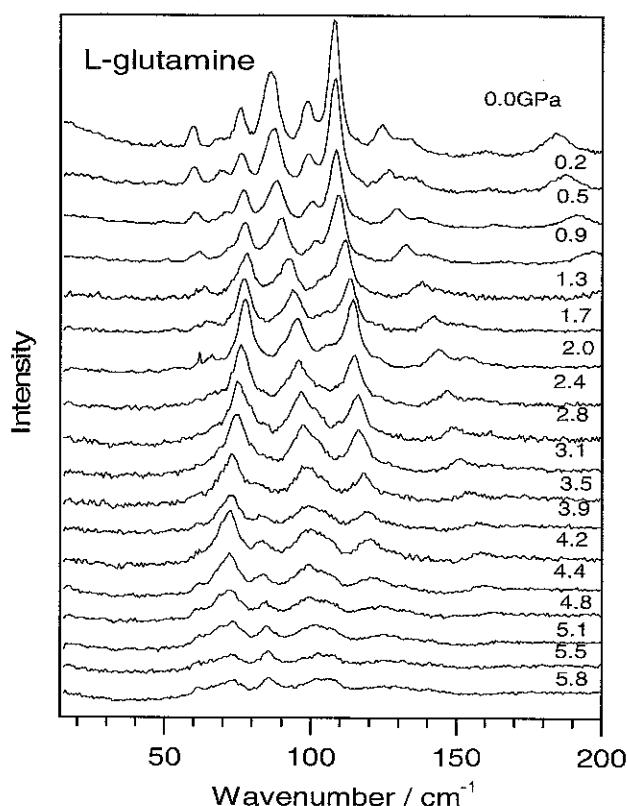


## Raman spectroscopy of L-glutamine under high pressure conditions

P. T. C. Freire<sup>1</sup>, R. O. Holanda<sup>1</sup>, C. Luz-Lima<sup>1</sup>, J. Mendes Filho<sup>1</sup>, F. E. A. Melo<sup>1</sup>

<sup>1</sup>Departamento de Física, Universidade Federal do Ceará, C.P. 6030, Fortaleza, 60455-760, Brazil

L-glutamine is an amino acid classified as conditionally essential substance that participates in the regulation of acid-base balance and in the formation of many substances. Additionally, it participates in proteins synthesis and the energy production. L-glutamine crystallizes in an orthorhombic structure  $P2_12_12_1$  with four molecules per unit cell [1, 2]. A recent study showed that up to 4.9 GPa the original orthorhombic structure undergoes any phase transition [3]. Additionally, it was observed that occurs a shortening of the N – H ... O hydrogen bonds, with a minimum distance of  $\sim 2.6$  ang. In this work we present the Raman spectra of L-glutamine crystal for many pressures (from 0.0 to 5.8 GPa) in the spectral range from 20 to 3200  $\text{cm}^{-1}$ . Beyond the previous informations presented in Ref. [3] our study allowed us to follow the pressure behavior of several bands associated to internal modes such as torsional vibrations of  $\text{NH}_3^+$  and  $\text{NH}_2$ , bending of  $\text{CONH}_2$ , out-of-plane vibrations of  $\text{CCN}$ , rocking of  $\text{NH}_3^+$ ,  $\text{NH}_2$  and  $\text{CH}_2$ , stretching vibrations of  $\text{CC}$ ,  $\text{CN}$ ,  $\text{CH}$ , among others. From the study of the low wavenumber bands it was possible to observe disappearance of two peaks, as well as, the appearance of a band at  $\sim 75$   $\text{cm}^{-1}$  (Fig. 1). This result is discussed in terms of both the X-ray data from Ref. [3] as well as the behavior of bands in the high wavenumber region. Also, a comparison with results previously presented in L-alanine and L-cysteine is discussed in the present work.



[1] W. Cochran, B.R. Penfold, Acta Cryst. 5 (1952) 644

[2] T.F. Koetzle, M.N. Frey, M.S. Lehmann, W.C. Hamilton, Acta Cryst. B 29 (1973) 2571

[3] P. Lozano-Casal, D.R. Allan, S. Parsons, Acta Cryst. B 64 (2008) 466



## Structure-reactivity relationship of $\text{Ca}^{2+}$ -carbohydrate solution complexes studied by $^1\text{H}$ , $^{13}\text{C}$ and $^{43}\text{Ca}$ NMR spectroscopy

A. Pallagi<sup>1,2</sup>, P. Sebők<sup>2</sup>, P. Sipos<sup>1\*</sup>, I. Pálinkó<sup>2</sup>

<sup>1</sup>Department of Inorganic and Analytical Chemistry, University of Szeged, Dóm tér 7, Szeged, H-6720 Hungary

<sup>2</sup>Department of Organic Chemistry, University of Szeged, Dóm tér 8, Szeged, H-6720 Hungary

Sugar derivatives are known to form weak complexes with  $\text{Ca}^{2+}$  ion. Their structures in solution have only been studied sporadically. Recently, we have been involved in a comprehensive study concerning the structure and equilibria of  $\text{Ca}^{2+}$ -gluconate complexes in aqueous solutions, using a broad range of  $\text{Ca}^{2+}$  and gluconate concentrations and ionic strengths [1]. Structural information was derived from multinuclear NMR measurements and stability constants were quantitatively estimated with the help of the PSEQUAD program [2].

In order to reveal the fine details of structure-reactivity relationships regarding these weak metal-carbohydrate complexes, we have decided to widen the scope of the sugar derivatives, *i.e.*, the prospective ligands. Results of this experimental work are communicated in this contribution.

A set of sugar derivatives was put together along various lines. One of the selection criteria was the oxidation states of the terminal groups and keeping the chain length of gluconic acid (*i.e.* 6). The group contained D(+)-glucose (partially oxidized at one end), mucic acid (fully oxidized at both ends), D-sorbitol (fully reduced at both ends), L-gulonic acid (fully oxidized at one end and fully reduced at the other). The other was keeping the oxidation states of the terminal group as in L-gulonic acid (or in D-gluconic acid) but increasing (D-heptagluconic acid) or decreasing (arabic acid) the chain length. The acid-base behavior of the relevant compounds (those having carboxylic groups) were investigated first, then, the  $\text{Ca}^{2+}$  complexation properties were studied both at constant (1.0 M NaCl) ionic strength. The main experimental tool was  $^1\text{H}$  and  $^{13}\text{C}$  NMR spectroscopy, but representative  $^{43}\text{Ca}$  NMR spectra were also recorded. The observed variations in the NMR spectra made possible to propose structures for the complexes and from the quantitative analysis of the stability constants factors influencing complex stability were deduced.

Our experiments proved that multinuclear NMR spectroscopy is a useful tool for the determination of the stability constant of these weak complexes. It was found that in these solutions  $\text{Ca}^{2+}$  complexes with 1:1 composition were formed and their stability constants increased with the increasing oxidation state of the ligand. It also could be observed that the formation of a six- or five-membered chelate ring (where it was possible at all) contributed to the stability increase.

[1] A. Pallagi, P. Sebők, P. Forgó, I. Pálinkó, P. Sipos, *Carbohydr. Res.* (submitted)

[2] PSEQUAD, A program for calculating equilibrium constants from experimental data, Update 5.10, L. Zékány, I. Nagypál, G. Peintler, 2008



## An IR and Raman spectroscopic investigation on $\alpha$ -difluoromethylornithine (DFMO), a potential target as chemotherapeutic agent

K. Balci<sup>1</sup>, Y. Akkaya<sup>1</sup>, S. Akyuz<sup>2</sup>, N. Palavan-Unsal<sup>3</sup>

<sup>1</sup> *Istanbul University, Department of Physics, Vezneciler 34134, Istanbul, Turkey*

<sup>2</sup> *Istanbul Kultur University, Department of Physics, Atakoy Campus, 34156 Bakirkoy, Istanbul, Turkey*

<sup>3</sup> *Istanbul Kultur University, Department of Molecular Biology and Genetics, Atakoy Campus, 34156 Bakirkoy, Istanbul, Turkey*

Polyamines are present in almost all living organisms. Cellular polyamine contents have been shown to have profound effects on growth and differentiation [1]. Ornithine decarboxylase is an enzyme that controls the formation of the polyamine putrescine in numerous of eucaryotic cells. This enzyme is involved in cellular response to growth, differentiation and stress [1]. Alpha-difluoromethylornithine (DFMO) is an irreversible inhibitor of ornithine decarboxylase and has been shown to affect differentiation in a number of systems. Recent studies indicate that long-term administration of DFMO causes inhibition on tumor growth and metastasis [2]. On the other hand, DFMO has been reported to inhibit the DMSO-induced induction of both heme synthesis and transcription of  $\alpha$ - and  $\beta$ -globin mRNA [3]. Despite its remarkable scientific importance, up to our knowledge, no vibrational spectroscopic data have been published on DFMO yet. A complete prediction of the recorded room-temperature IR (4000-400  $\text{cm}^{-1}$ ) and Raman (4000-50  $\text{cm}^{-1}$ ) spectra of the molecule in solid phase and also in aqueous suspensions was first reported in this study. The assignment of the fundamental bands observed in the obtained experimental spectra were given on the basis of the group frequency concept and in the light of the theoretical results obtained from the DFT based electronic structure calculations. At the first step of the calculations, the theoretically possible conformers for free DFMO molecule were searched by means of a molecular dynamics calculation performed using MM2 force field. At the next step, the most stable conformers were determined by means of thermochemistry calculations carried out first at B3LYP/6-31G(d) and then at B3LYP/6-311++G(d,p) level of theory, respectively. Afterwards, their equilibrium geometry and vibrational spectral data were calculated at the same levels of theory. In the correction of the overestimations of the calculated harmonic wavenumbers, two different empirical scaling approaches, called "dual scale factors" and "SQM FF methodology", were applied independently from each other. Considering that DFMO has a carboxyl group, the calculations were also repeated for the energetically most favorable dimer forms of the same conformers. For each vibrational mode of the conformers, the potential energy distributions (PEDs) were calculated within the scaled quantum mechanics force field (SQM FF) methodology.

[1] B. G. Katzung, Basic and Clinical Pharmacology, Appleton and Lange, 1989, Lebanon.

[2] S.K. Choudhary, D. Sharma and A. Dixit, Cell Biol. Cell Int., 23 (1999) 489-495.

[3] S.M. Aziz M.N. Gillespie, P.A. Crooks, S.F. Tofiq, C.P. Tusuboi, J.W. Olson, M.P. Gosland, J. Pharmacol. Exp. Therapeutics, 278 (1996) 185.

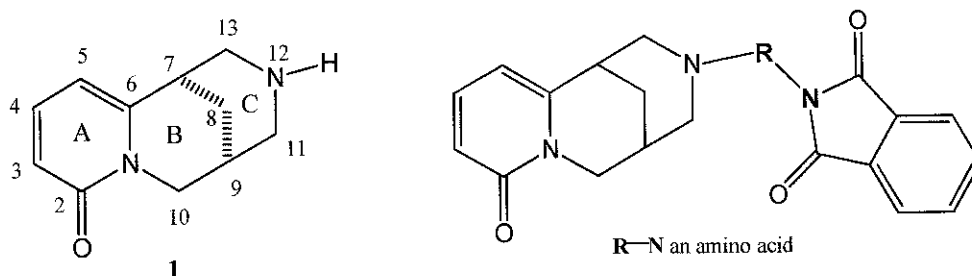


## A comparative study of EI-MS and NMR in analysis of the new derivatives of cytisine with aminoacids

A. K. Przybył, Z. Nowakowska

A. Mickiewicz University, Faculty of Chemistry, Grunwaldzka 6, 60-780 Poznań

(-)-Cytisine (1) is a naturally occurring quinolizidine alkaloid extracted from seeds of *Laburnum anagyroides* and other *Leguminosae* plants. (-)-Cytisine has been used as a smoking cessation aid (Tabex<sup>®</sup>), and is also a very promising compound for the development of new drugs for the potential treatment of CNS disorders, particularly Alzheimer's and Parkinson's diseases [1]. Moreover, some compounds of the *N*-substituted cytisine have been found to show analgesics properties [2]. Increased biological activity of particular derivatives is related to the interactions with amino acids making the structures of nAChR receptors [3]. The aim of this study was to obtain new amino acid derivatives of cytisine, expected to show potential biological activity, whose investigation can contribute to understanding of the interactions of ligands with nAChR receptors and bitter taste receptors.



It has been shown that the *N*-phthaloyl-amino acid cytisine esters occur in solutions at dynamical equilibrium as the mixtures of two conformers, which is manifested, as a double set of signals (both in <sup>1</sup>H-NMR and <sup>13</sup>C-NMR). 1D and 2D NMR spectra were taken of the cytisine derivatives studied and the chemical shifts were assigned to the corresponding atoms in the molecules of these compounds.

We focused our attention on the mass spectrometric properties of the new derivatives of cytisine substituted with amino acids. In particular, we hope that the recognition of the fragmentation pathways and relative abundances of the ions obtained will provide important information, useful for the identification and differentiation of the compounds discussed. The process of the EI-induced mass fragmentation explains the influence of *N*-substituents in ring C on the process of mass fragmentation of the molecular ions of the compounds investigated. The results reported in this presentation show that EI-MS is a very useful tool for differentiating between the isomeric compounds discussed. Only on the basis of the low-resolution spectra, we can easily establish the substituted enantiomers of *L* and *D* amino acids.

**Acknowledgements:** This project has been supported by the Scientific Research Committee of Poland Grant No. N N312 187835

- [1] C. C. Boido, B. Tasso, V. Boido, F. Sparatore, *Il Farmaco*, 58, (2003) 265-277  
 [2] T. S. Rao, L. D. Correa, R. T. Reid, G. K. Lloyd, *Neuropharmacology*, 35, (1996) 393-405; T. W. Seale, S. Singh, G. Basmadjan, *Neuroreport*, 9, (1998) 201-205  
 [3] B. Tasso, C. Canu Boido; E. Terranova, C. Gotti, L. Riganti, F. Clementi, R. Artali, G. Bombieri, F. Meneghetti, F. Sparatore, *J. Med. Chem.* 52 (2009) 4345-4357



## A Raman spectroscopic study on the DNA structure at reduced pH values, in the presence of $Mn^{2+}$ ions

C. M. Muntean<sup>1</sup>, R. Misselwitz<sup>2,3</sup> and H. Welfle<sup>2</sup>

<sup>1</sup> National Institute for Research & Development of Isotopic and Molecular Technologies, P.O. 5, Box 700, R-400293 Cluj-Napoca, Romania

<sup>2</sup> Max-Delbrück-Centrum für Molekulare Medizin Berlin-Buch, Robert-Rössle-Str. 10, D-13092 Berlin, Germany

<sup>3</sup> Present address: Institut für Immunogenetik, Charité-Universitätsmedizin Berlin, Campus Virchow-Klinikum, Humboldt-Universität zu Berlin, Spandauer Damm 130, 14050 Berlin, Germany

In this work Raman spectra of calf thymus DNA were measured at reduced pH values in the presence of divalent manganese ions.

The experimental results exemplify in detail the structural changes of calf thymus DNA induced by this pH treatment in the presence of  $Mn^{2+}$  ions.

Raman spectra were analyzed in the wavenumber region  $600-1150\text{ cm}^{-1}$  that contains information about nucleoside conformation, backbone geometry and  $PO_2^-$  interaction.

Besides, Raman spectrum of DNA contains many overlapping bands in the region  $1150-1600\text{ cm}^{-1}$ , which originate primarily from in-plane vibrations of base residues. Previous studies showed that these bands cannot be assigned unambiguously because of the peaks overlap and also because the intensity of the bands in this spectral range is in general sensitive to the base-stacking interactions.

In our study proton binding to N7 of guanine is indicated to start at pH 5.1 as judged from the trough around  $1492\text{ cm}^{-1}$  in the difference spectrum. However at this pH it is not a significant phenomenon. In mononucleotides, protonation of cytosine N3 ( $pK_a=4.24$ ) and adenine N1 ( $pK_a=3.80$ ) commences at a significantly higher pH than protonation of guanine N7 ( $pK_a=2.3$ ). However the results obtained in mononucleotide studies are not directly transferable to the case of nucleotides in the DNA double helix.

The intensity of the band at  $1375\text{ cm}^{-1}$  slightly decreases with lowering the pH, which results in the trough around  $1377\text{ cm}^{-1}$ . Purine (dA, dG) and dT residues contribute to this band. Therefore discrimination between the individual contributions of these bases is difficult.

Manganese(II) ions are expected to inhibit DNA protonation even at low concentrations.

Further studies on DNA model systems with modified counterion distributions would provide information for a better understanding of the equilibria between protonated and non-protonated DNA base pairs. Such studies may contribute to the elucidation of the possible significance of base pair protonation in cellular processes.

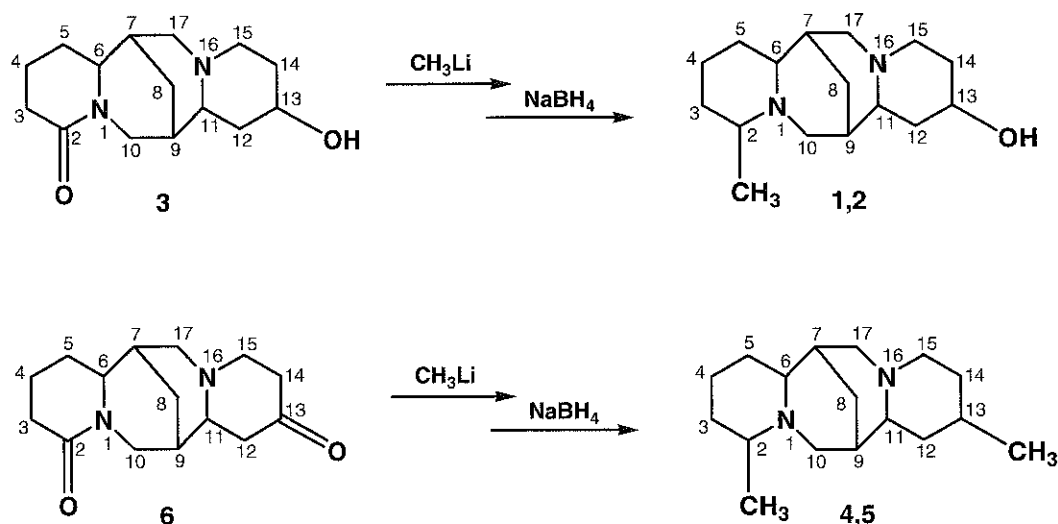


## New methyl sparteine derivatives as potential hypoglycemic agents

B. Jasiewicz, K. Skrycki

A. Mickiewicz University, Grunwaldzka 6, 60-780 Poznań, Poland

After cardiovascular diseases, diabetes is the second most important threat to the health of the present society. The compounds of plant origin which demonstrate the hypoglycemic activity include alkaloids occurring in plants of the *Fabaceae* family [1-3]. There are reports on sparteine sulfate [2], lupanine, 17-oxolupanine, 13-hydroxylupanine and 2-thionosparteine as the compounds increasing insulin secretion or decreasing the level of glucose in blood [4]. The main aim of our study was to synthesize new sparteine derivatives which would have hypoglycemic activity. New 2-methyl-13 $\alpha$ -hydroxysparteine (**1**) and 2-methyl-13 $\beta$ -hydroxysparteine (**2**) were synthesized from 13-hydroxylupanine (**3**) and new 2,13 $\alpha$ -dimethylsparteine (**4**) and 2,13 $\beta$ -dimethylsparteine (**5**) were synthesized from 13-oxolupanine (**6**) (Scheme 1). Stereochemistry of compounds **1**, **2**, **4** and **5** was established on the basis of their  $^{13}\text{C}$  and  $^1\text{H}$  NMR spectra as well as on DFT calculations. In solution, the conformation with ring C a boat predominates in all compounds studied. Pharmacological actions of new compounds have been found on the basis of the computer-aided drug discovery approach with the computer program Prediction of activity Spectra for Substances (PASS).



- [1] M. H. Mohamed, A.-N. A. El-Shorbegi, *J. Nat. Prod.* 56 (1993) 1999-2002  
 [2] J. Cabo, J. Jimenez, S. Risco, A. Zarzuelo, *Plant. Med. Phytother.* 18 (1984) 237-242  
 [3] G. Paolisso, S. Sgambato, N. Passariello, G. Pizza, R. Torella, P. Tesaro, M. Varricchio, F. D'Onofrio, *Eur. J. Clin. Pharmacol.* 34 (1988) 227-232  
 [4] P. M. Garcia Lopez, P. G. de la Mora, W. Wysocka, B. Maiztegui, M. E. Alzugaray, H. Del Zotto, M. I. Borelli, *Eur. J. Pharm.* 504 (2004) 139-142



## Characterization of changes in structure and stability of lysozyme caused by glycine and its methyl derivatives

P. Bruździak, J. Stangret

*Department of Physical Chemistry, Chemical Faculty, Gdańsk University of Technology,  
Narutowicza 11/12, 80-233 Gdańsk, Poland*

Osmolytes are small organic compounds possessing the ability to significantly affect proteins stability. Due to their properties, they are of interest to pharmaceutical and food industry. The exact mechanism of their influence on proteins is still not clear. However, it seems that water, as solution solvent, plays a great role in this phenomena.

A series of osmolyte-affected FTIR spectra of hen egg white lysozyme was investigate. Following osmolytes were investigated: glycine, N-methylglycine (NMG, sarcosine), N,N-dimethylglycine (DMG) and N,N,N-trimethylglycine (TMG, betaine). Protein and osmolytes solutions were prepared according to [1]. The chosen group of compounds would allow to draw conclusions concerning the influence of solute hydrophobicity on behaviour of protein.

To extract subtle changes in secondary structure of the hen egg white lysozyme, method of isolation of protein spectrum from ATR series of spectra was used, first introduced in [1]. Changes in the shape of the amide I band of particular glycine- and glycine derivative-affected protein spectrum were compared to changes (presented in [1]) developed in the presence of TMAO and urea, strong stabilizer and mild denaturant, respectively.

Unfortunately, presented FTIR studies cannot answer the question whether a selected osmolyte will affect thermal stability of protein. To gain an insight into this subject, DSC thermal denaturation experiments were performed and results were correlated to spectroscopic data.

**Acknowledgments:** This work was supported from the Republic of Poland scientific funds as a research project, within grant no. N N301 105438.

[1] A. Panuszko, P. Bruździak, J. Zielkiewicz, D. Wyrzykowski, J. Stangret, *J. Phys. Chem. B* 113 (2009) 14797–14809





## The use of FT-IR spectra in examination of structure and stability changes of *Taq*SSB protein and its complex with ssDNA

P. Rakowska<sup>1</sup>, M. Olszewski<sup>2</sup>, J. Stangret<sup>1</sup>, J. Kur<sup>2</sup>

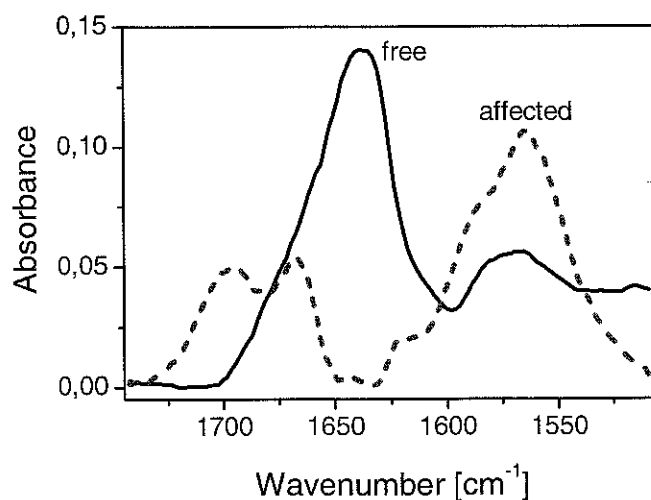
<sup>1</sup>Department of Physical Chemistry, Chemical Faculty, Gdańsk University of Technology, Narutowicza 11/12, 80-233 Gdańsk, Poland

<sup>2</sup>Department of Microbiology, Chemical Faculty, Gdańsk University of Technology, Narutowicza 11/12, 80-233 Gdańsk, Poland

Single stranded DNA – binding proteins (SSB) are vital components of cells in every living organisms. They play the essential part in replication, recombination and repair processes of DNA. One of them *Taq*SSB protein becomes a target of interest because of its characteristic properties. It was isolated from the thermophilic organism *Thermus aquaticus*. In contrast to other SSB proteins from mesophilic and eucariotic organisms, *Taq*SSB is a homodimer containing two single-stranded DNA (ssDNA) binding domains per monomer. This protein finds a wide application in molecular biology and analytic methods.

The infrared spectroscopy was used to carry out stability experiments. The *Taq*SSB protein in water solution and its complex with ssDNA was investigate. A series of FT-IR spectra of *Taq*SSB and *Taq*SSB-ssDNA complex was characterized to compare their structures and denaturation temperatures. FT-IR spectra of *Taq*SSB protein and its complex with ssDNA was measured in D<sub>2</sub>O.

The infrared studies show that binding of ssDNA causes changes in secondary structure of *Taq*SSB. The temperatures of unfolding of both *Taq*SSB and *Taq*SSB-ssDNA complex are very high. However, obtained results indicate that *Taq*SSB protein in complex with ssDNA unfolds in slightly lower temperatures than free *Taq*SSB. This rather unexpected result has been discussed in terms of denaturation thermodynamics.



Spectrum of the *Taq*SSB protein affected by ssDNA in water solution (affected) and the free protein in solution spectrum (free)

## Spectroscopic, calorimetric and ab initio study of water interactions with stabilizing and denaturing osmolytes

A. Panuszko<sup>1</sup>, D. Wyrzykowski<sup>2</sup>, J. Stangret<sup>1</sup>

<sup>1</sup>*Department of Physical Chemistry, Chemical Faculty, Gdańsk University of Technology, Narutowicza 11/12, 80-233 Gdańsk, Poland*

<sup>2</sup>*Faculty of Chemistry, University of Gdańsk, Sobieskiego 18, 80-952 Gdańsk, Poland*

Osmolytes are small organic compounds produced in living cells, reaching very high concentrations that exert influence on the stability of a protein [1]. It is believed that stabilizing osmolytes are excluded from protein surface. However, denaturing osmolytes preferentially interact with protein surface [2,3]. It is also proposed, that osmolytes do not interact with protein directly, but through surrounding water, modifying its properties. According to this theory, stabilizing osmolytes may be classified as water "structure-makers", while denaturing osmolytes as "structure-breakers" [4,5].

To investigate the hydration of stabilizing osmolytes (glycine and its methyl derivatives) and denaturing osmolytes (alkyl derivatives of urea) we used FT-IR spectroscopy. This technique is an ideal tool to observe subtle changes in the net of hydrogen bonds. Spectra of HDO isotopically diluted in H<sub>2</sub>O are free from most of experimental and interpretative problems connected with H<sub>2</sub>O spectra. The difference spectra method has been applied to remove the contribution of bulk water and thus to separate the spectra of solute-affected HDO [6,7].

To estimate the hydrogen-bond energies between water and the osmolytes studied, calorimetric measurements were carried out.

The experimental results were confronted with DFT-calculated structures of small gas-phase and polarizable continuum model (PCM) solvated aqueous clusters to obtain complementary picture of the osmolytes hydration spheres.

This work is supported by the scientific funds as a research project, within grant no. N N204 121338.

- [1] R. Kumar, Arch. Biochem. Biophys. 491 (2009) 1-6
- [2] S. N. Timasheff, Annu. Rev. Biophys Biomol. Struct. 22 (1993) 67-97
- [3] T. O. Street, D. W. Bolen, G. D. Rose, Proc. Natl. Acad. Sci. USA 103 (2006) 13997-14002
- [4] Q. Zou, B. J. Bennion, V. Dagget, K. P. Murphy, J. Am. Chem. Soc. 124 (2002) 1192-1202
- [5] E. A. Galiński, M. Stein, B. Amendt, M. Kinder, Comp. Biochem. Physiol. 117A (1997) 357-365
- [6] J. Stangret, Spectr. Letters 21 (1988) 369-381
- [7] J. Stangret, T. Gampe, J. Phys. Chem. B 103 (1999) 3778-3783



## Conformational preferences, experiment and theoretical vibrational spectra of cyclo(gly-val) dipeptide

S. Celik<sup>a</sup>, A. E. Ozel<sup>b</sup>, S. Akyuz<sup>c</sup>, S. Kecel<sup>b</sup> and G. Agaeva<sup>d</sup>

<sup>a</sup> *Electrical-Electronics Engineering Department, Engineering Faculty, Istanbul University, 34320, Avcilar, Istanbul, Turkey*

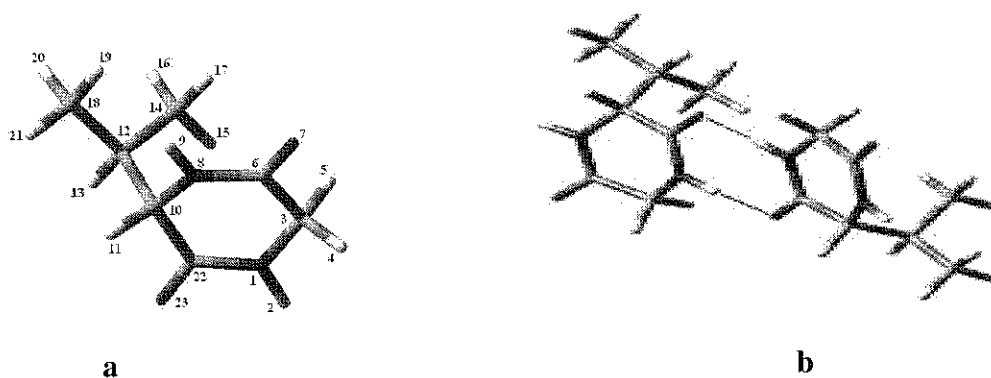
<sup>b</sup> *Department of Physics, Faculty of Science, Istanbul University, Vezneciler, 34134, Istanbul, Turkey*

<sup>c</sup> *Department of Physics, Faculty of Science and Letters, Istanbul Kultur University, Atakoy Campus, 34156, Istanbul, Turkey*

<sup>d</sup> *Institute of Physical Problems, Baku State University AZ- 1148, Baku /AZERBAIJAN*

The theoretical conformational analysis of cyclic dipeptide, glycine-valine, was performed by molecular mechanics method, in order to examine the energetically optimal conformational states of the cyclic dipeptide that has anticancer activity. The relative positions of the side chain residues of the stable conformations of dipeptide were obtained depending on the obtained conformational analysis results. The geometry of the most stable conformation of the cyclo(Gly-Val) was optimized using DFT method at B3LYP/6-31++G(d,p) level of theory. After then dimeric forms of the dipeptide were formed and their investigated, energetically optimal conformational states of dimers were obtained and the geometry of the global conformation of the dimer was optimized using the same method and the same level of theory.

The experimental IR and micro-Raman spectra of cyclo(Gly-Val) were reported for the first time. The vibrational normal modes and associated wavenumbers, IR intensities and Raman activities of the monomeric and dimeric forms of the dipeptide were calculated using DFT method at B3LYP/6-31++G(d,p) level of theory and the results were compared with the experimental data. The fundamental vibrational modes were assigned depending on their total energy distributions. The aim of this study is to give a complete description of the molecular geometry and molecular vibrations of monomer and dimer of cyclo(Gly-Val) in the framework of the density functional method and conformational analysis method to investigate the hydrogen bonding interactions and the coordination effects on the investigated molecule.



Global conformations of monomeric (a) and dimeric (b) forms of cyclo(Gly-Val) dipeptide. The hydrogen bonds that act important role for the formation of dimer are indicated by broken lines (b)

## Raman and infrared spectroscopy of amino acids and its implication for improvement of the protein secondary structure determination

T. Pazderka<sup>1</sup>, V. Kopecký Jr.<sup>1</sup>, K. Hofbauerová<sup>1,2</sup>, V. Baumruk<sup>1</sup>

<sup>1</sup>*Institute of Physics, Faculty of Mathematics and Physics, Charles University in Prague, Ke Karlovu 5, Prague 2, CZ-121 16, Czech Republic; pazderka@karlov.mff.cuni.cz*

<sup>2</sup>*Institute of Microbiology, Academy of Sciences, Vídeňská 1083, Prague 4, CZ-142 20, Czech Republic*

Determination of the protein structure represents one of the key tasks of present molecular biology. Raman and infrared (IR) spectroscopy can provide good wealth of information about protein structure in comparison to other methods of optical spectroscopy. Therefore, development and improvement in such spectroscopic techniques that can be used for characterization of proteins is becoming increasingly important in the rapidly expanding field of proteomics.

In this study Raman and IR spectra of all amino acids (AA) presented in proteins have been measured with a view to possible protein sequence dependent subtraction of vibration bands of AA side chains in the regions of amide I, II and III. The measurements were especially focused on new method of non-enhanced Raman spectroscopy – the drop coating deposition Raman (DCDR) spectroscopy [1] – based on a coffee ring effect, which enables measurements of solutions of biomolecules at very low concentrations. Even if the DCDR measurements may be slightly problematic [2], good quality spectra of molecules in glass phase can be obtained [3]. The Raman measurements were performed on extremely diluted amino acid samples (0.005 mg/mL) to avoid formation of microcrystals. The method of AA side chains spectral subtraction was tested on globular proteins and short peptide samples with known primary sequence. The influence of the subtraction on improvement of the secondary structure determination will be discussed as well.

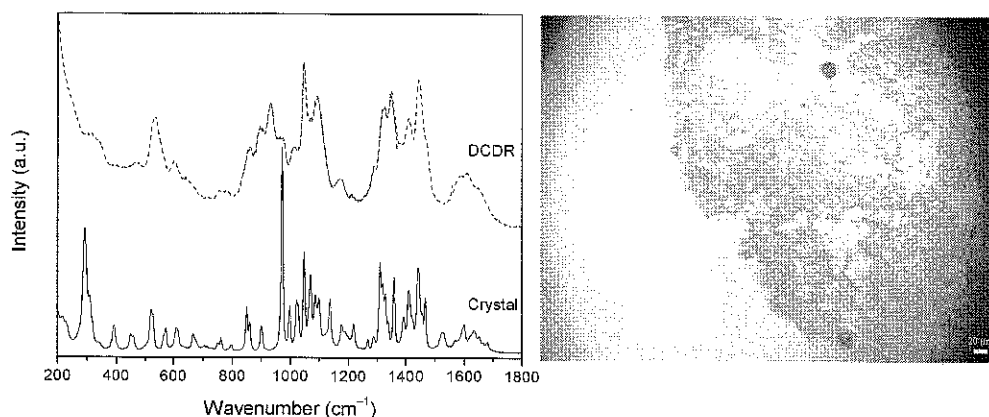


Fig. 1. – (left) Raman spectra of L-arginine measured from the polycrystalline sample and as DCDR deposit and (right) the detail view of DCDR sample (the white bar represents 20  $\mu\text{m}$ ).

**Acknowledgements:** The Grant Agency of the Academy of Sciences and the Ministry of Education of the Czech Republic are acknowledged for the support (Nos. KJB101120805 and No. MSM 0021620835, respectively).

[1] D. Zhang, Y. Xie, M. F. Mrozek et al., *Anal. Chem.* 75 (2003) 5703–5709

[2] V. Kopecký Jr., V. Baumruk, *Vib. Spectrosc.* 42 (2006) 184–187

[3] J. Kapitán J., V. Baumruk, V. Kopecký Jr. et al., *J. Am. Chem. Soc.* 128 (2006) 13451–13462

## Structural and spectroscopic elucidation of L-proline tyrosine (L-pro-tyr) dipeptide

S. Kecel<sup>1</sup>, A. E. Ozel<sup>1</sup>, S. Akyuz<sup>2</sup>, S. Celik<sup>3</sup> and G. Agaeva<sup>4</sup>

<sup>1</sup>Istanbul University, Faculty of Science, Department of Physics, Vezneciler, 34134, Istanbul, Turkey

<sup>2</sup>Istanbul Kultur University, Faculty of Science and Letters, Department of Physics, Atakoy Campus, 34156, Istanbul, Turkey

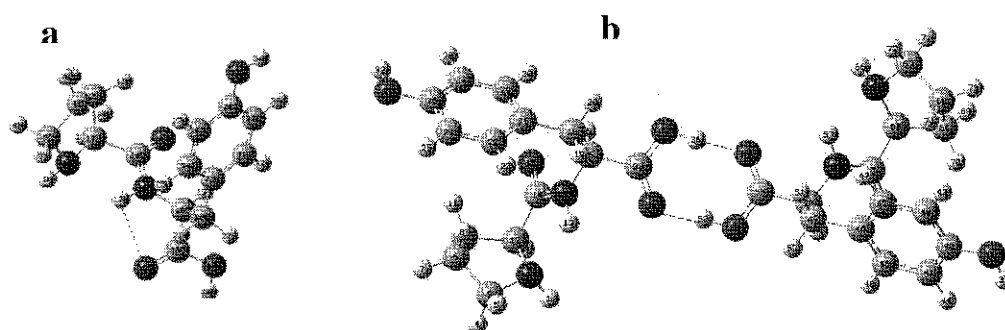
<sup>3</sup>Istanbul University, Engineering Faculty, Electrical-Electronics Eng. Department, 34320 - Avcilar, Istanbul, Turkey

<sup>4</sup>Institute of Physical Problems, Baku State University AZ- 1148, Baku /AZERBAIJAN

In this study the conformational properties of the drug based dipeptide L-proline tyrosine (L-Pro-Tyr) and its dimer have been investigated by molecular mechanics and ab-initio calculations. The calculation on Pro-Tyr dipeptide as a function of side chain torsion angles, enable us to determine their energetically preferred conformations. 108 possible conformations of Pro-Tyr dipeptide have been investigated theoretically by using program proposed by Godjaev et al[1]. The lowest energy conformation of the dipeptide has been determined by using the Ramachandran maps [2,3] and compared with the quantum chemical ab-initio results with the Gaussian03 program by using DFT with B3LYP functional and 6-31++G(d,p) basis set.

Raman (4000-50 cm<sup>-1</sup>) and IR (4000-400 cm<sup>-1</sup>) spectra of the biologically active molecule have been recorded in solid phase. The assignments of the vibrational spectra have been carried out with scaled quantum mechanical (SQM) method. In addition, the total energy distributions (TED) of the dipeptide have been calculated and the vibrational modes are determined. The experimental vibrational wavenumbers of solid dipeptide are found to be more close to the calculated wavenumbers of dimeric form of Pro-Tyr than its monomeric form.

This study was supported by the Research fund of Istanbul University (Project number ONAP-2423).



Monomeric (a) and dimeric (b) forms of Pro-Tyr dipeptide. The estimated H-bonds are indicated with broken lines.

[1] N.M Godjaev., I.S.Maksumov, I.Ismailoval., J.Chem.Struc. (Russian), 24 (1983) 147

[2] G.N. Ramachandran, Biopolymers 6 (1963) 1494.

[3] G.N. Ramachandran, C. Ramakrishnan, V. Sasisekharan, J. Mol. Biol. 7 (1963) 95.



## DCDR spectroscopy as efficient tool for study of liposome interaction with biomolecular complexes

E. Kočiřová, M. Procházka and J. Štěpánek

*Charles University, Faculty of Mathematics and Physics, Institute of Physics, Ke Karlovu 5, Prague 2, CZ-121 16, Czech Republic*

Drop coating deposition Raman (DCDR) spectroscopy is relatively new method based on deposition of a small drop of the sample in aqueous solution on a special hydrophobic surface consisting of a polished stainless steel base coated with a thin layer of Teflon (SpectRIM™, Tienta Sciences) [1]. This surface enables the droplet to dry in the manner of “coffee ring effect” [2]: The dispersed material is carried by the flow of a liquid in the evaporating droplet to its edge where it forms a ring. By using confocal Raman microspectrometer it is possible to obtain in this way Raman spectra of biomolecules present in very low concentration (down to 1  $\mu\text{M}$  [3]) in the original solution.

Liposomes represent interesting lipid-membrane system often employed as a model of real biological membrane. We have studied two kinds of liposomes, the first composed of pure phosphatidylcholine (PC) and the second prepared from asolectin that is a mixture of various lipids extracted from soybean, resembling the natural biomembrane. Dried deposited drops of both liposome samples form distinct rings with the majority of lipids accumulated at the edge and the salts of phosphate buffer separated in the central part of the dried drop. Although PC and asolectin solutions are at room temperature in the gel and the liquid crystalline phase, respectively, Raman spectra measured from the ring of the dried drops show formation of a new phase in both cases. Very good reproducibility of liposome DCDR spectra proves that dried deposited drops of aqueous liposome suspension represent well defined model system, promising for studies of liposome interactions with other biomolecules via vibrational spectroscopy.

Oligonucleotides, synthetically prepared short chains of nucleic acids, are potential candidates to specifically modulate gene expression inside living cells [4]. Water soluble cationic porphyrins can serve as enhancers of oligonucleotide penetration through the membrane [5]. We used DCDR technique to study interaction of the porphyrin/oligonucleotide complex, cationic copper 5,10,15,20-tetrakis (1-methyl-4-pyridyl) porphyrin (CuTMPyP) and 15 bases long oligothymidylate (dT<sub>15</sub>), with liposomes. Raman mapping of the dried droplet of this system revealed partial separation of the free CuTMPyP/dT<sub>15</sub> complexes and the CuTMPyP/dT<sub>15</sub> complexes bound to liposomes. This enabled us to obtain Raman spectra of particular components. Factor analysis displayed spectral changes mainly in the region of CH stretching vibration (2800-3000  $\text{cm}^{-1}$ ), which were attributable to a reorientation of lipid chains in liposome as a consequence of their interaction with the CuTMPyP/dT<sub>15</sub> complex.

- [1] D. Zhang, Y. Xie, M.F. Mrozek, C. Ortiz, V.J. Davisson, D. Ben-Amotz, *Anal. Chem.* 75 (2003) 5703-5709
- [2] R.D. Deegan, O. Bakajin, T.F. Dupont, G. Huber, S. R. Nagel, T.A. Witten, *Nature* 389 (1997) 827-829
- [3] V. Kopecký Jr., V. Baumruk, *Vib. Spectrosc.* 42 (2006) 184-187
- [4] J. Goodchild, *Curr. Opin. Mol. Ther.* 6 (2004) 120-128
- [5] P. Praus, E. Kočiřová, O. Seksek, F. Sureau, J. Štěpánek, P.-Y. Turpin, *Current Organic Chemistry* 11 (2007) 515 – 527 and references therein.

**Acknowledgements:** Financial support from the Czech Ministry of Education (project No. MSM0021620835) is gratefully acknowledged.



## Calculations of infrared spectra of the amide I band of proteins – method development and application to SR Ca<sup>2+</sup>-ATPase

E. L. Karjalainen, A. Barth

*Department of Biochemistry and Biophysics, Arrhenius Laboratories, Stockholm University,  
SE-106 91 Stockholm, Sweden*

The aim of the presented work is to improve the understanding of the correlation between the infrared absorbance in the amide I region and conformational changes of the protein backbone. The amide I region of infrared spectra is a crowded region with many overlapping bands and there is, in spite of previous efforts, not yet a clear understanding of the relationship between structure and band shape.

Our computational approach involves constructing the vibrational hamiltonian using a combination of published parameterised ab initio data of small peptides for the calculation of diagonal force constants as well as off-diagonal force constants for nearest neighbours in a polypeptide chain [1], and a transition dipole coupling model (“floating oscillator model”) [2] for describing long range interactions.

Ultimately, the calculations will be applied on structures of the SR Ca<sup>2+</sup>-ATPase and other proteins to calculate infrared difference spectra of the conformational changes and thereby advance our understanding of the SR Ca<sup>2+</sup>-ATPase and other P-type pump mechanisms. Improved understanding of the correlation between structure and band shape of the amide I band will also make infrared spectroscopy a more valuable tool in the study of proteins, especially of those that are too large for NMR or are difficult to crystallise.

[1] J-H. Choi, M. Cho, in (A. Barth, P.I. Haris, eds.) Biological and Biomedical Infrared Spectroscopy, IOS Press (2009) 224-260

[2] H. Torii, M. Tasumi, J. Chem. Phys. 96 (5) (1992) 3379-3387



## Surface-enhanced Raman study of the interactions between cationic polyamines and polynucleotides

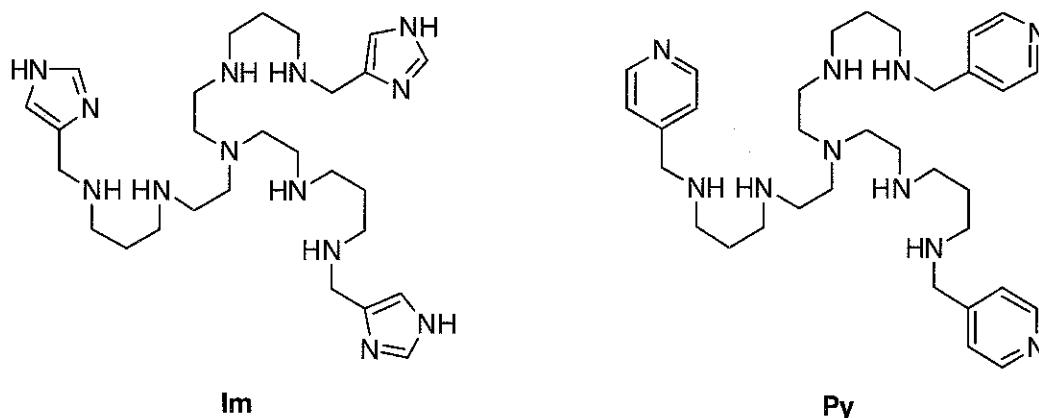
A. Dijanošić<sup>1</sup>, S. Miljanić<sup>1</sup>, Z. Meić<sup>1</sup>, I. Piantanida<sup>2</sup>, M. T. Albelda<sup>3</sup>, A. Sornosa-Ten<sup>3</sup>, E. García-España<sup>3</sup>

<sup>1</sup> Laboratory of Analytical Chemistry, Department of Chemistry, Faculty of Science, University of Zagreb, Horvatovac 102a, HR-10000 Zagreb, Croatia

<sup>2</sup> Laboratory of Supramolecular and Nucleoside Chemistry, Department of Chemistry and Biochemistry, Ruđer Bošković Institute, P.O.B. 1016, HR-10000 Zagreb, Croatia

<sup>3</sup> Departamento de Química Inorgánica, Instituto de Ciencia Molecular, Apartado de Correos 22085, 46071 Universidad de Valencia, Spain

Surface-enhanced Raman scattering (SERS) was used to study interactions of new DNA/RNA binding compounds with double-stranded DNA polynucleotides (poly dAdT-poly dAdT, poly dGdC-poly dGdC) and calf thymus DNA (ct-DNA).



SERS experiments with double-stranded polynucleotides revealed strong enhancement of the Raman scattering from the polyamine molecules attached on the colloidal silver particles as well as appearance of new bands associated mainly with nucleobases. **Im** and **Py** selectively interact with polynucleotides depending on their base pairs structures. Interactions within both, major and minor groove are recognized for poly dAdT-poly dAdT, while the polyamines prefer binding only to major groove of poly dGdC- poly dGdC.

In SERS spectra with ct-DNA downshift of the imidazole and pyridine ring vibrations supports aromatic stacking interactions of the aromatic moieties between the DNA base pairs.

Although the same binding mode was evidenced for both molecules, more spectral changes were observed for **Im**. Since **Im** and **Py** contain the same aminomethylene chains in molecular structure, differences originate from the aromatic rings. Unlike pyridine, the imidazole ring poses two potential binding sites, obviously responsible for stronger interactions.



## Studies on Valine-Tyrosine, antihypertensive dipeptide in Aqueous Solution by Raman Spectroscopy

Y. Akkaya<sup>1</sup>, K. Balci<sup>1</sup> and S. Akyuz<sup>2</sup>

<sup>1</sup> *Istanbul University, Faculty of Science, Department of Physics, Vezneciler, 34134, Istanbul, Turkey,*

<sup>2</sup> *Istanbul Kultur University, Faculty of Science and Letters, Department of Physics, Atakoy Campus, 34156 Istanbul, Turkey*

Hypertension is one of the important life style-related diseases, and has a major risk factor for cardiovascular disease (CVD) which is the number one cause of death and disability in most Western countries. Therefore the peptides, derived from foot proteins that exert antihypertensive activity, have attracted considerable interest. Valine-Tyrosine (Val-Tyr) dipeptide is molecule inhibiting the angiotensin converting enzyme (ACE) that was first identified from sardine muscle hydrolyzed by *Bacillus licheniformis* alkaline protease [1]. In addition, it is also known that Val-Tyr specifically inhibits angiotensin I (Ang I) evoked contraction through ACE inhibition and have an apparent blood pressure lowering effect in transgenic hypertensive mice [2]. Despite its great scientific and commercial value, only one vibrational spectroscopic study on H-Val-Tyr-OH molecule, which was based on the IR spectroscopy [3], is available. Moreover, no published study on the prediction of the room-temperature Raman spectra of the molecule could be found in the current literature. From this point of view, our study including a correct and complete prediction of the experimental Raman spectra of Val-Tyr dipeptide, separately recorded in solid phase as well as in water and heavy water solutions in the range 4000 – 100 cm<sup>-1</sup>, will provide significant contribution. In the recorded spectra, the characteristic Fermi doubled of tyrosine, due to phenolic moiety, was observed around 851 and 825 cm<sup>-1</sup>. The relative integrated intensity ratio of the higher- and lower-wavenumber components of this doubled is known to be sensitive to the nature of hydrogen-bonding state of the tyrosine OH group. The obtained Raman spectroscopic data have clearly indicated that both hydrogen and oxygen atoms of phenoxyl group involve in a hydrogen bonding, however, phenoxyl-oxygen involve in a remarkably stronger hydrogen bonding in solid phase of H-Val-Tyr-OH than its aqueous solutions. The hydrogen bonding state of the tyrosine phenoxyl group was determined to change, depending on the concentration of the dipeptide. In addition, amide I and amide III bands were also determined to alter, depending on the concentration of the solution.

[1] H. Matsufuji, T. Matsui, E. Seki, K. Osajima, M. Nakashima, Y. Osajima, *Biosci Biotechnol Biochem* 58 (1994) 2244-2245.

[2] T. Matsui, X. L. Zhu, K. Watanabe, K. Tanaka, Y. Kusano, K. Matsumoto, *Life Sciences* 79 (2006) 2492-2498

[3] B. B. Koleva, T. M. Kolev, M. Spitteller, *Spectrochimica Acta Part A* 68 (2007) 1187-1196.



## Evaluation of Existence of Biofilm in the Isolates of Pseudomonas with Spectrophotometer

G. Uraz, B. Çelik

*Gazi University, Faculty of Science and Arts, Department of Biology, Teknikokullar ANKARA*

Bacteria become more resistant against anti-microbial, anti-septic and industrial biosids, when they synthesize biofilm. Bacteria containing biofilm gain resistance against proteases, some chemical substances and environmental factors compared to those which do not contain.

In recent years, it is mentioned in literature about the existence of biofilm in Pseudomonas bacteria. Biofilm makes it easy for the pseudomonas spread in the environment. It is one of the leading factors of hospital infections due to the resistance it earns to the bacteria. Biofilm is also important in pseudomonas contained in the environmental samples. It causes pollution of environment and especially water contamination, due to the increase of bacteria population.

For this reason, the existence of biofilm was investigated in the study, by isolating the Pseudomonas bacteria from the water and soil samples. 16 P.aeruginosa, 7 P.fluorescens, 5 P.putida were isolated from the soil samples. And, 11 P.aeruginosa, 7 P.fluorescens, 5 P.putida was studied on in water samples. Biofilm formation in pseudomonas was investigated by way of using dyes called safranin and crystal violet. The micro-plate to which bacterium culture was added was washed for 3 times with distilled water by being taken out of incubator at the end of 24 hours and the crystal violet solution prepared as 0.1% was distributed to all tiny wells. A film layer which can be seen with naked eye was formed in the peripheries of tiny wells which had "biofilm positive." 200 microliters of ethanol with 95% was added to these tiny wells and it was left to thaw for 10 minutes. Then, it was read at 540 nm in spectrophotometer device. The same procedure was repeated by using safranin solution of 0.1%. The procedure of thawing was made with acetic acid of %50 and it was read at 470 nm in spectrophotometer device (Versamax Tunable, Microplate Reader; Moleküler Devices®).

In this research, strong positive at the ratio of 53.57% was found in the study carried out by way of using crystal violet in 28 soil samples with 24 hours measurements; and strong positive at the ratio of 57.14% was found in the study carried out by way of using safranin.

In totally 23 water samples, strong positive at the ratio of 47.82% was found in the study conducted by way of using crystal violet with 24 hours measurements; and strong positive at the ratio of 56.52% was found in the study conducted by way of using safranin. As a consequence, it was determined that there is biofilm secreted by Pseudomonas.



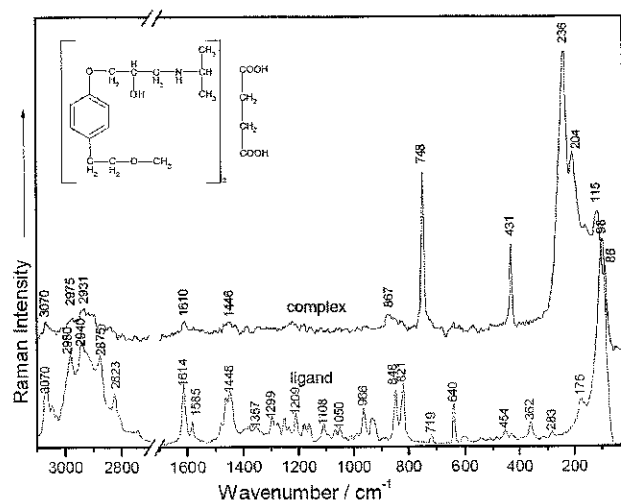
## Vibrational and DFT Study of Some Cardiovascular Drugs and Their Copper Complexes

O. Cozar, L. Szabó, I. B. Cozar, N. Leopold, V. Chiş, L. David

*Babeş-Bolyai University, Faculty of Physics, Kogălniceanu 1, 400084 Cluj-Napoca, Romania*

Atenolol (ATE) and metoprolol (MET) are selective beta receptor blockers used for various indications, but particularly for the management of cardiac arrhythmias, cardio protection after myocardial infarction (heart attack), and hypertension. These drugs block chemicals, such as adrenaline, and prevent thus from increasing heart rate, blood pressure, and oxygen use [1].

IR, Raman and surface-enhanced Raman scattering (SERS) spectra of protonated molecular forms of atenolol (ATE) and metoprolol (MET) were recorded, and the vibrational bands assigned by means of density functional theory (DFT) based calculations. The adsorption geometry to the silver surface of the investigated drugs was derived by considering the molecular electrostatic potential (MEP) map and the SERS surface selection rules [2,3]. Both molecules are adsorbed through the oxygen atoms and  $\pi$ -electrons of the ring to the silver surface. The whole structure of the molecules lies on the metal surface with the aromatic ring in a tilted and flat orientation for ATE and MET, respectively.



The ring characteristic bands ( $1614\text{ cm}^{-1}$  and  $1448\text{ cm}^{-1}$ ) from the Raman spectrum of MET (Fig. 1) are not meaningfully shifted by the complexation with copper ( $1610\text{ cm}^{-1}$  and  $1446\text{ cm}^{-1}$ ). This fact shows that oxygen atom directly bonded to the MET ring does not participate to the Cu coordination. On the other hand, bands which appear at  $431\text{ cm}^{-1}$ ,  $236\text{ cm}^{-1}$  and  $204\text{ cm}^{-1}$  in the spectrum of Cu-MET compound assigned to Cu-O bands clearly show the participation of the other MET and tartrate oxygens to copper coordination.

Molecular complexes with Cu (II) were prepared on going from the starting salts (sodium benzoate and copper sulphate) by coprecipitation procedure.

A comparative study of the FT-IR and Raman spectra of ligands (ATE, MET) and the corresponding metal complex allowed us to establish the molecular groups involved in the coordination and the local symmetry around the Cu(II) ions.

Thus in the case of Cu – ATE complex the  $\text{NH}_2$  and  $\text{C}=\text{O}$  groups are involved in the coordination by nitrogen and oxygen atoms.

[1] S.A.C. Wren, P. Tchelitcheff, J. Pharm. Biomed. Analysis 40, 571 (2006)

[2] N. Leopold, L. Szabo, A. Pirnau, M. Aluas, L. F. Leopold, V. Chis, O. Cozar, Journal of Molecular Structure, 919, 94 (2009)

[3] M. Moskovits, J. S. Suh, J. Phys. Chem., 88, 5526 (1984)



## Vibrational investigation on the *in vitro* bioactivity of commercial and experimental calcium-silicate cements for root-end endodontic therapy

P. Taddei<sup>1</sup>, E. Modena<sup>1</sup>, A. Tinti<sup>1</sup>, F. Siboni<sup>2</sup>, C. Prati<sup>2</sup>, M. G. Gandolfi<sup>2</sup>

<sup>1</sup>Dipartimento di Biochimica "G. Moruzzi", Sez. di Chimica e Prop. Biochimica, Via Belmeloro 8/2, University of Bologna, 40126 Bologna, Italy

<sup>2</sup>Dipartimento di Scienze Odontostomatologiche, Via S. Vitale 59, University of Bologna, 40126 Bologna, Italy

Portland cements are hydraulic calcium-silicate materials able to set in moist environment. White Portland cements are composed of tricalcium silicate (alite), dicalcium silicate (belite), tricalcium aluminate and calcium sulphate. Grey Portland cements also contain a ferrite phase (aluminoferrite) and other transition metals (Cr and Mn) and metalloids (As).

In the last decade, calcium-silicate hydraulic cements have received great attention in endodontics because able to set in presence of blood and other biological fluids. In the 1990s a first calcium-silicate cement MTA (Mineral Trioxide Aggregate) was developed as root-end filling material.

Recent investigations demonstrated that MTA and calcium-silicate cements are bioactive materials, i.e. they are able to spontaneously form a calcium-phosphate layer when immersed in physiological-like fluids. This bone-like apatite layer can support new tissue formation and the integration in bone tissue and represents an essential requirement for an artificial material to be considered osteoconductive and osteoinductive.

This study was aimed at comparatively investigating the bioactivity of commercial calcium-silicate cements (ProRoot white MTA, Angelus grey MTA, Angelus white MTA, TechBiosealer root end) and an experimental calcium-silicate cement (wTC) upon ageing for different times (from 1 to 28 days), at 37°C, in Dulbecco's Phosphate buffered saline (DPBS). With the exception of wTC, all the cements contained bismuth oxide for radiopacity. ATR/FT-IR and micro-Raman spectroscopy were used to investigate the presence of deposits on the cement surface and the composition changes as a function of storage time (hydration of anhydrite/gypsum and formation of ettringite; hydration of belite/alite and formation of hydrated silicates).

Spectroscopic analyses showed that after one day of ageing all the cements formed an apatite deposit on their surface, as revealed by the appearance of the bands at about 1030, 600 and 560 cm<sup>-1</sup> (IR) and 960 cm<sup>-1</sup> (Raman). The thickness of the deposit was evaluated by the  $I_{960(\text{phosphate})}/I_{990(\text{cement})}$  (Raman) and  $I_{1030(\text{phosphate})}/I_{950(\text{cement})}$  (IR) ratios obtained on the surfaces of the samples. After one day in DPBS, only in Angelus grey MTA the bands of the cement near 830-850 cm<sup>-1</sup> became undetectable due to the high thickness of the superficial apatite deposit suggesting that Angelus grey MTA possesses the highest bioactivity.

At increasing storage times in DPBS (14-28 days), the thickness of the deposit increased as well as its crystallinity and the bands of a B-type carbonated apatite appeared at 1460-1415, 1025, 960, 600-560 cm<sup>-1</sup> (IR) and 1074, 1050, 965, 606-595- 436 cm<sup>-1</sup> (Raman).

All cements produced and released Ca(OH)<sub>2</sub>. Its formation was monitored by the trend of the 3640 cm<sup>-1</sup> IR band and its release was detected by pH measurements.

In conclusion, all calcium-silicate cements resulted bioactive. The higher bioactivity found for Angelus grey MTA must be further investigated considering the presence in its composition of transition metals.



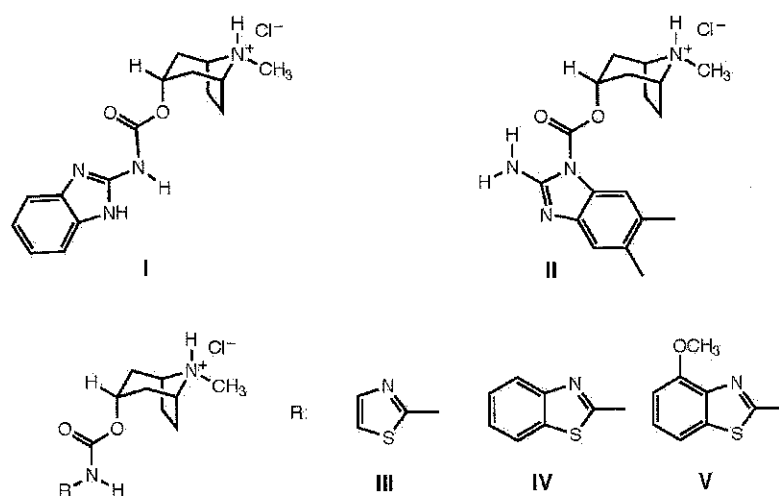
## Synthesis, conformational and pharmacological study of some carbamates derived from *endo*-8-methyl-8-azabicyclo[3.2.1]octan-3 $\alpha$ -ol hydrochlorides

I. Iriepa<sup>1</sup>, J. Bellanato<sup>2</sup>, E. Gálvez<sup>1</sup>

<sup>1</sup>Dpto. Química Orgánica, Universidad de Alcalá, Ctra. Madrid-Barcelona Km 33,600, 28871, Alcalá de Henares, Madrid, Spain

<sup>2</sup>Instituto de Estructura de la Materia, C.S.I.C., Serrano, 121, 28006 Madrid, Spain

A series of benzimidazole, thiazole and benzothiazole carbamates derived from *endo*-8-methyl-8-azabicyclo[3.2.1]octan-3 $\alpha$ -ol hydrochlorides (**I-V**) has been synthesized and studied by <sup>1</sup>H, <sup>13</sup>C and IR spectroscopy. To assist in the interpretation of the spectroscopic data, the crystal structure of compound **IV** was determined by X-ray diffraction.



From the <sup>1</sup>H and <sup>13</sup>C NMR data it can be deduced that compounds **I-V**, in DMSO-*d*<sub>6</sub>, show a preferred conformation where the pyrrolidine and piperidine rings adopt a flattened enveloped at N8 and a distorted chair conformation puckered at N8 and flattened at C3, respectively with the *N*-CH<sub>3</sub> group in equatorial position. This conformation found in solution agrees with that observed for compound **IV** in the solid state.

In the case of compound **IV**, X-Ray data show that molecules in the crystal are linked by hydrogen bonding through the Cl<sup>-</sup> ion, which is involved in two different hydrogen bonds. <sup>13</sup>C NMR data for compound **II** suggest intramolecular hydrogen bonding. To go further in the structural study of these compounds, IR spectroscopy of the corresponding bases has been used.

Compounds displaying 5-HT<sub>3</sub> antagonistic activities are agents in the treatment of vomiting and nausea resulting from anticancer therapy. The antagonistic activities of compounds **I-V** have been evaluated, *in vitro* and *in vivo*. Compounds **II-V**, *in vitro*, showed similar activities to the reference compound. Moreover, compound **III** displays, *in vivo*, more activity than metoclopramide.

## Chiral recognition and complexation behaviour of $\beta$ -CyDs vs. L-, D- and DL-serine by FTIR-ATR spectroscopy.

V. Venuti<sup>1</sup>, V. Crupi<sup>1</sup>, D. Majolino<sup>1</sup>, A. Mazzaglia<sup>2</sup>, A. Paciaroni<sup>3</sup>, R. Stancanelli<sup>4</sup>

<sup>1</sup>Dipartimento di Fisica & CNISM, Università di Messina, viale Ferdinando Stagno D'Alcontres 31, 98166 Messina, Italy.

<sup>2</sup>Istituto per lo Studio dei Materiali Nanostrutturati ISMN-CNR, c/o Dipartimento di Chimica Inorganica, Chimica Analitica e Chimica Fisica, Università di Messina, 98166, Messina Italy.

<sup>3</sup>Dipartimento di Fisica, Università di Perugia, CEMIN & INFN CRS SOFT, Via A. Pascoli, 06123 Perugia, Italy.

<sup>4</sup>Dipartimento Farmaco-Chimico, Università di Messina, Viale Annunziata, 98168 Messina, Italy.

Cyclodextrins are well known in supramolecular science as host molecules capable of encapsulating molecules in their hydrophobic cavity via noncovalent interactions. The chiral recognition properties of these macrocycles, not fully characterized yet, are of great relevance in pharmaceutical industry [1]. We performed an attenuated total reflection Fourier transform infrared FTIR-ATR investigation of the inclusion complexes of  $\beta$ -cyclodextrins ( $\beta$ -CyDs, host) with the amino acid serine (guest) in its chiral (D-serine, L-serine) and racemic (DL-serine) forms. The vibrational dynamics of the complexes has been compared with the single components and physical mixtures with the aim at characterizing the "host-guest" interactions involved in the chiral recognition mechanism.

[1] A. Yanagida, A. Shoji, Y. Shibusawa, H. Shindo, M. Tagashira, M. Ikeda, Y. Ito, J. Chromatogr. A 1112 (2006) 195-201.



## Flexibility of a Model Cyclic Hexapeptide Studied by the Raman and Raman Optical Activity

J. Hudecová<sup>1,2\*</sup>, J. Kapitán<sup>1,2</sup>, V. Baumruk<sup>1</sup> and P. Bouř<sup>2</sup>

<sup>1</sup>*Institute of Physics, Faculty of Mathematics and Physics, Charles University in Prague, Ke Karlovu 5, 121 16 Prague 2, Czech Republic*

<sup>2</sup>*Institute of Organic Chemistry and Biochemistry, Academy of Sciences, Flemingovo nám. 2, 166 10 Prague 6, Czech Republic*

Raman optical activity (ROA) measures the vibrational optical activity as an intensity difference in the Raman scattering for right and left circularly polarized light. The ROA and Raman spectra of the cyclo-(Phe-DPro-Gly-Arg-Gly-Asp) peptide were recorded on the ROA spectrometer built at the Institute of Physics of the Charles University that adopts an ICP modulation scheme and the backscattering geometry [1].

The model peptide has a distinct folded structure containing short  $\beta$ -hairpin and  $\beta$ -sheet patterns [2]. Geometry of the backbone is rather restricted. The spectra and molecular motions were analyzed with the aid of density functional theory (DFT) simulations combined with molecular dynamics (MD). According to the MD the side chains largely oscillate around several preferred conformations. Raman and ROA spectral intensities, band positions, and, in an extreme case, the ROA signs, are significantly modified by such molecular flexibility [3].

Spectral averaging of many MD structures provided a dramatic improvement in simulated spectral shapes, in comparison with a classical one conformer model. The Raman and ROA scattering was dominated by hydrophobic phenylalanine and proline groups, as could be verified both by the computations and an additional experiment with a model Phe-D-Pro dipeptide. Computational analyses suggest that the ROA spectrum mostly senses locally chiral side chains, whereas vibrational coupling between different side chains contributes less, and is restricted to specific vibrational regions.

The combination of the Raman and ROA spectroscopy with the multi-scale computational technique thus brings extended information about biologically relevant molecules. Future instrumental and computational improvements are nevertheless desirable to investigate further details in molecular structure and dynamics.

Support from Grant Agency of Charles University (project 126310), Grant Agency of the Czech Republic (203/06/0420), and Grant Agency of the Academy of Sciences (A400550702, M200550902) are gratefully acknowledged.

[1] J. Hanzlíková, P. Praus, V. Baumruk, *J. Mol. Struct.* 480-481 (1999) 431-435

[2] P. Bouř, J. Kim, J. Kapitán, R.P. Hammer, R. Huang, L. Wu and T. A. Keiderling, *Chirality* 20 (2008) 1104-1119

[3] J. Kapitán, V. Baumruk, V. Kopecký Jr., P. Bouř, *J. Phys. Chem. A* 110 (2006) 4689-4696



## Free radicals in gamma irradiated neurological drug topimarate: an EPR study

S. Osmanoglu, Y. Dicle<sup>1</sup>

*Siirt Univ., Faculty of Education, Siirt, Turkey*

Using high energy ionising radiation both for sterilization of pharmaceuticals and medical device or for improvement of the hygienic quality of foods is now a well established technology. The aim of this study is to investigate the spectroscopic and kinetic features of the species having unpaired electrons induced gamma irradiated gabaapentin at room and different temperatures in dose range 5-50 kGy using EPR spectroscopy. EPR measurements proved that gabapentin contained stable paramagnetic species after irradiation and relative yielding of free radicals depends on the absorbed dose. radical species responsible from observed EPR lines are investigated at room and different temperatures. The storage period of the gabapentin which it conserved its identity was determined. This permitted to discriminate irradiated gabapentin from unirradiated one. Some spectroscopic properties and suggestions concerning possible structure of the radicals are discussed in this study.





## Development of semi-conductor nanoparticle systems for Si-nanowire solar cells

J. Habinshuti<sup>1,2</sup>, S. Turrell<sup>1</sup>, C. Kinowski<sup>3</sup>, D. Stievenard<sup>2</sup>, B. Grandidier<sup>2</sup>, T. Xu<sup>2</sup>, O. Cristini<sup>3</sup>

<sup>1</sup>LASIR (UMR 8516, CNRS), Bât C5, Université de Lille 1, 59650 Villeneuve d'Ascq cedex (France)

<sup>2</sup>IEMN (UMR 8520, CNRS), Département ISEN, 41 Bd Vauban, 59046 Lille cedex (France)

<sup>3</sup>PhLAM (UMR 8523, CNRS), Bât P5, Université de Lille 1, 59650 Villeneuve d'Ascq cedex (France)

In order to increase the conversion efficiency of Si-based photovoltaic cells, a new hybrid structure is under design in which Si nanowires (NW) are coupled with semi-conductor (SC) nanoparticles (NP). In this approach, after absorbing incident energy, the NPs can then transfer this energy to nearby Si nanowires, thus enhancing the efficiency of the energy conversion. Hence, a first problem involves the development of NP systems which can be compatible with the NWs, which might also transfer energy to rare-earth (RE) ions and which can remain stable under functioning conditions.

A second problem is to assure the robustness of the system. In this aim, the NW/NP package must be encased in a non-conducting solid medium a few microns thick and this layer must then be covered by an equally thin conducting layer.

In the present work, data obtained using micro-Raman and UV-visible spectroscopies is combined with SEM measurements to show the effect of synthesis parameters on the size and size-distribution of the colloïdally-formed SC nanoparticles (CdSe, PbSe) which are to be grafted on to the Si nanowires.

Sol-gel techniques have been used to develop the protective non-conduction layer. Micro-Raman results combined with photoluminescence data will be used to discuss the adaptability of ZrO<sub>2</sub> and PMMA systems for the packaging of the NW/NP ensembles, as well as the compatibility of these systems with nanoparticle – rare earth energy exchanges.

[1] W. Hoffmann, *Solar Energy Materials and Solar Cells*, 90 (2006) 3285 -3311

[2] J. Li, H.Y. Yu, S.M. Wong, X. Li, G. Zhang P. Guo-Qiang Lo and L. Kwong, *Appl. Phys. Lett.* 95 (2009) 243113-243116



## Localized vs charge-transfer excited states of photosensitizers on TiO<sub>2</sub> nanoparticles. Stark effect spectroscopy

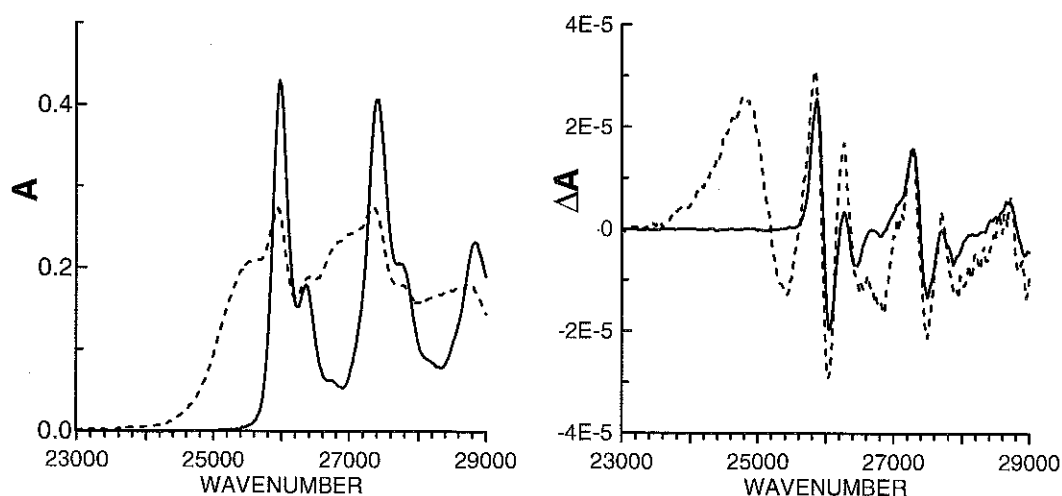
S. Krawczyk<sup>1</sup>, A. Zdyb<sup>2</sup>, A. Nawrocka<sup>1</sup>

1. Institute of Physics, Maria Curie-Skłodowska University, 20-031 Lublin, Poland

2. Institute of Physics, Lublin Polytechnic, Nadbystrzycka 38, 20-618 Lublin, Poland

The investigations of electronic processes at the molecule-solid interface with the participation of molecular electronic excited states are stimulated by their prospective applications in new type photocells and in the photocatalysis. The adsorption capacity and energetics of energy levels make the colloidal nanoparticles of TiO<sub>2</sub> very promising in this respect.

The interpretation of valuable spectroscopic observations for these systems requires the knowledge of the involvement of the oxide's metal atoms into the excited state orbital. Our data provide the most direct assessment of the excited state delocalization. This is obtained with the technique of electroabsorption which measures the difference dipole moments ( $\Delta\mu$ ) and difference polarizabilities ( $\Delta\alpha$ ) between the ground and excited states of the adsorbate. The examined photosensitizers were catechol, alizarin and 9-anthracenecarboxylic acid (9-ACA) which bind to Ti<sup>(IV)</sup> surface atoms through the dissociated hydroxy or carboxy groups.



Absorption and electroabsorption spectra of 9-ACA free (line) and adsorbed on TiO<sub>2</sub> (dots).

The dyes and their complexes with TiO<sub>2</sub> were prepared in ethanol or in ethylene glycol-water solvent and frozen between transparent electrodes to about 100 K. The electric field-induced features result from the large (7-10 Debye units) value of  $\Delta\mu$  in the molecule of 9-ACA when adsorbed on TiO<sub>2</sub>. This is similar to the observed dipole differences in the range  $\Delta\mu=9-12$  D for alizarin [1] and  $\Delta\mu\approx 16$  D for catechol [2]. The dependence of  $\Delta\mu$ 's on the surface potential of TiO<sub>2</sub>, modified by changing the pH of colloid, allows to assess the charge-transfer character of the electronic transitions and to estimate the electric field generated by the charged TiO<sub>2</sub> surface. Our experimental data also bear indirect information on the surface states in the TiO<sub>2</sub> and their possible role as traps for the injected electrons.

[1] A. Nawrocka, S. Krawczyk, J. Phys. Chem. C 112 (2008) 10233–10241

[2] A. Nawrocka, A. Zdyb, S. Krawczyk, Chem. Phys. Lett. 475 (2009) 272–276

## Spectroscopy study of exciton-phonon interaction in organic and semiconductor quantum dots

A.M. Yaremko, V.O. Yukhymchuk, V.M. Dzhagan

*Department of optics, Institute of Semiconductor Physics of the NASU, 45, Prospect Nauki, 03028 Kiev, Ukraine*

Optical and structural properties of crystal nanostructures (organic and semiconductor types) are intensively studied during last two decades. It is caused both the practical aim in developing of new elements of devices and fundamental physical reasons. In such structures the space confinement influence significantly on their properties, in particular on optical ones. The important characteristic for solids and nanostructures is the electron (exciton) – phonon interaction (EPI) which describes the response of electron system of crystal on the incident electromagnetic field.

Effect of space confinement on the value of EPI in QD's was investigated both the experimentally and theoretically. Obtained results concern to change of EPI constant are non-simple (contradictory) and there is no clear understanding of this problem. In the present communication we look on this problem once more and study it theoretically and experimentally for number of nano-dots with different size.

Response of system on EM field depends on the EPI which can be considered as weak ( $\beta_s < 1$ ) or strong ( $\beta_s \geq 1$ ) coupling depending on the parameter  $\beta_s = \chi_s / \Omega_s$ , which is the ratio of the EPI constant,  $\chi_s$ , to the corresponding phonon frequency,  $\Omega_s$ . For organic type crystals and crystal with hydrogen bonds, in which the Frenkel type exciton are realized,  $\beta_s \geq 1$  as usual, and many phonon replicas are observed experimentally in this case. The similar many phonon features are observed in Raman spectra of number semiconductors CdS, ZnO etc. Therefore in present work the problem of EPI we study in the framework of identical approach for organic and semiconductor structures. The idea of approach is to describe the spectrum (using developed in our works theory) by varying the coupling constant,  $\chi_s$ . After fitting theoretical spectrum one can make the conclusion concern to constant EPI,  $\beta_s$ . Such method is especially convenient if several phonons, having frequencies  $\Omega_s$ , take part in formation of spectrum. The corresponding analysis was made for number of quantum nanostructures. The numerical calculations showed that constants EPI depend strongly on the size and concentration of QD's. Beside take place the intermixing of vibrations in such structures.



## PAN-based carbon fibers modified with carbon nanotubes

A. Weselucha-Birczyńska<sup>1</sup>, A. Frączek-Szczypta<sup>2</sup>, S. Błażewicz<sup>2</sup>

<sup>1</sup> Faculty of Chemistry, Jagiellonian University, Ingardena 3, 30-060 Krakow, Poland

<sup>2</sup> Faculty of Material Science and Ceramics, AGH University of Science and Technology, Mickiewicza 30, 30-059 Krakow, Poland

Polyacrylonitrile (PAN)-based polymers belong to the most popular polymer precursors for carbon fibers applied in composite technologies, as well as for manufacturing porous and activated carbons for electrochemistry, separation processes, energy storage devices etc. [1].

New trends in development of composites technologies are to combine small amount of nanoparticles with polymeric matrix to form nanocomposites fibers. Carbon nanotubes are considered as potentially new class reinforcement to improve mechanical properties, thermal stability and conductivity of nanocomposites, and also to prepare anisotropic nanocomposites. The presence of carbon nanotubes in polymer solution can be located between the polymer chains and have influence on supramolecular structure of polymer. During converting of nanocomposites polymer fibers into nanocomposites carbon fibers the carbon nanotubes affect microstructure of carbon matrix [2].

Both single-walled carbon nanotubes and multi-walled carbon nanotubes may be viewed as single macromolecules and because of their nanosize, are potentially defect-free structures [3]. Depending on the size, chirality and orientation carbon nanotubes exhibit unique mechanical, electrical and thermal properties.

The work deals with preparation of PAN-based carbon fibers containing two different kinds of carbon nanotubes: single walled carbon nanohorns (SWCNHs) and multi walled carbon nanotubes (MWCNTs). The modified PAN fibers were spun from dimethylformamide (DMF) solution containing of 1wt% of carbon nanotubes. After that fibers were stabilized in an oxidizing atmosphere by a multistage process in the temperature range 140-200°C. The oxidized fibers were carbonized at 1000°C in argon atmosphere. The properties of CNTs and their influence on morphology, structure, microstructure and mechanical properties of the fibers were analyzed using several methods such as Raman spectroscopy, X-ray diffraction (XRD), scanning electron microscopy (SEM) and Zwick testing machine model 1435.

Additives of nanostructured carbons in carbon fibers brings changes in their microstructures. A comparison of pure carbon fibers and those containing nanotubes reveals differences in their structural ordering. The results from Raman spectroscopy and X-ray diffraction indicate that carbon nanotubes induce increase of graphitic ordering in nanocomposite carbon fibers compare to pure carbon fibers. The mechanical properties of the fibers were examined. The strength of carbon fibers containing CNTs was slightly lower than that of pure carbon fibers, while Young's modulus increases.

**Acknowledgements:** This work has been supported by the Polish Ministry of Science and Higher Education, Statutory Research.

[1] H.G. Chae, T.V. Sreeckumar, T. Uchida, S. Kumar *Polymers* 46 (2005) 10925

[2] A. Frączek-Szczypta, M. Bogun, S. Błażewicz *J Mater Sci* 44 (2009) 4721–4727

[3] A.H. Barber, S.R. Cohen, S. Kenig, H.D. Wagner *Compos Sci Tech* 64 (2004) 2283–2289



## Specific aspects of SERS and SERRS of Ag nanoparticles-polymer nanocomposites

O. Dammer<sup>1,2</sup>, B. Vlckova<sup>1</sup>, J. Pflieger<sup>2</sup>, M. Procházka<sup>3</sup>, M. Slouf<sup>2</sup>

<sup>1</sup> Dept. of Physical and Macromolecular Chemistry, Charles University in Prague, Hlavova 8, 12840 Prague 2  
Czech Republic

<sup>2</sup> Institute of Macromolecular Chemistry ASCR, Heyrovsky Sq. 2, 16206 Prague 6, Czech Republic

<sup>3</sup> Institute of Physics, Charles University in Prague, Ke Karlovu 5, Prague 2, 121 16, Czech Republic

Nanocomposites of conjugated polymers with plasmonic metal nanoparticles (NPs) are currently the subject of considerable interest due to their prospective applications in construction of sensors, light-emitting diodes and solar cells [1]. Since these systems are SERS-active, SERS spectroscopy appears to be a method of choice for investigation of their internal structure.

In this contribution, we pinpoint and explain several specific aspects which manifest themselves in SERS and SERRS of selected Ag NPs-conjugated polymer nanocomposites.

In the case of the nanocomposites of Ag NPs with a water soluble conjugated polymer poly(N-ethyl-2-ethynylpyridinium) iodide, we have revealed that, in the range of polymer concentrations at which the negative surface charges on Ag NPs are compensated by the cationic polymer, the effect of the polymeric nature of the adsorbate on the morphology of Ag nanoparticle assembly is so specific that it causes the SERS signal intensity (at  $\lambda_{exc}=514.5$  nm) to be inversely proportional to the polymer concentration in the composite [2]. The unusual concentration dependence stems from the polymer concentration dependent changes in the morphologies of Ag NP assemblies, in particular, from the presence of fractal aggregates in nanocomposites with the lower polymer concentrations, and of weakly interacting, widely spaced Ag NPs in composites with the higher polymer concentrations.

In our very recent study of the Ag NPs-P3OT /P3OT=poly(3-octylthiophene-2,5-diyl)/composites, the morphology of Ag NP in the composites is found to be strongly affected by the preparation pathway adopted. The M-composite prepared by a simple mixing of Ag NP organosol with a solution of P3OT contains large NP aggregates, while isolated NPs and their small aggregates are encountered in the R-composite prepared by Ag NP growth in the presence of P3OT. A systematic mutual comparison of relative band intensities in SERS of the composites and NRS of the neat polymer ( $\lambda_{exc}=632$  nm) with those in SERRS of the composites and RRS of the polymer ( $\lambda_{exc}=441.6$  nm, 514.5 nm) reveals that the very strong SERRS enhancements are experienced (i) by the ordered form of the polymer in the M-composite at  $\lambda_{exc}=514.5$  nm and (ii) by the disordered polymer in the R-composite at  $\lambda_{exc}=441.6$  nm. Additionally, the relative band intensity evaluation indicates a higher abundance of the disordered polymer structure in R-composite than in M-composite, which, most probably, stems from changes of the polymer molecular structure induced by the Ag NPs growth in the polymer environment during the composite preparation. Manifestation of the (resonance) Raman dispersion effect in the wavelength dependence of SERRS of a polymer in its nanocomposite with Ag NPs thus emerges as an important source of information about the actual polymer structure within a particular nanocomposite.

**Financial support:** KAN 100500652 (AVCR) and P208/10/0941 (GACR) grants.

[1] B. C. Sih, M.O. Wolf, Chem. Commun. (2005) 3375-3384.

[2] O. Dammer, B. Vlckova, M. Prochazka, J. Sedlacek, J. Vohlidal, J. Pflieger, Phys. Chem. Chem. Phys. 11 (2009) 5455-5461



## Raman microprobe imaging of submicron structures and interdisciplinary characterization of beam damage

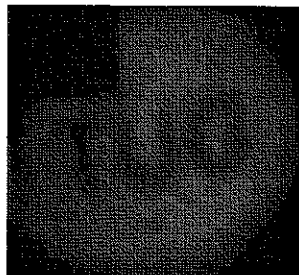
P. Wilhelm, B. Chernev, H. Plank, M. Sezen, M. Dienstleder, T. Haber, F. Hofer

*Institute for Electron Microscopy and Fine Structure, Graz University of Technology  
and Centre for Electron Microscopy Graz, Steyrergasse 17, A-8010 Graz, Austria*

Focused Ion Beam (FIB) has been used for device modification on nano-scaled functional materials. While, on the one hand, its high accuracy is a superior advantage as a preparation method, on the other hand, severe damage of sensitive samples may occur during the milling process. Raman spectroscopy provides information about chemical changes or stress of the material processed.

The spatial resolution of a standard dispersive confocal Raman microscope system is limited by the optical diffraction limit, resulting in an achievable spatial resolution in the order of somewhat below 1  $\mu\text{m}$ . Moving to the diffraction limit and beyond requires careful selection of the appropriate excitation wavelength, high numerical aperture objective and proper confocal arrangement. Special mapping and imaging techniques enable Raman microscopy to be pushed towards the true optical limit of resolution, which has been shown in detail in this study.

The figure below shows a Global Raman image of a FIB-modified silicon sample (area ca. 20  $\mu\text{m}$  x 20  $\mu\text{m}$ ). Due to the implantation of Ga ions the FIB-etched details are not Raman active (dark structures in the figure).



Furthermore the quantity of implanted Ga ions is proportional to the used FIB-parameters, like ion energy, beam current, spot dwell time or refresh time. Since the damaged silicon exhibits lowered Raman activity, it is possible to correlate the Raman intensity to the degree of beam damage. Moreover, since the damaged areas exhibit a surface structuring, those were examined with atomic force microscopy, to correlate the degree of surface roughness and sputtering dose with the FIB parameters. To complete a comprehensive picture, the Ga implantation in silicon has been qualitatively and quantitatively characterized by transmission electron microscopy with nm resolution.

[1] L.A. Gianuzzi, F.A. Stevie (Eds.) "Introduction to Focused Ion Beams" (2005), Springer New York

## Raman spectroscopy and luminescence of mesoporous ZrTiO<sub>4</sub> ceramics

A. Gajović<sup>1</sup>, R. Krsmanović<sup>2</sup>, J. Macan<sup>3</sup>, D. S. Su<sup>4</sup>, H. Ivanković<sup>3</sup>

<sup>1</sup> Rudjer boskovic Institute, Bijenička 54, HR-10002 Zagreb, Croatia

<sup>2</sup> Vinča Institute of Nuclear Sciences, P.O.Box 522, 11001 Beograd, Serbia

<sup>3</sup> University of Zagreb, Faculty of Chemical Engineering and Technology, Marulićev trg 19, P.O. Box 177, HR-10000 Zagreb, Croatia

<sup>4</sup> Fritz-Haber-Institut der Max-Planck-Gesellschaft, Faradayweg 4-6, D-14195 Berlin Germany

Zirconium titanate (ZrTiO<sub>4</sub>, ZT) is widely used in the electronic industry as high-performance dielectric materials for resonators in microwave region. This oxide also has applications for photo catalysis and for ceramics sensors.

ZrTiO<sub>4</sub> ceramics having different porosity were prepared by sintering the amorphous powder precursor, synthesized by sol-gel procedure, at different temperatures (1100, 1200, 1300 and 1400 °C). The structure of ceramics was investigated by X-ray diffraction (XRD), scanning electron microscopy (SEM) high resolution transmission electron microscopy (HRTEM) and Raman spectroscopy. Luminescence were observed by Raman spectroscopy and studied in details by luminescence spectroscopy.

Prepared ZT ceramics have  $\alpha$ -PbO<sub>2</sub> orthorhombic structure with a random distribution of the Zr<sup>4+</sup> and Ti<sup>4+</sup> cations at equivalent sites as observed by XRD. (HR)TEM observations show two different kinds of pores. The larger pores (100-300 nm) are open and situated between sintered grains (Fig. 1a), while smaller (2-10 nm) are closed and located inside sintered grains (Fig. 1b). During Raman spectroscopy measurements using 514 nm for excitation, the luminescence part of spectra was noticed in the region between 540 and 580 nm for all sintered ceramics, while the luminescence completely vanished in the case of precursor powder annealed at the same temperatures but without compaction (Fig. 1c). The luminescence spectroscopy of ceramics showed emission in the region up to 600 nm for 377.5 nm and 488nm excitation. The relative intensity and the shape of the observed luminescent bands depend on the sintering temperature.

The observed luminescence properties of ceramics will be discussed considering Zr<sup>4+</sup> and Ti<sup>4+</sup> cations' coordination in the vicinity of the closed pores as well as introduction of new surface electronic states formed by surface defects (e.g. ion vacancies, surface ions with low coordination numbers, and groups coordinated on the surface of materials).

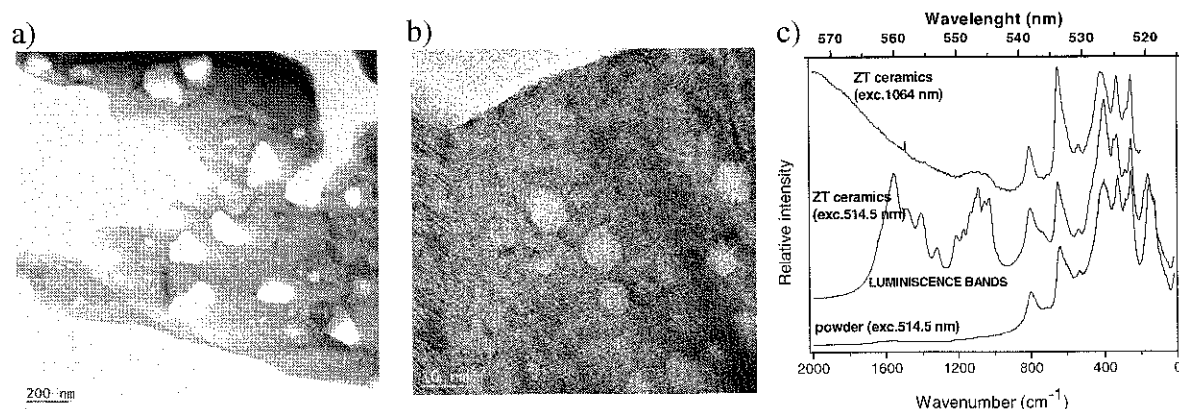


Figure 1: Porous ZT ceramics sintered at 1100 °C: a) large pores, b) small pores, c) Raman spectra and observation of luminescence

## Electronic absorption spectra of some phthalazinium ylids used to characterize the local ordering processes in liquid and solid solutions

A. Rogojanu, C. F. Dascalu, B. C. Zelinschi, D. O. Dorohoi

*Alexandru Ioan Cuza University, Faculty of Physics, 11 Carol I Blv., Iasi, RO-700506, Romania*

A spectral study of some phthalazinium ylids in different condensed media is presented here. Phthalazinium ylids are zwitterionic compounds having a visible absorption band due to the electronic intramolecular charge transfer (ICT) between the carbanion and the heterocycle.

The ICT band of phthalazinium ylids is very sensitive to the solvent action, showing a blue shift when passes from a non-polar to a polar solvent, or from an aprotic to a protic solvent. From the solvent influence on the electronic spectra of phthalazinium ylids solved in a pure solvent, the excited states dipole moments of the spectrally active molecules were estimated. The study of the ternary solutions of phthalazinium ylids can offer information about the molecular ordering in the vicinity of the spectrally active molecule and permits to evaluate the energy of interaction in a pair of molecules of the type solute-solvent. A pronounced local in-homogeneity in the ternary solutions was evidenced by the spectral means.

The dipolar molecules of phthalazinium ylids can be oriented in the stretched polymeric films. Poly-(vinyl alcohol) (PVA) films, colored with phthalazinium ylids and dried by water evaporation were stretched under the heating influence. The visible electronic spectra of the stretched films were measured for linearly polarized visible radiations having their electric field intensity parallel and perpendicular on the stretching direction. The dichroism of the colored PVA films depends on the stretching degree. The birefringence of each film was estimated by using a polarizing microscope equipped with a compensatory wedge.

The comparative analysis of the liquid and solid solutions of phthalazinium ylids demonstrates that the dipolar ylid molecules are partially oriented in condensed media.





## Micro-Brillouin scattering study of orthorhombic HEWL crystals in glycerol

T. Ishii, H. Kanazawa, S. Kojima

*Graduate School of Pure and Applied Sciences, University of Tsukuba, Tsukuba, Ibaraki, 305-8573, Japan*

We have studied the protein glass transition of lysozyme crystals in glycerol. Micro-Brillouin scattering is a useful tool to measure the elastic properties of a very small crystal over a wide temperature range[1,2]. The elastic properties of a HEWL(Hen egg white lysozyme) crystal with orthorhombic symmetry is studied in glycerol. Glycerol is known as a cryoprotective or bioprotective liquid which undergoes a liquid-glass transition around 185 K without any crystallization. Typical relaxation behavior is observed in the gigahertz frequency range, and the relaxation time obeys the Arrhenius law. The attempt relaxation time and the activation energy of HEWL tetragonal and orthorhombic crystals in glycerol are in agreement within experimental uncertainty. Those results suggest that two kinds of HEWL crystals have the same relaxation structure, which is probably localized in the vicinity of the interface between the hydrated glycerol, water molecules and a surface of a HEWL molecule.

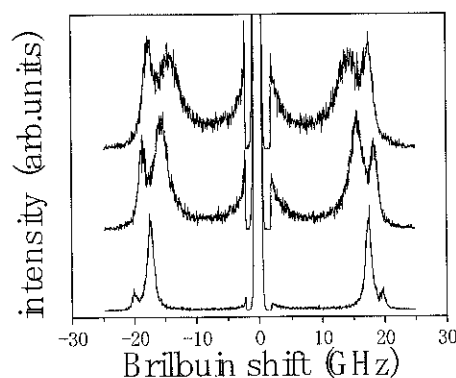


Fig.1. Temperature dependence of Brillouin scattering spectra.

- [1] Y. Ike, E. Hashimoto, Y. Aoki, K. Kanazawa, and S. Kojima, *J. Mol. Struct.* 924-926 (2009) 157-160.
- [2] I. E. Hahsimoto, Y. Aoki, Y. Seshimo, K. Sasanuma, Y. Ike and S. Kojima, *Jpn. J. Appl. Phys.* 47 (2008) 3839-3842.

## A SEM, EDX and XAS characterization of Ba(II)Fe(III) layered double hydroxides

D. Srankó<sup>1</sup>, M. Sipiczki<sup>2</sup>, É.G. Bajnóczy<sup>1</sup>, M. Darányi<sup>3</sup>, Á. Kukovecz<sup>3</sup>, Z. Kónya<sup>3</sup>, S.E. Canton<sup>4</sup>, K. Norén<sup>4</sup>, P. Sipos<sup>1\*</sup>, I. Pálinkó<sup>2\*</sup>

<sup>1</sup>Department of Inorganic and Analytical Chemistry, University of Szeged, Dóm tér 7, Szeged, H-6720 Hungary

<sup>2</sup>Department of Organic Chemistry, University of Szeged, Dóm tér 8, Szeged, H-6720 Hungary

<sup>3</sup>Department of Applied and Environmental Chemistry, University of Szeged, Rerrich B. tér 1, Szeged, H-6720 Hungary

<sup>4</sup>Chemical Physics Department, Chemical Centre, Lund University, PO Box 124, Lund, SE-221 00, Sweden

Recently, we have successfully prepared a novel layered double hydroxide (LDH) containing Ba(II) and Fe(III) ions in the positively charge layers [1; 2]. The synthesis required extreme conditions, *i.e.*, at least 10 M NaOH solution (but 20 M NaOH solution proved to be even better) was needed for co-precipitating the solid material from an aqueous solution of Ba(ClO<sub>4</sub>)<sub>2</sub> Fe(ClO<sub>4</sub>)<sub>3</sub> with varying Ba:Fe ratios. The synthesis was performed under N<sub>2</sub> blanket. This and the hyperalkaline conditions assured that the interlayer (counter) ions were exclusively OH<sup>-</sup> ions. The obtained materials were characterized by powder XRD, TG-DTG, <sup>57</sup>Fe Mössbauer, and qualitatively rationalized NEXAFS measurements. It was proven that layered materials were prepared indeed, and indirectly, through determining the local geometries of the cations, it was shown that they were double hydroxides.

In this contribution we show with a direct method that in these experiments double hydroxides were formed and also give a more quantitative interpretation of the recorded X-ray absorption spectra using the near edge region.

The direct method includes the combination of S(canning)E(lectron)M(icroscopy) and E(nergy)D(ispersible)S(pectroscopy). The former provides with topological information, while the latter is a microanalytical technique. The result of their combination can also be visualized giving a map of elements of the LDH particle under the microscope.

For scrutiny a sample prepared from a solution containing the Ba(II) and Fe(III) ions in 3:1 ratio and precipitated by 20 M NaOH was chosen. Its topology was examined at increasing magnifications (from 1000 to 25000) and lamellar particles were observed. EDX data obtained from two different parts of the same sample gave a ratio close to the synthesis mixture on the average. The elemental map displayed a close to even distribution of the Ba(II) and the Fe(III) ions, convincingly showing that no segregation of the monoionic oxides occurred during the synthesis, *i.e.*, layered hydroxide was formed indeed. The analysis of the near-edge spectrum at the Fe-K-edge allowed us to obtain quantitative data on the local coordination environment of the Fe(III) ion.

Results gained in the work leading to this contribution gave additional evidence that layered double hydroxide was formed. It is a new class of LDHs, since here the ionic radii of the cations are significantly different (in other LDHs they are close to each other), no wonder that the synthesis requires forcing conditions.

- [1] D. Srankó, A. Pallagi, I. Pálinkó, E. Kuzmann, S.E. Carton, M. Walczak, P. Sipos, Insights into Coordination, Bioinorganic and Applied Inorganic Chemistry (M. Melník, P. Segl'a, M. Tatarko, eds.), ISBN 978-80-227-3085-3, Press of Slovak University of Technology, Bratislava, 2009, pp. 380-385
- [2] D. Srankó, A. Pallagi, E. Kuzmann, S.E. Carton, M. Walczak, A. Sági, Á. Kukovecz, Z. Kónya, P. Sipos, I. Pálinkó, Appl. Clay Sci. 48 (2010) 214-217



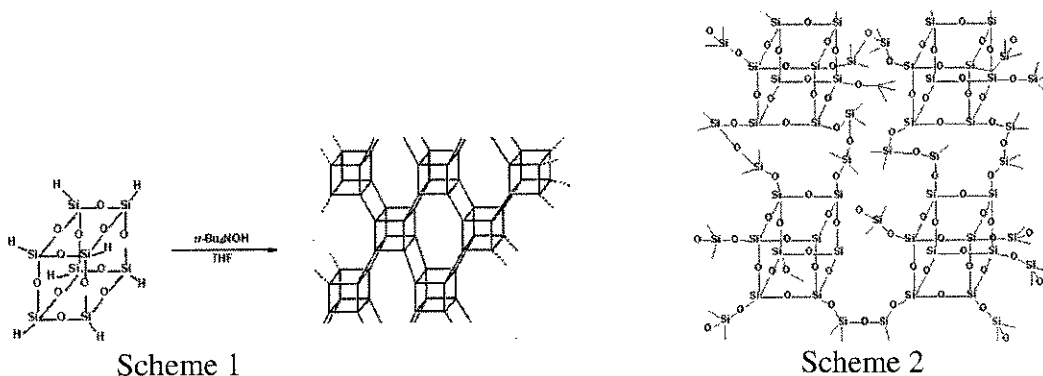
## Spectroscopy studies of mesotextured cross-linked octahydrodoctasilsesquioxanes materials

M. Handke<sup>1</sup>, M. Gajewicz<sup>1</sup>, A. Kowalewska<sup>2</sup>

<sup>1</sup>AGH University of Science and Technology; Faculty of Materials Science and Ceramics; Al. Mickiewicza 30, 30-059, Kraków, Poland

<sup>2</sup>Centre of Molecular and Macromolecular Studies; Polish Academy of Sciences; Sienkiewicza 112, Łódź, Poland

Mesoporous materials are obtained most frequently using ionic (electrostatic interactions) or neutral (hydrogen bonding) surfactants, that have been the most commonly used templates for directing the formation of mesopores. Since the mesostructure of silica-surfactant composites is fragile and may collapse during the decomposition of the surfactant, the research is focused on the preparation of structurally stable mesoporous silica that would yield mesostructure texture also after calcination. In our work we have obtained mesoporous materials without using any template or surfactant whatsoever. The mesopores are created due to hydrolytic condensation process of octahedral octahydrodoctasilsesquioxane ( $T_8^H$ ) alone and with siloxanes molecules as precursors molecules (Scheme 1 and 2). To our best knowledge mesoporous silica were never obtained in such an extremely simple way so far.



FTIR analysis of the obtained solid product revealed a complete condensation of  $T_8$  units, and virtually no SiH was left. The shape of Si-O-Si band in the FTIR spectrum corresponds closely to the one found for  $\text{SiO}_2$ . Residual SiOH groups can be also found and the crosslinked material is hydrophilic. Structural analysis has shown that the siliceous material is amorphous but mesoporous. Comparison of deconvoluted spectra of condensed  $T_8^H$  with the spectra of silica glass typically obtained at high temperature from liquid phase shows that the "short range" structure of these silicas is different.

The obtained materials have large surface area and pores distributed over the micro and meso range. BET surface area and pore distribution were measured using nitrogen adsorption methods. Mesopore surface areas, pore volumes and pore size distributions were determined from the adsorption branch using the BJH method. Micropore surface areas and volumes were calculated with t-Plot method. The cross-linked material obtained using  $T_8^H$  contained only about 10% of micropores and 90% of mesopores. Apparently, the mesopores are formed by assembling the fixed framework of octasilsesquioxanes.

## Kinetic studies for isothermal decomposition of un-irradiated and $\gamma$ -irradiated gallium acetylacetonate new route for synthesis of gallium oxide nanoparticles

Kh. M. Al-Khamis, Z. Al-Othman, N. M. Al-Andis, and R. M. Mahfouz\*

*Department of Chemistry, College of Science, King Saud University, PO Box 2455, Riyadh-11451, Saudi Arabia*

Isothermal decomposition of un-irradiated and  $\gamma$ -irradiated gallium acetylacetonate  $\text{Ga}(\text{acac})_3$  with  $10^3$  kGy total  $\gamma$ -ray dose were carried out in static air. The isothermal operating temperature were selected to be 160, 170, 180 and 190 °C. Kinetics of decomposition were followed using both model-fitting and model-free approaches. The results of model fitting application on the investigated data showed that the decomposition behavior was best described by phase-boundary controlled reaction ( $R_2$ ). Kinetic parameters of the decomposition process were calculated and evaluated. Analysis of the data using model free approach signify the dependency of  $E_a$  on extent of conversion ( $\alpha$ ). Pre- $\gamma$ -irradiation of gallium acetylacetonate  $\text{Ga}(\text{acac})_3$  with  $10^3$  kGy total  $\gamma$ -ray dose has almost no significant effect on the kinetic parameters.

Calcination of  $\text{Ga}(\text{acac})_3$  at 900 °C for 6 hours led to the formation of  $\text{Ga}_2\text{O}_3$  mono dispersed nanoparticles. X-ray diffraction, FTIR, SEM, and TEM techniques were employed for characterization of the synthesized nanoparticles. This is the first attempt to prepare  $\text{Ga}_2\text{O}_3$  nanoparticles by solid state thermal decomposition of  $\text{Ga}(\text{acac})_3$ .

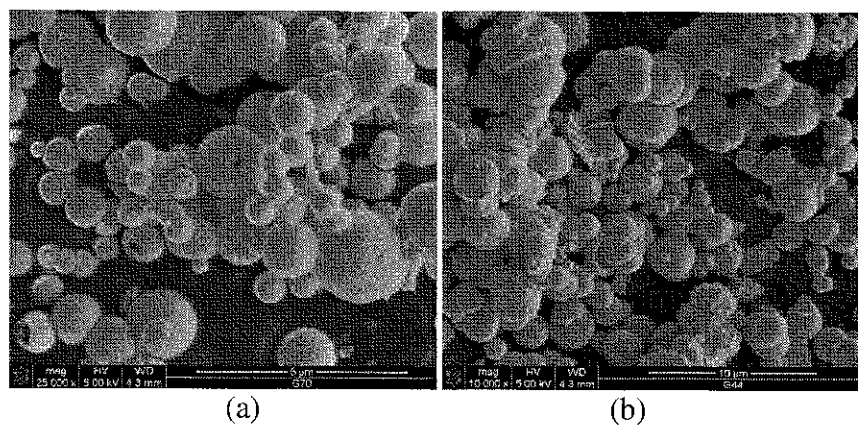


Figure 1. SEM image of  $\beta$ - $\text{Ga}_2\text{O}_3$  nanoparticles obtained by calcination at 900°C for 6 hours (a) un-irradiated sample (b)  $\gamma$ -irradiated sample with total dose 103 kGy.

- [1]. Mahfouz\*, R. M. Siddiqui, M. R. H. Al-Ahmari, Sh. A. Alkayali, W. Z. Progress in Reaction Kinetics and Mechanism. 2007, 32,1-27.
- [2]. Mahfouz\*, R. M. Al-Ahmari, SH. A. Al-Fawaz, A. M. Al-Othman, Z. Warad, I. Kh. Siddiqui, M. R. H. Radiation Effects & Defects in Solids. 2009, 164(4), 266-275.
- [3]. Al-Khamis, Kh. M. Mahfouz, R. M. Al-Warthan, A. M. R. H. Arabian Journal of Chemistry. 2009, 2, 73-77.

## Infrared and Raman spectroscopy investigation of high- $k$ metal oxide thin films: chemical stability, interfacial properties and solid state crystallization

M. Modreanu

*Tyndall National Institute, University College Cork, Lee Maltings, Prospect Row, Cork, Ireland*

As the semiconductor industry drives towards smaller device sizes while striving to maintain power consumption at acceptable levels, in particular for portable applications, the incorporation of new materials becomes inevitable. High dielectric constant (high- $k$ ) metal oxides materials are leading candidate to replace, or be combined with, silicon dioxide in many applications. Lanthanum oxide ( $\text{La}_2\text{O}_3$ ) is considered to be a potential candidate for gate oxide applications in the future high- $\kappa$ /metal gate MOSFET devices beyond the 45nm node while hafnium oxide ( $\text{HfO}_2$ ) is being already used in the 45nm CMOS technologies. One of the challenges associated with  $\text{La}_2\text{O}_3$  and  $\text{HfO}_2$  based high- $\kappa$  thin films is the moisture and  $\text{CO}_2$  absorption when exposed to air resulting formation of carbonates and hydroxyls. In this work we explore the solid phase crystallization of amorphous  $\text{HfO}_2$  and  $\text{La}_2\text{O}_3$  based thin films and their time dependence reaction with moisture and  $\text{CO}_2$ . Uncapped and  $\text{SiO}_2$ -capped (in-situ without breaking the vacuum)  $\text{HfO}_2$  and  $\text{La}_2\text{O}_3$  thin films were deposited on HF last terminated double side polished silicon (100) substrates by electron beam evaporation from solid  $\text{La}_2\text{O}_3$  and  $\text{HfO}_2$  pellets (99.9% purity, Cerac) at  $150^\circ\text{C}$ . After deposition the samples were exposed to forming gas (5% $\text{H}_2$ /95% $\text{N}_2$ ) Rapid Thermal Annealing and nitrogen gas annealing at several temperatures ranging from  $450^\circ\text{C}$  to  $1050^\circ\text{C}$ . High Resolution TEM, XRD, Time resolved FTIR and Raman measurements were performed to investigate the chemical stability and crystallisation of the  $\text{HfO}_2$  and  $\text{La}_2\text{O}_3$  based thin films. The films thickness and optical properties have been inferred from the spectroscopic ellipsometry. Carbonates and hydroxyls species have been detected by FTIR on  $\text{HfO}_2$  thin films after two weeks of air exposure. Kinetics FTIR and Raman measurements performed over a period of three weeks on uncapped  $\text{La}_2\text{O}_3$  thin films, indicate that the formation of  $\text{La}(\text{OH})_3$  is thickness dependent but is not as fast as was considered in the literature. For  $\text{HfO}_2$  thin films a transition to a crystalline phase occurs at a temperature greater than  $450^\circ\text{C}$  depending to the layer thickness. The crystalline grains consist of cubic and monoclinic phases already classified in the literature but this work provides the first evidence of amorphous-cubic phase transition at a temperature as low as  $500^\circ\text{C}$ . According to SE, XRR and FTIR results, an increase in the interfacial layer thickness can be observed only for high temperature annealing. We report on a different behaviour of crystallisation into pure  $\text{La}_2\text{O}_3$  hexagonal phase for uncapped and  $\text{SiO}_2$ -capped  $\text{La}_2\text{O}_3$  films. The  $\text{SiO}_2$ -capped  $\text{La}_2\text{O}_3$  films require a much lower temperature ( $700^\circ\text{C}$ ) while for uncapped films temperatures higher than  $900^\circ\text{C}$  are needed. Following the forming gas annealing the  $\text{La}_2\text{O}_3$  films exhibit a significantly enhanced resistance to  $\text{La}(\text{OH})_3$  formation. We report here the infrared and Raman active modes of both amorphous and crystalline  $\text{HfO}_2$  and  $\text{La}_2\text{O}_3$  thin films.



## Self-assembling of Z- $\alpha$ -pyridylcinnamic acid dimers over polycrystalline Ag and Au surfaces followed by FT-IR and atomic force microscopies

K. Csankó<sup>1</sup>, M. Darányi<sup>2</sup>, G. Kozma<sup>2</sup>, Á. Kukovecz<sup>2</sup>, Z. Kónya<sup>2</sup>, I. Pálinkó<sup>1\*</sup>

<sup>1</sup>Department of Organic Chemistry, University of Szeged, Dóm tér 8, Szeged, H-6720 Hungary

<sup>2</sup>Department of Applied and Environmental Chemistry, University of Szeged, Rerrich B. tér 1, Szeged, H-6720 Hungary

It is well-known that nitrogen has affinity towards transition metals, especially to gold and silver. Many nitrogen-containing compounds form self-assembled layers over these metals [1, 2]. In these layers nitrogen is covalently bonded to the metal and the rest of the molecule may or may not interact with neighbouring molecules. If they do, secondary interactions of various forms (hydrogen bonding, C–H... $\pi$ ,  $\pi$ ... $\pi$  and/or van der Waals) may organize the layer and/or help in depositing several layers on top of each other.

In our work leading to this contribution FT-IR microscopy and A(tomic)F(orce)M(icroscopy) imaging was used for studying the formation of self-assembling multilayers of Z-2(3'-pyridyl)-3-phenyl propenoic acid over Ag and Au surfaces prepared by laser evaporation. The compound was synthesized and purified in our laboratory. It was dissolved in CCl<sub>4</sub> and was deposited onto the phenomenologically smooth but atomically rough metal surfaces by the dip-coating technique under ambient conditions (room temperature, atmospheric pressure in air).

First, it was checked whether the deposition was successful and the molecule remained intact or not. FT-IR microscopy working in the reflectance mode was used for this purpose. It was found that the acid molecule could be placed onto both metal surfaces, even washing with the pristine solvent could not remove it. The molecule remained intact, moreover, it was bonded in the form of dimers – as it was expected.

Surface-subtracted AFM images revealed full coverage and a thin layer with an average height of 1.4 nm over the Au surface. Depending on the orientation of the adsorbed dimers this corresponds to mono or few layers only. In the first layer the pyridyl nitrogen was covalently attached to the Au surface, while the other layers (if any) were bonded to the first one with secondary forces. The small thickness of the layer indicates mainly  $\pi$ ... $\pi$  and C–H... $\pi$  interactions among them.

The situation over the Ag surface was very different, however. It was clear that the initially bonded layer served as starting points for the deposition of further molecules. The orientation of the dimers was also different, actually peaks with a prismatic structure were grown reaching the height of 160 nm. Thus, a bumpy surface was grown with quite extended chains. The agglomeration was more or less perpendicular to the surface. The thickness of the pillars at the base was several hundred nm, which means that many chains grew together. These chains are grouped together, thus, there must be extensive interaction among them. The immediate interaction between the silver surface and dimer layer must be covalent bonding between the metal and nitrogen atom of the pyridyl ring, while the chains growing to pillars interact through C–H...N hydrogen bonds and C–H... $\pi$  and/or  $\pi$ ... $\pi$  close contacts.

[1] R. Otero, M. Lukas, R.E.A. Kelly, W. Xu, Læksgaard, I. Stensgaard, L.N. Kantorovich, F. Besenbacher, *Science* 319 (2008) 312-315

[2] J.A.A.W. Elemans, S. Lei, S. De Feyter, *Angew. Chem. Int. Ed.* 48 (2009) 7298-7352



## STM/STS characterization of PTCDI/melamine self assembly on Si(111) - $\sqrt{3} \times \sqrt{3}$ Ag surface

R. Stiuftuc<sup>1,2</sup>, B. Grandidier<sup>3</sup>, G. Stiuftuc<sup>1</sup> and C.M. Lucaciu<sup>2</sup>

<sup>1</sup>"Babes-Bolyai" University, Faculty of Physics, Cluj Napoca, Romania

<sup>2</sup>University of Medicine and Pharmacy "Iuliu Hatieganu", Faculty of Pharmacy, Physics-Biophysics Department, Cluj-Napoca, Romania

<sup>3</sup>Institut d'Electronique et de Microélectronique et de Nanotechnologies, IEMN, Département ISEN, 41 bd Vauban, 59046 Lille Cedex, France

Scanning Tunneling Microscopy (STM) and Scanning Tunneling Spectroscopy (STS) are two complementary techniques capable of resolving structures and studying electronic transport on atomic scale [1]. Here we report on STM and STS measurements performed in UHV conditions at low temperatures (77K and 5K) investigating the electronic properties of PTCDI/melamine self-assembled macromolecular network on Si(111)- $\sqrt{3} \times \sqrt{3}$  Ag surface. The topographic images revealed the internal molecular structure while the conductivity spectra acquired on the bare surface and on different zones of the macromolecular arrangement combined with DFT calculation allowed the identification of molecular orbitals. By comparing the STS measurements performed on the Si/Ag surface and on the macromolecular network the LUMO molecular orbital has been identified as lying below the Fermi level of the surface. The modification of the density of states of Ag/Si(111)- $\sqrt{3} \times \sqrt{3}$  surface caused by the presence of the self-assembled molecular network at energies much higher than the height of the potential barriers induced by the molecules has also been observed [2].

- [1] M. Berthe, R. Stiuftuc, B. Grandidier, D. Deresmes, C. Delerue, D. Stievenard Science 318, 436 (2008)
- [2] R. Stiuftuc, L.M.A. Perdigão, B. Grandidier, D. Deresmes, G. Allan, C. Delerue, D. Stievenard, P.H. Beton, S.C. Erwin, M. Sassi, V. Oison, J.-M. Debierre, Phys. Rev. B, 2010



## A spectroscopic method to estimate the binding potency of amphiphile assemblies

W. Pohle<sup>1</sup>, D. R. Gauger<sup>1</sup>, V. Andrushchenko<sup>2</sup>, P. Bour<sup>2</sup>, F. Billes<sup>3</sup>

<sup>1</sup> *Institute of Biochemistry & Biophysics, Friedrich-Schiller University Jena, Philosophenweg 12, D-07743 Jena, Germany*

<sup>2</sup> *Institute of Organic Chemistry & Biochemistry, Academy of Sciences, Flemingovo nám. 2, 16610 Prague, Czech Republic*

<sup>3</sup> *Department of Physical Chemistry & Material Science, Budapest University of Technology and Economy, Budafoki út 8, H-1521 Budapest, Hungary*

A fast and convenient spectroscopic methodology to determine the water uptake capacity of amphiphile assemblies studied in multilayer films is presented. This method was developed to provide a reliable, but relatively simple tool for estimating the binding potency of such complex systems. The water binding potency represents a general propensity of higher-order systems to bind or embed relevant ligands, such as various non-lipid effectors in the case of artificial lipid membranes. In this sense, the binding potency might contribute to a specific functional role of certain lipids.

The essence of the new method is that the calibration of data measured by infrared (IR) spectroscopy against those directly obtained by Karl-Fischer titration (KFT) enables to replace the expensive chemical-analytical technique by a more comfortable and efficient IR-spectroscopic protocol. This approach combines the easy handling, versatility and availability of IR spectroscopy [1] with the high accuracy and sensitivity of KFT. The usefulness of the procedure is demonstrated on an example set of six amphiphiles with a common chain length of 18 carbon atoms. The set of compounds comprised the surfactants stearylamine and stearyltrimethylammonium (chloride), the lipids dioleoyltrimethylammoniumpropane (chloride) as well as distearoyl- and dioleoylphosphatidylcholine, and dioleoylglycerol (or diolein) biologically important as a second messenger. Despite the structural similarity given by the equal chain length, the binding potency data differ tremendously which can be correlated with the systematic variations introduced into the amphiphile structure.

Going further beyond the methodical aspect, the scientific relevance of the data is comprehensively discussed especially in terms of the structural factors that govern the binding potency of amphiphiles. This is favored mainly by fluidity and disfavored mainly by the formation of inter-amphiphile binding networks. For the phosphatidylcholines, our data which are complemented by the results of conjugated X-ray diffraction experiments [2] add new strong evidence in favor of a particular hydration model that involves both primary water binding to phosphate and the existence of water clusters hosting the trimethylammonium moiety as semi-clathrates [3]. Such water cluster formation seems to occur also in the small neurotransmitter acetylcholine as indicated by IR-spectroscopic hydration studies.

Interestingly, stearylamine and diolein assemblies did not take up any water at all. This unexpected hydrophobicity is referred to the unusual structures formed in these peculiar cases: rigid ammonium amide with a strong hydrogen bonding/salt bridge network in stearylamine [4], and, as revealed by related molecular dynamics simulations, aggregations of subunits resembling inverted micelle-like assemblies in diolein.

[1] W. Pohle, C. Selle, H. Fritzsche, H. Binder, *Biospectroscopy* 4 (1998) 267-280

[2] W. Pohle, C. Selle, D. R. Gauger, K. Brandenburg, *J. Biomol. Struct. & Dynam.* 19 (2001) 351-364

[3] G. A. Jeffrey, W. Saenger, *Hydrogen Bonding in Biological Structures*, 1991, Springer, Berlin

[4] W. Pohle, D. R. Gauger, *J. Mol. Struct.* 924-926 (2009) 144-147





## Vibrational spectroscopy in the study of self-assembled monolayers of thiols on gold. An example of 4-mercaptobenzoic acid

Do Thi Minh, K. Volka

*Department of Analytical Chemistry, Institute of Chemical Technology, Prague  
Technická 5, 166 28 Praha 6, Czech Republic*

Structure of the self-assembled monolayers of thiols on silver or gold surfaces is in focus of many papers and there is also a wide range of techniques used in these studies. For vibrational spectroscopy, it is no trivial task, but application of infrared reflection-absorption technique (IRRAS) or attenuated total reflection technique (ATR) surface-enhanced infrared-absorption reflectance (SEIRA) in infrared spectroscopy as well as surface enhanced Raman scattering (SERS) spectroscopy allow to obtain a whole range of interesting results.

One of the frequently studied objects is 4-mercaptobenzoic acid (MBA). The literature data agree in conclusion that the interaction with noble metal is realized through the thiol group, but what is the arrangement of the carboxyl groups seems to be an open question, as presence of monomeric, dimeric or of both forms is concluded from infrared spectra.

We tested a chance of SERS spectroscopy to clarify the self-assembling process of MBA. To overcome a crucial problem of reproducibility of SERS active surfaces, we used commercially available nanostructured gold substrates (Klarite™) and studied the MBA deposition from pure and acidified ethanol *in situ*. Parallel measurements were done under comparable conditions by surface plasmon resonance (SPR) technique. Low intensity of the carboxyl group bands does not allow any conclusion on the interactions of the carboxyl groups, but intensity changes of the phenyl bands during the deposition as well as SPR measurements demonstrate considerable complexity and low reproducibility of the process. Incorporation of ethanol into the early structures of monolayer is one of the complications encountered. Possible sources of this variability are pointed out.



## Temperature dependence of elastic properties in alkali borate binary glasses

M. Kawashima, S. Aramomi, Y. Matsuda, S. Kojima

Graduate School of Pure and Applied Sciences, University of Tsukuba, Tsukuba, Ibaraki, 305-8573, Japan

The additions of alkali oxide to pure  $B_2O_3$  induce the change of coordination number of boron atom from three to four and the increase of the network connectivity. Although the composition dependence of the elastic properties of alkali borate glasses have been reported systematically at room temperature [1], the study on elastic properties of alkali borate glasses at high temperatures, especially above glass transition ( $T_g$ ), is poor and the influence of alkali ions at high temperatures is still unknown. While the understanding of elastic properties at high temperatures is important for glass science or processing. In order to measure elastic properties at high temperatures, nondestructive and noncontact Brillouin scattering spectroscopy is a powerful tool. By combining a Brillouin apparatus and an IR compact image furnace, we can investigate the elastic properties in a GHz frequency range without any contact with a sample. Therefore, in the present paper, the temperature dependence of elastic property in alkali borate glasses  $xM_2O \cdot (100-x)B_2O_3$  ( $M = Li, Na, K, Rb, Cs$   $x = 14, 28$ ), where  $x$  denotes the molar concentration, are investigated by Brillouin scattering up to 1100 °C, and the influence of alkali ions and alkali dependence of fragility is discussed. Figs. 1 and 2 show the temperature dependence of the sound velocity ( $V_L$ ) and absorption coefficient of  $28M_2O \cdot 72B_2O_3$ .  $V_L$  is nearly constant below  $T_g$ , while it remarkably decreases above  $T_g$ . The decreasing rate becomes increase with the decrease of the ionic size of alkali ions. The slop of decrease of  $V_L$  just above  $T_g$  shows the correlation with fragility [2].

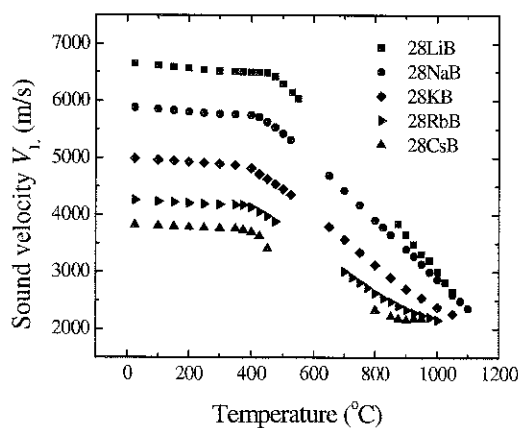


Fig. 1 Temperature dependence of sound velocity of  $28M_2O \cdot 72B_2O_3$

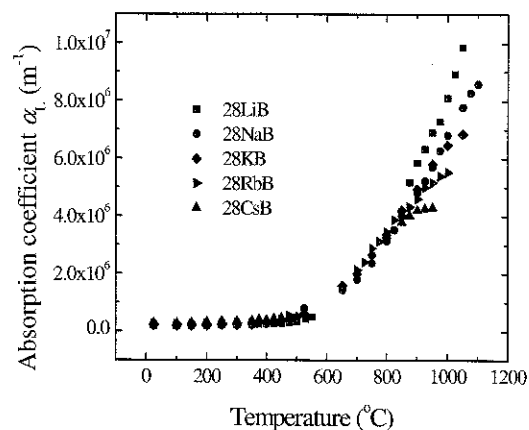


Fig. 2 Temperature dependence of absorption coefficient of  $28M_2O \cdot 72B_2O_3$

[1] M. Kodama, J. Non-Cryst. Solids 127 (1991) 65-74.

[2] J. E. Masnik, J. Kieffer, and J. D. Bass, J. Chem. Phys. 103 (1995) 9907-9917.

## Dichroic polymer foils analysed by spectral means

A. Rogojanu, R. E. Stanculescu and D.O. Dorohoi

*Faculty of Physics, Al.I.Cuza University, 11 Carol I Blvd. RO-700506, Romania*

Polymer foils stretched under hitting become anisotropic media and when they are colored with organic anisotropic molecules become dichroic and could be used in various displays. Polyvinyl alcohol (PVA) foils have different application in medical purposes and could be used as health indicators when they show dichroic properties.

Our purpose is to search the dichroism of the colored PVA foils by spectral means and to establish the influence of the foil thickness, the nature and concentration of dichroic molecules and of the degree of stretching on the dichroic properties of the polymer foils.

The dichroic ratio was considered as an indicator of the order degree induced by stretching in the polymer foils. Information of the electronic transition dipole moment was obtained from the dichroism studies.

Concomitantly, the PVA stretched foil birefringence was determined by using the implemented previously method of channeled spectrum. The obtained results were corroborated with the dichroic ratio.

Quantum chemical calculations applied to the dichroic molecules in free space and in polymer foils attested the experimental results. The studies regarding the ordered foil dichroism are very important in spectroscopy of the complex molecules from the point of view of their structural characterization in parallel with the theoretical results obtained by computational methods.



## Intermolecular interactions in pyridinium ylid ternary protic solutions. Theoretical and spectral study

E. Filip<sup>1</sup>, M. Dulcescu<sup>2</sup>, D. O. Dorohoi<sup>2</sup>

<sup>1</sup>*Faculty of Chemistry, Al.I.Cuza University, 11 Carol I Blvd. RO-700506, Romania*

<sup>2</sup>*Faculty of Physics, Al.I.Cuza University, 11 Carol I Blvd. RO-700506, Romania*

Pyridinium ylids are zwitterionic compounds having separated opposite charges on the heteroatom and on the ylid carbanion. They have multiple applications in organic chemistry as acid-basic indicators or as precursors in various reactions. The delocalization of the positive charge on the heterocycle and of the negative charge on the carbanion substituents determine the stability of these cycloimmonium ylids. Pyridinium ylids are spectrally active molecules with a visible electronic band due to an intramolecular charge transfer of the electronic charge from the carbanion towards the heterocycle. The mechanism of the visible band determines a decrease of the molecular electric dipole and consequently the decrease of the universal dipolar interactions of the solute with the solvent molecules. The visible electronic band of the pyridinium ylids shifts to blue in protic and in polar solvents compared to the non-protic and non-polar solvents. The solvent influence on the electronic visible spectra of pyridinium ylids in mixtures of various ethanol molar percentages in water was studied both from experiments and from quantum chemical evaluations. The strength of the universal interactions of the hydrogen bond complexes of pyridinium ylids with water or ethanol molecules was evaluated from the spectral shifts measured in electronic absorption spectra of ternary solutions. Concomitantly, the molecular electro-optical parameters for the hydrogen bond complexes of the types water-ylid and ethanol-ylid and also the interaction energies were estimated by methods of molecular orbitals with HyperChem Programs.



## Solvent influence on the zwitterionic solutes studied by electron spectroscopy

D. O. Dorohoi

*Alexandru Ioan Cuza University, Faculty of Physics, 11 Carol I Blv., RO-700506, Iasi, Romania*

Zwitterionic compounds such as cycloimmonium ylids are dipolar molecules having opposite charges localized on atoms or atomic groups. Recently, new cycloimmonium ylids were reported as having applications in pharmaceutical industry as bioactive molecules or as precursors in drug obtaining. They are also used in chemistry as acido-basic indicators or as initial substances in dimerization or other reactions. All reactions take place in situ and the knowledge about the intermolecular interactions between the zwitterionic compounds and the solvent become important.

The visible intramolecular charge transfer band of cycloimmonium ylids was used in our studies. The mechanism of the cycloimmonium ylids visible electronic band determines the decreasing of the dipole moment in the excited electronic states of cycloimmonium ylids and consequently a diminution of the intermolecular strength in the excited states of the zwitterionic compounds. This band has low intensity, shifts to blue in polar and protic solvents and disappears in acid solutions due to the blocking of the non-participant pair of electrons delocalized on the ylid carbanion.

The zwitterionic compound from the class of cycloimmonium ylids as dipolar molecules in their ground electronic state interact with the solvent molecules by orientation, induction, polarization and dispersive forces. Supplementary, in the protic solvents, specific interactions of the proton change type appear in the cycloimmonium solutions. The modifications induced by the intermolecular interactions in the molecular electron distribution are reflected in the electronic spectra as changes in the intensity or in the wavenumbers in the maxima of the electronic bands. The theoretical results obtained in describing the solutions were applied here in order to characterize the intermolecular interactions and to determine some electro-optical molecular parameters such as dipole moments and polarizability in the excited states of the studied zwitterionic compounds.



## Optical spectroscopy of Dy<sup>3+</sup> ions in heavy metal lead-based glasses and glass-ceramics

J. Pisarska, W. A. Pisarski

*University of Silesia, Institute of Chemistry, Szkolna 9, 40-007 Katowice, Poland*

Among trivalent lanthanides, the Dy<sup>3+</sup> ions have been successfully incorporated into several glasses and crystals in order to obtain two primary color yellow/blue luminescent materials. Dysprosium-doped solid-state systems can be quite easily excited by the commercial UV or blue LEDs, because their excitation spectra exhibit several 4f-4f electronic bands located in the 340-480 nm spectral range. Luminescence spectrum of Dy<sup>3+</sup> consists of two relatively intense bands, that correspond to the <sup>4</sup>F<sub>9/2</sub> - <sup>6</sup>H<sub>15/2</sub> (blue) and <sup>4</sup>F<sub>9/2</sub> - <sup>6</sup>H<sub>13/2</sub> (yellow) transitions, respectively. It has been observed that the intensity of the <sup>4</sup>F<sub>9/2</sub> - <sup>6</sup>H<sub>13/2</sub> (yellow) transition of Dy<sup>3+</sup> is strongly influenced by the environment. Thus, the relative intensities of the <sup>4</sup>F<sub>9/2</sub> - <sup>6</sup>H<sub>13/2</sub> transition to the <sup>4</sup>F<sub>9/2</sub> - <sup>6</sup>H<sub>15/2</sub> transition known as a yellow-to-blue luminescence intensity ratio Y/B can be modulated by varying the glass host and its chemical composition, activator (Dy<sup>3+</sup>) concentration and thermal treatment. The latter process leads to transformation from glasses to transparent glass-ceramics (TGC). The spectroscopic consequence of this transformation is the narrowing of spectral lines and the lengthening of luminescence lifetimes for the excited states of lanthanide ions. This behaviour can be explained by structural changes in the environment around lanthanide ions, giving important contribution to the luminescence intensities associated to <sup>4</sup>F<sub>9/2</sub> - <sup>6</sup>H<sub>13/2</sub> and <sup>4</sup>F<sub>9/2</sub> - <sup>6</sup>H<sub>15/2</sub> transitions of Dy<sup>3+</sup>.

In this work, we present new results for some dysprosium-doped heavy metal glasses before and after heat treatment. Correlation between structure and luminescence properties (especially Y/B ratios) of Dy<sup>3+</sup> in lead-based systems was examined using X-ray diffraction, FT-IR and optical spectroscopy. The excitation and luminescence spectra of Dy<sup>3+</sup> ions in glass samples before and after thermal treatment are presented and discussed in relation to potential application in the visible optoelectronics.

**Acknowledgments:** The Ministry of Science and Higher Education supported this work under research project N N204 313937.



## Structural phase transitions of BaTiO<sub>3</sub> nanorods' investigated by Raman spectroscopy *in situ* at different temperatures

A. Gajović<sup>1</sup>, J. Vukajlović<sup>1,2</sup>, K. Žagar<sup>3</sup>, M. Plodinec<sup>1</sup>, M. Čeh<sup>3</sup>

<sup>1</sup>Ruđer Bošković Institute, Bijenička 54, HR-1002 Zagreb, Croatia

<sup>2</sup>Department of Physics, Faculty of Science, University of Zagreb, Bijenička 32, HR-10000 Zagreb, Croatia

<sup>3</sup>Jožef Stefan Institute, Jamova 39, 1000 Ljubljana, Slovenia

Structural phase transitions of perovskite materials are often associated with phase transition of their ferroelectric or ferromagnetic properties. Typical example is BaTiO<sub>3</sub> (BTO), where phase transition from tetragonal to cubic phase induces the transition from ferroelectric to paraelectric state. This phase transition is expected at 132°C.

BTO nanorods were synthesized using sol-gel electrophoretic deposition into polycarbonate (PC) template membranes with pore diameters of 200 nm and thickness of 10-25 μm. After the deposition, the samples were annealed at elevated temperatures. This heating procedure was done in order to burn off the polycarbonate membrane and to make the nanorods dense and crystalline. Obtained nanorods were characterized by micro-Raman spectroscopy (RS) and X-ray diffraction, while their morphology and nano-structure were observed by High resolution transmission electron microscopy (HRTEM).

Tetragonal phase of BFO, having 4mm symmetry with *c/a* axis ratio close to one, is hard or impossible to distinguish from cubic phase by using diffraction techniques, so RS was applied as the main method for structural investigation. Since RS results suggest tetragonal structure with low *a/c* ratio, as well as possible coexistence of more phases in the nanorods [1], these results will be compared with HRTEM and SAED at the individual crystallites as building blocks of nanorods. Moreover, depending on the synthesis procedure, in some samples of BTO nanorods the Raman band at 630 cm<sup>-1</sup>, corresponding to hexagonal structure [1] was also observed and confirmed by HRTEM observations. Normally, hexagonal phase can be achieved in BTO by heating at temperatures higher than 1432 °C.

*In situ* high temperature RS was used for study of phase transitions from tetragonal to cubic structure in BTO nanorods having different amount of hexagonal phase. The influence of hexagonal phase to these phase transitions in BTO nanorods will be discussed. Moreover, the stability of hexagonal phase was investigated in temperature range from -95 °C to 200 °C.

[1] W. Satoshi et al., Jpn. J. Appl. Phys. 42 (2003) 6188-6195.



## Vibrational spectroscopic studies on the $T_d$ -type Clathrates: $Cd(2,5\text{-dimethylpyrazine})M(CN)_4 \cdot 2C_6H_6$ ( $M= Cd$ or $Hg$ )

C. Bayrak<sup>1</sup> and M.T. Aytakin Aydin<sup>2</sup>

<sup>1</sup>Hacettepe University, Faculty of Education, Department of Physics, 06800, Beytepe /Ankara, Turkey  
<sup>2</sup>Anadolu University, Science Faculty, Department of Physics, Eskişehir, 26470, Turkey

In this study the  $Cd(2,5\text{-dimethylpyrazine})M(CN)_4 \cdot 2C_6H_6$  ( $M=Cd$  or  $Hg$ ) clathrates of 2,5-dimethylpyrazine (2,5-dmpz) were prepared for the first time and their FT-IR (4000-50  $cm^{-1}$ ), FT-Raman (4000-50  $cm^{-1}$ ) spectroscopy, X-ray diffraction, thermal and elemental analyses were investigated. All the vibrational modes of coordinated 2,5-dmpz have upward shifts in frequencies compared to those in the free molecule, these shifts being metal dependent.

The assigned wavenumbers for the  $M(CN)_4$  group in the compounds studies appeared to be much higher than those for the  $M(CN)_4$  ion  $K_2M(CN)_4$  ( $M= Cd$  or  $Hg$ ) salts. The CH out-of-plane mode ( $A_{2U}$ ) of benzene in the infrared spectra of the clathrates was located at 681  $cm^{-1}$ . This band in the spectra of the clathrates was found shifting the higher frequency (681  $cm^{-1}$ ) from that of liquid benzene (670  $cm^{-1}$ ). Similar positive frequency shifts were observed for Hofmann- $T_d$ -type and Hofmann-type clathrates.

The thermal behavior of Hofmann- $T_d$ -type clathrates of 2,5-dmpz was studied in dynamic nitrogen atmosphere by DTA, DTG and TG techniques. Thermal decomposition of  $Cd(2,5\text{-dmpz})M(CN)_4 \cdot 2C_6H_6$  ( $M=Cd$  or  $Hg$ ) occur in the three separated stages.





## Vibrational Spectroscopic Studies on the Hofmann-type Clathrates: $M(C_4H_7NH_2)_2Pd(CN)_4 \cdot 2C_6H_6$ (M=Ni, Cd or Co; G=benzene)

Ö. Bağlayan,, M.T. Aytakin Aydın and, M. Şenyel

*Anadolu University, Science Faculty, Department of Physics, TR26470, Eskişehir, Turkey*

In this study the  $M(C_4H_7NH_2)_2Pd(CN)_4 \cdot 2G$  (M=Ni or Co; G=benzene) clathrates of cyclobutylamine (cba) were prepared for the first time and their FT-IR ( $4000-50\text{ cm}^{-1}$ ), FT-Raman ( $4000-50\text{ cm}^{-1}$ ) spectroscopy, X-ray diffraction, thermal and elemental analyses were investigated. Their spectral data are found to be consistent with the structure of the Hofmann-type clathrates. The FT-IR spectra were recorded in the range of  $4000-50\text{ cm}^{-1}$  on a Bruker IFS 66VS spectrometer with the resolution of about  $2\text{ cm}^{-1}$ . The samples were prepared as mulls in nujol and hexachloro-1,3-butadiene between CsI plates. The spectrometer was calibrated using polystyrene and indene. The FT-Raman spectra were recorded with 532nm laser source BRUKER Senterra Raman spectrometer in the spectroscopic region of  $4000\text{cm}^{-1}-50\text{cm}^{-1}$ .

From these spectra the vibrational wavenumbers of ligand molecule,  $Pd(CN)_4^{2-}$  group and guest molecule benzene were determined. Otherwise, the molecular structure was supported by making elemental analysis of the clathrates. By analysing the structures of the clathrates, ligand molecule cyclobutylamine was coordinated to M metal atom from cyclobutylamine's nitrogen atom, the guest molecule was enclathrated in the structural cavities between the sheets.

The thermal behavior of Hofmann-type clathrates of cba was studied in dynamic nitrogen atmosphere by DTA, DTG and TG techniques. Thermal decomposition of  $M(C_4H_7NH_2)_2Pd(CN)_4 \cdot 2G$  (M=Ni or Co; G=benzene) occur in the three separated stages.



## IR and 2D correlation spectroscopic investigation of CuO-V<sub>2</sub>O<sub>5</sub>-P<sub>2</sub>O<sub>5</sub>-CaF<sub>2</sub> glass system

N. Vedeanu<sup>1</sup>, D. A. Magdas<sup>2</sup>, O. Cozar<sup>3</sup>

<sup>1</sup>Iuliu Hațieganu University of Medicine and Pharmacy, RO-400023 Cluj-Napoca, Romania

<sup>2</sup>National Institute for Research and Development of Isotopic and Molecular Technologies, RO-400293 Cluj-Napoca, Romania

<sup>3</sup>Babes-Bolyai University, Faculty of Physics, RO-400028 Cluj-Napoca, Romania

Phosphate glasses containing calcium are intensely studied because of their multiple technical applications, but also for their medical potential as bio-glasses. Different properties of the phosphate glasses are induced by the different types of modifier ions introduced in the phosphate matrix and also by the depolymerization degree of the phosphate network [1].

It is well known from the literature that IR and Raman bands specific for phosphate glasses are large and overlapped compared with those specific to crystals and in consequence a correct and accurate band assignment is sometimes difficult.

The present work uses two methods – 2D correlation spectroscopy and spectral deconvolution of IR bands – in order to obtain a better band assignment, to establish the band shifts and to find correlations between various structural groups in the CuO-V<sub>2</sub>O<sub>5</sub>-P<sub>2</sub>O<sub>5</sub>-CaF<sub>2</sub> glass system.

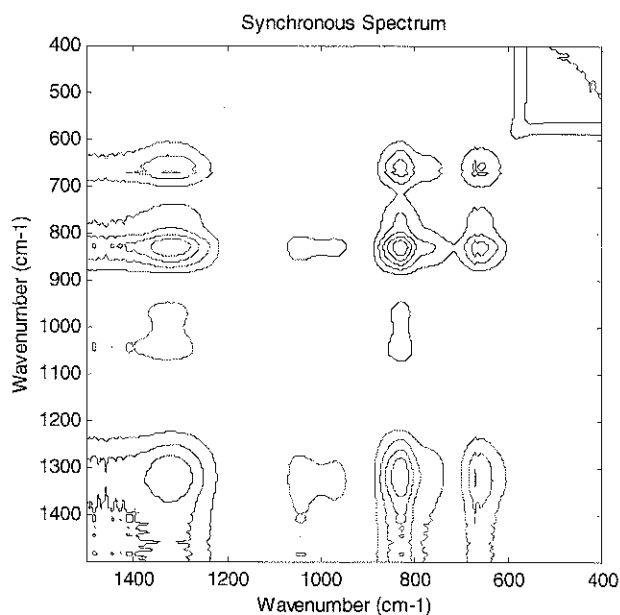


Fig. 1. IR 2D-COS synchronous spectrum for CuO-V<sub>2</sub>O<sub>5</sub>-P<sub>2</sub>O<sub>5</sub>-CaF<sub>2</sub> glass system

The two methods have pointed out that although the two oxides CuO and V<sub>2</sub>O<sub>5</sub> have both network modifier effect, V<sub>2</sub>O<sub>5</sub> effect is significantly higher. In addition, spectral deconvolution of the studied glass system evidenced that for high V<sub>2</sub>O<sub>5</sub> content ( $x > 20$  mol %) it acts not as a network modifier, but as a glass network former [2].

[1] G. Tricot, L. Montagne, L. Delevoye, G. Palavit, V. Kostoy, J. Non-Cryst. Solids 345-346 (2004) 56

[2] N. Vedeanu, O. Cozar, I. Ardelean, B. Lendl, D. A. Magdas, Vibr. Spectrosc. 48 (2008) 259



## Singlet Oxygen Photosensitization in Polymer Films

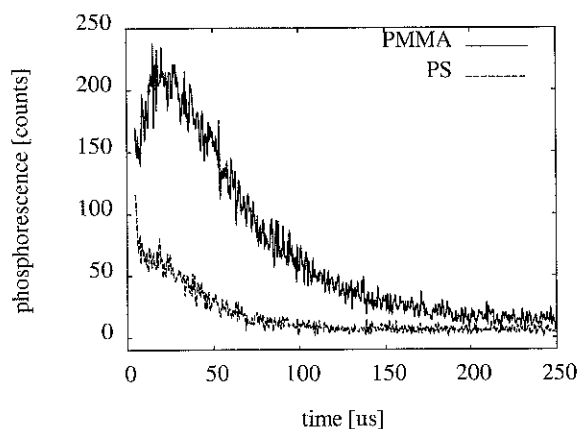
R. Dědic, V. Vyklický, A. Svoboda, and J. Hála

*Charles University in Prague, Faculty of Mathematics and Physics,  
Department of Chemical Physics and Optics, Ke Karlovu 3, Praha 2, 121 16, Czech Republic*

The photosensitizing properties of various photosensitizers in solutions as well as in complexes with biologically important molecules such as proteins or lipids were thoroughly investigated by our group in the past [1–4]. Direct detection of extremely weak near infrared luminescence of photosensitizers triplet states and of singlet oxygen with parallel spectral and temporal resolution was used to characterize production and quenching of both the excited states at room temperature. Unfortunately, our unique experimental set-up has been able to measure signals only from standard spectroscopic cells, which limited the investigations to solutions or suspensions. However, it is very important to observe the processes of photosensitization also from the surface of solid samples. This would enable to examine properties of photosensitizers bound to solid carriers as well as observe the processes of photosensitization and reactions of the excited states with biological environment directly in tissues. We have adapted our detection set-up to use bifurcated optic fiber with luminescence probe to both excite and collect the phosphorescence. Using this set-up, we have investigated photosensitization of singlet oxygen by protoporphyrin IX (PpIX) in polymer films.

The films were prepared from polystyrene (PS) and poly(methyl methacrylate) (PMMA). Both the polymers were dissolved in tetrahydrofuran (THF). Solution of PpIX in THF was added to obtain different concentrations of the photosensitizer in the films. The solutions were left in Petri dishes to evaporate under controlled conditions. Films ( $0.45 \pm 0.05$ ) mm thick were obtained this way.

Striking difference between PS and PMMA films was found. While only very weak signal of singlet oxygen luminescence at 1278 nm modulated on background luminescence was obtained in PS films, strong signal at the same wavelength was observed in PMMA films under the same conditions. This is demonstrated in the figure below, where kinetics of singlet oxygen luminescence is shown for both polymers with equal PpIX concentration of 100  $\mu\text{M}$ . Lifetimes of singlet oxygen of  $(42.2 \pm 1.7)$   $\mu\text{s}$  and PpIX triplets of  $(11.9 \pm 0.4)$   $\mu\text{s}$  can be resolved from the kinetics in PMMA.



- [1] R. Dědic, A. Molnár, M. Kořínek, A. Svoboda, and J. Hála. *J. Lumines.* 108 (2004) 117
- [2] M. Kořínek, R. Dědic, A. Molnár, and J. Hála. *J. Fluoresc.* 16 (2006) 355
- [3] A. Molnár, R. Dědic, A. Svoboda, and J. Hála. *J. Mol. Struct.* 834 (2007) 488
- [4] R. Dědic, V. Vyklický, A. Svoboda, and J. Hála. *J. Mol. Struct.* 924-926 (2009) 153



## Dependence of Singlet Oxygen Kinetics on Photosensitizer Concentration in Lipid Films

R. Dědic, V. Vyklický, and J. Hála

*Charles University in Prague, Faculty of Mathematics and Physics  
Department of Chemical Physics and Optics Ke Karlovu 3, Praha 2, 121 16, Czech Republic*

Lipids can form liposomes — vesicles that are often used for transport of lipophilic drugs (photosensitizers, PS) in the bloodstream for photodynamic therapy. Lipidic environment is able to substantially influence the lifetime of singlet oxygen ( $^1\text{O}_2$ ) [1]. Nevertheless, our previous efforts to investigate the photosensibilization of  $^1\text{O}_2$  in liposomes [2, 3] always provided shorter lifetimes of  $^1\text{O}_2$  than the ones previously published. Therefore, we have investigated the dependence of  $^1\text{O}_2$  kinetics under different TPP concentrations.

The thin lipid films were prepared by spin-coating of 200  $\mu\text{M}$  solution of phosphatidylcholine (PC) in chloroform with different concentrations of photosensitizer meso-tetraphenyl-porphine (TPP) on glass carriers. The infrared phosphorescence of both the photosensitizer and  $^1\text{O}_2$  was excited and collected using bifurcated optical fiber with luminescence probe. The signal was spectrally resolved using a high-luminosity monochromator and detected by an infrared-sensitive photomultiplier. The pulses from the photomultiplier were recorded by photon counter/multiscaler with time-resolution of 5 ns per channel [4].

Figure 1 shows typical  $^1\text{O}_2$  phosphorescence kinetics in dry lipid film. It was possible to resolve one rise- and one decay-time from the kinetics for all concentrations. The rise-times are increasing with TPP concentration from  $(1.3 \pm 0.5) \mu\text{s}$  to  $(3.6 \pm 0.5) \mu\text{s}$ . On the other hand, the decay-times are decreasing from  $(14 \pm 2) \mu\text{s}$  to  $(5.6 \pm 0.4) \mu\text{s}$ . The value at the lowest TPP concentration is equal to the  $^1\text{O}_2$  lifetime previously published by Baier [1].

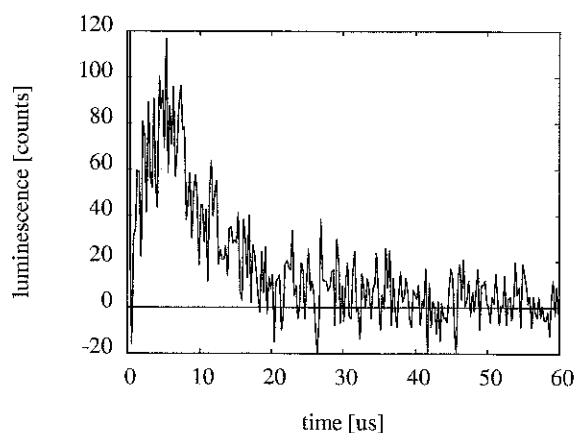


Figure 1:  $^1\text{O}_2$  phosphorescence kinetics at 1278 nm in sample with 1.75 TPP per 1000 PC

- [1] J. Baier, M. Maier, R. Engl, M. Landthaler, and W. Bäuml. *J. Phys. Chem. B* 109 (2005) 3041
- [2] A. Molnár, R. Dědic, A. Svoboda, and J. Hála. *J. Mol. Struct.* 834 (2007) 488
- [3] A. Molnár, R. Dědic, A. Svoboda, and J. Hála. *J. Lumines.* 128 (2008) 783
- [4] R. Dědic, V. Vyklický, A. Svoboda, and J. Hála. *J. Mol. Struct.* 924-926 (2009) 153

## Spectroscopic investigation on noble metal-organic nano hybrids with controlled shapes and properties

M. Alloisio<sup>1</sup>, A. Demartini<sup>1</sup>, S. Leporatti<sup>1</sup>, A. Rindi<sup>1</sup>, C. Cuniberti<sup>1</sup>, G. Dellepiane<sup>1</sup>, G. Margheri<sup>2</sup>, E. Giorgetti<sup>2</sup>, M. Muniz-Miranda<sup>3</sup>

<sup>1</sup>*INSTM and Dipartimento di Chimica e Chimica Industriale, Università di Genova, Via Dodecaneso 31, I-16146 Genova, Italy*

<sup>2</sup>*Istituto dei Sistemi Complessi – CNR, Via Madonna del Piano 10, I-50019 Sesto Fiorentino, Italy*

<sup>3</sup>*Dipartimento di Chimica, Università di Firenze, Via della Lastruccia 3, I-50019 Sesto Fiorentino, Italy, and European Laboratory for Non-linear Spectroscopy, Via Nello Carrara 1, I-50019 Sesto Fiorentino, Italy*

Hybrid compounds obtained by a bottom-up technique consisting of self-assembling properly functionalized organic molecules onto preformed nanosized cores of noble metals represent very promising materials for applications in both industrial and medical fields. Their optical, spectroscopic and functional properties can be easily modulated by mastering size and shape of the metal core as well as the chemical nature of the organic shell.

To this end we prepared gold and silver nanoclusters with different geometries (spheres, rods, cages, ribbon-like assemblies, stars) by reduction of the corresponding salt in aqueous solution, properly manipulating the synthesis protocol. The morphology of the as-prepared colloids was characterized by TEM technique and confirmed by spectroscopic analysis. The plasmonic absorption are tuned throughout the visible and near-infrared (NIR) region in relation to nanostructure size, shape, aggregation state and local environment. The so prepared nanostructures were then passivated with properly functionalized molecules like chromophores and diacetylenic monomers by taking advantage of the well-established monolayer chemistry. The optical properties of the novel nano hybrids were investigated by UV-Vis and Raman techniques in order to evaluate the role of the metal nanostructures on the behaviour of the chemisorbed molecules and on their sensitivity to the environmental changes [1].

Photopolymerized diacetylene monomers bonded to these nanostructures [2,3] represent promising materials with strong electromagnetic field enhancements in the NIR region without need of properly structured metallic nanoparticulates to induce hot-spots [4]. This opens the way to the implementation of nonlinear optical effects and to devices, like switches or modulators, for telecom applications. Moreover, the use of these nanostructures allows the extension of well established spectroscopic diagnostics, like SERS, in this spectral region.

- [1] M. Alloisio, A. Demartini, C. Cuniberti, G. Dellepiane, *Sensor Letters* (2010) in press.
- [2] A. Demartini, M. Alloisio, C. Cuniberti, G. Dellepiane, S. A. Jadhav, S. Thea, E. Giorgetti, C. Gellini, M. Muniz-Miranda, *J. Phys. Chem. C* 113 (2009) 19475
- [3] G. Dellepiane, C. Cuniberti, M. Alloisio, A. Demartini, *Phys. Chem. Chem. Phys.*, (2010), DOI: 10.1039/b912921a
- [4] F. Hao, C. L. Nehl, J. H. Hafner, P. Nordlander, *Nano Letters* 3 (2007) 729



## Kinetics of crystallization of SnO<sub>2</sub> nanoparticles in sol-gel -based glass ceramics: comparison of thin films and bulk systems

T. V. Tran<sup>1</sup>, S. Turrell<sup>1</sup>, C Kinowski<sup>2</sup>, O. Cristini<sup>2</sup>, B. Capoen<sup>2</sup>, M. Bouazaoui<sup>2</sup>, P. Roussel<sup>3</sup>, S. Berneschi<sup>4</sup>, G. Righini<sup>4</sup>, M. Ferrari<sup>5</sup>, S. N. B. Bhaktha<sup>6</sup>

<sup>1</sup>LASIR (CNRS, UMR 8516) Université Lille 1 et CERLA, 59650 Villeneuve d'Ascq cedex, France

<sup>2</sup>PhLAM (CNRS, UMR 8523) Université Lille 1 et CERLA, 59650 Villeneuve d'Ascq cedex, France

<sup>3</sup>UCCS (CNRS, UMR 8181), Bât. C-7a, ENSCL, 59652 Villeneuve d'Ascq, France

<sup>4</sup>MDF Lab., IFAC-CNR, Via Madonna del Piano 10, 50019 Sesto Fiorentino, Florence, Italy

<sup>5</sup>CSMFO Lab., IFN-CNR, Via alla Cascata 56/c, 38050 Trento, Italy

<sup>6</sup>LPMC, CNRS UMR6622 and Université de Nice-Sophia Antipolis, Parc Valrose, 06108, Nice cedex 02, France

Silica-based nanostructured glass ceramics are of great interest due to their applications towards various photonic devices. The production of active rare earth (RE) species in a glass matrix can give rise to high luminescence efficiency, if one can avoid clustering of and energy exchange between the RE ions. The use of glass ceramics offers an ideal solution as this class of materials combines the mechanical and optical properties of the glass with a crystal-like environment for the RE ions, thus eliminating the cluster effects.

In the present work, SiO<sub>2</sub> – SnO<sub>2</sub> systems have been chosen as the glass-ceramic because the semiconductor nanoclusters of SnO<sub>2</sub> can also be used to transfer energy to RE ions. In effect, by doping the RE ions into the semiconductor nanoclusters, then band gap excitation may result in efficient energy transfer thus yielding enhanced luminescence from the RE ion [1,2].

This communication presents recent results obtained for high-Sn content thin-film and bulk systems. All syntheses are based on sol-gel techniques and the samples are activated by rare-earth ions (Eu<sup>+3</sup>, Er<sup>+3</sup>). Use of the m-line technique provided the determination of the thicknesses and refractive indices of the films. Data obtained using a combination of Raman, FTIR and photoluminescence spectroscopies as well as *in situ* high-temperature XRD and TEM microscopy, makes it possible to show that:

- a) the doped RE ions are indeed located within the SnO<sub>2</sub> NC
  - b) in the case of the thin films, the growth kinetics of the SnO<sub>2</sub> NCs vary with the densification temperature and the concentration of SnO<sub>2</sub>.
  - c) for the bulk systems, the NC size seems to be controlled by the pore size of the gel.
- Discussion will be made on the origin of these differences.

[1] J. Castillo, V. D. Rodriguez, A. C. Yanes and J. Méndez-Ramos, J. Nanopart. Res. 10 (2008) 499 - 506

[2] S.N.B. Bhaktha, F. Beclin, M. Bouazaoui, B. Capoen, A. Chiasera, M. Ferrari, C. Kinowski, G.C. Righini, O. Robbe and S. Turrell, Appl. Phys. Lett. 93 (2008) 211904-1 – 211904-3



## Nanoparticle enhanced FTIR spectroscopy of polymer interfaces

C. Zimmerer<sup>1</sup>, G. Steiner<sup>2</sup>, V. Šablinskas<sup>3</sup>, G. Heinrich<sup>1</sup>

<sup>1</sup> *Leibniz Institute of Polymer Research Dresden e.V., Dresden, Germany*

<sup>2</sup> *Dresden University of Technology, Medical Faculty, Clinical Sensing and Monitoring, Dresden, Germany*

<sup>3</sup> *Vilnius University, Department of General Physics and Spectroscopy, Vilnius, Germany*

The development of new classes of polymers composite materials with emphasis on their rich molecular architecture and molecular interactions requires methods for a non-destructive characterization. In particular knowledge of molecular organization at the polymer interfaces is essential for material properties. Methods that are relevant to characterization molecular structure are Raman and infrared spectroscopy. However, a disadvantage of the spectroscopic methods lies in their sensitivity to bulk phases and less to the thin interface layer.

Surface enhanced infrared absorption is a relatively new technique whereby the spectra of very thin layers are enhanced by interaction of vibrational modes with the collective motion of electrons of metal nanoparticles. When nanoparticles are incorporated into the polymer interface vibrational modes become more intense. The infrared spectra measured in this way allow a characterization of molecular processes between different polymers of the blend.

In this contribution, we demonstrate the potential of metal nanoparticle enhanced FTIR spectroscopic imaging to study molecular processes in amino functionalized polymeric modifier for Bisphenol-A based Polycarbonate. Infrared spectra reveal chemical reactions and a formation of covalent bindings when the temperature is increased. Obtained reaction products at the interface are urethane, urea and more complex structures dicarbonic acids. In addition, changes in the  $\nu$  (C=O) mode of the carbonate group at an initial wavenumber of  $1775\text{ cm}^{-1}$  give rise to chain scissions or association by hydrogen bond formation of polycarbonate by the modifier. This fundamental study confirmed the suitability of metal nanoparticle enhanced FTIR spectroscopy to assess molecular processes between polymers in a non-destructive manner, and open the possibility for the in-situ characterization of polymer composite materials.



## Spectroscopic study of tetracationic porphyrin H-aggregation on polyanionic matrix

O. Ryazanova, I. Voloshin and V. Zozulya

*Department of Molecular Biophysics, B. Verkin Institute for Low Temperature Physics & Engineering of NAS of Ukraine, 47 Lenin ave., 61103, Kharkov, Ukraine*

Self-assembly of tetracationic porphyrin TMPyP4 onto polyanionic matrix of inorganic polyphosphate (PPS) in aqueous solutions has been studied in a wide range of molar phosphate-to-dye ratios by means of polarized fluorescence, absorption, and static light scattering techniques [1].

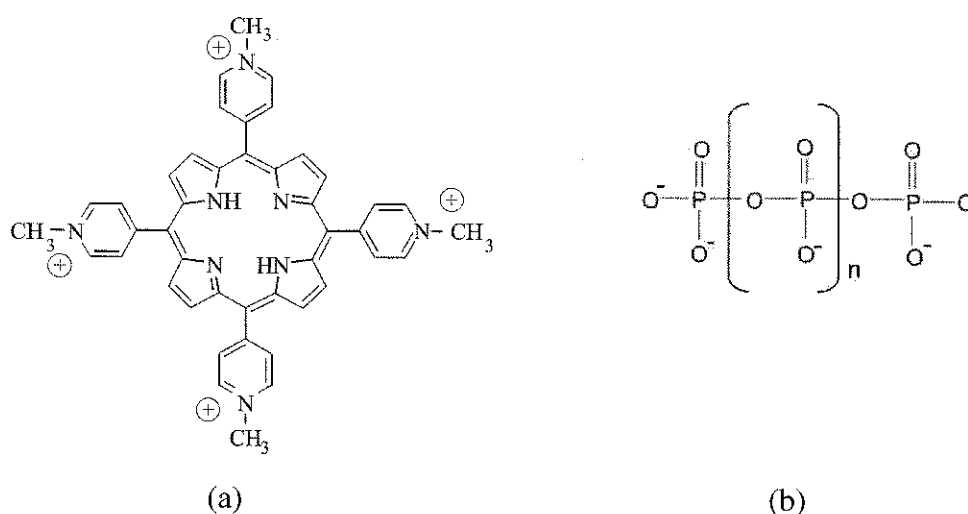


Fig. 1. Molecular structure of tetracationic porphyrin TMPyP4 (a) and polyphosphate (b).

It was established that the binding of  $\text{TMPyP}^{4+}$  to PPS is characterized by the binding constant of  $3 \times 10^5 \text{ M}^{-1}$  and the cooperativity parameter of about 150. The fluorescence quenching of the bound  $\text{TMPyP}^{4+}$  evidences the stacking of the porphyrine chromophores. Under the stoichiometric binding ratio  $\text{TMPyP}^{4+}$  forms extended continuous face-to-face aggregates (so-called H-aggregates) which are manifested themselves by a 12 nm blue shift and a 51% hypochromicity of the Soret absorbance band. Each face-to-face  $\text{TMPyP}^{4+}$  stack is formed with participation of four PPS chains. Formation of such columnar aggregates is promoted by the ability of PPS chains to take a helix conformation where negative charges are arranged along two oppositely situated rows with intercharge distance of 0.36 nm which corresponds to the thickness of the porphyrin  $\pi$ -electronic system. The ability of each PPS strand to be template for formation of two porphyrin stacks results in the integration of the adjacent stacks into higher-order aggregates which dimension was estimated from the fluorescence polarization data.

[1] V.N. Zozulya, O.A. Ryazanova, I.M. Voloshin, A.Yu. Glamazda, V.A. Karachevtsev, *J. Fluoresc.* (2010), accepted.



## FTIR, UV-VIS spectroscopy and DFT calculations on the structure of the gadolinium-lead-germanate glasses

S. Rada<sup>1</sup>, V. Dan<sup>1</sup>, M. Rada<sup>1</sup>, M. Culea<sup>2</sup>, T. Rusu<sup>1</sup>, M. Bosca<sup>1</sup>, L. Pop<sup>1</sup>, E. Culea<sup>1</sup>

<sup>1</sup>Department of Physics, Technical University of Cluj-Napoca, 400020 Cluj-Napoca, Romania

<sup>2</sup>Physics Department, Babes-Bolyai University, 400084 Cluj-Napoca, Romania

Glasses in the system  $x\text{Gd}_2\text{O}_3 \cdot (100-x)[7\text{GeO}_2 \cdot 3\text{PbO}]$  with  $0 \leq x \leq 40\text{mol}\%$  have been prepared from melt quenching method. Lead-germanate glasses are particularly interesting in the context of the germanate anomaly. In this paper, we investigated changes in germanium coordination number in gadolinium-lead-germanate glasses through molar volume analysis, measurements of densities, investigations of FTIR and UV-VIS spectroscopy and calculations of density functional theory (DFT).

Despite some inconsistencies the coordination change model remains the currently accepted model for the anomalous behavior of the lead-germanate glasses. Based on these experimental results, we propose the following answerable mechanisms of germanate anomaly: i) smaller thermodynamic stability of the  $[\text{GeO}_6]$  structural units and the occupation of the interstices of larger dimensions (the six-coordinated interstices of the  $[\text{PbO}_6]$  structural units) in lead-germanate network yield the apparition with promptitude of the  $[\text{GeO}_5]$  structural units with higher thermodynamic stability and larger ionic radius and ii) unaccommodating with the terminal oxygens of the  $[\text{GeO}_5]$  structural units and with the formation of smaller network cavities of the lead-germanate glasses needs links with  $[\text{GeO}_4]$  tetrahedrons for stabilization generating the formation of 3-membered rings of  $[\text{GeO}_4]$  tetrahedral structural units.



## FTIR, UV-VIS and EPR spectroscopy investigations of the copper-lead-germanate glasses

R. Chelcea, S. Rada, E. Culea

*Department of Physics, Technical University of Cluj-Napoca, 400020 Cluj-Napoca, Romania*

Glasses in the system  $x\text{CuO} \cdot (100-x)[7\text{GeO}_2 \cdot 3\text{PbO}_2]$  with  $0 \leq x \leq 60$  mol% have been prepared from melt quenching method. In this paper, we investigated changes in germanium coordination number in copper-lead-germanate glasses through investigations of FTIR, UV-VIS and EPR spectroscopy.

Our FTIR spectroscopic studies on copper-lead-germanate glasses suggest that  $[\text{CuO}_6]$  octahedral and  $[\text{CuO}_4]$  tetrahedral units exist in these materials. The decreasing trends of the IR bands located in the  $360\text{-}500\text{cm}^{-1}$  and  $670\text{-}1100\text{cm}^{-1}$  region towards lower wavenumber show the increase of polymerization degree of the network by interconnection of Pb-O-Ge and Pb-O-Pb linkages.

By increasing of the CuO content up to 60mol%, decreasing trend was observed for the UV band situated in the 250-400nm domain. This might be due to the formation of the  $[\text{CuO}_6]$  structural units by conversion of some  $[\text{GeO}_6]$  to  $[\text{GeO}_4]$  structural units. The intensity of the signal decreases because it is possible a gradual adaptation of  $\text{Cu}^{+2}$  ions from covalent to ionic environment.

All EPR spectra exhibit parallel ( $g_{\parallel}$ ) and ( $g_{\perp}$ ) perpendicular features along with hyperfine lines. The presence of the lead oxide, acting as a network modifier, influences the transformations of the microenvironment of the paramagnetic ions. The compositional dependence of  $\text{Cu}^{+2}$  EPR parameters is related to the structural modifications in the glass network.



## FTIR, UV-VIS and EPR investigations of the gadolinium-lead-tellurate unconventional glasses

S. Rada, R. Chelcea, A. Dehelean, P. Pascuta, T. Ristoiu, I. Coroiu, M. Barlea, E. Culea

*Department of Physics, Technical University of Cluj-Napoca, 400020 Cluj-Napoca, Romania*

In this paper, we have examined and analyzed the effects of systematic gadolinium ions intercalation on lead-tellurate glasses with interesting results. Modifications of gadolinium-environment in  $x\text{Gd}_2\text{O}_3 \cdot (100-x)[7\text{TeO}_2 \cdot 3\text{PbO}]$  glasses system, where  $0 \leq x \leq 40$  mol% have been investigated by FTIR, UV-VIS and EPR spectroscopy.

The gadolinium and lead ions have an affinity pronounced towards  $[\text{TeO}_3]$  structural units yielding the deformation of the Te-O-Te linkages. Structural changes, as recognized by analyzing band shapes of IR spectra, revealed that the increase of the  $\text{Gd}^{+3}$  content causes the intercalation of  $[\text{GdO}_n]$  entities in the  $[\text{TeO}_4]$  chain network. The excess of oxygen can be supported into the glass network by the formation of  $[\text{PbO}_n]$  and  $[\text{GdO}_n]$  structural units.

The UV-VIS spectroscopy data show that the  $\text{Pb}^{+2}$  ions absorb strongly in the ultraviolet.

Then, the gadolinium ions will coordinate more with the excess of oxygen yield the formation of network formers ( $g \approx 4.8$ ) and modifiers sites ( $g \approx 2$ ). It can be pointed that the  $\text{Gd}^{+3}$  ions are generally suspected to improve their environment.



## Redox processes in iron-lead-tellurate glasses

A. Dehelean<sup>1,2</sup>, S. Rada<sup>2</sup>, E. Culea<sup>2</sup>

<sup>1</sup>Department of Physics, Technical University of Cluj-Napoca, 400020, Romania  
<sup>2</sup>Nat. Inst. For R&D of Isotopic and Molec. Technologies, Cluj-Napoca, Romania

In this paper, we have analyzed the effects of iron ions intercalations on lead-tellurate glasses by investigations of FTIR and UV-VIS spectroscopy. The homogeneous glass system has compositions  $x\text{Fe}_2\text{O}_3 \cdot (100-x)[4\text{TeO}_2 \cdot \text{PbO}_2]$  where  $x = 0-60\text{mol}\%$ .

The presented observations in these mechanisms show that the lead ions have an affinity pronounced towards  $[\text{TeO}_3]$  structural units yielding the deformation of the Te-O-Te linkages and pursuant to the intercalation of  $[\text{PbO}_n]$  ( $n=3, 4$ ) and  $[\text{FeO}_n]$  ( $n=4, 6$ ) entities in the  $[\text{TeO}_4]$  chain network. The formation of  $[\text{FeO}_4]^{-1}$  structural units with negative charge implies the attraction of  $\text{Pb}^{+2}$  ions for charge compensation. Thus, some  $\text{Pb}^{+2}$  ions decontrol of the  $[\text{TeO}_3]$  structural units. By increasing of the  $\text{Fe}_2\text{O}_3$  content up to 60mol%, the accommodation of the network with excess of oxygen can be supported by the conversion of  $[\text{TeO}_3]$  to  $[\text{TeO}_4]$  structural units and the formation of  $[\text{FeO}_6]$  structural units.

Our UV-VIS spectroscopic data show two mechanisms: i) the conversion of the  $\text{Fe}^{+3}$  to  $\text{Fe}^{+2}$  species in same time with the oxidation of  $\text{Pb}^{+2}$  to  $\text{Pb}^{+4}$  ions for sample with smaller  $\text{Fe}_2\text{O}_3$  content; ii) when the  $\text{Fe}_2\text{O}_3$  content is higher ( $x \geq 50\text{mol}\%$ ), the  $\text{Fe}^{+2}$  ions capture positive holes and are transferred to  $\text{Fe}^{+3}$  ions through photochemical reaction while the  $\text{Pb}^{+2}$  ions are formed by reduction of the  $\text{Pb}^{+4}$  ions.



## Novel photochromic properties of the tungsten-lead-borate glasses

M. Rada<sup>1</sup>, V. Maties<sup>1</sup>, S. Rada<sup>2</sup>, I. V. Simiti<sup>2</sup>, E. Culea<sup>2</sup>

<sup>1</sup>*Mechanics Department, Technical University of Cluj-Napoca, 400641 Cluj-Napoca, Romania*

<sup>2</sup>*Physics Department, Technical University of Cluj-Napoca, 400641 Cluj-Napoca, Romania*

Glasses and glass ceramics were prepared in the system  $x\text{WO}_3 \cdot (100-x)[3\text{B}_2\text{O}_3 \cdot \text{PbO}]$  where  $0 \leq x \leq 40$  mol% by conventional melting-quenching method. Influence of tungsten ions on structural behavior in lead-borate glasses has been investigated using infrared spectroscopy and DFT calculations.

These tungsten-lead-borate systems exhibit a photochromic effect which can be induced through laser exposures ( $\lambda=633\text{nm}$ ) directly on the bulk sample. Structural investigations by FTIR spectroscopy show that the photosensitive effect are due to a reduction of  $\text{W}^{+6}$  to  $\text{W}^{+5}$  and/or  $\text{W}^{+4}$  promoted by the oxidation of  $\text{Pb}^{+4}$  and some structural changes of the borate network.

By the substitution of the lead ions with tungsten ions, tungsten ions would occupy the six-coordinated interstices. The expanded thermodynamic stability of the  $[\text{W}_2\text{O}_7]$  and  $[\text{WO}_4]$  polyhedrons comparative with the  $[\text{WO}_6]$  polyhedron yield the formation of the  $\text{PbMoO}_4$  crystalline phase and of the  $[\text{W}_2\text{O}_7]$  structural units in the glass ceramic.



## Hydrothermal synthesis of iron oxide nanorings by Mn-doping

M. Gotić and S. Musić

*Ruder Bošković Institute, Bijenička c. 54, HR-10002 Zagreb, Croatia*

Jia et al. (*Angew. Chem. Int. Ed.* **2005**, 44, 4328-33) showed that the phosphate anions could induce the preferential dissolution of the hematite spindle precursor to give single-crystalline iron oxide nanotubes. Recently the same authors (*J. Am. Chem. Soc.* **2008**, 130, 16968-77) introduced sulphate anions into the system in order to achieve better control of its morphology and this double anion mediation resulted in the synthesis of iron oxide nanorings. In this work, we successfully control the morphology of iron oxide nanotubes by cation doping. With increased Mn-doping the aspect ratio of iron oxide nanotubes gradually decrease and as a result iron oxide nanorings are formed (Fig. 1). The impact of Mn-dopant on the microstructural properties of iron oxide nanoparticles having spindle and nanotube shapes were studied using Mössbauer, FT-IR, FE-SEM and XRD techniques.

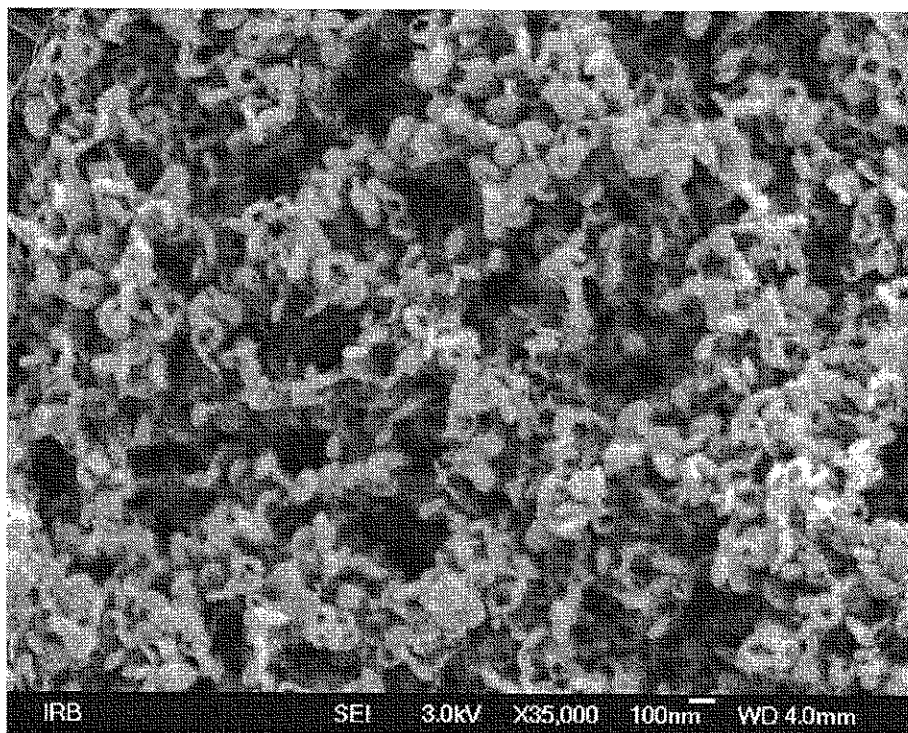


Fig. 1 Mn-doped  $\alpha$ -Fe<sub>2</sub>O<sub>3</sub> particles in the form of nanorings.

## Development of copper nanostructured materials for surface-enhanced Raman scattering spectroscopy

M. Vyskovska<sup>1</sup>, V. Prokopec<sup>1</sup>, M. Clupek<sup>1</sup>, A. Kokaislova<sup>1</sup>, J. Cejkova<sup>2</sup>, P. Matejka<sup>1</sup>

<sup>1</sup>Dept. of Analytical Chemistry, Institute of Chemical Technology, Technicka 5, 166 28 Prague 6, Czech Republic

<sup>2</sup>Dept. of Chemical Engineering, Inst. Chemical Technology, Technicka 3, 166 28 Prague 6, Czech Republic

Surface enhanced Raman scattering (SERS) spectroscopy is a powerful and widely used technique in chemical, analytical or bioanalytical applications. SERS spectra can be observed on surfaces of some metals (Ag, Au and Cu) with appropriate morphology (roughness, size and shape of nanostructures). Copper nanomaterials have been used in different studies recently.

In this study Cu nanostructured surfaces have been prepared by electrochemical deposition of copper onto platinum target [1]. Cu large-scaled SERS-active nanostructured substrates were modified with different analytes (aliphatic and aromatic thiols). Substrate morphology has been studied systematically by scanning electron microscopy (SEM). The chemical reduction Cu<sup>2+</sup> salt (sulphate, nitrate or chloride) in aqueous medium has been carried out using an excess of sodium borohydride in citrate solution. CuNP systems were modified by selected thiol derivatives at various concentrations. Due to quite limited stability of systems CuNP sols have been prepared at ca. 0°C in the ice bath. Systems were stable for about one hour under cooling in the ice bath. Afterwards CuNPs oxidized or aggregated. The prepared modified CuNP sols were of different colours: from light brown to dark reddish brown. Absorption spectra exhibited a maximum located at about 560 nm (Fig. 1). It was observed that absorption maximum of surface plasmon resonance (SPR) was shifted by analyte modification in UV/VIS spectra. CuNP systems can be characterized by microscopic methods, e.g. by atomic force microscopy (AFM) or transmission electron microscopy (TEM). SERS activity of Cu nanostructured systems has been investigated by Raman spectral measurements at 1064 nm, 785 nm and 488 nm excitation wavelengths.

It was observed that CuNPs gave rise to enhancement of Raman signal. SERS spectra of modified systems were collected (Fig. 2) and exhibited all characteristic Raman bands even at low concentration of the analyte. These systems can be used for characterization and detection of different low-molecular compounds with the structure similar to studied analytes.

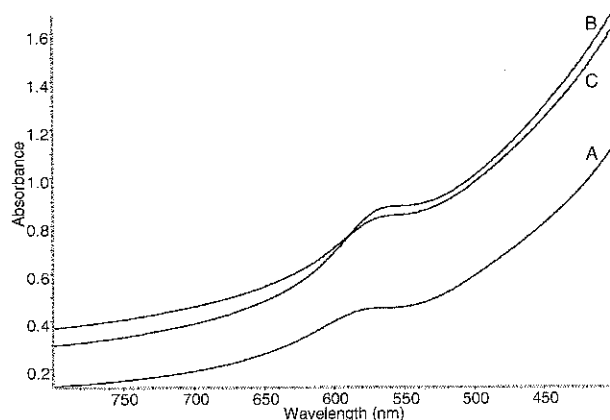


Fig. 1. UV/VIS spectra CuNP with 16-MHDA (A), unmodified CuNP (B), CuNP with 4-ATP (C)

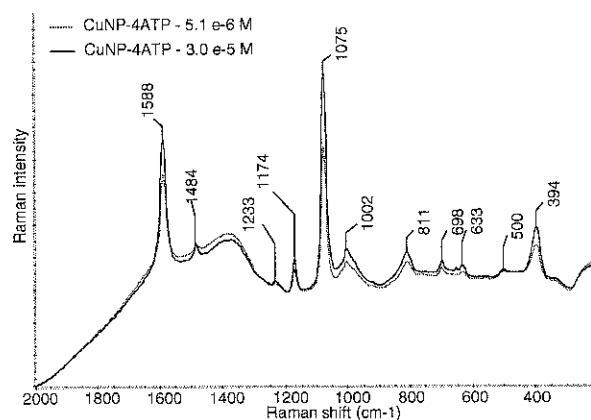


Fig. 2. SERS spectra CuNP with 4-ATP excited at 785 nm (conc. ~ 10<sup>-5</sup> M)

[1] J. Cejkova, V. Prokopec, S. Brazdova, A. Kokaislova, P. Matejka, F. Stepanek, Appl. Surf. Sci. 255 (2009) 7864



## Molecular aggregation of naphthalimide dyes in Langmuir-Blodgett films

D. Bauman, N. Bielejewska

*Faculty of Technical Physics, Poznan University of Technology, Nieszawska 13A, 60-965, Poznan, Poland*

Langmuir-Blodgett (LB) technique [1] is a unique method which allows to fabricate nanosized ordered layers from some molecules and colloid particles, the architecture of which can be manipulated with easy. This gives possibility to optimize the physical (especially electro-optical) parameters of a material used and therefore LB films are today the integral part of the knowledge area connected with the molecular electronics. The LB technique was also proposed to obtain the ordered layer for organic light emitting diodes (OLEDs) [2,3], which constitute today the largest competition with respect to liquid crystal displays (LCDs). On the other hand, the fabrication of ultra-thin layers by LB technique is very useful to study molecular aggregates, especially of organic compound molecules. These layers give the molecules the opportunity to be in highly oriented environments, similarly as it takes place in solid matrices, where the phenomenon of the molecular aggregation frequently occurs [4]. In the recent years, molecular aggregates have attracted a considerable attention because of very interesting optical properties of these systems and their possible application as novel functionalized materials in molecular electronics and photonics.

We present here the results of the spectroscopic study of Langmuir-Blodgett (LB) films formed of some naphthalimide dyes (derivatives of 4-aminonaphthalimide) and of their mixtures with arachidic acid, used as supporting matrix. The derivatives of 4-aminonaphthalimide under investigation are known as organic dyes with very high quantum fluorescence yield [5,6]. The electronic absorption, excitation, and fluorescence spectra were recorded. On the basis of these spectra, the spectral properties of the dyes and the intermolecular interactions in nanosized ordered films were determined. The shape and band position of the absorption spectra of the derivatives of 4-aminonaphthalimide, pure and mixed with the arachidic acid, suggest a tendency to formation of J-type aggregates [7] between the dye molecules in the ground electronic state. The fraction of these aggregates rises with the increase of the layer number in the LB film. The detailed analysis of the fluorescence spectra allow to conclude that in the excited state at enough high concentration, the dyes can create molecular configurations giving the excimer emission. The fraction of excimers strongly depends on the dye content as well as on the dye molecular structure. On the basis of the results obtained the possibility of the utilization of LB films formed of the derivatives of 4-aminonaphthalimide as an active layer in OLEDs has been discussed.

- [1] M.C. Petty, *Langmuir-Blodgett Films-An Introduction*, Cambridge University Press, Cambridge, 1996.
- [2] J.R. Sheats, H. Antoniadis, M. Hueschen, W. Leonard, J. Miller, R. Moon, D. Roitman, A. Stocking, *Science* 273 (1996) 884-888.
- [3] I.H. Stapff, V. Stuempflen, H. Wendorff, D.B. Spohn, D. Moebius, *Liq.Cryst.* 23 (1997) 613-617.
- [4] *Organic Molecular Aggregates: Electronic Excitation and Interaction Processes*, Eds. P. Reineker, H. Haken, and H.C. Wold, Springer, Berlin, 1983.
- [5] R. Stolarski, *Fibres and Textiles in Eastern Europe* 17 (2009) 91-95.
- [6] N. Bielejewska, E. Wolarz, R. Stolarski, D. Bauman, *Opto-electronics Rev.* 16 (2008) 367-378.
- [7] D. Moebius, *Adv.Mater.* 5 (1995) 437-444.





## EPR and IR structural investigation of $V_2O_5 - P_2O_5 - BaO$ glass system with opto-electronic potential

R. Stanescu<sup>1</sup>, N. Vedeanu<sup>2</sup>, S. Filip<sup>1</sup>, O. Cozar<sup>1</sup>

<sup>1</sup>Babes-Bolyai University, Faculty of Physics, RO-400028 Cluj-Napoca, Romania

<sup>2</sup>Iuliu Hațieganu University of Medicine and Pharmacy, RO-400023 Cluj-Napoca, Romania  
University of Oradea, Faculty of Physics, RO-410087 Oradea, Romania

The interest for phosphate glasses increased because of a great variety of opto-electronic applications in which they are involved, the presence in different organic or inorganic composites, as nuclear waste hosts or for medical applications. Most of the applications are related to the molecular level structure of these glasses. The addition of transition metal (TM) oxides leads to the depolymerization of the phosphate chains and to the formation of new P – O – TM which can change the electrical, optical or magnetic properties of these glasses [1].

The present work is a structural study of some phosphate glasses containing vanadium. The following glass systems was prepared and investigated by EPR and IR spectroscopy:  $xV_2O_5(1-x)[0.8P_2O_5 \cdot 0.2BaO]$ .

According to the calculated EPR parameters ( $g_{\parallel} \sim 1.92$ ,  $g_{\perp} \sim 2.00$  and  $A_{\parallel} = 197 \cdot 10^{-4} \text{ cm}^{-1}$ ) vanadium ions are present in this glasses in a square pyramidal ( $C_{4v}$ ) site as  $VO^{2+}$  ions for  $x < 10 \text{ mol } \%$ . The shape of the EPR spectra is changed with the increasing of the vanadium content, this consisting in a progressive disappearance of the hyperfine structure characteristic to the  $V^{4+}$  ions. The changes observed in the EPR spectra of these glasses are explained supposing the superposition of two EPR signals, one with a well-resolved hyperfine structure typical for isolated  $V^{4+}$  ions and the other one consisting in a broad line without hyperfine structure characteristic for clustered ions [2].

IR spectra of the studied glass system show for low concentration of ions the specific bands belonging to the phosphate groups, but at high concentration of  $V^{4+}$  ( $x \geq 10 \text{ mol } \%$ ) the bands belonging to the vibration of  $V_2O_5$  groups dominates the spectra. In the same time the bands belonging to the phosphate groups are strongly reduced except the specific bands of the short chain phosphate units. This suggest that in the studied glasses vanadium act as network modifier for low concentration ( $x < 10 \text{ mol } \%$ ) but may act also as a network former at high concentration of  $V_2O_5$  [3].

- [1] J. E. Garbarczyk, P. Machowski, M. Wasiucioneck, L. Tykarski, R. Bacewicz, A. Aleksiejuk, Sol. State Ionics 136-137 (2000) 1077-1083
- [2] V. R. Kumar, R. P. S. Chakradhar, A. Murali, N. O. Gopal, J. L. Rao, Int. L. Mod. Phys. B 16 (2003) 3033-3047
- [3] O. Cozar, N. Vedeanu, D. A. Magdas, I. Ardelean, J. Optoelectronics Adv. Mat. V. 10, 4 (2008) 871-875



## Preparation and photophysical study of fluorophore modified gold nanoparticles

P. Angelova<sup>1</sup>, N. Kuchukova<sup>1</sup>, G. Dobrikov<sup>1</sup>, I. Petkova<sup>2</sup>, E. Giorgetti<sup>3</sup>, I. Timtcheva<sup>1</sup>, K. Kostova<sup>1</sup>, E. Vauthey<sup>2</sup>

<sup>1</sup>*Institute of Organic Chemistry with centre of Phytochemistry – Bulgarian Academy of Sciences, Acad.G.Bonchev Str. Bl.9, Sofia 1113, Bulgaria*

<sup>2</sup>*Universite de Geneve, Department de Chimie Phisique, 30 Quai Ernest Ansermet, CH-1211 Genève 4*

<sup>3</sup>*Istituto dei Sistemi Complessi – CNR, Via Madonna del Piano 19, I-50019 Sesto Fiorentino, Italy*

Tailoring the optoelectronic properties of noble metal nanoparticles by organizing chromophores of specific properties and functions on their surface can lead to the preparation of photoresponsive organic-inorganic nanohybrid materials with possible application in new devices for sensing, switching and drug delivery.<sup>1</sup> Close vicinity of the noble metal nanoparticle influences the excited state's deactivation pathways of the organic fluorophores capped on their surface. In many of the examples studied to date, the energy transfer process is considered to be the major deactivation pathway for excited fluorophores bound on metal surfaces.<sup>2</sup> The energy transfer depends strongly on the nanoparticle's size and shape, on the distance between the dye molecule and the nanoparticle, as well as on the overlap of the fluorophore emission and the noble metal nanoparticle's surface plasmon absorption.<sup>3-7</sup>

Design and synthesis of new organic compounds with desired structure and photophysical properties for application as fluorescent markers for noble metal nanoparticles is performed. The novel fluorophores are derivatives of 4-methoxy-1,8-naphthalimide bearing at the imide N atom long methylene chains with SH end groups, which enables their covalent binding to noble metals. The methylene chains consist of 6, 8, 12 and 16 groups respectively. The novel organic luminophores are applied for fluorescent labeling of both synthetically prepared Monolayer Protected Clusters (MPCs) of Au nanoparticles, and of Au nanoparticles, obtained by picosecond laser ablation. The influence of the chain length and the size of the nanoparticles on the fluorescent ability of the MPCs is studied by UV-Vis absorption, steady state and picosecond time resolved fluorescence spectroscopy.

- [1]. G.J. Hutchings, M. Brust, H. Schmidbaur, *Chem. Soc. Rev.*, 37 (2008), 1759–1765
- [2]. K. G. Thomas, Prashant V. Kamat, *Acc. Chem. Res.*, 36 (2003), 888-898
- [3]. Chen, Y.; Munechika, K.; Ginger, D.; *NANOLETTERS* 2007, 7, 3, 690
- [4]. Drexhage, K. H.; Kuhn, H.; Shafer, F. P.; *Ber. Bunsen-Ges. Phys. Chem.* 1968, 72, 329.
- [5]. Ishida, A.; Sakata, Y.; Majima, T.; *Chem. Commun.* 1998, 57.
- [6]. Saito, K.; *J. Phys. Chem. B* 1999, 103, 6579.
- [7]. Pagnot, T.; Barchiesi, D.; Tribillon, G.; *Appl. Phys. Lett.* 1999, 75, 4207.



## *In situ* high temperature Raman spectroscopy of modified titanate nanotubes

M. Plodinec<sup>1</sup>, D. Iveković<sup>2</sup>, D. S. Su<sup>3</sup>, A. Gajović<sup>1</sup>

<sup>1</sup> Ruđer Bošković Institute, Zagreb, Bijenička 54, HR-10000 Zagreb, Croatia

<sup>2</sup> Faculty of Food Technology and Biotechnology, University of Zagreb, Pierottijeva 6, HR-10000 Zagreb, Croatia

<sup>3</sup> Fritz-Haber-Institut der Max-Planck-Gesellschaft, Faradayweg 4-6, 14195 Berlin, Germany

Titanate nanotubes have wide field of applications; as catalyst supports, for photo catalysis, as gas sensors, high efficiency solar cells, etc. Titanate nanotubes are particularly interesting due to its large surface area. We studied modified titanate nanotubes with application as catalysts carrier. With the aim to study their stability during further processing and during final catalytic reactions. We also investigate temperature region in which the structure of modifier and nanotubes will be unchanged.

Titanate nanotubes (TiNT-H) were synthesized by hydrothermal method. Chemical modification of TiNT-H was performed through the reaction of surface -OH groups with (3-aminopropyl) triethoxy silane (APTES) (Fig. 1a). The structure and morphology of modified nanotubes were studied by Raman spectroscopy (RS) and high resolution transmission electron microscopy (HRTEM). High temperature behavior was examined by thermal gravimetric analysis and differential scanning calorimetry (TGA-DSC), while structural changes *in situ* at high temperature were studied by RS.

During *in situ* Raman spectroscopy of modified nanotubes we observed that hydrogen titanate crystal structure were stable up to 400 °C, which is much higher than the phase transition temperature of 175 °C for pure TiNT-H [1]. We conclude that organic part which is built-in on the surface of TiNT nanotubes contribute to higher temperature stability of titanate nanotubes (Fig. 1b), while the organic part starts to decompose at temperatures higher than 150 °C (Fig. 1c).

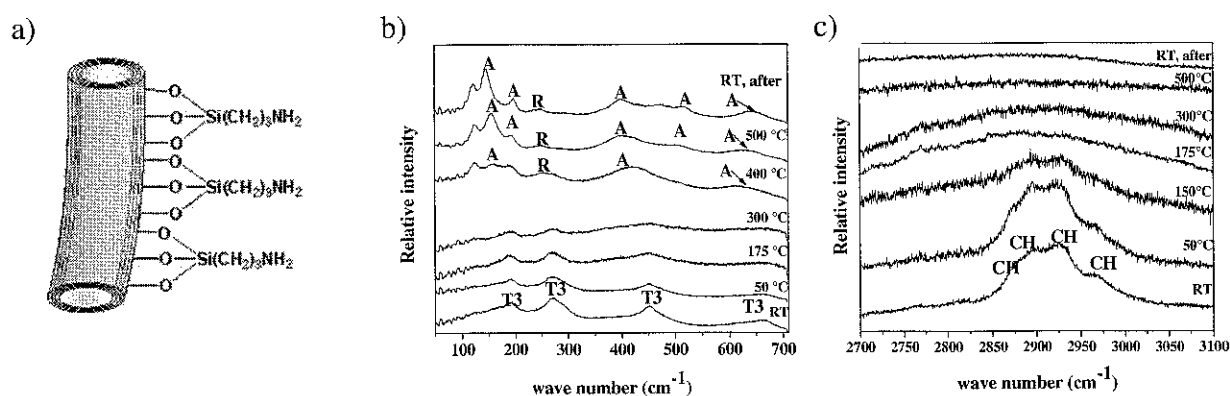


Figure 1: Modified nanotubes schematic view (a), high temperature RS, inorganic part (b), organic part (c).

[1] A. Gajović, I. Friščić, M. Plodinec, D. Iveković, J. Mol. Struct. 183 (2009) 924-926

## FT-IR and MAS-NMR spectra of $\text{SiC}_x\text{O}_y$ glass materials

M. Handke, M. Sitarz, E. Długoń

*AGH University of Science and Technology; Faculty of Materials Science and Ceramics; Al. Mickiewicza 30, 30-059, Kraków, Poland*

Polysiloxane and/or polysilsesquioxane polymers pyrolysis is very promising method for advanced ceramics processing. Xerogels obtained by polycondensation of siloxane contain methyl groups bonded to silicon atoms are precursors for such method. The ratio of Si-O and Si-C bonds depends on the type of xerogels. In the presented work the xerogel materials of ladder-like structure were chosen. Pyrolysis carried out for several hours in argone (absolutely free from oxygen) at  $600^\circ\text{C}$ . The glassy  $\text{SiC}_x\text{O}_y$  ceramics (black glass) with intrinsic homogeneity on the atomic level was obtained.

Measured IR spectra of these black glass sample remind the spectrum of silica glass. The three main bands at about  $1100$ ,  $800$  and  $450\text{ cm}^{-1}$  due to Si-O vibration are complex and relatively broad, but their numeric deconvolution allowed for acquisition of important information on the structure of glassy materials. Some dissimilarities can be found on their careful comparison with the spectra of silica glass typically obtained at high temperature from liquid phase. It means that the "short range" structures of these silica glasses are not alike. The most significant difference in IR spectra of samples pyrolysed in argon can be observed in the range  $850 - 550\text{ cm}^{-1}$  these bands can be associated with OSiC bonds vibrations. These findings were confirmed by NMR measurements. The strong band at chemical shift around  $-65.0\text{ ppm}$  is due to T ( $\text{CSiO}_3$ ) units and less intense peaks around  $-25\text{ ppm}$  and  $-102\text{ ppm}$  indicate the presence of the D ( $\text{C}_2\text{SiO}_2$ ) and Q ( $\text{SiO}_4$ ) units, respectively. These results indicate development of  $\text{SiC}_x\text{O}_y$  homogenous glass material.



## Spherical vibrational modes of amorphous and crystalline $\text{ZrO}_2\text{-CuO}$ nanoparticles

L. Mikac<sup>1</sup>, M. Ivanda<sup>1</sup>, G. Štefanić<sup>2</sup>, S. Musić<sup>2</sup>, K. Furić<sup>1</sup>

<sup>1</sup>Division of Materials Physics, Rudjer Boskovic Institute, Bijenicka 54, 10000 Zagreb, Croatia

<sup>2</sup>Division of Materials Chemistry, Rudjer Boskovic Institute, Bijenicka 54, 10000 Zagreb, Croatia

The spherical vibrational modes of nanosized amorphous and crystalline  $\text{ZrO}_2\text{-CuO}$  (ZC) particles were analyzed by low frequency Raman spectroscopy. The amorphous precursors of the ZC system at the  $\text{ZrO}_2$ -rich side of the concentration range were prepared by co-precipitation from aqueous solutions of the corresponding salts [1]. Thermal behavior of the amorphous precursors was monitored using Raman spectroscopy, field emission scanning electron microscopy (FE-SEM) and transmission electron microscopy (TEM) measurements.

The symmetric ( $l=0$ ) spherical vibrational mode of amorphous and crystalline ZC nanoparticles were observed. On the basis of recently developed approach [2], the size distributions of the ZC nanoparticles were determined and compared with FE-SEM and TEM measurements. It has been found that longitudinal sound velocity in amorphous nanoparticles does not differ from those in crystalline nanoparticles. The intensity of the low frequency Raman scattering peak normalized to the optical vibrational modes showed to be a good indicator for determination of a degree of sintering of the nanosized powder particles.

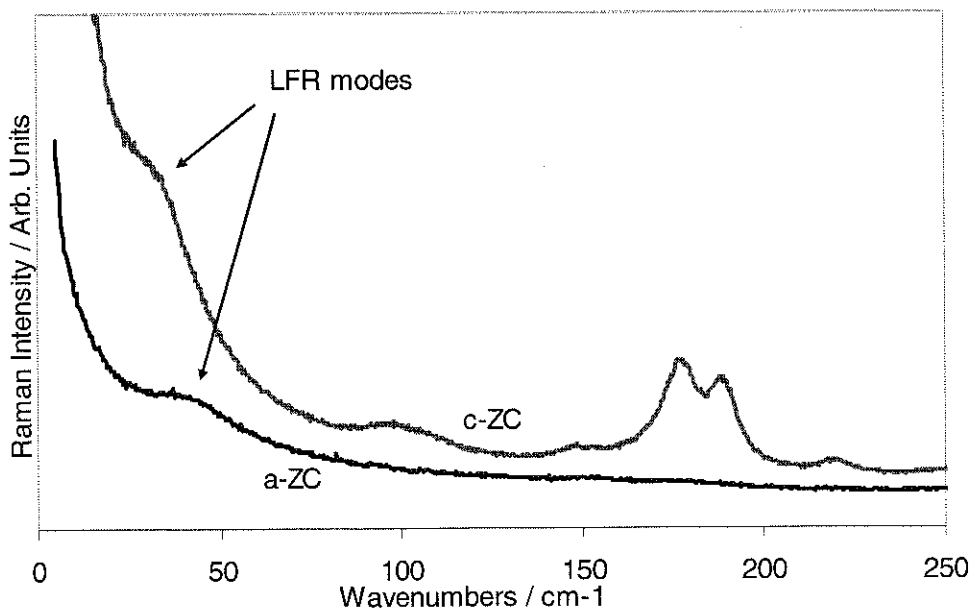


Figure 1. Raman spectra of amorphous (a-ZC) and crystalline (c-ZC) samples. Low frequency modes are marked with arrows.

[1] G. Štefanić, S. Musić, M. Ivanda, *Journal of Alloys and Compounds* 491 (2010) 536-544.

[2] M. Ivanda, K. Furić, S. Musić, M. Ristić, M. Gotić, D. Ristić, A. Tonejc, I. Djerdj, M. Mattarelli, M. Montagna, F. Rossi, M. Ferrari, A. Chiasera, Y. Jestin, G. C. Righini, W. Kiefer, R. R. Gonçalves, *Journal of Raman Spectroscopy* 38 (2007) 647-659

## Porous silicon prepared by electrochemical etching of silicon epitaxial layer

M. Ivanda<sup>1</sup>, M. Balarin<sup>2</sup>, O. Gamulin<sup>2</sup>, V. Đerek<sup>1</sup>, D. Ristić<sup>1</sup>, S. Musić<sup>1</sup>, M. Ristić<sup>1</sup>, and K. Furić<sup>1</sup>

<sup>1</sup>Division of Materials Physics, Rudjer Boskovic Institute, Bijenicka 54, 10000 Zagreb, Croatia

<sup>2</sup>Department of Physics and Biophysics, University of Zagreb, Medical School, Šalata 3b, 10 000, Zagreb, Croatia

Porous silicon (PS) samples were prepared by electrochemical etching of p-type (111) silicon epitaxial layer on silicon (111) substrates, by varying the concentration of 48% HF in ethanol solution and by varying the etching time. Electrical resistivity of epitaxial layer was  $\sim 2 \Omega \text{ cm}$  and of silicon substrate was  $\sim 0.015 \Omega \text{ cm}$ . Within the epitaxial layer and on the substrate surface the micro- and nano-pores of different sizes in dependence on HF concentration and etching time were obtained. The structural and optical properties of prepared samples were investigated by Raman spectroscopy, photoluminescence and field emission scanning electron microscopy (FE-SEM). The photoluminescence peak shows blue shift with the decrease of size of the basic silicon structural unit. The FE-SEM images showed high density of micrometer sized pores on the epitaxial layers separated by the fine nanometer sized cobweb-like silicon structures whose morphology and density depend on the HF concentration and etching time. The Raman spectra of such structures show transversal optical (TO) phonon bands that broaden and red-shift depending on the size of silicon nanostructures. The size distributions of the silicon basic structural units were determined by applying the phonon confinement model and were compared with those determined by FE-SEM.

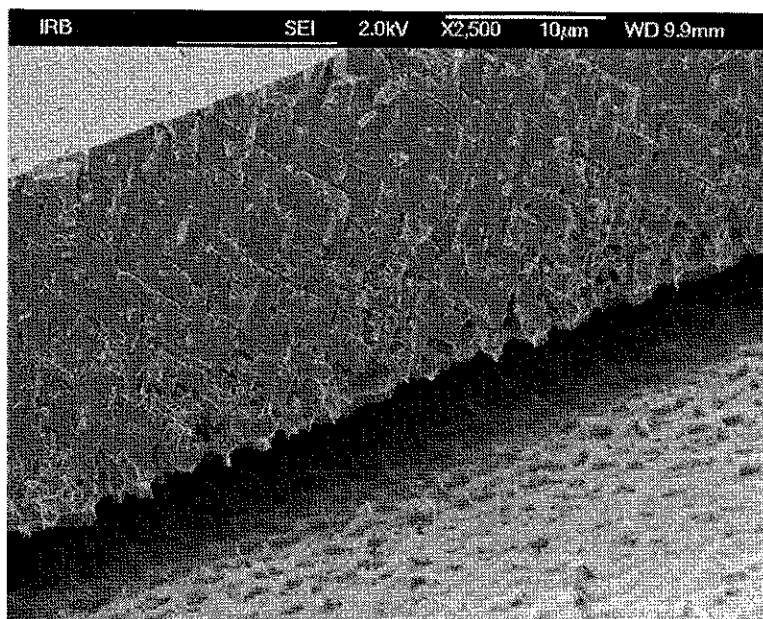


Figure 1. The FE-SEM image of porous epitaxial layer of silicon produced by electrochemical etching in 25% of 48% HF in 96% ethanol solution.

## Spectroscopic studies of Mo-Cu-Pb-P<sub>2</sub>O<sub>5</sub> glass system

D. A. Magdas<sup>1</sup>, N. Vedeanu<sup>2</sup>, O. Cozar<sup>3</sup>

<sup>1</sup>National Institute for Research and Development of Isotopic and Molecular Technologies, Donath, 71-103, P.O. 700, RO-400293, Cluj-Napoca, Romania

<sup>2</sup>Iuliu Hatieganu University of Medicine and Pharmacy, Department of Physics-Biophysics, RO- 400023, Cluj-Napoca, Romania

<sup>3</sup>Faculty of Physics, Babes-Bolyai University, 400084 Cluj-Napoca, Romania

In order to evidence the structural changes induced by CuO and MoO<sub>3</sub> in the phosphate glass network and their modifier or former role, x (CuO·MoO<sub>3</sub>)(1-x)[2P<sub>2</sub>O<sub>5</sub>·PbO] glass system was prepared and investigated using Raman and EPR spectroscopies.

Raman spectra present the specific bands of phosphate glasses at low concentration of modifier oxides meanwhile at higher concentration a strong depolymerization of the phosphate network appears. The addition of copper oxide leads to more P=O bond breakage and the formation of the P-O-Cu bonds. We concluded that at high content of CuO it acts in the structure of glasses as a network former. Similar trend was observed in iron-lead-phosphate glasses with addition of iron oxide [1,2]. The presence of the Cu-O-P and Fe-O-P bonds for higher content of modifier oxide in these glass systems is consistent with the improving of their chemical durability.

The shape of EPR spectra is also changed with the increase of modifier oxides content, this consist in a progressive disappearance of the hyperfine structure. This fact may be explained by the superposition of two EPR signals, one with a well resolved hyperfine structure and the other one consisting in a broad line without hyperfine structure characteristic for clustered ions.

[1] O. Cozar, D. A. Magdas, I. Ardelean, J. Non-Cryst. Solids, 354 (2008) 1032-1035

[2] D.A. Magdas, O. Cozar, V. Chis, I. Ardelean, N. Vedeanu, Vibrational spectroscopy 48 (2008) 251-254



## FTIR spectroscopy analysis of oxidation process of coal tar pitches

D. Mikociak, C. Paluszkiewicz, S. Błażewicz

*AGH University of Science and Technology, Faculty of Materials Science and Ceramics,  
Al. Mickiewicza 30, 30-059 Krakow, POLAND*

Composite materials with polymer matrix have gained wide applications in civil engineering. Particular family of composites constitute carbon fibre reinforced carbon matrix. This type of composite is becoming more and more prevalent in modern structural materials. Their evolution is particularly depended on development of new and improved precursor components of matrices having better mechanical property and low technological cost. In processing of carbon composites coal tar pitch- based precursors and their derivatives including mesophase pitches are being used. Pitches are cheaper than polymer materials, moreover they retain high carbon residue after carbonisation process. Pitches subjected to thermal treatment may develop different structures, from glass-like carbon to fully graphitizing mesophase structures depending upon the initial pitch properties and its source of origin.

This paper discusses results of an experimental study of oxidation process of coal tar pitch. Carbon pitches with Melting Point ( $T_{Mett}$ ) ranging between 80-300°C were subjected to analysis. Five days lasting oxidation process in temperature of 200°C was conducted for all samples. An oxidative treatment of pitch is the first step in carbon composite technology and has strong influence on the mechanical properties of carbon composites obtained from pitch matrix. The optimal time and stabilization temperature for pitch samples were determined. The samples after different oxidative treatments were verified using FTIR spectroscopy in the range from 4000 to 400  $\text{cm}^{-1}$  using KBr technique of FTS-60 V Bio Rad. Following gradual oxidization of analyzed samples, an increase of band intensity in the range of 1600-1800 $\text{cm}^{-1}$ , corresponding to creation of formation C=O was observed. An observed 'degradation' of intensity of C-H group bands is being noticed in the range of 2800-3200 $\text{cm}^{-1}$ . The fastest oxidization occurred for pitch characterized with the highest Melting Point.

**Acknowledgements:** This work was supported by The Ministry of Science and Education, project No N N507 466637





## Synthesis and characterization of the novel heteropolyoxotungstates based on $[\text{BiW}_9\text{O}_{33}]^{9-}$ units

D. Rusu,<sup>1</sup> A. R. Tomsa,<sup>2</sup> M. H. Dickman,<sup>3</sup> U. Kortz,<sup>3</sup> O. Baban,<sup>4</sup> M. Rusu<sup>4</sup>

<sup>1</sup> Medicine and Pharmacy Iuliu Hatieganu University, Faculty of Pharmacy, 400023 Cluj-Napoca, Romania.

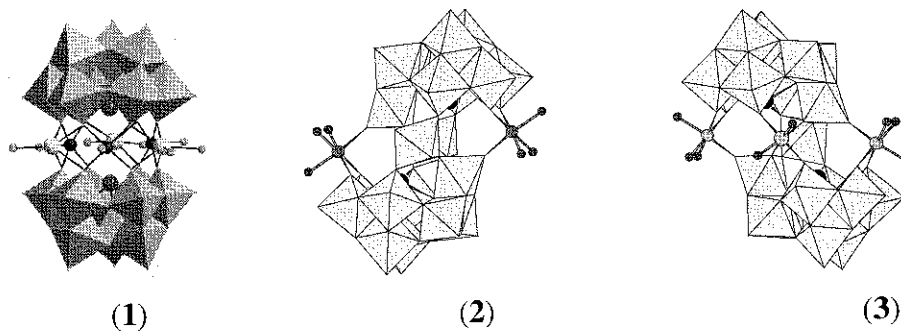
<sup>2</sup> Raluca Ripan Institute for Research in Chemistry 30, Fantanele St., RO-400294 Cluj-Napoca, Romania

<sup>3</sup> Jacobs University, School of Engineering and Science, 28725 Bremen, Germany.

<sup>4</sup> Babes-Bolyai University, Faculty of Chemistry and Chemical Engineering, 400028 Cluj-Napoca, Romania.

Lacunary polyoxometalates exhibit an increased reactivity towards transition metal ions, thus forming a broad variety of substituted polyoxometalates in which the polyoxoanion framework remain unchanged or may rearrange in the course of the reaction with transition metal cations. Trivacant polyoxometalates  $\alpha\text{-B-}[\text{BiW}_9\text{O}_{33}]^{9-}$  are suitable building blocks for the synthesis of sandwich-type complexes  $[\text{M}_3^{n+}(\text{H}_2\text{O})_x(\text{BiW}_9\text{O}_{33})_2]^{(12-3n)-}$  on the one hand and the transition metal substituted complexes  $[(\text{M}^{n+}(\text{H}_2\text{O})_3)_2(\text{WO}_2)_2(\text{BiW}_9\text{O}_{33})_2]^{(14-2n)-}$  on the other hand. These complexes have been obtained by straightforward routes from lacunary polyoxotungstates [1].

Three novel heteropolytungstates,  $[\text{Cu}_3^{2+}(\text{H}_2\text{O})_3(\text{BiW}_9\text{O}_{33})_2]^{12-}$  (1),  $[(\text{Mn}^{2+}(\text{H}_2\text{O})_3)_2(\text{WO}_2)_2(\text{BiW}_9\text{O}_{33})_2]^{10-}$  (2) and  $[\text{Co}_3(\text{H}_2\text{O})_8(\text{WO}_2)(\text{BiW}_9\text{O}_{33})_2]^{10-}$  (3) have been synthesized by same method from precursor  $[\text{BiW}_9\text{O}_{33}]^{9-}$  and transition metal cations in hot slightly acidic aqueous solution. These polyoxoanions were characterized by elemental and thermogravimetric analysis, FT-IR, UV, Vis, EPR spectroscopies, X-ray Diffraction and cyclic voltammetry. This allowed for determining subsequently the behavior of the encapsulated transition metal ions, their coordination by the tungstobismutate(III) fragments, the corresponding local symmetry and the type of metal-metal interactions. Polyoxoanion (1) (see Figure), consist from two  $\alpha\text{-B-}[\text{BiW}_9\text{O}_{33}]^{9-}$  units, which are linked by an equatorial belt of three  $\text{Cu}(\text{H}_2\text{O})^{2+}$  units. Three  $\text{Na}(\text{H}_2\text{O})_2^+$  units are also attached in the equatorial plane. The bond geometry is square-pyramidal against each Cu atom and trigonal-prismatic against each Na atom.



Polyoxoanions (2) and (3) are isostructural similarly and consist from two  $\beta\text{-B-}[\text{BiW}_9\text{O}_{33}]^{9-}$  framework which are linked by an equatorial belt of two  $\text{Mn}(\text{H}_2\text{O})_3^{2+}$  unit and two  $\text{WO}_2$  groups for (2) and from two  $\beta\text{-B-}[\text{BiW}_9\text{O}_{33}]^{9-}$  framework which are linked by an equatorial belt of two  $\text{Co}(\text{H}_2\text{O})_3^{2+}$ , one  $\text{Co}(\text{H}_2\text{O})_2^{2+}$  and one  $\text{WO}_2$  units for (3). The bond geometry is octahedral against each Mn and Co atoms.

[1] Xue, G.; Vaisserman, J.; Gouzerh, P. *J. Cluster Science*, 2002, 13, 409-421.



## Covalently grafted, silica gel supported mixed amino acid iron complexes – syntheses, structural characterization and catalytic testing

Z. Csendes<sup>1</sup>, N. Földi<sup>1</sup>, N. Varga<sup>1</sup>, J.T. Kiss<sup>1</sup>, I. Labádi<sup>2</sup>, I. Pálinkó<sup>1\*</sup>

<sup>1</sup>Department of Organic Chemistry, University of Szeged, Dóm tér 8, Szeged, H-6720 Hungary

<sup>2</sup>Department of Inorganic and Analytical Chemistry, University of Szeged, Dóm tér 7, Szeged, H-6720 Hungary

In order to satisfy the need for novel highly active, and, even more importantly, highly selective catalysts various strategies may be followed. One promising way may be to mimic the active sites of enzymes [1]. To ease the work-up procedure, facilitating the recovery as well as increasing the ruggedness of the catalyst, immobilizing these active site mimics seems to be advantageous. In this contribution we describe such a biomimetic approach: our work concerns the covalent anchoring of Fe(III)-mixed C-protected amino acid complexes prepared in various ways onto a modified silica gel support. Previously, we applied for anchoring of various copper-amino acid complexes onto silica gel [2] and montmorillonite [2-4] hydrogen bonding and ionic interactions, respectively. Although immobilization was successful, we hoped for a better control of synthesis using covalent grafting. Our initial results with Fe(III)-single amino-acid complexes and chloropropylated silica gel were encouraging [5].

The components of the anchored complexes [methylesters of L-histidine (chis), L-cysteine (ccys), L-cystine (ccysccys)], FeCl<sub>3</sub>, chloropropylated silica gel (SG) and the isopropanol solvent were commercial products. Covalent grafting was performed at the N-terminal of the amino acid (N-alkylation-like transformation) with the chlorine of the chloropropylated SG followed by complexation. Two C-protected amino acid pairs were used as ligands: chis-ccys and ccys-ccysccys. The synthesis of the immobilized materials was done in three ways: (A): the first amino acid from the respected pairs was anchored followed by complexation, then the second amino acid was added in excess, (B): the same as (A) but now the second amino acid was anchored, (C): a 1:1 mixture of the amino acid was anchored and complexes were prepared applying either ligand-poor conditions (only the immobilized protected amino acids were available for coordination) or circumstances abundant in non-anchored protected amino acid molecules. Structural information on each step of the synthesis procedure was obtained by mid-range infrared spectroscopy, measuring diffuse reflectance (4000–400 cm<sup>-1</sup> wavenumber range, BIO-RAD Digilab Division FTS-65 A/896 FT-IR spectrophotometer, 2 cm<sup>-1</sup> resolution, 126 scans, Win-IR package).

It was found that covalent anchoring was successful applying either method. The structure of the obtained immobilized materials proved to be different. Coordinating groups could be determined through the analysis of the IR spectra. The materials were found to be active in a superoxide dismutase test reaction. Some of them displayed remarkable catalytic performance making them promising electron transfer catalysts.

- [1] A.J. Kirby, *Angew. Chem. Int. Ed. Engl.* 35 (1996) 706-724
- [2] I. N. Jakab, K. Hernadi D. Méhn, T. Kollár, I. Pálinkó, *J. Mol. Struct.* 651-653 (2003) 109-114
- [3] K. Hernadi, I. Pálinkó, E. Böngyik, I. Kiricsi, *Stud. Surf. Sci. Catal.* 135, 366; CD-ROM edition 27P10 (2001)
- [4] I. Szilágyi, I. Labádi, K. Hernadi, T. Kiss, I. Pálinkó, *Stud. Surf. Sci. Catal.* 158 (2005) 1011-1018
- [5] Z. Csendes, V. Bugris, P. Sebök, Zs. Major, J.T. Kiss, I. Pálinkó, *Insights into Coordination, Bioinorganic and Applied Inorganic Chemistry* (M. Melník, P. Segl'a, M. Tatarko, eds.), ISBN 978-80-227-3085-3, Press of Slovak University of Technology, Bratislava, 2009, pp. 54-61



## Optical properties of porous silicon on an insulator layer

M. Balarin<sup>1</sup>, O. Gamulin<sup>1</sup>, M. Ivanda<sup>2</sup>, M. Kosović<sup>1</sup>, D. Ristić<sup>2</sup>, M. Ristić<sup>2</sup>, S. Musić<sup>2</sup>, K. Furić<sup>2</sup>

<sup>1</sup>University of Zagreb, School of Medicine, Dpt of Physics and Biophysics, Šalata 3, 10000 Zagreb, Croatia

<sup>2</sup>Division of Materials Physics, Rudjer Bosković Institute, Bijenička 54, 10000 Zagreb, Croatia

Silicon wafers, consisting of 280  $\mu\text{m}$  thick n-type (Sb doped) upper layer and 20  $\mu\text{m}$  n-type (P doped) lower layer, were electrochemically etched in hydrofluoric acid (HF) ethanol solution. The resistivity of upper layer was 0.015  $\Omega\text{cm}$ , while the lower layer was much worse conductor with resistivity 2  $\Omega\text{cm}$ . Porous silicon (PS) samples were produced by etching the non polished side of wafers at the constant current density. The etching process was performed with different concentration of HF in ethanol solution. It was found that such n-type silicon on insulator can be selectively etched without illumination. The possible mechanism of the etching phenomenon is discussed.

Samples were investigated by Raman spectroscopy, photoluminescence (PL) and scanning electron microscopy (SEM). The most intensive photoluminescence peak showed samples which were etched with the lowest HF concentration. The Raman spectra of all samples showed broadened and red-shifted transversal optical (TO) phonon bands. SEM images showed high density of less than 100 nm sized pores whose density and morphology depended on HF concentration. The etching of the unpolished side of wafers caused interesting topography, presented in electron micrograph Fig. 1 b), and inhomogeneous luminescence presented in Fig. 1 a). Figure 1 c) shows the high magnification FE-SEM micrograph of strong luminescence region with nanometers pores in silicon.

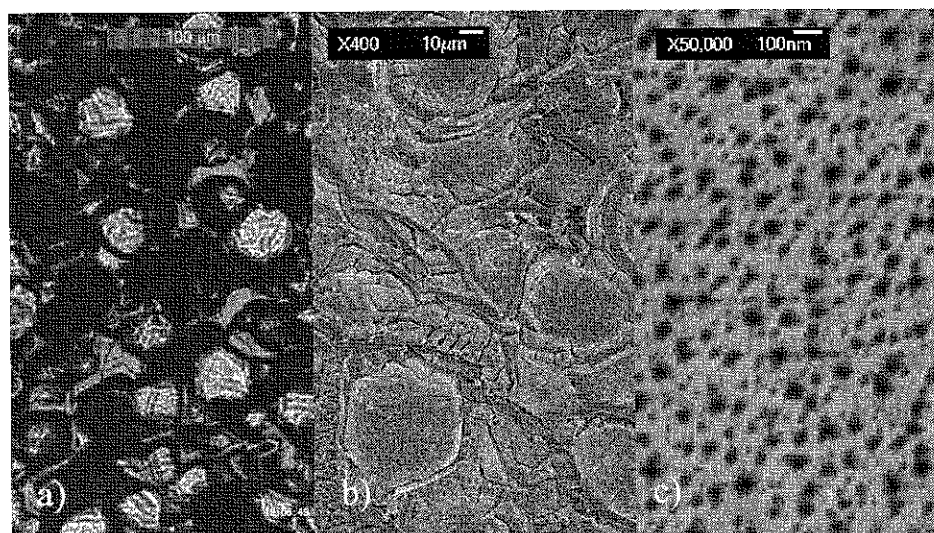


Figure 1. Inhomogeneous luminescence at the PS surface (a), topography of the PS surface (b) and high magnification FE-SEM micrograph of strong photoluminescence region (c)

## The crystal and molecular structure of new hybrid material: 2-amino-4-methyl-3-nitropyridinium hydrogen oxalate

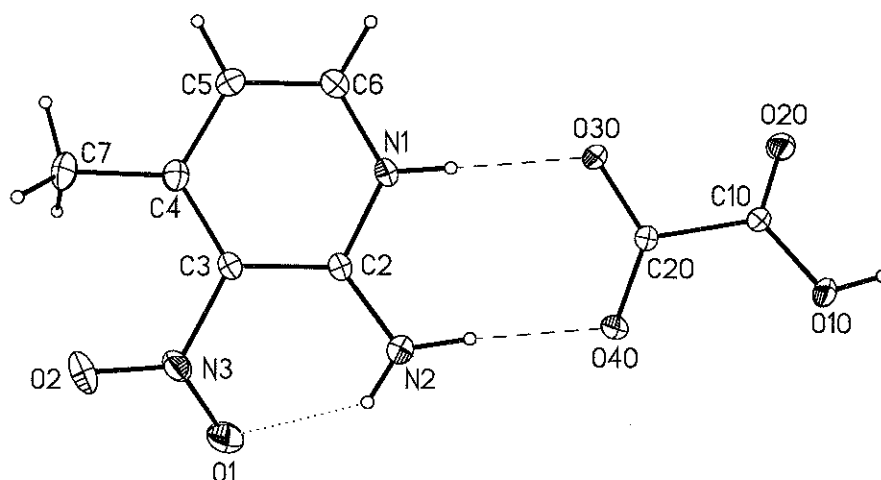
I. Bryndal<sup>1</sup>, E. Kucharska<sup>1</sup>, K. Hermanowicz<sup>2</sup>, M. Maczka<sup>2</sup>, M. Wandas<sup>1</sup>, J. Hanuza<sup>1,2</sup>

<sup>1</sup>Department of Bioorganic Chemistry, Institute of Chemistry and Food Technology, Faculty of Engineering and Economy, University of Economic, Komandorska 118/120, 53-345 Wrocław, Poland

<sup>2</sup>Institute of Low Temperature and Structure Research, Polish Academy of Sciences, Okólna 2, 50-422 Wrocław, Poland

New organic-organic salt, 2-amino-4-methyl-3-nitropyridinium hydrogen oxalate, and its deuterium discharge form have been synthesised and characterised by means of FT-IR, FT-Raman, DSC and single crystal X-ray crystallography. The temperature dependence of the IR and Raman spectra has been studied in the range 4-295 K. The 2-amino-4-methyl-3-nitropyridinium hydrogen oxalate belongs to a big family of organic-organic hybrid salts that have attracted considerable attention in the last years. These are novel materials possessing interesting optical properties [1-4].

The structure determination revealed that 2-amino-4-methyl-3-nitropyridinium hydrogen oxalate crystallizes in noncentrosymmetric space group  $P2_1$ . The crystal structure is built of the 2-amino-4-methyl-3-nitropyridinium cations and oxalate monoanions. The crystal structure displays a hydrogen-bonded network structure involving primarily  $-NH$  and  $-OH$  moieties as donors and carboxylate O-atom as acceptors. The 6-311G(2d,2p) and 6-31G(d,p) basis set with B3LYP functional have been used to discuss the structure and dynamics of the compound studied. The wavenumbers of characteristic bands of the HB in the studied salt have been calculated in quantum chemical DFT procedure and compared with the experimental data. The normal modes of the  $NH$ ,  $NH_2$ ,  $OH$ ,  $CO$ ,  $CH_3$  and  $NO_2$  groups and pyridine ring assigned with the use of PED contributions.



- [1] G. R. Desiraju, *Crystal Engineering: The Design of Organic Solids*, vol. 54, New York, Amsterdam 1989, Elsevier.  
 [2] J. M. Lehn, *Angew. Chem., Int. Ed. Engl.*, 29 (1990) 1304-1319.  
 [3] J. C. MacDonald and G. M. Whitesides, *Chem. Rev.* 94 (1994) 2383-2420.  
 [4] C.B. Aakeröy, *Acta Crystallogr.*, B 53 (1997) 569-586.



## Surface characterisation of thin silicon rich oxide thin films

D. Ristić<sup>1,2</sup>, V. Holy<sup>3</sup>, M. Ivanda<sup>2</sup>, M. Marciuš<sup>2</sup>, M. Buljan<sup>2</sup>, O. Gamulin<sup>4</sup>, K. Furić<sup>2</sup>, M. Ristić<sup>2</sup>, S. Music<sup>2</sup>, M. Mazzola<sup>1</sup>, A. Chiasera<sup>1</sup>, M. Ferrari<sup>1</sup>, G.C. Righini<sup>5</sup>

<sup>1</sup>*CSMFO Lab, Istituto di fotonica e nanotecnologie (IFN-CRN), Via alla Cascata 56/C, Povo, 38123 Trento, Italy*

<sup>2</sup>*Division of Materials Physics, Rudjer Boskovic Institute, Bijenicka 54, 10000 Zagreb, Croatia*

<sup>3</sup>*Department of Condensed Matter Physics, Faculty of Mathematics and Physics, Charles University in Prague, Ke Karlovu 5, 121 16 Praha, Czech Republic.*

<sup>4</sup>*Medical School, Dept. Physics and Biophysics, University of Zagreb, Šalata 3b, 10000, Zagreb, Croatia*  
<sup>5</sup>*MDF Lab, "Nello Carrara" Institute of Applied Physics (IFAC-CNR), Via Madonna del Piano 10, 50019 Sesto Fiorentino, Firenze, Italy*

The silicon rich oxide (SiO<sub>x</sub>) films were deposited using the LPCVD (Low Pressure Chemical Vapour Deposition) method by thermal oxidation of silan in an oxygen atmosphere at the temperature of 570°C. The films were deposited on silicon (111) substrates. The flows of oxygen and silan in the horizontal tube reactor were varied in order to deposit films with different values of oxygen content  $x$ . The deposition temperature of 570°C was chosen in order to obtain highly homogeneous thin films. The roughness of the film surfaces and of the substrate-film interfaces were determined by X-Ray specular reflection. The films were found to have a very homogeneous surface. Scanning electron microscopy was used to study the surface morphology of the thin films. Infrared absorption measurements of the thin films were made, and they showed the absence of the broad band at 1260 cm<sup>-1</sup> in the infrared spectra, which is an indication of low surface roughness. Raman spectroscopy was used to determine the structure of the deposited films. The measured Raman spectra showed broad bands typical of the Raman spectra of amorphous materials.



## Varying the microstructural properties of ZnO particles using different synthesis routes

A. Šarić, S. Musić, M. Ivanda

*Ruder Bošković Institute, P. O. Box 180, HR-10002 Zagreb, Croatia*

Zinc oxide (ZnO) is an important technological material due to its excellent chemical, electrical and optical properties. It can be applied in the production of paints, rubbers, cosmetics, catalysts, gas sensors, varistors, LEDs, acoustic wave devices, etc. In all cases the particle morphology and size are important parameters for specific applications of ZnO.

In the present work ZnO particles were precipitated at 90 °C by hydrolysis of zinc acetylacetonate ( $\text{Zn}(\text{acac})_2$ ) in water at pH~9 to pH~5. Hydrolyses were also performed for different ratios of  $\text{Zn}(\text{acac})_2$  : Na-citrate. In dependence on the precipitation conditions different shapes and sizes of ZnO particles were obtained. The correlation between these ZnO particles and their FT-IR and Raman spectra were investigated. In the presence of Na-citrate, a plate-like precursor was obtained and spectroscopy showed a coordinated citrate group at the surface of the particles. Upon heating of this precursor at 300 °C, nanosize and monodisperse ZnO particles were produced.

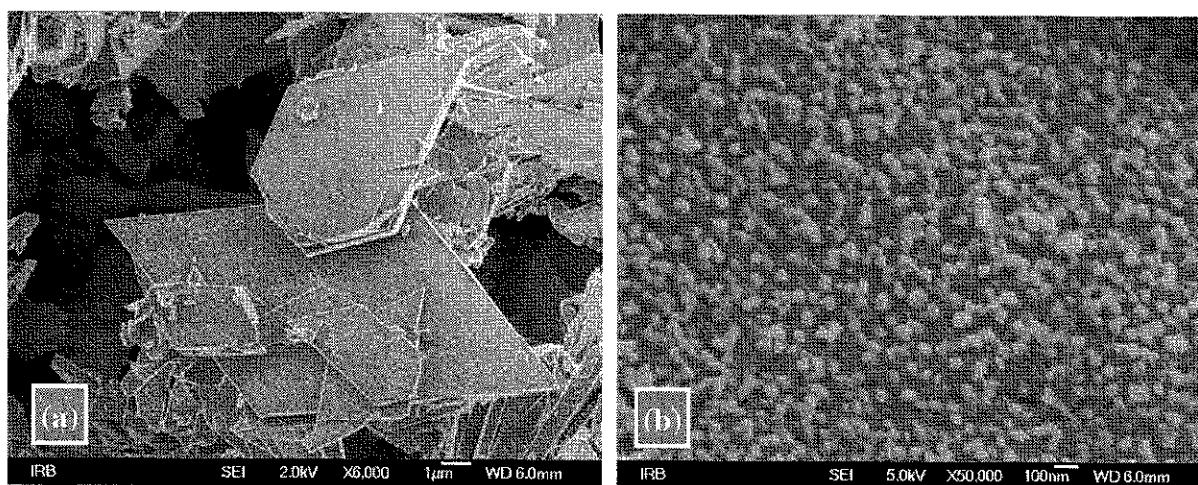


Fig. 1. FE SEM images of (a) the precursor obtained in the presence of sodium citrate and (b) nanosize ZnO particles produced upon heating at 300 °C.

## Lattice dynamics and high-pressure Raman scattering studies of cation-deficient Aurivillius compounds

M. Maczka<sup>1</sup>, M. Ptak<sup>1</sup>, W. Paraguassu<sup>2</sup>, P. T. C. Freire<sup>3</sup>, A. G. Souza Filho<sup>3</sup>, J. Mendes Filho<sup>3</sup>, J. Hanuza<sup>4</sup>

<sup>1</sup>Institute of Low Temperature and Structure Research, Polish Academy of Sciences, P.O. Box 1410, 50-950 Wrocław 2, Poland

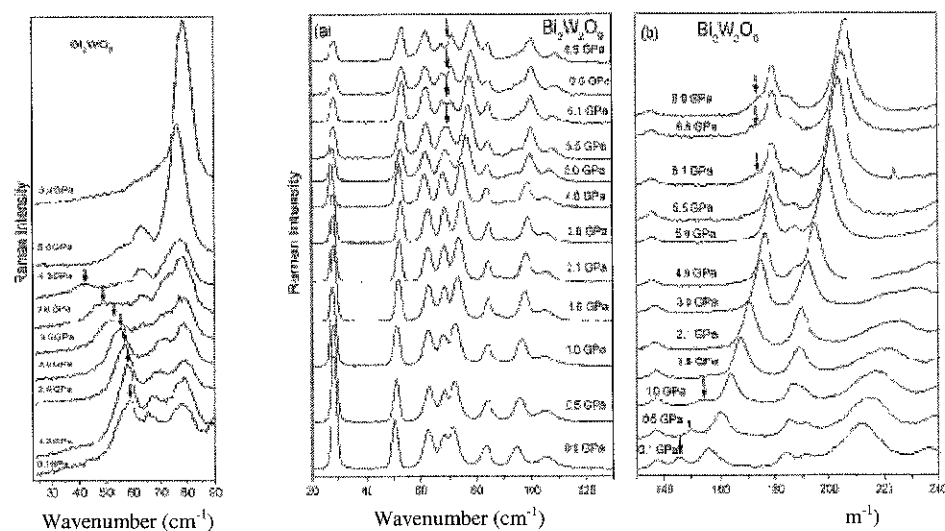
<sup>2</sup>Departamento de Física, Universidade Federal do Maranhão, São Luis-MA, 65085-580, Brazil

<sup>3</sup>Departamento de Física, Universidade Federal do Ceará, P.O. Box 6030, Fortaleza-CE, 60455-970, Brazil

<sup>4</sup>Department of Bioorganic Chemistry, University of Economics, 53-345 Wrocław, Poland

Bismuth layered compounds (Aurivillius family) of general formula  $(\text{Bi}_2\text{O}_2)(\text{A}_{m-1}\text{B}_m\text{O}_{3m+1})$  have received much attention since these materials are candidates for the development of ferroelectric random access memories [1]. Recently,  $\text{Bi}_2\text{WO}_6$  and  $\text{Bi}_2\text{MoO}_6$  have been found to be excellent photocatalytic materials whereas  $\text{Bi}_2\text{W}_2\text{O}_9$  has been found to be a promising candidate for microwave applications [2-4].

Although this family of compounds is very large, up to now only three cation-deficient phases, i.e. phases that have no voluminous A cation, have been identified. These are  $\text{Bi}_2\text{WO}_6$ ,  $\text{Bi}_2\text{MoO}_6$  and  $\text{Bi}_2\text{W}_2\text{O}_9$ . In the present presentation we will discuss results of lattice dynamics calculations in order to assign the modes to respective motions of atoms. We will show using high-pressure Raman scattering that these crystals undergo second-order pressure-induced phase transitions. Our results give strong evidence that the first phase transition observed in these crystals involves the loss of the  $\text{WO}_6$  or  $\text{MoO}_6$  tilt mode. The second transition is related to shifts of the W(Mo) and Bi atoms. Our results also show that symmetry increases upon application of pressure for  $\text{Bi}_2\text{WO}_6$  and  $\text{Bi}_2\text{MoO}_6$  but decreases for  $\text{Bi}_2\text{W}_2\text{O}_9$ . We also show that in contrast to  $\text{Bi}_2\text{WO}_6$  and  $\text{Bi}_2\text{MoO}_6$ , no soft mode behaviour is observed for  $\text{Bi}_2\text{W}_2\text{O}_9$ .



- [1] Y. Noguchi, K. Murata, M. Miyayama, *Appl. Phys. Lett.* 89 (2006) 242916  
 [2] L. Zhang, W. Wang, L. Zhou, H. Xu, *Small* 3 (2007) 1618-1625  
 [3] M.C. Long, W.M. Cai, H. Kisch, *Chem. Phys. Lett.* 461 (2008) 102-105  
 [4] A. Feteira, D.C. Sinclair, *J. Am. Ceram. Soc.* 91 (2008) 1338-1341



## Vibrational properties of hexagonal bronze systems: high pressure and polarized Raman spectra

W. Paraguassu,<sup>1\*</sup> M. Maczka,<sup>2</sup> K. Pereira da Silva,<sup>1</sup> A. G. Souza-Filho,<sup>3</sup> P. T. C. Freire,<sup>3</sup> J. Mendes Filho,<sup>3</sup> and J. Hanuza<sup>2,4</sup>

<sup>1</sup>Departamento de Física, Universidade Federal do Maranhão, São Luis-MA, 65085-580, Brazil

<sup>2</sup>Institute of Low Temperature and Structure Research, Polish Academy of Sciences, P.O.Box 1410, 50-950 Wrocław 2, Poland

<sup>3</sup>Departamento de Física, Universidade Federal do Ceará, P.O. Box 6030, Fortaleza-CE, 60455-970, Brazil

<sup>4</sup>Department of Bioorganic Chemistry, University of Economics, 53 - 345 Wrocław, Poland

$\text{Cs}_4\text{W}_{11}\text{O}_{35}$  and  $\text{Rb}_4\text{W}_{11}\text{O}_{35}$  belongs to the class of hexagonal bronzes whose structure derives from  $\text{K}_x\text{WO}_3$  superconductor hexatungstate. Charge Imbalanced tungsten bronzes are dielectric materials with rich polymorphism, ferroelectric properties and second harmonic generation. In this work we report polarized Raman spectra results for both system and results of high pressure Raman scattering experiment (0.0 – 11.0 GPa) on  $\text{Cs}_4\text{W}_{11}\text{O}_{35}$  system, for which we have observed two structural phase transitions at about 4 GPa and 7.5 GPa (Figure 1). We discuss these transformations, and polarized Raman spectra, on basis on lattice dynamics calculation in the related system  $\text{KNbW}_2\text{O}_9$  (Figure 2). Polarized Raman spectra provide strong indicative that the highest wavenumber modes observed in these systems originates from tungsten or oxygen vacancies. The observation of a soft like mode indicates that the observed phase transitions present displacive type behavior, what further indicates that these transformations are likely related to reorientations of octahedral units. The soft mode nature is discussed on basis on lattice dynamics calculations.

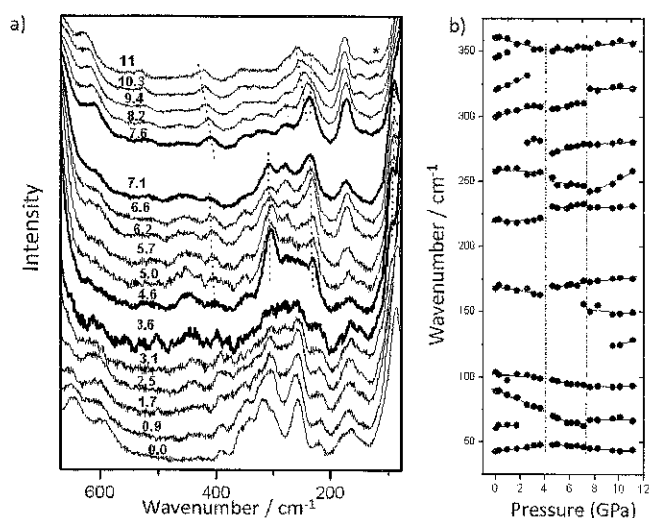


Figure 1

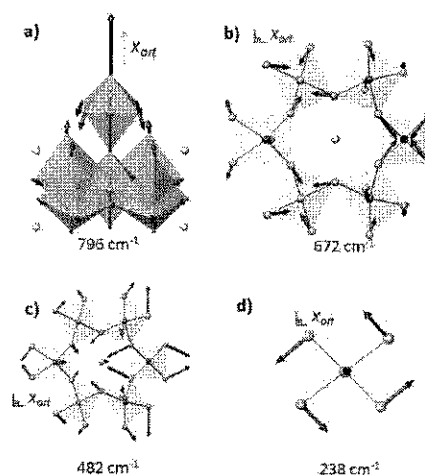


Figure 2



## Reconsideration of the $^{13}\text{C}$ absolute nuclear magnetic shielding scale from NMR measurements of CO/He and CH<sub>4</sub>/He gas phase mixtures

W. Makulski

*Laboratory of NMR Spectroscopy, Faculty of Chemistry, University of Warsaw, Pasteura 1, 02-093 Warszawa, Poland*

The absolute shielding scales are of high significance when experimental NMR results are to be compared with quantum chemical calculations. For obvious reasons carbon-13 scale belongs to the more important scales from organic chemistry and biochemical points of view.

The carbon monoxide is an experimental reference molecule for the carbon-13 absolute nuclear magnetic shielding scale [1]. This is because its spin-rotation constant has for long been known with relatively high accuracy [2]. This value  $\langle C \rangle_{01} = 32.70(12)$  kHz has served for precise calculation of  $^{13}\text{C}$  nuclear magnetic shielding constant in  $^{13}\text{CO}$  isolated molecule and consequently in TMS (tetramethylsilane) liquid sample usually taken as external reference [3].

In this work we measured  $^{13}\text{C}$ ,  $^1\text{H}$  and  $^3\text{He}$  Larmor frequencies in CO/He and CH<sub>4</sub>/He gaseous mixtures by high resolution NMR spectroscopy. A new approach in establishing the dipole magnetic moments from gas phase NMR spectra and calculated shielding constants was utilized in the carbon-13 case [4]. Our method utilizes the free helium magnetic moment as reference. The  $^1\text{H}$ ,  $^{13}\text{C}$  and  $^3\text{He}$  radiofrequencies are strictly linear dependent on densities of gaseous buffers used: Xe, CO<sub>2</sub> and SF<sub>6</sub>. The methane/helium mixtures serve as a source of more accurate than the presently accepted value of  $^{13}\text{C}$  dipole magnetic moment  $\mu(^{13}\text{C}) = 0.70236944(63)\mu_{\text{N}}$ . This new value and chemical shifts/frequencies in carbon monoxide/helium mixtures were utilized to recalculation of  $^{13}\text{C}$  nuclear magnetic shielding for the  $^{13}\text{CO}$  molecule at 300K. The reference absolute shielding constant value  $\sigma(^{13}\text{CO})^{300\text{K}} = 1.67(2)$  ppm is established with a much higher accuracy and differ by  $\sim 1$  ppm from the result used up to now  $\sigma(^{13}\text{C})^{300\text{K}} = 0.6(0.9)$  ppm.

Our experiments demonstrate that a new experimental  $^{13}\text{C}$  shielding scale should be established. It could be done ultimately when new theoretical calculations with new spin-rotation experimental/theoretical values in  $^{13}\text{CO}$  molecule will be made. By employing small amounts of CO<sub>2</sub> as impurity in CO material it was possible to estimate  $\sigma_0(^{13}\text{CO}_2) = 60.31(2)$  ppm in the new absolute shielding scale proposed. The  $^{13}\text{C}$  shielding results for both carbon oxides were compared with the different theoretical values reported in the literature.

[1] W.T.Raynes, Mc Vay, Wright, J.Chem.Soc., Faraday Trans 2, 85 (1989) 759.

[2] W.L.Meerts, F.H. de Leeuw, A.Dymanus, Chem.Phys.22 (1977) 319.

[3] K.Jackowski, M.Wilczek, M.Pecul, J.Sadlej, J.Phys.Chem.A 104 (2000) 5955; J.Phys.Chem.A 104 (2000) 9806 erratum.

[4] M.Jaszuński, K.Jackowski, Lecture Notes in Physics, Springer: Berlin, Vol.745 (2008) p.233.



## FTIR study of PGLA modified with nanoadditives

M. Ziabka<sup>1</sup>, C. Paluszkiwicz<sup>2</sup>, J.Chlopek<sup>1</sup>

<sup>1</sup>AGH University of Science and Technology, Faculty of Materials Science and Ceramics,  
Department of Biomaterials, Mickiewicza 30Av., 30-059Krakow, Poland,

<sup>2</sup>AGH University of Science and Technology, Faculty of Materials Science and Ceramics,  
Department of Silicate Chemistry, Mickiewicza 30Av., 30-059Krakow, Poland,

Poly(lactide-co-glicolide) (PGLA) currently plays an essential role in modern medicine. Due to its very good biological properties such as high biocompatibility, resorbability, lack of inflammatory reaction and no pathological tissue response, PGLA is successfully applied in drug delivery systems, scaffolds for tissue engineering, reconstructive implants and bone fracture fixation devices [1-2]. Silver ions ( $\text{Ag}^+$ ) have been investigated for a long time in the biomedical area because of their bactericidal properties. They readily bind to negatively charged proteins, RNA, DNA, and chloride ions. Currently, silver agent is frequently applied as a viable treatment option for infections encountered in burns, open wounds, and chronic ulcers [3]. Hydroxyapatite is widely used for bone implant and bone cement applications due to its compositional and biological similarities to native tissues [4]. Compounding of hydroxyapatite and silver nanoparticles with polymeric binders can provide improved bioactivity and bactericidal properties.

Copolymer of lactide and glycolide was prepared using  $\text{Zr}(\text{acac})_4$  initiator (Center of Polymer and Carbon Materials, PAN - Zabrze, Poland). Commercially available silver nanopowder (Sigma Aldrich, particle size < 100nm) and nanohydroxyapatite (n-Gimat, particle size < 100nm) were used as modifiers. PGLA and PGLA/Ag, PGLA/HAp and PGLA/HAp/Ag composites with 3wt.% of HAp and 5wt.% of Ag contents were obtained in the form of foils by slip-casting method.

Fourier Transform Infrared Spectroscopy (FTIR) in the attenuated total reflection mode (ATR) was used for spectra measurements (Digilab FTS60v; Excalibur). All samples (pure polymer and composites) were analyzed before and after incubation in immersion solution (ultra high quality  $\text{H}_2\text{O}$ ). Analyses were performed in the range of  $550\text{-}4000\text{cm}^{-1}$  with a  $4\text{cm}^{-1}$  resolution.

Results of FTIR analysis for PGLA/HAp and PGLA/HAp/Ag showed additional bands at  $572\text{cm}^{-1}$  and  $602\text{cm}^{-1}$  which corresponded to  $\text{PO}_4^{3-}$  bending vibrations. In the range of  $1040\text{-}1080\text{cm}^{-1}$  changes in the bands intensities correlation related to  $\text{PO}_4^{3-}$  stretching vibrations were revealed. After incubation, there were differences in spectra intensities in the range of  $1000\text{-}1250\text{cm}^{-1}$ , attributed to C-O and C-O-C stretching vibrations [1,2]. Such behaviour was more evident for pure PGLA than for PGLA/Ag. It might be assumed that addition of silver nanoparticles to the PGLA matrix moderates degradation process.

This work was financially supported by The Ministry of Science and Education, project No 5047/B/T02/2010/38

[1] E. Pamuła, M. Błażewicz, C. Paluszkiwicz, P. Dobrzyński, J. Mol. Struct. 596 (2001) 69.

[2] J. Chlopek, A. Morawska-Chochol, C. Paluszkiwicz et al., Pol. Deg. and Stab. 94 (2009) 1479

[3] B.S. Atiyeh, M. Costagliola, et.al, Burns 33 (2007) 139.

[4] N. Degirmenbasi, D.M. Kalyon, E. Birinci, Colloids and Surfaces B: Biointerfaces 48 (2006) 42.



## Headgroup hydrocarbon groups are involved in water binding as revealed by isotope IR spectroscopy

W. Pohle<sup>1</sup>, D. R. Gauger<sup>1</sup>, E. Mrazkova<sup>2</sup>, P. Hobza<sup>2</sup>

<sup>1</sup> Institute of Biochemistry and Biophysics, Friedrich-Schiller University, Philosophenweg 12, D-07743 Jena, Germany

<sup>2</sup> J. Heyrovsky Institute of Physical Chemistry, Academy of Sciences of the Czech Republic and Center for Complex Molecular Systems and Biomolecules, Dolejskova 3, Prague 8, C-18223, Czech Republic

Water is an ideal probe molecule to explore the binding behavior of lipid aggregates (as of any molecule with polar regions) since it combines many H bonding potentialities (altogether 4) with a small size largely excluding steric problems. We have applied infrared spectroscopy to study the hydration of phosphatidylcholines (PCs) according to a previously developed methodology [1] in terms of the specific contributions of the different lipid components for water binding.

Beside the well known binding sites, as phosphate and carbonyl groups, the polar lipid region comprises also CH (i.e. methyl, methylene and methine) groups, which are, however, not easily accessible by experimental means. To visualize the pertinent CH vibrational bands, which are practically hidden in the spectra of common lipids because of complete overlap by the predominant chain CH bands, both a truncated model compound, methyl-PC [2] and dimyristoyl-PCs with different specific deuterations as real lipid molecules have been studied. Systematic variation of the isotopic-exchange pattern made it possible to disentangle the CH stretching-vibration bands by separating the different molecular regions of a phospholipid, namely headgroup, glycerol backbone and hydrocarbon chains, from each other [3]. CH (or CD) stretching vibration bands due to methyl and methylene groups located in methyl-PC or in the polar region of dimyristoyl-PCs undergo surprisingly dramatic hydration-driven wavenumber upshifts of 6-20 cm<sup>-1</sup>. These shifts are relatively strong referred to the 2 cm<sup>-1</sup> wavenumber increase commonly found for the lipid chain-melting process, which in fact represents a conformationally fairly demanding (i.e. the main) transition. Therefore, the shifts of these headgroup CH (or CD) stretching vibration bands can be considered as indicating a direct water binding to the CH groups in the polar lipid domain rather than only conformational changes.

This suggestion is supported by the results of theoretical calculations performed for methyl-PC. The data reveal, among other structural and molecular-physical phenomena, the existence of (lipid-)C-H...OH<sub>2</sub> hydrogen bonding suitable to explain the spectroscopic findings [4]. The formation of such weak C-H...O hydrogen bonds might be promoted by the presence of electrophilic substituents located next to the CH groups in the polar lipid domain.

[1] W. Pohle, C. Selle, H. Fritzsche, H. Binder, *Biospectroscopy* 4 (1998) 267-280

[2] W. Pohle, D. R. Gauger, H. Fritzsche, B. Rattay, C. Selle, H. Binder, H. Böhlig, *J. Mol. Struct.* 563-564 (2001) 463-467

[3] D.R. Gauger, W. Pohle, *J. Mol. Struct.* 744-747 (2005) 211-21.

[4] E. Mrazkova, P. Hobza, M. Bohl, D. R. Gauger, W. Pohle, *J. Phys. Chem. B* 109 (2005) 15126-15134



## Polysiloxane networks formation studied by FTIR spectroscopy

A. Nyczyk, C. Paluszkiwicz, M. Hasik

*Faculty of Materials Science and Ceramics, AGH-University of Science and Technology, Al. Mickiewicza 30, 30-059 Kraków, Poland*

Polymer networks are formed by cross-linked macromolecules. Depending on their chemical composition as well as cross-linking density, such networks show versatile physical and chemical properties and therefore find various applications, e.g. as absorbent materials, drug carriers, sensors, composite matrices [1].

Polysiloxanes, i.e. the polymers containing Si-O bonds in the main chain, are the most important class of macromolecular compounds with inorganic backbone. Polysiloxane networks, particularly those based on poly(dimethylsiloxane), are well-known for their elastomeric properties [2]. The networks obtained by hydrolytic polycondensation of alkoxy silanes (the so-called sol-gel method) have been widely studied as precursors to silica or Si-O-C ceramics [3].

In the work, preceramic polysiloxane networks have been prepared by cross-linking of linear polysiloxanes containing vinyl groups in their molecules. The polymers have been obtained by ring-opening polymerization of two cyclic monomers: 1,3,3,5,5-pentamethyl-1-vinylcyclotrisiloxane (D<sub>2</sub>V) and 1,3,5-trimethyl-1,3,5-trivinylcyclotrisiloxane (V<sub>3</sub>). They have been cross-linked with hydrogen siloxanes using the so-called hydrosilylation reaction, which is a catalytic addition of Si-H bonds to multiple ones. Hydrogen siloxanes of various structures (linear, cyclic, cubic) and containing various numbers of hydrogen atoms in their molecules (two, four, eight) have been applied as cross-linking agents.

The reactions have been carried out at 60 °C, in toluene, using platinum(0)-1,3-divinyl-1,1,3,3-tetramethyldisiloxane complex as catalyst (Karstedt's catalyst). FTIR spectroscopy has been applied to follow the network formation process. Spectra recorded for the samples of reaction mixtures at selected times of the process have confirmed that - as expected for hydrosilylation - Si-H bonds have gradually disappeared from the systems and Si-CH<sub>2</sub>-CH<sub>2</sub>-Si linkages between the polymer chains have been formed. This has been manifested by lowering in intensities of the bands at ~2100 cm<sup>-1</sup> and ~900 cm<sup>-1</sup> originating from Si-H bond stretching and asymmetric bending vibrations, respectively as well as the by the appearance of the band at ~1130 cm<sup>-1</sup> assigned to the bending vibrations of CH bonds in Si-CH<sub>2</sub>-CH<sub>2</sub>-Si linkages. Based on quantitative FTIR spectra analysis, it has been concluded that the rate of network formation depends on the type of the polymer as well as on the hydrogen siloxane used as the cross-linking agent. Results of the studies have also shown that the efficiency of hydrosilylation, which decides on the suitability of the cross-linked polymer formed for use as preceramic material, is strongly influenced by the functionality of the hydrogen siloxane.

The work was financially supported by Polish Ministry of Science and Higher Education Grant No. NN507 457837.

- [1] A. Fernandez-Barbero, I. J. Suarez, B. Sierra-Martin, A. Fernandez-Nieves, F. Javerr de las Nieves, M. Marquez, J. Rubio-Retama, E. Lopez-Cabarcos, *Adv. Colloid Interf. Sci.* 147-148 (2009) 88-108
- [2] S. J. Clarson, J. E. Mark, in: "Polymeric Materials Encyclopedia", ed. J. C. Salomone, CRC Press 1996, vol. 10, 7663-7677
- [3] C. G. Pantano, A. K. Singh, H. Zhang, *J. Sol-Gel Sci. Technol.* 14 (1999) 7-25



## Characterization of ceramic/poly- $\epsilon$ -caprolactone nanocomposite materials by FTIR spectroscopy

C. Paluszkiwicz, E Sołtysiak, M. Blazewicz

*AGH – University of Science and Technology, Faculty of Materials Science and Ceramics, Al. Mickiewicza 30, 30-059 Krakow, Poland*

The bone tissue is the second most frequently transplanted human tissue and in the medical market a demand is growing for new materials for reconstitution of bone defects. Polymer nanocomposites belong to a new class of hybrid materials consisting of polymer matrix and inorganic nanoparticles. Nanocomposites consisting of resorbable polymer and bioactive nanoparticles are very attractive materials for medical applications.

The aim of this work was to obtain and characterize new nanocomposite materials consisting of resorbable polymer (poly- $\epsilon$ -caprolactone) matrix and ceramic (wollastonite or montmorillonite) nanoparticles for medical use in the field of bone tissue regeneration. Poly- $\epsilon$ -caprolactone (PCL) is a biodegradable polymer belonging to the aliphatic polyesters group. It is a non-toxic material, which has a good ability to mix, and is mechanically compatible with many other polymers and organic and inorganic compounds. This biocompatible polymer has been widely used also in the tissue engineering. Wollastonite and montmorillonite are bioactive and biocompatible materials, which may become an interesting alternative to hydroxyapatite, in particular due to higher than in the case of other bioactive materials rate of apatite formation on its surface after incubation in SBF, and due to their ability of chemical integration with the bone.

Nanocomposite polycaprolactone/wollastonite and polycaprolactone/montmorillonite foils with a varying content of the ceramic nanoparticles were prepared. The nanocomposites and ceramic nanoparticles were investigated using FT-IR techniques.

The FTIR microscopy spectra were collected using Bio-Rad Excalibur with microscope UMA500 equipped with MCT detector. FTIR measurements of the samples were carried out on the transmission and reflection modes. Spectra were measured at  $4\text{ cm}^{-1}$  resolution in the region from  $4000\text{ cm}^{-1}$  to  $700\text{ cm}^{-1}$ . FT-IR method is a particularly efficient tool for the surface analysis of nanosized and nanocomposite materials. This technique was used to determine structural changes of the polymer caused by the presence of ceramic nanoparticles.

We observed a correlation between the concentration of nanoparticles and structural changes of the nanocomposite surface. These results were confirmed by SEM/EDS, DSC and AFM studies.

This work was supported by The Ministry of Science and Higher Education, Grant No. N N507 370735



## Tuning the photophysical properties of pyrene-based systems: a theoretical study

M. Piccardo, M. Ottonelli, D. Duce, S. Thea, G. Dellepiane

*INSTM and Dipartimento di Chimica e Chimica Industriale, Università di Genova,  
via Dodecaneso 31, I-16146 Genova, Italy.*

In these years,  $\pi$ -conjugated systems have been the object of an increasing interest due to their particular electronic properties, which make these molecules suitable for advanced electronic and photonic applications. For this reason, knowledge of structure-property relationship for these molecular systems has gained a key role for the molecular design of new high performance materials [1,2]. In this framework, theoretical modelling gives a powerful test bench for screening new potentially useful molecules showing the desired electronic properties, through the prediction/correlation of the modifications induced in reference structures by the introduction of appropriate chemical substituents. The choice of such modifications can be addressed by the analysis of the electronic properties of the reference molecule.

Here we are considering the pyrene moiety, one of the  $\pi$ -centers that has been more extensively studied and widely used in many applications such as sensors [3], organic light emitting diodes (OLED) [4-6], hole-transporting materials [7] and in solar cells [8-11]. An increase of the efficiency of new pyrene-based systems in the above devices implies a modulation of the electronic properties in order to obtain appreciable absorption cross sections in the visible spectra region, blue-light emitting properties or efficient photoinduced charge separation. Using a time dependent density functional (TDDFT) approach and a suitable electron density analysis, we will show that tuning of the electronic properties of the pyrene moiety can be achieved in order to obtain new molecules for OLED or photovoltaic applications.

- [1] M. M. Haley, R. R. Tykwinski (Eds.), Carbon-Rich Compounds: From Molecules to Materials, Wiley-VCH, Weinheim, Germany, 2006.
- [2] H. Kang, G. Evrenenko, P. Dutta, K. Clays, K. Song, T.J. Marks, J. Am. Chem. Soc. 128 (2006) 6194-6205.
- [3] R. Martinez-Manez, F. Sancenon, Chem. Rev. 103 (2003) 4419-4476.
- [4] J. N. Moorthy, P. Natarajin, P. Venkatakrisnan, D.F. Huang, T. J. Chow, Org. Lett. 9 (2007) 5215-5218.
- [5] C. Tang, F. Liu, Y.J. Xia, J. Lin, L.H. Xie, G.Y. Zhong, Q.L. Fan, W. Huang, Org. Electron. 7 (2006) 155-162.
- [6] J. Daub, R. Engl, J. Kurzawa, S.E. Miller, S. Schneider, A. Stockmann, M.R. Wasielewski, J. Phys. Chem. A, 105 (2001) 5655-5665.
- [7] K. R. J. Thomas, M. Velusamy, J.T. Lin, C. H. Chuen, Y. T. Tao, J. Mater. Chem. 15 (2005) 4453-4459.
- [8] S.K. Pal, V. Sundström, E. Galoppini, P. Persson, Dalton Trans. 45 (2009) 10021 - 10031.
- [9] P.G. Hoertz, R.A. Carlisle, G.J. Meyer, Nano Lett. 3 (2003) 325-330.
- [10] Y. Matsunaga, K. Takechi, T. Akasaka, A.R. Ramesh, P.V. James, K. George Thomas, P.V. Kamat, J. Phys. Chem. B 112 (2008) 14539-14547.
- [11] O. Taratula, J. Rochford, P. Piotrowiak, E. Galoppini, R.A. Carlisle, G.J. Meyer, J. Phys. Chem. B 110 (2006) 15734-15741.



## Metal-organic platforms for photonic applications based on poly-10,12 dicosadienedioic acid (PDCDA)

A. Rindi<sup>1</sup>, G. Margheri<sup>2</sup>, M. Muniz-Miranda<sup>3</sup>, G. Dellepiane<sup>1</sup>, M. Alloisio<sup>1</sup>

<sup>1</sup>Department of Chemistry and Industrial Chemistry, University of Genova, Via Dodecaneso 31, 16146, Genova, Italy

<sup>2</sup>Institute for Complex System s, CNR, Via Madonna del Piano 10, 50019, Sesto Fiorentino (Fi), Italy

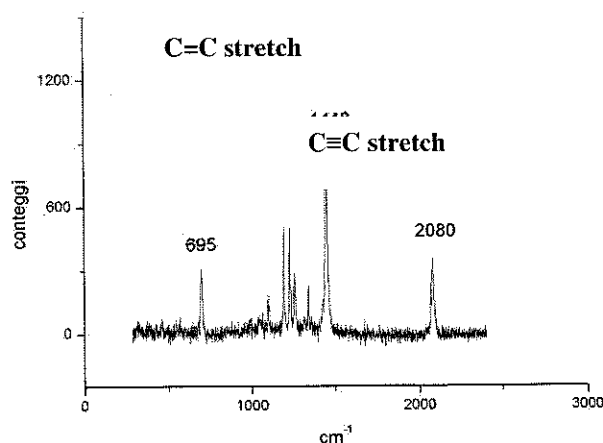
<sup>3</sup>Department of Chemistry, University of Florence, Via della Lastruccia 3, 50019 Sesto Fiorentino, Italy

The modification of metal surfaces with monolayers of polydiacetylenes (PDAs) or with PDAs-based nanohybrids [1] is a subject of great interest, in particular for applications in nonlinear optics, sensing [1,2] nanolithography and nanophotonics.

For the functionalization of metal we have chosen the 10,12 dicosadienedioic (DCDA) monomer for the following reasons. First, the presence of a symmetric COOH functionality makes it possible to use either of the DCDA terminals as linker to a surface, while the other one is free to interact with other molecules or other metal surfaces. Second, the absence of cumbersome lateral moieties enables the polymerization in the more conjugated form, highly desirable for nonlinear optical applications.

In this work, we report on the realization of metal-organic surfaces via functionalization of a planar Ag surface through 1) Self Assembly (SA) of a molecular monolayer of DCDA, and 2) SA of a layer of Ag-DCDA capped particles. The functionalization is followed in both cases by the UV polymerization of the monomeric units.

The formation of a self-assembled monolayer (SAM) of DCDA on the flat Ag surface and the UV polymerization are *in-situ* monitored via Surface Plasmon Resonance Spectroscopy (SPRS). The polymerization process is confirmed by Surface Enhanced Raman Scattering (SERS) measurements (see figure below).



The DCDA-capped nanoparticles used for the second step have been chemically synthesized, their water dispersion has been analyzed by UV-vis extinction spectroscopy and their shapes and dimensions were investigated by electron microscopy. The SA of these particles on the Ag surface was *in-situ* monitored by SPRS. After UV irradiation of the surface the final product, a metal-polymer composite, is obtained and analyzed by SERS spectroscopy. In both cases, a bluish-green PDCDA is formed, that results to be quite stable even after prolonged UV irradiation.

[1] M. Alloisio, A. Demartini, C. Cuniberti, G. Dellepiane, *Sensor Letters*, (2010), in press.

[2] T. Kim, R. M. Crooks. *Tetrahedron Lett.*, 35 (1994) 9501



## The influence of platinum(IV) ions on the formation of iron oxides in a highly alkaline medium

S. Krehula, S. Musić

*Division of Materials Chemistry, Ruđer Bošković Institute, P.O. Box 180, HR-10002 Zagreb, Croatia*

The effect of the presence of platinum(IV) ions, in the form of  $\text{Pt}(\text{OH})_6^{2-}$  at a high pH, on the formation of iron oxides in a highly alkaline precipitation system was investigated using X-ray powder diffraction (XRD),  $^{57}\text{Fe}$  Mössbauer and FT-IR spectroscopies, field emission scanning electron microscopy (FE-SEM) and energy dispersive X-ray spectroscopy (EDS). Acicular  $\alpha\text{-FeOOH}$  particles precipitated by hydrothermal treatment in a highly alkaline medium with the addition of tetramethylammonium hydroxide (TMAH) were used as reference material [1, 2].

In the presence of 1 or 5 mol % of platinum ions in the precipitation system lath-like  $\alpha\text{-FeOOH}$  (goethite) particles were formed as a single phase after a short autoclaving time (2 hours). No significant change in the size and shape of these particles in comparison to the reference sample was observed. After 6 hours of autoclaving the formation of platinum nanoparticles at the surface of  $\alpha\text{-FeOOH}$  particles via reduction by TMAH and/or its decomposition products became visible. These nanoparticles acted as a catalyst for the reduction of Fe(III) ions into Fe(II) and gradual transformation of  $\alpha\text{-FeOOH}$  into a mixed Fe(II)-Fe(III) oxide ( $\text{Fe}_3\text{O}_4$  magnetite) by the dissolution-recrystallization mechanism. The presence of a higher concentration of platinum ions accelerates the process of  $\alpha\text{-FeOOH} \rightarrow \text{Fe}_3\text{O}_4$  transformation with the appearance of  $\alpha\text{-Fe}_2\text{O}_3$  (hematite) particles as an intermediate product.

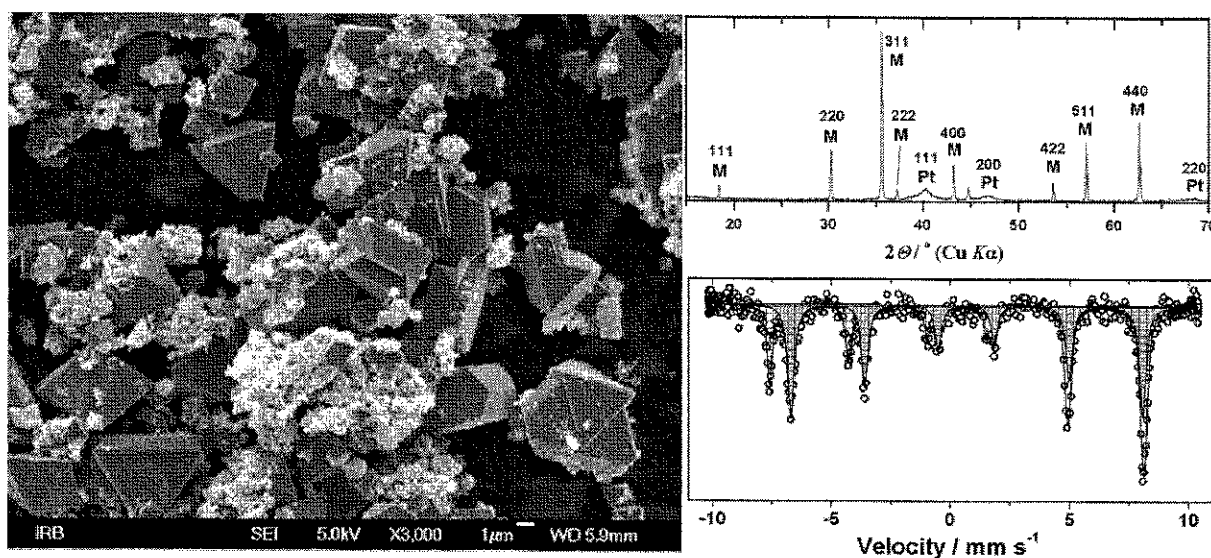


Fig. 1: FE-SEM image, XRD pattern and Mössbauer spectrum of the sample consisting of  $\text{Fe}_3\text{O}_4$  crystals and platinum nanoparticles.

[1] S. Krehula, S. Popović, S. Musić, *Mater. Lett.* 54 (2002) 108-113

[2] S. Krehula, S. Musić, *J. Cryst. Growth* 310 (2008) 513-520



## Influence of alkaline earth metals on molecular structure of 3-nitrobenzoic acid in comparison with alkali metals effect

M. Samsonowicz, E. Regulska, W. Lewandowski

*Department of Chemistry, Białystok Technical University, Zamenhofa 29, 15-435 Białystok, Poland*

The influence of magnesium, calcium, strontium and barium ions on the electronic system of 3-nitrobenzoic acid was studied in comparison with studied earlier alkali metal ions [1]. The vibrational (FT-IR) and NMR ( $^1\text{H}$  and  $^{13}\text{C}$ ) spectra were recorded for 3-nitrobenzoic acid and its salts. Characteristic shifts in IR and NMR spectra along Mg→Ba metal series were compared with Li→Cs series. Good correlations between the wavenumbers of the vibrational bands in the IR spectra for 3-nitrobenzoates and ionic potential, electronegativity, inverse of atomic mass, atomic radius and ionization energy of metals were found for alkaline earth metals as well as for alkali metals.

Optimized geometrical structures of studied compounds were calculated by B3LYP method using 6-311++G\*\* basis set. The theoretical wavenumbers and intensities of IR spectra were obtained. The calculated parameters were compared to experimental characteristic of studied compounds.

This work was supported by Białystok Technical University (theme no. W/WBiIŚ/10/2010)

- [1] R. Świsłocka, E. Oleksiński, E. Regulska, M. Kalinowska, W. Lewandowski, *J. Mol. Struct.*, 834-836 (2007) 380-388



## Experimental and theoretical study of molecular structure of alkali metal para substituted benzoates

E. Regulska, M. Kalinowska, W. Lewandowski

*Department of Chemistry, Białystok Technical University, Zamenhofa 29, 15-435 Białystok, Poland*

The present work is a continuation of our recent reports on the vibrational and NMR spectra as well as geometric characteristic of benzoic acid derivatives [1-4]. The influence of amino-, nitro-, methoxy-, hydroxy- and halogeno- substituents in para position towards the carboxylic group as well as alkali metal on molecular structure of benzoates were estimated. FT-IR, FT-Raman and NMR spectra of the title compounds were recorded and analyzed. Data of chemical shifts in  $^1\text{H}$  and  $^{13}\text{C}$  NMR as well as wavenumbers and intensities in IR and Raman spectra of studied benzoate derivatives were analyzed in comparison with alkali metal benzoates. Optimized geometrical structures were calculated by B3LYP/6-311++G\*\* method. The calculated parameters are compared with experimental characteristics of these molecules.

Presented work was supported by Białystok Technical University (theme no. W/WBiŚ/9/2010)

- [1] M. Kalinowska, G. Świdorski, W. Lewandowski, *Polyhedron*, 28 (2009) 2206-2218.
- [2] E. Regulska, M. Samsonowicz, R. Świsłocka, W. Lewandowski, *J. Phys. Org. Chem.*, 20 (2007) 93-108.
- [3] R. Świsłocka, M. Samsonowicz, E. Regulska, W. Lewandowski, *J. Mol. Struct.*, 792-793 (2006) 227-238.
- [4] W. Lewandowski, L. Fuks, M. Kalinowska, P. Koczoń, *Spectrochim. Acta A*, 59 (2003) 3411-3420.



## Phosphoenolpyruvate and $Mg^{2+}$ binding to pyruvate kinase monitored by infrared spectroscopy

S. Kumar, A. Barth

*Department of Biochemistry and Biophysics, The Arrhenius Laboratories for Natural Sciences, Stockholm University, SE – 10691 Stockholm, Sweden*

Infrared spectroscopy is a powerful technique to detect ligand induced changes in biomolecules as it has distinct signals and provides different levels of structural information. A dialysis accessory to attenuated total reflection infrared spectroscopy makes this technique more universal for ligand binding studies. We used this to investigate the binding of phosphoenolpyruvate (PEP) and  $Mg^{2+}$  to pyruvate kinase (PK), where conformational changes of PK were revealed upon binding of PEP and  $Mg^{2+}$ . Isotopically labeled PEP helped to assign and evaluate the infrared absorption bands. The difference spectrum of bound and free PEP indicates specific interactions between ligand and protein. The quantitative evaluation revealed that the enzyme environment has little influence on the P-O bond strengths of the band substrate PEP, which are weakened by less than 3% upon binding. The carboxylate absorption bands indicate also little perturbation of the C-O bands. The binding mode of PEP to PK is slightly different in presence of different monovalent cations  $K^+$  and  $Na^+$ . We also investigate the enzyme activity of PK by using infrared spectroscopy.



## FTIR-ATR analysis of synthetic iron(II-III) hydroxysalts green rusts

C. Rémazeilles, P. Refait

*Laboratoire d'Etude des Matériaux en Milieux Agressifs, Université de La Rochelle, Avenue Michel Crépeau, F-17042 La Rochelle cedex 01, France*

Iron (II-III) hydroxysalts green rusts (GRs) are intermediate compounds in the aqueous corrosion process of ferrous materials. Very reactive towards oxygen, they are difficult to characterise and they often transform during analysis when experiments are carried out without any protection against air. This certainly explains the lack of spectroscopic data. The various studies devoted to the crystal structures of green rusts established that these compounds can be classified as layered double hydroxides. The chemical composition of GR(SO<sub>4</sub><sup>2-</sup>) is for instance Fe<sup>II</sup><sub>4</sub>Fe<sup>III</sup><sub>2</sub>(OH)<sub>12</sub>SO<sub>4</sub> • 8H<sub>2</sub>O, [1] which can be developed as [Fe<sup>II</sup><sub>4</sub>Fe<sup>III</sup><sub>2</sub>(OH)<sub>12</sub>]<sup>2+</sup> [SO<sub>4</sub> • 8H<sub>2</sub>O]<sup>2-</sup> to remind that the crystal structure is built on positive hydroxide layers alternating with negative interlayers.

This poster presents a survey of infrared spectra of green-rusts including different anions (chloride, carbonate, sulphate, methanoate, bromide) acquired from synthetic compounds by Attenuated Total Reflection (ATR) Infrared spectroscopy under nitrogen atmosphere. A quite simple system adapted to the ATR accessory allowed us to obtain good quality spectra. For instance, in the 3000-3700 cm<sup>-1</sup> region, OH vibrations of the Fe(OH)<sub>2</sub> hydroxide-like sheets and of interlaying water molecules could be differentiated. Otherwise, a particular behaviour of GR(SO<sub>4</sub><sup>2-</sup>) could be clearly demonstrated. During the drying step under nitrogen, carried out directly on the ATR crystal, an instantaneous evolution of the spectrum was observed, which can be attributed to a structural change of the compound. As a matter of fact, the crystal structure of GR(SO<sub>4</sub><sup>2-</sup>) differs from that of most of GRs [1,2]. This change is more likely due a dehydration of the interlayers, initially composed of 8 water molecules per SO<sub>4</sub><sup>2-</sup> anion [1].

This study demonstrates that the FTIR spectral analysis of green rusts is of great interest not only to identify them but also to bring some structural complementary information.

[1] L. Simon, M. François, Ph. Refait, G. Renaudin, M. Lelaurain, J.-M. Génin, *Solid State Sciences* 5 (2003) 327-334

[2] Ph. Refait, M. Abdelmoula, J.-M. Génin, *Corrosion science* 40 (1998) 1547-1560

## Experimental and Theoretical Vibrational Spectroscopic Investigation of Zn(II) Halide Complexes of Pyridine Derivatives

E. Akalin<sup>1</sup>, S. Akyuz<sup>2</sup>

<sup>1</sup> *Istanbul University, Science Faculty, Physics Department, Vezneciler, 34134, Istanbul, Turkey*

<sup>2</sup> *Istanbul Kultur University, Faculty of Science and Letters, Department of Physics, Atakoy Campus, 34156 Istanbul, Turkey*

Pyridine bases are well known as ligands in complexes of transition metals. Formations of such complexes are likely to be closely related to the base strength. It is known that electron releasing substituent increases the base strength whereas electron withdrawing one decreases it. The position of the substituent is also important for determining the base strength of pyridine derivative. It is well known that several modes of coordinated pyridine derivatives show upward shifts in frequency compared to those of free molecule and the shifts are metal dependent.

The aim of this study is to analyse the influence of the formation of metal–ligand bond through the ring nitrogen on the vibrational wavenumbers of pyridine derivatives, depending on the electron releasing (NH<sub>2</sub>) or electron withdrawing (Cl) substituent, in the same position. As pyridine derivatives, 3-aminopyridine and 3-chloropyridine were used. Moreover, determination of the wavenumbers of metal–ligand bond vibrations has a separate interest. In order to investigate the influence of the counter ligand, halide, on pyridine derivative vibrations, calculations were carried out on both ZnCl<sub>2</sub>(L)<sub>2</sub> and ZnBr<sub>2</sub>(L)<sub>2</sub> (where L= 3-aminopyridine or 3-chloropyridine) compounds.

In this study the vibrational spectra of monomeric Zn(L)<sub>2</sub>X<sub>2</sub> (X=Cl and Br; L= 3-aminopyridine or 3-chloropyridine) compounds are reported and discussed. Full assignment of the spectra is presented and the analysis of the experimental data are supported by DFT calculations performed with B3LYP functional and the 6-311++G(d,p) basis set. The FT-IR (400–4000 cm<sup>-1</sup>) and Raman (0–3200 cm<sup>-1</sup>) spectra of compounds are recorded and are compared with that of the calculated spectra. Anharmonic corrections to the harmonic wavenumbers are done with the same method and level of theory. The coordination effects on vibrational wavenumbers of 3-aminopyridine and 3-chloropyridine were discussed in detail by comparing the spectra of free and coordinated molecules.



## IR and EPR study of copper(II) complexes with $^{15}\text{N}$ -labelled lysine and ornithine

O. Cozar<sup>1</sup>, I. Bratu<sup>2</sup>, L. Szabó<sup>1</sup>, I.B. Cozar<sup>1</sup>, M. Culea<sup>1</sup>, L. David<sup>1</sup>

<sup>1</sup>Babeş-Bolyai University, Faculty of Physics, RO-400084, Cluj-Napoca, Romania

<sup>2</sup>National Institute for Research and Development of Isotopic and Molecular Technologies, RO-400293, Cluj-Napoca, Romania

Copper(II) amino acids complexes have received the attention because they proved to be useful antibacterial agents, nutritive supplies for humans and animals, and also as models for metalloproteins [1].

Labelled stable isotopes ( $^{15}\text{N}$ -lysine,  $^{15}\text{N}$ -ornithine) are used in a variety of studies offering the ideal internal standards in quantitative informations, in isotopic tracers for nutrition investigations, to elucidate details of nitrogen metabolism in vivo and protein metabolism in different diseases [2].

The structural results obtained by IR and EPR investigations of  $^{15}\text{N}$ -lysine and  $^{15}\text{N}$ -ornithine copper(II) complexes adsorbed on NaY and HY zeolites are reported.

C-N stretching vibrations are observed in the  $1230\text{-}1030\text{cm}^{-1}$  region, whereas the out of plane bending vibrations are present in the  $650\text{-}900\text{cm}^{-1}$  range. As concerned the isotopic shift of the vibrational frequencies, N-H bending vibrations are the most sensible being located at  $1636\text{cm}^{-1}$  and  $1631\text{cm}^{-1}$  for  $^{14}\text{N}$ -H and  $^{15}\text{N}$ -H bending vibrations, respectively. In the spectra of copper complexes these bands are shifted compared to those of the ligands, which show the implication of  $\text{NH}_2$  group in the metal-ligands coordination. The shift of the  $\nu(\text{C}=\text{O})$  stretching vibration for complexes suggest also the involvement of the carboxylic group in covalent bonding to the copper ion [3].

Powder EPR spectra of both copper(II) complexes at room temperature suggest the presence of dimeric species. The aqueous solutions spectra show a well resolved copper hyperfine structure and also the ligand hyperfine structure due to the two  $^{15}\text{N}(I=1/2)$  nuclei for lysine compound.

EPR spectra of both compounds adsorbed on HY and NaY type zeolites are anisotropic due to the very low mobility in the faujasite cavities of the zeolites. Two different monomeric species were evidenced in the case of HY zeolite. One of them is localized in the middle of the large cavity (site III) of the zeolites and the other one on the walls (site II) of these cavities, respectively.

All the MO coefficients for metal-ligand bonds in the identified monomeric species were estimated assuming a square-planar local symmetry around the metal ion [4].

[1] M.Z.Iqbal, S.Khurshid, M.S.Iqbal, J.Pak., Med. Assoc., 40 (1990) 221

[2] F.Mesnard, R.G.Ratcliffe, Photosynth. Res., 83 (2005) 163

[3] A.Stanila, A.Marcu, D.Rusu, M.Rusu, L.David, J. Molec. Structure, 834-836 (2007) 364

[4] O.Cozar, V.Grecu, V.Znamirovski, Electron Spin Resonance of Metal Complexes, Ed. Acad. Bucuresti, 2001



## Spectral and ESR study of Cu(II), Co(II) and Ni(II) theophyllinato complexes containing propanolamine ligands

A. Bebu<sup>1</sup>, A. Kozma<sup>2</sup>, E. Forizs<sup>2</sup>, M. Toderas<sup>3</sup>, L. David<sup>1</sup>

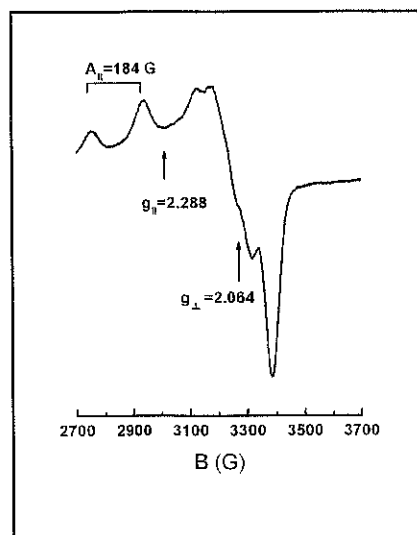
<sup>1</sup>"Babes Bolyai" University, Dpt of Physics, 400084 Cluj Napoca, Romania

<sup>2</sup>"Babes Bolyai" University, Dpt of Chemistry, 400028 Cluj Napoca, Romania

<sup>3</sup>University of Oradea, faculty of Science, 410087 Oradea, Romania

The transition metal complexes containing theophylline (th = 1,3-dimethylxantine) are intensely studied for modeling metal ions interactions with the guanine base of nucleic acid. As a part of our research on the theophyllinato complexes containing aminoalcohol ligands, we have already reported preparation and structural characterization of some new mixed ligand complexes of Cu (II), Co(II) and Ni(II) with 2-aminoethanol [1, 2].

Five new mixed ligand complexes  $[M(\text{th})_2(\text{ap})_2] \cdot n\text{H}_2\text{O}$  ( $M = \text{Cu}$ ,  $n = 2$ ;  $M = \text{Co}$ ,  $\text{Ni}$ ,  $n = 1$ ),  $[\text{Ni}(\text{th})_2(\text{pa})_2] \cdot \text{H}_2\text{O}$  and  $[\text{Cu}(\text{th})(\text{pa})]_2$  containing deprotonated theophylline and 1-amino-2-propanol (ap) or 3-amino-1-propanol (pa) as ligands were prepared and investigated by elemental analysis, spectroscopic methods (FT-IR, UV-VIS, ESR) and thermal studies. The results of spectroscopic studies indicated that the Co(II) and Ni(II) centers, are hexacoordinated by two theophyllinate-anions (coordinated through N(7)-atom) and two propanolamine molecules in a distorted octahedral geometry. The propanolamine are coordinated as bidentate ligands (through N and O atoms) to the metal center [3].



The spectral data and thermal behavior of  $[\text{Cu}(\text{th})_2(\text{ap})_2] \cdot 2\text{H}_2\text{O}$  shows that copper(II) ions are penta-coordinated with a square-pyramidal symmetry. One of the 1-amino-2-propanol ligands acts as a monodentate, and the second acts as a bidentate ligand. The room temperature powder ESR spectrum of this complex as shown in the figure above exhibits four hyperfine lines in the  $g_{\parallel}$  region and a strong absorption signal in the  $g_{\perp}$  region. The shape of the spectrum and the obtained values of ESR parameters ( $g_{\parallel}=2.288$ ,  $g_{\perp}=2.064$ ,  $A_{\parallel}=184\text{G}$ ) suggest a  $\text{CuN}_2\text{N}_2\text{O}^*$  chromophore.

The spectral and thermoanalytical data for  $[\text{Cu}(\text{th})(\text{pa})]_2$  suggest dinuclear structure. Each Cu(II) ion is four-coordinated with  $\text{N}_2\text{O}_2$  coordination environments. The 3-amino-1-propanol acts as monoanionic bidentate ligand bridging by oxygen atom. The room temperature powder ESR spectrum confirm the pseudotetrahedral local symmetry ( $g_{\parallel}=2.305$ ,  $g_{\perp}=2.061$ ).

[1] S. Gál, J. Madarász, E. Forizs, I. Labádi, V. Izvekov, G. Pokol, J. Therm. Anal. Cal., 53 (1998) 343

[2] P. Bombicz, J. Madarász, E. Forizs, I. Foch, Polyhedron, 16 (1997) 3601

[3] S. B. Sanni, A. T. H. Lenstra, V. C. Patel, Acta Crystallogr., Sect.C: Cryst. Struct. Commun., 41 (1985) 199

## Spectroscopic investigations of some transitional metals complexes with methionine as ligand

A. Stanila and L. F. Leopold

*University of Agricultural Sciences and Veterinary Medicine, No.3-5 Manasturstr. 400372 Cluj-Napoca, Romania*

Minerals such as zinc, copper, iron and others can chemically bond to amino acids resulting chelates. Amino acids are ideal chelators or ligands from both chemical and nutritional points of view. Metal amino acid chelates resemble these compounds which allow the minerals to be carried in with the amino acids during absorption. Finally, the amino acids, once released from the metal, can be used to build proteins or provide energy.

Methionine is the only sulfur-containing amino acid that is essential for mammals and must therefore be derived entirely from the diet. A preliminary study has suggested that methionine (6 grams per day) may improve memory recall in people with AIDS-related nervous system degeneration and also may help treat some symptoms of Parkinson's disease.

The  $[\text{Cu}(\text{L})_2]\cdot\text{H}_2\text{O}$ ,  $[\text{Co}(\text{L})_2]\cdot 2\text{H}_2\text{O}$ ,  $[\text{Zn}(\text{L})_2]\cdot\text{H}_2\text{O}$  complexes with methionine (L) as ligand, were synthesized in water solution and analyzed by means of: elemental analysis, atomic absorption spectroscopy, differential scanning calorimetry, FT-IR, UV-VIS and EPR spectroscopies.

The atomic absorption spectroscopy and elemental measurements confirm the ratio 1:2 metal ion: methionine composition for the synthesised compounds.

The IR spectra show that amino acids act as bidentate ligands with coordination involving the carboxylic oxygen and the nitrogen atom of the amino group. The  $\nu(\text{N-H})$  stretching vibration appears at  $3146\text{ cm}^{-1}$  in the ligand spectrum and is shifted at  $3229\text{ cm}^{-1}$  for Cu-L and  $3172\text{ cm}^{-1}$  for Co-L, proving the involvement of the  $-\text{NH}_2$ - group in the complexes formation. The  $\nu(\text{C=O})$  stretching vibration which appear in the ligand spectrum at  $1610\text{ cm}^{-1}$  is shifted with  $38\text{ cm}^{-1}$  for Cu-L,  $30\text{ cm}^{-1}$  for Co-L toward higher frequencies and with  $24\text{ cm}^{-1}$  for Zn-L complex toward lower frequencies which involves the carboxylic group in covalent bonding with metal ions.

Spectral UV-VIS data confirmed the covalent metal-ligand bonds, the pseudotetrahedral symmetry around the copper and zinc ions and the octahedral symmetry for the cobalt ion.

Powder EPR spectrum at room temperature are typically for pseudotetrahedral symmetry around the copper ion with the g tensor value:  $g=2.094$  corresponding to a  $\text{CuN}_2\text{O}_2$  chromophore. The Co-L powder EPR spectrum revealed the presence of monomeric compounds, with octahedral symmetry around the cobalt ion, the g tensor value is  $g=2.201$ .

[1] S. Bandyopadhyaya, G.N. Mukherjeea, M.G.B. Drewb, *Inorganica Chimica Acta*, 359 (2006) 3243.

[2] A. Shoveller, B. Stoll, R. Ball, D. Burrin, *J. Nutr.*, 135, (2005) 1609

[3] G. Mohamed, N. El-Gamel, *Spectrochimica Acta*, 60 (2004) 3141.





## FT-Raman analysis of luteolin and its complexes with Al (III)

A. Baran, E. Mrozek, M. Baranska

Faculty of Chemistry, Jagiellonian University, Ingardena 3, 30-060 Cracow, Poland

Luteolin (Fig. 1) is a yellow flavonoid occurring in a few plant species i.e. *Reseda luteola*. It is considered to play an important role in the human body e.g. as an antioxidant and a free radical scavenger. This compound is also commonly known as a traditional dye used in the past especially in Europe, Middle East and North Africa [1]. The technology of dyeing requires to use metal ions called mordants to fix and stabilize colorant on the textile. The most popular mordant was alum but other metal salt e.g. copper and iron were used also [2]. Due to the interesting properties of this dye, the synthesis and then analysis of luteolin complexes with Al(III) was put as an aim of this research.

Several flavonoids were investigated by various spectroscopic techniques [3, 4] but vibrational analysis of luteolin has not been reported yet. The issue what is the chemistry of luteolin complexes has not been answered in contrast to other flavonoid compounds e.g. quercetin [3]. Therefore in this work we demonstrate Raman spectroscopy analysis of luteolin and its complexes with aluminum (III). It is supposed that luteolin can form different complexes depending on the ratio of metal:ligand. Additionally, vibrational analysis of deprotonation process of this compound in respect to pH is carried out. Raman spectroscopy was chosen in regard to its sensitivity in detection of any structural changes of molecules in the solvent environment.

The samples are investigated using FT-Raman spectroscopy. The experimental work is supported by quantum-chemical calculations performed at the B3LYP/6-311++g(d,p) level and the assignment of vibration modes is based on the potential energy distribution.

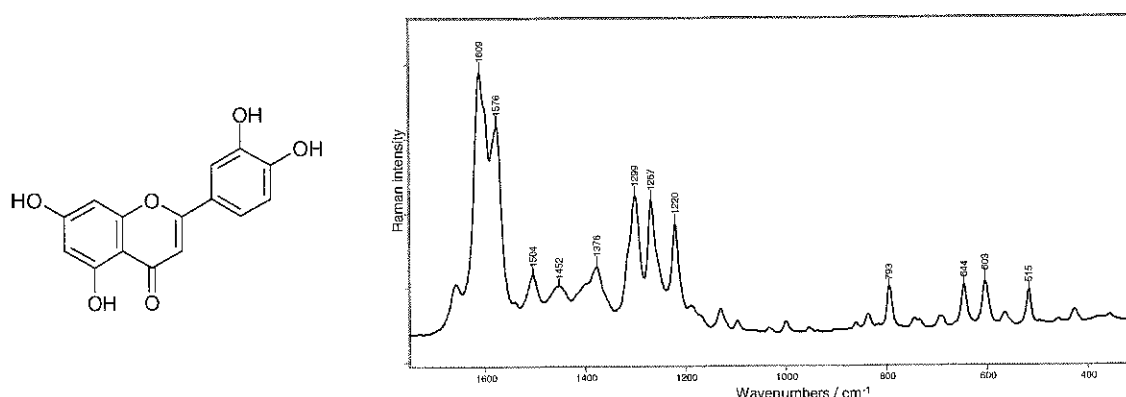


Fig. 1. The structure of luteolin and its Raman spectrum.

- [1] H. Scheppe, *Handbuch der Naturfarbstoffe*, 1993, Nikol Verlagsgesellschaft, Hamburg
- [2] G. Favaro, C. Clementi, A. Romani, V. Vickackaite, *J. Fluoresc.* 17 (2007) 707-714
- [3] J.P. Cornard, J.C. Merlin, *J. Inorg. Biochem.* 92 (2002) 19-27
- [4] J.E. Brown, H. Khodr, R.C. Hider, C.A. Rice-Evans, *Biochem. J.* 330 (1998) 1173-1178

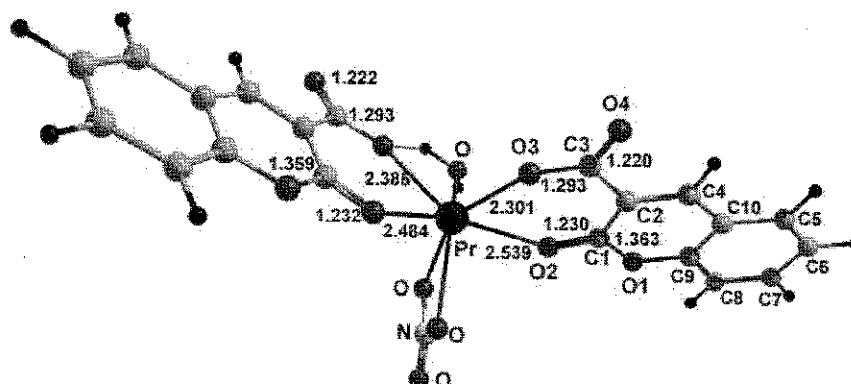
## FTIR, Raman, NMR and theoretical studies of lanthanide complexes with coumarin-3-carboxylic acid

I. Georgieva<sup>1</sup>, N. Trendafilova<sup>1</sup>, I. Kostova<sup>2</sup>, Tz. Mihaylov<sup>1</sup>

<sup>1</sup>*Institute of General and Inorganic Chemistry, Bulgarian Academy of Sciences, Acad. G. Bonchev, 11, 1113 Sofia, Bulgaria*

<sup>2</sup>*Department of Chemistry, Faculty of Pharmacy, Medical University, 2 Dunav St., Sofia 1000, Bulgaria*

The interaction of Ln(III) cations (Ln(III) = La(III), Ce(III), Pr(III), Nd(III), Sm(III), Eu(III) and Tb(III)) with the deprotonated form of the coumarin-3-carboxylic acid (L) was studied with DFT/B3LYP, MP2 and CCSD(T) methods. FTIR, Raman and NMR spectroscopies were applied to clarify the structure and molecular properties of Ln(III) complexes. Molecular modeling of the complex structures was performed in agreement with the general formulae predicted from elemental analyses. The ligand binding mode was suggested based on energy calculations of different model structures. Geometrical parameters, vibrational frequencies, IR intensities and Raman activities as well as <sup>1</sup>H and <sup>13</sup>C NMR chemical shifts of the ligand and Ln(III) complexes were calculated at DFT/B3LYP level and sufficiently accurate basis sets. To approach the experimental environment the calculations were performed in DMSO solution using polarizable continuum model. The comparative vibrational and NMR analyses, based on both experimental and theoretical data of two hypothetical Ln(III) structures predicted the metal polyhedron and bidentate binding of the two ligands to Ln(III) through the deprotonated carboxylic oxygen and the carbonylic oxygen. Specific vibrational and <sup>1</sup>H and <sup>13</sup>C NMR data were established able to distinguish the two bidentate ligand binding modes. The strength and character of the Ln(III)-L bidentate bonding were characterized by calculated LnO bond lengths, binding energies, ligand deformation energies, energy partitioning analysis,  $\sigma$ -donation contributions and natural population analyses. The energy decomposition calculations predicted predominant electrostatic interaction terms to the Ln-L bonding (ionic character) and showed variations of the orbital interaction term (covalent contributions) for the Ln(III) complexes studied. Electron distribution analysis suggested that the covalent contribution comes mainly from the interaction with the carboxylate moiety of the ligand.



## Zn(II), Cd(II) and Hg(I) complexes of biologically important ligands: FT-IR, FT-Raman, $^1\text{H}$ and $^{13}\text{C}$ NMR studies

M. Kalinowska, R. Świsłocka, W. Lewandowski

*Department of Chemistry, Białystok Technical University, Zamenhofa 29,  
15-435 Białystok, Poland, w-lewando@wp.pl*

Transition metal ions, including also heavy toxic metals, are of great importance in biology and medicine because they play a significant role determining the enzymatic activity. In this study zinc (II), cadmium (II) and Hg (I) cinnamates were synthesized and the composition of these compounds was determined. The FT-IR, FT-Raman,  $^1\text{H}$  and  $^{13}\text{C}$  NMR spectra of these compounds were registered, assigned and analyzed (Fig. 1). The effect of Zn(II), Cd(II) and Hg(I) ions on the molecular structure of ligand was discussed. Studies of differences in the number and position of bands from the IR, Raman spectra and chemical shifts from NMR spectra lead to conclusions concerning the distribution of electron charge in molecule, the delocalization energy of  $\pi$  electrons and the reactivity of ligands in metal complexes. This allows for a more precise interpretation of the mechanism by which particular metals, e.g., heavy metals, affect the chemical and biochemical properties of ligands. The above differences make it possible to predict what kind of deformation an electronic system of ligands would undergo during complexation.

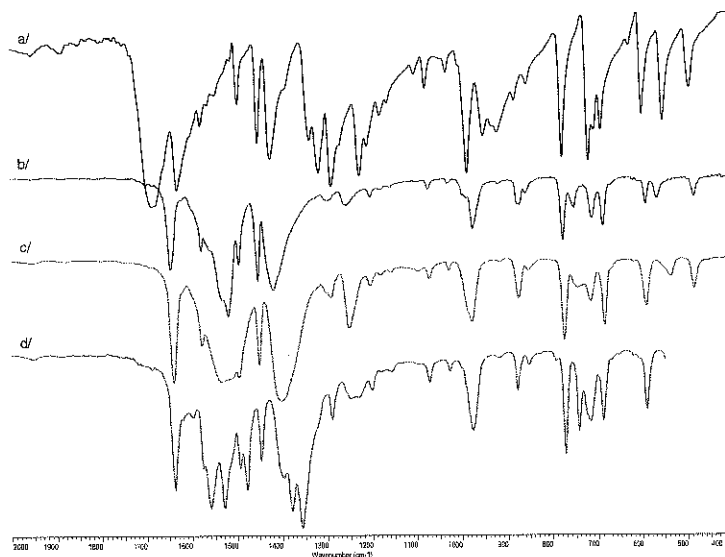


Fig. The FT-IR spectrum registered in KBr pellet for: a/ cinnamic acid,  
b/ Zn(II) cinnamate, c/ Cd(II) cinnamate, d/ Hg(I) cinnamate.

This work was supported by N N305 384538, W/WBiIS/6/2010



## Molecular structure of alkali metal salts of *p*-coumaric acid: spectroscopic (FT-IR, FT-Raman, $^1\text{H}$ and $^{13}\text{C}$ NMR) and theoretical (in B3LYP/6-311++G\*\* level) studies

R. Świsłocka, M. Kowczyk, M. Kalinowska, W. Lewandowski

*Department of Chemistry, Białystok Technical University, Zamenhofa 29,  
15-435 Białystok, Poland*

The evaluation of the electronic charge distribution in metal complexes enables more precise interpretation of mechanism by which particular metal ions affect biochemical properties of ligands [1,2]. In this paper we investigated the influence of alkali metal cations (lithium, sodium, potassium, rubidium and cesium) on the electronic structure of *p*-coumaric acid. It allowed observing the systematic changes in the spectra of investigated complexes depending on the position of the element in the periodic table. *P*-coumaric acid is a derivative of cinnamic acid that occurs in several plant species. Li, Na, K, Rb and Cs *p*-coumarates were synthesized and the experimental and theoretical FT-IR, FT-Raman,  $^1\text{H}$  and  $^{13}\text{C}$  NMR spectra of *p*-coumaric acid and its salts were registered and analyzed. The structures of *p*-coumaric acid and Li, Na, K salts were calculated by B3LYP/6-311++G\*\* method.

This work was supported by NN312 111838, W/WBiIS/13/2010

[1] W. Lewandowski, M. Kalinowska, H. Lewandowska, J. Inorg. Biochem., 99 (2005) 1407-1423

[2] M. H. Borawska, P. Koczoń, J. Piekut, R. Świsłocka, W. Lewandowski, J. Mol. Struct., 919 (2009) 284-289



## Surface-enhanced spectroscopic methods on metal nano-surfaces: What is the role of oxidation reduction cycles?

P. Matejka<sup>1</sup>, M. Vyskovska<sup>1</sup>, A. Kokaislova<sup>1</sup>, V. Prokopec<sup>1</sup>, J. Cejkova<sup>2</sup>, M. Clupek<sup>1</sup>

<sup>1</sup>Dept. of Analytical Chemistry, Institute of Chemical Technology, Technicka 5, 166 28 Prague 6 -Dejvice, Czech Republic

<sup>2</sup>Dept. of Chemical Engineering, Institute of Chemical Technology, Technicka 3, 166 28 Prague 6 – Dejvice, Czech Republic

Surface-enhanced Raman scattering (SERS) and surface-enhanced infrared absorption (SEIRA) spectroscopies are methods allowing detection and identification of molecular species on nanostructured surfaces of several metals, especially Au, Ag and Cu. To achieve required enhancement of the spectral signal a proper preparation procedure has to be tailored. This study is aimed at comparison of series of electrochemically prepared Au, Ag and Cu nano-/micro-structured surfaces on Pt targets [1 – 3] used for both SERS and SEIRA.

Each preparation procedure started with cathodic metal coating from an appropriate bath [1]. We tried to improve the morphology of the surface in terms of SERS enhancement via subsequent treatment by oxidation reduction cycles (ORC) [2-3] under various conditions. Nowadays we include the study of SEIRA-activity of substrates using the diffuse reflectance accessory. We monitor the surface morphologies by scanning electron microscopy (SEM) and/or atomic force microscopy (AFM) as well as the SERS- and SEIRA-activities to correlate the surface enhancement factors with morphological parameters.

Generally, every kind of ORC treatment of any metal substrate causes significant morphological changes on both micro- and nano- scale (e.g., see Fig. 1). However, ORC treatments give rise to the formation of the substrates with either apparently improved (as expected) or somewhat downgraded SERS-activity. Furthermore, we should notify that substrates with good surface enhancement of Raman signal do not show corresponding SEIRA-activity. The principal component analysis (PCA) of spectral data shows the crucial role of cathodic coating conditions on the quality of spectral information comparing to the relatively minor role of ORC treatment procedures.

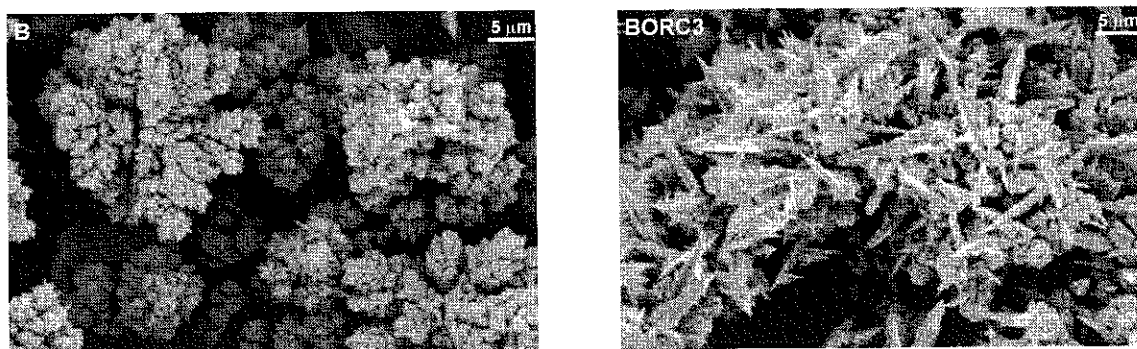


Fig. 1: Morphology of copper substrate prepared by cathodic reduction without ORC (B) and by combination of cathodic reduction with ORC treatment (BORC3). SEM images

- [1] M. Clupek, V. Prokopec, P. Matejka, K. Volka, J. Raman Spectrosc. 39 (2008) 515-524
- [2] V. Prokopec, J. Cejkova, P. Matejka, P. Hasal, Surf. Interface Anal. 40 (2008) 601-607
- [3] J. Cejkova, V. Prokopec, S. Brazdova, A. Kokaislova, P. Matejka, F. Stepanek, Appl. Surf. Sci. 255 (2009) 7864-7870

## Surface-Enhanced Raman Scattering of aromatic amides

J.L. Castro, J.F. Arenas, M.R. López-Ramírez and J.C. Otero

*Department of Physical Chemistry, Faculty of Science, University of Málaga, E-29071 Málaga, Spain.*

Surface-enhanced Raman scattering (SERS) of benzamide and salicylamide recorded on silver colloids have been studied and compared with the observed behaviour of the parent molecules benzoic and salicylic aromatic acids.

In the SERS of the benzamide, mode  $1; \nu_{\text{ring}}$  is observed at  $830 \text{ cm}^{-1}$  and undergoes a blue shift of  $+53 \text{ cm}^{-1}$  with respect to the Raman spectrum of the crystalline solid. Benzoic acid is adsorbed on silver as benzoate anion and its respective mode 1 is registered at  $845 \text{ cm}^{-1}$  being shifted in SERS towards the blue some  $+50 \text{ cm}^{-1}$  with respect to the wavenumber recorded in the Raman of the solid [1].

Concerning the SERS of salicylamide, mode  $1; \nu_{\text{ring}}$ , is observed at  $798 \text{ cm}^{-1}$ , i.e.  $+48 \text{ cm}^{-1}$  blue shifted with respect to the Raman of the solid, whereas in the SERS of the salicylic acid, which is adsorbed as hydroxybenzoate anion, we have detected a shift of  $+37 \text{ cm}^{-1}$  with respect to the respective band recorded in the Raman spectrum of the solid [2].

These results indicate that, in spite of the high  $\text{pK}_a$  values of the amide function group, benzamide and salicylamide are adsorbed on silver nanoparticles as anions linking to the metal through both the nitrogen and the oxygen atoms of the ionized carboxamide group. In order to confirm this unexpected conclusion, theoretical DFT calculations have been carried out on these molecules.

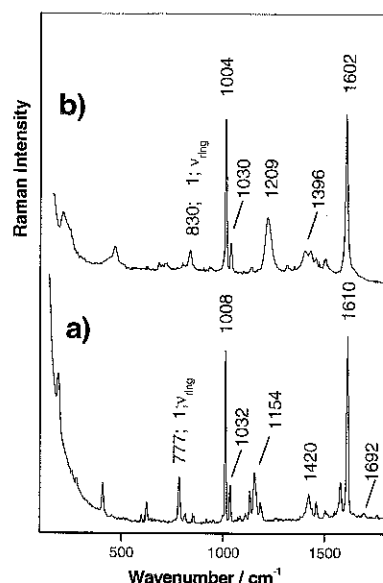


Fig. 1. a) Raman spectrum of solid benzamide; b) SERS spectrum of a  $10^{-3} \text{ M}$  solution

[1] M. Pagannone, B. Fornari, G. Mattei, *Spectrochim. Acta* 43A (1987) 621.

[2] J.L. Castro, J.F. Arenas, M.R. López-Ramírez, J.C. Otero, *Biopolymers* 82 (2006) 379.



## SERS/SERRS spectra and excitation profiles of Ru (II) bis(2,2-bipyridine)(4,4-dicarboxybipyridine) complex in systems with Ag nanoparticles: chemisorption versus electrostatic bonding

M. Kokoskova<sup>1</sup>, M. Procházka<sup>2</sup> B. Vlckova<sup>1</sup>

<sup>1</sup> Dept. of Physical and Macromolecular Chemistry, Charles University in Prague, Hlavova 8, 12840 Prague 2 Czech Republic

<sup>2</sup> Institute of Physics, Charles University in Prague, Ke Karlovu 5, Prague 2, 121 16, Czech Republic

Ru(II) polypyridine complexes are currently widely employed as sensitizers in dye-sensitized solar cell and as luminiscent probes of various types of microenvironment [1]. Our interest in these complexes stems from our effort to develop versatile SERRS and surface-modified luminescence probes for various systems with plasmonic metal nanoparticles (NPs).

In this contribution, we employ SERS/SERRS spectra and SERS/SERRS excitation profiles to explore bonding of the dicationic Ru (II) bis(2,2-bipyridine)(4,4-dicarboxybipyridine) /Ru(bpy)<sub>2</sub>(dcbpy)/ complex to unmodified and to chloride-modified surfaces of borate-stabilized Ag NPs, and to evaluate the effect of different types of dye-Ag NP surface bonding on the geometric as well as electronic structure of the dye.

Both SERRS ( $\lambda_{exc}=441.6$  nm) and SERS ( $\lambda_{exc}=532$  nm) spectra of Ru(bpy)<sub>2</sub>(dcbpy) obtained from the Ag NP hydrosol/ Ru(bpy)<sub>2</sub>(dcbpy) ( $1 \times 10^{-6}$  M) system show doublets of closely spaced bands, namely 1256, 1273; 1474, 1488 and 1534, 1559 cm<sup>-1</sup>. The 1273, 1488 and 1559 cm<sup>-1</sup> bands match those in SERRS, SERS and RRS spectra of Ru(bpy)<sub>3</sub> [2] and are assigned to the Ru-bpy unit of the complex. On the other hand, the 1253, 1474 and 1534 cm<sup>-1</sup> bands correspond to those encountered in the RRS spectra of Ru(dcbpy)<sub>4</sub>(NSC)<sub>2</sub> chemisorbed on TiO<sub>2</sub> surfaces [3], and are attributed to the Ru-dcbpy unit of adsorbed Ru(bpy)<sub>2</sub>(dcbpy). Chemisorption of Ru(bpy)<sub>2</sub>(dcbpy) on Ag NP surfaces is witnessed also by the 1367 cm<sup>-1</sup> band of  $\nu_s$  (COO<sup>-</sup>) of the bidentately coordinated carboxylate units. In contrast to that, both the SERRS and SERS spectra of Ru(bpy)<sub>2</sub>(dcbpy) obtained from the Ag NPs/NaCl/complex system show neither the doublets, nor the chemisorbed carboxylate band, and are virtually identical with those of Ru(bpy)<sub>3</sub>. These results indicate that modification of Ag NPs by adsorbed chlorides prevents chemisorption of Ru(bpy)<sub>2</sub>(dcbpy) by the two carboxylate groups, while it allows for the electrostatic attachment of this complex dication to the negatively charged surface of chloride-modified Ag NPs /in the same manner as Ru(bpy)<sub>3</sub>/.

To obtain a deeper insight into the structural changes undergone by the complex upon its chemisorption onto unmodified Ag NP surfaces, SERRS/SERS excitation profiles of the its spectral bands have been constructed from the SERRS/SERS spectra measured as a function of  $\lambda_{exc}$ . The maxima of the profiles of Ru-bpy unit bands at 458 nm nearly coincide with the 455 nm maximum of the absorption band of the free Ru(bpy)<sub>2</sub>(dcbpy) complex. In contrast to that, the Ru-dcbpy unit band profiles maximize at 488 nm. Further experiments targeted on specification of the electromagnetic and of the molecular resonance mechanism contributions to the Rudcbpy band profiles are currently in progress.

**Financial support:** P208/10/0941 grant awarded by GACR.

- [1] K. Kalyanasundaram, Photochemistry of Polypyridine and Porphyrin Complexes; Academic Press inc., London, 1992  
[2] I. Srnova, B. Vlckova, T.L. Snoeck, D.J. Stufkens, P. Matejka, Inorg. Chem. 39 (2000) 3551  
[3] M. K. Nazeeruddin, S. M. Zakeeruddin, R. Humphry-Baker, M. Jirousek, P. Liska, N. Vlachopoulos, V. Shklover, C. Fischer, M. Graetzel, Inorg. Chem. 38 (1999) 6298



## Computation of electromagnetic properties of plasmonic metamaterials with relevance in SERS by using S-parameter retrieval approach

M. Giloan<sup>1</sup>, S. Astilean<sup>1</sup>

<sup>1</sup> Babes-Bolyai University, Institute for Interdisciplinary Research in Bionanoscience, Nanobiophotonics Center, T. Laurian 42, 400271 Cluj-Napoca, Romania

Surface-enhanced Raman scattering (SERS) is a an excitation process that results in the enhancement of Raman scattering of molecules near nanostructured metallic surfaces. A great interest was stimulated in understanding and quantifying such processes. The main mechanism behind this enhancement is based on the enhancement of the electric field due to localized surface plasmon excitation.

In this work, we investigate the correlation between the substrate electromagnetic parameters and the localization of the electric field enhancement, the so called hotspots, on a SERS substrate prepared by using metal resonant nanoparticles. We considered a substrate made from gold bow-tie structures in a hexagonal lattice. This substrate is suitable for fabrication using nanosphere lithography and it has been previously demonstrated that it presents SERS activity [1]. In this study, the local electromagnetic parameters of the substrate, electric permittivity, magnetic permeability, and the index of refraction were computed using the numerical S-parameter retrieval approach, a well know method used for metamaterials characterization [2, 3]. Computer simulations were performed using FDTD algorithm [4]. Raman enhancement factors of about  $10^6$  are achieved for both OY and OZ polarization (see fig. 1). We analyzed the phase of a propagating wave incident on the substrate as a function of the propagation distance. Our simulations proved that in a hotspot area, at frequencies close to the resonant frequency, the phase of the electromagnetic wave propagates backward. This negative phase velocity of the wave confirms the local negative index of refraction.

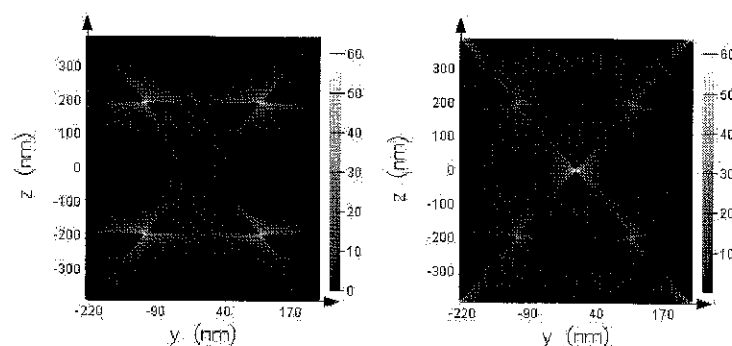


**Figure 1** Field enhancement (left) polarization OY direction, (right) polarization OZ direction, wavelength 764 nm.

**Acknowledgements:** The authors wish to thank for the financial support provided from programs co-financed by The SECTORAL OPERATIONAL PROGRAMME HUMAN RESOURCES DEVELOPMENT, Contract POSDRU 6/1.5/S/3 – „Doctoral studies: through science towards society”.

- [1] M. Baia, L. Baia, S. Astilean, J. Popp, Appl. Phys. Lett. 88 (2006) 143121
- [2] X. Chen, T. M. Grzegorezyk, B. Wu, J. Pacheco Jr., J. A. Kong, Phys. Rev. E 70 (2004) 016608
- [3] T. Koschny, P. Markos, D. R. Smith, C. M. Soukoulis, Phys. Rev. E 68 (2003) 016608
- [4] <http://www.lumerical.com>





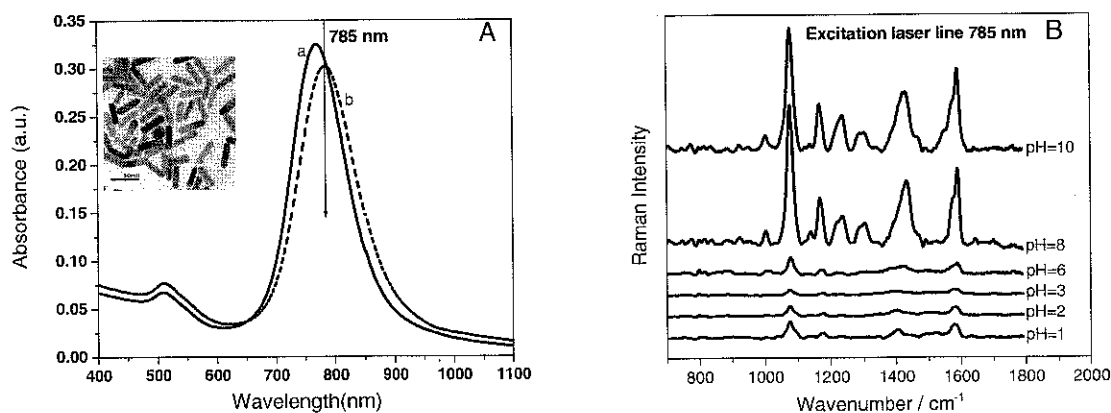
## A pH-dependent SERS study of 4-aminothiophenol adsorbed on gold nanorods

A.M. Gabudean, S. Astilean

*Babes-Bolyai University, Faculty of Physics and Institute for Interdisciplinary Research in Bionanoscience, Nanophotonics Center, T. Laurian 42, 400271 Cluj-Napoca, Romania*

The fabrication of nano-sized optical probes, capable of providing information on their biological environment in addition to their targeted spatial localization is a major field of interest in biochemistry and cell biology [1]. Gold nanorods (GNRs) have attracted considerable attention due to their unique properties related to a large surface-enhanced Raman scattering (SERS), high sensitivity of localized surface plasmon resonance (LSPR), biocompatibility, easy synthesis and functionalization, with great applicability in bioimaging, biosensing and optical spectroscopy applications.

In the present work we study the effect of pH on SERS of 4-Aminothiophenol (p-ATP) labeled GNRs. The GNRs were prepared by employing a modified version of the seed-mediated growth method developed by Nikoobakht et al. [2]. Here, p-ATP molecule was chosen as a model adsorbate since it adsorbs strongly onto gold through the formation of an Au-S bond and the pH-sensitive amino group ( $-NH_2$ ) remains exposed to be acted upon through protonation. Fig. A illustrates the extinction spectra of as-prepared Au NRs at pH=6 before (curve a) and after (curve b) labeling with p-ATP. The spectral shift to red of longitudinal LSPR clearly indicates that thiol-containing molecules are selectively bound to the end of individual Au nanorods.



As revealed in Fig. B, drastic changes occur in SERS spectra of p-ATP as a function of pH when varied from acidic to basic environment. Actually, both SERS and LSPR spectra exhibits a rich pH-dependent behavior which will be discussed in our presentation. We believe that the sensitivity of the SERS spectral pattern of p-ATP/GNRs conjugates toward pH of the surrounding medium can make them suitable candidates for the use as nanoscale pH meter device applicable in monitoring in vivo biological process within single cells.

**Acknowledgments.** This work was supported by CNCSIS in the frame of the PN-II research programs under the project PCCE No 129/2008. A. M. Gabudean also acknowledges Ph.D. scholarship, project co-financed by the Sectoral Operational Program for Human Resources Development 2007 – 2013, Contract nr. POSDRU/88/1.5/S/60185 – “Innovative doctoral studies in a knowledge based society”, Babeş-Bolyai University, Cluj-Napoca, Romania

- [1] Z. Wang, A. Bonoiu, M. Samoc, Y. Cui, P. N. Prasad, *Biosensors & Bioelectronics* 23 (2008) 886  
 [2] B. Nikoobakht, M. A. El-Sayed, *Chem.Mater.* 15 (2003) 1957-1962.

## SERS of benzenesulfonamide adsorbed on silver nanoclusters

J.L. Castro, M.R. López-Ramírez, J.F. Arenas, J.C. Otero

*Department of Physical Chemistry, Faculty of Science, University of Málaga, E-29071 Málaga, Spain*

In this work, the Raman and SERS spectra of benzenesulfonamide have been recorded on silver sols and analyzed on the basis of the electromagnetic (EM) and charge transfer (CT) enhancement mechanisms. Figure 1b shows the Raman spectrum of the  $\text{Ph-S(=O)}_2\text{NH}^-$  anion in aqueous solution ( $\text{pK}_a=8,97$ ) where important wavenumber shifts are observed with respect to the Raman of the solid (Fig. 1a), namely, the  $\nu_s(\text{OSO})$  and  $\nu(\text{C-S})$  vibrations, which are observed in SERS at 1119 and 1072  $\text{cm}^{-1}$ , undergo a redshift of -48 and -28  $\text{cm}^{-1}$ , respectively, whereas  $\nu(\text{S-N})$ , registered in SERS at 978  $\text{cm}^{-1}$ , is blueshifted +66  $\text{cm}^{-1}$ . These shifts agree with the theoretical predictions obtained by carrying out DFT calculations and with the expected changes in the involved bond lengths when the molecule is ionized, which consist of a lengthening of the S=O and C-S bonds and a shortening of the S-N bond [1], respectively.

The SERS spectrum shown in Fig. 1c is obtained at  $\text{pH}=7$  and correlates very well with the Raman spectrum of the anion (Fig. 1b). Therefore, it can be deduced that the species adsorbed on the silver nanoparticles is the deprotonated  $\text{Ph-S(=O)}_2\text{NH}^-$  system and that the interaction with the metal must be established through the nitrogen atom.

According to the selection rules of the EM mechanism [2], the drastic decrease of the relative SERS intensity of the band assigned to  $\nu(\text{S-N})$  and the enhancement of the bands attributed to the vibrations  $\nu(\text{CS})$  and  $\delta(\text{OSO})$  could be interpreted as a result of the parallel arrangement of the S-N bond with respect to the surface of the metal. In addition, it is found that the relative enhancement of some SERS bands with respect to the Raman spectrum of the anion, especially the mode  $\delta a; \nu_{\text{ring}}$ , is related to the contribution of a resonant CT enhancement mechanism [3].

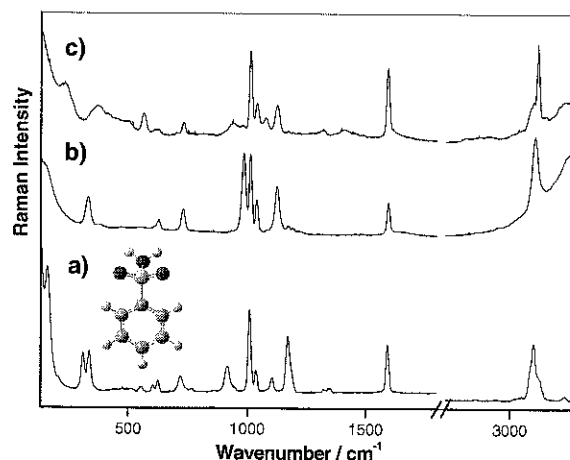


Fig. 1. Raman spectra of benzenesulfonamide: a) solid, b) aqueous solution at  $\text{pH}=14$ , and c) SERS spectra on silver colloid.

- [1] A.D. Popova, M.K. Georgieva, O.I. Petrov, K.V. Petrova, E.A. Velcheva, *Int. J. Quantum Chem.* 107 (2007) 1752.
- [2] M. Moskovits, D.P. DiLella, K.J. Mainard, *Langmuir* 4 (1988) 67.
- [3] J.F. Arenas, D.J. Fernández, J. Soto, I. López-Tocón, J.C. Otero, *J. Phys. Chem. B* 107 (2003) 13143.

**SERRS microspectroscopy of porphyrins on Ag immobilized nanoparticles**

P. Šimáková and M. Procházka

*Charles University in Prague, Faculty of Mathematics and Physics, Institute of Physics,  
Ke Karlovu 5, CZ-121 16, Prague 2, Czech Republic*

Porphyrins are important biomolecules whose synthetic derivatives are or can potentially be applied in photodynamic therapy of cancer, antiviral treatment, specific sensing of DNA sequences, selective cleavage of nucleic acids, etc. Porphyrins have been extensively studied by using surface-enhanced resonance Raman scattering (SERRS) spectroscopy, employing various metal surfaces including silver colloids [1]. They exhibit strong SERS signal and therefore can also be used for testing properties of metal surfaces.

In this contribution SERRS spectra of cationic free-base 5,10,15,20-tetrakis(1-methyl-4-pyridyl) porphyrin (TMPyP) were measured from immobilized Ag colloidal nanoparticles (borohydride- and hydroxylamine-reduced) using integrated confocal Raman microspectrometer (LabRam HR800, Horiba Jobin-Yvon, 514.5 nm Ar<sup>+</sup> laser line used). The nanoparticles were immobilized on a glass plate either by silane [2] or by drying of a colloid/TMPyP droplet.

In the case of silanized substrates, the limit of detection (LOD) of TMPyP was determined as  $\sim 1 \times 10^{-8}$  M (for 60s acquisition time). Nevertheless, we struggled with decreasing of the analyte signal as well as with a frequent presence of spurious bands assigned to carbonaceous compounds (two broad bands at  $\sim 1300$ - $1600$  cm<sup>-1</sup> and/or rapidly fluctuating peaks) coming from decomposition of silane. The Ag colloid/TMPyP droplets on a glass plate have tendency to form a ring at the edge of the droplet in which almost all nanoparticles and aggregates are clustered [3] similar to the coffee ring effect used in the drop coating deposition Raman (DCDR) technique [4]. This behaviour is observed for all measured TMPyP concentrations ( $1 \times 10^{-6}$  M -  $1 \times 10^{-10}$  M), i.e. for different aggregation states of the colloid, although for particular TMPyP concentrations the rings differ in width and shape. This unique structure provides substantially higher SERRS signal (TMPyP spectra are obtained even for  $1 \times 10^{-10}$  M TMPyP concentration and 1s acquisition time) and substantially less problems with spurious bands than the silanized substrates.

**Acknowledgment:** Financial support from Grant Agency of the Czech Republic (grant No. P208/10/0941) is gratefully acknowledged.

- [1] M. Procházka, J. Štěpánek, P.-Y. Turpin, J. Bok, J. Phys. Chem. B 106 (2002) 1543-1549 and references therein
- [2] N. Hajduková, M. Procházka, J. Štěpánek, P. Molnár, Vib. Spectrosc. 48 (2008) 142-147
- [3] J.-Y. Jung, Y. W. Kim, J. Y. Yoo, Anal. Chem. 81 (2009) 8256-8259
- [4] D. Zhang, Y. Xie, M. F. Mrozek, C. Ortiz, V. J. Davisson, D. Ben-Amotz, Anal. Chem. 75 (2003) 5703-5709



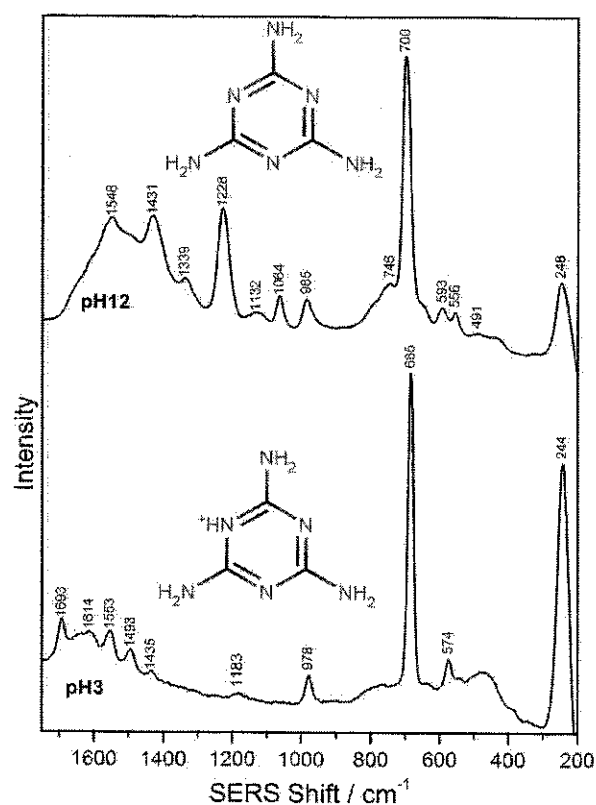
## Surface-enhanced Raman and DFT study on melamine

N. Mircescu, L. Szabó, N. Leopold, O. Cozar, V. Chiş

Faculty of Physics, Babeş-Bolyai University, Kogalniceanu 1, 400084 Cluj-Napoca, Romania

Melamine (2,4,6-triamino-1,3,5-triazine) is a relatively cheap industrial chemical, mostly used in the production of plastics and glues. It contains 67% nitrogen per mass unit and has been used to fraudulently increase the apparent protein content, as protein in food products is typically measured by analysis of total nitrogen [1].

A joint experimental and theoretical study, using surface-enhanced Raman spectroscopy (SERS) and density functional theory (DFT) calculations, was performed on melamine, in order to determine valuable physico-chemical properties of the molecule. Also, the possibility of melamine SERS detection at  $\mu\text{g/l}$  (ppb) level was assessed.



SERS spectra of neutral (top) and protonated melamine (bottom).

band at  $1228\text{ cm}^{-1}$  in the SERS spectrum of neutral melamine is missing in the SERS spectrum of the protonated molecular species. The complete assignment of the SERS spectra is performed based on DFT calculations. Other valuable physico-chemical properties, like optimized geometry, ionization potentials and electron and proton affinities or molecular electrostatic potential have been obtained from DFT calculations on the two melamine molecular species. These properties are essential when the geometry of the adsorbed molecule on colloidal silver particles is envisaged.

Melamine is only slightly soluble in water, therefore the normal Raman spectra of melamine aqueous solutions could not be recorded. SERS spectroscopy is a valuable tool to overcome such lack of sensitivity inconveniences. SERS spectra of neutral melamine, and in the protonated molecular form were successfully recorded, melamine having a  $\text{pK}_a$  value of 6.76 [2].

Silver colloid was prepared following a simple procedure, reducing silver nitrate with hydroxylamine at room temperature [3]. The pH of the colloids was then adjusted to acid or basic pH's using hydrochloride or sodium hydroxide solutions. The spectra were recorded using a 532 nm, frequency-doubled Nd:YAG laser of a DeltaNu Advantage Raman spectrometer.

Comparing the SERS spectra of the two melamine molecular species several differences can be observed. The total symmetric ring stretching (breathing) vibration is shifted  $5\text{ cm}^{-1}$  to lower wavenumbers, at  $685\text{ cm}^{-1}$ , in the protonated molecular form. Also, the strong intensity

[1] A. Breidbach, K. Bouten, K. Kröger, F. Ulberth, Anal. Bioanal. Chem. 396 (2010) 503

[2] MarvinSketch software, ChemAxon Kft. Budapest, Hungary

[3] N. Leopold, B. Lendl, J. Phys. Chem. 107 (2003) 5723



## Trace-detection of triphenylene by SERS spectroscopy using functionalized silver nanoparticles with bis-acridinium lucigenine.

I. López-Tocón<sup>1</sup>, J.C. Otero<sup>1</sup>, J. F. Arenas<sup>1</sup>, J.V. García-Ramos<sup>2</sup>, S. Sánchez-Cortés<sup>2</sup>

<sup>1</sup>Department of Physical Chemistry, Faculty of Science, University of Málaga, E-29071 Málaga, Spain.

<sup>2</sup>Instituto de Estructura de la Materia, CSIC, Serrano 121, E-28006 Madrid, Spain.

Surface Enhanced Raman Scattering (SERS) of triphenylene (TP) has been recorded on Ag nanoparticles functionalized [1] with the molecular assembler bis-acridinium lucigenine dication (LG) which approaches this hydrophobic adsorbate to the metal surface allowing for its detection (Figure 1). The self-assembly of the LG viologen on metallic surface leads the formation of intramolecular cavities where TP can be hosted (Figure 2) and has been checked by analyzing SERS intensities of TP bands at different LG concentrations. The limit of detection at trace-level concentration (20 ppb) is confirmed by the presence of their characteristic fingerprint vibrational bands and the LG-analyte affinity is deduced from the analysis of TP bands intensities at different concentrations of pollutant. It is shown that the adsorption isotherm for TP at LG cavities fits very well to a Langmuir isotherm.

On the other hand, optimized structure and force field of LG and TP have been calculated at B3LYP/6-31G\* level of theory by using GAUSSIAN03 program package. All this allows us to extract structural information on the host and the analyte from the SERS spectra of LG and LG/TP complex taking into account EM selection rules [2]. The two acridinium planes of LG are rotated one to each other 90.10°. Given that, no wavenumber shifts of LG bands are observed in SERS spectra with or without TP, it is expected that the structural conformation of LG does not change when TP is hosted. However, the orientation of LG respect to the metallic surface changes from a perpendicular to a tilted position when TP concentration decreases.

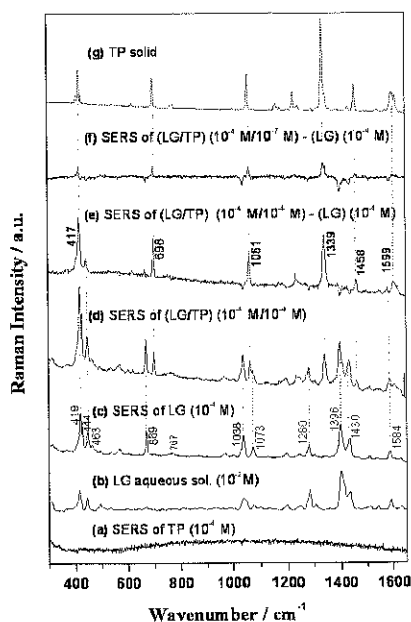


**Figure 1:** SERS spectra recorded at 785 nm excitation line.

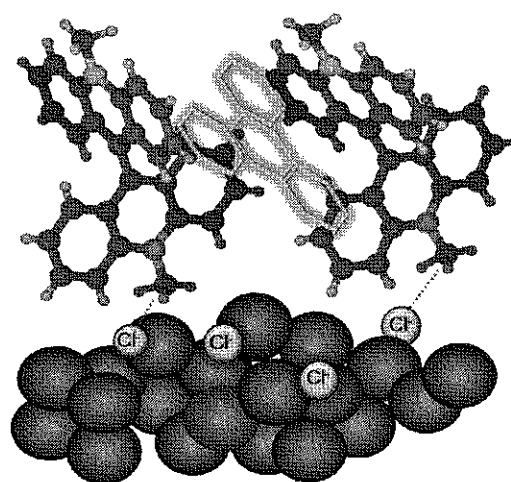


**Figure 2:** Intermolecular cavities of LG adsorbed on metal surface.

- [1] P. Leyton, S. Sánchez-Cortés, J.V. García-Ramos, C. Domingo, M. Campos-Vallette, C. Saitz, R.E. Clavijo, *J. Phys. Chem. B* 108 (2004) 17484  
 [2] M. Moskovits, *Rev. Mod. Phys.* 57 (1985) 783



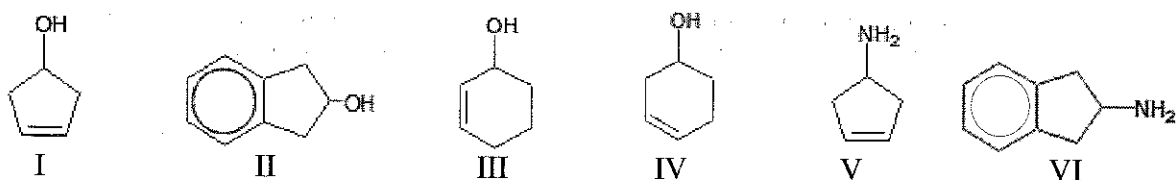
## Spectroscopic and theoretical investigation of intramolecular $\pi$ -type hydrogen bonding in 3-cyclopentenol and related molecules

E. J. Ocola<sup>1</sup>, A.A. Al-Saadi<sup>2</sup>, and J. Laane<sup>1</sup>

<sup>1</sup>Department of Chemistry, Texas A&M University, College Station, TX 77843-3255 USA

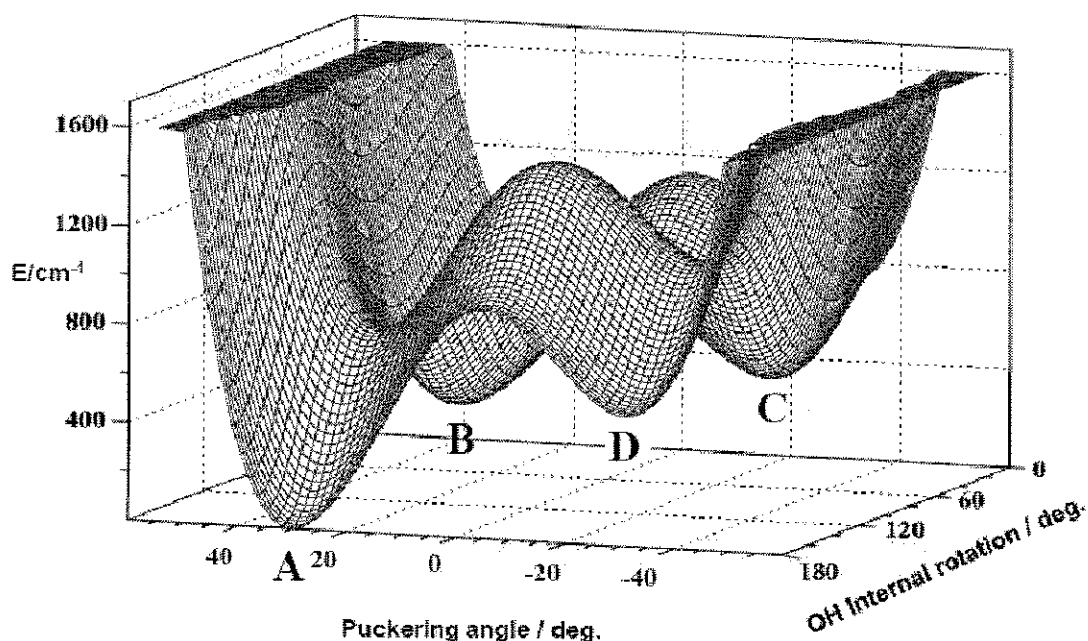
<sup>2</sup>Chemistry Department, King Fahd University of Petroleum & Minerals, Dhahran 31261, Saudi Arabia

Infrared, Raman, and jet-cooled fluorescence spectroscopies have been used to investigate the  $\pi$ -type intramolecular hydrogen bonding of several molecules including those shown below.



The infrared and Raman spectra of 3-cyclopentenol (I) show almost all of the expected vibrational bands from each of the four conformations predicted by *ab initio* and DFT calculations. The correlation between experimental and computed frequencies is excellent. The conformer with the intramolecular hydrogen bonding is predicted to be  $401\text{ cm}^{-1}$  lower in energy than any of the other conformations, and the spectra support that.

For 2-indanol (II) the fluorescence excitation spectra show the presence of four conformers with the hydrogen bonded species of lowest energy. Two-dimensional potential energy surfaces in terms of the ring-puckering and  $-\text{OH}$  torsional motions were calculated for both I and II. That for I is shown below. The spectra and computational results for III, IV, V, and VI will also be discussed.



## The photodissociation of CH<sub>3</sub>I in the edges of the A-band: Comparison between slice imaging experiments and multisurface wave packet calculations

L. Rubio-Lago,<sup>1,2</sup> A. García-Vela,<sup>3</sup> A. Arregui,<sup>1</sup> G. A. Amaral,<sup>1</sup> J. Rodríguez<sup>1</sup>, M. González and L. Bañares<sup>1</sup>

<sup>1</sup>Departamento de Química Física I, Facultad de Ciencias Químicas, Universidad Complutense de Madrid, Madrid 28040, Spain

<sup>2</sup>Instituto de Estructura de la Materia, CSIC, C/Serrano, 123, Madrid 28006, Spain

<sup>3</sup>Instituto de Física Fundamental, CSIC, C/Serrano, 123, Madrid 28006, Spain

The photodissociation of methyl iodide at different wavelengths in both edges of the A-band has been studied using a combination of slice imaging and resonance enhanced multiphoton ionization detection of the methyl fragment in the vibrational ground state ( $v = 0$ ). In the red edge (305 – 333 nm) the kinetic energy distributions (KED) of the produced CH<sub>3</sub> ( $v = 0$ ) fragments show a vibrational structure, both in the I ( $^2P_{3/2}$ ) and I ( $^2P_{1/2}$ ) channels, due to the contribution to the overall process of initial vibrational excitation in the  $\nu_3$  (C–I) mode of the parent CH<sub>3</sub>I. The structures observed in the KEDs shift toward upper vibrational excited levels of CH<sub>3</sub>I when the photolysis wavelength is increased. In the blue edge (205 – 235 nm) the I ( $^2P_{1/2}$ ) KEDs show two contributions of different anisotropy whose ratio strongly depends on the photolysis wavelength.

The I ( $^2P_{3/2}$ ) / I ( $^2P_{1/2}$ ) branching ratios, photofragment anisotropies, and the contribution of vibrational excitation of the parent CH<sub>3</sub>I are explained in terms of the contribution of the three excited surfaces involved in the photodissociation process,  $^3Q_0$ ,  $^1Q_1$ , and  $^3Q_1$ , as well as the probability of nonadiabatic curve crossing  $^1Q_1 \leftarrow ^3Q_0$  and inverse curve crossing  $^3Q_0 \leftarrow ^1Q_1$ . The experimental results are compared with multisurface wave packet calculations carried out using the available *ab initio* potential energy surfaces, transition moments, and nonadiabatic couplings, employing a reduced dimensionality (pseudotriatomic) model. A general qualitative good agreement has been found between theory and experiment, the most important discrepancies being in the I ( $^2P_{3/2}$ ) / [I ( $^2P_{1/2}$ ) + I ( $^2P_{3/2}$ )] branching ratios. Inaccuracies of the available potential energy surfaces are the main reason for the discrepancies.



## Dissociation of the ethyne dication: the case of $C^+ - H^+ - CH$ channel

R. Flammini<sup>1</sup>, E. Fainelli<sup>1</sup>, L. Avaldi<sup>1</sup> and M. Satta<sup>2</sup>

<sup>1</sup>IMIP-CNR Istituto di Metodologie Inorganiche e dei Plasm, Via Salaria km 29.300, 00010 Montelibretti, Italy

<sup>2</sup>ISMN-CNR Istituto dei Materiali Nanostrutturati, Via dei Taurini 19, 00185 Roma, Italy

A study on the fragmentation of the ethyne dication is presented. The ethyne molecule has recently attracted a lot of interest due to its peculiar structure which bends upon electron or photon excitation before dissociation, producing weird multiple-ion coincidence diagrams. These experimental findings have been rationalized in terms of isomerization [1], trans- and cis-bending motions [2].

Here we face the problem of the charge localization when the molecule is doubly ionized. Contrary to the common belief, before the dissociation occurs, the measurements [3,4] show that the double charge can also localize on one side of the molecule instead to obey to the Coulomb repulsion which would have suggested to maximize the distance between the two positive charges.

We report experimental evidence (Auger electron-ion-ion coincidence spectroscopy) and theoretical calculations (based on TDDFT theory) for the localization of the charges, leading to the anomalous fragmentation of the ethyne dication.

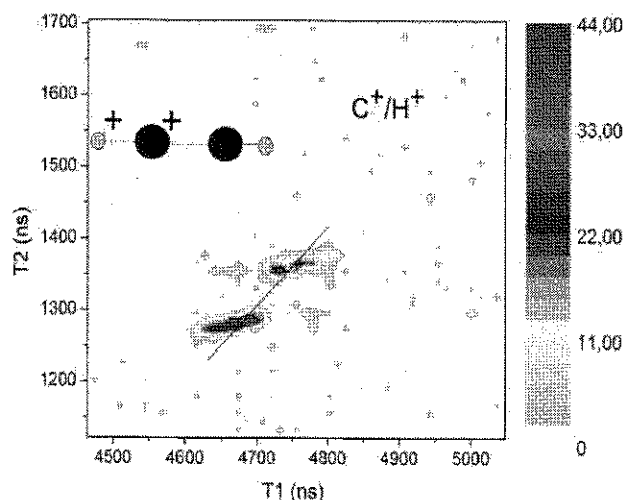


Figure1: Auger electron-ion-ion coincidence spectrum of the ethyne molecule for the ( $C^+/H^+$  channel). The spectrum has been recorded at 260 eV Auger electron energy. The positive slope of the feature indicates that the two positive charges have been generated from the same side of the molecule.

- [1] A. Hishikawa *et al.*, J. Chem. Phys. 128 (2008) 084302,  
R. Flammini *et al.* Phys. Rev. A 77 (2008) 044701
- [2] N. Saito *et al.*, Chem. Phys. Lett. 393 (2004) 295
- [3] R. Thissen *et al.* J. Chem. Phys. 99 (1993) 6590
- [4] S. De *et al.* Phys. Rev. A 77(2008) 022708



## Micro-solvation effects in ultrafast relaxation. Application to photochromic molecules

G. Piani, L. Poisson, B. Soep, J. M. Mestdagh

<sup>1</sup>Laboratoire Francis Perrin, CEA-CNRS URA2453, CE Saclay,  
IRAMIS/SPAM Bât 522 91191 Gif-sur-Yvette Cedex

A gas phase study of isolated molecules is a way to access their intrinsic properties and to perform direct comparison with calculations. Our concern is to unravel the dynamics of photoexcited molecules at the femtosecond timescale as it relaxes its internal energy along a reaction pathway. Time resolved photoelectron spectroscopy deserves fundamental information on the series of excited state, which is experienced by the molecule during such a relaxation process.

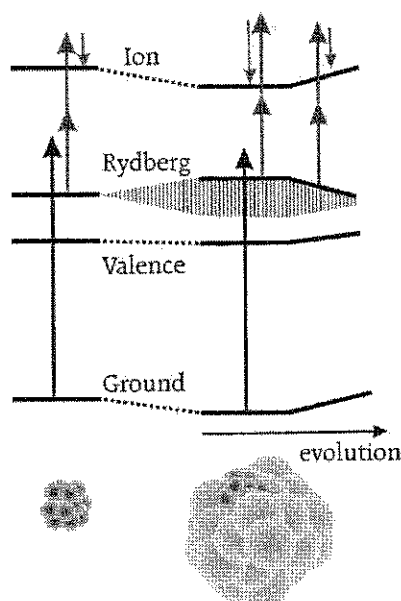


Fig 1: Solvation effects on electronics states

Study of the microsolvation effects (influence of a single or several solvent molecules) of the reaction pathway is challenging in the gas phase because the number or solvent molecules attached to the reacting system is hard to control<sup>1</sup>. Deposition of the Molecules on large argon clusters is an elegant way to turn around these difficulties

The study of microsolvation effects on relaxation dynamics of model molecules and photochromic molecules<sup>2</sup> will be presented at the conference.

- [1] Poisson, L.; Gloaguen, E.; Mestdagh, J.-M.; Soep, B.; Gonzalez, A.; Chergui, M., *J. Phys. Chem. A* **2008**, 112, (39), 9200-9210.  
[2] Poisson, L.; Raffael, K. D.; Soep, B.; Mestdagh, J. M.; Buntinx, G., *J. Am. Chem. Soc.* **2006**, 128, (10), 3169-3178.

## Forward-to-backward differential-cross-section ratio in electron-impact vibrational excitation via the $^2\Sigma_u^+$ resonance of $H_2$

G. B. Poparić<sup>1</sup>, M. Ristić<sup>2</sup>, D. S. Belić<sup>1</sup>

<sup>1</sup>Faculty of Physics, University of Belgrade, Studentski trg 12, P.O. Box 368, 11000 Belgrade, Serbia

<sup>2</sup>Faculty of Physical Chemistry, University of Belgrade, Studentski trg 12, P.O. Box 137, 11000 Belgrade, Serbia

Electron-impact vibrational excitation of the hydrogen molecule has been investigated by use of a crossed beam double trochoidal electron spectrometer. Forward and backward scattered electrons from the  $^2\Sigma_u^+$  shape resonance in the  $v=0 \rightarrow 1$  vibrational excitation channel are analyzed. These two contributions are separated by electron beam modulation and time-of-flight detection of scattered electrons. Backward electrons are additionally delayed in time by introduction of a decelerator device. The operation of this device is tested by the measurements performed on the  $^2\Pi_g$  resonance in  $N_2$  molecule and  $^2\Pi$  resonance in CO [1]. An obtained time-of-flight spectrum of electrons scattered at 0 and 180 degrees from the  $v = 1$  level excitation in  $H_2$ , at incident energy of 2.5 eV is shown in figure 1. The ratio of forward-to-backward scattered electrons is measured for the incident electron energies from 1 to 5 eV. Present results are normalized and absolute values of differential cross sections at critical angles of 0 and 180 degrees are obtained. The results of our measurements of differential cross-sections for the vibrational excitation at incident energy of 2.5 eV with results of other authors are shown in figure 2.

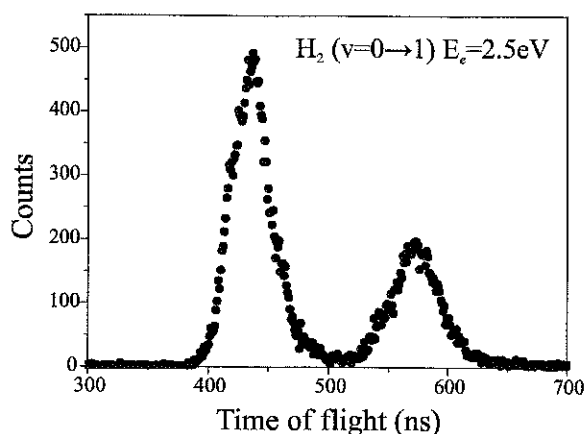


Figure 1. Time-of-flight spectrum

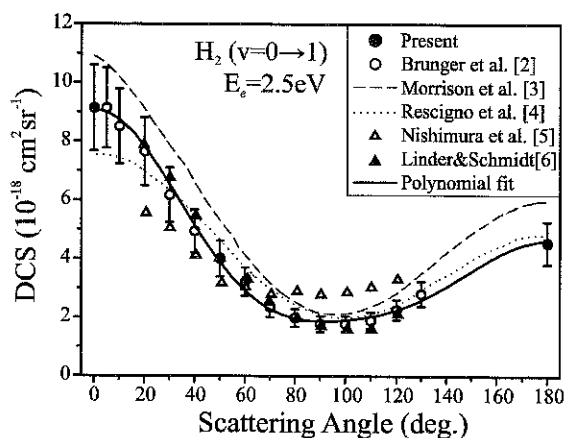


Figure 2. Differential cross sections spectra

- [1] G. B. Poparić, S. M. D. Galijaš, D. S. Belić, Phys. Rev. A, 70 (2004) 024701  
 [2] M. J. Brunger, S. J. Buckman, D. S. Newman, D. T. Alle, J. Phys. B, 24 (1991) 1435  
 [3] M. A. Morrison, R. W. Crompton, B. C. Saha, Z. L. Petrovic, Z. Aust. J. Phys. 40 (1987) 239  
 [4] T. N. Rescigno, B. K. Elza, B. H. Lengsfeld, B. J. Phys. B 26 (1993) L567  
 [5] H. Nishimura, A. Danjo, H. Sugahara, Phys. Soc. Japan 54 (1985) 1757  
 [6] F. Linder, H. Schmidt, Naturforsch. 16a (1971) 1603



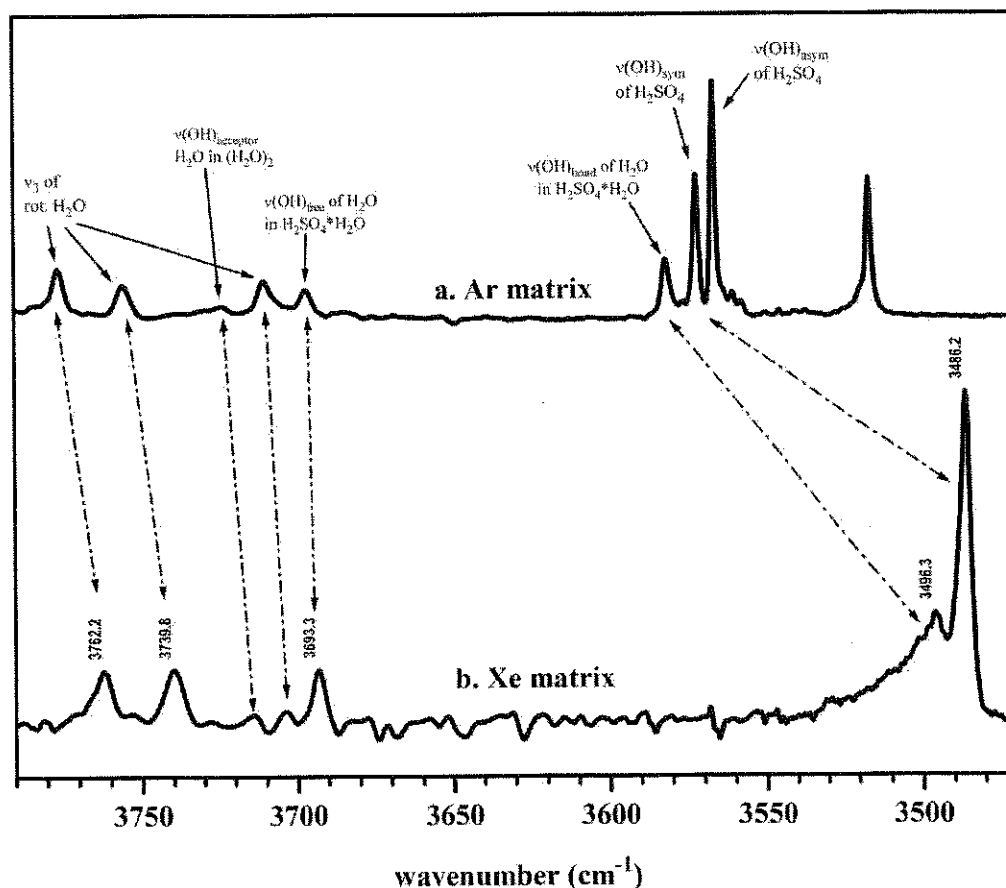
## Hydrogen Bonding in Solid Xenon. A Matrix Isolation Study

A. Loewenschuss<sup>1</sup>, M. Rozenberg<sup>1</sup>, and C.J. Nielsen<sup>2</sup><sup>1</sup>Institute of Chemistry, The Hebrew University of Jerusalem, Jerusalem, Israel 91904; loewena@huji.ac.il<sup>2</sup>Centre for Theoretical and Computational Chemistry, Department of Chemistry, University of Oslo, 1033 Blindern, N-0315 Oslo, Norway. c.j.nielsen@kjemi.uio.no

For argon and xenon matrices, in the same matrix layer the  $\nu(\text{OH})$  stretches of highly acidic species ( $\text{H}_2\text{SO}_4$  and  $\text{H}_2\text{SO}_4 \cdot \text{H}_2\text{O}$ ) show distinctly larger red shifts as opposed to species of lower acidity or of modes which do not directly involve the O-H bond. (Figure 1)

A correlation is obtained of the spectral shifts with interaction energies, empirically estimated from the acidic properties attributed to a variety of molecular species. The spectral interpretation and empirical calculations are complemented by B3LYP and MP2 model calculations of the interaction energies and fundamental modes of vibration.

The hydrogen bonding observed between acidic species and Xe atoms is considered of relevance to the formation of xenon hydrides in irradiated matrices.



## Molecular photoionization spectroscopy with synchrotron radiation

M. Coreno<sup>1,3</sup>, K. C. Prince<sup>2,3</sup>

<sup>1</sup> *CNR-IMIP, sez Montelibretti 00016 Monterotondo S. (RM)*

<sup>2</sup> *Sincrotrone Trieste ScpA, Basovizza Area Science Park, I-34149 Trieste, Italy,*

<sup>3</sup> *GasPhase beamline, Lab. Elettra, I-34149, Trieste, Italy*

Synchrotron radiation in the VUV and Soft-X-Ray energy region is a valuable tool for the investigation of electronic properties of isolated systems. The flux and energy resolution achievable at third generation facilities, like the Gas Phase beamline of the Elettra storage ring (Trieste, Italy) [1], enable studies of inner-shell electron excitation in experiments that have been so far traditionally characterized by intrinsic low signal level due to the low density of the targets like biomolecules [2] and clusters [3].

Recent examples will be discussed, where photoionization techniques have been used in investigations on gas phase molecular targets of increasing complexity, ranging from molecules of biological interest, to metal containing systems.

[1] K.C. Prince, et al *J. Synch. Rad.* 5 (1998) 565-568 .

see also at <http://www.elettra.trieste.it/beamlines/GAPH/>

[2] V. Fever, O. Plekan, R. Richter, M. Coreno , K.C. Prince, V. Carravetta, *J. Phys. Chem. A* 113 (2009) 10726-10733

[3] P. Piseri, T.Mazza, G.Bongiorno, M. Devetta, M.Coreno, P.Milani, *J. Electron Spectr. and Related Phen.* 166-167(2008) 28-37.



## Hyperfine structure of rotational spectra: interplay of experiment and theory

C. Puzzarini<sup>1</sup>, G. Cazzoli<sup>1</sup>, J. Gauss<sup>2</sup>

<sup>1</sup>Dipartimento di Chimica "G. Ciamician", Università di Bologna, Via F. Selmi 2, I-40126 Bologna, Italy

<sup>2</sup>Institut für Physikalische Chemie, Universität Mainz, D-55099 Mainz, Germany

The determination of (hyper)fine parameters such as quadrupole-coupling, spin-spin coupling, and spin-rotation constants is one of the aims of high-resolution rotational spectroscopy. These parameters are relevant not only from a spectroscopic point of view, but also from a physical and/or chemical viewpoint, as they might provide detailed information on the chemical bond, structure, etc. Furthermore, the hyperfine structure of rotational spectra is so characteristic that its analysis may help in assigning the spectra of unknown species [1]. However, the experimental determination of hyperfine constants can be a challenge not only for actual problems in resolving hyperfine structures themselves, but also due to the lack of reliable estimates or the complexity of the hyperfine structure itself. It is thus important to be able to rely on good predictions for such parameters, which can nowadays be provided by quantum-chemical calculations [2]. In fact, the aim of this presentation is to show how fruitful the interplay between experiment and theory can be in this field. A number of examples will be presented to illustrate this interplay in the investigation of hyperfine structures of rotational spectra. Those include isotopic species of water and formic acid as well as heavy-element-containing species, as CH<sub>2</sub>FI.

From an experimental point of view, we focus on the Lamb-dip technique. This technique allows to improve the resolving power in the millimeter- and submillimeter-wave frequency range by at least one order of magnitude, thus making it possible to perform sub-Doppler measurements as well as to resolve narrow hyperfine structures. In particular, the high resolution that can be achieved by our experimental set up will be demonstrated by a few representative examples [3,4].

Concerning theory, the theoretical background for the required quantum-chemical calculations will be briefly reviewed, and a particular emphasis on the computational requirements will be given [2]. It will be demonstrated that high-level calculations can provide very reliable values for hyperfine parameters (quadrupole coupling constants, spin-rotation tensors, spin-spin couplings, etc.) and how theoretical predictions are often essential for a detailed analysis of the hyperfine structure of the recorded spectra [5].

[1] G. Cazzoli, C. Puzzarini, A. Gambi, *J. Chem. Phys.* 120 (2004) 6495-6501

[2] C. Puzzarini, J. F. Stanton, J. Gauss, *Int. Rev. Phys. Chem.* 29 (2010) 273-367

[3] G. Cazzoli, C. Puzzarini, *J. Mol. Spectrosc.* 226 (2004) 161-168

[4] G. Cazzoli, L. Dore, C. Puzzarini, *Astron. Astrophys.* 507 (2009) 1707-1710

[5] C. Puzzarini, G. Cazzoli, M. E. Harding, J. Vázquez, J. Gauss, *J. Chem. Phys.* 131 (2009) 234304/1-11.



## The shape of biomolecules and their weakly bound molecular complexes revealed by microwave spectroscopy

S. Melandri<sup>1</sup>, A. Maris<sup>1</sup>, A. Merloni<sup>1</sup>, B. M. Giuliano<sup>2</sup>, L. B. Favero<sup>3</sup>, W. Caminati<sup>1</sup>

<sup>1</sup> "G. Ciamician" Department of Chemistry, University of Bologna, Via Selmi 2, I-40126 Bologna, Italy

<sup>2</sup> Departamento de Química, Universidade de Coimbra, 3004-535 Coimbra, Portugal

<sup>3</sup> I.S.M.N.-C.N.R., Via Gobetti 101, I-40129 Bologna, Italy

2-Phenylethylamine (PEA) is a prototype system for the study of the conformational behavior of the adrenergic neurotransmitters including: dopamine, noradrenaline and adrenaline and various other substances such as tyramine, serotonin, amphetamine and the ephedras. The common structural feature of these substances is the presence of the ethylamino group in the side chain which, due to its flexibility, gives rise to a complex conformational surface which contains several minima at relatively low energy.

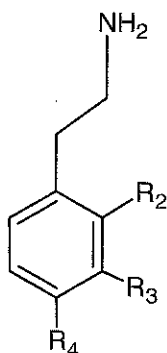
For the isolated molecule the shape is the result of the intramolecular interactions, which in the case of phenylethylamine are dominated by the presence of the aromatic ring, the ethylamino side chain and the possible substituents on the aromatic ring. Substitution with fluorine atoms is particularly interesting as it is used in medicinal chemistry to modulate the physical chemical physics properties of the molecule.

When the molecules are in different environments, such as in solution or when interacting with their receptors, the shape is the result of a delicate balance between intra and intermolecular interactions, and an understanding of this balance is particularly important for bioactive molecules.

As examples, we report the rotational spectrum of the 1:1 molecular adduct between 2-phenylethylamine and water (PEA-W; normal and H<sub>2</sub><sup>18</sup>O species) and various fluoro substituted phenylethylamines by Free Jet Absorption Millimeter Wave spectroscopy (FJAMMW) and Molecular Beam Fourier Transform (MB-FTMW). The results have been rationalized and confirmed with the help of *ab initio* calculations.

In the case of PEA-W, the dominant spectrum belongs to the structure where the PEA moiety is in the most stable *gauche* conformation and the water molecule is hydrogen bound to the nitrogen lone pair. The orientation of the water molecule is such that the oxygen atom is almost equidistant (ca 2.5 Å) from the closest methylenic and aromatic hydrogen atoms.

From the theoretical approach and from the observed microwave spectrum we report evidence of the effect of substitution in the different positions for the three fluoro phenylethylamines.



R<sub>2</sub>, R<sub>3</sub>, R<sub>4</sub>=H; 2-phenylethylamine

R<sub>2</sub>= F; R<sub>3</sub>, R<sub>4</sub>=H; 2-Fluoro-2-phenylethylamine

R<sub>3</sub>= F; R<sub>2</sub>, R<sub>4</sub>=H; 3-Fluoro-2-phenylethylamine

R<sub>4</sub>= F; R<sub>2</sub>, R<sub>3</sub>=H; 4-Fluoro-2-phenylethylamine

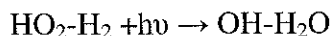


## The vibration structure of OH radical and OH-H<sub>2</sub>O complex: A Matrix Isolation Study

P. R. Joshi, L. Krim

*UMR 7075; Laboratoire de Dynamique, Interactions et Réactivité (LADIR); Université Pierre et Marie Curie, Bât F74; 3eme étage; 4 place, Jussieu; 75252 Paris, France*

Hydroxyl radical, 'the detergent of atmosphere', the title is acquired due to capability of transformation of trace component present in atmosphere mainly troposphere into water soluble forms and also plays vital role in chemistry of the interstellar medium. The infrared spectra of OH radical isolated in solid neon have been investigated by Fourier Transform infrared spectroscopy (FTIR). OH monomer was prepared by microwave discharge of a mixture of water and neon gas at different concentrations prior to deposition on the cold mirror at 5 K. The microwave discharge of H<sub>2</sub>O/Ne system is remarkable due to its propensity to form OH radical and other species like H<sub>2</sub>, HO<sub>2</sub>, OH-HO<sub>2</sub>, OH-H<sub>2</sub>O and (OH)<sub>n</sub>-H<sub>2</sub>O and IR spectroscopy reveals a variety of phenomena far from being fully understood. OH concentration studies, D/H isotopic substitution and subsequent annealing leads to the characterization of the different species trapped in the neon matrix. All vibrationnal modes of OH-H<sub>2</sub>O complex have been detected. The presence of species such as H<sub>2</sub> and HO<sub>2</sub> after matrix deposition led us to carry subsequent UV photolysis of our samples where the complex OH-H<sub>2</sub>O may also be formed by following reaction:



## Conformational Stability of some Organoamines by Utilizing Variable Temperature Infrared Spectra of Rare Gas Solutions

J. R. Durig, A. Ganguly, S. S. Panikar, I. D. Darkhalil, T. Iwata

Department of Chemistry, University of Missouri-Kansas City, Kansas City, MO 64110, USA

The variable temperature infrared spectra of krypton and/or xenon solution have been utilized to obtain the conformational stability of isopropylamine (two conformers), 2,2-difluoroethylamine (five possible conformers) and ethylenediamine (ten possible conformers). To obtain reliable enthalpy determinations from variable temperature infrared spectra it is essential to have confident assignments for the possible forms present particularly in the spectral region where the conformer pairs will be selected for the enthalpy determination. By utilizing the *ab initio* predicted intensities, fundamental frequencies and gas phase contours as well as data from xenon or krypton solutions with the sharp bands made it possible to assign a large number of closely spaced fundamentals. The infrared spectra were predicted from the MP2(full)/6-31G(d) calculations and scaled frequencies were used together with a Lorentzian function to obtain the simulated spectra. A very large number of fundamentals in the "fingerprint" region were assigned for the two conformers of isopropylamine as well as for three conformers of the other two molecules. The variable temperature infrared spectra of krypton or xenon solutions have been utilized to obtain the enthalpy differences between the two conformers of isopropylamine and the three conformers of 2,2-difluoroethylamine and ethylenediamine. These experimental results will be compared to the values predicted from *ab initio* calculations from a variety of basis sets.

We [1] have shown that *ab initio* MP2/6-311+G(d,p) calculations predict the structural parameters for fifty substituted hydrocarbons for the carbon-hydrogen distances better than 0.002 Å compared to the experimentally determined  $r_0$  values from isolated CH stretching frequencies [2] which agree with previously determined values from earlier microwave studies. Therefore, all of the carbon-hydrogen distances can be taken from the MP2/6-311+G(d,p) predicted values for the three molecules. We have also shown [3] that we can obtain good structural parameters by adjusting the structural parameters obtained from the *ab initio* calculations to fit the rotational constants obtained from microwave experimental data. By utilizing the previously reported microwave rotational constants for isopropylamine [4] and the two forms of 2,2-difluoroethylamine [5] and ethylenediamine [6] along with *ab initio* MP2(full)/6-311+G(d,p) predicted structural values, adjusted  $r_0$  parameters for the heavy atoms have been obtained for these three molecules. The results will be discussed and compared to the corresponding properties of some similar molecules wherever possible.

[1] J. R. Durig, K. W. Ng, C. Zheng, S. Shen, Struct. Chem.15 (2004) 149.

[2] D. C. McKean, M. W. Mackenzie, A. R. Morrison, J. Mol. Struct. 116 (1984) 331.

[3] G. A. Guirgis, X. Zhu, Z. Yu, J. R. Durig, J. Phys. Chem. A 104 (2000) 4383.

[4] S. C. Mehrotra, L. L. Griffin, C. O. Britt, J. E. Boggs, J. Mol. Spectrosc. 64 (1977) 244.

[5] K. M. Marstokk, H. Mollendal, Acta Chem. Scand. A 36 (1982) 517.

[6] K. M. Marstokk, H. Mollendal, J. Mol. Struct. 49 (1978) 221.





## Small Water/Alcohol Clusters: A Combined Raman- and FTIR-Jet Study

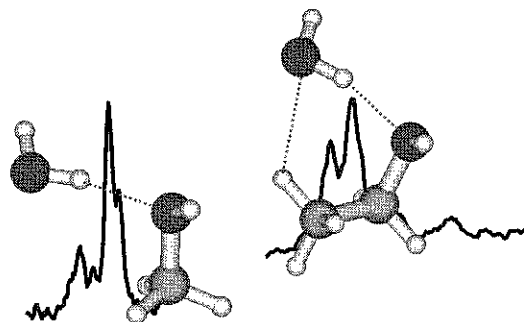
M. Nedić, T. N. Wassermann, R. W. Larsen, M. A. Suhm

*Georg-August-Universität Göttingen, Institut für Physikalische Chemie, Tammannstr. 6, 37077 Göttingen, Germany*

Water/alcohol mixtures exhibit several physical anomalies which were extensively studied on the macroscopic scale [1]. To rationalize the origin of these peculiarities, a fundamental understanding of their microscopic properties, like the constitution and conformation of small clusters, is crucial. In this context, mixtures of water with methanol or ethanol are the simplest and most interesting model cases which are accessible to accurate quantum chemical investigations. Ethanol represents the first case where internal conformational degrees of freedom influence the cluster formation.

In this study we prepare and isolate mixed dimers and trimers at low temperatures in supersonic jet expansions and investigate them by spontaneous Raman scattering [2]. FTIR spectra assist the assignment due to partially complementary selection rules [3, 4]. Mixtures of deuterium oxide with methanol-OD ( $\text{CH}_3\text{OD}$ ) were measured for a closer analysis of dynamic effects.

Relaxation studies show that water takes the role of a hydrogen bond donor in the mixed water/alcohol dimers [5]. In case of the water/methanol dimer a splitting due to an interchange of the water donor between the (equivalent) methanol acceptor lone pairs is observed. Furthermore, we can show that the mixed water/ethanol dimer prefers ethanol in a gauche conformation as the hydrogen bond acceptor although this is not the most stable conformation in the isolated ethanol molecule. This represents a simple case of adaptive aggregation. In mixed trimers a strongly negative mixing enthalpy, a property well known from bulk solutions [6, 7, 8], is also reflected on the microscopic scale.



- [1] F. Franks, and D. J. G. Ives, *Q. Rev. Chem. Soc.* 20 (1966) 1-44
- [2] P. Zielke, and M. A. Suhm, *Phys. Chem. Chem. Phys.* 8 (2006) 2826-2830
- [3] R. W. Larsen, P. Zielke, and M. A. Suhm, *J. Chem. Phys.* 126 (2007) 194307
- [4] T. N. Wassermann, P. Zielke, J. J. Lee, C. Cézar, and M. A. Suhm, *J. Phys. Chem. A* 111 (2007) 7437-7448
- [5] M. Nedić, T. N. Wassermann, Z. Xue, P. Zielke, and M. A. Suhm, *Phys. Chem. Chem. Phys.* 10 (2008) 5953-5956
- [6] J. A. Larkin, *J. Chem. Thermodynamics* 7 (1975) 137-148
- [7] A. J. Easteal, *J. Chem. Thermodynamics* 17 (1985) 69-82
- [8] D. Gonzalez-Salgado, and I. Nezbeda, *Fluid Phase Equilib.* 240 (2006) 161-166



## Conformational Stability, Structural Parameters and Vibrational Assignment from Variable Temperature Infrared Spectra of Krypton Solution of Ethylisocyanate

S. X. Zhou, J. R. Durig

Department of Chemistry, University of Missouri–Kansas City, Kansas City, MO 64110 USA

Infrared spectra of the gas, variable temperature studies of krypton solution and solid have been investigated. These spectroscopic data indicate two conformers in the fluid states which are the *cis* and *trans* forms with a large proportion of molecules in the gas phase executing nearly free internal rotation of the NCO group. From variable temperature at  $-110$  to  $-155^{\circ}\text{C}$ , studies of krypton solutions were carried out and by using two conformer pairs, an enthalpy difference of  $100 \pm 10 \text{ cm}^{-1}$  ( $1.20 \pm 0.12 \text{ kJ/mol}$ ) was obtained with the *cis* conformer the more stable form. *Ab initio* calculations have been carried out by the perturbation method to the second order (MP2) with full electron correlation with the basis sets 6-311+G(2d,2p) and larger. The barrier at the *cis* position ranged from a low value of  $11 \text{ cm}^{-1}$  to a high value of  $31 \text{ cm}^{-1}$  with a value of  $19 \text{ cm}^{-1}$  from the largest basis set of cc-PVQZ indicating that the *gauche* well is probably so shallow that it does not contain a bound vibrational state. This results in the *cis* conformer as the most stable form which is consistent with the experimental rotational [1] and vibrational data [2]. By utilizing the previously reported microwave rotational constants [1] with the structural parameters predicted by the *ab initio* MP2(full)/6-311+G(d,p) calculations, adjusted  $r_0$  structural parameters have been obtained for the *cis* [*trans*] form. The determined heavy atom parameters are:  $r(\text{C}=\text{N}) = 1.211(5)$  [ $1.212(5)$ ],  $r(\text{C}=\text{O}) = 1.167(5)$  [ $1.166(5)$ ],  $r(\text{C}-\text{N}) = 1.448(5)$  [ $1.452(5)$ ],  $r(\text{C}-\text{C}) = 1.516(5)$  [ $1.513(5)$ ] Å for the distances and angles of  $\angle\text{CCN} = 112.6(5)$  [ $109.6(5)$ ],  $\angle\text{CNC} = 137.5(5)$  [ $136.1(5)$ ]. The centrifugal distortion constants, dipole moments, conformational stability, vibrational frequencies, infrared intensities and Raman activities have been predicted from *ab initio* calculations and compared to experimental quantities when available. These results are compared to the corresponding quantities of some similar molecules.

[1] T. Sakaizumi, O. Ohashi, K. Ushida, O. Ohashi, I. Yamaguchi, Bull. Chem. Soc. Jpn. 49 (1976) 2908-1912

[2] J. F. Sullivan, D. T. Durig, J. R. Durig, S. Craddock, J. Phys. Chem. 91 (1987) 1770-1778



## 30-fs hole-transfer dynamics in polymer/PCBM bulk heterojunction

A. A. Bakulin<sup>1</sup>, J. C. Hummelen<sup>2</sup>, P. H.M. van Loosdrecht<sup>1</sup>, M. S. Pshenichnikov<sup>1</sup><sup>1</sup>Zernike Inst. for Advanced Materials, Univ. of Groningen, Nijenborgh 4, 9747 AG Groningen, The Netherlands<sup>2</sup>Stratingh Inst. for Chemistry, Univ. of Groningen, Nijenborgh 4, 9747 AG Groningen, The Netherlands

Plastic photovoltaic devices are promising candidates for renewable energy sources [1]. In the most efficient plastic solar cells, light is harvested and converted to electricity in a “bulk-heterojunction” active layer, consisting of a mixture of organic electron donor and acceptor materials. For the electron donor, various types of conjugated polymers can be used, while the overwhelming majority of the photovoltaic blends utilizes the same soluble fullerene derivative, PCBM, as an acceptor which makes it the most used material in the organic photovoltaics.

The most widely studied charge generation process in polymer/PCBM blends is the ultrafast electron transfer (ET) after polymer excitation [2]. However, apart from the absorption by the polymer, the methanofullerenes also have a substantial contribution into the overall blend absorption in the blue, red, and even visible parts of the solar spectrum. Optical excitation of PCBM in PCBM:polymer blends leads to the creation of an exciton on the PCBM molecule, which can subsequently dissociate into charge excitations through the so-called hole-transfer (HT) process (Fig.1). The HT time and efficiency are thought to be intimately related to the structure of donor and acceptor valence bands and, in particular, to the polymer-PCBM HOMO-HOMO energy offset. Despite the obvious fundamental interest and practical importance for solar cell applications, HT dynamics have received surprisingly little attention so far.

Here we employ ultrafast visible-pump/IR-probe spectroscopy together with AFM microscopy to study the hole dynamics in light-harvesting of MDMO-PPV:PCBM blends. For the first time, we directly resolve the 30-fs hole-transfer following PCBM excitation, and show that PCBM exciton harvesting depends on the blend morphology [3]. The obtained results are instrumental for future design of fullerene-derivatives-based photovoltaic devices.

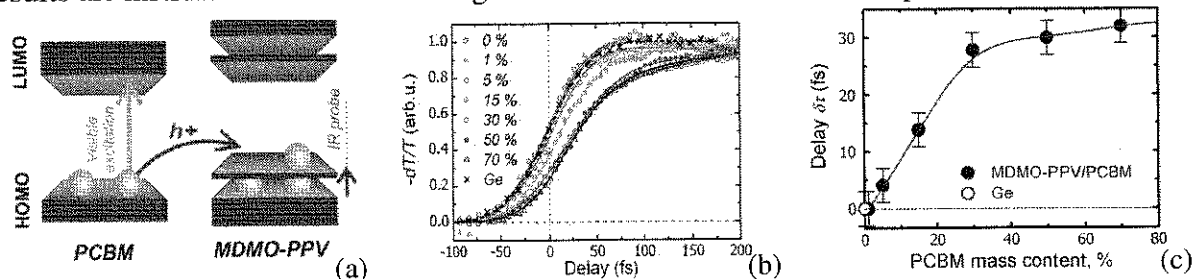


Fig. 1. (a) Schematics of the energy diagrams for the hole-transfer process in the PPV:PCBM bulk heterojunction and its spectroscopic interrogation. The excitation wavelength is tuned into the PCBM absorption band at 630 nm while the probe wavelength corresponds to the low-energy hole-associated band of the MDMO-PPV at 3  $\mu\text{m}$ . (b) PIA transients for MDMO-PPV:PCBM films with different PCBM weight fractions. Crosses show instantaneous response obtained from the Ge thin film for the calibration purposes. (c) The delay of PIA response at half maximum of the amplitude as a function of PCBM concentration.

[1] G. Dennler, M. C. Scharber, C. J. Brabec, *Advanced Materials* 21 (2009) 1323

[2] C. J. Brabec, G. Zerza, G. Cerullo, S. De Silvestri, S. Luzzati, J. C. Hummelen, S. Sariciftci, *Chem. Phys. Lett.* 340 (2001) 232

[3] A. A. Bakulin, J. C. Hummelen, M. S. Pshenichnikov, P. H. M. van Loosdrecht, *Advanced Functional Materials* (2010), to be published

## Two-dimensional coherent electronic spectroscopy of electron-phonon coupling

T. Mančal<sup>1</sup>, F. Šanda<sup>1</sup>, N. Christensson<sup>2</sup>, V. Butkus<sup>1,3</sup>, J. Olšina<sup>1</sup>, V. Balevicius Jr.<sup>1,3</sup>, L. Valkunas<sup>3,4</sup>

<sup>1</sup>*Faculty of Mathematics and Physics, Charles University in Prague Ke Karlovu 5, 121 16 Prague 2, Czech Republic*

<sup>2</sup>*Dep. Fakultät für Physik, Universität Wien, Sensengasse 8, Wien 1090, Austria*

<sup>3</sup>*Department of Theoretical Physics, Faculty of Physics of Vilnius University Sauletekio Avenue 9, build. 3, LV-10222 Vilnius, Lithuania*

<sup>4</sup>*Institute of Physics, Savanoriu Avenue 231, LV-02300 Vilnius, Lithuania*

Two-dimensional (2D) coherent electronic spectroscopy has become an important tool for probing excited state dynamics in photo-induced processes such as photosynthesis. The aim of this contribution is to discuss how the evolution of 2D spectra reveals details of electron-phonon coupling.

We study theoretically two- and three electronic level systems coupled explicitly to some effective vibrational degrees of freedom (DOF). Standard response function theory of non-linear spectra is able to treat systems interacting with a boson bath exactly, as long as this interaction leads to pure dephasing only [1]. The central quantity of the theory is the so-called energy gap correlation function. Once a general relaxation between electronic states is allowed, a direct calculation of the spectroscopic signals from density matrix equation of motion based on the same correlation function is necessary. We will discuss inherent limitation of this approach, which forces neglecting of the bath evolution memory between interaction of the system with exciting light, and thus prevents exact calculation of the response from equation of motion even for a two-level system. We will present a theory based on parametric projection operators to overcome this limitation [2].

Motivated by experiments on bacterial photosynthetic antennae [3,4] we apply the method of parametric projection operators to derive equations of motion for a complex of molecules (chromophores) coupled to each other by electrostatic resonance interaction. We apply the method in the limits of weak and strong resonance interaction. The case of weak resonance interaction allows for the strong coupling treatment of the system bath interaction [5], and enables to utilize the full strength of the parametric projector method. In case of the strong resonance coupling, the system-bath interaction is treated perturbatively, but some corrective terms that describe the memory of the bath evolution can still be derived.

We will present calculations of 2D spectra and electronic state dynamics for model systems consisting of several chromophores interacting with boson bath in order to demonstrate subtle effects of the system bath interaction on the measured time dependent 2D line shapes. Our results enable to link electron-phonon coupling parameters with the characteristic features of the ordinary 2D spectra and the recently introduced Double Quantum 2D spectra.

[1] R. Doll, D. Zueco, M. Wubs, S. Kohler, P. Hanggi, *Chem. Phys.* 347 (2008) 243

[2] T. Mančal, F. Šanda, in preparation

[3] D. Zigmantas, E. L. Read, T. Mančal, T. Brixner, A. T. Gardiner, R. J. Cogdell, G. R. Fleming, *P. Natl. Acad. Sci. USA* 103 (2006) 12672

[4] G. S. Engel, T. R. Calhoun, E. L. Read, T. K. Ahn, T. Mančal, Y. -C. Cheng, R. E. Blankenship, G. R. Fleming, *Nature* 446 (2007) 782

[5] T. Mančal, V. Balevicius Jr., L. Valkunas, *New J. Phys.* (2010), submitted



## Mixed numerical/analytic solution of the anharmonic vibrational problem for a polyatomic molecule using high orders of canonical perturbation theory

S.V. Krasnoshchekov, E.V. Isayeva, N.F. Stepanov

*Chemistry Department, Moscow State University, Leninskiye Gory, 119991, Moscow, Russia*

For a polyatomic molecule, second-order canonical perturbation theory (CPT2) [1] expresses spectroscopic constants such as  $\omega_e$  and  $\omega_e x_e$  in the form of analytical expressions using parameters of the original vibrational Hamiltonian and readily supports the calculation of energy levels for fundamentals, overtones and combination bands. The problem remains that the treatment of resonances is complicated and analytic expressions for spectroscopic constants for higher orders of perturbation theory are almost impossible to deduce.

A powerful technique of using ladder operators significantly simplifies the procedure of canonical transformations for high orders of perturbation theory [2]. Combination of this technique with the one of normal ordering of operators allows developing an efficient computational algorithm for solving the anharmonic problem for a polyatomic molecule [3,4]. Within this method, the ladder operator representation of the transformed Hamiltonian is preserved during the whole algorithmic procedure until the stage of evaluation of diagonal matrix elements, while numerical coefficients are kept as real numbers.

In our Fortran computer implementation of the general scheme suggested by Sibert [3,4], we lifted some limitations of the original program, including the maximum size of a molecule. Evaluation of vibrational transition probabilities in IR and Raman spectra could be efficiently accomplished using transformation S-functions obtained during canonical transformations. This technique allows obtaining reliable values of vibrational intensities in IR and Raman spectra in high orders of perturbation theory.

In the traditional way of conducting CPT2 calculations using analytical formulas, the resonances are treated using a simple variational procedure, for which matrix elements of first (Fermi-type) and second-order (Darling-Dennison type) resonances are required. Analytical expressions for the latter ones are quite difficult to evaluate free of errors [5]. In the framework of the method employed by us, it is straightforward to introduce the uniform procedure of both detecting resonances, taking them into account in the final variational procedure, and presenting the final perturbative Hamiltonian in the form of a sum of the main diagonal Dunham-type expansion in powers of  $(v_r + 1/2)$  plus resonance-type expansions of the special general form, the number of which is equal to the number of resonances.

It is shown that for molecules studied the coefficients of perturbative Dunham-type Hamiltonians at 4th and 6th orders of CPT conform to the same rules as for diatomic molecules. Namely, at 4th order coefficients  $Y_0$  and  $\omega_e x_e$  coincide with ones at CPT2 level, while at 6th order coefficients  $\omega_e$  and  $\omega_e y_e$  coincide with ones at CPT4 level.

The advantages and limitations of this method are illustrated by results of vibrational analysis of several molecules, including *trans*- and *cis*-1,2-difluoethylene.

[1] H.H. Nielsen, Encyclopedia of Physics, Ed. S.Flügge, XXXVII/1 (1959) 173-313

[2] Y.S.Makushkin, V.G. Tyuterev, "Methods of Perturbations and Effective Hamiltonians in Molecular Spectroscopy", Novosibirsk (1984)

[3] E.L. Sibert III, J. Chem. Phys., 88 (1988) 4378-4390

[4] E.L. Sibert III, Comput. Chem. Commun., 51 (1988) 149-160

[5] D.A. Matthews, J. Vázquez, J.F. Stanton, Mol. Phys., 105 (2007) 2659-2666



**Theoretical study of proton tunneling in the excited state of tropolone**

M. J. Wójcik, Ł. Boda and M. Boczar

*Faculty of Chemistry, Jagiellonian University, 30-060 Kraków, Ingardena 3, Poland*

Ab initio CIS/6-311++G(d,p) calculations of geometry and vibrational frequencies have been carried out in the  $\tilde{A}$  state of tropolone. The grids of potential energy surfaces along the coordinates of high frequency-tunneling vibration and the low-frequency coupled vibration have been calculated. Two-dimensional model potentials, formed from symmetric mode coupling potential and squeezed double well potential, have been fitted to the calculated potential energy surfaces and used to analyze proton dynamics. The tunneling splittings for different vibrationally excited states have been calculated and compared with the available experimental data. The model potential energy surfaces, based on the CIS/6-311++G(d,p) calculations, give good estimation of the tunneling energy splittings in the vibrationally ground and excited states of tropolone, and explain monotonic decrease in tunneling splittings with the excitation of low-frequency out-of-plane modes and increase of the tunneling splittings with the excitation of low-frequency planar modes.



## DFT Calculation of Low Frequency Vibrational Modes of Polypeptides Consisting of L- and D-Alanine Residues

K. Itoh

Waseda University, 3-43-8, Sekimachi-kita, Nerimaku, Tokyo 177-0051, Japan

Recently, terahertz (THz) time-domain spectroscopy has been developed and low-frequency vibrational modes observed by the method are expected to give new insight into conformational states and dynamics of polypeptides and proteins. In this respect it is of importance to know how the low-frequency vibrational modes reflect secondary and tertiary structures of polypeptide chains. Although normal modes of globular proteins such as bovine pancreatic trypsin inhibitor (BPTI) have been calculated [1,2], the calculations were based on experimental parameters and their reliability have not always been confirmed by experimental data. On the other hand, *ab initio* quantum mechanical calculation performed by a density functional theory (DFT) well reproduces vibrational spectra of molecules and becomes one of the useful methods for analyzing the spectra. In a previous paper [3] we applied the DFT method based on the B3LYP/6-31G level to calculate the far-IR spectra in the  $700 - 0 \text{ cm}^{-1}$  region for  $\alpha$ -helical L-alanine oligomer models with the amino and carboxyl ends blocked by  $\text{CH}_3\text{CO}$  and  $\text{NHCH}_3$  groups ( $\text{CH}_3(\text{CONHC}_\alpha\text{H}(\text{CH}_3))_{n-1}\text{CONHCH}_3$ ,  $n = 8 - 24$ ); the results for the model with  $n = 24$  are in a reasonable agreement with the far-IR dichroic spectra of an  $\alpha$ -helical poly-L-alanine film in the  $700 - 60 \text{ cm}^{-1}$  region [4], indicating the high reliability of the DFT calculation. The THz time-domain spectra in the  $150 - 5 \text{ cm}^{-1}$  region were also measured for poly-L-alanines, and IR bands appearing in this region could be related to the average lengths of the  $\alpha$ -helical segments in the samples.

In the present paper the DFT calculation was extended to oligomer models consisting of L- and D-alanine residues and the results were compared with the far-IR spectra of poly-DL-alanines with various D/L mixing ratios ( $x = \text{D}/(\text{L}+\text{D})$ ,  $0.03 - 0.5$ ). The models with 24 peptide bonds are designated by positions taken by the D-alanine residues such as (12- and 13-D)<sub>24</sub>, where the D-alanine residue takes the 12th and 13th positions from the amino end. The calculations have indicated so far the following points. (i) The right-handed  $\alpha$ -helical oligomer models, (12-D)<sub>24</sub>, (12-, 13- and 14-D)<sub>24</sub> and (4-, 8-, 12, 16- and 20-D)<sub>24</sub> give a spectral feature below  $200 \text{ cm}^{-1}$ , which is similar to the feature calculated for the  $\alpha$ -helical model consisting of the L-alanine residues ( $n = 24$ ). The result indicates that the far-IR spectra in this region reflect the  $\alpha$ -helical backbone structure irrespective of the side chain configurations. (ii) The spectra in the  $700 - 200 \text{ cm}^{-1}$  region calculated for the models, (12-D)<sub>24</sub> and (4-, 8-, 12, 16- and 20-D)<sub>24</sub>, give IR bands at 585, 489 and  $434 \text{ cm}^{-1}$ , which are ascribable the D-alanine residues incorporated into the right-handed  $\alpha$ -helix. The spectra in the  $700 - 200 \text{ cm}^{-1}$  observed for poly-DL-alanines consist of the corresponding bands at 580, 478 and  $428 \text{ cm}^{-1}$  and IR bands observed for the  $\alpha$ -helical poly-L-alanine. Although poly-DL-alanine ( $x = 0.5$ ) has been considered to exist in a so-called random coil state due to the amide I band observed at  $1660 \text{ cm}^{-1}$ , the above-mentioned results suggest that it is more reasonable to consider that the backbone of the sample is virtually a composite of the right- and left handed  $\alpha$ -helices, which comprise mainly the L- and D-residues, respectively.

[1,2] J. Smith *et al.*, J. Chem. Phys. 93 (1990), 2974 and A. Roitberg *et al.* Science 268 (1995), 1319.

[3] K. Itoh *et al.*, 5th International Conference of Advanced Vibrational Spectroscopy, Melbourne, Australia, July, 2009, O4.

[4] K. Itoh and T. Shimanouchi, Biopolymers 9 (1970), 383.



## Quantum-mechanical analysis of intensity distribution in resonance hyper Raman spectra of polyatomic molecules

T. Burova, A. Anashkin

*Saratov state university, Astrakhanskaya str.83, 410026, Saratov, Russia*

It's proposed to exceed the quantum-mechanical method previously used for calculation of intensity distribution in electron-vibrational absorption spectra and resonance Raman (RR) spectra to analysis of resonance hyper Raman (RHR) spectra of polyatomic molecules. It makes possible to describe all these spectra from one point of view with the same set of parameters. The main steps in realizing the quantum-mechanical method [1] are to obtain vibrational characteristics including frequencies and Dushinsky's parameters; to obtain electronic characteristic including excitation energies, density matrix, matrix elements of electron-vibrational interaction; and, finally, to calculate the intensity distribution in RHR spectrum.

Calculations of relative line intensities in resonance hyper Raman spectra of fluorobenzene, chlorobenzene and adenine were made in Herzberg-Teller approximation as well as in Frank-Condon approximation. The results obtained in different approximations gave an opportunity to make some consequences. 1) The Frank-Condon data do not correspond to the experimental values for the most intensive lines. 2) The intensity distribution is corrected if we take into account the influence of electronic states adjacent to the resonance state. The influence of the excited electronic states is important because of significant values of oscillator strengths and the little energy gap between these states and the resonance electronic state. RHR spectra of fluorobenzene (resonance with the lowest excited electronic state), chlorobenzene (resonance with the second excited electronic state) and adenine (resonance with the third excited electronic state) were calculated taking into account the contribution of 5-10 excited electronic states. 3) The electron-vibrational interaction and intensity redistribution by Herzberg-Teller mechanism are quite strong.

Our results showed that the intensity distribution in RHR and RR spectra of each molecule (fluorobenzene, chlorobenzene and adenine) had the same characteristic features. The most intensive lines in RRS are most intensive in RHRS too. The intensity distribution between lines of medium intensity is also the similar. This fact confirmed conclusions [2-3] concerning the same character of intensity distribution in RHR and RR spectra of low symmetry molecules.

Comparison of theoretical results for fundamentals, overtones and combinations and experimental data [4-6] showed the satisfactory agreement that makes advisable using of the quantum-mechanical method for analysis of intensity distribution in resonance hyper Raman spectra of polyatomic molecules.

[1] T. Burova, *Khim.Fiz.(Rus)* 13 (1994) 29-35.

[2] Y Chung, L.Ziegler, *J. Chem. Phys.* 88 (1988) 7287-7294.

[3] T.Dines, *Chem. Phys. Lett.*459 (2008) 180-182.

[4] C.Bonang, S.Cameron, *Chem. Phys. Lett.* 192 (1992) 303-310.

[5] C.Bonang, S.Cameron, *Chem.Phys.Lett.*187 (1991) 619-622.

[6] A.Toyama, N.Harada, Y.Abe, H.Takeuchi, I.Harada, *J. Raman Spectr.*25 (1994) 623-630.





## Atomic charges and charge fluxes derived from IR intensities

A. Milani, C. Castiglioni

*Politecnico di Milano, Dip. Chimica, Materiali, Ing. Chimica "G.Natta",  
P.zza Leonardo da Vinci, 32 – 20133, Milano, Italy*

The determination and the analysis of molecular charge distribution is of outstanding importance for the investigation of molecular properties either at the intramolecular and intermolecular level, especially for the rationalization of the physical/chemical behaviour. Since the birth of quantum chemistry different methods were developed, ranging from standard Mulliken population analysis to many other different schemes, based either on the analysis of the molecular wavefunction/electronic density or on the fitting of molecular electrostatic potentials. These methods, while being widely adopted, share an intrinsic limitation due to the fact that these charges are not directly related to any experimentally measurable quantity. About forty years ago, accurate spectroscopy studies, devoted to the determination and analysis of the absolute IR band intensities of simple organic molecules, started to appear in the literature. These experimental investigations were supported by many theoretical studies aimed at an interpretation of the intensity data; on this basis several models were developed for a description of the molecular charge distribution and its mobility from IR intensities [1]. In particular, the Electro-Optical Parameters model (EOP) and the related Equilibrium Charges and Charge Fluxes (ECCF) model gave powerful but simple methods to describe the effect of the intramolecular chemical environment on the electrical features of bonds and atoms in molecules. Moreover, Atomic Polar Tensors (APT), which can be directly derived from IR intensities (and equilibrium electrical dipole moment), were used to the same purpose. The IR parameters so derived and in particular ECCF parameters, have been used successfully for the description of intramolecular effects such as inductive effects, hyperconjugation, charge backdonation as well as intermolecular interactions by the identification of atomic sites able to form hydrogen bonds or responsible of strong electrostatic interactions. However, the determination of reliable ECCF parameters from experimental IR intensities is partially hindered by the difficulty to obtain accurate absolute intensity data and by intrinsic spectroscopic problems related to the derivation of the intensity parameters (e.g. good vibrational force fields required a number of unknowns which largely exceeds that of the experimental data available, etc.).

We discuss here the possible application of IR intensity parameters obtained by DFT computed APTs. Several organic molecules, for which accurate experimental intensity data (and often intensity parametrizations) are available, will be considered and computed IR intensities will be compared with their experimental counterpart [2]. Moreover, a general analytical model based on ECCF parameters will be used to obtain atomic charges and charge fluxes from the APTs [2,3]. The atomic charges derived from DFT computed APTs give an accurate description of charge distribution, since they are comparable with those previously derived from experimental intensities. Moreover, they show a good agreement with charges derived by means of other widely used schemes. In addition, the IR charges have the advantage of being directly connected to experimentally measurable quantities.

- [1] M. Gussoni, C. Castiglioni, G Zerbi in "Handbook of Vibrational Spectroscopy", J. Chalmers and P. Griffiths Eds. (2001), John Wiley & Sons, Chichester UK Vol.3 pp. 2040 and references therein.
- [2] A. Milani, C. Castiglioni, *J. Phys. Chem. A* 114 (2010) 624
- [3] A. Milani, D. Galimberti, C. Castiglioni, G. Zerbi, *J. Mol. Struct.*, submitted.



## CCFOM and CCFDF models to interpret infrared intensities: A Comparative Study

V. H. Rusu, M. N. Ramos and R. L. Longo

Departamento de Química Fundamental, Universidade Federal de Pernambuco, Av. Prof. Moraes Rego, 1235 - Cidade Universitária, Recife - PE, Brazil

The beginning of the measurement of absolute infrared intensities (IR) by experimentalists was accompanied by the birth of theoretical models to interpret these experimental intensities. Some theoretical models have been proposed to interpret IR intensities. Particularly, our group has used the charge-charge flux-overlap modified (CCFOM) model [1]. More recently, Bruns et al. [2] have proposed the charge-charge flux-dipole flux (CCFDF) model. Both have a quantum-mechanical basis and have been successful in interpreting IR intensities [3,4]. The atomic charge derived from CCFOM model is obtained from the Mulliken charge corrected by an element of the overlap tensor, whereas that CCFDF is derived from the QTAIM methodology [5]. The dynamic part of the CCFDF model is represented by two terms: charge-flux and dipole-flux. The CCFOM model does not separate this dynamic part into two, i.e., both are represented as simply charge-flux.

In order to better compare these two models, we have performed MP2/aug-cc-pVTZ calculations to interpret IR intensities of the HX diatomic molecules (X= F, Cl, Br, CN and NC). Table 1 shows the CCFOM and CCFDF results for these HX molecules. The CCFOM charge fluxes are small, i.e., near zero. This is expected to acid molecules to taking into account experimental results obtained from the equilibrium charge – charge flux (ECCF) model [6] for infrared intensities. The charge-flux and dipole flux terms from CCFDF are large and with opposite signs, except to HF. For this latter, both have the same sign.

We can also verify that the equilibrium hydrogen charges from CCFOM are smaller than the CCFDF ones. The greater difference is verified in HF. Its CCFDF value is comparable to the corresponding values obtained for lithium and sodium atoms. On the other hand, this is not chemically expected. For this reason, we have compared CCFOM and CCFDF hydrogen charges to the  $\mu/R_{A-X}$  ratios, where  $\mu$  is the dipole moment and  $R_{A-X}$  is the A-X bond length with A= H, Li and Na. This analysis has revealed that the CCFOM charges show a better linear consistence with  $\mu/R_{A-X}$  than those derived from the CCFDF model.

| Molecules | CCFOM model |   | CCFDF model |   |                                     |
|-----------|-------------|---|-------------|---|-------------------------------------|
|           | $q_H$       | $\frac{\partial q_H}{\partial r_H} r_H$ | $q_H$       | $\frac{\partial q_H}{\partial r_H} r_H$ | $\frac{\partial m_H}{\partial r_H}$ |
|           | (e)         | (e)                                     | (e)         | (e)                                     | (e)                                 |
| HF        | 0.409       | -0.057                                  | 0.753       | -0.304                                  | -0.106                              |
| HCl       | 0.182       | 0.044                                   | 0.298       | 0.356                                   | -0.431                              |
| HBr       | 0.127       | 0.006                                   | 0.105       | 0.887                                   | -0.857                              |
| HCN       | 0.255       | 0.027                                   | 0.223       | 0.789                                   | -0.757                              |
| HNC       | 0.404       | 0.109                                   | 0.565       | -0.173                                  | 0.040                               |

- [1] M. Gussoni, M. N. Ramos, C. Castiglioni, and G. Zerbi, Chem. Phys. Lett., 142, (1987) 515.  
 [2] R. L. A. Haiduke, A. E. de Oliveira, and R. E. Bruns, J. Phys. Chem. A, 108, (2004) 6788.  
 [3] V. H. Rusu, J. B. P. Da Silva and M. N. Ramos, Vib. Spectrosc., 46, (2009) 52.  
 [4] J. V. Da Silva, A. E. Oliveira, Y. Hase and R. E. Bruns, J. Phys. Chem. A, 113, (2009), 7972.  
 [5] R. F. W. Bader and P. M. Beddall, J. Chem. Phys., 56, (1972), 3320.  
 [6] M. Gussoni, M. N. Ramos, C. Castiglioni, and G. Zerbi, J. Mol. Struct., 174, (1988), 47.



**Spectroscopic properties of hydrogen-bonded systems by wavelet analysis**F. Muniz-Miranda<sup>1</sup>, M. Pagliai<sup>2</sup>, G. Cardini<sup>1,2</sup>, V. Schettino<sup>1,2</sup><sup>1</sup>*European Laboratory for Non-Linear Spectroscopy (LENS), via Nello Carrara 1, I-50019, Sesto Fiorentino (FI), Italy*<sup>2</sup>*Dipartimento di Chimica "Ugo Schiff", via della Lastruccia 3, I-50019, Sesto Fiorentino (FI), Italy*

Propane-1,3-diol and ethane-1,2-diol are two homologous glycols of industrial interest that interact with the water environment mainly through hydrogen bonds. Car-Parrinello molecular dynamics (CPMD) simulations have been carried out to characterize the structural and spectroscopic properties of these glycols in relation with the H-bond interactions.

In order to obtain useful insights on their vibrational properties, CPMD simulation data have been analyzed by wavelet transform (WT). This is a mathematical tool able to perform time-frequency localization and could also be exploited in non-linear time-resolved spectroscopy.

Through a preliminary time-frequency analysis by WT, we have correlated the O-H stretching frequency of glycols with the hydrogen bond length, creating 2D spectrograms that spread the vibrational density of states along the inter-molecular bond axis: the resulting 2D spectrograms show how the vibrational modes evolve due to modifications in the solvation cage, confirming the fundamental assumption that the vibrational frequencies are mainly determined by the structural evolution.

This method of obtaining correlation spectrograms is completely general and can be applied to different structural time-dependent properties, allowing the simultaneous interpretation of both dynamic and structural quantities.



## Conformational study of arbutin by quantum chemical calculations and multivariate analysis

C. Araujo-Andrade<sup>1</sup>, S. Lopes<sup>2</sup>, R. Fausto<sup>2</sup> and A. Gómez-Zavaglia<sup>2,3</sup>

<sup>1</sup>Unidad Académica de Física de la Universidad Autónoma de Zacatecas, Zacatecas, Mexico

<sup>2</sup>Department of Chemistry, University of Coimbra, 3004-535 Coimbra, Portugal

<sup>3</sup>Centro de Investigación y Desarrollo en Criotecnología de Alimentos (Conicet La Plata, UNLP), 1900 La Plata, Argentina

Arbutin (IUPAC name: (2R,3S,4S,5R,6S)-2-hydroxymethyl-6-(4-hydroxyphenoxy)oxane-3,4,5-triol, also known as hydroquinone- $\beta$ -D-glucopyranoside) is an abundant solute in the leaves of many freezing- or desiccation-tolerant plants (Figure 1) [1].

Taking into account the protective role of arbutin in such plants and the importance of OH groups on the physico-chemical and biological function of sugars as cryoprotectants, a deep analysis of the molecular structure of arbutin may be very useful for the elucidation of the molecular mechanisms involved in its role as cryoprotectant.

Arbutin has eight conformationally relevant dihedral angles, five of them related with the orientation of the hydroxyl groups and the remaining three taking part in the skeletal of the molecule. In this study, a systematic search on the conformational space of arbutin was performed. Conformers were grouped according to structural similarities using multivariate analyses and correlations between their structures and several properties established [2].

Intramolecular interactions involving OH groups were also investigated and correlations between spectroscopic, structural and thermodynamic properties established.

The strategy here used might be useful to investigate the structure and structure/properties correlations in other biologically relevant conformationally flexible molecules, in particular carbohydrates.

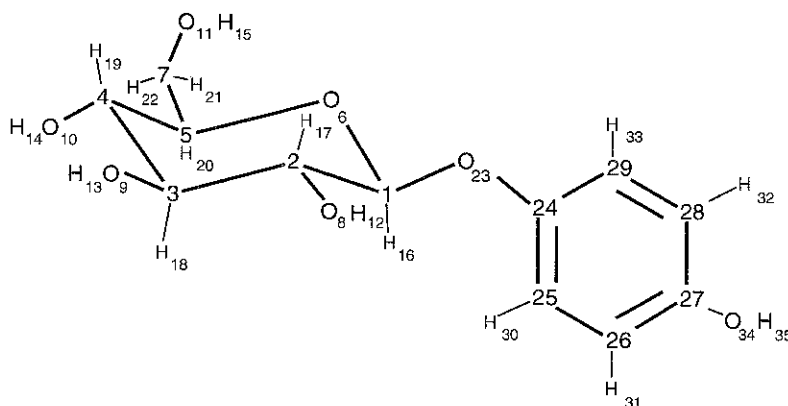


Figure 1 – Arbutin molecule, with atom numbering scheme.

[1] D. Hinch, A. E. Oliver, J. H. Crowe, *Biophys. J.* 77 (1999) 2024.

[2] The Unscrambler software (v9.8) (2009) CAMO Software AS, Nedre Vollgate 8, 0158 Oslo (Norway).



## Conformational equilibria and intramolecular proton transfer in hydrogenmalonate anion: influence of the crystalline environment. a combined vibrational spectroscopic and quantum chemical study

M. Ristova<sup>1</sup>, J. Petreska<sup>1</sup>, L. Pejov<sup>1</sup>, B. Šoptrajanov<sup>2</sup>

<sup>1</sup> *Institute of Chemistry, Faculty of Science, SS. Cyril and Methodius University, Arhimedova 5, 1000 Skopje, Republic of Macedonia*

<sup>2</sup> *Macedonian Academy of Sciences and Arts, Bul. Krste Misirkov 2, 1000 Skopje, Republic of Macedonia*

Conformational equilibria and intramolecular proton transfer in the hydrogenmalonate anion in the gas phase and in a crystalline environment were studied by combined theoretical and experimental approaches.

The computational study involved several aspects. Full geometry optimizations of the possible conformers of the free hydrogenmalonate anion as well as of the anion placed within a particular crystalline environment were carried out with gradient methodology at B3LYP/6-31++G(*d,p*) and BPBE/6-31++G(*d,p*) as well as at B3LYP/6-311++G(*d,p*) and BPBE/6-311++G(*d,p*) levels of theory, followed by harmonic vibrational analyses. The influence of crystalline environment on the conformational equilibria was studied by the finite-cluster approach, *i.e.* modeling the anion neighborhood as a finite cluster cut out from the periodic structure. In the case of the *Z*-isomer, the atom-centered density matrix propagation (ADMP) scheme was used to study the dynamics of intramolecular proton transfer in the free hydrogenmalonate anion and of the anion placed in a crystalline environment. The dynamical studies were performed at B3LYP/6-31++G(*d,p*) and BPBE/6-31++G(*d,p*) levels of theory.

Some of the result of the theoretical study were correlated with the experimental ones obtained from the Fourier transform infrared spectra of several hydrates of metal(II) hydrogenmalonates. The FT IR measurements were carried out at room temperature (RT) and the boiling temperature of liquid nitrogen (LNT).



## Vibrational frequencies studied as a function of pressure near the i-ii phase transition in solid benzene

H. Yurtseven, B. Raşitoğlu

*Department of Physics, Middle East Technical University, 06531 Ankara, Turkey*

Vibrational frequencies are analysed as a function of pressure according to a power-law formula close to the I-II transition (critical pressure  $\sim 1.4$  Gpa) in solid benzene. The Raman frequencies measured in the pressure range 0 to 5 Gpa at 300K, as reported in the literature, are used for this analysis and the values of the critical exponent  $\gamma$  for the frequency shifts  $(1/\nu)(\partial\nu/\partial P)_T$  are determined. The  $\gamma$  values determined from the Raman frequencies of the three lattice modes, vary from 0.4 to 0.5. By a constant mode Grüneisen parameter which relates the frequency shifts  $(1/\nu)(\partial\nu/\partial P)_T$  to the isothermal compressibility  $\kappa_T = (-1/V)(\partial V/\partial P)_T$ , the  $\gamma$  exponent values can also describe the critical behaviour of  $\kappa_T$  near the I-II transition in solid benzene.

This shows that the critical behaviour of the thermodynamic quantities such as the isothermal compressibility  $\kappa_T$  studied here, can be predicted from the vibrational frequencies measured spectroscopically to high accuracy.



**Critical behaviour of the order parameter from birefringence and raman intensity data close to the  $\lambda$ -transition in  $\text{NH}_4\text{Br}$**

H. Yurtseven

*Department of Physics, Middle East Technical University, 06531 Ankara, Turkey*

The critical behaviour of the order parameter is investigated using the birefringence and Raman intensity data near the  $\lambda$ -phase transition ( $T_\lambda=235$  K) in  $\text{NH}_4\text{Br}$ . From the analysis of the experimental data using the mean field theory, the critical exponent for the order parameter is determined as  $\beta \approx 0.5$ . This indicates a second order transition between the phases II (CsCl) and III (tetragonal) in  $\text{NH}_4\text{Br}$ , as expected.

Our results show that the mean field model is capable of describing the order-disorder phase transition in the  $\text{NH}_4\text{Br}$  crystal.



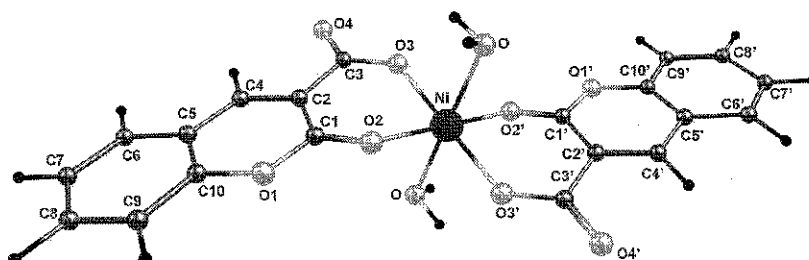
## Structure and spectroscopic properties of Ni(II), Co(II) and Zn(II) complexes with coumarin derivative predicted by DFT calculations

N. Trendafilova<sup>1</sup>, I. Georgieva<sup>1</sup>, B. S. Creaven<sup>2</sup>

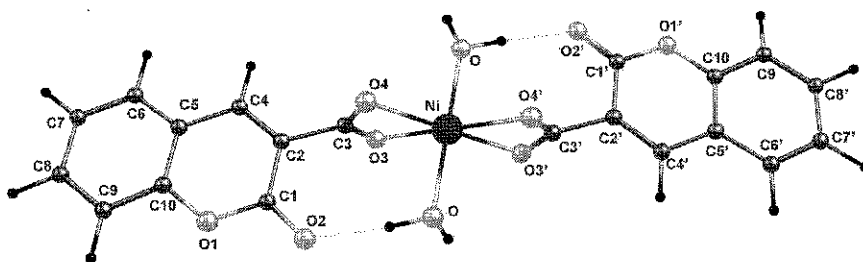
<sup>1</sup>*Institute of General and Inorganic Chemistry, Bulgarian Academy of Sciences, Acad. G. Bonchev, 11, 1113 Sofia, Bulgaria*

<sup>2</sup>*Department of Applied Science, Institute of Technology, Tallaght, Dublin 24, Ireland*

Ni(II), Co(II) and Zn(II) complexes of coumarin 3-carboxylic acid with potential biological activities are characterized by FTIR, <sup>1</sup>H NMR, <sup>13</sup>C NMR, electronic spectroscopic data and DFT calculations. The molecular electrostatic potential calculations of the active deprotonated ligand form, CCA<sup>-</sup>, have suggested two possible bidentate binding types: (a) CCA1 - through the carboxylic O3 and lactone carbonylic O2 atoms and (b) CCA2 - through the carboxylic O3, O4 atoms. The first type of coordination was proposed for lanthanide complexes ((Dy(III), Er(III), Eu(III), Gd(III), Tb(III), Sm(III))), whereas the second one was predicted for Cu(II) and Sn complexes. In the present study, the two possible manners of coordination of HCCA to Ni(II), Co(II) and Zn(II) have been modeled at B3LYP level with 6-311+G(d) basis for Ni(II), 6-31+G(d) basis for O, C1,C2,C3 and 6-31G(d) basis for other C and H atoms. The complex geometries were optimized for the possible spin states and the minimum structures were used to calculate molecular properties, IR, NMR and electronic spectra. There is a lack of X-ray diffraction analysis data about the complexes studied and thus no comparison with experimental structural data was possible. NMR, electronic and vibrational spectra calculations revealed better coincidence of the experimental spectra with the calculated spectra of CCA2 type coordination, namely, bidentate through the carboxylic O3, O4 atoms. Characteristic IR and NMR parameters of CCA1 and CCA2 are specified and used to distinguish the two ligand coordination types in metal complexes.



(a) Ni(CCA1)<sub>2</sub>(H<sub>2</sub>O)<sub>2</sub>



(b) Ni(CCA2)<sub>2</sub>(H<sub>2</sub>O)<sub>2</sub>





## Structural and Vibrational Study of 2-benzyl-4,5-dihydro-1H-imidazole

C. D. Contreras<sup>1</sup>, A. E. Ledesma<sup>1</sup>, J. Zinzuk<sup>2</sup> and S. A. Brandán<sup>1</sup><sup>1</sup>*Cátedra de Fisicoquímica I. Instituto de Química-Física. Facultad de Bioquímica, Química y Farmacia. Universidad Nacional de Tucumán. Tucumán. R. Argentina,*<sup>2</sup>*Instituto de Química Rosario (CONICET-UNR), Facultad de Ciencias Bioquímicas y Farmacéuticas, Universidad Nacional de Rosario, Santa Fé. R. Argentina.*

The 2-benzyl-4,5-dihydro-1H-imidazole (**1**), that is a vasodilator broadly used in hypertensive therapy, has been theoretically studied and its molecular structures are observed in the Figure 1. The infrared and Raman spectra were registered in solid state. The corresponding geometries for the compound were calculated using the Gaussian 03 [1] program at B3LYP theory level. The harmonic vibrational frequencies for the optimized geometries of the compound were calculated using 6-31G\* and 6-311++G\*\* basis sets in the approximation of the isolated molecule. Then, for a complete assignment of the IR and Raman spectra, Density Functional Theory (DFT) calculations were combined with Pulay's Scaled Quantum Mechanics Force Field (SQMFF) methodology in order to fit the theoretical wavenumber values to the experimental ones.

The force constants were calculated for the compound using the Pulay et al. [2] methodology from the Scaling Quantum Mechanic Force Field (SQM). The assignment of the observed bands in the vibrational spectra was performed. Furthermore, the analysis of the Natural Bond Orbitals (NBO) [3] was carried out to study the charge transference interactions between the benzyl and dihydroimidazole rings of the compound.

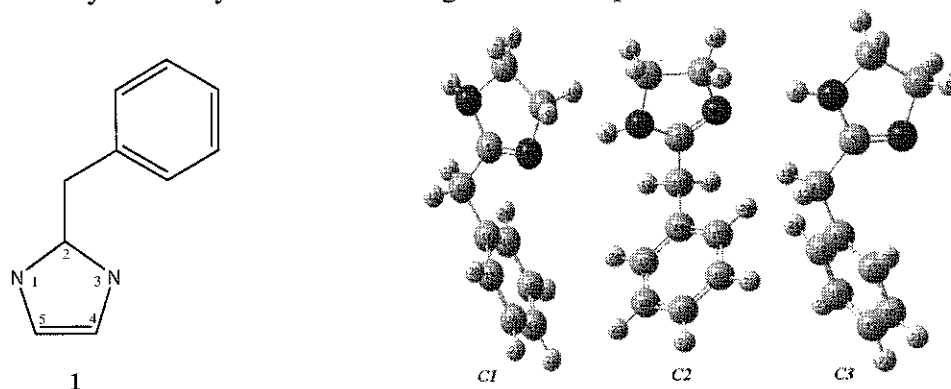


Fig. 1: Theoretical structures of 2-benzyl-4,5-dihydro-1H-imidazole.

[1] Program Gaussian 03, GAUSSIAN, Inc. Pittsburgh, PAA, USA, 2003.

[2] P. Pulay, G. Fogarasi, F. Pang, E. Boggs, *J. Am. Chem. Soc.*, 101(10) (1979) 2550.

[3] E.D. Glendening, J.K. Badenhoop, A.D. Reed, J.E. Carpenter, F.F. Weinhold, NBO 3.1; Theoretical Chemistry Institute, University of Wisconsin; Madison, WI, 1998.

## A Theoretical Interpretation of the Infrared Intensities of Maleimide

E. C. Aguiar, J. B. P. da Silva, M. N. Ramos

Departamento de Química Fundamental – Universidade Federal de Pernambuco  
Av. Prof. Moraes Rego, 1235 - Cidade Universitária, ZIP: 50670-901 Recife - Pernambuco – Brasil.

Maleimide presents an interesting molecular structure due to presence of three important functional groups: carbonyl, imide and ethylenic groups, which are inter-bonded through an aromatic five-membered ring, as can be seen in Figure 1. As consequence maleimide and its N-derivatives have been largely used in a variety of photochemical applications, which are based on their electron accepting properties [1]. In this study we have employed MP2/6-31++G(d,p) and B3LYP/6-31++G(d,p) calculations to electronically interpret the molecular structure of maleimide in terms of atomic charges and charge fluxes obtained from its IR intensities using the charge-charge flux-overlap modified (CCFOM) model [2].

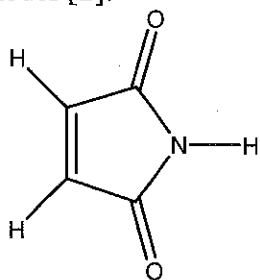


Figure 1: Maleimide and its functional groups.

According with the CCFOM model the equilibrium atomic charge ( $q_{\alpha}^{\circ}$ ) is given by the  $P_{\alpha}^{xx}$  element of the atomic polar tensor of  $\alpha$  atom. Here  $x$  is the Cartesian axis perpendicular to the molecular plane. The charge-flux ( $\partial q_{\alpha} / \partial z_{\alpha}$ ) due to the  $\alpha$ - $\beta$  stretching along the  $z$  Cartesian axis is given by the  $P_{\alpha}^{zz}$  element. From this we have derived values of  $q_H^{\circ}$  and ( $\partial q_H / \partial z_H$ ) for the N–H imide group in maleimide in using the hydrogen polar tensors. For instance, their MP2 values are 0.34 e and -0.02 e/Å, respectively, which are typical values for acid hydrogen atoms. The

N–H stretching intensity can be adequately represented by:

$$A^{NH, str} = K \cdot \left( q_H^{\circ} + \left( \partial q_H / \partial z_H \right) r_{NH}^{\circ} \right)^2$$

where  $K = 975$  for intensity values in  $\text{km mol}^{-1}$  and  $r_{NH}^{\circ}$  stands for the equilibrium N–H bond length. Its MP2 calculated value is  $104 \text{ km mol}^{-1}$ , whereas that obtained from Eq. (1) is  $101 \text{ km mol}^{-1}$ , which are in excellent agreement. Analogously, we have derived values of  $q_H^{\circ}$  and ( $\partial q_H / \partial z_H$ ) for the hydrogen atoms in ethylenic group. For instance, their corresponding MP2 values are 0.16 e and -0.13 e/Å, i.e., they are almost equals but of opposite signs. Thus it is expected that the symmetric and asymmetric C–H intensities in maleimide are predicted to be very weak. In fact, their MP2 values are  $0.1 \text{ km mol}^{-1}$  and  $0.2 \text{ km mol}^{-1}$ , respectively. The out-of-plane X–H bending intensities are essentially determined by equilibrium hydrogen charge.

The asymmetric C=O intensity dominates the IR spectrum of maleimide. This band is observed to be very strong at  $1756 \text{ cm}^{-1}$  in vapour phase since the C=O charge flux vectors ( $\partial q_O / \partial r_{CO}$ ) are in the same sense, in contrast to what occurs with the symmetric mode. Thus, the symmetric C=O stretching intensity is predicted to be medium-weak at  $1770 \text{ cm}^{-1}$ . Indeed, the corresponding MP2 values for these asymmetric and symmetric modes are  $683.8 \text{ km mol}^{-1}$  and  $16.2 \text{ km mol}^{-1}$ , respectively. Finally, we have performed anharmonicity calculations to analyze its effect on the vibrational spectrum of maleimide.

[1] J. Von Sonntag, W. Knolle, J. Photochem, Photobiol. A: Chem. 136 (2000) 133–139;

[2] M. Gussoni, C. Castiglioni, M. N. Ramos, M. Rui, G. Zerbi, J. Mol. Struct. 224 (1990) 445–470.



## Performance of polarized continuum solvation models in DFT prediction of IR band polarization properties for anisotropic LC solutions

G. Keresztury<sup>1</sup>, T. Sundius<sup>2</sup>, M. Rogojerov<sup>3</sup>, Cs. Németh<sup>1</sup>

<sup>1</sup>Chemical Research Center, HAS, P.O. Box 17, H-1525 Budapest, Hungary,

<sup>2</sup>Department of Physics, University of Helsinki, P.O. Box 64, FIN-00014 Helsinki, Finland

<sup>3</sup>Institute of Organic Chemistry, Bulgarian Academy of Sciences, 1113 Sofia, Bulgaria

Computational prediction of the *frequencies* of internal vibrations of molecules based on the scaled quantum mechanical force field (SQM FF) method applying the density functional theory (DFT) has proven to be very popular and successful in recent years. The reliability of vibrational band assignments is greatly facilitated by the use of infrared and Raman intensities as well during the comparison of calculated and observed spectra, even if the relative band *intensities* can be predicted as yet with about an order of magnitude greater percentage errors compared to frequencies. However, while the calculation of IR intensities is part of a routine computational task, few publications deal with theoretical prediction of the underlying basic quantities, the *vibrational transition moments* (TMs) and their directional property that cannot be measured directly but may be deduced from polarized IR spectra [1].

In recent years we have worked on computational prediction of transition moment directions of slightly *asymmetric molecules* (of  $C_s$  symmetry) using the SQM FF method applying the DFT//B3LYP method (see e.g. [2-6]). The experimental data on transition moment directions of IR active vibrations have been extracted from polarized IR spectra of oriented samples, i.e., from infrared linear dichroism (IR-LD) spectra of solute molecules aligned in a nematic liquid crystal as anisotropic solvent. To eliminate the sign ambiguity of the determination of the angle of orientation ( $\pm\phi_i$ ), we have developed a joint evaluation procedure of the measured and theoretically predicted, calculated spectral parameters.

Determination of the average orientation of  $C_s$  molecules and their experimental transition moment directions is facilitated by corrections introduced through comparison with quantum chemically calculated vibrational transition moments of two strong absorption bands. According to the accumulated evidence, TM directions calculated by DFT (B3LYP/6-31G\* or higher level) for medium intense or stronger bands agree with experimental data within 5-10°, i.e. they are much more reliable than what can be anticipated from structural considerations alone.

Further improvement in the performance of this method is expected from DFT calculations taking into account the influence of the anisotropic dielectric field surrounding the solute molecules in the LC medium [7]. This is being tested now through computations using the new features of the Gaussian-09 program package associated with the polarizable continuum model (PCM). Our earlier experimental data obtained for p-Cl-acetophenone and asymmetrically deuterated (1-D- and 2-D-) naphthalene derivatives are re-evaluated in view of the new computational results.

- [1] J. Michl, E. W. Thulstrup: *Spectroscopy with Polarized Light*. VCH Publishers, New York, 1986.
- [2] G.Keresztury, F.Billes, M.Kubinyi, and T.Sundius: *J. Phys. Chem. A*, 102 (1998) 1371-1380.
- [3] M. Rogojerov, G. Keresztury and B. Jordanov: *J. Mol. Structure*, 661-662 (2003) 227-234.
- [4] M. Rogojerov, G. Keresztury, and B. Jordanov: *Spectrochim. Acta Part A* 61 (2005) 1661-1670.
- [5] G. Keresztury and M. Rogojerov: *Bulgarian Chem. Comm.* 37/4 (2005) 327-331.
- [6] M. Rogojerov, P. Angelova, G. Keresztury, D. Tsankov, *Vibr. Spectrosc.*, 43 (2007) 64-70.
- [7] C. Cappelli, F. Corni, B. Mennucci, J. Tomasi, R. Cammi, *Int. J. Quantum Chem.*, 104 (2005) 716-726.



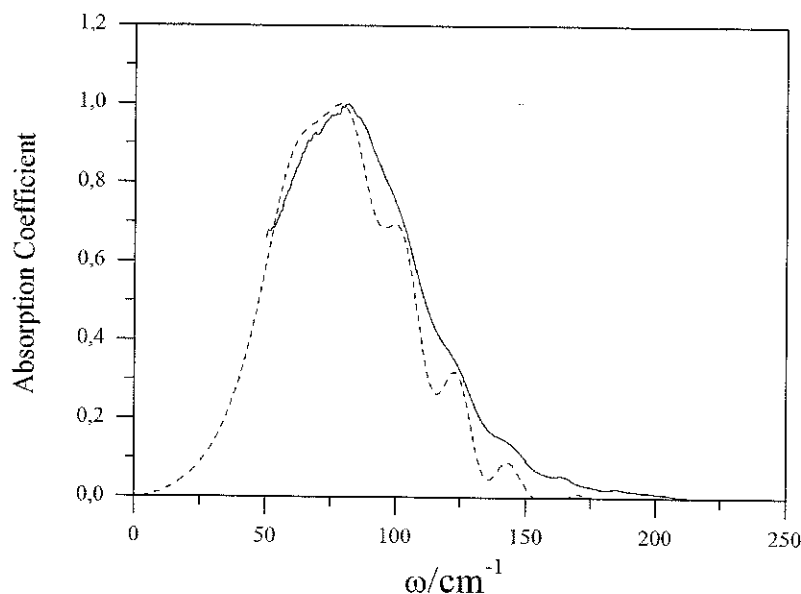
## A simulation study of the far-infrared absorption spectra of HCl diluted in liquid Ar

A. Padilla and J. Pérez

*Departamento de Física Fundamental y Experimental, Electrónica y Sistemas, Universidad de la Laguna, Av. Astrofísico Francisco Sánchez, 38205, La Laguna, Spain*

The far-infrared absorption coefficient of HCl diluted in liquid Ar has been calculated at different experimental conditions by using a mixed quantum-classical stochastic simulation technique recently developed [1]. This technique employs a model to represent the HCl-solvent(Ar) anisotropic interaction, in terms of the directing intermolecular field (DIF) approach which is assumed an stochastic Gaussian process. The characteristic main parameters: the anisotropic interaction strength and the binary autocorrelation time, are calculated by means of molecular dynamic simulation, while the binary HCl-Ar anisotropic interaction is taken as the Holmgren et al. potential [2].

The theoretical spectra have been compared with the available experimental data (see figure) as well as with the classical stochastic simulation and molecular dynamic simulation spectra. The statistical parameters of the HCl-Ar anisotropic interaction and the orientational times associated to the rotational spectral density have been calculated allowing a comparative analysis of the temporal scales involved in the rotational spectra.



Experimental (continuous line) and theoretical (dashed line) absorption coefficients of HCl diluted in liquid Ar.

- [1] A. Padilla, J. Pérez, W. A. Herrebout, B. J. Van der Veken and M. O. Bulanin, *J. Mol. Struct.* doi:10.1016/j.molstruc.2009.09.012  
 [2] S. L. Holmgren, M. Waldman and W. Klemperer, *J. Chem. Phys.* **67**, 4414 (1977); **69**, 1661 (1978).



## Raman spectra of polyynes and cumulenes: a computational investigation

A. Milani, F. Innocenti, C. Castiglioni

*Politecnico di Milano - Dip. Chimica, Materiali, Ing. Chimica "G. Natta" -  
P.zza Leonardo da Vinci 32, 20133 Milano, Italy.*

In the last few years, molecular systems based on linear carbon chains became an interesting subject in nanoscience and nanotechnology. Their stability, non-linear optical, electronic transport and vibrational properties have been widely studied both experimentally and theoretically. Raman spectroscopy proved to be an useful method for the investigation of linear carbon chains: recently the modulation of the phonon dispersion curves as a function of the degree of bond length alternation (BLA) of an infinite carbyne chain has been described in terms of electron-phonon coupling [1]. Furthermore, the Raman features of polyynes of different chain lengths have been interpreted in the frame of the Effective Conjugation Coordinate model (ECC) [2], revealing the importance of long range dynamical interactions. It has been indeed proved how Raman frequencies, bond length alternation and the electronic gap are strongly and analytically related.

In spite of the fact that a comprehensive understanding of the electronic and vibrational structure of polyynes has been reached, it is still debated whether linear carbon chains characterized by vanishing BLA value (i.e. cumulenic structures, with quasi equivalent CC bonds along the whole chain) could exist and be observed by Raman spectroscopy, as for the widely occurring polyynic molecules (alternated chains). If existing, cumulenes are particularly intriguing structures, since they represent the finite size molecular parents (oligomers) of an ideally infinite, zero gap (i.e. metallic) 1-D chain. While the infinite cumulenic chain is expected to relax into the alternated polyynic form due to Peierls distortion, the existence of finite length cumulenic chains cannot be excluded "a priori", thanks to the introduction of end-effects which can force a structure different from that of the infinite limit. For this reason, a systematic investigation of short linear  $C_n$  chains (whose existence has been experimentally verified) and of vinyl-capped chains has been carried out with the help of DFT calculations [3]. The optimized molecular structures of such chains present very small BLA values also in the case of relatively long carbon sequences (we considered chains as long as  $C_{30}$ ); moreover the calculated Raman spectra show low CC stretching frequencies when compared to polyynes of the same length. Using the results obtained for oligomers, phonon dispersion branches for an infinite cumulene model are built and they are compared to the phonon branches of the infinite polyyne.

According to DFT calculations, the Raman cross sections of cumulenes result to be systematically much lower than polyynes, but they are large enough to be observed, at least in principle. A relationship between bond length alternation and local Raman parameters (change of the molecular polarizability with individual CC stretchings) is found, thus allowing a comprehensive rationalization of the Raman intensity behavior of the different molecular species considered, ranging from polyynes, un-capped chains and vinyl capped carbon chains. Also in this case the effect of the end groups is shown to play a key role.

[1] A. Milani, M. Tommasini, G. Zerbi, *J. Chem. Phys.* 128 (2008) 064501[2] M. Tommasini, D. Fazzi, A. Milani, M. Del Zoppo, C. Castiglioni, G. Zerbi, *J. Phys. Chem. A* 111 (2007) 11645[3] F. Innocenti, A. Milani, C. Castiglioni, *J. Raman Spectrosc.* 41 (2010) 226

## Theoretical and experimental vibrational study of anhydrous citric acid as monomer and dimer

L. C. Bichara<sup>1</sup>, E. G. Ferrer<sup>2</sup>, H. E. Lanús<sup>1</sup>, C. G. Nieto<sup>3</sup> and S. A. Brandán<sup>1</sup>

<sup>1</sup>*Cátedra de Fisicoquímica I. Instituto de Química Física. Facultad de Bioquímica, Química y Farmacia. Universidad Nacional de Tucumán. San Lorenzo 456. T4000CAN, S. M. de Tucumán. R. Argentina.*

<sup>2</sup>*Centro de Química Inorgánica. CEQUINOR. CCT. Departamento de Química. Facultad de Ciencias Exactas. Universidad Nacional de La Plata. 47 y 115. CC. 962 (B1900AVV), 1900. La Plata.*

<sup>3</sup>*Cátedra de Microbiología General. Instituto de Microbiología. Facultad de Bioquímica, Química y Farmacia. Universidad Nacional de Tucumán. Ayacucho 471. T4000CAN, S. M. de Tucumán. R. Argentina.*

A new structural and vibrational theoretical study of the anhydrous citric acid as monomer and dimer (Figure 1) was performed employing the Density Functional Theory (DFT) method with Pople's basis sets. The new vibrational spectra registered in solid state were compared with those obtained for the monohydrated acid. The geometries of monomers and dimer in gas phase were fully optimised at the B3LYP/6-31G\* and B3LYP/6-311++G\*\* levels of theory by using the Gaussian 03 program [1] and the harmonic wavenumbers were evaluated at the same levels. For a complete assignment of the vibrational spectra, DFT calculations were combined with Pulay's Scaled Quantum Mechanics Force Field (SQMFF) methodology [2] in order to fit the theoretical wavenumber values to the experimental ones. In this way, a complete assignment of all the observed bands in the vibrational spectra was performed. The scaled force constants for monomer and dimer species are also reported.

The natural bond orbital (NBO) study [3] reveals the characteristics of the electronic delocalization of the dimeric species of the acid while the corresponding topological properties of electronic charge density are analysed by employing Bader's Atoms in Molecules theory (AIM) [4].

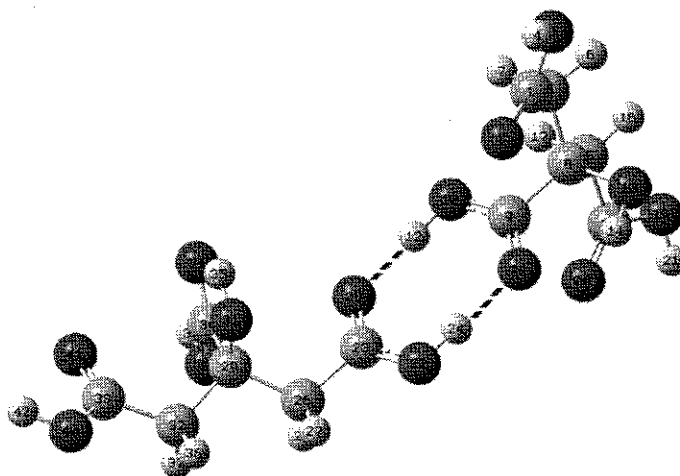


Fig. 1: Theoretical structure of dimer citric acid.

[1] Program Gaussian 03, GAUSSIAN, Inc. Pittsburgh, PAA, USA, 2003.

[2] P. Pulay, G. Fogarasi, F. Pang, E. Boggs, *J. Am. Chem. Soc.*, 101(10) (1979) 2550.

[3] E.D. Glendening, J.K. Badenhoop, A.D. Reed, J.E. Carpenter, F.F. Weinhold, NBO 3.1; Theoretical Chemistry Institute, University of Wisconsin; Madison, WI, 1998.

[4] F. Biegler-König, J. Schönbohm, D. Bayles, AIM2000; A Program to Analyze and Visualize Atoms in Molecules, *J. Comput. Chem.* 22 (2001) 545.

**Spectral and quantum – chemical characterization of some carbanion monosubstituted cycloimmonium ylids**

T. Teslaru, A. Sebi, R. E. Stanculescu and D. O. Dorohoi

*“Alexandru Ioan Cuza” University, Faculty of Physics, 11 Carol I Blv., RO-700506*

The carbanion monosubstituted cycloimmonium ylids are few stable compounds, but they are used in organic chemistry as precursors in obtaining new heterocyclic compounds or as acid-basic indicators.

Recently were revealed anti-inflammatory, antiseptic and antifungal action of the studied compounds.

Hyperchem 8.0.6. Program was used for electro-optical characterization of the carbanion monosubstituted cycloimmonium ylids. The bond lengths, the charged near molecular atoms, the HOMO and LUMO energies, dipole moments, polarizabilities and so on were obtained and discussed in correlations with spectral characteristics obtained experimentally by using electronic, IR and NMR Spectra of carbanion monosubstituted substances.

The dimerization reaction of carbanion monosubstituted pyridazinium ylids was spectrally studied and the geometry of the obtained dimmers was optimized by quantum mechanical procedures. The computed and the experimental spectra were compared and a good accordance between the obtained data was revealed.



**Electro-optical parameters of some thio-semicarbazides studied by spectral and computational means**

R. E. Stanculescu<sup>1</sup>, V. Sunel<sup>2</sup>, D. O. Dorohoi<sup>1</sup>

<sup>1</sup>*Alexandru Ioan Cuza University, Faculty of Physics, 11 Carol I Blv., RO-700506*

<sup>2</sup>*Alexandru Ioan Cuza University, Faculty of Chemistry, 11 Carol I Blv., RO-700506*

Thio semicarbazides are substances with biological activity obtained by N-(p-nitrobenzyl)-L-phenylalanine, considered as precursor, after many reaction steps. The energetic and electro-optical parameters of the studied thio-semicarbazide were established by quantum-chemical software. HyperChem 8.6 with Polak Ribiere algorithm and RMS 0.001 kcal/mol was used for optimization the structure of studied molecules by AM1, PM3 and RM1 semi-empirical methods. The results obtained by these semi-empirical methods are discussed and compared with those experimentally determined.

The chemical reactivity and the biological activity of the studied compounds were appreciated by the difference between LUMO and HOMO energies. The results referring to the atomic charges and bond lengths obtained through computational means are correlated with the signals from NMR and FTIR spectra. The electronic and vibration spectra were simulated and compared with those experimentally obtained. The IR bands were attributed to various types of vibration movements as a result of simulation. The computed oscillator strengths and the surfaces of the electronic absorption bands are also in a good accordance.





## Crystal polymorphism: a combined approach using vibrational spectroscopy and *ab initio* calculations.

N.F.C. Mendes, P. Ribeiro-Claro

*CICECO, Departamento de Química, Universidade de Aveiro, P-3810-193 Aveiro, Portugal*

The study of polymorphism among molecular crystals constitutes a field of increasing scientific and commercial interest. In particular, the characterization and prediction of the properties of crystals of biological and pharmaceutical relevance represents both a challenge and an opportunity available to spectroscopists and computational chemists.

The combined use of computational and experimental data constitutes a powerful tool to solve the structure of molecular crystals and to perform a thorough assignment of their spectra. In particular, the combined use of vibrational spectroscopy and *ab initio* calculations has proven to be a valuable tool in the assignment of vibrational spectra of polymorphic and pseudo-polymorphic forms of different systems [1-3] and can be used to assist the resolution of unknown solid state structures by providing the identification of the most relevant motifs in the intermolecular potential energy landscape [4].

Our approach – shortly described as “PiMM: Pairs in Molecular Materials” – assumes that intermolecular interactions in the crystal promote perturbations to the isolated molecule spectrum, and these perturbations are additive. Within the PiMM approach, the *i*th spectroscopic observable  $\sigma_i$  of a solid sample (*e.g.*, vibrational wavenumber, NMR shift, and electronic transition) is given by its calculated value for the isolated molecule, corrected for the perturbations resulting from the contacts with neighboring molecules in the crystal,  $\Delta\sigma_i$ . Assuming that only the neighbours in the first shell will significantly affect the spectroscopic observables of the isolated molecule, each spectroscopic observable is given by the simplified equation

$$\sigma_i(\text{crystal}) = \sigma_i(\text{isolated}) + \sum_{j=1}^M \Delta\sigma_i$$

Following previous works [1-4], the PiMM approach is herein applied to pharmaceutical active drugs, addressing a set of problems related with (pseudo)polymorphism, from hydrogen bonding interaction patterns, dynamics of solid state transitions, solubility and bioavailability.

- [1] M.M. Nolasco, A. M. Amado, P. Ribeiro-Claro, *ChemPhysChem*, 7 (2006) 2150-2161
- [2] M. M. Nolasco, A. M. Amado, P. Ribeiro-Claro, *J. Raman Spectrosc.*, 40 (2009) 394-400.
- [3] M. Sardo, A. M. Amado, P. Ribeiro-Claro, *J. Raman Spectrosc.*, 40 (2009) 1956-1965
- [4] M. M. Nolasco, P. Vaz, P. Ribeiro-Claro, *THEOCHEM* 946 (2010) 65-69



## Transformation of spectral radiance by inelastic and elastic scattering in the gaseous atmosphere

O. V. Postylyakov

*A. M. Obukhov Institute of Atmospheric Physics, Pyzhevsky per.3, Moscow 119017, Russia*

The transfer of radiance through gaseous media may significantly distort its spectral structure due to absorption and scattering. For example, filling (reduction of depth) of the Fraunhofer lines [1] in the observations of the scattered solar radiation has been called the Shefov-Ring effect. Several inelastic scattering processes, such as rotational Raman scattering (RRS), inelastic Rayleigh-Brillouin scattering [2] and aerosol fluorescence are responsible to this effect in the Earth atmosphere.

To quantitatively simulate inelastic scattering, the radiative transfer (RT) model MCC++ [3] was upgraded with inelastic scattering block.

The RT model MCC++ takes into account multiple scattering (using Monte Carlo methods) and polarization. The model is linearized, i.e. it solves the equation in derivatives of radiance simultaneously with the transfer equation in radiance. Gained experience proved that a simultaneous solution of these equations can be greatly faster than the traditional algorithm of the finite difference approach based on multiple runs of a radiative model with perturbed optical properties. It was shown in paper [1], that this feature allows the fast calculation of the spectrum of the *elastically* scattered radiance basing on the full RT simulation at only one wavelength, if variations of absorption cross section and scattering of the media with wavelength are small in the target spectral range.

A method of the fast calculation of the spectrum of the *inelastically* scattered radiance using the full simulation at only one wavelength by *linearized* RT model is proposed. It works if variations of optical properties of the media with wavelength are small in the target spectral range. The proposed method was applied to Monte Carlo simulation of rotational Raman scattering in the Earth atmosphere, which gives the main contribution in the Shefov-Ring effect as shown in [2].

The work was partially supported by RFBR grant #08-05-01046.

[1] N. N. Shefov, Izd. Akad. Nauk 1 (1959) 25, in Russian

[2] G. W. Kattawar, A. T. Young, T. J. Humphreys, *Astrophys. J.* 243 (1981) 1049-1057

[3] O. V. Postylyakov, *J. Quant. Spectrosc. Radiat. Transfer* 88 (2004) 297-317



## 7-[2-hydroxy-3(-4-acetyl-amino)-phenoxy-propyl]-1,3 dimethyl xantine derivatives characterized by HyperChem 8.0.6 and spectral means

M. Avadanei<sup>1</sup>, V. Barboiu<sup>1</sup>, M. Dulcescu<sup>2</sup>, L. Profire<sup>3</sup>, D. O. Dorohoi<sup>2</sup>

<sup>1</sup>"Petru Poni" Institute of Macromolecular Chemistry, 41A Aleea Grigore Ghica Voda, Iasi, RO-700487, Iasi, Romania

<sup>2</sup>"Alexandru Ioan Cuza" University, Faculty of Physics, 11 Carol I Blv, Iasi, RO-700506, Romania

<sup>3</sup>"Gr.T. Popa" University of Medicine and Pharmacy, Faculty of Pharmacy, Iasi

Xanthine derivatives are alkaloids commonly used for their effects as mild stimulants and as bronchia-dilatators notably in treating the asthma symptoms. Some xanthine derivatives are active at the levels of central nervous, cardio-vascular or bronchia-pulmonary systems. The 8-substituted of 7-[2-hydroxy-3(-4-acetyl-amino)-phenoxy-propyl]-1,3-dimethyl-xanthine derivatives are new pharmacological products, synthesized from theophiline and paracetamol, with enhanced properties compared with their precursors.

The electro-optical and spectral characteristics of the studied 8-substituted of 7-[2-hydroxy-3(-4-acetyl-amino)-phenoxy-propyl]-1,3-dimethyl-xanthine derivatives were established by theoretical means, utilizing HyperChem 8.0.6 programs and also experimentally, on the basis of UV-VIS, FTIR and NMR spectra.

This study is devoted to a complete characterization of these new products with pharmacological action. Some structural and electro-optical features of the studied compounds were established by quantum-mechanical calculations such as: molecular optimized geometry, length of the covalent bonds, atomic charges, dipole moment in the ground state, polarizability, index of refraction, refractivity, HOMO and LUMO levels, molecular surface, molecular volume and so on. The energetic characteristics of the compounds under the study are relevant both for their chemical reactivity and for biological action. The computed spectral characteristics of the studied compounds were compared by the recorded UV-VIS, FTIR and NMR spectra. A good accordance between the computed and the experimentally recorded spectra was obtained.



## Structural and theoretical studies of 2-amino-3-nitropyridine.

R. M. Mahfouz, N. S. Al-Hokbany, S. M. Akriche and M. Rzaigui.

King Saud University, Department of chemistry, College of Science, P.O.Box 2455, Riyadh, 11451 Kingdom of Saudi Arabia.

Geometrical optimization, spectroscopic analysis, electronic structure and nuclear magnetic resonance of 2-amino-3-nitropyridine were investigated by utilizing density functional theory (DFT) with the standard B3LYP/6-31++G(d,p) level of theory and basis set combinations geometrical parameters (bond lengths, bond angles and torsion angles) were computed and compared with the experimental values obtained using x-ray single crystal measurements of the little compound. IR spectra were obtained and assigned by vibrational analysis comparing the calculated IR spectral with these of experiments known, all the IR data obtained in this investigation were considered to be reliable<sup>1</sup>.

The <sup>1</sup>H and <sup>13</sup>C nuclear magnetic resonance (NMR) chemical shifts of 2-amino-3-nitropyridine were calculated using GIAO method in DMSO solution using IEF-PCM model and compared with experimental data. Hydrogen bonding C-H...N interaction in this compound was investigated by means of the NBO analysis. The electronic transition energies and intensities of spectral lines were carried out using TD-DFT and ZINDO methods.

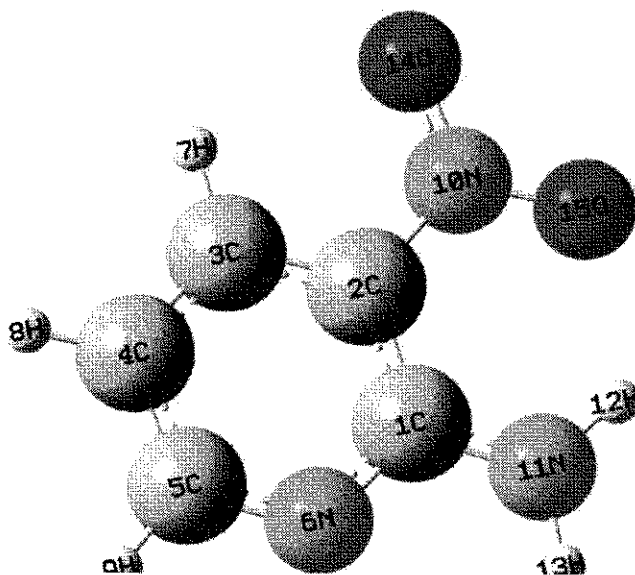


Figure 1. Optimized molecular structure of 2-amino-3-nitropyridine.

- [1] Aakeröy, C.B.; AliciaM, B.; Nieuwenhuyzen, M.; Zou, M., *Journal of Material Chemistry* 1998, 8(6), 1385-1389.

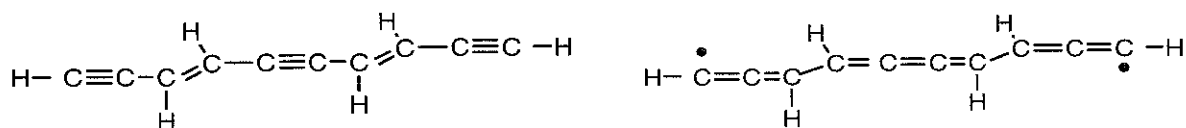
## Structural and Vibrational properties of Photochromic Polydiacetylenes

C. Gellini<sup>1</sup>, M. Muniz-Miranda<sup>1</sup>, P. R. Salvi<sup>1</sup>, M. Alloisio<sup>2</sup>, G. Dellepiane<sup>2</sup><sup>1</sup>Dipartimento di Chimica Università di Firenze, Via della Lastruccia 3, I-50019 Sesto Fiorentino, Italy, and European Laboratory for Non-linear Spectroscopy, Via Nello Carrara 1, I-50019 Sesto Fiorentino, Italy<sup>2</sup>INSTM and Dipartimento di Chimica e Chimica Industriale, Università di Genova, Via Dodecaneso 31, I-16146 Genova, Italy

Polymers with extended  $\pi$ -electron conjugation have attracted strong interest since long time, due to their wide use as active materials in electronic devices [1,2]. Between all the organic conjugated polymers, polydiacetylenes represent one of the most experimentally and theoretically investigated class of systems [3]. Their peculiar optical and electronic properties depend highly on the conformation of the polymer chains. Two are the main factors which account for the large differences in the optical behaviour of these compounds: the first corresponds to a different  $\pi$ -electron delocalization along the polymer backbone, which identifies the single constitutive chromophores; the second is the distribution of the chromophores along the chain, which depends on the conformational properties of the chain and is related to the stiffness of the polymer and the strength of attractive interactions between separated segments of the chain.

A study on the time-dependent photo-polymerization of 10,12-pentacosadiynoic acid,  $\text{CH}_3-(\text{CH}_2)_{11}-\text{C}\equiv\text{C}-\text{C}\equiv\text{C}-(\text{CH}_2)_8-\text{COOH}$  (PCDA), on Ag nanoparticles (AgNPs) has been recently reported, where different chromatic phases are obtained as a function of the irradiation time [4]. At the very first stage of polymerization, the polymer exhibits a blue form that quickly changes into a most delocalized bluish-green form, which becomes predominant at long irradiation time together with the red form. Even though the bluish-green phase was already observed in LB films of PCDA [5], its effective structure is still an open question. The debate proposes a structural rearrangement of the skeleton structure from a polydiacetylenic towards a butatrienic form (see Figure), or more simply a more effective interaction between chromophoric segments of the chain resulting from a more planar arrangement of the segments.

In this paper we want to address the issue of the structural properties in the bluish-green form of PCDA-AgNPs deposited on alumina discs by means of a comparison between the Raman frequencies of the three different chromatic phases observed after UV irradiation and the *ab-initio* DFT calculations (rb3lyp/6-31G) on enyne oligomers, chosen for modelling the polymer chain.



- [1] H. Meier, F. Diederich, *Angew. Chem. Int. Ed.* 44 (2005) 2482
- [2] M. Gholami, R.R. Tylwinski, *Chem.Rev.* 106 (2006) 4997
- [3] Z.G. Soos, D.S. Galvao, S. Etemad, *Adv. Mater.* 6 (1994) 280
- [4] C. Raimondo, M. Alloisio, A. Demartini, C. Cuniberti, G. Dellepiane, S.A. Jadhav, G. Pettrill, E. Giorgetti, C. Gellini, M. Muniz-Miranda, *J. Raman Spectrosc.* 40 (2009) 1831
- [5] A. Fujimori, M. Ishitsuka, H. Nakahara, E. Ito, M. Hara, K. Kanai, H. Ishii, Y. Ouchi, K. Seki, *J. Polym. Sci. Part B: Polym. Phys.* 42 (2004) 2329



## A theoretical study on the spectroscopical effects of rhodamine b and noble metals nanoparticles interactions

D. Duce, M. Ottonelli, M. Piccardo, G. Dellepiane

*INSTM and Dipartimento di Chimica e Chimica Industriale, Università di Genova,  
via Dodecaneso 31, I-16146 Genova, Italy;*

The development of new chemical sensors is a task of great interest for their wide use in many fields, with biological [1], medical [2] and technological [3] applications. Two are the main characteristics that are requested for high performance sensors: selectivity and sensitivity. While the former can be easily achieved through the choice of an appropriate molecular species, the sensitivity, which is generally related to the absorbance or fluorescence properties of the chromophores, could be limited by the intrinsic value of the organic absorption cross section. In fact for organic systems the latter seldom exceeds about  $10^{-16}$  cm<sup>2</sup>, and moreover their fluorescent properties could be decreased due to photobleaching effects. Recently these limitations have been overcome by realizing that noble-metal nanoparticles do not suffer such limitations, and as a function of their size, shape, composition and local environment can give (due to scattering and absorption effects) intense signals with apparent absorption cross sections of about  $10^{-10}$  cm<sup>2</sup>. In this way, integration between the characteristic properties of the organic chromophore and those of the nanoparticles can give hybrid systems to build new efficient sensors for biological and chemical targets [4,5].

The optimization of these hybrid systems it is of interest to understand how the variation of the local environment, due to the interaction or binding between the organic chromophores and the nanoparticle, could modify in a synergic way the properties of the single components. Using as a model system Rhodamine B in the presence of noble-metals nanoparticles, we will show the results of a quantum chemical study focused on the correlations between the variation of electronic and optical properties of the organic dye due to the interaction with the metal-system. In connection with this study, some pertinent experimental results will be discussed.

- [1] J.N. Anker, W.P. Hall, O. Lyandres, N.C. Shah, J. Zhao, R.P. Van Duyne, *Nature Mater.* 7 (2008) 442-453.
- [2] C. McDonagh, C.S. Burke, B.D. MacCraith, *Chem. Rev.* 108 (2008) 400-422.
- [3] B.S. Sherigara, W. Kutner, F. D'Souza, *Electroanalysis* 15 (2003) 753-772.
- [4] S.W. Thomas, G.D. Joly, T.M. Swager, *Chem. Rev.* 107 (2007) 1339-1386.
- [5] D.T. McQuade, A.E. Pullen, T.M. Swager, *Chem. Rev.* 100 (2000) 2537-2574.



## Hydrogen bond dynamics of methyl acetate in methanol

M. Pagliai<sup>1</sup>, F. Muniz-Miranda<sup>2</sup>, G. Cardini<sup>1,2</sup>, R. Righini<sup>1,2</sup>, V. Schettino<sup>1,2</sup>

<sup>1</sup>*Dipartimento di Chimica, Università di Firenze, Via della Lastruccia 3, 50019, Sesto Fiorentino, Italy*

<sup>2</sup>*European Laboratory for Non-Linear Spectroscopy (LENS), Via Nello Carrara 1, 50019, Sesto Fiorentino, Italy*

The interactions of methyl acetate in methanol have been studied by means of *ab initio* molecular dynamics simulations within the Car-Parrinello approach. These simulations have been shown to be particularly suitable to describe the H-bond dynamics of methyl acetate in water, leading to a complete characterization of the observed mono- and bi-dimensional IR spectra, reported by Candelaresi *et al.* [1].

Banno *et al.* [2, 3] have recently shown that the C=O stretching band of methyl acetate in methanol splits in a doublet as a consequence of the H-bond interaction as it occurs in water, although the position of the band differs in the two solvents. This behavior has been explained by considering the solvation structure and dynamics of methyl acetate in both solvents. Methyl acetate forms one or two H-bond in water solution, whereas in methanol it can interact at most with only one molecule.

The H-bond effects on the spectroscopic properties of methyl acetate in methanol have been interpreted by wavelet transform analysis. An algorithm has been set up to correlate the C=O stretching frequency during the simulations with the function for the description of the H-bond, introduced by Pagliai *et al.* [4]. Since wavelet transforms localize the signal in the frequency and time domains, it is possible to obtain the frequency and the bond length of the C=O stretching at the same time step of the simulations.

The Car-Parrinello molecular dynamics simulations, in conjunction with wavelet transforms, have shown to satisfactorily characterize the structural and vibrational properties of H-bonded systems, helping to elucidate at atomic level the interactions that take place in the sample dissolved in different media and their spectroscopic features.

[1] M. Candelaresi, M. Pagliai, M. Lima, R. Righini, *J. Phys. Chem. A* 113 (2009) 12783-12790

[2] M. Banno, K. Otha, S. Yamaguchi, S. Hirai, K. Tominaga, *Acc. Chem. Res.* 42 (2009) 1259-1269

[3] M. Banno, K. Otha, K. Tominaga, *J. Raman Spectrosc.* 39 (2008) 1531-1537

[4] M. Pagliai, G. Cardini, R. Righini, V. Schettino, *J. Chem. Phys.* 119 (2003) 6655-6662



**Ab-initio studies of the homodimers of methane and silane,  
and of methyl and silyl fluoride and chloride**

T. A. Ford

*School of Chemistry, University of KwaZulu-Natal, Durban 4000, South Africa*

The structures and vibrational spectra of the weakly bound homodimers of methane and silane have been determined by means of a series of ab initio calculations at the level of second order Møller-Plesset perturbation theory and with a triple-zeta split valence Gaussian basis set with polarization and diffuse functions on all atoms. The similarities and differences in the structures have been rationalized on the basis of the differing polarities of the CH and SiH bonds. The calculations have been extended to include the dimers of methyl and silyl fluoride and chloride, in order to explore the effect of the presence of a halogen atom on the dimerization process, and on the structures and spectra of the aggregates.





**Effect of alkali metal ions on the pyrrole and pyridine  $\pi$ -electron systems in pyrrole-2-carboxylate and pyridine-2-carboxylate molecules: : FT-IR, FT-Raman, NMR and theoretical studies**G. Świdorski<sup>1</sup>, S. Wojtulewski<sup>2</sup>, M. Kalinowska<sup>1</sup>, R. Świśtocka<sup>1</sup>, W. Lewandowski<sup>1</sup><sup>1</sup>*Department of Chemistry, Białystok Technical University, Zamenhofa 29, 15-435 Białystok, Poland*<sup>2</sup>*Institute of Chemistry, University of Białystok, Al. J. Piłsudskiego 11/4, 15-443, Białystok, Poland*

The FT-IR, FT-Raman and <sup>1</sup>H and <sup>13</sup>C NMR spectra of pyrrole-2-carboxylic acid (PCA), pyridine-2-carboxylic as well as lithium, sodium, potassium, rubidium and caesium pyrrole-2-carboxylates and pyridine-2-carboxylates were recorded, assigned and compared in the Li → Na → K → Rb → Cs salt series. The effect of alkali metals on the electronic system of ligands was discussed. Moreover the calculation for pyrrole-2-carboxylic acid and Li, Na, K pyrrole-2-carboxylates in B3LYP/6-311++G\*\* level and Møller-Plesset method in MP2/6-311++G\*\* level were made. Bond lengths, angles and dipole moments as well as aromaticity indices (HOMA, EN, GEO, I<sub>6</sub>) for the optimized structures of pyrrole-2-carboxylic acid (PCA) and lithium, sodium, potassium pyrrole-2-carboxylates were also calculated. The degree of perturbation of the aromatic system of ligand under the influence of metals in the Li → Cs series was investigated with the use of statistical methods (linear correlation), calculated aromaticity indices and Mulliken, NBO and ChelpG population analysis method. Additionally, the Bader theory (AIM) was applied to setting the characteristic of the bond critical points what confirmed the influence of alkali metals on the pyrrolic ring.

This work was supported by S/WBiŚ/21/07



**Theoretical and spectroscopic study of hydrogen bond vibrations in imidazole and its deuterated derivative**

M. J. Wójcik<sup>1</sup>, J. Kwiendacz<sup>1</sup>, M. Boczar<sup>1</sup>, Ł. Boda<sup>1</sup>, Y. Ozaki<sup>2</sup>

<sup>1</sup>*Faculty of Chemistry, Jagiellonian University, 30-060 Kraków, Ingardena 3, Poland*

<sup>2</sup>*Department of Chemistry, School of Science and Technology, Kwansai-Gakuin University, Gakuen, Sanda 669-1337, Japan*

Theoretical simulation of the bandshape and fine structure of the N-H(D) stretching band is presented for imidazole and its deuterated derivative taking into account adiabatic coupling between the high-frequency N-H(D) stretching and the low-frequency N...N stretching vibrations, anharmonicity of the potentials for the low-frequency vibrations in the ground and excited state of the N-H(D) stretching mode, Fermi resonance between the N-H(D) stretching and the first overtone of the N-H(D) bending vibrations, and electric anharmonicity. The vibrational potential functions describing N-H and N...N stretching modes have been obtained from *ab initio* calculations. The effect of deuteration has been successfully reproduced by our model calculations. Infrared, far-infrared, Raman and low-frequency Raman spectra of the polycrystalline imidazole have been recorded. The geometry and experimental frequencies are compared with the results of harmonic MP2/6-311++G\*\* and anharmonic B3LYP/6-311++G\*\* calculations.



## Potential energy curves for PTCDI and PTCDA dimers obtained by MP2 and DFT methods with dispersion correction

G. Mile, M. Oltean, V. Chiş

Babeş-Bolyai University, Faculty of Physics, Kogălniceanu 1, RO-400084, Cluj-Napoca, Romania

Perylene derivative PTCDA (perylene-3,4,9,10-tetracarboxylic-3,4,9,10-dianhydride) and its imide analogue PTCDI have attracted growing scientific interest as candidate materials for organic electronic devices. The characterization of their intermolecular interactions is extremely important, particularly for the understanding of organic thin film formation.

While MP2 or coupled cluster methods, able to capture dispersive effects, are computationally very expensive for large molecules, pure DFT methods fail to describe such interactions. However, very recent advances in density functional theory led to DFT methods which account for dispersion effects. Such methods were derived by explicitly including an attractive dispersion term (DFT-D methods) [1], by using parametrized functionals [2] or by developing dispersion-correcting potentials (Cpots methods) [3].

In this work, analytical potential energy functions were obtained for stacked PTCDI and PTCDA dimers by using MP2 method (with and without BSSE correction) and different variations of DFT-D and Cpots approaches. The main conclusions of this study can be summarized as follows:

- i) The method used for the monomer geometry optimization has a minor influence on the PES parameters (binding energy and equilibrium distance) obtained by all the tested methods.
- ii) Equilibrium distances and corresponding interaction energies of the stacked dimers at different levels of theory were obtained by fitting the calculated intermolecular potentials with modified Morse, Lenard-Jones or Murrell-Sorbie potentials. For example, Cpot-Morse combination gives  $R_{eq}=3.580 \text{ \AA}$ ,  $E_{eq}=0.662 \text{ eV}$  and  $R_{eq}=3.56$ ,  $E_{eq}=0.641 \text{ eV}$ , respectively, for PTCDI and PTCDA dimers.
- iii) MP2 method overbinds the dimers; however, BSSE correction brings the binding energy and equilibrium distance in a fairly good agreement with the values given by DFT-D and Cpot methods.
- iv) Partial optimized dimers in which the relative rotation of the two component molecules is allowed ( $\theta_{eq}=29.6^\circ$ ) are almost two times more stable ( $E_{eq}=1.265 \text{ eV}$  for PTCDI) than the parallel stacked dimers.

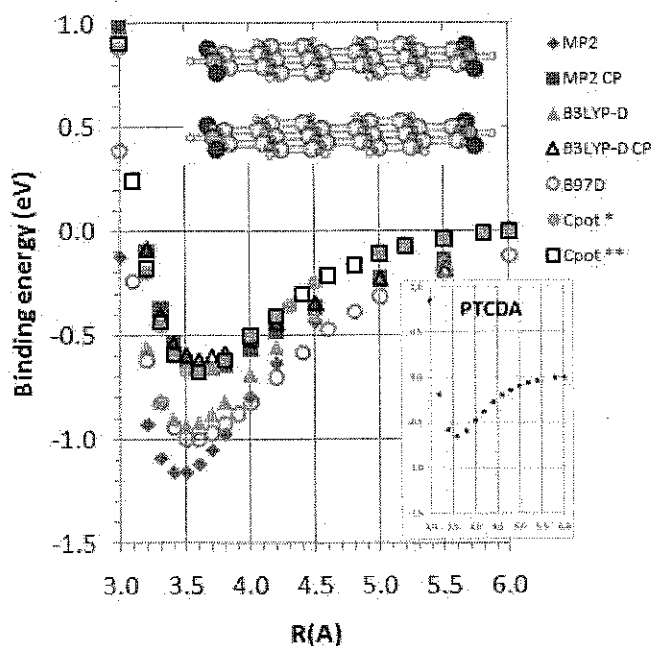


Fig.1 Calculated potential energy curves for PTCDI and PTCDA (bottom inset) at different levels of theory

[1] S. Grimme, J. Comput. Chem., 25 (2004) 1463-1473

[2] Y. Zhao, D.G. Truhlar, Theor. Chem. Acc., 120 (2008) 215-241

[3] G. A. DiLabio, Chem. Phys. Lett., 455 (2008) 348-353



**Methanol under moderate pressures: a dynamical study by femtosecond transient spectroscopy**

M. Candelaresi<sup>1,2</sup>, L. Bussotti<sup>2</sup>, M. Paolantoni<sup>3</sup>, P. Foggi<sup>2,3</sup>

<sup>1</sup>*Department of Physics, Univ. of Strathclyde, Glasgow (United Kingdom)*

<sup>2</sup>*LENS, Univ. of Florence, Florence (Italy)*

<sup>3</sup>*Department of Chemistry, Univ. of Perugia, Perugia (Italy)*

Pressure as well as temperature are known to strongly influence the dynamics in condensed phase. Spectroscopic studies as a function of pressure and temperature are helpful in disentangling the complexity of condensed systems dynamical properties as in the case of hydrogen-bonded liquids. Methanol is the model prototype in the study of hydrogen-bonding phenomena and it is the simplest system exhibiting both polar and non-polar intermolecular interactions. Its spectroscopic properties has been extensively investigated; nevertheless, to our knowledge, no studies combining high pressure and sub-picosecond time-resolution techniques have been published yet, even if methanol dynamics occurs mostly in the picosecond and sub-picosecond temporal range. For this reason we have undertaken a study of methanol in the range 1-3000 bar by femtosecond stimulated fluorescence Stokes shift (SFSS). SFSS is the stimulated (two-pulse) counterpart of spontaneous fluorescence Stokes shift and allows to fully exploit the time resolution provided by our ultrashort laser-pulse system. A popular method of studying solvation dynamics consists in measuring the shift of the fluorescence emission of a solute molecule following short pulse excitation. The solvation response can be directly related to correlation functions describing the equilibrium fluctuations in the potential of the solvent molecule. It has been demonstrated that the content of information of this type of measurements is the same of that achieved by stationary spectroscopic techniques, e.g. depolarized light scattering or by time-resolved techniques such as transient optical Kerr effect. In this research we have chosen SFSS because it better adapts to the experimental constrains of the high pressure apparatus.



**Energy Transfer across metal films mediated by Surface Plasmon Polaritons: a time-resolved fluorescence study**

E. Collini, F.Todescato, C.Ferrante, R. Bozio

*Dipartimento di Scienze Chimiche and INSTM, Università di Padova, via Marzolo 1, 35131 - Padova (Italy)*

Surface plasmon polaritons (SPPs) on the opposite interfaces of a metal film can mediate efficient radiative energy transfer (ET) from donor to acceptor molecules, located on opposite sides of the metal film. The most promising feature of this ET process is that, while in the conventional nonradiative (Förster) mechanism the distance between donor and acceptor molecules is usually less than 10 nm, in the case of SPPs mediated ET, the excitation energy can migrate through metal films up to 150 nm thick. [1] Highly efficient SP-mediated radiative ET can be exploited, for example, to increase the spectral coverage of OLEDs output, to enhance the optical absorption in organic photovoltaic devices, to directionally control the energy flow in artificial photosynthesis, and in general for all the applications of photochemistry near surfaces.

In this work we studied the efficiency of SPP-mediated ET across Ag films between a suitable dye and the conjugated polymer MEH-PPV, largely employed in opto-electronic devices, with the aim of finding the optimum conditions in order to exploit SPP-mediated ET for the aforementioned applications.

We investigated ET between MEH-PPV and a series of dyes acting both as donors (dichloroanthracene, diphenylanthracene, rubrene) and acceptor (styryl-9, sulfurhodamine640, cresyl violet) with respect to the polymer. Structures with different thickness of Ag were also considered. The presence and the efficiency of ET processes across the metal was ascertained looking at variation in the fluorescence lifetimes of the involved species by means of time-correlated single photon counting (TCSPC). The results confirmed the presence of efficient SPP-mediated ET in the employed configurations.

[1] P. Andrew, L. Barnes, Science 306 (2004) 1002-1005



## **Vibrational dynamics at the phospholipid – water interface**

**B. Brożek-Płuska<sup>1</sup>, P. Ciąćka<sup>1</sup>, H. Abramczyk<sup>1,2</sup>**

<sup>1</sup>*Technical University of Lodz, Institute of Applied Radiation Chemistry, Laboratory of Laser Molecular Spectroscopy, Wroblewskiego 15, 93-590 Lodz, Poland.*

<sup>2</sup>*Max Born Institute, Max-Born Strasse 2A, D 12489 Berlin, Germany.*

It is known that lipid molecules play a key role in activity of biological membranes and decide about the health-disease balance in living creatures.

Stability, structure, dynamics and biological function activity are largely determined by interactions, energy transfer and orientation of water molecules in the restricted environments that differ significantly from bulk water properties. However, the confinement of water in biological structures does not represent a single pattern of behavior. For example, the water confined in reverse micelles differs from the confinement of water in phospholipid membranes. The interactions with water modify physical properties, both static and dynamical of the lipid bilayer. Moreover, the interactions lead to the modification of the diffusion barrier across the membrane to ions, oxygen and other small ions. The modification by water may play an important role in the energy dissipation in lipids that is a key mechanism in maintaining the photostability of the biological tissue.

We report on the IR pump-probe measurements on vibrational dynamics of Dipalmitoyl phosphatidylcholine (DPPC) and water at membrane interfaces as well as the energy flow in DPPC/water membranes. We report on the vibrational relaxation of the CH<sub>2</sub> and CH<sub>3</sub> modes of DPPC lipid and OH mode of water as well as the dynamics of energy transfer between the water and the lipid. The two-color experiments with the excitation at OH water stretching region and probing with a second pulse at C-H chain region were used to investigate the relaxation dynamics at the water-lipid interface for a controlled humidity of the sample.

[1] A. Pevsner, M. Diem, *Biopolymers (Biospectroscopy)* 72 (2003) 282-289

[2] F.S. Parker *Applications of Infrared, Raman, and Resonance Raman Spectroscopy in Biochemistry*, Plenum, New York, 1983

[3] J. Liquier, E. Taillander, In *Infrared Spectroscopy of Biomolecules*, H. H. Mantsch, D. Chapman, Eds., Wiley, New York, 1996



## Photophysical characterization of low molecular weight organogels for energy transfer and light harvesting

T. Atsbeha<sup>1,2</sup>, L. Bussotti<sup>1</sup>, A. Marcelli<sup>1</sup>, P. Foggi<sup>1,3</sup>, S. Cicchi<sup>4</sup>, G. Ghini<sup>5</sup>, P. Fabbrizi<sup>4</sup>

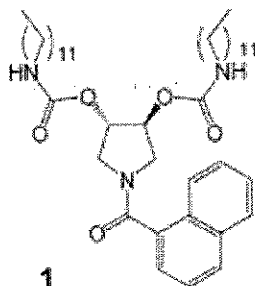
<sup>1</sup>European Laboratory for Nonlinear Spectroscopy (LENS), Via Nello Carrara 1, 50019 Sesto F. no (ITALY)

<sup>2</sup>Department of Chemistry, Addis Ababa University, P.O.Box 1176, Addis Ababa (Ethiopia)

<sup>3</sup>Dipartimento di Chimica, Università di Perugia, Via Elce di sotto 8, 06100 Perugia (ITALY)

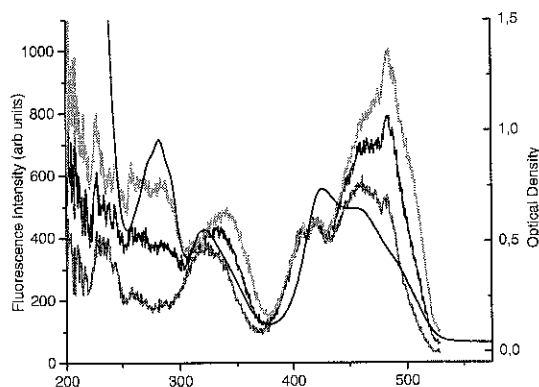
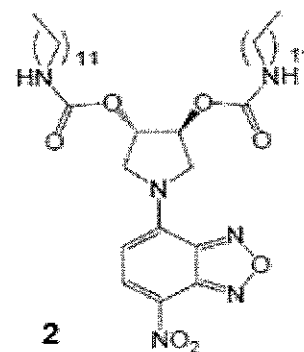
<sup>4</sup>Dipartimento di Chimica "Ugo Schiff" Università di Firenze, Via della Lastruccia 13, 50019 Sesto F.no (ITALY)

<sup>5</sup>ISC-CNR Via Madonna del Piano, 50019 Sesto F.no (ITALY)



The choice of a donor and an acceptor with suitable optical and self assembly properties is extremely important in the design of an organogel-based light harvesting assembly. In particular, the use of chromophore based organogels as scaffolds can provide supramolecular structures capable of enhancing energy transfer processes. In this work, we present the synthesis and characterization of *N*-(naphthalene-1-carboxamide)-(3*S*,4*S*)-pyrrolidin-(3,4)-bisdodecyl-carbamoyldiester (1) and *N*-(4-

nitrobenzofurazan-7-amino)-(3*S*,4*S*)-pyrrolidin-(3,4)-bisdodecyl-carbamoyldiester (2) which are used as donor and acceptor moieties respectively. The donor molecule is hardly capable of gelifying a solvent on its own but it can be assembled at a reasonable concentration with the acceptor gelator to form a two-component donor-acceptor organogel in cyclohexane. A stable organogel is formed from cyclohexane at concentrations as low as  $\approx 10^{-3} M$ . The optical changes during the sol-gel transition, examined by temperature dependent UV-vis and fluorescence spectroscopy, are an indication of the sol-gel transition. Excitation energy transfer processes are confirmed by comparison of the excitation and absorption spectra.



Fluorescence excitation spectra of donor-acceptor gel (2:1 ratio) taken at different times during cooling process (from high to low temperature: red, blue, green) and absorption spectrum (black line) recorded after several hours of jellification.



## **Characterization of a cobalt-dioxolene complex by Transient Infrared Spectroscopy**

A. Lapini<sup>1</sup>, P. Tourón Touceda<sup>1</sup>, S. Mosquera Vázquez<sup>1</sup>, M. Lima<sup>1</sup>, A. Dei,<sup>2</sup>  
P. Foggi<sup>1,3,4</sup>, R. Righini<sup>1</sup>

<sup>1</sup> *European Laboratory for Non Linear Spectroscopy (LENS), University of Florence, Via Nello Carrara 1, 50019 Sesto Fiorentino, Italy.*

<sup>2</sup> *LAMM Laboratory, Dipartimento di Chimica dell' Università di Firenze, UDR INSTM, Via della Lastruccia 3, 50019 Sesto Fiorentino (Firenze), Italy.*

<sup>3</sup> *Dipartimento di Chimica, University of Perugia, 06100 Perugia, Italy.*

<sup>4</sup> *CNR-INO, Largo E. Fermi 6, 50125 Firenze, Italy.*

We report on a time-resolved spectroscopic study aimed to shed light on the photoinduced valence tautomeric interconversion occurring in [Co(Me<sub>4</sub>cyclam)DBSQ]<sup>+</sup>. This compound belongs to the family of cobalt-dioxolene complexes, a class of compounds that was shown to undergo interconversion between the diamagnetic species Co<sup>III</sup>-Cat and the paramagnetic one Co<sup>II</sup>-Sq by the effect of several different perturbations: temperature, pressure, light absorption.

Previous studies, with nanosecond-picosecond time resolution and femtosecond transient absorption spectroscopy, have demonstrated the feasibility of light-induced interconversion in such systems and measured the charge recombination time.





## Transient absorption spectroscopy of heteroaromatic Donor-Acceptor $\pi$ -conjugated 2,2'-bipyridines

S. Mosquera Vázquez<sup>1</sup>, P. Foggi<sup>1,2,3</sup>, A. Lapini<sup>1</sup>, P. Tourón Touceda<sup>1</sup>, A. Abbotto<sup>4</sup>,  
F. De Angelis<sup>5</sup>, M. Lobello<sup>5</sup>

<sup>1</sup>LENS, University of Florence, Via Nello Carrara 1, 50019 Sesto Fiorentino, Italy.

<sup>2</sup>Dipartimento di Chimica, University of Perugia, 06100 Perugia, Italy.

<sup>3</sup>CNR-INO, Largo E. Fermi 6, 50125 Firenze, Italy

<sup>4</sup>Dipartimento Scienze dei Materiali, University Milano Bicocca, 20125 Milan, Italy

<sup>5</sup>CNR-ISTM and Dipartimento di Chimica, University of Perugia, Via Elce di Sotto 8, 06123, Perugia, Italy.

Understanding the dynamics of electron transfer (ET) processes is relevant for subjects like solar cells and molecular electronics devices construction [1]. One of the main processes is the ET occurring in the ligands of metal complexes, which is accompanied by isomerizations and conformational changes.

In this presentation we show our results on recent investigations of the dynamics of excited states in heteroaromatic donor-acceptor  $\pi$ -conjugated 2,2'-bipyridines dyes by UV-visible pump probe transient absorption spectroscopy. The dyes have a pyridine or pyridinium as  $\pi$ -acceptor, a pyrrole as  $\pi$ -donor and ethilenic units used as spacers [2]. Such dyes can be utilized in the synthesis of new metal complexes for DSC's.

The excitation wavelengths were 400 nm or 480 nm, in resonance with the intramolecular charge transfer band. The transient UV-vis spectra are collected between 420 and 700 nm (Figure 1). They show 4 main features: i) two positive bands around 450 and 550 nm corresponding to the bleaching of the ground state and to the stimulated emission respectively. ii) two negative bands at 520 nm and between 600 and 700 nm. The kinetics was probed at the maxima of the most characteristic bands. In all the collected kinetics traces, three time constants were needed for a satisfactory fit of the data. The results of the fitting process are shown in Table 1. The shortest time constant is attributed to an efficient vibrational relaxation in the excited state. The second time constant is attributed to a change in the geometry within the excited state. The third process is the relaxation toward the ground state. As it can be seen, the third process occurs in the hundreds of picosecond regime. This ensures an efficient charge transfer process from the ligand to the metal. Ab-initio calculations are in progress to confirm the nature of the intermediate dynamics.

|            |            | $\tau_1$ | $\tau_2$ | $\tau_3$ |
|------------|------------|----------|----------|----------|
| Compound 1 | ESA        | -        | 11.8     | 118      |
|            | SE         | 0.8      | 73       | -        |
|            | Blue shift | 1.08     | -        | -        |
| Compound 3 | B          | 1.2      | 21.6     | 329      |
|            | ESA        | -        | 13       | 303      |
|            | SE         | 0.6      | 6.5      | 208      |
|            | Blue Shift | -        | 22       | -        |
| Compound 4 | ESA        | 1.66     | -        | 160      |
|            | SE         | 2.08     | -        | 141      |
|            | Red shift  | -        | 22       | -        |

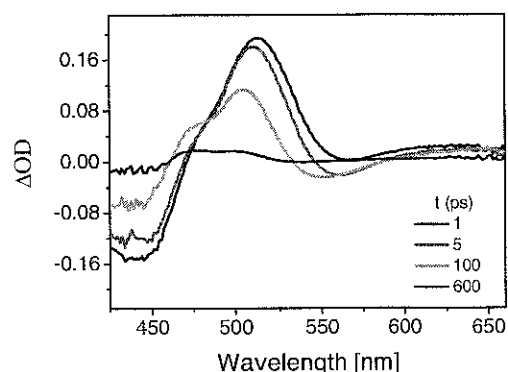


**Table 1.** Picosecond dynamics time constants of transient absorption and stimulated emission of three compounds.

**Figure 1.** Transient absorption spectra collected at various delay times for compound 3.

[1] R. D. Pensack, K. M. Banyas, L. W. Barbour, M. Hegadorn, J. B. Asbury, PCCP 11 (2009) 2575

[2] A. Abbotto, L. Bellotto, F. De Angelis, N. Manfredi, C. Marinzi, Eur. J. Org. Chem. (2008) 5047–5054



## **Cross Phase modulation in visible-pump/infrared-probe spectroscopy**

M. Lima, A. Lapini, P. Tourón Touceda, S. Mosquera Vázquez

*European Laboratory for Non-linear Spectroscopy, Via Carrara 1, 50019 Sesto Fiorentino (Fi), Italy*

Visible-pump/infrared-probe spectroscopy is one of the most powerful tools to investigate structural dynamics of molecular systems. When performing these experiments one must be aware of the artefacts deriving from the non-linear response of the solvent and of the sample cell itself. The intensity of these effects can be comparable to the signal to be measured. Cross phase modulation is observed when a strong pump pulse modulates the refraction index seen by the probe<sup>1</sup>. This effect is amplified when the probe pulse is chirped. Because of the experimental difficulties in recovering the chirping in the infrared region, it is convenient to characterize the cross phase modulation in order to subtract it from the overall transient signal. For this reason we undertook a detailed simulation of cross phase modulation in the mid-infrared region and in the conditions of our experiments. Our simulation takes into account the different group velocities of the pump and probe pulses and includes the influence of the linear chirp of the mid-infrared pulse. The results of our numerical calculations fit the experimental signal measured in 2 mm thick CaF<sub>2</sub> window.

[1] G. P. Agrawal, P.L. Baldeck and R.R. Alfano, Phys. Rev. A, 40, 5063 (1989)

## 2D Raman correlation and NMR spectroscopy study of liquid crystalline ionogel phase formation in ionic liquid/H<sub>2</sub>O mixtures

V. Aleksa<sup>1</sup>, J. Kausteklis<sup>1</sup>, Z. Gdaniec<sup>2</sup>, V. Balevicius<sup>1</sup>

<sup>1</sup>Vilnius university, Faculty of Physics, Sauletekio al. 9-3, LT-10222 Vilnius, Lithuania

<sup>2</sup>Institute of Bioorganic Chemistry, Polish Academy of Sciences, Z. Noskowskiego 12/14, PL-61704 Poznan, Poland

Some of imidazolium-based room-temperature ionic liquids (RTILs) with long alkyl chains can form various liquid crystalline (LC) phases in water solution [1, 2]. For [C<sub>10</sub>mim][Br] it was identified as LC ionogel [1]. It exists at room temperature over the wide range of water concentrations (5 – 40 % w/w). In these sample conditions a complex-shaped contour of strongly overlapped O–H stretching bands can be detected in 2D Raman correlation spectrum (Fig. 1), as well as several new signals appear in <sup>1</sup>H, <sup>13</sup>C and <sup>81</sup>Br NMR spectra.

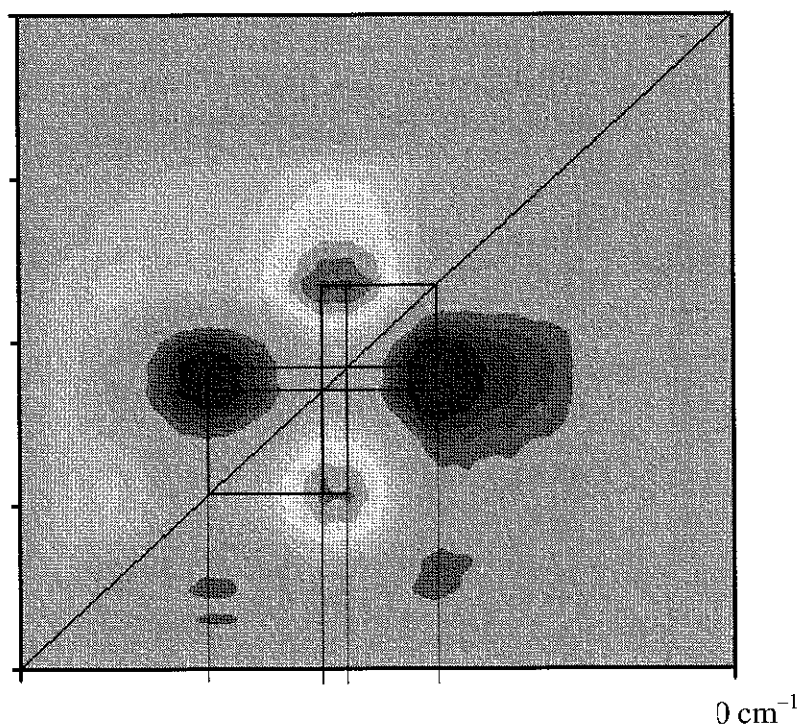


Fig. 1. Asynchronous 2D Raman correlation spectrum of [C<sub>10</sub>mim][Br]/water in vOH region.

These peaks can be originated from the H<sub>2</sub>O molecules trapped in inhomogeneous regions of the sample or due to the appearance of non-equivalent water sites in LC ionogel, the exchange between those is highly restricted or even frozen. The situation is rather close to that in the reverse microemulsion [C<sub>4</sub>mim][BF<sub>4</sub>]/Triton X-100/Cyclohexane [3], where water molecules were found located mainly in the periphery of the polar core of the microemulsion droplets.

[1] M.A. Firestone, J.A. Dzelawa, P. Zapol, L.A. Curtiss, S.Seifert, M.L. Dietz, Langmuir 18 (2002) 7258 - 7260

[2] T. Inoue, B. Dong, L.Q. Zheng, J. Coll. Int. Sc. 307 (2007) 578 - 581

[3] Y. Gao, L. Hilfer, A. Voigt, K. Sundmacher, J. Phys. Chem. B 112 (2008) 3711 – 3719



## Challenging SERS from biomolecules to tissue

S. Cîntă Pînzaru<sup>1</sup>, A. Falamas<sup>1</sup>, N. Leopold<sup>1</sup>, C. Dehelean<sup>2</sup>, C. Lehene<sup>1</sup>

<sup>1</sup>Faculty of Physics, Babes-Bolyai University, Kogalniceanu 1, RO-400084 Cluj-Napoca, Romania

<sup>2</sup>Victor Babes University of Medicine and Pharmacy, Eftimie Murgu Square 2, RO-30004 Timisoara, Romania

Significant progress has been recently reported concerning the Raman spectroscopy applied in areas related to natural tissues or cell biology. Raman spectroscopy provides direct biochemical information with an extremely high spatial resolution, being an attractive method especially for early cancer diagnostic. However, the Raman signal from tissue is rather poor and statistical methods are required to obtain the desired degree of sensitivity and specificity in tissue discrimination. In order to increase the quality of the signal, surface enhanced Raman scattering (SERS) seems to be a considerable candidate in ultrasensitive characterization and discrimination of the tissue components, and consequently, a valuable technique in disease diagnostic [1]. In this work we resume our recent results concerning SERS of tissue. High quality SERS spectra of skin from different mice specimens exposed to cancer promoters [2] or from human colon carcinoma have been obtained. Strategies to improve the signal to noise ratio are presented. A challenging task is the correct interpretation of the SERS spectra from such complex biosystems starting from the well known signal of the molecular components. In this presentation we discuss our recent approach concerning the SERS results on tissue.

**Acknowledgement:** The financial support from grant PN-II-ID 2284 nr. 537/ 2009, ANCS Romania is highly acknowledged.

[1] S. Cîntă Pînzaru, L. M. Andronie, I. Domsa, O. Cozar, S. Astilean, J. Raman Spectrosc., 39 (2008) 331–334.

[2] A. Falamas, S. Pinzaru, C. Dehelean, Ch Krafft, J. Popp, Romanian J. Biophys., 20, 1 (2010) 4-12.



## Backbone Structures of 19 Dipeptides in Aqueous Solution

J. Grdadolnik

*National institute of Chemistry, Hajdrihova 19, SI-1000 Ljubljana, Slovenia*

It has been shown recently that the distinct conformational preferences displayed by amino acid residues in proteins exist already in dipeptides in aqueous solution. Determination of structures of dipeptides in aqueous solution is therefore important for understanding the structures of proteins. Moreover, accurate energy calculations for flexible peptides are needed both to describe and to predict the folding of  $\alpha$ -helices,  $\beta$ -hairpins and reverse turns. The first necessary step in producing a force field that will reliably describe the folding energetics of flexible peptides is to obtain accurate experimental data for the fractional populations in the major backbone conformations. The  $\phi, \psi$  maps of residues in flexible peptides have three major conformational basins, like the  $\phi, \psi$  maps of most amino-acid residues found by superposition of all residue conformations of a given amino-acid type in high-resolution PDB structures. Dipeptides, single amino acids, blocked by acetyl and N-methyl groups, represent the ideal molecules for such conformational studies. They adopt several distinct backbone conformations in aqueous solution; however, the exact probability distributions of the conformations in dipeptides of all naturally occurring amino-acids have been yet unknown.

We used the amide III region of Raman and infrared spectra to determine the backbone structures of 19 dipeptides in aqueous solution (all except proline dipeptide). The analysis reveals that three distinct backbone conformations exist in dipeptides [1]: the  $P_{II}$ ,  $\alpha_R$ , and  $\beta$  conformations, which correspond to the bands that appear in both infrared and Raman spectra near:  $1309\text{ cm}^{-1}$ ,  $1299\text{ cm}^{-1}$ , and  $1288\text{ cm}^{-1}$ , respectively. The assignment of the bands was checked by changing temperature, pH, and solvent. The distributions of the  $P_{II}$ ,  $\alpha_R$ , and  $\beta$  conformations depend on the type of side-chain. The  $P_{II}$  is the prevailing conformation of alanine and leucine dipeptides; however, threonine, and histidine dipeptides adopt predominantly the  $\beta$  conformation. The least populated conformation of dipeptides in aqueous solution is the  $\alpha_R$  conformation (exception is glycine dipeptide). The experimental populations of dipeptides derived from the infrared spectra and Raman spectra agree well with the  $^3J_{HN\alpha}$  NMR coupling constants [2] and are in accord with the electrostatic screening model of conformational preferences of residues [3]. The influences of surrounding, cosolvents, metal ions and aesthetics on preferential conformations of representative dipeptides will be also presented.

[1] Grdadolnik J, Golič Grdadolnik S, Avbelj F., J Phys Chem B. 2008; 112: 2712-18.

[2] Avbelj F, Golič Grdadolnik S, Grdadolnik J, Baldwin LR., Proc Natl Acad Sci USA. 2006; 103: 1272-77.

[3] Avbelj F., J Mol Biol. 2000; 300: 1335-59.



## Noncovalent interaction of carbon nanotubes with DNA and polynucleotides: UV absorption spectroscopy and molecular dynamic simulation

V.A. Karachevtsev, A.M. Plokhotnichenko, M.V. Karachevtsev and V. S. Leontiev

*B.I. Verkin Institute for Low Temperature Physics and Engineering, National Academy of Science of Ukraine, 47 Lenin ave., 61103, Kharkov, Ukraine*

The unique physical and chemical properties of carbon nanotubes provide an opportunity to design new miniature chemical/biological sensors targeting specific molecular systems and reactions. The central issue in designing and forming such devices is the understanding of the mechanism of interactions between nanotubes and the recognition biosystems. The problem is closely related to nanotube functionalization. Native DNA and synthetic oligonucleotides with artificial nucleic base sequences are also applied to nanotube functionalization. It is supposed that adsorption of the single-stranded DNA (ss-DNA) with the helix structure takes place upon polymer wrapping around the tube during the ultrasonic treatment. Under wrapping the hydrophobic nitrogen bases are adsorbed to the nanotube surface via  $\pi$ - $\pi$  stacking, and the hydrophilic sugar-phosphate backbone is directed to water. Despite of availability and abundance of the optical absorption method, the direct manifestation of  $\pi$ - $\pi$  stacking interaction between single-walled carbon nanotubes (SWNTs) and  $\pi$ -conjugated systems in spectral properties of nanotubes was not observed earlier.

UV-visible absorption spectra of hybrids formed by carbon single-walled nanotubes (SWNTs) and ss-DNA, double-stranded DNA (ds-DNA), and synthetic homopolynucleotides (poly(rC) and poly(rG)) have been studied. In 300-400 nm spectral range a decrease of SWNTs light absorption because of their interaction with polymers was observed. The strongest attenuation of the light absorption is observed in the spectrum of ss-DNA-adsorbed nanotubes while in the case with ds-DNA adsorption this effect is significantly weaker. This weakness is because of the double helix conformation in which nitrogen bases are hidden inside polymer and direct stacking with tube makes difficult. The formation of stacking structures between the bases and the nanotube surface is mainly possible due to unpicked double strands at the polymer ends. The revealed decrease of nanotubes absorption is explained by SWNTs hypochromism that results from  $\pi$ - $\pi$  stacking interaction of polymer nitrogen bases with the tube surface. The hypochromic effect is manifested more markedly for the pyrimidine polynucleotide (poly(rC)) than for purine polymer (poly(rG)), because of a higher propensity of pyrimidine bases for structural re-orientation.

Molecular dynamic simulation demonstrates a spontaneous wrapping of polynucleotides around the nanotube. Simulation showed that pyrimidine oligonucleotide (d(C)<sub>25</sub>) manifests a higher rate of minimizing the hybrid structure with the wrapped polymer structure around the tube than purine one (d(G)<sub>25</sub>). Such a polymer behavior can be explained by the pyrimidine oligonucleotides property to form the stable ordering self-stacking structure which prevents from structural re-orientation, in contrast to pyrimidine polynucleotides.

This work was partially supported by Grants 4950 of the Science and Technology Center in Ukraine and National Academy of Sciences of Ukraine



## Intermolecular interactions in water-aliphatic halogen systems – vibrational spectroscopy studies.

M. Kozanecki<sup>1</sup>, P. Zawadzka<sup>1</sup>, R. Kisiel<sup>1</sup>, M. Pastorzak<sup>1</sup>

<sup>1</sup>*Department of Molecular Physics, Faculty of Chemistry, Technical University of Lodz, Zeromskiego 116, 90-924 Lodz, Poland*

Supramolecular structure of liquid water resulting from the formation of H-bond network is a key factor determining anomalous properties of water. Many reports devoted to liquid water showed that it is very sensitive to temperature, pH, ions and also for organic compounds [1-3]. Currently proposed models assumed that the water molecules form clusters in liquid phase [3-5]. Computer simulations confirmed such possibility, however size of such clusters and arrangement of water molecules has been still widely discussed in literature [3-7]. Explanation of supramolecular structure of water seems to be fundamental for better understanding of many chemical, physical and especially biochemical processes. Probably it is also a key for explanation of properties of hydrogels.

This work is devoted to study intermolecular interactions in water-aliphatic halogen systems. Influence of chemical structure of organic compounds (number of halogen atoms) on water-halogen interactions will be discussed. Such model systems are interesting not only from cognitive point of view, but also for environmental protection technologies (problem of volatile organic compounds in water). Formation of water clusters in organic phase was investigated in solutions containing small amount of distilled water (between 0.01% to 2% w/w) dispersed by vigorous mixing and then by ultrasound treatment in organic phase. Vibrational spectroscopy (UV-Vis-NIR spectrometer – Cary 5000, Varian; Raman spectrometer T-64000, Jobin-Yvon) commonly regarded as the most powerful tool to study intermolecular interaction was applied to characterize investigated systems.

For low concentrations, water is dispersed molecularly in aliphatic halogens what is confirmed by the presence of only two peaks (corresponding to  $\nu_1$  and  $\nu_3$  modes of water) in vibrational spectra. Increasing water content in organic phase leading to cluster formation. It is manifested by appearing of additional broad band at lower frequency which may be assigned to OH groups forming H-bonds. Obtained results shows an influence of chemical structure of aliphatic halogens on stability of water clusters. Apolar environment ( $\text{CCl}_4$ ) favors strong interactions between water molecules while the water-halogen interactions are relatively weak. Decreasing number of chlorine atoms in halogen molecules results in increasing of the dipole moment and simultaneously in stronger water-halogen interactions. These effects are manifested by the shift of vibrational bands assigned to molecularly dispersed water to lower frequency and simultaneously shift of band corresponding to H-bonded water molecules to higher frequency. These results are in agreement with observations reported by Scatena [8] and devoted to water-tetrachloromethane and water-hexane interfaces.

- [1] V. S. Marinov, H. Matsuura, J.Mol.Struct. 610 (2002) 105-112
- [2] D. V. Luu, L. Cambon, M. Mathlouthi, J.Mol.Struct.237 (1990) 411
- [3] R. C. Dougherty, L. N. Howard, J. Chem. Phys. 109 (1998) 7379-7393
- [4] M. Chaplin, Biophys. Chemist. 83 (2000) 211-221
- [5] O. Mishima, H. E. Stanley Nature 396 (1998) 329-335
- [6] A. Soper, Science 297 (2002) 1298-1299
- [7] S. Xantheas, Chem. Phys. 258 (2000) 225-231
- [8] L. F. Scatena, M. G. Brown, G. L. Richmond, Science 292 (2001) 908-91



## Spectroscopic study of MADS box and its interaction with DNA

B. Řezáčová<sup>1,2</sup>, Ch. Zentz<sup>2</sup>, P. Y. Turpin<sup>2</sup>, J. Štěpánek<sup>1</sup>

<sup>1</sup>Charles Univ. in Prague, Faculty of Math. and Physics, Ke Karlovu 3, CZ-121 16 Prague 2, Czech Republic

<sup>2</sup>Laboratoire Acides Nucléiques & Biophotonique, FRE CNRS 3207, Université Pierre et Marie Curie  
5 rue Henri Desbrières, 91030 Evry, France

MADS box is a family of transcription factors that play an essential role in the gene regulation of higher organisms, binding to multiple target gene sequences in a complex manner. It derives its name from initials of four of the originally identified members: MCM1, AG, DEFA and SRF [1]. Among MADS box transcription factors, the serum response factor (SRF) plays an important role in the activation of genes that respond to mitogenes and in the regulation of muscle specific genes [2]. MADS box is a DNA binding region showing wide sequence homology of 56 amino acids with many eukaryotic regulatory proteins. One of the most extensively characterized DNA binding sequence recognized by these proteins is the CArG box element: CC(A/T)<sub>6</sub>GG. Preceding studies have disclosed that the initial recognition is a dynamical process [3]. Recent works on 20-mer oligonucleotides bearing the specific high affinity CArG box of the c-fos enhancer revealed a bend-linear interconversion dynamics [4], which is even partly kept after the SRF/SRE complex formation [5]. Still not much is though known about the recognition. Therefore the conserved MADS box motif serves as a study basis of common functional properties of DNA recognition within the whole protein family (over 200 members).

UV absorption, fluorescence and Raman spectroscopies were employed to study structural and dynamic properties of the SRF protein active domain - MADS box and of the CArG box containing DNA segment (SRE). Advanced data processing by using factor analysis enabled us to detect weak spectral changes, mainly those caused by temperature shifts within small temperature intervals that indicated sensitively the flexibility of molecular motifs and/or complexes. Our attention was focused on effects caused by variations of environmental conditions like the concentrations of particular small ions. MADS box was studied at different pH. Emission spectra of its intrinsic fluorophores (tyrosines) provided information about its structural stability and protonation state of intrinsic tyrosines. In addition, different quenchers were employed in order to assign fluorescence components to the individual tyrosine residues of MADS.

The MADS – SRE interaction has been found to be so strong that the sample precipitates if the concentrations necessary for Raman measurements are used. We had thus to concentrate our effort to measurements of the MADS fluorescence. Its quenching by SRE indicated formation of a complex between both partners that remained dissolved in the buffer.

**Acknowledgements:** This work is supported by the Czech Science Foundation (project 202/09/0193). B.R. thanks the Institut Français de Prague for financial support of her stay in ANBioPhi.

- [1] Z. Schwarz-Sommer, P. Huijser, W. Nacken, H. Saedler, H. Sommer, *Science* 250 (1990) 931-936
- [2] J. M. Miano, *J. Mol. Cell. Cardiol.* 35 (2003) 57-593
- [3] A. Huet et al., *FEBS Journal* 272 (2005) 3105-3119
- [4] J. Stepanek, M. Vincent, P-Y Turpin, D. Paulin, S. Femandjian, B. Alpert, C. Zentz, *FEBS Journal* 274 (2007) 2333-2348
- [5] J. Stepanek, V. Kopecky, A. Mezzetti, P.-Y. Turpin, D. Paulin, B. Alpert, C. Zentz, *BBRC* 391 (2010), 203-208





## Can drop coating deposition Raman spectroscopy distinguish shortcomings or inaccuracies in protein crystals?

V. Kopecký Jr.<sup>1</sup>, K. Hofbauerová<sup>1,2</sup>, J. Kohoutová<sup>3</sup>, J. Štěpánek<sup>1</sup>, R. Ettrich<sup>3</sup>

<sup>1</sup>*Institute of Physics, Faculty of Mathematics and Physics, Charles University in Prague, Ke Karlovu 5, Prague 2, CZ-121 16, Czech Republic; hofbauer@biomed.cas.cz*

<sup>2</sup>*Institute of Microbiology, Academy of Sciences, Vídeňská 1083, Prague 4, CZ-142 20, Czech Republic*

<sup>3</sup>*Institute of Systems Biology and Ecology, Academy of Sciences of the Czech Republic, Zámek 136, Nové Hradky, CZ-373 33, Czech Republic*

Raman spectroscopy gives a unique opportunity to study protein samples in different phases. It is possible to measure intact protein crystals directly in hanging drops in crystallization boxes they were grown and to study the protein structure as well as chemical reactions in single crystals [1]. Moreover, we apply a new technique of Raman spectroscopy – a drop coating deposition Raman (DCDR) method [2, 3], based on a coffee ring effect, that enables measurements of solutions down to 1  $\mu\text{M}$  concentrations. However, our recent work adverted to subtle differences which correspond to the glass-like phase of the deposited samples [3, 4]. Thus, DCDR protein samples represent a "transition phase" between oversaturated protein solutions and crystals. This enables to distinguish spectral differences given by the density of molecules in crystals from those caused by protein crystal artifacts. We illustrate, on several examples, applicability of the method for distinguishing these differences and improving X-ray protein structures by molecular modeling based on information from Raman spectroscopy.

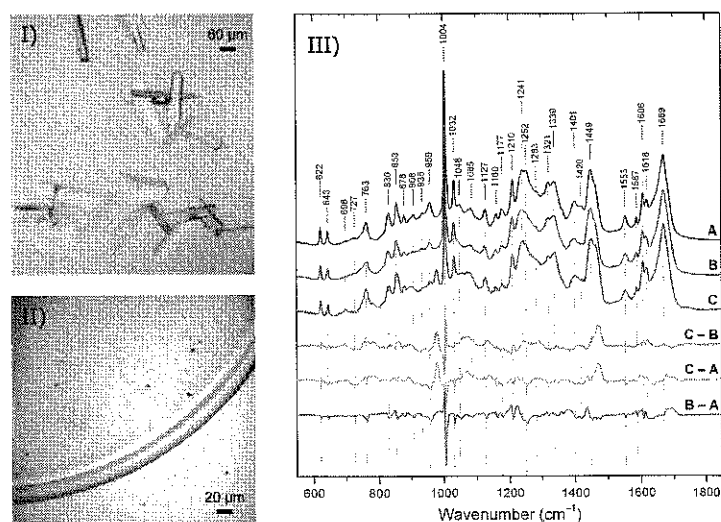


Fig. 1 – I) Crystals of PsbP protein; II) DCDR ring of PsbP protein; III) Raman spectra of PsbP protein measured in (A) solvent, as (B) DCDR deposit and in (C) the crystal form. Appropriate spectral differences are depicted down the figure.

**Acknowledgements:** The Grant Agency of the Academy of Sciences and the Ministry of Education of the Czech Republic are acknowledged for the support (Nos. KJB101120805 and No. MSM 0021620835, respectively).

[1] P. R. Carey, J. Dong, *Biochemistry* 43 (2004) 8885–8893

[2] D. Zhang, Y. Xie, M. F. Mrozek et al., *Anal. Chem.* 75 (2003) 5703–5709

[3] V. Kopecký Jr., V. Baumruk, *Vib. Spectrosc.* 42 (2006) 184–187

[6] [4] J. Kapitán J., V. Baumruk, V. Kopecký Jr. et al., *J. Am. Chem. Soc.* 128 (2006) 13451–13462



## DFT molecular force field of acetazolamide compound

S. A. Brandán<sup>1</sup>, E. Eroğlu<sup>2</sup>, A. E. Ledesma<sup>1</sup>, O. Oltulu<sup>2</sup>, O. B. Yalçinkaya<sup>3</sup>

<sup>1</sup>*Cátedra de Fisicoquímica I, Instituto de Química Física, Facultad de Bioquímica, Química y Farmacia, Universidad Nacional de Tucumán, San Lorenzo 456, T4000CAN, S. M. de Tucumán, R. Argentina.*

<sup>2</sup>*Harran University, Faculty of Sciences and Arts, Department of Physics, 63300, Şanlıurfa, Turkey.*

<sup>3</sup>*Istanbul University, Faculty of Sciences, Department of Physics, 34134, Vezneciler, Istanbul, Turkey.*

A theoretical structural and experimental vibrational study for the acetazolamide compound is presented (Figure 1). The Density functional theory (DFT) has been used to study its structures and vibrational properties.

The geometries were fully optimized at the B3LYP/6-31G\* and B3LYP/6-311++G\*\* levels of theory and the harmonic vibrational frequencies were evaluated at the same levels by using the Gaussian 03 [1] program. The calculated harmonic vibrational frequencies for the compound are consistent with the experimental IR and Raman spectra. These calculations gave us precise knowledge of the normal modes of vibration of this compound. A complete assignment of all the observed bands in the infrared and Raman spectra for the acetazolamide compound was performed by using the Pulay et al. SQMFF methodology [2].

The characteristic and nature of the different bonds in the compound was quantitatively investigated by means of Natural Bond Orbital (NBO) analysis [3]. The topological properties of electronic charge density are analysed by employing *Bader's* Atoms in the Molecules theory (AIM) [4].

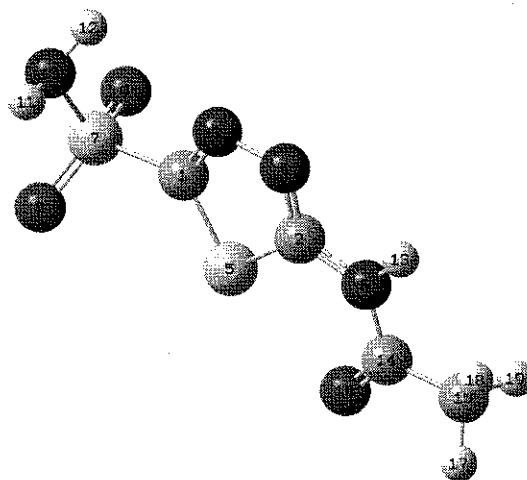


Figure 1: Theoretical structure of acetazolamide.

[1] Program Gaussian 03, GAUSSIAN, Inc. Pittsburgh, PAA, USA, 2003.

[2] G. Fogarasi, X. Zhou, P.W. Taylor and P. Pulay, *J. Am. Chem. Soc.* 105 (1992) 7037.

[3] E.D. Gledening, J.K. Badenhoop, A.D. Reed, J.E. Carpenter, F.F. Weinhold, NBO 3.1; Theoretical Chemistry Institute, University of Wisconsin; Madison, WI, 1998.

[4] R.F.W. Bader, *J. Phys. Chem. A*, 102 (1998) 7314.

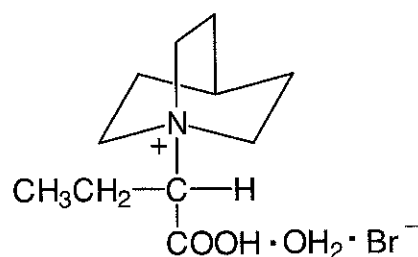


## Spectroscopic and structural studies of 2-(quinuclidinium)-butyric acid bromide hydrate

Z. Dega-Szafran, A. Katrusiak, M. Szafran, P. Barczyński

*Faculty of Chemistry, Adam Mickiewicz University, 60-780 Poznań, Poland*

Quinuclidine (1-azabicyclo[2,2,2]octane) is a strong base ( $pK_a = 11.15$ ). The Menshutkin reaction results in the formation of a variety of quaternary quinuclidinium salts by the action of alkyl electrophiles. The reaction of quinuclidine with 2-bromo-alkanocarboxylic acids results in homologues of 2-(quinuclidinium)-alkanocarboxylic bromides [1,2]. The subject of our interest is 2-(quinuclidinium)-butyric acid bromide (QNBu·HBr) which crystallizes as a hydrate. Its structure has been determined by X-ray diffraction.



The chiral center at the CH atom, is responsible for the non-magetical equivalence of the  $\text{CH}_2$  methylene protons in the substituent and two resonance signals in the  $^1\text{H}$  NMR spectrum are observed. The structures of monomer and dimeric cation of the title complex have been optimized by the B3LYP/6-31G(d,p) approach. The solid-state FTIR spectra of the complex and its deuterated analogue have been measured and compared with the theoretical spectrum. The assignments of the observed and predicted bands have been proposed. The  $pK_a$  values of quinuclidinium-acetate (quinuclidine betaine), 2-(quinuclidinium)-propionate and 2-(quinuclidinium)-butyrate determined by the potentiometric titration of their hydrohalides have been compared.

- [1] Z. Dega-Szafran, A. Katrusiak, M. Szafran, *J. Mol. Struct.* 929 (2009) 182.  
[2] Z. Dega-Szafran, A. Katrusiak, M. Szafran, *J. Mol. Struct.* (2010),  
doi:10.1016/j.molstruc.2010.03.029

## Infrared spectroscopic studies of $\text{Ca}^{2+}$ ATPase phosphoenzyme

N. Eremina, A. Barth

*Department of Biochemistry and Biophysics, The Arrhenius Laboratories for Natural Sciences, Stockholm University, SE – 10691 Stockholm, Sweden*

Muscle relaxation is mediated by the sarcoplasmic reticulum (SR)  $\text{Ca}^{2+}$  ATPase, an ion pump, which transports  $\text{Ca}^{2+}$  from the cytoplasm into SR against the concentration gradient. ATP is the energy source for this transport process. It phosphorylates the pump, which sequentially adopts two phosphorylated states,  $\text{Ca}_2\text{E1P}$  and  $\text{E2P}$ , with different properties.

Earlier work has determined vibrational frequencies of the transiently bound phosphate group of the  $\text{E2P}$  state, by monitoring  $\text{E2P}$ 's oxygen exchange with isotopically labelled water [1]. This approach however does not work for the  $\text{Ca}_2\text{E1P}$  state, because it is not reactive with water. So a new method has been developed, which involves a helper enzyme to initiate an isotope exchange [2]. In this study we use this method to investigate the  $\text{Ca}_2\text{E1P}$  state.

Previously two bands of the  $\text{Ca}_2\text{E1P}$  phosphate state have been tentatively identified at 1175 and 1113  $\text{cm}^{-1}$ , by comparison of spectra obtained with labelled and unlabelled ATP. These originate from the P-O stretching vibrations of the P-O terminal bonds [3]. The goal of the present work is to confirm the two bands mentioned above as well as to search for third expected P-O band with isotope exchange.

[1] A. Barth, N. Bezlyepkina, *J. Biol. Chem.* 279 (2004) 51888-51896

[2] E-L. Karjalainen, A. Hardell, A. Barth, *Biophys. J.* 91 (2006) 2282-2289

[3] M. Liu, M. Krasteva, A. Barth, *Biophys. J.* 89 (2005) 4352-4363



## Experimental and theoretical study of molecular structure of magnesium, calcium, strontium and barium 4-nitrobenzoates

M. Samsonowicz, E. Regulska, R. Świsłocka, W. Lewandowski

*Department of Chemistry, Białystok Technical University, Zamenhofa 29,  
15-435 Białystok, Poland*

The effect of alkali metals on the electronic system of 4-nitrobenzoic acid was investigated and reported previously [1]. In this paper the influence of magnesium, calcium, strontium and barium ions on the electronic system of 4-nitrobenzoic acid was studied. The vibrational (FT-IR) and NMR ( $^1\text{H}$  and  $^{13}\text{C}$ ) spectra were recorded for 4-nitrobenzoic acid and its salts. The assignment of vibrational spectra was done. Characteristic shifts of band wavenumbers and changes in band intensities along the metal series  $\text{Mg} \rightarrow \text{Ba}$  were observed. Good correlations between the wavenumbers of the vibrational bands in the IR spectra for 4-nitrobenzoates and ionic potential, electronegativity, inverse of atomic mass, atomic radius and ionization energy of metals were found. The chemical shifts of protons ( $^1\text{H}$  NMR) and carbons ( $^{13}\text{C}$  NMR) in the series of studied alkali earth metals 4-nitrobenzoates were observed too.

Optimized geometrical structures of studied compounds were calculated by B3LYP method using 6-311++G\*\* basis set. The theoretical wavenumbers and intensities of IR spectra were obtained. The calculated parameters were compared to experimental characteristic of studied compounds.

This work was supported by grant no. N N305 267534

- [1] E. Regulska, M. Samsonowicz, R. Świsłocka, W. Lewandowski, *J. Phys. Org. Chem.*, 20 (2007) 93-108



## Isomerizational and conformational study of methyl-2-cyano-3-methoxyacrylate (MCMA) and methyl-2-cyano-3-aminoacrylate (MCAA) and its N-methyl derivatives

A. Gatíal<sup>1</sup>, H. Juhásová<sup>1</sup>, M. Gróf<sup>1</sup>, J. Kožíšek<sup>1</sup>, V. Milata<sup>2</sup>, N. Prónayová<sup>3</sup>, P. Matejka<sup>4</sup>

<sup>1</sup>Department of Physical Chemistry, <sup>2</sup>Department of Organic Chemistry, <sup>3</sup>Central Laboratories, Faculty of Chemical and Food Technology, Slovak University of Technology, SK-81237 Bratislava, Slovakia

<sup>4</sup>Department of Analytical Chemistry, Institute of Chemical Technology, CZ-16628 Prague, Czech Republic

H<sub>3</sub>C-O-CH=C(CN)(COOCH<sub>3</sub>) (MCMA) and H<sub>2</sub>N-CH=C(CN)(COOCH<sub>3</sub>) (MCAA) and its N-methyl derivatives belong to the push-pull ethylenes intensively used in synthetic organic chemistry. The electron donor methoxy and amino groups in the investigated compounds seem to have a special influence on their conformational and configurational equilibria due to the different possibility to create an intramolecular hydrogen bond.

Whereas MCMA and methyl-2-cyano-3-dimethylaminoacrylate (MCDMAA) (H<sub>3</sub>C)<sub>2</sub>N-CH=C(CN)(COOCH<sub>3</sub>) have no such possibility and were prepared as *E* isomers confirmed by X-ray analysis, MCAA and methyl-2-cyano-3-methylaminoacrylate (MCMAA) H<sub>3</sub>C-NH-CH=C(CN)(COOCH<sub>3</sub>) can form intramolecular hydrogen bond between aminohydrogen and carbonyl oxygen and therefore *Z* isomer is more stable. MCAA and MCMAA were prepared as a mixture of both isomers and by heating or dissolving in solvent of different polarity it is possible to shift not only conformational but also isomerizational equilibrium as confirmed by NMR and IR and Raman spectroscopy.

Using ab initio MP2 and DFT B3LYP calculations in different basis sets four conformers of MCMA and MCMAA and two conformers of MCAA and MCDMAA have been found for each *Z*-isomer and *E*-isomer (the first *Z* or *E* letters will denote isomer, i.e. *cis* and *trans* position of methoxy or amino and methyl ester groups, the second *Z* or *E* and the third *s* or *a* letters denote the conformational orientation of carbonyl oxygen and methoxy or methylamino group towards or from double C=C bond, respectively). As shown by the calculations, they significantly differ in energy and their behaviour in polar surrounding was estimated by solvent effect calculations using IEFPCM model in different basis sets.

The isomerization was not found out for MCMA and with the most stable *EZa* conformer the second *EEa* conformer of *E*-isomer was observed in DMSO solution as well as in solid phase. Similarly, the isomerization was not observed for MCDMAA and only very weak arguments for the presence of the second less stable *EE* conformer in very polar solutions from IR spectra were obtained. For MCMAA, three conformers were found in very polar DMSO and isomerizational shift between *ZZa* and *EZa* and *EEa* isomers was explained by the solvent effect calculations.

Table 1: MP2/6-311G\*\* calculated ab initio relative energies ΔE of the conformers of studied compounds.

|              |            |            |            |            |               |            |            |            |           |
|--------------|------------|------------|------------|------------|---------------|------------|------------|------------|-----------|
| <b>MCMA</b>  | <i>EZa</i> | <i>EZs</i> | <i>EEa</i> | <i>EEs</i> | <i>ZZa</i>    | <i>ZZs</i> | <i>ZEa</i> | <i>ZZs</i> |           |
| ΔE(kJ/mol)   | 0.00       | 1.40       | 5.63       | 7.04       | 15.36         | 23.01      | 19.41      | 32.43      |           |
| <b>MCMAA</b> | <i>EZa</i> | <i>EZs</i> | <i>EEa</i> | <i>EEs</i> | <i>ZZa</i>    | <i>ZZs</i> | <i>ZEa</i> | <i>ZEs</i> |           |
| ΔE(kJ/mol)   | 7.41       | 14.27      | 13.31      | 21.26      | 0.00          | 36.00      | 15.99      | 47.62      |           |
| <b>MCAA</b>  | <i>EZ</i>  | <i>EE</i>  | <i>ZZ</i>  | <i>ZE</i>  | <b>MCDMAA</b> | <i>EZ</i>  | <i>EE</i>  | <i>ZZ</i>  | <i>ZE</i> |
| ΔE(kJ/mol)   | 6.01       | 11.69      | 0.00       | 15.34      | ΔE(kJ/mol)    | 0.00       | 7.54       | 20.03      | 31.47     |

**Acknowledgement.** This work has been supported by Slovak Grant Agency VEGA (Projects No. 1/0127/09, 1/0817/08 and 1/0225/08).



## Propanol in argon matrix: 2D FTIR correlation spectroscopy

V. Šablinskas<sup>1</sup>, I. Doroshenko<sup>2</sup>, V. Pogorelov<sup>2</sup>, V. Balevicius<sup>1</sup>

<sup>1</sup>Vilnius university, Faculty of Physics, Sauletekio al. 9-3, LT-10222 Vilnius, Lithuania

<sup>2</sup>National Taras Shevchenko University of Kiev, Faculty of Physics, Glushkova av. 2, build.1, Kiev, Ukraine

The dynamic FTIR spectra of propanol in argon matrix have been measured by heating the sample from  $T = 11$  K to 30 K stepping by 1 K (for 3000 - 3700  $\text{cm}^{-1}$  region, i.e. the range of H-bond stretching vibrations, see Fig. 1) till the argon matrix starts to evaporate at 31 K. The original spectra were baseline corrected. The zero-absorbance was used as the reference spectrum.

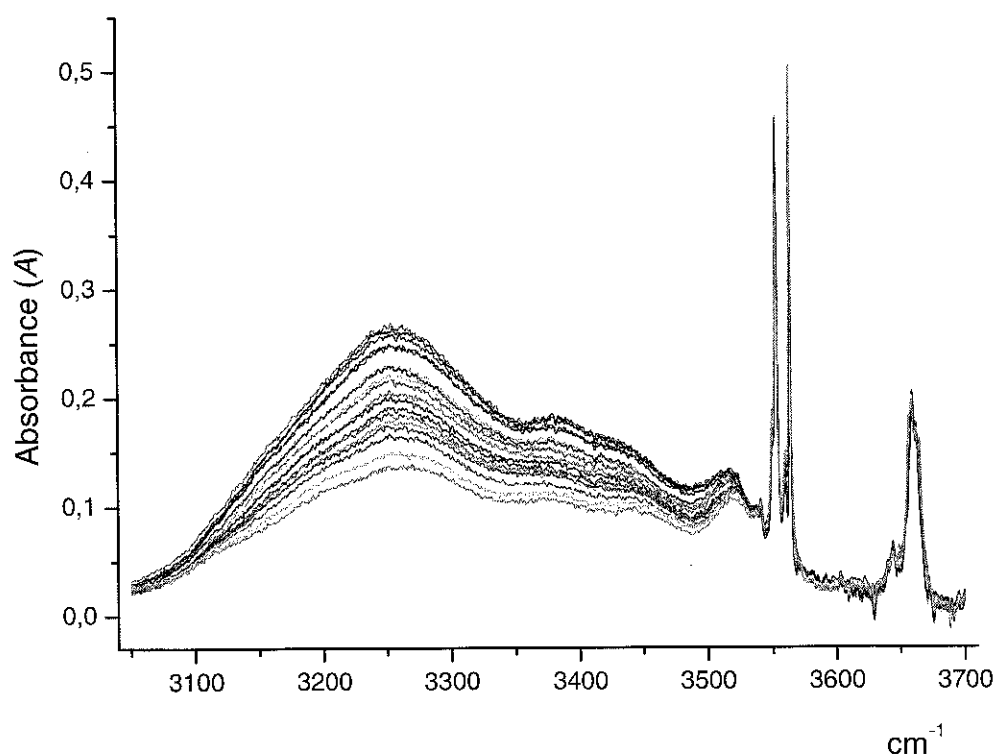


Fig. 1. FTIR spectra of propanol in argon matrix in O-H stretching region over the temperature range 11 - 30 K (from bottom to upper, by stepping  $\Delta T = 1$  K).

The synchronous 2D FTIR correlation spectrum was obtained by the inner product of two spectrum vectors, while the asynchronous correlation spectrum was calculated by a cross product of the spectrum vector and its Hilbert transformation [1]. New information concerning the formation and stoichiometry of the H-bond clusters as well as the conformational changes was obtained.

[1] I. Noda, Y. Ozaki, *Two-Dimensional Correlation Spectroscopy: Applications in Vibrational and Optical Spectroscopy* (Wiley: Chichester, 2004).

## Vibrational and structural study of 6,6'-diacetyl-2,2'-bipyridine dioxime using FT-IR Raman and quantum chemical calculations

A. Şengül<sup>1</sup> and E. Eroğlu<sup>2</sup>

<sup>1</sup>Karaelmas University, Faculty of Sciences and Arts, Department of Chemistry, 67100, Zonguldak, Turkey.

<sup>2</sup>Harran University, Faculty of Sciences and Arts, Department of Physics, 63300, Şanlıurfa, Turkey.

The Fourier transforms infrared and Raman spectra of 6,6'-diacetyl-2,2'-bipyridine dioxime were recorded in the solid phase. Optimized geometry, frequency and intensity of the vibrational bands of the title compound were investigated by utilizing ab initio and DFT calculations with 6-31G\* basis set at HF, MP2 and DFT-BLYP levels of the theory using the Gaussian 03 [1] program. The calculated structure and scaled theoretical wavenumber showed very good agreement with the experimental values. Normal coordinate calculations were carried out and potential energy distributions were calculated for the title compound using MOLVIB [2] program. A detailed interpretation of the infrared and Raman spectra was reported based on a normal mode analysis of fundamental frequencies.

[1] Program Gaussian 03, GAUSSIAN, Inc. Pittsburgh, PAA, USA, 2003.

[2] T. Sundius, MOLVIB Program, J. Mol. Struct. 218 (1990) 321; Vib. Spectrosc. 29 (2002) 89.





**NMR, IR and Raman investigation of 3-[2-(4-Methyl-2-phenyl-thiazol-5-yl)-2-oxo-ethyl]-thiazolidine-2,4-dione compound with antimicrobial potential**

N. Vedeanu<sup>1</sup>, A. Pîrnău<sup>2</sup>, I. B. Cozar<sup>3</sup>, O. Oniga<sup>1</sup>, C. Moldovan<sup>1</sup>, C. M. Lucaciu<sup>1</sup>

<sup>1</sup>Iuliu Hațieganu University of Medicine and Pharmacy, RO-400023 Cluj-Napoca, Romania

<sup>2</sup>National Institute for Research and Development of Isotopic and Molecular Technologies, RO-400293 Cluj-Napoca, Romania

<sup>3</sup>Babes-Bolyai University, Faculty of Physics, RO-400028 Cluj-Napoca, Romania

The treatment of infectious diseases is an important and challenging problem due to a combination of factors, including emerging infectious diseases and the increasing number of multi-drug resistant microbial pathogens. Bacterial resistance has become a serious public health problem, demanding new classes of antibacterial agents. Thiazoles and their derivatives have attracted the interest over the last decades because of their varied biological activities: antibacterial, antiviral, antifungal, inflammation or in the treatment of allergies.

A new synthesized compound 3-[2-(4-Methyl-2-phenyl-thiazol-5-yl)-2-oxo-ethyl]-thiazolidine-2,4-dione was investigated by <sup>1</sup>H NMR and vibration spectroscopy [1].

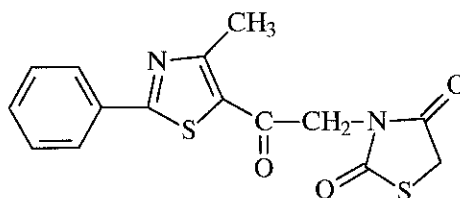


Fig. 1. 3-[2-(4-Methyl-2-phenyl-thiazol-5-yl)-2-oxo-ethyl]-thiazolidine-2,4-dione

The <sup>1</sup>H and <sup>13</sup>C NMR spectra of this new compound was recorded at room temperature on a Bruker Avance III NMR spectrometer operating at 500 MHz for <sup>1</sup>H and 125.76 MHz for <sup>13</sup>C, internal standard TMS. The sample was prepared by dissolution in DMSO-d<sub>6</sub> (signal for <sup>1</sup>H at 2.512 ppm and at 39.476 ppm for <sup>13</sup>C). The spectra were recorded using a single excitation pulse of 10.1 μs for <sup>1</sup>H and 8 μs for <sup>13</sup>C. The FID signal was acquired 32 times for <sup>1</sup>H and 1024 times for <sup>13</sup>C [2].

In addition, vibrational techniques (IR and Raman) were used to evidence the structure of the new synthesized compound and the spectra obtained present the bands corresponding to the structural units of this compound. Vibrational spectroscopy offers functional group analysis through direct observation of the chemical bond itself. It can also determine the formation of the reaction products through spectra obtained. In pharmaceutical discovery research, vibrational spectroscopy can indicate intermolecular hydrogen bonding through appropriate placement of ligand substituents [3].

[1] D. A. Shinabarger, *Exp. Opin. Invest. Drugs* 8 (1999) 1195

[2] V. Chis, A. Pîrnău, O. Oniga, N. Leopold, L. Szabo, M. Baias, O. Cozar, *Vib. Spectrosc.* 48 (2008) 289

[3] H. Deng, A. Lewandowicz, S. M. Cahill, R. H. Furneaux, P. C. Tyler, M. E. Girvin, R. H. Callender, V. L. Schramm, *Biochemistry* 43 (2004) 1980



**Paramagnetic species generated by near IR as possible intermediates in molecular mechanism of optical nonlinearity in 1,3-dinitrobenzene crystal. NIR, EPR, CD and quantum chemical studies**

M. M. Szostak<sup>1</sup>, K. Piela<sup>1</sup>, H. Chojnacki<sup>1</sup>, E. Bidzińska<sup>2</sup>, K. Dyrek<sup>2</sup>

<sup>1</sup> *Wrocław University of Technology, Wybrzeże Wyspiańskiego 27, 50-370 Wrocław, Poland*

<sup>2</sup> *Jagiellonian University, Ingardena 3, 30-060 Kraków, Poland*

A few minutes storage of electric charges generated by the exposure to near IR (NIR) (photoelectret property) was recently detected by us in the weakly conducting 3-nitroaniline (m-NA) crystal [1]. The occurrence of paramagnetic species (polarons) and motions of molecular fragments lead to conformational chirality of the solid m-NA confirmed by the recorded and calculated circular dichroism (CD) spectra [2]. Our spectroscopic research on 1,3-dinitrobenzene (m-DNB) crystal revealed its many features similar to those of m-NA suggesting an easy formation of charged species also in this crystal [3].

In this work the polarized NIR spectra of a single crystal, EPR spectra of powders, and CD spectra of m-DNB in KBr pellets were recorded before and after the illumination by two NIR diode lasers beams. The spectroscopic results are discussed taking into account calculated band structure as well as calculated CD spectra and first hyperpolarizabilities ( $\beta$ ) for neutral molecule and radical anion. The role of polarons in molecular mechanism of m-DNB crystal optical nonlinearity will be proposed.

- [1] M.M.Szostak, H. Chojnacki, E. Staryga, M. Dłużniewski, G. Bąk, *Chem. Phys.* 365 (2009) 44-57  
[2] M.M. Szostak, H. Chojnacki, *Book of Abstracts of First Polish-French Workshop on Organic Electronics and Nanophotonics, Świeradów-Zdrój, Poland. 2010, P-16, 53*  
[3] M. Trzebiatowska-Gusowska, K. Piela, T. Misiaszek, M.M. Szostak, J. Baran, *J. Raman Spectrosc.*, in press 2010, DOI 10.1002/jrs

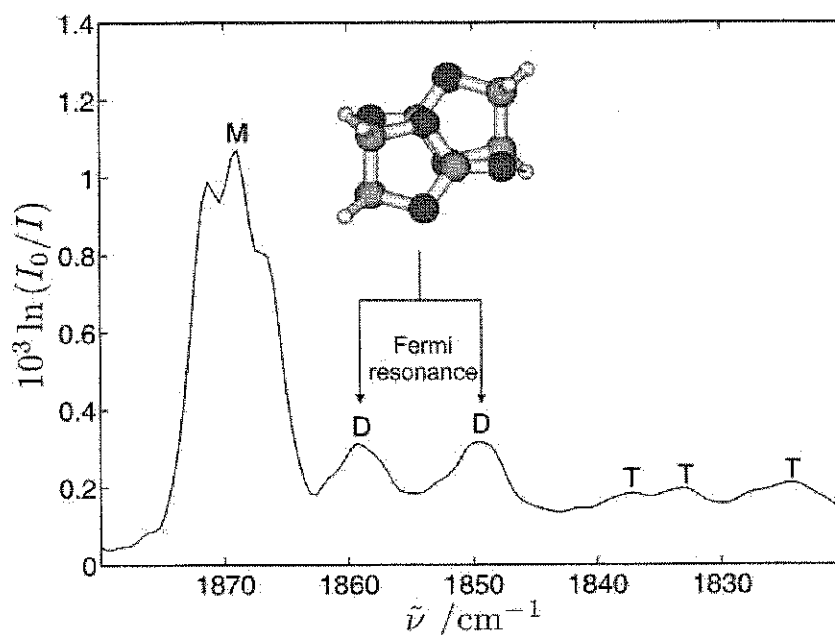


## Dimers of Cyclic Carbonates: Chirality Recognition in Battery Solvents

F. Kollipost, S. Hesse, J. J. Lee, M. A. Suhm

*Institut für Physikalische Chemie, Tammannstraße 6, 37077, Göttingen, Germany*

Dimers of ethylene carbonate and propylene carbonate are created in supersonic jet expansions and characterized by FTIR spectroscopy. The study continues an earlier investigation of the related lactones [1]. While there is a unique centrosymmetric dimer of ethylene carbonate in a pronounced case of complementary chirality synchronization, two chiral propylene carbonate molecules combine in more intricate ways. If they have the same handedness, one of them is forced into an axial conformation and the binding partner stays in the more stable equatorial structure. If they have opposite handedness, centrosymmetric dimers of either axial or equatorial conformations are formed.



[1] S. Hesse, M. A. Suhm, *Phys. Chem. Chem. Phys.* 11 (2009), 11157-11170

## The reactivity of nitromethane under high static pressure

M. Citroni<sup>1,2</sup>, R. Bini<sup>1,2</sup>, M. Pagliai<sup>1,2</sup>, G. Cardini<sup>1,2</sup>, V. Schettino<sup>1,2</sup>

<sup>1</sup>European Laboratory for Non-Linear Spectroscopy (LENS), via N. Carrara 1, 50019 Sesto Fiorentino (FI), Italy

<sup>2</sup>Dipartimento di Chimica, Università di Firenze, via della Lastruccia 3, 50019 Sesto Fiorentino (FI), Italy

Nitromethane is the simplest explosive compound containing the NO<sub>2</sub> group linked to a C atom. Understanding its reactivity induced by static or dynamic compression has been a major unresolved issue, fundamental for the general purpose of understanding, mastering and designing safe and efficient explosive compounds.

We have investigated the reactivity of nitromethane induced by high static pressure at ambient temperature by means of infrared spectroscopy and *ab initio* molecular dynamics simulations. The evolution of the IR spectrum during the reaction has been monitored at 32.2 and 35.5 GPa performing the measurements in a diamond anvil cell.

The simulations have allowed the characterization of the onset of the reaction mechanism at high pressure, showing that it involves the formation of aci-ion forms of nitromethane through a bimolecular process. The reaction gives rise to an extended amorphous polymer. From the point of view of solid state chemistry, the reaction mechanism is fully consistent with the known crystal structure at the reaction pressure [1].

The decompression of the sample after the reaction has been monitored by IR spectroscopy, observing a continuous evolution of the product. The disordered and extended network obtained during the high-pressure reaction decomposes releasing the pressure in smaller molecules. This behavior has been confirmed by the simulations and represents an important novelty in the scene of the known high-pressure reactions of molecular systems.

The major reaction product has been identified as N-methylformamide, the smallest molecule containing the peptide bond.

[1] M. Citroni, F. Datchi, R. Bini, M. Di Vaira, Ph. Pruzan, B. Canny, V. Schettino, J. Phys. Chem. B 112 (2008) 1095-1103.



## Rotational spectrum of glycolamide-water and glycolamide-ammonia molecular complexes.

A. Maris<sup>1</sup>, S. Melandri<sup>1</sup>, W. Caminati<sup>1</sup>, L. B. Favero<sup>2</sup>

<sup>1</sup> "G. Ciamician" Department of Chemistry, University of Bologna, Via Selmi 2, I-40126 Bologna, Italy.

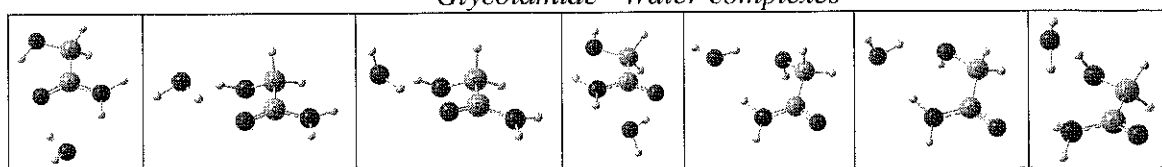
<sup>2</sup> I.S.M.N.-C.N.R., Via Gobetti 101, I-40129 Bologna, Italy

Hydrogen bonds play important roles in many chemical and bio-chemical processes. Hydrogen-bonded complexes involving small organic molecules and water or ammonia can be formed in adiabatic expansions and probed spectroscopically. The hydrogen bonding interactions in these species can be used as models for the hydrogen bonding networks observed in larger systems. Rotationally resolved spectroscopy has been employed in numerous studies to gain insights into hydrogen bonds at the molecular level as an effective approach for the study of hydrogen bonds [1].

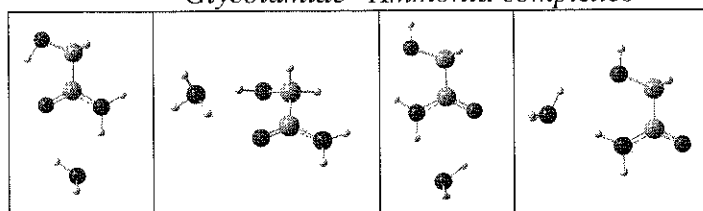
The rotational spectra of glycolamide...H<sub>2</sub>O (<sup>16</sup>O and <sup>18</sup>O) and glycolamide...NH<sub>3</sub> have been measured and assigned by free-jet millimeter-wave absorption spectroscopy in the 58.9-78.3 GHz region. Among all the possible conformers (see figure), only one was observed. In the observed form the solvent moiety is bound to the amidic group, acting both as a proton donor to the carbonyl and proton acceptor from the amine group. Additionally an intramolecular interaction takes place between the hydroxyl and the carbonyl groups of glycolamide.

The strong preference of the solvent molecule to form a closed ring structure stabilized by two intermolecular hydrogen bonds with the amide group rather than the aldol or β-aminoalcohol unit of glycolamide was confirmed by *ab initio* (MP2) and density function theory (B3LYP) calculations performed both at 6-311++G\*\* and aug-cc-pVTZ level, using the Gaussian 09 suite of programs [2].

Glycolamide...Water complexes



Glycolamide...Ammonia complexes



[1] W. Caminati and Jens-Uwe Grabow, in "Frontiers of Molecular Spectroscopy"; J. Laane Ed. (Elsevier, Amsterdam, The Netherlands), 2009.

[2] Gaussian 09, Revision A.02, M. J. Frisch et al., Gaussian, Inc., Wallingford CT, 2009.

## Synthesis, structural characterization and some applications of immobilized organocatalysts

A. Mayer<sup>1</sup>, M. Sipiczki<sup>1</sup>, Gy. Szöllösi<sup>2</sup>, J.T. Kiss<sup>1</sup>, I. Pálinkó<sup>1\*</sup>

<sup>1</sup>Department of Organic Chemistry, University of Szeged, Dóm tér 8, Szeged, H-6720 Hungary

<sup>2</sup>Stereochemistry Research Group of the Hungarian Academy of Sciences, University of Szeged, Dóm tér 8, Szeged, H-6720 Hungary

Organocatalysis may be defined as the acceleration of chemical reactions through adding organic molecules in less than the stoichiometric amount to the reacting mixture [1]. The catalysts are small organic molecules containing nitrogen, sulfur, or phosphorous beside carbon, hydrogen and oxygen. In recent years this area has been buzzing, the number of published paper vs. year function is by far over the linear relationship [2]. The majority of the work applies organocatalysts in the same phase as the reactants and the products, and thus, the recovery and recycling of the catalytic molecules is difficult if not impossible. Scarcely appearing papers only describe the synthesis and use immobilized organocatalysts [3, 4]. In this contribution the synthesis and structural characterization of covalently anchored organocatalysts is described and some examples for their catalytic applications are also given.

For immobilization N-protected or C-protected L-proline was used and the solid phase was chloropropylated silica gel. The compounds were covalently grafted onto the silica gel surface, esterification or N-alkylation reactions proceeded. Then, the protecting groups were removed and the resulting substances were structurally characterized with FT-IR spectroscopy (BIORAD FTS 65/896 spectrophotometer, 4000–400 cm<sup>-1</sup> range, diffuse reflectance measurements, WinIR package). A commercially available substance, the resin-anchored L-prolinol-2-chlorotrityl ether was also studied with this method. For the proline derivatives it was found that anchoring was successful and the anchored compounds remained intact, i.e. no decomposition took place. The IR spectrum of the resin-anchored material also showed the features of the immobilized organic material.

The catalytic effects of the solid substances were probed in aldol dimerization reactions of acetone with various aldehydes (benzaldehyde, 2-nitro- and 4-nitrobenzaldehyde and 2-thiophene carbaldehyde). The reactions were run at room temperature, analysis was done with a gas chromatograph (YL6100GC-6000) equipped with a chiral capillary column (Cyclosil B). Identification and quantitative analysis of the products was done with a mass selective and a flame ionization detector, respectively. Proline immobilized at the N atom was not active, while the silica-anchored proline efficiently and with high selectivity catalyzed the aldol dimerization of acetone and 2-nitrobenzaldehyde. The resin-immobilized material catalyzed the reaction with all the reactants, however, occasionally appreciable dehydration of the aldol dimer occurred. In some cases substantial enantioselectivity was observed in the dimerization reaction.

The experiments showed that the properly anchored organocatalysts do not lose their activity and their recovery and reuse are significantly helped by the heterogenization.

[1] K.A. Ahrendt, C.J. Borths, D.W.C. Macmillan, *J. Am. Chem. Soc.* 122 (2000) 4243-4244

[2] B. List, *Chem. Rev.* 107(2007) 5413-5415

[3] S.E. Park, E.A. Prasetyano, *Top. Catal.* 52 (2009) 91-100

[4] M. Gruttadauria, F. Giacalone, R. Noto, *Chem. Soc. Rev.* 37 (2008) 1666-1688

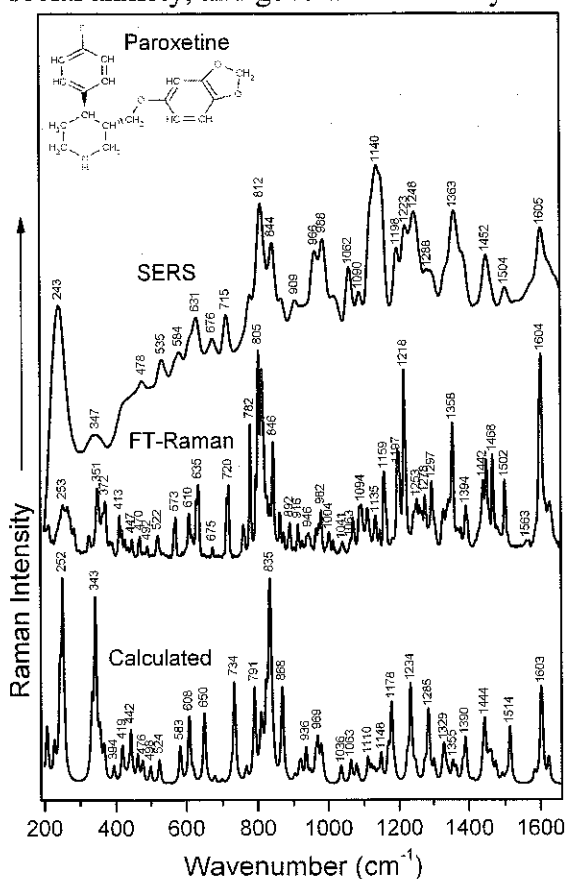


## Vibrational spectroscopic and DFT study of paroxetine

I. B. Cozar, L. Szabó, N. Leopold, D. Mare, V. Chiş, L. David

*Faculty of Physics, Babeş-Bolyai University, Kogălniceanu 1, 400084 Cluj-Napoca, Romania*

Paroxetine (trade names Seroxat, Paxil) (3*S*,4*R*) -3- [(2*H*-1,3- benzodioxol -5-yloxy) methyl] -4-(4-fluorophenyl) piperidine is a selective serotonin reuptake inhibitor (SSRI) antidepressant. Paroxetine is used to treat major depression, obsessive-compulsive, panic, social anxiety, and generalized anxiety disorders in adult outpatients.



Structural investigations by different vibrational spectroscopic methods (FT-IR, Raman and SERS), as well as density functional theory (DFT) based calculations were performed on paroxetine. These studies contribute to the understanding of the structure-activity relationships and the physico-chemical behavior of the investigated system [1].

The inserted figure shows the Raman and SERS spectra of paroxetine recorded using the 532 nm laser line. In the SERS experiments, the paroxetine molecules adsorbed to hydroxylamine reduced colloidal silver nanoparticles.

Experimental data were interpreted with the aid of quantum chemical calculations based on density functional theory (DFT). After the identification of the lowest energy conformer of the molecule, vibrational IR and Raman spectra of the paroxetine molecule were assigned based on DFT calculations at B3LYP level of theory using the 6-31G(d) and cc-pVTZ basis sets. The very good correlation found between the experimental and theoretical data is a clear evidence for a reliable assignment of all

vibrational bands.

The molecular electrostatic potential was calculated and used as a reactivity map for the prediction of preferred adsorption sites of the investigated molecule.

The enhancement in the SERS spectra of the ring stretching vibrations in the 810-850 and 1605  $\text{cm}^{-1}$  region, indicate a preponderant perpendicular adsorption geometry of the paroxetine aromatic rings to the silver surface.

[1] L. Szabó, V. Chiş, A. Pîrnău, N. Leopold, O. Cozar, Sz. Orosz, *J. Mol. Struct.*, 924–926, 361–370 (2009)



## Analysis of the frequency shift and the linewidth as a function of temperature in solid nitrogen

M. Kurt<sup>1</sup>, H. Yurtseven<sup>2</sup>

<sup>1</sup>*Department of Physics, Çanakkale 18 Mart University, 17100 Çanakkale, Turkey*

<sup>2</sup>*Department of Physics, Middle East Technical University, 06531 Ankara, Turkey*

The temperature dependence of the frequency shift and the linewidth is studied using the expressions derived from the anharmonic self energy. The functional form of the frequency shift is fitted in the study to the experimental data for the R<sub>1</sub> fluorescence line of ruby sample as a function temperature at zero pressure, instead of using empirical  $\nu - P$  and  $\nu - T$  relations in the ruby-fluorescence method as given in the literature, in particular, for the solid nitrogen.

We also demonstrate in the study the temperature dependence of the E<sub>g</sub> librational frequency and its linewidth by fitting the functional forms of both frequency shift and the linewidth to the experimental data for the  $\alpha$  phase of solid nitrogen.





FT-IR and RAMAN studies on the  $P_2O_5$ -BaO- $Li_2O$  glass system

C. Ivascu, L. Daraban, O. Cozar and I. Ardelean

*Babeş-Bolyai University, Faculty of Physics, RO-400084, Cluj-Napoca, Romania*

In this paper, were investigated through FT-IR and Raman spectroscopies the  $P_2O_5 \cdot 2xBaO \cdot (1-2x) Li_2O$  glass system where  $0 \leq x \leq 0.5$  mol%. FT-IR and Raman spectra show structural modifications with the variation of studied glasses composition. The characteristic bands of the FT-IR spectra of these glasses due to the stretching and bending vibrations were identified and analyzed by the increasing of  $Li_2O$  content.

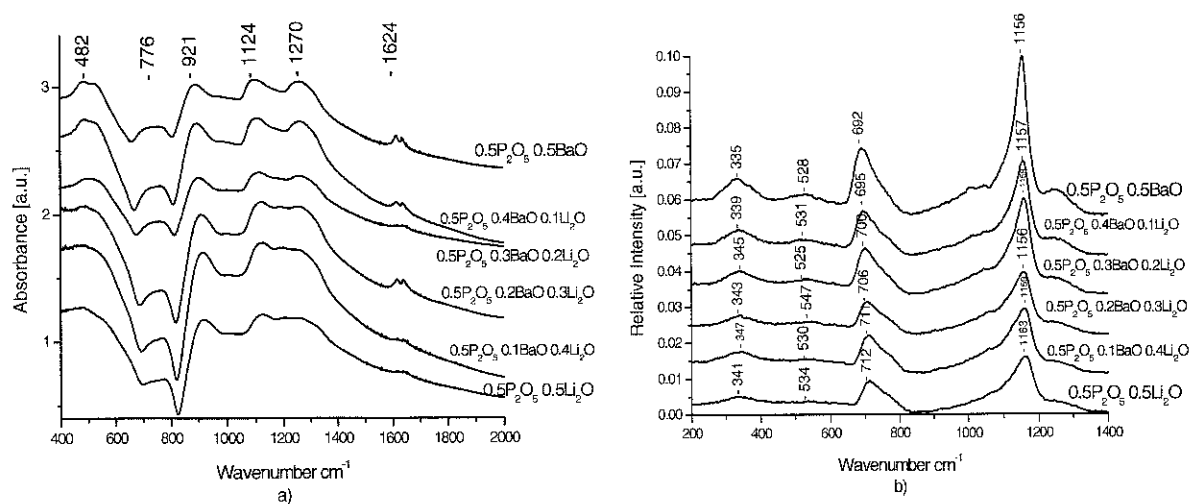


Fig.1: FT-IR(a) and Raman(b) spectra of  $P_2O_5 \cdot 2xBaO \cdot (1-2x) Li_2O$  glass system.

In the typical infrared spectra of studied glasses, the predominant absorption band are attributed to the symmetric stretching vibrations of P=O double bonds. Raman spectra of the studied glasses contain typical bands attributed to the phosphate glasses. The band at  $\sim 700$   $cm^{-1}$  is assigned to symmetric stretching vibrations of P-O-P groups. The band from  $\sim 1158$   $cm^{-1}$  is attributed to symmetric stretching motions of the non-bridging oxygen (NBO) atoms bonded to phosphorous atoms ( $PO_2$ ) in phosphate tetrahedron [1]. FT-IR and Raman spectroscopies revealed a local network structure mainly based on  $Q^2$  and  $Q^3$  tetrahedrons connected by P-O-P linkages [2].

- [1] N. Vedeanu, O. Cozar, I. Ardelean, B. Lendl, D.A. Magdas, *Vibrational Spectroscopy*, 48 (2008) 259.  
 [2] D. Ilieva, B. Jivov, G. Bogachev, C. Petkov, I. Penkov and Y. Dimitriev, *Journal of Non-Crystalline Solids*, 283 (2001) 195.



## DFT, FT-Raman, FT-IR and NMR studies of 4-(substituted phenylazo)-3,5-diacetamido-1H-pyrazoles

S. Demirci<sup>1</sup>, S. Kınalı<sup>2</sup>, Z. Çalışır<sup>3</sup>, M. Kurt<sup>3</sup>, A. Ataç<sup>4</sup>

<sup>1</sup>Ahi Evran University, Faculty of Science and Art, Department of Chemistry, 40100, Kırşehir, Turkey

<sup>2</sup>Gazi University, Faculty of Science and Art, Department of Chemistry, 06500, Ankara, Turkey

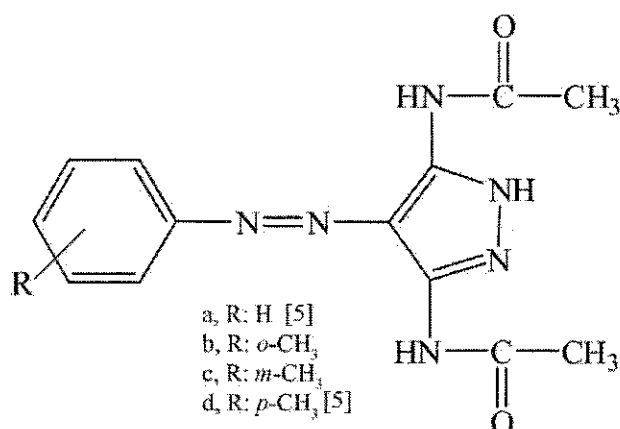
<sup>3</sup>Ahi Evran University, Faculty of Science and Art, Department of Physics, 40100, Kırşehir, Turkey

<sup>4</sup>Celal Bayar University, Faculty of Science and Art, Department of Physics, 45043, Manisa, Turkey

Azo dyes are very important class of synthetic chemicals [1] known as organic colorants commonly prepared by coupling of a diazonium compound with a phenol or an aromatic amine [2]. The azo dyes containing heterocyclic rings result in brighter and often deeper shades than their benzene analogs. On the other hand, they are very important in applications such as disperse dyes for polyester fibers, reprography, functional dye and nonlinear optical systems, photodynamic therapy, and lasers [3,4].

In this study, 2-(substituted phenylazo)malononitriles were synthesized by the coupling reaction of the diazonium salts, which were prepared with the use of various aniline derivatives with malononitrile, and then some novel (b and c) 4-(substituted phenylazo)-3,5-diamino-1H-pyrazoles were obtained via the ring closure of the azo compounds with hydrazine monohydrate.

The experimental and theoretical vibrational spectra of 4-(substituted phenylazo)-3,5-diacetamido-1H-pyrazoles were studied. The Fourier transform Raman and Fourier transform infrared spectra of the 4-(substituted phenylazo)-3,5-diacetamido-1H-pyrazoles molecules were recorded in the solid phase. The structural and spectroscopic analysis of the molecules were carried out by using Hartree-Fock and density functional harmonic calculations. The <sup>1</sup>H and <sup>13</sup>C nuclear magnetic resonance (NMR) chemical shifts of the 4-(substituted phenylazo)-3,5-diacetamido-1H-pyrazoles molecules were calculated using the Gauge-Invariant-Atomic Orbital (GIAO) method. Finally, geometric parameters, vibrational wavenumbers and chemical shifts were compared with available experimental data of the molecules.



- [1] R.A. Hoodles, K.G. Pitman, T.E. Stewart, J. Thompson, J.E. Arnold, J. Chromatogram 54 (1971) 393-404.
- [2] K. Golka, S. Kopps, Z.W. Myslak, Toxicol. Lett. 151 (2004) 203-210.
- [3] P.C. Tsai, I.J. Wang, Dyes and Pigments 74 (2007) 578-584
- [4] A.C. Razus, L. Birzan, N.M. Surugiu, Dyes and Pigments 74 (2007) 26-33
- [5] M.H. Elnagdi, E.M. Kandeel, E.M. Zayed, Z.E. Kandil, J. Heterocyclic Chem. 14 (1977) 155-157



## Theoretical and experimental vibrational analysis of hydantion

G. Ogruc-Ildiz

*Istanbul Kultur University, Faculty of Science and Letters, Department of Physics, Atakoy Campus, Bakirkoy 34156, Istanbul, Turkey*

Hydantoin is a biologically active molecule widely used in medicine as antiepileptic, antischistosomal, antiarrhythmic, antibacterial and tuberculostatic drugs [1,2]. It is also an effective medication for the treatment of metastatic prostate cancer. Beside its medical usage it is also used as herbicides and fungicides [3,4].

In this study the geometry optimization of monomeric and dimeric forms of hydantoin molecule were done using DFT method employing 6-31++G(d,p) basis set. Harmonic and anharmonic wavenumbers and infrared intensities were computed at the same theory level. Experimental IR spectra were recorded. The hydrogen bond interaction of hydantoin was investigated via dimers of hydantoin and vibrational frequency shifts were reported. Total energy distribution (TED%) calculations were done to characterize the fundamentals.

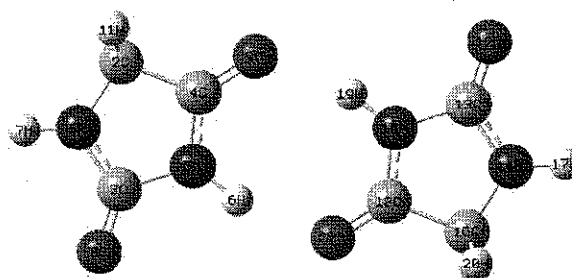


**Fig.1.** The dimeric form of hydantoin molecule

- [1] M.V.P. Santos, M.R.S. Junior, S.M Oliveira, J.B.P. Silva, M.T.C. Lima, M.C.A. Lima, S.L. Galdino, I.R. Pitta J. Mol. Struct. 715 (2005) 191-198
- [2] H.G. Kruger, P.Mdluli, T. D. Power, T. Raasch, A. Singh, , J. Mol. Struct. 771(2006) 165-170
- [3] N. Opacic, M. Barbaric, B. Zorc, M. Cetina, A. Nagl, D. Frkovic, M. Kralj, K. Pavelic, J. Balzarini, G. Andrei, R. Snoeck, E. D. Clercq, S. Raic-Malic, M. Mintas, J. Med. Chem 48 (2005) 475-482
- [4] P. Dapporto, P. Paoli, P.Rossi, M. Altamura, E. Perrotta, R. Nannicini, J. Mol. Struct. 532 (2000) 194-204

## Spectral and ESR study of Cu(II), Co(II) and Ni(II) theophyllinato complexes containing propanolamine ligands

A. Bebu<sup>1</sup>, A. Kozma<sup>2</sup>, E. Forizs<sup>2</sup>, M. Toderas<sup>3</sup>, L. David<sup>1</sup>

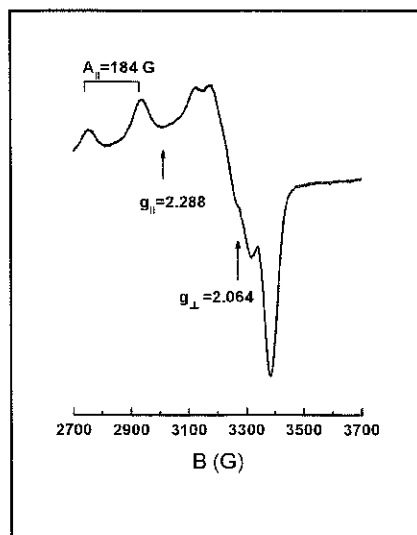
<sup>1</sup>"Babes Bolyai" University, Dpt of Physics, 400084 Cluj Napoca, Romania

<sup>2</sup>"Babes Bolyai" University, Dpt of Chemistry, 400028 Cluj Napoca, Romania

<sup>3</sup>University of Oradea, faculty of Science, 410087 Oradea, Romania

The transition metal complexes containing theophylline (th = 1,3-dimethylxantine) are intensely studied for modeling metal ions interactions with the guanine base of nucleic acid. As a part of our research on the theophyllinato complexes containing aminoalcohol ligands, we have already reported preparation and structural characterization of some new mixed ligand complexes of Cu (II), Co(II) and Ni(II) with 2-aminoethanol [1, 2].

Five new mixed ligand complexes  $[M(th)_2(ap)_2] \cdot nH_2O$  ( $M = Cu, n = 2; M = Co, Ni, n = 1$ ),  $[Ni(th)_2(pa)_2] \cdot H_2O$  and  $[Cu(th)(pa)_2]$  containing deprotonated theophylline and 1-amino-2-propanol (ap) or 3-amino-1-propanol (pa) as ligands were prepared and investigated by elemental analysis, spectroscopic methods (FT-IR, UV-VIS, ESR) and thermal studies. The results of spectroscopic studies indicated that the Co(II) and Ni(II) centers, are hexacoordinated by two theophyllinate-anions (coordinated through N(7)-atom) and two propanolamine molecules in a distorted octahedral geometry. The propanolamine are coordinated as bidentate ligands (through N and O atoms) to the metal center [3].



The spectral data and thermal behavior of  $[Cu(th)_2(ap)_2] \cdot 2H_2O$  shows that copper(II) ions are penta-coordinated with a square-pyramidal symmetry. One of the 1-amino-2-propanol ligands acts as a monodentate, and the second acts as a bidentate ligand. The room temperature powder ESR spectrum of this complex as shown in the figure above exhibits four hyperfine lines in the  $g_{||}$  region and a strong absorption signal in the  $g_{\perp}$  region. The shape of the spectrum and the obtained values of ESR parameters ( $g_{||}=2.288, g_{\perp}=2.064, A_{||}=184G$ ) suggest a  $CuN_2N_2^*O$  chromophore.

The spectral and thermoanalytical data for  $[Cu(th)(pa)_2]$  suggest dinuclear structure. Each Cu(II) ion is four-coordinated with  $N_2O_2$  coordination environments. The 3-amino-1-propanol acts as monoanionic bidentate ligand bridging by oxygen atom. The room temperature powder ESR spectrum confirm the pseudotetrahedral local symmetry ( $g_{||}=2.305, g_{\perp}=2.061$ ).

[1] S. Gál, J. Madarász, E. Forizs, I. Labádi, V. Izvekov, G. Pokol, J. Therm. Anal. Cal., 53 (1998) 343

[2] P. Bombicz, J. Madarász, E. Forizs, I. Foch, Polyhedron, 16 (1997) 3601

[3] S. B. Sanni, A. T. H. Lenstra, V. C. Patel, Acta Crystallogr., Sect.C: Cryst. Struct. Commun., 41 (1985) 199



## Adsorption of 2- and 3-Chloropyridine on Sepiolite and Loughlinitite: An Infrared Spectroscopic Study

S. Akyuz and T. Akyuz

*Istanbul Kultur University, Science and Letters Faculty, Physics Department, Atakoy Campus, 34156, Bakirkoy, Istanbul Turkey*

Sepiolite and loughlinitite (natural Na-sepiolite) are in palygorskite-sepiolite group of phyllosilicates class of clay minerals [1, 2]. They have fibrous structures consisting talc-like ribbons parallel to the fibre axis. Each ribbon alternates with channels along the fibre axis. Structurally they are formed by an alteration of blocks and channels that grow up in the fibre direction (c-axis). The chemical formula of sepiolite is  $Mg_4Si_6O_{15}(OH)_2 \cdot 6H_2O$  and that of loughlinitite is  $Na_2Mg_3Si_6O_{16} \cdot 8H_2O$  [1,2]. Loughlinitite is virtually identical in appearance to sepiolite both in a hand specimen and microscopically. However, field observations and mineralogical determinations indicate that loughlinitite and sepiolite are formed authigenically and independently in different physicochemical environments rather than being the product of transformation of one to the other [3].

Compounds containing pyridine rings are distributed over widely in nature and have several important applications. 2- and 3-Chloropyridine are used as intermediates in synthetic organic, pharmaceutical and agricultural chemical manufacture. In the present paper, IR spectroscopic results for adsorption of 2- and 3-chloropyridine onto sepiolite and loughlinitite are reported. Chloropyridines are weaker bases than pyridine, thus protonation is only expected on strongly acidic surface sites. The most probable binding sites of sepiolite and loughlinitite are surface hydroxyls, Lewis or Brønsted acid sites, and water molecules. It is well known that the broken Si-O-Si bonds of the terminal silica tetrahedra on the external surfaces compensate their residual charge by accepting a proton or hydroxyl group and form Si-OH groups. If adsorbed organic molecule interacts with surface silanol groups of sepiolite or loughlinitite, the Si-OH stretching and deformation bands must be altered.

The adsorption of 2- and 3-chloropyridine showed a considerable alteration on both Si-OH stretching and deformation peaks of the clay structure. On the other hand the perturbation observed on the zeolitic and bound water vibrations of sepiolite and loughlinitite indicates that some of the adsorbed chloropyridine molecules enter the interior channels and replace zeolitic water molecules. The spectroscopic results indicate that chloropyridine molecules adsorbed on sepiolite and loughlinitite are coordinated to Lewis acidic centers or surface hydroxyls by H-bonding interaction through the pyridine ring nitrogen lone pairs. Moreover, some of the adsorbed chloropyridine molecules may enter the interior channels of the clay structure and replace zeolitic water. Presence of pyridinium surface species is also detected as a lesser extent in the case of loughlinitite.

[1] J.J. Fahey, M. Ross, J.M. Axelrod, *Am. Miner.* 45 (1960) 270-281.

[2] Serratos, In *Proceedings of International Clay Conference, 1978*, edited by M. M. Mortland and V. C. Farmer, p. 99. Elsevier, Amsterdam (1979).

[3] S. Kadir, H. Bas, Z. Karakas, *Can. Miner.* 40 (2002) 1091-1102.



## Mid-infrared stimulated emission spectroscopy and its Applications

E. L. Terpugov, O. V. Degtyareva

*Institute of Cell Biophysics Russian Academy of Sciences, 142290, Institutskaj st.,3, Pushchino, Moscow Region, Russian Federation;*

Mid- Infrared stimulated emission spectroscopy (MISES) is a novel technique, which allows the spectra of the biomolecules and inorganic materials to be obtained in situ at room temperature [1-3]. The emission arises in the excited molecules of sample during optical excitation by a low intense visible light. The IR-radiation usually was trapped from a front surface of the sample. The intensity of vibration modes is sensitive to the channels and the mechanism of energy flow following a vibrational excitation.

In this work, we present spectral analysis of liquids (carbon tetrachloride and benzol) using MISES: effects of lamp and laser light excitation. We have measured the sample (IR-emission and absorption as well as Raman) spectra in the range 500-1700  $\text{cm}^{-1}$  with a resolution of 4  $\text{cm}^{-1}$  using a FTIR-spectrometer. The comparative work on the emission characteristics – line narrowing, emission intensity and composition of the eigenstates – was carried out by the use of two different light sources (continuous-wave (cw) 100 W Xenon lamp - (320-700) nm; and cw laser (Nd:YAG, 1064 nm). In both cases, we obtained high – quality vibrational spectra with the set of spatially resolved spectral lines. The characteristics of the infrared emission produced by different wavelength radiation on liquids are presented.

Application of the MISES technique to enable the weak (in IR-absorption or Raman) lines to be observed in the spectra of carbon tetrachloride as well of benzol. Also we pointed out the presence of pure infrared (IR-active) and Raman (Raman-active) vibrational modes in the spectra, which relative proportions were varied with modification excitation conditions. The differences in intensity of radiation and line narrowing phenomena in the spectra of the carbon tetrachloride as well as benzol were explained by distinct wave-driven excitation mechanism for their molecules. Advantages and disadvantages of the technique are discussed.

[1] E.L. Terpugov, O.V. Degtyareva, Proc. of SPIE 4129 (2000) 659-665

[2] V.S. Gorelik, A.G. Gagarinov, O.V. Degtyareva, V.V. Savransky, E.L. Terpugov, Inorgan. Mater. 42 (2006) 1251-1254

[3] A.G. Gagarinov, O.V. Degtyareva, A.A. Khodonov, E.L. Terpugov, Vibrat. Spectrosc. 42 (2006) 231-238

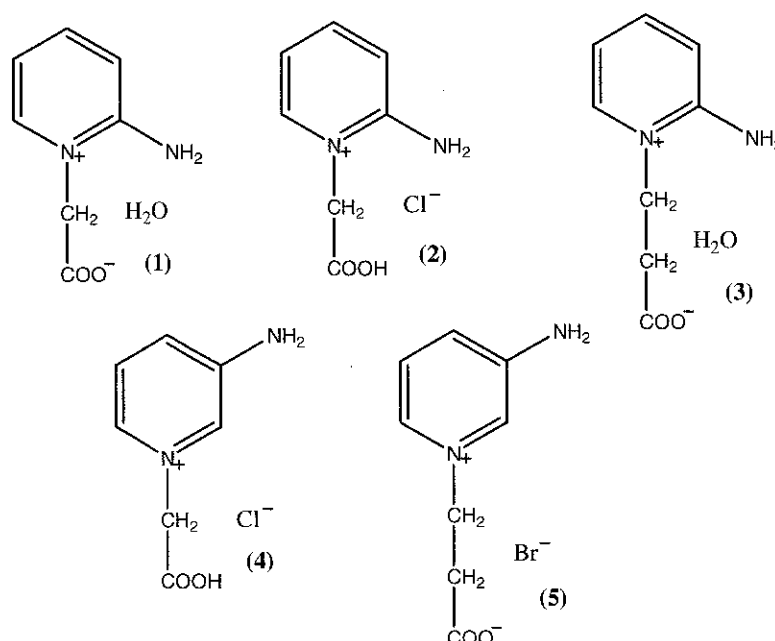


## Aminopyridine betaines and their hydrohalides studied by FTIR and NMR spectroscopy and DFT calculations

I. Kowalczyk and M. Szafran

*Faculty of Chemistry, A. Mickiewicz University, 60780 Poznań, Poland*

The assignments of the anharmonic experimental solid state vibrational frequencies of 2-aminopyridine betaine (**1**) (2-NH<sub>2</sub>PB), its hydrochloride (**2**) (2-NH<sub>2</sub>PBH·Cl), 3-(2-aminopyridinium)propionate (**3**) (2-NH<sub>2</sub>PB<sup>2</sup>), 3-aminopyridine betaine hydrochloride (**4**) (3-NH<sub>2</sub>PBH·Cl) and 3-(3-aminopyridinium)propionate hydrobromide (**5**) (2-NH<sub>2</sub>PB<sup>2</sup>H·Br), based on the calculated frequencies in vacuum at the the B3LYP/6-311G(d,p) level of theory for optimized structure, have been made. The overestimation of the computed wavenumbers was corrected by scaling equation,  $v_{\text{exp}} = a + bv_{\text{cal}}$ , recommended by Alcolea Palafox.



Correlations between the experimental <sup>13</sup>C and <sup>1</sup>H NMR chemical shifts ( $\delta_{\text{exp}}$ ) and the GIAO/B3LYP/6-311G(d,p) calculated magnetic isotropic shielding tensors ( $\sigma_{\text{cal}}$ ) in vacuum and DMSO,  $\delta_{\text{exp}} = a + b \cdot \sigma_{\text{calc}}$ , are reported.

[1] M. Alcolea. Palafox, M. Gill, N.J. Nunez, V.K. Rastogi, L. Mittal, R. Sharma, *Int. J. Quant. Chem.* 103 (2005) 394



## Synthesis, spectroscopic and structural properties of trichoromethyl trifluoromethanesulphonate, $\text{CF}_3\text{SO}_2\text{OCCl}_3$

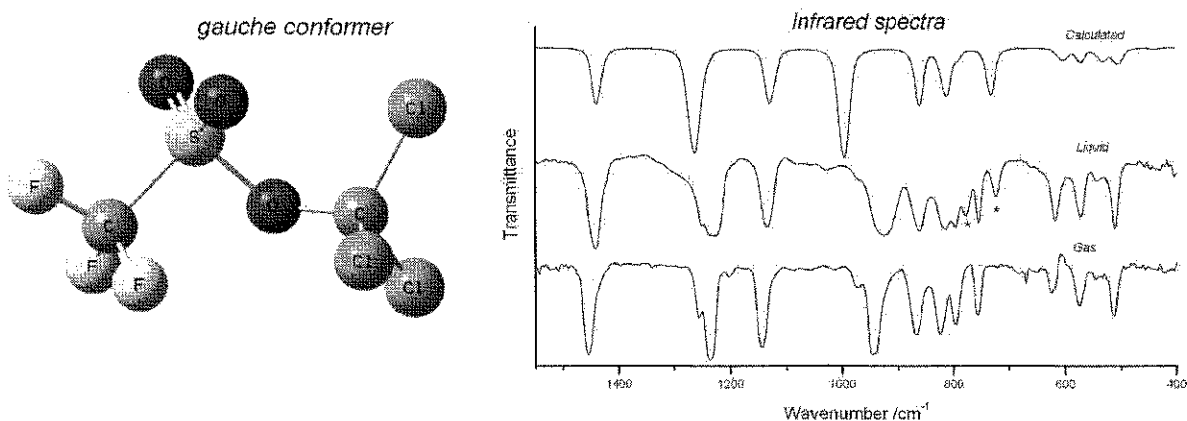
M. E. Defonsi Lestard<sup>1</sup>, L. A. Ramos<sup>2</sup>, M. E. Tuttolomondo<sup>1</sup>, S. E. Ulic<sup>2,3</sup> and A. Ben Altabef<sup>1</sup>

<sup>1</sup>INQUINOA- CONICET, Instituto de Química Física, Facultad de Bioquímica, Química y Farmacia, Universidad Nacional de Tucumán, San Lorenzo 456, T4000CAN, Tucumán, R. Argentine

<sup>2</sup>CEQUINOR, Departamento de Química, Facultad de Cs. Exactas. UNLP C. C. 962 1900, La Plata., R. Argentine

<sup>3</sup>Departamento de Cs. Básicas, Univ. Nacional de Luján. Ruta 5 y 7, 6700, Luján, Buenos Aires, R. Argentine.

Trichoromethyl trifluoromethanesulphonate,  $\text{CF}_3\text{SO}_2\text{OCCl}_3$ , was synthesized by reacting  $\text{Ag}(\text{OSO}_2\text{CF}_3)$  and  $\text{BrCCl}_3$ . This compound was characterized by NMR ( $^{13}\text{C}$ ,  $^{19}\text{F}$ ) and vibrational spectroscopy. Quantum chemical calculations<sup>1</sup> were used to predict the geometry of the most stable conformation of  $\text{CF}_3\text{SO}_2\text{OCCl}_3$ . Potential energy curves around the S-O bond were calculated at the MP2 and DFT (B3LYP and mPWIPW91) levels with different basis sets. Two structurally equivalent conformers were identified with  $C_1$  symmetry and *gauche* conformation (CSOC dihedral angle of about  $130^\circ$ ). The shallow rotational barrier between both conformers is  $4 \text{ kJ mol}^{-1}$  at B3LYP/6-311++G(d,p) level. This result is in agreement with geometric parameters of other covalent sulphonates. This conformational preference was analyzed using the total energy and natural bond orbital partition schemes. Additionally, the total potential-energy was deconvoluted using six fold Fourier-type expansion. The infrared (gas and liquid) and Raman (liquid) spectra of  $\text{CF}_3\text{SO}_2\text{OCCl}_3$  allowed to assign 28 of the  $3N-6=30$  fundamental vibrational modes. The harmonic vibrational wavenumbers and the force field were also calculated.<sup>2</sup>



[1] *Gaussian 03*, Revision B.02, Gaussian, Inc., Pittsburgh PA, 2003.

[2] P. Pulay, G. Fogarasi, G. Pongor, J. E. Boggs, A. Vargha, *J. Am. Chem. Soc.*, 105 (1983) 7037



## Experimental and theoretical investigation of 2-phenyl-thiazole-4-yl-methyl-quinolinium iodine

A. Pîrnău<sup>1</sup>, M. Bogdan<sup>1</sup>, M. Palage<sup>3</sup>, L. Szabó<sup>2</sup>, N. Leopold<sup>2</sup>, R. A. Varga<sup>4</sup>, O. Cozar<sup>2</sup>, V. Chiş<sup>2</sup>

<sup>1</sup>National Institute for Research and Development of Isotopic and Molecular Technologies, Donath 65-103, RO-400293, Cluj-Napoca, Romania

<sup>2</sup>Babeş-Bolyai University, Faculty of Physics, Kogălniceanu 1, RO-400084, Cluj-Napoca, Romania

<sup>3</sup>Iuliu Haţieganu University of Medicine and Pharmacy, Department of Therapeutical Chemistry, Ion Creanga 12, RO-400010, Cluj-Napoca, Romania

<sup>4</sup>Babeş-Bolyai University, Faculty of Chemistry and Chemical Engineering, Arany Janos 11, RO-400028 Cluj-Napoca, Romania

The synthesis of 2-phenyl-thiazole-4-yl-methyl-quinolinium iodide compound (2PTMQI) was performed by the alkylation of some nitrogen heterocycles, with halogen compounds, having in their structure 2-Aryl-thiazolic system [1,2]. The bactericide activity of the new compound has been evaluated against two strains of germs: *Staphylococcus aureus* and *Pseudomonas aeruginosa*.

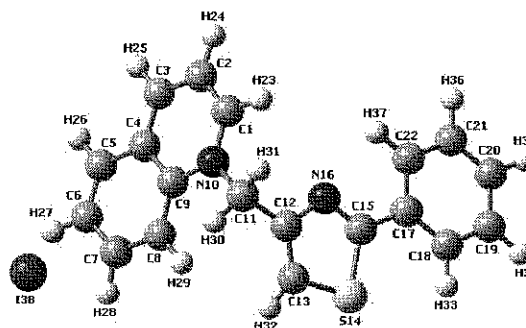
In this work, experimental methods (NMR, FT-IR, Raman and SERS spectroscopies, and X-ray diffraction technique) coupled with quantum chemical calculations based on density functional theory (DFT) are used for structural and electronic characterization of phenyl-thiazole-4-yl-methyl-quinolinium iodide compound (2PTMQI).

X-ray diffraction technique indicates that 2PTMQI crystallized in the triclinic space group *P-1*, with *Z*=2 and cell parameters: *a* = 8.044(4)Å, *b* = 8.479(4)Å, *c* = 13.559(6)Å,  $\alpha$  = 82.078(8)°,  $\beta$  = 83.526(8)° and  $\gamma$  = 74.350(7)°.

The lowest energy conformer of this compound in gas phase was obtained by a potential energy surface scan performed at B3LYP/6-31G(d) level of theory.

The molecular vibrations of 2PTMQI were investigated by FT-IR, FT-Raman and SERS spectroscopies and a complete assignment of the experimental vibrational bands was possible on the basis of B3LYP/6-31G(d) calculations. The molecular electrostatic potential of this molecule has been calculated and used for predicting site candidates of electrophilic attack. By Raman and SERS spectroscopies, coupled with DFT calculations it was shown that this molecule adsorbs to the silver colloid through the sulfur atom.

<sup>1</sup>H and <sup>13</sup>C NMR spectra of 2PTMQI were obtained in DMSO solution and they were also calculated using the GIAO (Gauge-Including Atomic Orbitals) method and by considering the solvent effects within the PCM solvation model. For a reliable prediction of the <sup>13</sup>C NMR spectrum of the investigated compound in DMSO solution, it is essential to use a correlation consistent basis set (cc-pVDZ) for carbon atoms.



Molecular structure and atom numbering scheme of 2PTMQI

[1] G. McDonnell and D. Russell, *Clinical Microbiology Reviews*, Jan., (1999) 147

[2] C. Moldovan, O. Oniga, B. Tipericiu, P. Verite, A. Pîrnău, M. Bojiţă, *Farmacia*, 57 (2009) 452



## Raman and IR studies of melilite-type crystals $\text{Ca}_2\text{MgSi}_2\text{O}_7$ , $\text{Ca}_2\text{ZnSi}_2\text{O}_7$ and $\text{Sr}_2\text{MgSi}_2\text{O}_7$

M. Ptak<sup>1</sup>, M. Maczka<sup>1</sup>, J. Hanuza<sup>2</sup>, A. A. Kaminskii<sup>3</sup>, P. Becker<sup>4</sup>, L. Bohaty<sup>4</sup>

<sup>1</sup>*Institute of Low Temperature and Structure Research, Polish Academy of Sciences, P.O. Box 1410, 50-950 Wrocław 2, Poland*

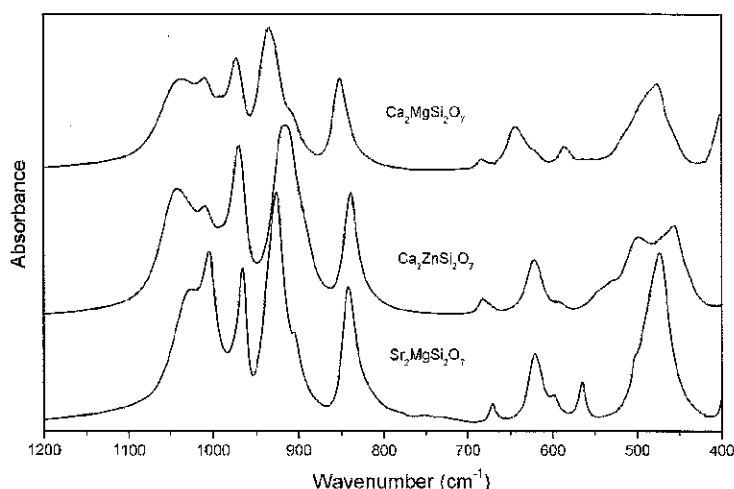
<sup>2</sup>*Department of Bioorganic Chemistry, University of Economics, 53-345 Wrocław, Poland*

<sup>3</sup>*Institute of Crystallography, Russia Academy of Sciences, Leninsky prospect 59, 119333 Moscow, Russia*

<sup>4</sup>*Institute of Crystallography, University of Cologne, 50674 Cologne, Germany*

Melilite-type compounds with the general composition  $\text{X}_2\text{YZ}_2\text{O}_7$  (X=Ca, Sr, Ba; Y=Mg, Zn; Z=Ge, Si) have received much attention since these materials exhibit both laser and nonlinear optical properties [1]. At high temperatures all melilite-type crystals crystallize in the space group  $P-42_1m$  [1]. However some of them undergo phase transitions with decreasing temperature leading to a sequence of incommensurate and commensurate phases. For instance, incommensurate-to-normal phase transition occurs in  $\text{Ca}_2\text{MgSi}_2\text{O}_7$  at  $T=355$  K and in  $\text{Ca}_2\text{ZnSi}_2\text{O}_7$  at  $T=405$  K [2].

Although these materials have been extensively studied, these studies were focused mainly on structural properties but phonon properties are still not well known. Present report shows results of Raman and IR studies for three silicates:  $\text{Ca}_2\text{MgSi}_2\text{O}_7$ ,  $\text{Ca}_2\text{ZnSi}_2\text{O}_7$  and  $\text{Sr}_2\text{MgSi}_2\text{O}_7$ . Our polarized studies performed on single crystals allowed us to identify symmetries of observed modes and propose the detailed assignment for majority of them. We have also performed temperature-dependent Raman and IR studies in order to get deeper insight into mechanism of the phase transitions.



[1] A. A. Kaminskii, L. Bohaty, P. Becker, J. Liebertz, P. Held, H. J. Eichler, H. Rhee, J. Hanuza, *Laser. Phys. Lett.* 5 (2008) 845

[2] B. Bagautdinov, K. Hagiya, S. Noguchi, M. Ohmasa, N. Ikeda, K. Kusaka, K. Lishi, *Phys. Chem. Minerals* 29 (2002) 346



## Effect of methyl group and N-H...N hydrogen bond on IR and Raman spectra of 2-(N-ethylamino)- 3(or 5)-methyl-4-nitropyridine

J. Lorenc

*Department of Bioorganic Chemistry, Institute of Chemistry and Food Technology, Faculty of Engineering and Economics, University of Economics, Komandorska 118/120, 53-345 Wrocław, Poland*

2-(N-ethylamino)-3-methyl-4-nitropyridine (EN3MP) and its isomer 2-(N-ethylamino)-5-methyl-4-nitropyridine (EN5MP) belong to wide class of amino derivatives of nitropicolines and their N-oxides [1-3]. They are intensively studied due to their wide applications in organic syntheses and use as bioactive agents in pharmaceuticals [4,5]. Their molecular structure and vibrational spectra have been discussed in terms of quantum chemical DFT calculations (B3LYP/6-311++G(d,p) approach) and related to the XRD data obtained for the EN5MP crystal. The EN3MP isomer was studied in the liquid phase in which it forms a stable state.

The structures as well as the role of the intermolecular interactions in their stabilisation have been compared for the both isomers. Properties of the  $N_A-H \cdots N_P$  interactions between the nitrogen and the hydrogen atoms of the pyridine ring ( $N_P$ ) and amino group have been characterised for both molecules.

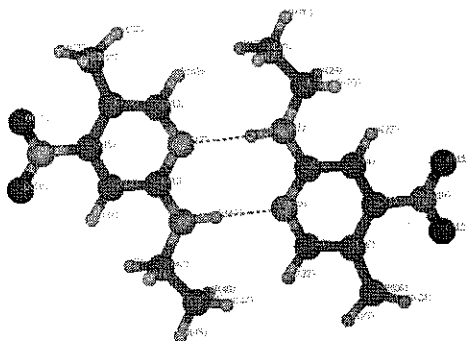


**Fig. 1:** The molecular structure of EN5MP dimer with atom-numbering scheme.

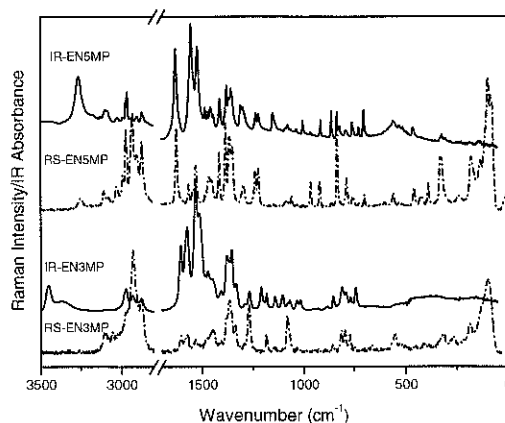


**Fig. 2:** IR and Raman spectra of EN5MP and EN3MP isomers in the region 3200-30  $\text{cm}^{-1}$

The EN5MP crystallizes in triclinic space group  $P\bar{1}$  with two molecules per unit-cell. The crystal structure of EN5MP is stabilized by  $N_A-H \cdots N_P$  and  $C-H \cdots O$  hydrogen bonds. The symmetry-related  $N_A-H \cdots N_P$  system generates the formation of the dimeric motifs built of eight-membered rings. The significant difference in the position of the  $\nu(\text{NH})$  IR bands observed as a singlet at  $3262 \text{ cm}^{-1}$  and as a doublet at  $3452, 3370 \text{ cm}^{-1}$  for EN5MP and EN3MP, respectively, is the result of different strength and nature of the  $N_A-H \cdots N_P$  hydrogen bonds in these isomers.

- [1] J. Oszust, Z. Talik, A. Pietraszko, M. Marchewka, J. Baran, *J. Mol. Struct.* 415 (1997) 53
- [2] J. Lorenc, B. Palasek, J. Hanuza, M. Mączka, A. Waškowska, *J. Raman Spectrosc.* 40 (209) 323
- [3] E. Lorenz, M. Mączka, K. Hermanowicz, A. Waškowska, A. Puszko, J. Hanuza, *Vibrational Spectrosc.* 37 (2005) 195
- [4] C. Hayes *et al.*, *J. Clin. Pharmacol.* 43 (2003) 379
- [5] H. Camp, J. Derc, *Handbook of Am. Chem. Soc.*, 2001, p31



## C-H...S hydrogen bonds as the organizing force in 2,3-thienyl- and phenyl- or 2,3-dithienyl-substituted propenoic acid aggregates studied by the combination of FT-IR spectroscopy and computations

L. Illés, K. Felföldi, J.T. Kiss, I. Pálinkó\*

*Department of Organic Chemistry, University of Szeged, Dóm tér 8, Szeged, H-6720 Hungary*

It has been found previously that short-range ordering prevails in  $\alpha$ -phenylcinnamic acid (*E*- or *Z*-2,3-diphenyl propenoic acid) solutions (the organizing force is strong O-H...O hydrogen bonds), while weak (aromatic)C-H...O hydrogen bonds are responsible for long-range ordering in the solid state [1]. If substituents are present in the molecules that are capable to act as hydrogen bond donors and acceptors (the oxygen of the methoxy group [2] and/or fluorine [3] on the aromatic rings or a furyl group in position 3 instead of the phenyl group [4]), they take part in forming extended aggregates, but only in the solid state. In this contribution the scope is further extended, experimental and computational results concerning the aggregate-forming properties of a range of propenoic acid stereoisomers having thienyl and phenyl or dithienyl groups in positions 2 and 3 are communicated.

Eight stereoisomer pairs of molecules have been synthesized covering all possibilities of 2,3-substitution enabling us to explore all possible hydrogen bonding interactions in solution and the solid state too. The molecules were synthesized in our laboratory applying a modified version of the Perkin condensation. In the experimental part of the work FT-IR spectroscopy (BIORAD FTS 65/896 spectrophotometer, 4000–400  $\text{cm}^{-1}$  range) was the tool of structural investigation. For the solution-phase studies  $\text{CCl}_4$  or (occasionally, when solubility properties of the compounds required)  $\text{CHCl}_3$  was chosen as solvent and the  $10^{-2}$  -  $10^{-4}$   $\text{mol/dm}^3$  concentration range was investigated. For measurements in the solid-state the KBr technique was applied. Molecular modeling was performed with semiempirical and *ab initio* codes included in the *Hyperchem* package [5].

The combination of experimental and computational approaches proved to be powerful in exploring hydrogen bonding possibilities. It was found that large aggregates were formed, but again only in the solid state. They were kept together by hydrogen bonds. The major organizing force was C-H...S hydrogen bonding. It connected the acid dimers (which were the basic unit of the hydrogen-bonded aggregates kept together with strong O-H...O hydrogen bonds). The donor atom was always aromatic carbon, (olefinic)C-H...S bonds were not found. Modeling of extended aggregates was possible in some cases applying the PM3 semiempirical method and the dimers and the dimer of the dimers could be studied with *ab initio* methods applying the 6-31 G\* and the 3-21 G basis sets, respectively. Although the C-H...S interactions were weak they played crucial role in keeping together the extended aggregates in the solid state.

- [1] I. Pálinkó, B. Török, M. Rózsa-Tarjányi, J.T. Kiss, Gy. Tasi, *J. Mol. Struct.* 348 (1995) 57-60; (b) I. Pálinkó, J.T. Kiss, *Mikrochim. Acta [Suppl.]* 14 (1997) 253-255  
[2] J.T. Kiss, K. Felföldi, I. Hannus, I. Pálinkó, *J. Mol. Struct.* 565-566 (2001) 463-468  
[3] B. Tolnai, J.T. Kiss, K. Felföldi, I. Pálinkó, *J. Mol. Struct.* 924-926 (2009) 27-31  
[4] J.T. Kiss, K. Felföldi, Z. Paksi, I. Pálinkó, *J. Mol. Struct.* 651-653 (2003) 253-258  
[5] *Hyperchem 8.0*, Hypercube, Inc., Gainesville, Florida, 2007



## Hydrogen bonds and mesomorphism of cholesteryl formiate

A. A. Yakubov

*Faculty of Physics, Samarkand State University, 15, University blvd, Samarkand, 140100, Uzbekistan*

Cholesteryl formiat (ChF) is the first member of cholesteryl n-alkanoates homologous series. ChF has a monotrop cholesteric liquid crystal phase which appears under cooling of the isotropic ChF phase [1]. IR spectra have shown [2] that in ChF there are intermolecular hydrogen bonds. The purpose of the given work is to provide more detailed and correct, as compared with [2], study of hydrogen bonding in ChF and its influence on mesomorphism of ChF.

ChF in solid crystal, cholesteric liquid crystal, and isotropic liquid phases as well as in solution in the CCl<sub>4</sub> was investigated by IR spectroscopic method. Infrared absorption spectra in the 4000-400 cm<sup>-1</sup> region were measured by spectrophotometer UR-20. Besides, ChF was studied by a method of semi empirical quantum-chemical calculations.

Changes of IR spectra in the basic in the 1750-1700 cm<sup>-1</sup> region of C=O stretching vibration at phase transitions show that in ChF there are intermolecular hydrogen bonds of type C=O...H-C. In solid crystalline phase all molecules are associated on dimers. In isotropic liquid phase almost all dimers are dissociated on monomers. In cholesteric liquid crystal phase the number of dimers and monomers is almost equal. Semi empirical quantum-chemical calculations confirm these results.

Formation of intermolecular hydrogen bonds in solid crystal phase of ChF leads to increase of forces of intermolecular interactions, and, as consequence, to rise in temperature of melting of ChF. Transition from at solid crystal phase to isotropic liquid phase without formation liquid crystal phase at heating of crystal ChF can be explained by the fact that the temperature of melting of ChF lies above temperature of area of existence of the mesophase.

[1] M.V. Kurik, A.A. Rudenko, V.G. Tishenko, Zhurn. Fiz. Khim. 54(1980) 79 (in Russian).

[2] L.S. Gorbatenko, T.P. Myasnikova, R.Ya. Evseeva, Zhurn. Prikl. Spektros. 24(1976) 153 (in Russian).



## The O–D/HDO stretchings in the $\text{Li}_2(\text{S,Se})\text{O}_4 \cdot (\text{H,D})_2\text{O}$ system: employing the double isolation method

V. M. Petruševski<sup>1</sup>, D. Sazdov<sup>1</sup>, B. Šoptrajanov<sup>2</sup>

<sup>1</sup> *Ss Cyril & Methodius University, Faculty of Natural Sciences and Mathematics, Arhimedova 5, 1000 Skopje, R. Macedonia*

<sup>2</sup> *Macedonian Academy of Sciences and Arts, Bul. Krste Misirkov 2, 1000 Skopje, R. Macedonia*

The IR spectra of mixed crystals of the monohydrates of lithium sulfate and lithium selenate have already been studied by us [1]. The attention was paid to various problems: (a) the differences in the hydrogen bond strength for the isomorphous sulfate/selenate pairs, (b) decrease of frequencies of the bending HOH modes on lowering the temperature, and (c) the symmetry of the tetrahedral anions.

The present study is a more thorough investigation regarding the problems of hydrogen bonding in the above pair of isomorphous compounds. The hydrogen bond strength was studied spectroscopically (i.e. based on the O–D stretchings of the isotopically isolated HDO molecules) in compounds containing selenate ions isolated in a sulfate matrix and vice versa (the above are examples for *double isolation* [2]). The results obtained show that for selenate ions isolated in a sulfate matrix, the hydrogen bonds built with the selenate oxygens are stronger than in the pure selenate compound. The opposite holds for the sulfate ions isolated in a selenate matrix: here the hydrogen bonds are weaker when compared with those in the pure sulfate compound. A simple explanation was offered for the above results, expected to hold for systems with high symmetry (as is the  $T_d$  symmetry for the ideal sulfate and selenate tetrahedra).

[1] B. Šoptrajanov, V. Petruševski, *J. Mol. Struct.* 142 (1986) 67–70.

[2] H. D. Lutz, *J. Mol. Struct.* 704, 71–78 (2003).



## Reaction monitoring of entacapone synthesis by in-line Raman spectroscopy and principal component analysis

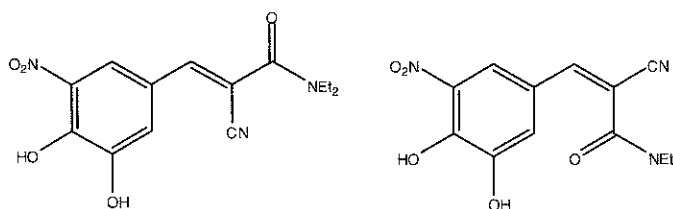
T. Jednačak,<sup>1</sup> P. Novak,<sup>1</sup> A. Kišić,<sup>1</sup> T. Hrenar,<sup>1</sup>  
S. Miljanić<sup>1</sup> and G. Verbanec<sup>2</sup>

<sup>1</sup> Department of Analytical Chemistry, Faculty of Natural Sciences, University of Zagreb, Horvatovac 102a, HR-10000 Zagreb, Croatia

<sup>2</sup> PLIVA Hrvatska d.d, Prilaz baruna Filipovića 29, HR-10000 Zagreb, Croatia

Entacapone is a strong and selective inhibitor of catechol-*O*-methyltransferase and therefore it is clinically used for the treatment of Parkinson's disease [1, 2].

An advantage of Raman spectroscopy is the possibility of using remote detection through fiber optics for the in-line monitoring of chemical reactions and crystallization processes.



*Cis*- and *trans*- stereoisomers of entacapone.

A combination of in-line Raman spectroscopy and principal component analysis [3, 4] was used to monitor Knoevenagel condensation reaction which was the final step in preparation of entacapone. The reaction gave two stereoisomeric forms of entacapone *E*- and *Z*- [1,5]. Both stereoisomeric forms are bioactive. Raman spectroscopy combined with chemometrics was proven to be useful to differentiate between the two isomers in the reaction mixture. The in-line spectra of the reaction mixture were compared to those obtained off-line for *E*- and *Z*-isomers. The reaction was also monitored by the off-line liquid chromatography.

[1] J. Leppänen, E. Wegelius, T. Nevalainen, T. Järvinen, J. Gynther, J. Huuskonen, *J. Mol. Struct.* 562 (2001) 129-135.

[2] A. Kwokal, T. T. H. Nguyen and K. J. Roberts, *Cryst. Growth Des.*, 9, 4324-4334 (2009).

[3] L. Nørgaard, M. H. Hahn, L. B. Knudsen, I. A. Farhat and S. B. Engelsen, *Int. Dairy J.* 15 (2005) 1261-1270.

[4] N. N. Daéid and R. J. H. Waddell, *Talanta* 67 (2005) 280-285.

[5]. P. Novak, A. Kišić, T. Hrenar, T. Jednačak, S. Miljanić and G. Verbanec, submitted.



## Cyanogen isocyanate, NCNCO; the infrared conundrum

N. P. C. Westwood, J. Wang

*Guelph-Waterloo Centre for Graduate Work in Chemistry, Department of Chemistry,  
University of Guelph, N1G 2W1, Guelph, Ontario, Canada*

The unstable NCNCO molecule is structurally and spectroscopically interesting as a molecule with large amplitude motion, and as a species that can form polymeric species in the solid state possibly leading to  $C_3N_4$  (carbon nitride). A problem of some concern over the years has been the gas-phase infrared spectrum [1] which has been suggested [2,3,] to not be in accord with matrix IR and DFT calculations. The present work has been undertaken to qualify these concerns and establish reasons for this unsatisfactory situation. NCNCO has thus been generated by two independent methods, pyrolysis of AgNCO(s) at 350°C and reaction of BrCN(g) with AgNCO(s) at 230°C and the corresponding gas-phase IR spectra have been obtained.

The present gas-phase IR spectrum is totally different from the previous spectrum [1] which we now demonstrate to be that of carbonyl diisocyanate ( $O=C(NCO)_2$ ). Earlier work of Mayer [4] had identified some IR bands of NCNCO, but admixed in that spectrum were bands now shown to be  $O=C(NCO)_2$ . The present work distinguishes these molecules and discusses the assignments for NCNCO, including the observation of new fundamentals and combination bands.

[1] T.C. Devore, *J. Mol. Struct.* 162 (1987) 287-304.

[2] M. Barbieux, S. Vandevorode, R. Flammang, M.W. Wong, H. Bibas, C.H.L. Kennard, C. Wentrup, *J. Chem. Soc. Perkin Trans. 2* (2000) 473-478.

[3] E.G. Robertson, D. McNaughton, *J. Phys. Chem. A.* 107 (2003) 642-650.

[4] E. Mayer, *Monatsh.* 101 (1970) 834-845.





## Antioxidant Chromones – A Conformational Study

N. F. L. Machado<sup>1</sup>, L. A. E. Batista de Carvalho<sup>1</sup> and M. P. M. Marques<sup>1,2</sup>

<sup>1</sup>Research Unit "Molecular Physical Chemistry", University of Coimbra – Portugal

<sup>2</sup>Department of Life Sciences, Faculty of Science and Technology, University of Coimbra – Portugal

Benzopyrane-type heterocyclic compounds are natural products, widely distributed in plants, with recognised antioxidant properties. In particular, 1,4-benzo-pyrones (also known as chromones) display a wide range of pharmacological activities, from anti-inflammatory to antimicrobial, anti-allergic, antispasmodic and antitumour [1,2]. These potential health benefits of chromones, arising from their antioxidant activity, are ruled by strict structure-activity/structure-property relationships (SAR's/SPR's). These, apart from determining their biological action, modulate their systemic distribution and bioavailability in sites of oxidation within the cell. This urges for an accurate conformational analysis of this kind of systems, that will allow to clearly understand their mechanisms of action and establish reliable SAR's allowing a rational design of efficient chemopreventive and anticancer agents.

The present work aims at gathering accurate conformational data on chromone derivatives using vibrational spectroscopy techniques in combination with quantum-mechanical calculations (at the Density Functional Theory level). For each compound, the harmonic vibrational frequencies were calculated for every conformer, while the corresponding intensities were obtained for the most stable geometries. All vibrational spectroscopic techniques were available to this study – FTIR, Raman and Inelastic Neutron Scattering (INS) – enabling a complete spectral assignment of the compounds. As a complementary technique to the vibrational optical methods, INS is particularly well suited to the study of hydrogenous compounds such as the ones presently investigated, and allows the observation of the low frequency vibrational modes. Furthermore, the INS pattern is easily predicted for each calculated minimum energy conformation, using dedicated programs (a-Climax [3]).

This study reports a conformational analysis of chromone and two acid derivatives comprising a carboxylic moiety in different positions of the heterocyclic ring – chromone-2-carboxylic acid (2CA) and chromone-3-carboxylic acid (3CA) (Fig. 1). In particular, the H-bonding profile of these substituted chromones was investigated, since it is determinant of their antioxidant behaviour.

N.F.L. Machado acknowledges his FCT Ph.D. grant (SFRH/BD/40235/2007).

[1] A. Foroumadi et al., *Bioorg.&Med.Chem.Lett.* 17, 6764-6769 (2007).

[2] N.F.L. Machado et al., *Current Bioactive Compounds* in press.

[3] A. J. Ramirez-Cuesta, *Comput.Phys.Commun.* 157(3), 226-238 (2004).



## Monitoring of structural phase transition of $(\text{Ge}_2\text{S}_3)_x(\text{As}_2\text{S}_3)_{1-x}$ chalcogenide glass with Raman spectroscopy

O. Gamulin<sup>1</sup>, M. Ivanda<sup>2</sup>, V. Mitsa<sup>3</sup>, M. Balarin<sup>1</sup>, and M. Kosović<sup>1</sup>

<sup>1</sup>University of Zagreb, School of Medicine, Dpt of Physics and Biophysics, Šalata 3, 10000 Zagreb, Croatia

<sup>2</sup>Division of Materials Physics, Rudjer Bosković Institute, Bijenička 54, 10000 Zagreb, Croatia

<sup>3</sup>Uzhhorod National University, Research Institute of Solid State Physics and Chemistry, 54 Voloshyn str., Uzhhorod 88000 Ukraine

The  $(\text{Ge}_2\text{S}_3)_x(\text{As}_2\text{S}_3)_{1-x}$  chalcogenide glass thin films, with  $x=0.1, 0.7$  and  $0.9$  were prepared by flash thermal evaporation of glass powder. Their average coordination numbers were  $Z=2.52, 2.68, 2.78$  respectively. Samples were deposited on c-Si substrate with an Al interlayer. The Raman spectra were recorded with a Jobin Yvon T 64000 triple monochromator spectrometer and FT-Raman module of Perkin-Elmer GX spectrometer. The excitations were green line  $\lambda = 514.5$  nm ( $E=2.41$  eV) from Ar-ion laser and near infrared line  $\lambda=1064$  nm ( $E=1.17$  eV) from Nd:YAG laser. Fig. 1 shows Raman spectra of  $(\text{Ge}_2\text{S}_3)_x(\text{As}_2\text{S}_3)_{1-x}$  samples with different coordination numbers excited with two different photon energies. Two major bands can be identified in those spectra, one between  $200$  and  $280$   $\text{cm}^{-1}$  and the other between  $300$  and  $450$   $\text{cm}^{-1}$ . Band positions in Raman spectra, recorded from sample with phase transition coordination number  $Z=2.68$  [1], are similar for both excitation energies. On the contrary, the spectra of samples with  $Z=2.52$  and  $Z=2.78$  exhibit shift of peak positions in dependence to the excitation energy. That shift is discussed in terms of structural ordering at the threshold  $Z$  and its connection with the band-tail states.

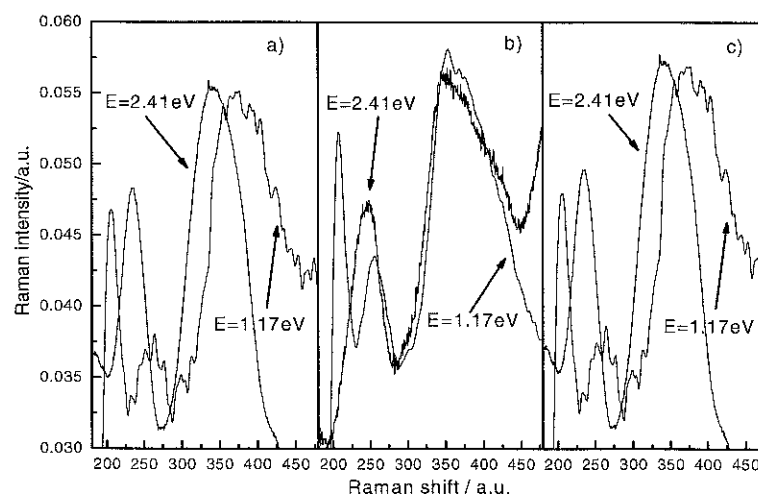


Fig. 1. Raman spectra of  $(\text{Ge}_2\text{S}_3)_x(\text{As}_2\text{S}_3)_{1-x}$  thin films a)  $Z=2.52$ , b)  $Z=2.68$  and c)  $Z=2.78$

[1] K. Tanaka, Phys. Rev B **39** (1989) 1270.



## Bent polyynes: ring strain studied by Raman and infrared spectroscopies

A. Lucotti<sup>1</sup>, M. Tommasini<sup>1</sup>, W.A. Chalifoux<sup>2</sup>, D. Fazzi<sup>4</sup>, G. Zerbi<sup>1</sup>, R.R. Tykwinski<sup>2,3</sup><sup>1</sup>Dipartimento di Chimica, Materiali e Ingegneria chimica "G. Natta", Politecnico di Milano, Piazza, Leonardo da Vinci 32, 20133 Milano, Italy and INSTM UdR Polimi<sup>2</sup>Department of Chemistry, University of Alberta, Edmonton, Alberta, T6G 2G2, Canada<sup>3</sup>Institut für Organische Chemie, Friedrich-Alexander-Universität, Erlangen-Nürnberg, Henkestrasse 42, D-91054, Erlangen, Germany<sup>4</sup>Center for NanoScience and Technology CNST IIT@PoliMi, via Pascoli 70/3, 20133 Milano, Italy

The structure of sp-carbon chains (polyynes) in solid state has been extensively studied by means of X-ray crystallography. These investigations typically show that a linear polyyne is rarely found and, in some cases, quite dramatic deviations from linearity can be observed.

Recently [1] we have shown that polyynes in solution are bent such that inversion symmetry is lost (series of polyynes **1**, see Figure 1) and the mutual exclusion principle between IR and Raman spectroscopy is not upheld. In order to assess whether different polyyne curvatures give intensity variations for those bands which violate the mutual exclusion principle, we have synthesized bent polyynes coupling the acetylenic skeleton (in our case 8 carbon atoms in the polyynic chain) with C10, C11, C12 alkyl chains in order to obtain a "ring" system (see Figure 1, systems **3a-c**). Different alkyl chain lengths produce different head-tail distances ( $R$ ) and therefore different curvatures of the polyyne chain.

The joint use of Raman and IR spectroscopies in solution allows to reliably probe the bending of the sp chain controlled by the imposed chemical structure. In particular we have proven that both the band positions and the relative intensities in the IR and Raman spectra are *curvature sensitive*. Furthermore, also the Raman depolarization ratio  $\rho$  is curvature sensitive and this fact can be exploited for a purely Raman quantification of chain bending. Density Functional Theory (DFT) calculations have been also carried out on model systems. This allows to nicely interpret and reproduce the experimental observations.

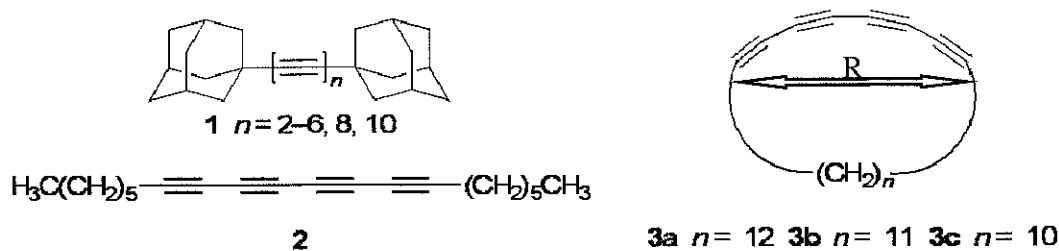


Figure 1. Sketch of the polyynes considered in this work.

[1] A. Lucotti, M. Tommasini, D. Fazzi, M. Del Zoppo, W. A. Chalifoux, M. J. Ferguson, G. Zerbi, R. R. Tykwinski, J. Am. Chem. Soc. 131 (2009), 4239-4244



## Weeding the Cosmos - FTIR synchrotron spectroscopy of methanol isotopologues at the Canadian Light Source

R.M. Lees<sup>1</sup>, Li-Hong Xu<sup>1</sup>, B.E. Billinghamurst<sup>2</sup>

<sup>1</sup>*Centre for Laser, Atomic and Molecular Studies (CLAMS), University of New Brunswick, Saint John, NB E2L 4L5, Canada*

<sup>2</sup>*Canadian Light Source Inc., 101 Perimeter Road, Saskatoon, SK S7N 0X4, Canada*

New astronomical facilities such as HIFI on the Herschel Space Observatory, the SOFIA airborne IR telescope and the ALMA mm telescope array will yield spectra from interstellar and protostellar sources with vastly increased sensitivity and frequency coverage. This creates the need for major enhancements to laboratory databases for the more prominent interstellar "weed" species in order to model and account for their lines in observed spectra in the search for new and more exotic interstellar molecular "flowers". With its large-amplitude internal torsional motion, methanol has particularly rich spectra throughout the FIR and IR regions and, being very widely distributed throughout the galaxy, is perhaps the most notorious interstellar weed. Thus, we have recorded new Fourier transform spectra for several methanol isotopic species on the high-resolution spectrometer on the CLS FIR beamline. The aim is to extend quantum number coverage of the data, improve our understanding of the energy level structure, and provide the astronomical community with better databases and models of the spectral patterns with greater predictive power for a range of astrophysical conditions.



## Raman microspectroscopy of inclusions in bituminous salts

A. Wesełucha-Birczyńska<sup>1</sup>, T. Tobała<sup>2</sup>

<sup>1</sup> Faculty of Chemistry, Jagiellonian University, Ingardena 3, 30-060 Kraków, Poland

<sup>2</sup> Faculty of Geology, Geophysics and Environmental Protection AGH University of Science and Technology, Mickiewicza 30, 30-059 Kraków, Poland

Fluid migration in sedimentary basins is of high interest, both from a scientific and an economic point of view. In various salt formations some amounts of organic matter and hydrocarbons occur. In Kłodawa Salt Dome (Central Poland) there are concentrations of so called "bituminous salt". These salts characterized by colour changes from light honey to dark brown and form very different shapes. Most of them occur in the form of irregular aggregates or streaks, rarely in the form of layers.

Microscopic observations carried out in thick plates of halite crystals showed the presence of relatively numerous fluid inclusions assemblage (FIA). They show great diversity in terms of size, shapes and filling material. Most are filled with hydrocarbons, which in varying proportions are accompanied by the brine and gas phase. Hydrocarbons found in the individual FIA display different fluorescence under the UV light which suggests the presence of different organic matter.

Raman spectroscopic studies of hydrocarbon-rich inclusions are very few in number because such studies are in general considered to be very difficult or even impossible. The reasons for this outlook are the usual presence of laser-induced fluorescence from many natural hydrocarbons as well as the laser-induced degradation of such inclusions and finally the very low Raman signal obtained from the necessarily low laser power used on such inclusions.

The inclusions in analyzed samples were investigated with Renishaw InVia Raman spectrometer. The samples were excited with an HP NIR 785 nm laser. There was detected CO<sub>2</sub> along with hydrogen sulfide among sometimes undefined hydrocarbons.

**Acknowledgements:** This work has been supported by the Polish Ministry of Science and Higher Education, Statutory Research.



## Structural and microstructural changes in the zirconium-indium mixed oxide system during thermal treatment

G. Štefanić, I. I. Štefanić, S. Musić and M. Ivanda

*Ruđer Bošković Institute, P. O. Box 180, HR-10002 Zagreb, Croatia*

The amorphous precursors of the zirconium-indium mixed oxide system at the zirconium-rich side of the concentration range were prepared by co-precipitation from aqueous solutions of corresponding chloride salts, followed by washing and drying. The dried samples were calcined in air at different temperatures up to 1200 °C and analyzed at room temperature using X-ray powder diffraction, Raman spectroscopy, Fourier transform infrared spectroscopy, field emission scanning electron microscopy and energy dispersive X-ray spectrometry. The phase analysis results indicated that the incorporation of In<sup>3+</sup> ions partially stabilized both the tetragonal and cubic ZrO<sub>2</sub> polymorphs. Maximum solubility of In<sup>3+</sup> ions in the ZrO<sub>2</sub> lattice (more than 50 mol%) occurred in the metastable products obtained after crystallization of the amorphous precursors. Temperature treatment caused a decrease in the solubility limits followed by the transition of the metastable tetragonal or cubic ZrO<sub>2</sub> into a thermodynamically stable monoclinic ZrO<sub>2</sub> polymorph. Precise unit-cell parameters of the ZrO<sub>2</sub>-type solid solutions were determined by using both Rietveld and Le Bail refinements of the powder diffraction patterns with added silicon as an internal standard. The influence of thermal treatment on the crystallization of the amorphous precursors was also examined by differential thermal analysis and thermogravimetric measurement. The obtained results show that the crystallization temperature of the amorphous precursors increased with an increase in the indium content from 435 °C (0 mol% InO<sub>1.5</sub>) to 468 °C (~50 mol% InO<sub>1.5</sub>). A comparison with the results obtained for the mixed oxides of zirconium and undersized trivalent metals (systems ZrO<sub>2</sub>-FeO<sub>1.5</sub>, ZrO<sub>2</sub>-GaO<sub>1.5</sub>, ZrO<sub>2</sub>-CrO<sub>1.5</sub> and ZrO<sub>2</sub>-AlO<sub>1.5</sub>) indicates that the crystallization temperature of the amorphous co-gels depends on the amount of the dopant cation (crystallization temperature increases with an increase in the dopant content) and the ionic radius of the dopant cation (crystallization temperature increases with a decrease in the ionic radius of the dopant cation).



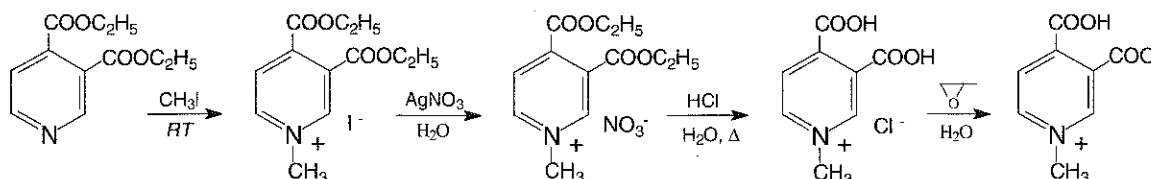
## Structure of 3,4-dicarboxy-1-methylpyridinium betaine studied by X-ray diffraction, DFT calculations, NMR and FTIR spectra

P. Barczyński, M. Szafran

Faculty of Chemistry, Adam Mickiewicz University, ul. Grunwaldzka 6, 60-780 Poznań, Poland

3,4-Pyridinedicarboxylic acid (cinchomeric acid) is one of the six isomers of pyridinedicarboxylic acids. All isomers are widely utilized in the construction of coordination networks and some of these are biologically active. 2,3-Pyridinedicarboxylic acid (quinolinic acid) has a very short intramolecular O-H...O hydrogen bond in the solid state, while two polymorphs of cinchomeric acid display exclusively intermolecular hydrogen bonds. The molecule is present as a zwitterion with one acid hydrogen on the ring nitrogen. In our earlier works, we have described the structures of 1-methyl, 1-carboxymethyl and 1-carboxyethyl derivatives of various pyridine carboxylic acids which form a group of betaines with interesting topologies and physical properties. This work continues our structural and vibrational studies of multicarboxylate ligands and hydrogen bonded complexes, and is focused on 3,4-dicarboxy-1-methylpyridinium betaine.

3,4-Dicarboxy-1-methylpyridinium betaine (34MePy) was obtained by acidic hydrolysis of its diethyl ester followed by treatment with propylene oxide.



The FTIR spectrum of 34MePy has a broad and strong absorption in the 1500-400  $\text{cm}^{-1}$  region, typical of hydrogen bonds shorter than 2.5 Å and the intense band at 1675  $\text{cm}^{-1}$  in the carboxyl/carboxylate region. The molecular and crystal structures of 34MePy have been determined by X-ray diffraction and by the B3LYP calculations and both confirmed the presence of an intramolecular O-H...O hydrogen bond. Both proton and carbon NMR shifts of 34MePy and its complex with HCl (34MePyHCl) were analyzed. The GIAO/B3LYP/6-311G(d,p) calculations in vacuum, DMSO- $d_6$  and  $\text{H}_2\text{O}$  solutions using the solvation model, are reported.

The structure of 3,4-dicarboxy-1-methylpyridinium chloride (34MePyHCl) has been recently studied [1].

[1] M. Szafran, A. Katrusiak, Z. Dega-Szafran, P. Barczyński, J. Mol. Struct. 934 (2009) 79-85

## The Studies of Molecular Structures and Vibrational Spectra of Sudan Orange G and Sudan Red G

A. Esme<sup>1</sup>, S. Sagdinc<sup>2</sup>

<sup>1</sup>Kocaeli University, Education Faculty, Umuttepe, 41380, Kocaeli, TURKEY

<sup>2</sup>Kocaeli University, Science and Art Faculty, Department of physics, Umuttepe, 41380, Kocaeli, TURKEY

Sudan azo-dyes are commonly used as synthetic organic colorants in chemical industries such as oils, plastics, waxes, petrol, shoes, among others[1]. The structural and electronic properties of the Sudan Orange G {4-(Phenylazo)resorcinol} and the Sudan Red G {amethoxybenzenazo- $\beta$ -naphthol} have been investigated by performing Hartree-Fock (HF) and B3LYP theoretical methods with 6-31G(d,p) basis set. The vibrational study of these molecules has been performed by FT-Raman and FT-IR spectroscopy. The observed FT-IR wave numbers were analyzed in light of the computed vibrational spectra. On the basis of the comparison between calculated and experimental results and the comparison with related molecules, assignments of fundamental vibrational modes are examined. The scaled theoretical wavenumbers showed very good agreement with the experimental values.

The nonlinear behaviors of Sudan Orange G and Sudan Red G as azo dyes have been investigated. The dipole polarizability ( $\alpha$ ) and first-order hyperpolarizability ( $\beta$ ) were calculated with Hartree-Fock and DFT methods.

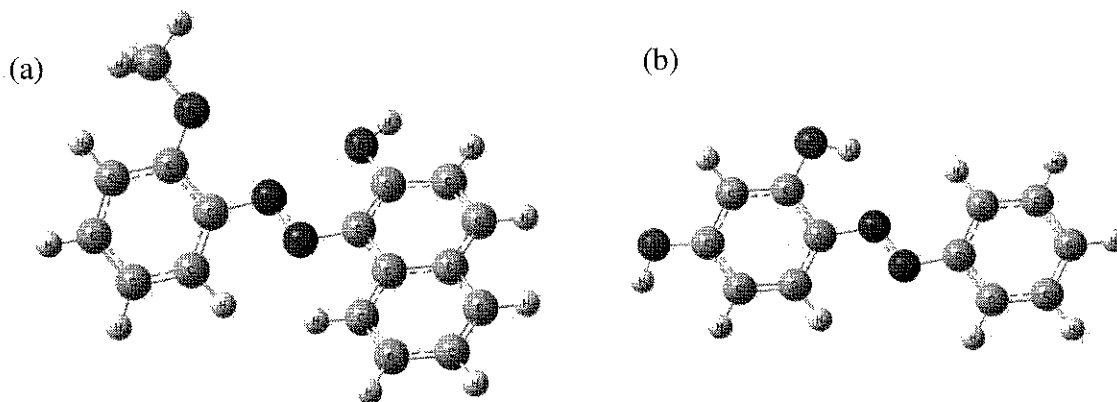


Fig 1. The optimized structures obtained using B3LYP/6-31G(d,p) level of (a) Sudan Red G and (b) Sudan Orange G.

[1] Society of Dyers and Colourists. (3rd ed.) Colour index (Vol 3). Badford, U.K. : Society of Dyery and Colourists (1971)



## Structural behavior of selected ionones upon thermal stress conditions

K. Chruszcz-Lipska, A. Kaczor

Jagiellonian University, Faculty of Chemistry, Ingardena 3, 30-060 Krakow, Poland

Ionones are one of the oldest groups of aroma chemicals that have a powerful, sweet, violet aroma and were amongst the first 'synthetics' to be used in perfumery [1]. In nature, the ionones are key intermediates of carotenes degradation. Extraction of carotenes out of plants and further food processing (blanching, pasteurization, heating, canning) results frequently in their degradation or isomerization to *cis* isomers, that in general have lower bioavailability and antioxidant capacity [2,3]. This work is a part of our study upon isomerization of carotenes in which small terpenes are treated as models of carotenes.

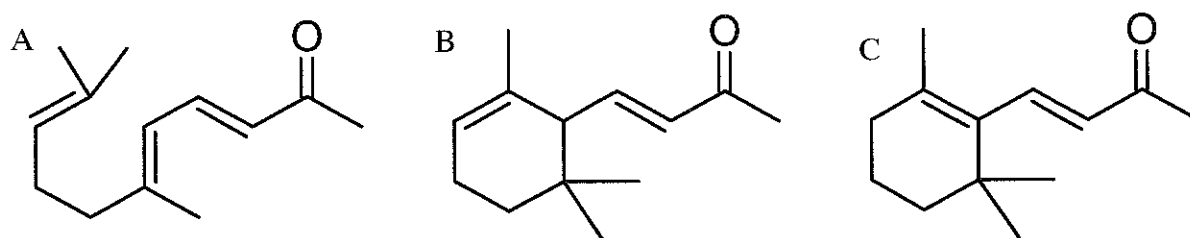


Figure 1. Structures of studied ionones.

The aim of this work is to determine the effect of the temperature stress on the selected ionones (Fig. 1): pseudoionone (6,10-Dimethyl-3,5,9-undecatrien-2-one) (A), alpha-ionone ((3*E*)-4-(2,6,6-Trimethylcyclohex-2-en-1-yl)but-3-en-2-one) (B) and beta-ionone ((3*E*)-4-(2,6,6-Trimethylcyclohex-1-en-1-yl)but-3-en-2-one) (C). The structural changes of ionones were monitored by NIR FT-Raman spectroscopy in the temperature range of -150 - +150°C and the experimental results were analyzed with the aid of quantum-chemical calculations (B3LYP/6-311++G(d,p)).

**Acknowledgments:** This research was supported by the Polish Ministry of Science and High Education in years 2009-2012 (grant no. N N204 311037). Computational center "Cyfronet" (Krakow, Poland) is acknowledged for CPU time.

[1] Kraft, P., *Synthesis*, 1999, 695.

[2] Schieber, A.; Carle, R. *Trends Food Sci. Technol.* 2005, 16, 416.

[3] Yeum, K. J.; Russell, R. M. *Annu. Rev. Nutr.* 2002, 22, 483.



## Infrared spectroscopy and photochemistry of 2-phenylethylamine and its derivatives isolated in noble gas matrices.

B. M. Giuliano<sup>1</sup>, I. Reva<sup>1</sup>, R. Fausto<sup>1</sup>, S. Melandri<sup>2</sup>

<sup>1</sup> Departamento de Química, Universidade de Coimbra, 3004-535 Coimbra, Portugal;

<sup>2</sup> Dipartimento di Chimica "G. Ciamician", Università di Bologna, 40126 Bologna, Italy

2-Phenylethylamine (hereinafter abbreviated as PEA) is the parent structure of a variety of important neurotransmitters including dopamine, amphetamine, serotonin, histamine and adrenaline. The common structural feature of PEA and the neurotransmitters cited above is the presence of the ethylamino group in the side chain which, due to its flexibility, gives rise to a complex conformational surface which contains several minima of relatively low energy.

Spectroscopic studies of monomeric molecules (in gas phase or isolated in cryogenic matrices) allow the precise determination of intrinsic molecular properties that can be directly compared to high level quantum chemical calculations.

The infrared spectra of PEA and its derivatives, 4-methoxyphenylethylamine (4MPEA) and tyramine (see Scheme 1), trapped in argon matrix have been recorded. Their interpretation was based on theoretical calculations of the vibrational spectra and relative energies of various stable conformers. The experimental spectra confirm the presence of several conformers in the samples. Photoreactions of these systems induced by UV irradiation have been investigated. Preliminary results show different photochemical behaviour related to the presence of oxygen containing substituents. Identification of decomposition products suggests the ring opening mechanism of the photoreaction.

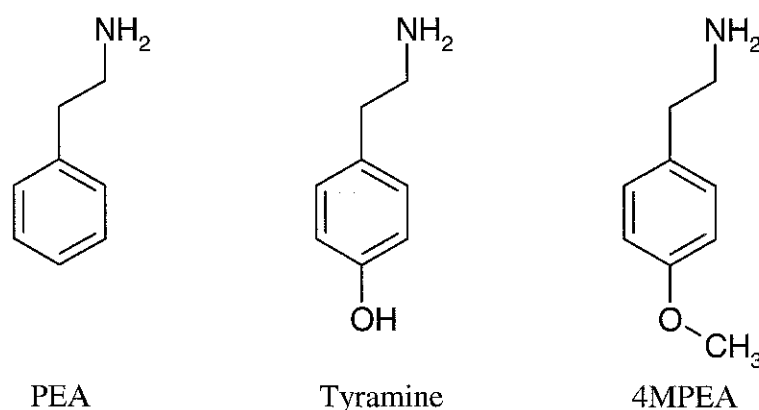


Figure 1. Sketch of the studied compounds.

## Flash vacuum pyrolysis of isoxazole. a low temperature matrix isolation infrared spectroscopy study.

C. M. Nunes, I. Reva, R. Fausto and T. M.V.D. Pinho e Melo

*Department of Chemistry, University of Coimbra, P-3004-535 Coimbra, Portugal.*

The gas-phase flash vacuum pyrolysis (FVP) is an important technique for studies of intramolecular reactions, such as cyclizations and eliminations. These types of reactions have great potential in heterocyclic chemistry. The use of FVP connected with an adequate method for trapping the produced unusual species and a suitable detection technique allows the investigation of many important reaction intermediates, which are not easily accessible to investigation under other experimental conditions. Low temperature matrix isolation is an experimental technique which permits the stabilization of reactive species resulting from FVP, allowing their detection and characterization by conventional spectroscopic methods. The combination of FVP and Matrix Isolation-IR Spectroscopy approach is then a powerful method, with a great potential for expanding the chemical knowledge of reactive intermediate species.

A pyrolysis system with a pulse hyperthermal nozzle, based upon the design conceived by Chen *et al.*,<sup>1</sup> was recently coupled to a home-made cryostat in our lab. In this communication we present the results obtained with this technique for isoxazole (**1**) (Figure 1).

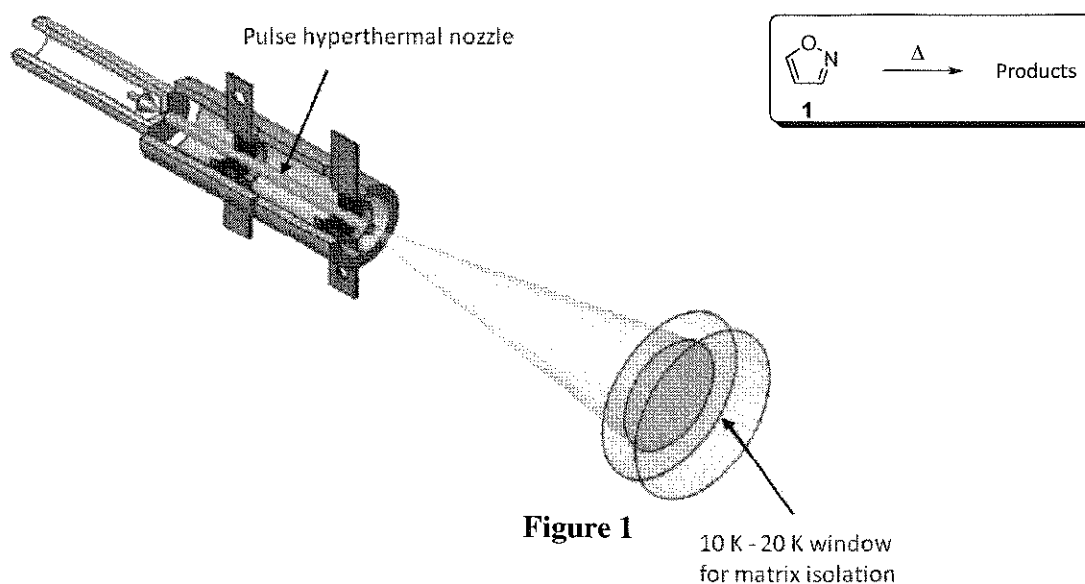


Figure 1

10 K - 20 K window  
for matrix isolation

Isoxazole was isolated in low-temperature argon matrices and characterized by infrared spectroscopy. The thermal reactivity was then explored by using the hyphenated FVP-Matrix Isolation-IR Spectroscopy under different experimental conditions (temperature of hot nozzle, concentration of sample in a pre-mixture with the noble gas and a variety of pulse parameters). To complement the experimental results, theoretical studies have been done in order to identify and characterize in greater detail the thermal reactivity paths of isoxazole.

**Acknowledgements:** This work was funded by FCT (Projects PTDC/QUI/71203/2006 and PTDC/QUI/64470/2006). C. M. Nunes acknowledges FCT the Ph.D. grant (SFRH/BD/28844/2006).

[1] X. Zang, *et al.* Rev. Sci. Inst. 74 (2003) 3077-3086.



## Infrared spectra of matrix-isolated 4-methoxybenzaldehyde (*p*-anisaldehyde) conformers

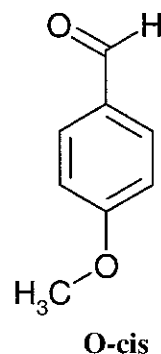
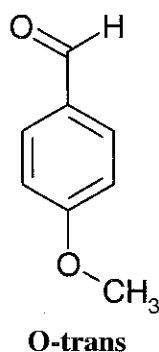
A. Sharma<sup>1</sup>, N. Kuş<sup>2</sup>, I. Reva<sup>1</sup>, L. Lapinski<sup>3</sup> and R. Fausto<sup>1</sup>

<sup>1</sup> Department of Chemistry, University of Coimbra, 3004-535 Coimbra, Portugal

<sup>2</sup> Department of Physics, Anadolu University, 26470 Eskişehir, Turkey

<sup>3</sup> Institute of Physics, Polish Academy of Sciences, Warsaw, Poland

In gas phase, at room temperature, 4-methoxybenzaldehyde (*p*-anisaldehyde) exists in two almost isoenergetic forms, *O-trans* and *O-cis* (shown below). The similarity of their structures results in very similar infrared absorption spectra and hence poses some difficulties in their experimental assignment. In the present study, monomers of the compound were trapped from the room-temperature gas phase into cryogenic argon and xenon matrices. Increasing the temperature of a Xe matrix to about 55 K led to conversion of the less stable *O-cis* form to the *O-trans* conformer, allowing the reliable assignment of the spectral signatures due to the individual forms. We have demonstrated that the minor *O-cis* conformer can be repopulated by irradiation of the matrix with UV light. UV irradiations of matrix-isolated *p*-anisaldehyde were leading to photostationary states and the photostationary ratio of *O-trans* and *O-cis* forms was found to be dependent on the wavelength range of the applied UV-light. The UV-induced *O-cis* → *O-trans* as well as *O-trans* → *O-cis* population changes were observed. The net direction of these changes depends on the initial ratio of the two conformers as well as on the intrinsic position of the photostationary equilibrium, being a function of the UV wavelength. The isomerization processes were probed by infrared spectroscopy. The interpretation and assignment of the experimental data was supported by quantum chemical calculations of the vibrational spectra and the barriers to intramolecular rotation. The absorption bands observed in the infrared spectra of *p*-anisaldehyde isolated in argon and xenon matrices were assigned to the theoretically predicted normal modes.



## Temperature controlled kinetics of growing and relaxation of alcohol clusters in Argon matrix

I. Doroshenko<sup>1</sup>, V. Pogorelov<sup>1</sup>, P. Uvdal<sup>2</sup>, V. Balevicius<sup>3</sup>, V. Šablinskas<sup>3</sup>

<sup>1</sup>*Department of Physics, Kyiv National Taras Shevchenko University, Glushkova av., 2, build.1, Kyiv, 03022, UKRAINE*

<sup>2</sup>*MAX-lab, Lund University, P.O. box 124, S-22100, Lund, SWEDEN*

<sup>3</sup>*Department of Physics, Vilnius University, Sauletkio, 9-3, Vilnius, LITHUANIA*

The clustering processes of monohydric alcohols (from methanol to hexanol) were investigated by FTIR using isolation in argon matrix technique. The transformation of the FTIR bands of free O–H ( $3600 - 3800 \text{ cm}^{-1}$ ) into diffuse bands ( $3000 - 3600 \text{ cm}^{-1}$ ), which were assigned to the stretching vibrations of the H-bonded O–H groups in various clusters, was monitored in its initial stage during softening the matrices by heating from 20 K to 50 K. The changes in spectra at increasing temperature were analyzed, expecting that such experiments may be considered as the proof of structural transformations in alcohols during the gas - liquid phase transition. The band shape analysis was carried out for investigated systems. The magnitude of inhomogeneous broadening due to the matrix effect was evaluated from the bandwidth of monomer species. The values of hydrogen bond dissociation time of alcohols trapped in Ar matrices were estimated from the bandwidths of dimers, trimers and higher aggregates. These data correlate with those directly measured in ultra fast infrared experiments of alcohols in solutions.



## Spectral indicators of structural flexibility of matrix isolated methyl isocyanate

I. Reva<sup>1</sup>, L. Lapinski<sup>1,2</sup>, R. Fausto<sup>1</sup>

<sup>1</sup>Department of Chemistry, University of Coimbra, 3004-535 Coimbra, Portugal

<sup>2</sup>Institute of Physics, Polish Academy of Sciences, 02-668 Warsaw, Poland

The infrared spectra of methyl isocyanate (MIC, O=C=N-CH<sub>3</sub>) monomers isolated in cryogenic argon, xenon and nitrogen matrices were studied. The observed infrared spectra were interpreted by comparison with the results of harmonic and anharmonic calculations carried out at the DFT, MP2 and CCSD levels of approximation.

In spite of the fact that MIC is a flexible molecule and some of its vibrations have a large-amplitude character, the IR spectrum in the 1600–500 cm<sup>-1</sup> range is very well reproduced by the calculations carried out within the harmonic approximation (Figure 1).

Clear indications of the structural flexibility of the molecule were observed in the experimental IR spectra. The most striking of these spectral features is the multiplet structure of the most intense band due to the antisymmetric stretching vibration of the N=C=O group. This band appears (in the spectra of MIC isolated in Ar, Xe or N<sub>2</sub> matrices) as a quadruplet spanning at *ca.* 2300 cm<sup>-1</sup> over the frequency range of nearly 100 cm<sup>-1</sup>. The very unusual structure of this band was interpreted in terms of coupling with the torsion of the methyl group, which is the lowest frequency vibration in the molecule.

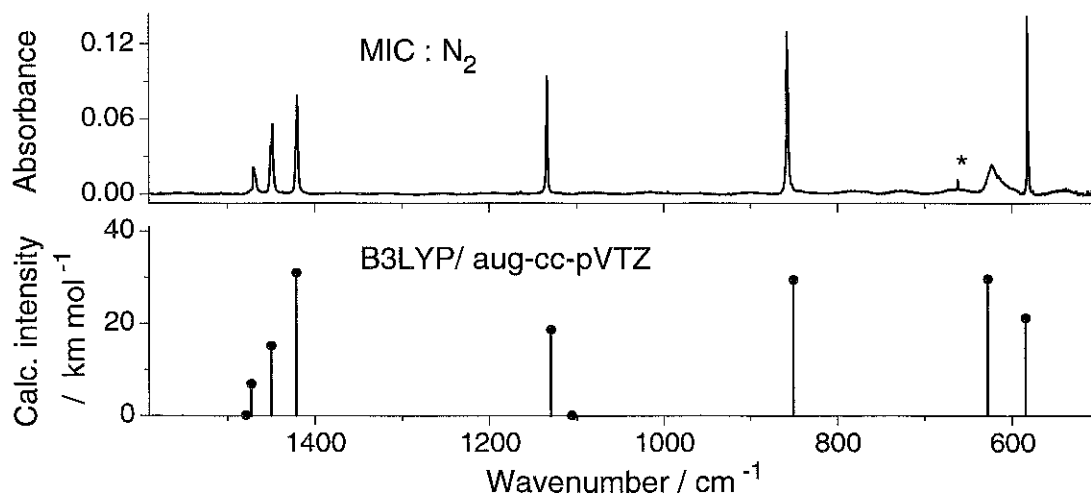


Figure 1. Fingerprint region of the experimental FTIR spectrum of MIC monomers isolated in a nitrogen matrix at 8 K compared with the spectrum calculated at the B3LYP/aug-cc-pVTZ level of theory. Theoretical wavenumbers were scaled by a factor of 0.977. Asterisk in the experimental spectrum designates a band due to traces of the matrix-isolated CO<sub>2</sub> impurity.



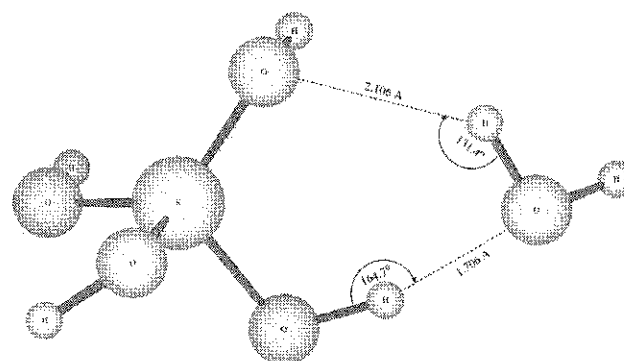
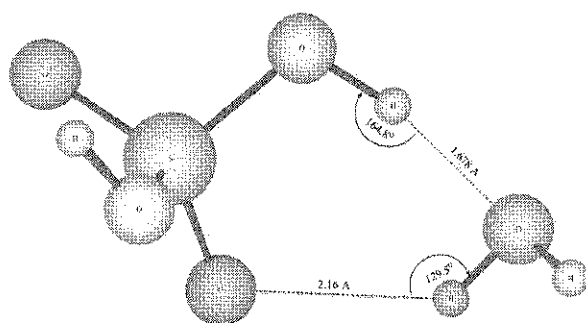
## The Matrix Isolation Infrared Spectrum of the Sulfuric Acid-monohydrate Complex: New assignments and resolution of "missing H-bonded $\nu(\text{OH})$ band" issue.

M. Rozenberg and A. Loewenschuss

*Institute of Chemistry, The Hebrew University of Jerusalem, Jerusalem 91904, Israel*

The matrix isolation infrared spectrum of "dry" and "wet" vapors of sulfuric acid have been investigated as trapped in solid argon matrices.

The availability of a spectrum of trapped anhydrous acid vapor and its comparison with the spectra of trapped water containing vapors of the acid, allowed the identification of the hydrogen bonding shifted hydroxyl bands for both the acid and the water moieties of the monohydrated  $\text{H}_2\text{SO}_4 \cdot \text{H}_2\text{O}$  complex. The experimental results are compared to the various theoretically calculated wavenumber values of the acid and its monohydrated complex. The complex stabilization energies as obtained from calculations and empirical correlations are compared.



## Infrared spectrum and photochemistry of matrix-isolated 3-furaldehyde

N. Kuş<sup>1,2</sup>, I. Reva<sup>1</sup> and R. Fausto<sup>1</sup>

<sup>1</sup> Department of Chemistry, University of Coimbra, 3004-535 Coimbra, Portugal

<sup>2</sup> Department of Physics, Anadolu University, 26470 Eskişehir, Turkey

Structure and reactivity of 3-furaldehyde (3FA) monomers isolated in argon matrices at 10 K were studied using FTIR spectroscopy and theoretically. The molecule can adopt two conformers, with trans and cis orientation of the O=C–C=C dihedral angle. At the B3LYP/6-311++G(d,p) level, the energy difference between the trans and cis conformers was computed to be *ca.* 4 kJ mol<sup>-1</sup>. The relative stability of the two conformers was explained using the natural bond orbital (NBO) method. In agreement with their relative energies, trans and cis conformers are populated in the gas phase at room temperature in proportion 5:1. They were found to be trapped in the same ratio in the cryogenic matrix, since they are separated by a high barrier to intramolecular rotation (34 kJ mol<sup>-1</sup>). The experimentally observed vibrational signatures of the two forms are in a good agreement with the theoretically calculated spectra.

Broad-band UV-irradiations with long-pass optical filters ( $\lambda > 375, 337, 283$  nm) did not induce any changes in the spectra of the matrix-isolated compound. A more energetic UV-irradiation ( $\lambda > 234$  nm) resulted in the partial trans→cis transformation, which ended in a photostationary state with trans:cis ratio being *ca.* 1.4:1. Further irradiation of the sample with UV-light of even higher energies ( $\lambda > 200$  nm) led to decarbonylation of 3FA (both conformers) and formation of furan and carbon monoxide.

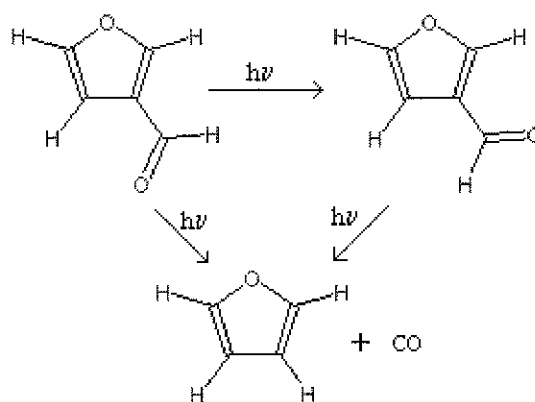


Figure 1. Trans (top, left) and cis (top, right) conformers of 3-FA and its photoproducts (furan + CO).



## IR Low-Temperature Matrix, X-ray and ab Initio Study on L-Isoserine Conformations

J. Cz. Dobrowolski<sup>1,2</sup>, M. H. Jamróz<sup>2</sup>, R. Kołos<sup>3,4</sup>, J. E. Rode<sup>2</sup>, M. K. Cyrański<sup>5</sup>, J. Sadlej<sup>1,5</sup>

<sup>1</sup>National Medicines Institute, 30/34 Chełmska Street, 00-725 Warsaw, Poland, E-mail: janek@il.waw.pl

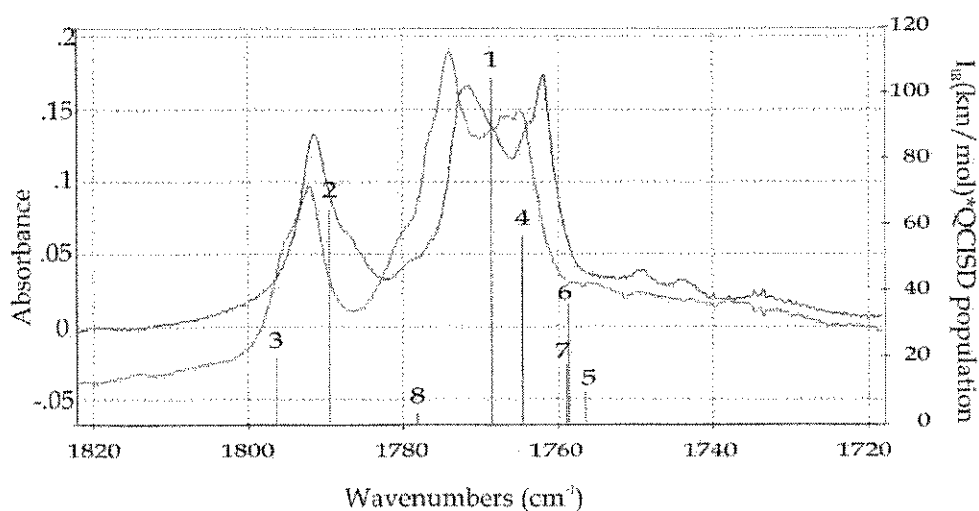
<sup>2</sup>Industrial Chemistry Research Institute, 8 Rydygiera Street, 01-793 Warsaw, Poland

<sup>3</sup>Institute of Physical Chemistry, PAN, 44 Kasprzaka Street, 01-224 Warsaw, Poland

<sup>4</sup>Cardinal S. Wyszyński University, Faculty of Mathematics and Natural Sciences, Wóycickiego 1/3, 01-938 Warsaw, Poland

<sup>5</sup>Faculty of Chemistry, Warsaw University, 1 Pasteura Street, 02-093 Warsaw, Poland

The IR low-temperature Ar and Kr matrix spectra of L-isoserine were registered for the first time and interpreted by means of the anharmonic DFT frequencies calculated at the B3LYP/aug-cc-pVTZ and B3LYP/aug-cc-pVDZ levels. 54 L-isoserine conformers were predicted to be stable at the B3LYP/aug-cc-pVDZ and MP2/aug-cc-pVDZ levels. Population of the 8 most stable conformers was based on the QCISD/aug-cc-pVDZ energies, corrected for anharmonic thermochemical factors obtained at the B3LYP/aug-cc-pVDZ level. We found several conformers to be present in the measured matrices and conformer **1** to be dominating. Presence of the conformer **2** is well confirmed by the  $\nu(\text{C}=\text{O})$  band at  $1790\text{ cm}^{-1}$  and two bands at  $1380$  and  $1350\text{ cm}^{-1}$ . Presence of the conformer **4** is quite well confirmed by the  $\nu(\text{C}-\text{O})$  bands at  $1120$  and  $1095\text{ cm}^{-1}$ . Slightly weaker arguments are found for the observation of conformers **6** and **3**. Calculations on 54 neutral and 5 zwitterionic conformers in water at the IEF-PCM/B3LYP/aug-cc-pVDZ level suggest that one neutral and one zwitterionic conformer co-exist in the aqueous environment.



The crystal structure of L-isoserine was solved by x-ray diffraction analysis. The compound crystallizes without solvent in the chiral  $P2_12_12$  space group. The asymmetric unit contains a single molecule. The molecule is in its zwitterionic form with the  $\text{CH}_2\text{-NH}_3$  side chain in the gauche conformation with respect to the hydroxyl group and in the anti conformation with respect to the carboxylate group. The structure of L-isoserine is dominated by a set of intermolecular hydrogen bonds. The strongest one appears between the OH and COOH groups of two neighbouring molecules: the  $\text{O}\cdots\text{H}$  contact is of  $1.66(2)\text{ \AA}$ , which is amongst the shortest H-bonds of this kind observed in amino acid crystal structures.



## Photoinduced reactivity of liquid ethanol at high pressure

M. Ceppatelli, S. Fanetti, M. Citroni, R. Bini

*European Laboratory for Non-Linear Spectroscopy (LENS), via N. Carrara 1, 50019 Sesto Fiorentino (FI), Italy  
and Dipartimento di Chimica, Università di Firenze, via della Lastruccia 3, 50019 Sesto Fiorentino (FI), Italy*

The lowest electronic excited states of simple alcohols, like ethanol and methanol, have dissociative character. Excitation to these states, possible through two-photon absorption of near UV radiation, leads to the formation of reactive radicals, that can trigger chemical reactions.

In this work, we have studied the high pressure photoinduced reactivity of liquid ethanol at room temperature as a function of irradiation power, wavelength and pressure in the range 0.005-1.7 GPa by means of infrared and Raman spectroscopy. All the measurements were performed in a diamond anvil cell. In these conditions, liquid ethanol was stable under laser irradiation using wavelength  $\lambda \geq 458$  nm. A complex reactivity, depending on pressure and on the reactant amount, was observed when the sample was irradiated with laser wavelength at 350 nm and power exceeding 100 mW, revealing also the existence of a threshold wavelength for the reaction.

In these conditions, we observed the formation of a few specific products among which molecular hydrogen has to be remarked especially for the mild pressure conditions required for its synthesis. Indeed, hydrogen is an important energy vector and its synthesis from a renewable source, like ethanol, has a strong appeal from the pollution point of view, because that would allow a net-zero greenhouse gases emission. On the basis of the products formed during the irradiation cycles at various pressures in the investigated range, the active dissociation channels of ethanol can be identified and the relative weight of several reactive paths, depending both on pressure and on irradiation time, was evidenced.



## Study of tetrazole derivatives by UV photoelectron spectroscopy and outer-valence Green's function methods

R. M. Pinto<sup>1</sup>, A. A. Dias<sup>1</sup> and M. L. Costa<sup>1</sup>

<sup>1</sup>CFA, Departamento de Física, Faculdade de Ciências e Tecnologia-UNL, 2829-516, Caparica, Portugal

Molecules containing the tetrazole ring are used in a wide range of applications [1, 2] where its chemical properties represent invaluable assets. Therefore, its electronic structure, tautomerism [3] and charge delocalization upon ionization is a matter of great interest. In this study, 5-aminotetrazole (5-ATZ) and 1H-tetrazole-5-acetic acid (T5A) electronic properties are investigated through UV photoelectron spectroscopy (UVPES) and quantum chemical calculations.

The He(I) photoelectron (PE) spectra of 5-ATZ and T5A have been recorded and compared with the simulated spectra based on the outer-valence Green's function (OVGF) and partial third-order (P3) methods. The thermochemistry properties of the two compounds were also calculated with the G2(MP2) multilevel procedure. The Mulliken charge distribution upon ionization was investigated and the character and shape of the molecular orbitals (MOs) was analyzed. The results show that 1H- and 2H-tautomers coexist in the gas phase, in similar proportions, against theoretical calculations prediction. Also, it is shown that T5A presents an almost symmetrical charge distribution, between the carboxylic and tetrazole groups. Finally, the P3 method proves to be suited to simulate the PE spectra of molecules with high nitrogen content.

- [1] G. Koldobskii, V. Ostrovskii, Russ. Chem. Rev. 63 (1994), 797-814.
- [2] R. Herr, J. Bioorg. Med. Chem. 10 (2002), 3379-3393.
- [3] R. M. Balabin, J. Chem. Phys. 131 (2009), 154307.



## Thermal decomposition of benzyl azide and its methyl derivatives studied by UV photoelectron spectroscopy and theoretical calculations

R. M. Pinto<sup>1</sup>, G. Copeland<sup>2</sup>, A. A. Dias<sup>1</sup>, M. L. Costa<sup>1</sup> and J. M. Dyke<sup>2</sup>

<sup>1</sup>CFA, Departamento de Física, Faculdade de Ciências e Tecnologia-UNL, 2829-516, Caparica, Portugal

<sup>2</sup>School of Chemistry, University of Southampton, Highfield, SO17 1BJ, Southampton U.K.

During the past three decades, several compounds containing the azido group ( $-N_3$ ) have drawn considerable attention [1] mainly because of their role as primary agents in explosive reactions. If subjected to a sudden increase in temperature or a strong mechanical stimulus, they react violently, releasing a large amount of energy through the elimination of  $N_2$  from the azide chain. Although much has already been done in studying several azides systems [2, 3], the aromatic ones, such as the benzyl azide (BA), lack the full theoretical and experimental characterization that already covered other simpler systems.

The thermal decomposition of benzyl azide,  $C_6H_5CH_2N_3$ , and its methyl derivatives, 2-, 3- and 4-methyl benzyl azide, (2-, 3- and 4-MBA),  $(CH_3)C_6H_4CH_2N_3$ , up to 1400 °C, has been studied by UV photoelectron spectroscopy (UVPES) and theoretical calculations.

The results show that the decomposition onset of the aforementioned molecules is marked by the elimination of  $N_2$ , at approximately 300 °C. Aside from molecular nitrogen, the pyrolysis spectra of BA shows the presence of several intermediates species, namely N-phenylmethanimine, N-methylenedianiline, benzene and benzonitrile, which further decompose into hydrogen cyanide, HCN, and molecular hydrogen,  $H_2$ . 2-MBA pyrolysis gives rise to the formation of a cyclic compound, isoindoline, for which an outer-valence photoelectron (PE) spectrum had to be simulated, based on outer-valence Green's function (OVGF) and partial third-order (P3) methods. 3- and 4-MBA thermal decomposition leads to the formation of toluene, m-, p-tolunitrile and m-, p-methyl benzylidene imine. Finally, some mechanisms for explaining the formation of these compounds are also introduced.

[1] S. Brase, C. Gil, K. Knepper, V. Zimmermann, *Angew. Chem. Int. Ed.*, 44 (2005) 5188-5240.

[2] J. M. Dyke, G. Levita, A. Morris, J. S. Ogden, A. A. Dias, M. Algarra, J. P. Santos, M. L. Costa, P. Rodrigues, M. M. Andrade, M. T. Barros, *Chem. Eur. J.*, 11 (2005), 1665-1676.

[3] R. M. Pinto, A. A. Dias, M. L. Costa, J. P. Santos, *J. Mol. Struct: THEOCHEM*, (2010), DOI: 10.1016/j.theochem.2010.02.011.



## Excited electronic states, crystal structure and DFT quantum chemical calculations of 2-amino-4-methyl-3-nitropyridine

W. Sasiadek<sup>1</sup>, E. Kucharska<sup>1</sup>, I. Bryndal<sup>1</sup>, M. Wandas<sup>1</sup>, J. Hanuza<sup>1,2</sup>

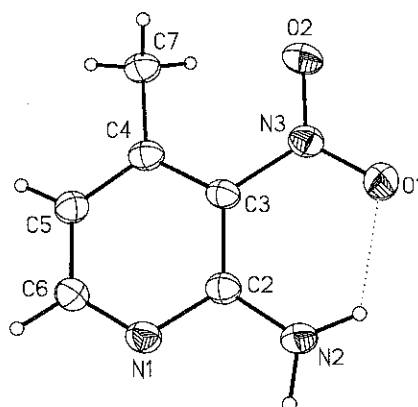
<sup>1</sup>Department of Bioorganic Chemistry, Institute of Chemistry and Food Technology, Faculty of Engineering and Economy, University of Economic, Komandorska 118/120, 53-345 Wrocław, Poland

<sup>2</sup>Institute of Low Temperatures and Structure Research, Polish Academy of Sciences, Okólna 2, 50-422, Wrocław, Poland

The electronic absorption, emission and excitation spectra of 2-amino-4-methyl-3-nitropyridine in chloroform (1.08 D), water (1.84 D), n-heptane (0 D) solution as well as solid state have been measured at room temperature. The influence of the solvent on optic properties has been discussed. The energy sequence of the singlet and triplet states has been calculated for optimized geometry of the molecule and compared to the experimental values. The results obtained by TD DFT quantum chemical calculations using MPW1PW91 and B3LYP functionals and 6-311G (2d,2p) basis have been compared with those of experimental values.

The structure determination revealed that 2-amino-4-methyl-3-nitropyridine crystallizes in centrosymmetric space group P2<sub>1</sub>/n. The crystal structure is stabilized by a combination of N-H...N hydrogen bonds and C-H...O interactions, and dispersive and electrostatic interlayer interactions.

The experimental absorption spectra in the region 20,000 – 50,000 cm<sup>-1</sup> consist of three bands with the maxima at 27,100 – 26,042, 39,216 – 35,282 and 45,045 – 41,152 cm<sup>-1</sup>. Moreover, fourth band appears in n-heptane and nujol mull at 51,813 – 51,282 cm<sup>-1</sup>. The excitation spectra in the region 20,000 – 40,000 cm<sup>-1</sup> consist of two bands with the maxima at about 33,333 and 23,256 cm<sup>-1</sup>. The emission spectra in the region 14,286 – 33,333 cm<sup>-1</sup> consist of two bands with the maxima at about 28,571 and 23,810 cm<sup>-1</sup>. The optic properties of the studied compound are compared to the spectra of other studied by us compounds [1, 2]. This compound includes three substituents: the nitro group (strong electron acceptor), the amino group (strong electron donor) and the methyl group, which interact by hyperconjugation and steric effect.



**Acknowledgement:** This work was financially supported by Ministry of Science and Higher Education (Grant No. PBZ/MEiN/01/2006/21).

[1] J. Lorenc, E. Kucharska, J. Hanuza, H. Chojnacki, J. Mol. Struct. 707 (2004) 47-57

[2] J. Lorenc, J. Mol. Struct. 748 (2005) 91-100



## Revisiting the electronic spectra of anthracene

D. O. Dorohoi<sup>1</sup>, A. Airinei<sup>2</sup>, R. I. Tigoianu<sup>1,2</sup>

<sup>1</sup>"Al. I. Cuza" University, Faculty of Physics, 11 Bldv. Carol I, Iasi-700506

<sup>2</sup>"Petru Poni" Institute of Macromolecular Chemistry Aleea Grigore Ghica Voda, 41A, Iasi-700487

Polycyclic aromatic hydrocarbons are of interest in various domains due to their unique characteristics such as high photoreactivity, strong  $\pi$ - $\pi^*$  absorption coupled with high fluorescence yield and high solubility in organic solvents. Like most polycyclic aromatic hydrocarbons, anthracene can be used to obtain dyes, scintillation counters, insecticides, coating materials, etc. The visible electronic (absorption and fluorescence) band of anthracene is assigned to a  ${}^1B_{2u} \leftarrow {}^1A_{1g}$  transition (p-band) with the transition moment polarized along the short molecular in plane axis. This band has a well resolved vibration structure consisting of five vibration sub-bands. Modifications of the electron density in the molecular electronic states responsible for the visible electronic band appearance determine changes both in the dipole moments and in polarizability of the spectrally active molecules in homogeneous solutions.

The purpose of this paper is both to verify the applicability of Takehiro Abe model in studying the solvent influence on the anthracene absorption and emission electronic spectra and to determine the dipole moment and the polarizability of anthracene in its vibronic states. The spectral method derived from the Abe model of a simple liquid was successfully used to estimate dipole moment and polarizability in the excited vibronic states of anthracene. One can affirm that the model proposed by T. Abe can be applied to study the solvent influence both in the absorption and fluorescence spectra of anthracene. The obtained values of the excited states dipole moments and polarizabilities are in a good agreement with the large delocalization of the anthracene  $\pi$ -electronic cloud. They are of the same order of magnitude with other similar determinations.

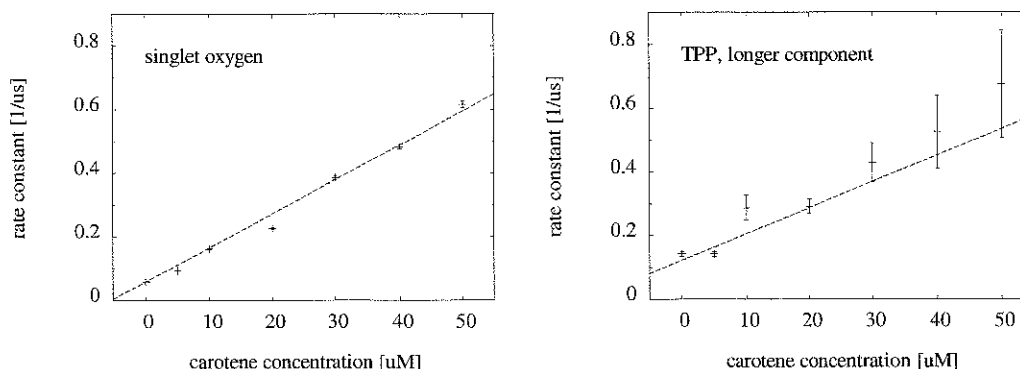


## TPP and Singlet Oxygen Quenching by Carotene in Solution

M. Scholz, R. Dědic, A. Svoboda and J. Hála

Charles University in Prague, Faculty of Mathematics and Physics Department of Chemical Physics and Optics,  
Ke Karlovu 3, 121 16, Praha 2, Czech Republic

Reactive oxygen species (ROS) participate in many destructive and degenerative processes in biological systems. One possible way of ROS production is photosensitization: ROS are generated by energy transfer from excited states of other molecules, so-called photosensitizers. This way singlet oxygen ( $^1\text{O}_2$ ) and a range of free radicals can be created. The emergent reactive substances are usually toxic and cause cell death. ROS production occurs either as a undesirable side-product of normal photoreactions (e.g. in photosynthesis under excessive light levels, in retina, or in skin) or as a helpful agent in various processes, such as immune responses of the body or photodynamic therapy of different severe illnesses. On the other hand, antioxidants are chemical substances occurring in the body naturally and protecting organisms against ROS. In this contribution, antioxidant properties of naturally occurring species,  $\beta$ -carotene, are investigated by examining its ability to quench  $^1\text{O}_2$  and triplet states of photosensitizer 5,10,15,20-tertaphenyl-porphin (TPP) in THF solutions. The quenching is evaluated using direct spectral- and temporal-resolved detection of weak near infrared phosphorescence of both triplet TPP ( $^3\text{TPP}$ ) and  $^1\text{O}_2$ . Dependencies of lifetimes of  $^3\text{TPP}$  and  $^1\text{O}_2$  on concentration of  $\beta$ -carotene were established (figure on the left). Quenching constant of  $(10.9 \pm 0.5) \times 10^9 \text{ M}^{-1} \text{ s}^{-1}$  for bimolecular quenching of  $^1\text{O}_2$  by carotene was determined. This value fits well with previously published one [1] and corresponds to its theoretically predicted diffusion limit in the order of magnitude. Kinetics of TPP phosphorescence in THF exhibit two components, opposed to the same photosensitizer in acetone which was studied earlier [2]. The portion of the longer one increases with emission wavelength. The lifetime of the shorter component of  $(0.34 \pm 0.03) \mu\text{s}$  fits well with  $(0.30 \pm 0.01) \mu\text{s}$  risetime of  $^1\text{O}_2$  kinetics and is not influenced by carotene concentration. On the other hand, lifetimes of the longer component decrease from  $(7.0 \pm 0.4) \mu\text{s}$  with increasing concentration of carotene (figure on the right). This decrease corresponds well to bimolecular quenching with quenching constant of  $(8 \pm 3) \times 10^9 \text{ M}^{-1} \text{ s}^{-1}$ .



[1] B. R. Nielsen, A. Mortensen, K. Jørgensen, and L. H. Skibsted. *J. Agric. Food Chem.* 44 (1996) 2106

[2] M. Koříněk, R. Dědic, A. Svoboda, and J. Hála. *J. Fluoresc.* 14 (2004) 71



## The EPR study of humic acid extracted from sediment collected at various seasons

J. Polak, M. Bartoszek, M. Żądło, W.W. Sułkowski

*Department of Environmental Chemistry and Technology, Institute of Chemistry, University of Silesia  
Szkolna 9, 40-006 Katowice, Poland*

Goczałkowice Reservoir is the biggest reservoir in the south of Poland. The main task of this dam reservoir is to supply water to the inhabitants of the Upper Silesia agglomeration.

Bottom sediment for studies were collected according to Polish standards at various seasons from eight places of the Goczałkowice Reservoir.

Humic acids (HA) were extracted by conventional procedures. The EPR spectroscopy was applied for both quantitative (free radical concentration) and qualitative (g factor) analysis of humic substances.

EPR spectra of the extracted humic substances exhibit broad lines from the paramagnetic metal ions (eg.  $\text{Fe}^{3+}$ ,  $\text{Mn}^{2+}$ ,  $\text{Cu}^{2+}$ ) and narrow lines from free radicals (Fig 1).

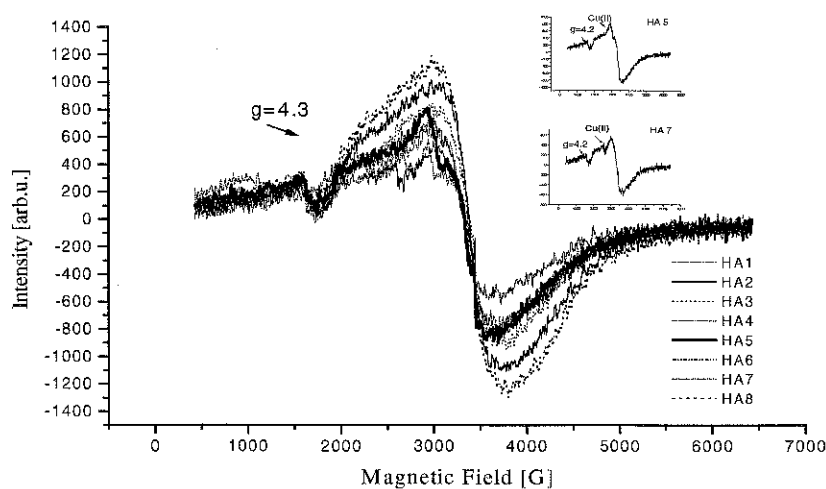


Fig. 1 The EPR spectra of humic acid (HA) extracted from bottom sediment taken at 8 points of the Goczałkowice Reservoir

The values of free radical concentration obtained for humic acids amount to  $1.14\text{-}13.6 \cdot 10^{16}$  spin/g depending on the season and the point of sample collection. These values are comparable with those obtained for aquatic HA ( $\sim 10^{16}$  spin/g) and for HA extracted from sewage sludge ( $\sim 10^{16}\text{-}10^{17}$  spin/g). The values of the g factor obtained for HA equals 2.0027 - 2.0035.

The EPR studies show that HA extracted from the bottom sediment collected at various points of the Goczałkowice Reservoir have similar physico-chemical properties. The influence of the reservoir depth on the content of oxygen functional groups and free radical concentration in humic and fulvic acids was noticed.

**Acknowledgements:** This work was supported by the Ministry of Science and Higher Education (MNiSW Poland) under Project No. N N204 1932 33.



## Comparison of a Pulsed-Excitation and a Phase-Modulation Method for Estimating Fluorescence Lifetimes Using a Convolved-Autoregressive Model and a High-Gain PMT

T. Iwata and Y. Mizutani

*Division of Energy System, Institute of Technology and Science, The University of Tokushima,  
2-1 Minami-Jyosanjima, Tokushima, 770-8506, Japan*

A comparative study between a pulsed excitation (PE) and a phase modulation (PM) method has been carried out numerically and experimentally for estimating values of fluorescence lifetimes. In order to enhance the sensitivity in light detection, we have connected a large value of a load resistor at the output of a photomultiplier tube (PMT), which also brings about improvement in signal-to-noise ratio (SNR) in measurements. The application of a convolved-autoregressive (C-AR) model to time-series data obtained from such a high-gain PMT enabled us to estimate the fluorescence lifetime values in a nanosecond region with precision. Finally, we have found that the PM method is somewhat preferable for a screening purpose of fluorescent samples used in the field of biology or biochemistry.

By the C-AR model, we can obtain fluorescence lifetimes directly by a linear-least-squares method from exponentially-decay time-series data that are measured by a time-correlated single-photon counting instrument [1]. Recently, we have proposed a frequency-multiplexed phase-modulation fluorometer for measuring lifetimes of fluorescent samples that have moderately-high quantum yields [2], where we have applied a normal AR (N-AR) model to several periods of time-series data. This is because we have found that the individual phase values can be derived at a time from the frequency-multiplexed sinusoidal waveform. Then we have proposed a method to connecting a large value of a load resistor after the PMT for the PE method [3]. Capability of the use of the large value of the load resistor for the PMT means also that we can use a conventional high-gain PMT instead of a high-speed one for measuring fluorescence lifetimes. By employing such a technique, enhancement in sensitivity in light detection and improvement in the SNR can be attained.

Although the effectiveness of the proposed technique has been demonstrated, there is a one unclear point: which method, between the PE and the PM method, is more suitable for obtaining the fluorescence lifetime values in the field of biology or biochemistry as the screening purpose? This is because precision and accuracy in estimation depend on many parameters. In order to give a guideline, we have carried out a comparative study. In the present report, numerical simulation results and an actual measurement result of  $1.0 \times 10^{-4}$  M/ml coumarin in ethanol are shown. Figure 1(a) and (c) are reference waveforms and (b) and (d) fluorescence ones obtained from the PE and the PM method, respectively, when  $R = 1.0 \text{ k}\Omega$ . For both methods, a fluorescence lifetime value of  $1.90 \pm 0.2$  ns was obtained from the AR-model-base data-analysis procedure.

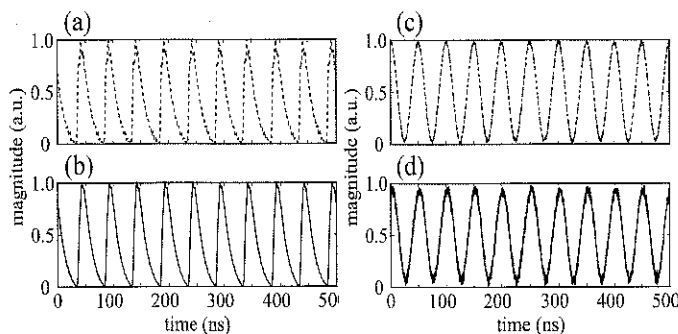


Fig.1 One of the experimentally-obtained waveforms.

[1] K.Sasaki, H. Masuhara, Appl. Opt. 30 (1991) 977

[2] T. Iwata, A. Muneshige, T. Araki, Appl. Spectrosc. 54 (2007) 950

[3] T. Iwata, R. Ito, Y. Mizutani, T. Araki, Appl. Spectrosc. 63 (2009) 1256



## Solvent effects on 3-hydroxyflavone photophysics / photochemistry. Relevance to its application in optical devices and its use as a (bio-)sensor.

A. Mezzetti<sup>1,2</sup>, S. Protti<sup>2,3</sup>, J.-P. Cornard<sup>2</sup>, C. Lapouge<sup>2</sup>, A. Idrissi<sup>2</sup>, M. Fagnoni<sup>3</sup>, A. Albini<sup>3</sup>

<sup>1</sup>Service de Bioénergétique, Biologie Structurale et Mécanismes, URA 2096, IBItec-S, Bat 532, CEA-Saclay, 91191 Gif-sur-Yvette cedex, France

<sup>2</sup>LASIR UMR 8516, Bat C5, Université Lille 1, 59655 Villeneuve d'Ascq, France

<sup>3</sup>Department of Organic Chemistry, Pavia, The University, Viale Taramelli 10, 27100 Pavia, Italy

We have used a multidisciplinary strategy combining different spectroscopic techniques (FTIR, Raman, Resonance Raman, UV-Vis, fluorescence, flash-photolysis) with theoretical calculations and a conventional physical organic chemistry approach to investigate the photophysical and photochemical properties of 3-hydroxyflavone (3HF).

Results have shown that the solvent can have a strong influence both on 3HF photophysical properties and on its photochemical reactivity. A systematic spectroscopic investigation has shown that in several polar solvents the corresponding 3HF anion is formed [1,2 & refs therein]. Quantum yield, relative intensity and peak position of the two emission bands from the N\*, T\* states (see fig. 1) were also measured in several solvents and were found to be strongly solvent-dependent [3].

Also 3HF photoreactivity is modulated by the solvent. Polar solvents favor a unimolecular photorearrangement whereas apolar solvents favor a photo-oxygenation reaction [3]. The reaction rate is also strongly solvent-dependent and affected by other parameters such as O<sub>2</sub> concentration [1].

The experimental results have been interpreted relying on molecular dynamics and quantum chemistry calculations. It has therefore been possible which to describe in terms of specific molecular interactions with the solvent how 3HF properties are influenced by its surrounding medium.

The results are discussed in the framework of the relevance of 3HF in many fields: pure physical chemistry (3HF is a model system to study excited-state proton transfer [4 and refs therein]), applications in biophysics, material science, supercritical fluids (fields in which 3HF is used as a fluorescent sensor [5,6,7 and refs. therein]), and also technology (3HF emitting properties are exploited in optical devices [8 and refs therein]).

- [1] S. Protti, A. Mezzetti, C. Lapouge, J. P. Cornard, *Photochem. Photobiol. Sci.* 7 (2008)109-119
- [2] S. Protti, A. Mezzetti, J. P. Cornard, C. Lapouge, M. Fagnoni, *Chem Phys Lett* 467 (2008) 88-93
- [3] S. Protti, A. Mezzetti, S. Lazzaroni, in preparation
- [4] R. Lehnig, D. Pentlehner, A. Vdovin, B. Dick, A. Slenczka, *J. Chem. Phys* 131 (2009) 194307
- [5] A. Sytnik, I. Litvinyuk, *Proc. Natl. Acad. Sci. USA* 93 (1996) 12959
- [6] N. Chattopadhyay, M. Barroso, C. Serpa, M. I. Silva, L.G. Arnaut, S. J. Formosinho, *Chem. Phys. Lett.* 387 (2004) 263-266
- [7] A. Quaranta, S. Carturan, G. Maggioni, R. Ceccato, G. Della Mea, *J. Non Cryst. Solids* 322 (2003) 1-6
- [8] S. Carturan, A. Quaranta, G. Maggioni, M. Bonafini, G. Della Mea, *Sensor. Actuat. A-Phys.* A113 (2004) 288



## Spectroscopic investigation of flavonoids of biomedical relevance in solution and inside lipid nanocapsules

A. Mezzetti<sup>1,2</sup>, S. Protti<sup>2,3</sup>, S. Lazzaroni<sup>2</sup>, A. Barras<sup>4,5</sup>, N. Montfillette-Dupont<sup>4</sup>,  
C. Lapouge<sup>2</sup>, J. P. Cornard<sup>2</sup>

<sup>1</sup>Service de Bioénergétique, Biologie Structurale et Mécanismes, URA 2096, IBItec-S, Bat 532, CEA-Saclay, 91191 Gif-sur-Yvette cedex, France

<sup>2</sup>LASIR UMR 8516, Bat C5, Université Lille 1, 59655 Villeneuve d'Ascq, France

<sup>3</sup>Department of Organic Chemistry, Pavia, The University, Viale Taramelli 10, 27100 Pavia, Italy

<sup>4</sup>Laboratoire de Chimie et MicroNanotechnologie à visée thérapeutique, UMR 8161 « Institut de Biologie de Lille », 1 rue du Pr. Calmette, BP 447, 59021 Lille Cedex, France

<sup>5</sup>Present address: Institut de Recherche Interdisciplinaire (IRI, USR 3078), Parc de la Haute Borne, 50 Avenue de Halley, BP 70478, 59658 Villeneuve d'Ascq and Institut d'Electronique, de Microélectronique et de Nanotechnologie (IEMN, UMR 8520), Cité Scientifique, Avenue Poincaré - BP. 60069, 59652 Villeneuve d'Ascq, France

Quercetin and (–)-epigallocatechin-3-gallate ((–)-EGCG) are two flavonoids with promising pharmacological potential. Two limiting factors for their use are the limited solubility in water (for quercetin) and its instability inside the human body (for (–)-EGCG). For all these reasons, it is necessary to find an alternative delivery method to increase the solubility of quercetin and stability of (–)-EGCG in order to facilitate their pharmacological effect. Lipid nanocapsules containing quercetin or (–)-EGCG have been recently realised by some of the authors [1,2]. In this communication we will present a detailed spectroscopic study (UV-Vis, fluorescence, Raman, FT-Raman) which has permitted, together with dynamic light scattering measurements and chromatographic analysis to characterize these nanocapsules. It has been possible to understand the structure of the nanocapsule as well as the localization of the flavonoids inside it.

A particular aspect is the possible formation of quercetin anions inside the nanocapsule. This pushed us to carry out a detailed spectroscopic and DFT study on deprotonation of OH moieties of quercetin in aqueous and organic solutions, as already performed for the parent molecule 3-hydroxyflavone [3]. Very interestingly, we have found that anion formation entails a strong modification of quercetin reactivity and of quercetin photophysics. The results will be discussed in the framework of the current studies of quercetin in chemical and biological contexts, especially investigations where fluorescence microscopy is used to localize quercetin distribution inside cells [4] and investigations where optical spectroscopy is used to follow quercetin binding to proteins and other biomolecules [5,6 and refs therein].

- [1] A Barras, A. Mezzetti, A. Richard, S. Lazzaroni, S. Roux, P. Melnyk, D. Betbeder, N. Montfillette-Dupont, *Int. J. Pharm.* 379 (2009) 270–277
- [2] The realisation of the flavonoid-loaded nanocapsules has been performed by adaptation (for the inclusion of flavonoids) of the method developed by Heurtault et al., 2000. (B. Heurtault, P. Saulnier, B. Pech, J.E. Proust, J. Richard, J.P. Benoit, 2000. Patent FR 0002688)
- [3] S. Protti, A. Mezzetti, J. P. Cornard, C. Lapouge, M. Fagnoni, *Chem. Phys. Lett.* 467 (2008) 88–93
- [4] A.-P. Nifli, P. A. Theodoropoulos, S. Munier, C. Castagnino, E. Roussakis, H. E. Katerinopoulos, J. Vercauteren, E. Castanas, *J. Agr. Food. Chem.* 55 (2007) 2873–2878
- [5] C. Dufour, O. Dangles, *Biochim. Biophys. Acta – General subjects* 1721 (2005) 164–173
- [6] O. J Rolinski, A. Martin, D. J. Birch, *J. Biomed. Optics* 12 (2007) 034013



## Reactivity of Carbamates in the Alkaline Hydrolysis Reaction

D. Cheshmedzhieva, B. Hadjieva, S. Ilieva, D. Nalbantova, B. Galabov

*Department of Chemistry, University of Sofia, 1164 Sofia, Bulgaria*

The quantitative characterisation of the reactivity of organic compounds in various chemical interactions is of key importance. It emphasises the conceptual link between properties of reactants and their behaviour in chemical reactions and supports the notion of organic chemistry as a fully quantitative science. In the present study we explore the application of Hammett sigma constants and several alternative theoretically estimated indices that characterize the reactivity of series of N-phenyl aryl substituted carbamates in the alkaline hydrolysis reaction.

A series of N-phenyl arylcarbamates with different substituents in the aromatic ring from the ester group were synthesised. The rate constants (at 25 °C) for the alkaline hydrolysis of a series of substituted N-phenyl arylcarbamate derivatives were spectrophotometrically determined. The obtained kinetic data were then correlated with the Hammett sigma constants and different theoretically estimated reactivity indices: Mulliken and NBO atomic charges, the Parr electrophilicity index ( $\omega$ ), and the electrostatic potential at the carbon and oxygen atoms of the reaction center ( $V_C$ ,  $V_O$ ).

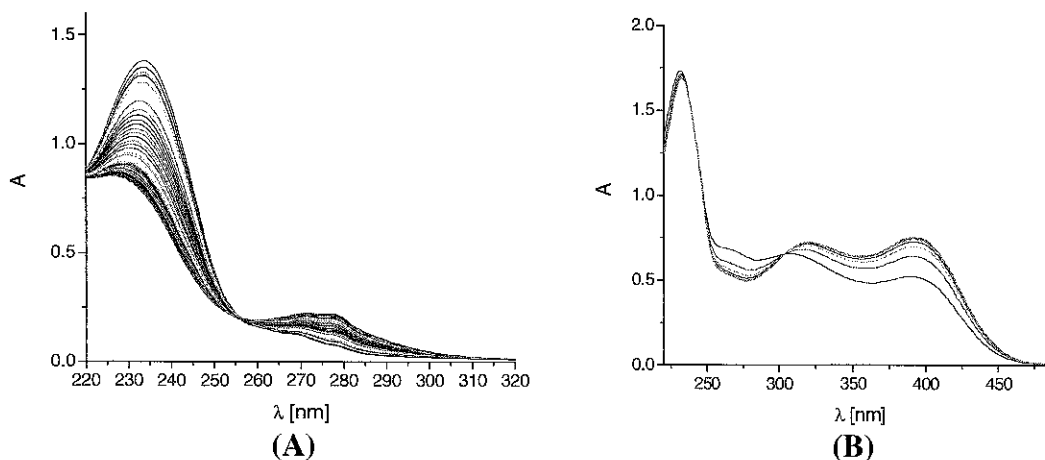


Figure 1. The change in the UV spectrum of (A) 3-methylphenyl phenylcarbamate and (B) 3-methyl-4-nitrophenyl phenylcarbamate as a function of time.

## CT Chromophores and Complexes: Spectra and Models

L. Grisanti, C. Sissa, F. Terenziani and A. Painelli

*Dipartimento di Chimica GIAF – Università di Parma e INSTM-UdR Parma  
v.le Usberti 17/A – 43124 Parma – ITALY*

The low energy spectral properties of conjugated molecules  $\pi$  with electron donor (D) and acceptor (A) groups is characterized by the presence of charge transfer (CT) optical transitions. This feature is well described adopting essential-state models for the electronic structure and accounting for the coupling between electrons and slow degrees of freedom, including molecular vibrations and polar solvation. Essential-state models have been developed for different families of compounds. These models accurately describe linear and non linear optical spectra of polar (DA) and multipolar chromophores in solution, rationalizing the subtle effects of solvent polarity on spectral properties including band shapes. Essential-state models also apply to the rationalization of linear and nonlinear optical spectra metalorganic complexes.

Essential-state models are semi-empirical in nature and provide a natural bridge between theoretical approaches and experimental data. Relevant model parameters are obtained from a detailed analysis of optical spectra: the proper choice of diabatic molecular states allows the definition of a reliable set of environment independent molecular parameters, while solvent effects are described by the solvent relaxation energy. This opens the way to the so called bottom-up modeling strategy where the information obtained from the analysis of solution spectra represents the basis to define models for molecular crystals, films or aggregates or, more generally, for materials where several molecules interact via electrostatic forces.

To exemplify the power of the proposed approach we address here recent results on metalorganic complexes of interest for NLO applications [1], as well as for an organic chromophore and the relevant bichromophoric specie. The models offer a simple and coherent physical picture to explain and rationalize the evolution of the optical spectra with the solvent polarity and/or upon complexation by a metal.

- [1] L. Grisanti, C. Sissa, F. Terenziani, A. Painelli, D. Roberto, F. Tessore, R. Ugo, S. Quici, I. Fortunati, E. Garbin, C. Ferrante and R. Bozio; *Phys. Chem. Chem. Phys.*, 2009, 11 (41), pp. 94509457



## Different methods for ionization threshold determination

G. Piani<sup>a</sup>, M. Pasquini<sup>b</sup>, G. Pietraperzia<sup>b</sup>, E. M. Castellucci<sup>b</sup>, M. Becucci<sup>b</sup>

*LENS – European Laboratory for Non-linear spectroscopy,  
Polo Scientifico e Tecnologico dell'Universita', via Nello Carrara, 1, Sesto Fiorentino (Firenze), Italy*

*<sup>a</sup> now at Laboratoire Francis Perrin, CEA Saclay, France*

*<sup>b</sup> also at Dipartimento di Chimica, Universita' di Firenze, Italy*

We are comparing different results about the determination of the ionization threshold of a simple aromatic molecule, like anisole, looking at both the ions and the electrons produced in the photoionization event.

We have measured the ionization threshold using a R2P2CI experiment: in this pump-probe experiment, by taking the pump laser tuned on the  $S_1 \leftarrow S_0$  transition energy and scanning the probe one, we are able to observe the rising up of ion production, and so directly determine the ionization threshold.

We have also performed some photoelectron imaging experiments, both 1C and 2C. Thanks to the 2C experiments, probing the ionization at different wavelengths, we have been able to energy calibrate the obtained photoelectron images, and so to acquire information on the anisole<sup>+</sup> energy levels.



## Velocity dependence of C<sub>2</sub>H<sub>2</sub> rotational temperature in a supersonic expansion

M. Scotoni, A. Mazzalai

*Dipartimento di Fisica Università di Trento , via Sommarive 14, 38123 Trento, Italy,*

Understanding and controlling the alignment of the of molecular rotational angular momentum  $J$  could play an important role for the characterization of stereodynamics of elementary processes both in gas phase and at surfaces.

This phenomenon can be exploited using different methodologies, i.e. by interaction with electromagnetic fields (stark effect, laser field) [1] or by using collisions in a supersonic beam expansion where an anisotropic velocity distribution creates a preferential axis for relaxation processes [2].

Collisional rotational orientation of acetylene molecules has already been observed in our lab, measuring the differential absorption of laser light with linear polarization variable respect to the molecular beam axis [3]. The degree of alignment resulted different for different  $J$  values, confirming that the alignment process is the result of the relaxation history .

In the parallel experiment, described in the same paper and performed in Perugia (Pirani et al.), the rotational orientation was measured observing the scattering cross section of the oriented acetylene with argon target at different collision energies. There clearly came out that the degree of orientation depend on the final velocity of expanded molecules. In order to investigate velocity dependence of relaxation process we measured rotational temperature of expanded acetylene as a function of velocity and observed a significant difference of rotational populations between head and tail of velocity distribution . Measurements, still in preliminary stage, as well interpretation, still going on, will be presented at the meeting.

[1] B. Friedrich and D. R. Herschbach, Phys. Rev. Lett. 74, 4623 (1995)

[2] M. J. Weida and D. J. Nesbitt, J. Chem. Phys. 100, 6372 (1994)

[3] Cappelletti, D.; Bartolomei, M.; Aquilanti, V.; Pirani, F.; Demarchi, G.; Bassi, D.; Iannotta, S.; Scotoni, M., Chemical Physics Letters , 420 (1-3), 47-53. (2006)



## A laser system for efficient excitation of positronium towards Rydberg levels

M. Becucci, G. Ferrari, M. Prevedelli, I. Boscolo, F. Castelli, S. Cialdi, F. Villa, M.G. Giammarchi

*LENS, Università di Firenze, Italy*

Antihydrogen production by charge exchange between positronium atoms in Rydberg levels and antiprotons is predicted to be much more effective than the direct recombination of positrons and antiprotons. Here we present a pulsed laser system suited for the two step positronium excitation  $n=1 \rightarrow n=3$  (wavelength of 205 nm) and  $n=3 \rightarrow n=20 \dots 30$  (wavelength of about 1670 nm), and with spectral properties suited to account for the various broadening mechanisms typically present in experiments dealing with cold antimatter.





## Tautomerism in pyrimidine derivatives investigated with core level spectroscopy techniques.

B. M. Giuliano<sup>1</sup>, V. Feyer<sup>2</sup>, K. C. Prince<sup>2</sup>, M. Coreno<sup>3</sup>, L. Evangelisti<sup>4</sup>, S. Melandri<sup>4</sup>, W. Caminati<sup>4</sup>

<sup>1</sup>Departamento de Química, Universidade de Coimbra, 3004-535 Coimbra, Portugal

<sup>2</sup>Sincrotrone Trieste, 34149 Basovizza, Italy

<sup>3</sup>CNR-IMIP, 10-00016 Montelibretti, Italy

<sup>4</sup>Dipartimento di Chimica "G. Ciamician", Università di Bologna, 40126 Bologna, Italy

The nucleobases cytosine, thymine and uracil are pyrimidine derivatives. They pair with their complementary purines, guanine and adenine, through hydrogen bonding to form DNA and RNA chains.

In the present communication we report the application of X-ray photoemission spectroscopy (XPS) to the study of the prototypical system 2-hydroxypyrimidine and the related molecules S-methyl-2-thiouracil and 2-thiouracil in the vapor phase (molecular sketches are shown in Fig.1). These systems have been previously studied in laboratory experiments mainly using microwave, infrared and UV photoelectron spectroscopy [1-3], which gave very precise information about the geometry of tautomers and about their relative stabilities. But previous experiments were performed in conditions far from thermal equilibrium and therefore the measured populations of tautomers could not easily be related to equilibrium thermodynamic parameters. XPS is a quantitative technique and the populations ratio of the keto-enol tautomers at the sample temperature can be found experimentally, which is extremely difficult otherwise.

Two different chemical shifts can be determined from our O1s XPS spectrum for the keto and enol tautomers of 4-hydroxypyrimidine and S-methyl-2-thiouracil. For both systems the analysis of the XPS spectra reveals that the relative population of the keto tautomer is 2.3 times higher than that of the hydroxy one. The XPS spectra of 2-thiouracil can instead be interpreted with the presence of a single tautomer, the diketo form, which is calculated to be the most stable one.

In addition, the high resolution valence photoemission and NEXAFS spectra have been measured to gain more information about the electronic structure of the tautomers.

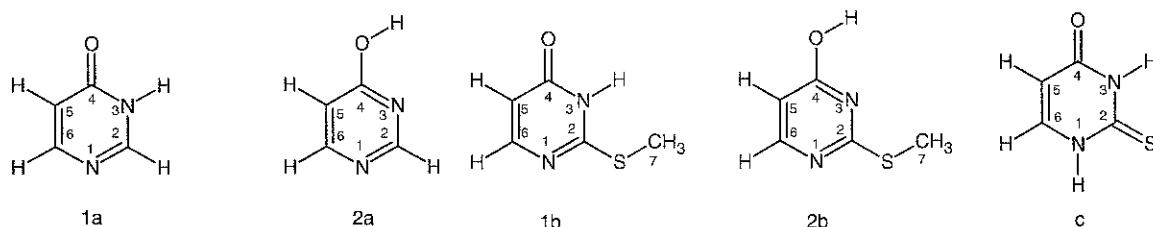


Figure 1. Chemical structures of the a) 4-Hydroxypyrimidine, b) S-methyl-2-thiouracil and c) 2-Thiouracil.

- [1] R. Sanchez, B. M. Giuliano, S. Melandri, L. B. Favero, W. Caminati, J. Am. Chem. Soc. 129 (2007) 6287.  
[2] A. R. Katritzky, M. Szafran, G. Pfisterguillouzo, J. Chem. Soc. Perkin Trans. 2 (1990), 871.  
[3] L. Lapinski, M. J. Nowak, J. Fulara, A. Les, L. Adamowicz, J. Phys. Chem. 96 (1992) 6250-6254.



## Time-resolved spectroscopy of native and mutated *Thermobifida fusca* hemoglobins

S. Abbruzzetti<sup>1</sup>, A. Bonamore<sup>2</sup>, A. Boffi<sup>2</sup>, A. Feis<sup>3</sup>, P. Foggi<sup>4</sup>, C. Gellini<sup>3</sup>, A. Marcelli<sup>5</sup>,  
P.R. Salvi<sup>3</sup>, C. Viappiani<sup>1</sup>

<sup>1</sup>Department of Physics, University of Parma, Italy

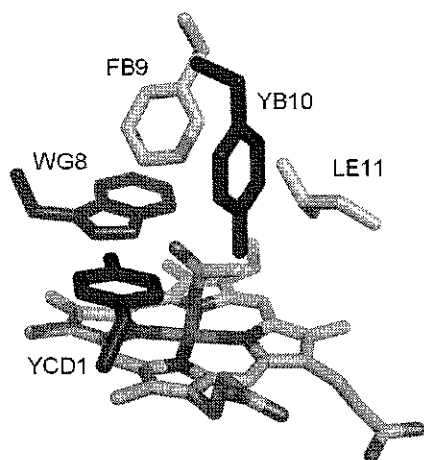
<sup>2</sup>Department of Biochemical Sciences, University of Rome "La Sapienza", Italy

<sup>3</sup>Department of Chemistry "Ugo Schiff", University of Florence, Italy

<sup>4</sup>Department of Chemistry, University of Perugia, Italy

<sup>5</sup>LENS, European Laboratory for Non-linear Spectroscopy, Florence, Italy

*Thermobifida fusca* hemoglobin (TFH) is a prototypical bacterial (class 2) hemoglobin. It has been identified in a thermophilic actinobacterium [1] and overexpressed. The heme cavity structural properties are mainly related to the polarity and H-bonding capability of the "distal" amino acids: tyrosine (B10 in the myoglobin helix notation), tyrosine (CD1), tryptophan (G8).



Single, double and triple phenylalanine (Phe) mutants of these key residues have recently become available. We have applied several techniques of time-resolved optical spectroscopy to study the dynamics following the photolysis of carbon monoxide-bound TFH.

1. Femtosecond transient absorption has shown that CO can rebind from TFH distal cavity in few ns. TrpG8 substitution with the apolar Phe accelerates the recombination, which takes place in hundreds of ps.

2. Laser flash photolysis measurements have allowed to extend the study of the dynamics to the ns and  $\mu$ s range. The yield of the geminate rebinding and the kinetics of recombination from the solvent are both influenced by the single TrpG8  $\rightarrow$  Phe mutation.

Further changes are observed when the three polar amino acids are replaced by Phe. Rate constant distributions have been obtained by the maximum entropy method [2].

3. Photoacoustic measurements have yielded both volume and enthalpy changes [3] following CO photodissociation in the ns -  $\mu$ s range. The thermodynamic parameters for the observed intermediates can be related to those measured by laser flash photolysis.

All the results point to an overwhelming role for TrpG8. This is in agreement with a recent study on a related bacterial hemoglobin from *Bacillus subtilis* [4].

- [1] A. Bonamore, A. Ilari, L. Giangiacomo, A. Bellelli, V. Morea, A. Boffi, FEBS J. 27 (2005) 4189-4201.
- [2] S. Abbruzzetti, S. Bruno, S. Faggiano, E. Grandi, A. Mozzarelli, C. Viappiani, Photochem. Photobiol. Sci. 5 (2006) 1109-1120.
- [3] R.W. Larsen, J. Mikšovská, Coord. Chem. Rev. 254 (2007) 1101-1127.
- [4] A. Feis, A. Lapini, B. Catacchio, S. Brogioni, P. Foggi, E. Chiancone, A. Boffi, G. Smulevich Biochemistry 47(2008) 902-910.



## High pressure photoinduced reactivity in clathrate hydrates

M. Ceppatelli<sup>1,2</sup>, R. Bini<sup>1,2</sup>, V. Schettino<sup>1,2</sup>

<sup>1</sup>LENS – European Laboratory for Non-Linear Spectroscopy, Via Nello Carrara 1, 50019, Sesto Fiorentino (FI), Italy

<sup>2</sup>Dipartimento di Chimica dell'Università degli Studi di Firenze, Via della Lastruccia 3, 50019, Sesto Fiorentino (FI), Italy

High pressure reactivity has been observed in several clathrate hydrates at room T and P of several tenths of GPa under irradiation with the Ar ion laser wavelength at 350 nm. The high pressure has been generated using a Membrane Diamond Anvil Cell (MDAC) and the reactivity has been monitored by means of FTIR and Raman spectroscopy. We have studied clathrate hydrates of different model hydrocarbons (ethane, ethylene, acetylene and propene) as well as the clathrate hydrates of two inorganic systems like nitrogen and carbon monoxide. The formation of CO<sub>2</sub> is observed in all the systems containing carbon atoms and direct evidence for the formation of molecular hydrogen is reported in some cases. The CO<sub>2</sub> produced during the reaction can be sequestered in situ as clathrate hydrate. The reaction is triggered by the two-photon excitation of the water molecules, leading to the formation of highly reactive OH radicals. Such species are able to induce a partial cleavage of the triple bond in the extremely stable nitrogen molecule.

[1] M. Ceppatelli, R. Bini, V. Schettino, P. Natl. Acad. Sci. USA, **106**, 11454-11459 (2009).

[2] M. Ceppatelli, R. Bini, V. Schettino, J. Phys. Chem. B, **113**, 14640-14647 (2009).



## Raman Spectroscopy for the evaluation of structural changes of peptides

G. Das<sup>1</sup>, M. L. Coluccio<sup>2</sup>, A. Nicastrì<sup>3</sup>, F. Gentile<sup>2</sup>, F. De Angelis<sup>1</sup>, E. Di Fabrizio<sup>1,2</sup> and G. Cuda<sup>3</sup>

<sup>1</sup>*Istituto Italiano di Tecnologia, Via Morego 30 Genova, ITALY*

<sup>2</sup>*BIONEM Lab., Università Magna Graecia di Catanzaro, Catanzaro, ITALY*

<sup>3</sup>*Proteomics Lab., Università "Magna Graecia" di Catanzaro, Catanzaro, ITALY*

Raman spectroscopy has become a versatile tool in protein science and biotechnology, and its role in the detection of malignant tissues is reported in several studies [1]. It is well known that the alteration of the protein primary structure due to the substitution of one amino acid with a different one can determine the alteration of protein folding, leading to the change of its biological function. For example, in BRCA1 (Breast Cancer Associated Gene 1) protein, several missense mutations that alter protein folding predispose to breast cancer [2]. A protein Raman spectrum comprises discrete bands representing vibrational modes of the peptide backbone and its side chains. In the present work, we analyzed through Raman spectroscopy four synthetic peptides sixteen amino acids in length designed on the basis of specific position of the sequence of BRCA1/BRCT (BRCA1 C-terminal) protein domain; of those four peptides, two corresponded to the wild-type form of BRCA1/BRCT protein domain (M1775 and W1837) and two corresponded to the mutated form (M1775R and W1837R). Both missense mutations have been detected in patients with hereditary breast cancer. We used gold-coated silicon nanostructures as SERS (Surface Enhanced Raman Scattering) substrates and DCDR (Drop Coating Deposition Raman) technique [3] to investigate structural changes in the primary structure of the mutated peptides compared to the wild-type. Data from synthetic peptides spectra show clear differences between wild-type and mutated peptides (fig.1a-1b). Analysis of the synthetic peptides through Raman spectroscopy play an important role for correct interpretation and functional evaluation of molecular alterations of proteins from cellular samples of patients with breast cancer.

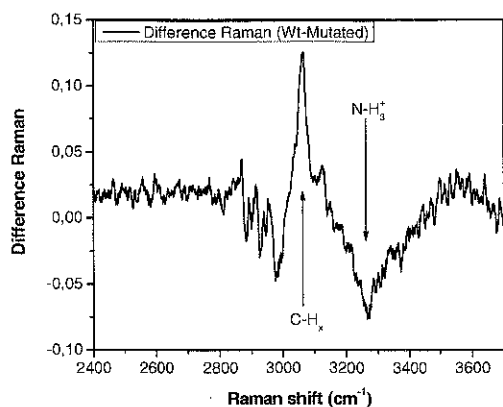


Fig. 1a Difference between spectra of the M1775 and M1775R peptides

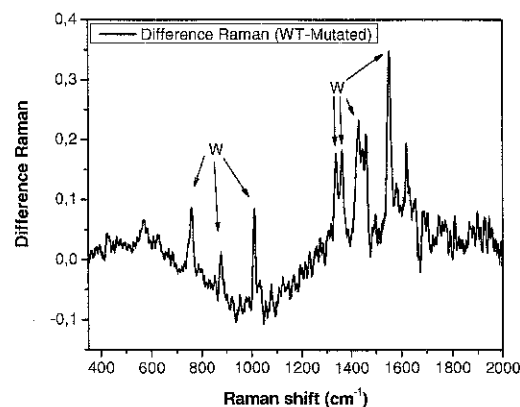


Fig. 1b Difference between spectra of the W1837 and W1837R peptides

- [1] A. Nijssen, S. Koljencic, T.C. Bakker Schut, P.J. Caspers, G.J. Puppels, *J. Biophotonics*. 2 (2009) 29-39.
- [2] R.S. Williams, D.I. Chasman, D.D. Hau, B. Hui, A.Y. Lau, J.N. Glover, *J. Biol. Chem.* 278 (2003) 53007-53016.
- [3] D. Zhang, Y. Xie, M.F. Mrozek, C. Ortiz, V.J. Davisson, D. Ben-Amotz, *Anal. Chem.* 75 (2003) 5703-5709.



## Main refractive indices of some carpathian crystals

C. F. Dascalu, B. C. Zelinschi, D. O. Dorohoi

*Alexandru Ioan Cuza University, Faculty of Physics, 11 Carol I Blv., Iasi, RO-700506, Romania*

Some Carpathian crystals were characterized from the point of view of their visible birefringence by using optical methods based on compensation of the optical way or by using interferometric devices. For the uniax crystals the previously described methods were applied and the main refractive indices and birefringence were estimated.

The obtained results were compared by those obtained by a new method based on polarizing microscope.

For the biaxials crystals a new method based on the inclined propagation of light was implemented. Two indices of refraction were estimated for propagation directions different to the normal incidence by solving the equation of the refractive indices ellipsoid. The other two were determined for the normal incidence on the crystalline plate cut parallel to one of main crystalline plane. The two pairs of refractive indices have a common value. The determined values were used to characterize the crystal from the point of view of optical axes orientation.

The obtained results were analyzed in correlation with the chemical composition of the Carpathian crystals. They can be used in Optics of anisotropic substances for projecting and obtaining devices working in polarized light.



## Development of copper nanostructured materials for surface-enhanced Raman scattering spectroscopy

M. Vyskovska<sup>1</sup>, V. Prokopec<sup>1</sup>, M. Clupek<sup>1</sup>, A. Kokaislova<sup>1</sup>, J. Cejkova<sup>2</sup>, P. Matejka<sup>1</sup>

<sup>1</sup>Dept. of Analytical Chemistry, Institute of Chemical Technology, Technicka 5, 166 28 Prague 6, Czech Republic

<sup>2</sup>Dept. of Chemical Engineering, Inst. Chemical Technology, Technicka 3, 166 28 Prague 6, Czech Republic

Surface enhanced Raman scattering (SERS) spectroscopy is a powerful and widely used technique in chemical, analytical or bioanalytical applications. SERS spectra can be observed on surfaces of some metals (Ag, Au and Cu) with appropriate morphology (roughness, size and shape of nanostructures). Copper nanomaterials have been used in different studies recently.

In this study Cu nanostructured surfaces have been prepared by electrochemical deposition of copper onto platinum target [1]. Cu large-scaled SERS-active nanostructured substrates were modified with different analytes (aliphatic and aromatic thiols). Substrate morphology has been studied systematically by scanning electron microscopy (SEM). The chemical reduction Cu<sup>2+</sup> salt (sulphate, nitrate or chloride) in aqueous medium has been carried out using an excess of sodium borohydride in citrate solution. CuNP systems were modified by selected thiol derivatives at various concentrations. Due to quite limited stability of systems CuNP sols have been prepared at ca. 0°C in the ice bath. Systems were stable for about one hour under cooling in the ice bath. Afterwards CuNPs oxidized or aggregated. The prepared modified CuNP sols were of different colours: from light brown to dark reddish brown. Absorption spectra exhibited a maximum located at about 560 nm (Fig. 1). It was observed that absorption maximum of surface plasmon resonance (SPR) was shifted by analyte modification in UV/VIS spectra. CuNP systems can be characterized by microscopic methods, e.g. by atomic force microscopy (AFM) or transmission electron microscopy (TEM). SERS activity of Cu nanostructured systems has been investigated by Raman spectral measurements at 1064 nm, 785 nm and 488 nm excitation wavelengths.

It was observed that CuNPs gave rise to enhancement of Raman signal. SERS spectra of modified systems were collected (Fig. 2) and exhibited all characteristic Raman bands even at low concentration of the analyte. These systems can be used for characterization and detection of different low-molecular compounds with the structure similar to studied analytes.

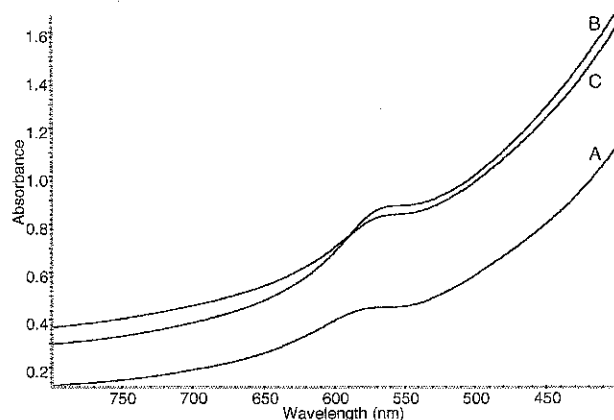


Fig. 1. UV/VIS spectra CuNP with 16-MHDA (A), unmodified CuNP (B), CuNP with 4-ATP (C)

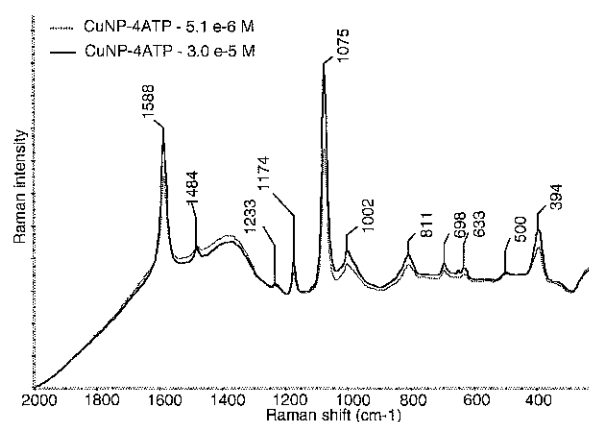


Fig. 2. SERS spectra CuNP with 4-ATP excited at 785 nm (conc.  $\sim 10^{-5}$  M)

- [1] J. Cejkova, V. Prokopec, S. Brazdova, A. Kokaislova, P. Matejka, F. Stepanek, Appl. Surf. Sci. 255 (2009) 7864.



## Electro-optical parameters of some thio-semicarbazides studied by spectral and computational means

R. E. Stanculescu<sup>1</sup>, V. Sunel<sup>2</sup>, D. O. Dorohoi<sup>1</sup>

<sup>1</sup>Alexandru Ioan Cuza University, Faculty of Physics, 11 Carol I Blv., RO-700506

<sup>2</sup>Alexandru Ioan Cuza University, Faculty of Chemistry, 11 Carol I Blv., RO-700506

Thio semicarbazides are substances with biological activity obtained by N-(p-nitrobenzyl)-L-phenylalanine, considered as precursor, after many reaction steps. The energetic and electro-optical parameters of the studied thio-semicarbazide were established by quantum-chemical software. HyperChem 8.6 with Polak Ribiere algorithm and RMS 0.001 kcal/mol was used for optimization the structure of studied molecules by AM1, PM3 and RM1 semi-empirical methods. The results obtained by these semi-empirical methods are discussed and compared with those experimentally determined.

The chemical reactivity and the biological activity of the studied compounds were appreciated by the difference between LUMO and HOMO energies. The results referring to the atomic charges and bond lengths obtained through computational means are correlated with the signals from NMR and FTIR spectra. The electronic and vibration spectra were simulated and compared with those experimentally obtained. The IR bands were attributed to various types of vibration movements as a result of simulation. The computed oscillator strengths and the surfaces of the electronic absorption bands are also in a good accordance.



## Raman spectroscopic study of the effects of ion solvation on liquid phase structure and dynamics of LiI–acetone solutions

F. Palombo<sup>1</sup>, P. Sassi<sup>1</sup>, M. Paolantoni<sup>1</sup>, A. Morresi<sup>1</sup>, and M. G. Giorgini<sup>2</sup>

<sup>1</sup>Department of Chemistry, University of Perugia, Via Elce di sotto 8, 06123, Perugia, Italy

<sup>2</sup>Department of Physical and Inorganic Chemistry, University of Bologna, Viale del Risorgimento 4, 40136, Bologna, Italy

Electrolyte solutions of halide and perchlorate salts, mainly lithium, in non-aqueous solvent have attracted much attention in the past decades due to their employment in electrochemical field. Both ion–solvent and ion–ion interactions may contribute to the structure and dynamics of such systems at an ionic/molecular level, and their specific role depends on the involved species. Acetone is a widely-used solvent with fairly low electron donicity and relative permittivity, and these properties can account for the occurrence of ion aggregates along with single ions in solution. Lithium iodide is moderately soluble in acetone; with its strong -almost covalent- bonds, it is a good candidate to study the modulation of intermolecular (dipolar) interactions in acetone by ion addition.

The vibrational spectroscopic investigation of electrolyte systems, such as LiI–acetone solutions at different concentration, constitutes an important approach to the study of solvation and association processes. Raman and depolarized Rayleigh scattering (DRS) are especially suitable for physicochemical studies in condensed phase allowing information to be obtained on system structure as well as molecular dynamics[1-4]. Low frequency Raman spectra of LiI–acetone solutions will be presented and ion association in this system will be discussed for very low concentrations of the electrolyte.

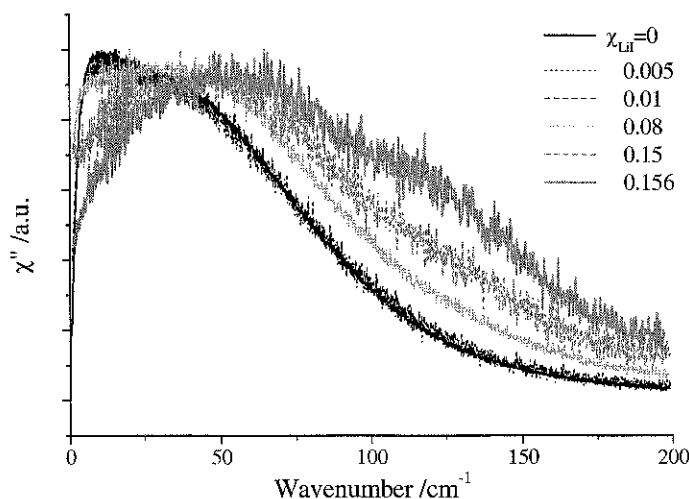


**Figure.** Evolution of the susceptibility representation of the low-frequency Raman spectrum of the LiI–acetone solution as a function of solute mole fraction, in the range  $5 \times 10^{-3}$  to 0.156 (saturated solution). The spectrum of neat acetone is also presented.

- [1] M. Paolantoni, P. Sassi, A. Morresi, S. Santini, *J. Chem. Phys.* 127 (2007) 024504
- [2] M. Paolantoni, L. Comez, D. Fioretto, M.E. Gallina, A. Morresi, P. Sassi, F. Scarponi, *J. Raman Spectrosc.* 39 (2008) 238-243
- [3] P. Sassi, M. Paolantoni, S. Perticaroli, F. Palombo, A. Morresi, *J. Raman Spectrosc.* 40 (2009) 1279-1283
- [4] M. Paolantoni, L. Comez, M. E. Gallina, P. Sassi, F. Scarponi, D. Fioretto, A. Morresi, *J. Phys. Chem. B* 113 (2009) 7874-7878





## Phosphoenolpyruvate and $Mg^{2+}$ binding to pyruvate kinase monitored by infrared spectroscopy

S. Kumar, A. Barth

*Department of Biochemistry and Biophysics, The Arrhenius Laboratories for Natural Sciences, Stockholm University, SE – 10691 Stockholm, Sweden*

Infrared spectroscopy is a powerful technique to detect ligand induced changes in biomolecules as it has distinct signals and provides different levels of structural information. A dialysis accessory to attenuated total reflection infrared spectroscopy makes this technique more universal for ligand binding studies. We used this to investigate the binding of phosphoenolpyruvate (PEP) and  $Mg^{2+}$  to pyruvate kinase (PK), where conformational changes of PK were revealed upon binding of PEP and  $Mg^{2+}$ . Isotopically labeled PEP helped to assign and evaluate the infrared absorption bands. The difference spectrum of bound and free PEP indicates specific interactions between ligand and protein. The quantitative evaluation revealed that the enzyme environment has little influence on the P-O bond strengths of the band substrate PEP, which are weakened by less than 3% upon binding. The carboxylate absorption bands indicate also little perturbation of the C-O bands. The binding mode of PEP to PK is slightly different in presence of different monovalent cations  $K^+$  and  $Na^+$ . We also investigate the enzyme activity of PK by using infrared spectroscopy.



## Combination of circular dichroism spectroscopy with theoretical spectra simulations as a tool for structural studies of macromolecules

V. Andrushchenko<sup>1</sup>, H. Wieser<sup>2</sup>, M. Straka<sup>1</sup>, P. Bour<sup>1</sup>

<sup>1</sup>Institute of Organic Chemistry and Biochemistry, Flemingovo nam. 2, 166 10 Prague, Czech Republic

<sup>2</sup>University of Calgary, 2500 University Dr. NW, Calgary, AB, T2N 1N4, Canada

Circular dichroism (CD) spectroscopy, both in the electronic (ECD) and in vibrational (VCD) regions of the spectrum provides rich information about structure of chiral molecules. Intrinsically not chiral molecules, such as residues in nucleic acids or proteins, can also produce a strong and informative CD signal upon their organization into ordered chiral structures, e.g. DNA double helix or protein alpha-helix. In this case the signal originates from the secondary structure of macromolecules, which results in high sensitivity of CD spectroscopy to minor structural changes, often not sensed by other techniques. CD signal can also be induced in intrinsically achiral molecules by external magnetic field, resulting in magnetic CD (MCD), which further expands applicability of CD spectroscopy.

Due to complexity of all types of CD spectra, it is often difficult to establish a direct and unambiguous connection between spectra and molecular structure. Theoretical simulations may significantly simplify this task, and additionally provide information on the energetics and other properties of studied systems. Unfortunately, large size of macromolecules prevents direct spectral simulation with sufficient precision. To avoid this limitation, we have developed ab initio-based methods allowing for reliable computations of large systems.[1] Several examples of VCD spectra calculations for various nucleic acid structural forms will be presented (Fig. 1). Potential of the CD technique for studies of electronic states of aromatic systems will be tested in MCD of fullerene (C<sub>60</sub>).

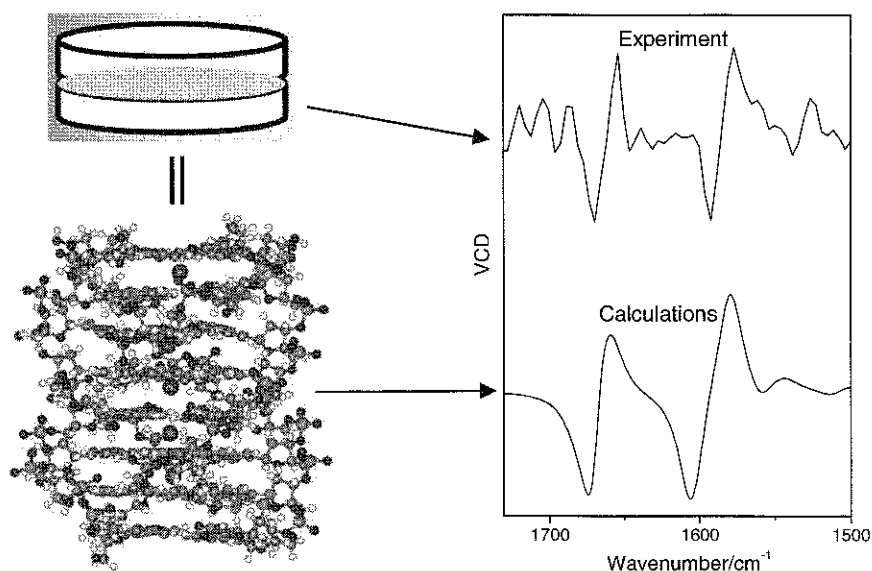


Figure 1. Experimental and simulated VCD spectra of d(G)<sub>8</sub> and the quadruplex structure giving rise to the simulated spectra.

[1] P. Bour, J. Sopkova, L. Bednarova, P. Malon, T.A. Keiderling, *J. Comput. Chem.* 18 (1997), 646.

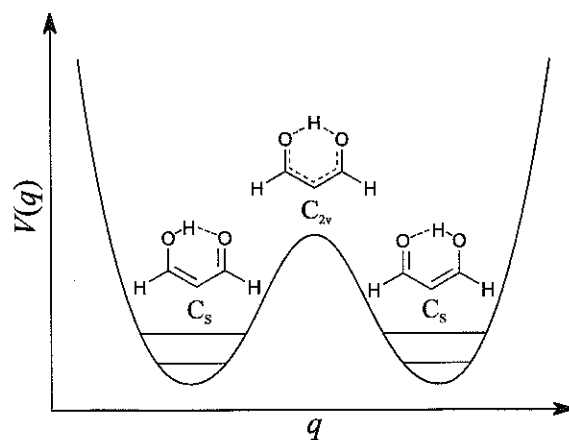
## Environmental and vibrational influence on the proton transfer in malonaldehyde

N. O. B. Lüttchwager<sup>1</sup>, T. N. Wassermann<sup>1</sup>, S. Coussan<sup>2</sup>, M. A. Suhm<sup>1</sup>

<sup>1</sup>*Institut für Physikalische Chemie, Tammannstraße 6, D-37077 Göttingen*

<sup>2</sup>*Laboratoire PIIM, Université de Provence, Centre Saint-Jérôme, Marseille F-13 397, cedex 20, France*

Enolic malonaldehyde is a prototypical system for strong intramolecular hydrogen bonding where the bridging hydrogen performs a fast transfer in a symmetric double-well potential. The two equivalent  $C_S$ -symmetric global minimum structures are separated by a relatively small barrier corresponding to a  $C_{2v}$ -symmetric transition state (see figure below). In consequence of the proton transfer process, the vibrational ground state shows a tunneling splitting  $\Delta$  of  $21.5831383(6) \text{ cm}^{-1}$  [1]. This ground state tunneling splitting can be translated to a tunneling period  $t_p$  of  $1.54548467(5) \text{ ps}$  via  $t_p = 1/(c_0\Delta)$  (with the speed of light  $c_0$ ). The tunneling coordinate  $q$  involves complicated rearrangement motions of the molecular backbone. It is therefore strongly coupled to different vibrational motions and the tunneling splitting is particularly sensitive to vibrational excitation. From complementary IR [2] and Raman [3] gas phase and supersonic jet spectra, aided by IR spectra of matrix-isolated malonaldehyde [2] we derive tunneling splittings of vibrationally excited states which reach from total quenching of the proton transfer ( $\Delta = 0 \text{ cm}^{-1}$ ) to acceleration by a factor of 3 ( $\Delta = 69 \text{ cm}^{-1}$ ). In the latter case, the periodic bond breaking and formation events are pushed to sub-picosecond time scales.



- [1] T. Baba, T. Tanaka, I. Morino, K. M. T. Yamada and K. Tanaka, *J. Chem. Phys.* 110 (1999) 4131-4133
- [2] T. N. Wassermann, D. Luckhaus, S. Coussan and M. A. Suhm, *Phys. Chem. Chem. Phys.* 8 (2006) 2344-2348
- [3] J. J. Lee, S. Höfener, W. Klopper, T. N. Wassermann and M. A. Suhm, *J. Phys. Chem. C* 113 (2009) 10929-10938; Z. Xue and M. A. Suhm, *J. Chem. Phys.* 131 (2009) 054301; N. O. B. Lüttchwager, T. N. Wassermann, S. Coussan and M. A. Suhm, *Phys. Chem. Chem. Phys.* (submitted 2010)



## Coherent dynamics in energy migration at room temperature: Evidence for subtle quantum-mechanical strategies for energy transfer optimization

E. Collini<sup>1</sup>, G.D. Scholes<sup>2</sup>

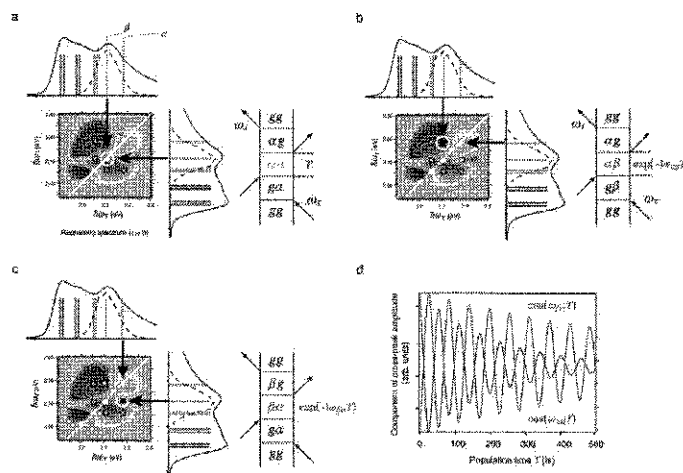
<sup>1</sup>Dipartimento di Scienze Chimiche and INSTM, Università di Padova, via Marzolo 1, 35131 - Padova (Italy)

<sup>2</sup>Department of Chemistry, Institute for Optical Sciences and Centre for Quantum Information and Quantum Control, University of Toronto, 80 St George Street, Toronto, Ontario, M5S 3H6 (Canada)

Electronic energy transfer (EET) is a process whereby the energy of absorbed light is transmitted between molecules. EET is a key photoinduced process for multichromophoric systems in biological photosynthesis, photovoltaic devices, photocatalysis, and sensors. For this reason in the recent years there have been many studies of EET phenomena and attempts to gain further insights into the mechanism of efficient EET. The pathways and timescales of EET for various multichromophoric systems ranging from photosynthetic complexes to conjugated polymers, to multibranch systems, are now well characterized in the frame of semiclassical theories (Förster model), in which the transfer rate can be calculated assuming incoherent quantum mechanical transitions.

However, the role of quantum coherences in determining the efficiency of energy transfer is still not well understood. This is especially true in the case of the so-called intermediate coupling, a particular regime for EET rising lot of interest because excitation moves in space, like in classical hopping mechanism, but still conserving quantum phase information.[1]

In this work we exploit two-dimensional photon echo experiments (2DPE) to observe quantum coherence dynamics in energy transfer on two evolutionarily related light-harvesting proteins isolated from marine cryptophyte algae. The data, recorded at room temperature, revealed exceptionally long-lasting excitation oscillations with distinct correlations and anti-correlations even at ambient temperature. These observations provide compelling evidence for quantum-coherent sharing of electronic excitation across the 5-nm-wide proteins under biologically relevant conditions, suggesting that distant molecules within the photosynthetic proteins are 'wired' together by quantum coherence for more efficient light-harvesting in cryptophyte marine algae.[2]



[1] E. Collini, G.D. Scholes, *Science* 323 (2009) 369-373

[2] E. Collini, C.Y. Wong, K.E. Wilk, P.M.G. Curmi, P. Brumer, G.D. Scholes, *Nature* 463 (2010) 644-648



## Energy transfer processes in homo and hetero dimers of porphyrins

E. Garbin<sup>1</sup>, E. Lubian<sup>1</sup>, S. Kovalenko<sup>2</sup>, N. Ernsting<sup>2</sup>, T. Carofiglio<sup>1</sup>, C. Ferrante<sup>1</sup>

<sup>1</sup>*Dipartimento di Scienze Chimiche, Università di Padova, via Marzolo 1, 35131 Padova, Italy*

<sup>2</sup>*Department of Chemistry, Humboldt University, Brook-Taylor-Str. 2, D-12489 Berlin, Germany*

The interest towards the energy transfer (ET) processes in structure containing porphyrinic moieties is due to the desire to investigate the natural photosynthetic processes through simple model systems and to emulate the high efficiency characteristic of biological light harvesting and electron transfer systems in order to exploit them in artificial devices.

One of the investigated system, reported in Figure 1, is a covalently linked dimer made by a tetra-phenyl-porphyrin (TPP) and a Zn-TPP unit, in which an energy transfer is expected from ZnTPP to TPP in the Q bands region. First evidence of ET in this dimer is shown by linear fluorescence measurement, from which an efficiency of about 80% can be expected.

To confirm these findings we performed transient absorption (TA) experiments exciting the Soret band at 403 nm with 80 fs pulses and probing the excited state dynamic using white light in the range 250-690 nm. TA provides information on the excited state dynamic confirming the efficiency of the transfer and measuring the ET rates. Two different mechanisms of ET can be recognized in this system: a first ultrafast transfer involving the B bands of approximately 600 fs, whose origin and nature is currently investigated, and a longer transfer of approximately 200 ps in the Q bands region, confirming the 80% efficiency found in linear measurements.

Homo-dimers of Zn-TPP and TPP with the same structure as the hetero-dimer in Figure 1 were also investigated through TA experiments performed with polarized light. Through the study of the evolution of the anisotropy signal, ET dynamics can be revealed.

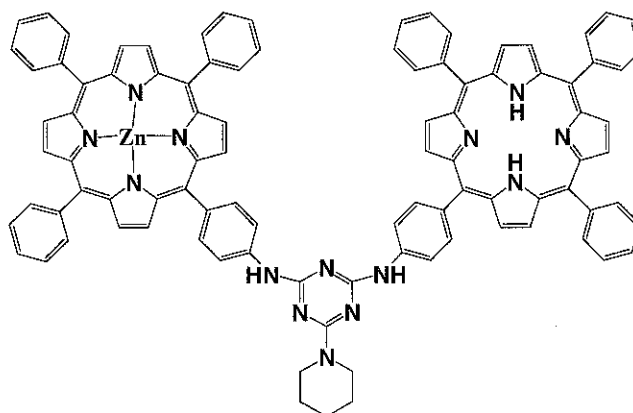


Figure 1: Molecular structure of the hetero dimer investigated.

## One- and two-mode behavior of the $\nu(\text{C}=\text{O})$ band in N,N-dimethylformamide isotopic mixtures: DMF/DMF- $\text{d}_1$ , DMF/DMF- $\text{d}_6$ , and DMF/DMF- $^{13}\text{C}$ O

H. Torii<sup>1</sup>, M. G. Giorgini<sup>2</sup> and M. Musso<sup>3</sup>

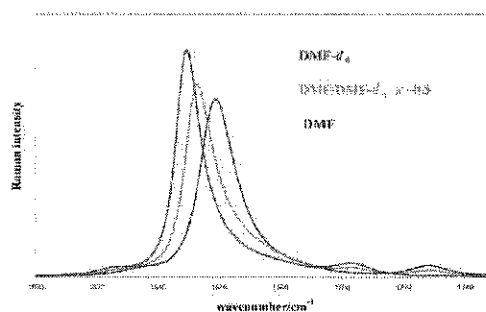
<sup>1</sup> Department of Chemistry, School of Education, Shizuoka University, 836 Ohya, Shizuoka 422-8529, Japan.

<sup>2</sup> Dipartimento di Chimica Fisica ed Inorganica, Università di Bologna, Viale del Risorgimento 4, I-40136 Bologna, Italy

<sup>3</sup> Fachbereich Materialwissenschaften, Abteilung Physik und Biophysik, Universität Salzburg, Hellbrunnerstraße 34, A-5020 Salzburg, Austria.

Observation of the Raman spectrum of some binary isotopic liquid mixtures may cause a great surprise: the spectral merging of the bands associated with a given normal mode having slightly different intrinsic frequency in the two neat liquids, to only one band with a frequency located in between (one-mode behavior). It was noticed in the Raman spectrum of the amide I [ $\nu(\text{C}=\text{O})$ ] band of formamide- $\text{d}_2$ /formamide- $\text{d}_3$  liquid mixtures [1]. Both the overlap of the two bands and the dynamical D/H exchange could be excluded as possible origins of merging. The onset of this phenomenon requires the occurrence of very critical spectral conditions, because, while it is observed in the amide I band of the formamide- $\text{d}_2$ /formamide- $\text{d}_3$  [1] mixtures, it is absent in the same mode of the analogous formamide/formamide- $^{13}\text{C}$ O mixtures [1] where the two-mode behavior is observed.

To unveil the origin of this phenomenon and recognize which and how spectral conditions discriminate between the observation of the one- or two mode behavior, a computational procedure has been envisaged [2] based on the parametrization of the vibrational modes in a liquid coupled by transition dipole coupling mechanism (TDC). It is well known, in fact, that the  $\nu(\text{C}=\text{O})$  mode in liquid carbonyl compounds, and more notably in the amide I band present in amides, is affected by intermolecular resonant vibrational coupling as manifested by the frequency splitting between the Raman aniso- and isotropic components (termed noncoincidence effect, NCE), particularly large ( $15\text{ cm}^{-1}$ ) in these carbonyl compounds. It has been found [3] that the ingredient for the onset of the one-mode behavior is the extent of resonance condition (the magnitude of the resonant coupling compared with the separation of the wavenumber positions) between the vibrations of the two species and their bandwidths. With the present investigation we intend to analyse and discuss the one-/two-mode behavior of the amide I band in isotopic mixtures of N,N- dimethylformamide (DMF) in the light of general results obtained in [3] on the basis of a parametric analysis of a coupled oscillator system. Among the results obtained for the three types of isotopic mixtures under study we report, on the right, the case of the isotropic Raman spectra of DMF/DMF- $\text{d}_6$  mixtures where the occurrence of the one-mode behavior is clearly seen.



[1] Mortensen A., Faurskov Nielsen O., Yarwood J., Shelley V., J. Phys. Chem. 1995, 99, 4435-4440

[2] Torii H., J. Phys. Chem. A 2006, 110, 4822-4832.

[3] Torii H., Osada Y., Iwami M., J. Raman Spectrosc. 2008, 39, 1592-1599



## Transient infrared spectroscopy: a new approach to investigate valence tautomeric interconversion

A. Lapini<sup>1</sup>, P. Tourón Touceda<sup>1</sup>, S. Mosquera Vázquez<sup>1</sup>, M. Lima<sup>1</sup>, A. Dei<sup>2</sup>,  
P. Foggi<sup>1,3,4</sup>, R. Righini<sup>1</sup>

<sup>1</sup> *European Laboratory for Non Linear Spectroscopy (LENS), University of Florence, Via Nello Carrara 1, 50019 Sesto Fiorentino, Italy.*

<sup>2</sup> *LAMM Laboratory, Dipartimento di Chimica dell'Università di Firenze, UdR INSTM, Via della Lastruccia 3, 50019 Sesto Fiorentino (Firenze), Italy.*

<sup>3</sup> *Dipartimento di Chimica, University of Perugia, 06100 Perugia, Italy*

<sup>4</sup> *CNR-INO, Largo E. Fermi 6, 50125 Firenze, Italy.*

Cobalt-dioxolene complexes may show redox isomerism (valence tautomerism). This phenomenon is due to intramolecular electron transfer within the cobalt(III)-catecholato moiety yielding a cobalt(II)-semiquinonato species. The relative stability of the two redox isomers is determined by temperature and it is possible to stimulate the interconversion from the stable isomer to the metastable one upon irradiation at appropriate wavelengths. Since the energies of the two isomers are different, irradiation is followed by a decay process to the ground state. Theory predicts that dynamics of relaxation should be basically controlled by the energy gap between the two interconverting isomers. A series of cobalt complexes of general formula  $[\text{Co}(\text{Me}_{(n)}\text{tpa})(\text{diox})]\text{PF}_6$  (diox = 3,5-di-tert-butyl-1,2-dioxolene), has been prepared using as an ancillary ligand the tripod-like  $\text{Me}_{(n)}\text{tpa}$  ( $n = 0, 1, 2, 3$ ), derived by tris(2-pyridylmethyl)amine (tpa) by successive introduction of methyl groups into 6-position of pyridine moieties. The steric hindrance induced by this substitution modulates the redox properties of the metal acceptor, thus determining the charge distribution of the metal-dioxolene moiety at room temperature.

We performed room temperature transient infrared measurements on a  $\text{CD}_3\text{CN}$  solution of  $[\text{Co}(\text{Me}_{(n)}\text{tpa})(\text{diox})]$  complexes ( $n = 0, 2, 3$ ) exciting the sample with 800 nm and 400 nm pump pulses to investigate the mechanism involved in the photoconversion process.



## A Semi-Quantitative LIBS Analysis on *Terra Sigillata* Wares

C. Lofrumento<sup>1</sup>, Ph. Sciau<sup>2,3</sup>, Y. Leon<sup>2,3</sup>, E. M. Castellucci<sup>1,4</sup>

<sup>1</sup>Department of Chemistry, Polo Scientifico e Tecnologico, University of Florence, via della Lastruccia 3, 50019, Sesto Fiorentino (Fi), Italy

<sup>2</sup>CNRS, CEMES, BP 94347, 29 rue J.Marvig, F-31055 Toulouse, France

<sup>3</sup>Université de Toulouse, UPS, INSA, CEMES, F-31055 Toulouse, France

<sup>4</sup>LENS- European Laboratory for Non-Linear Spectroscopy, University of Florence, via Nello Carrara 1, 50019, Sesto-Fiorentino (Fi), Italy

Former studies on terra sigillata fine wares of the Roman period revealed systematic differences in the mineral composition between central Italian and south Gaul productions by showing that, apart from the hematite content, the Gallic slips embody a significant content of corundum, while the Italian productions contain a great proportion of spinel [1].

A recent Raman investigation [2] demonstrates that, by the occurrence of an upshift of bands, the Raman spectrum of these *sigillata* slips can be associated with a substituted hematite. This premise has been confirmed by comparing the crystallization of hematite in four annealed clays to that of the ancient slips, thus establishing Raman scattering to be a fine technique to evaluate small variations in clays compositions and firing temperature.

Laser Induced Breakdown Spectroscopy (LIBS) capabilities to perform qualitative analysis have been shown widely together with the demonstration of its versatility and thoroughness [3]. Another feature of great interest is the capacity to perform elemental quantitative analysis, particularly interesting for the characterization of homogeneous materials [4]. Calibration-Free LIBS (CF-LIBS), based on calculations assuming stoichiometric ablation and thermal equilibrium within the plasma, provided a useful fast tool for the differentiation of the relative concentration *terra sigillata* samples.

On the basis of the results obtained by means of the other applied analytical techniques on *terra sigillata* wares, we tested the potentiality of LIBS. This checking was aimed at utilizing LIBS technique to study the different chemical compositions of the *terra sigillata* specimens by employing a simple, micro-destructive, as long as fast semi-quantitative analytical procedure.

[1] P. Sciau, S. Relaix, C. Mirguet, P. Goudeau, A. M. T. Bell, R. L. Jones, E. Pantos, Appl. Phys. A, (2008) 90, 61-66

[2] Y. Leon, C. Lofrumento, A. Zoppi, R. Carles, E. M. Castellucci, Ph. Sciau, J. Raman Spectr., accepted, DOI 10.1002/jrs.2678

[3] I. Osticioli, M. Wolf, D. Anglos, Appl. Spectr., (2008) 62, 1242-1249

[4] E. Tognoni, V. Palleschi, M. Corsi, G. Cristoforetti, Spectrochim. Acta B, (2002) 57, 115-1130





## Raman Spectroscopy for the evaluation of structural changes of peptides

G. Das<sup>1</sup>, M. L. Coluccio<sup>2</sup>, A. Nicastrì<sup>3</sup>, F. Gentile<sup>2</sup>, F. De Angelis<sup>1</sup>, E. Di Fabrizio<sup>1,2</sup>  
and G. Cuda<sup>3</sup>

<sup>1</sup>*Istituto Italiano di Tecnologia, Via Morego 30 Genova, ITALY*

<sup>2</sup>*BIONEM Lab., Università Magna Graecia di Catanzaro, Catanzaro, ITALY*

<sup>3</sup>*Proteomics Lab., Università "Magna Graecia" di Catanzaro, Catanzaro, ITALY*

Raman spectroscopy has become a versatile tool in protein science and biotechnology, and its role in the detection of malignant tissues is reported in several studies [1]. It is well known that the alteration of the protein primary structure due to the substitution of one amino acid with a different one can determine the alteration of protein folding, leading to the change of its biological function. For example, in BRCA1 (Breast Cancer Associated Gene 1) protein, several missense mutations that alter protein folding predispose to breast cancer [2]. A protein Raman spectrum comprises discrete bands representing vibrational modes of the peptide backbone and its side chains. In the present work, we analyzed through Raman spectroscopy four synthetic peptides sixteen amino acids in length designed on the basis of specific position of the sequence of BRCA1/BRCT (BRCA1 C-terminal) protein domain; of those four peptides, two corresponded to the wild-type form of BRCA1/BRCT protein domain (M1775 and W1837) and two corresponded to the mutated form (M1775R and W1837R). Both missense mutations have been detected in patients with hereditary breast cancer. We used gold-coated silicon nanostructures as SERS (Surface Enhanced Raman Scattering) substrates and DCDR (Drop Coating Deposition Raman) technique [3] to investigate structural changes in the primary structure of the mutated peptides compared to the wild-type. Data from synthetic peptides spectra show clear differences between wild-type and mutated peptides (fig.1a-1b). Analysis of the synthetic peptides through Raman spectroscopy play an important role for correct interpretation and functional evaluation of molecular alterations of proteins from cellular samples of patients with breast cancer.



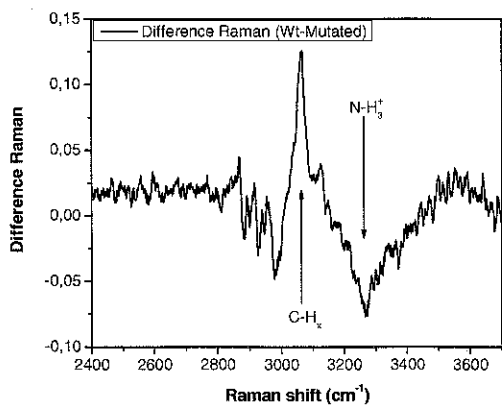


Fig.1a Difference between spectra of the M1775 and M1775R peptides

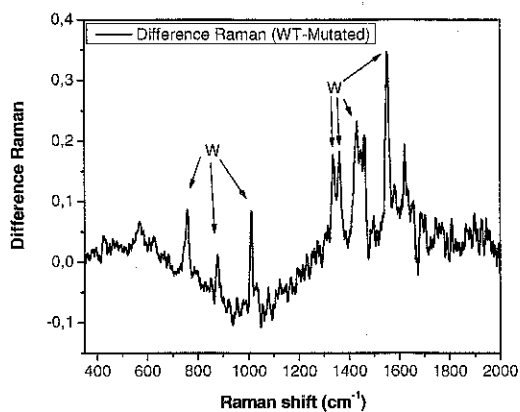


Fig.1b Difference between spectra of the W1837 and W1837R peptides

- [1] A. Nijssen, S. Koljencic, T.C. Bakker Schut, P.J. Caspers, G.J. Puppels, J. Biophotonics. 2 (2009) 29-39.
- [2] R.S. Williams, D.I. Chasman, D.D. Hau, B. Hui, A.Y. Lau, J.N. Glover, J. Biol. Chem. 278 (2003) 53007-53016.
- [3] D. Zhang, Y. Xie, M.F. Mrozek, C. Ortiz, V.J. Davisson, D. Ben-Amotz, Anal. Chem. 75 (2003) 5703-5709.

## High pressure photoinduced reactivity in clathrate hydrates

M. Ceppatelli<sup>1,2</sup>, R. Bini<sup>1,2</sup>, V. Schettino<sup>1,2</sup>

<sup>1</sup>*LENS – European Laboratory for Non-Linear Spectroscopy, Via Nello Carrara 1, 50019, Sesto Fiorentino (FI), Italy*

<sup>2</sup>*Dipartimento di Chimica dell'Università degli Studi di Firenze, Via della Lastruccia 3, 50019, Sesto Fiorentino (FI), Italy*

High pressure reactivity has been observed in several clathrate hydrates at room T and P of several tenths of GPa under irradiation with the Ar ion laser wavelength at 350 nm. The high pressure has been generated using a Membrane Diamond Anvil Cell (MDAC) and the reactivity has been monitored by means of FTIR and Raman spectroscopy. We have studied clathrate hydrates of different model hydrocarbons (ethane, ethylene, acetylene and propene) as well as the clathrate hydrates of two inorganic systems like nitrogen and carbon monoxide. The formation of CO<sub>2</sub> is observed in all the systems containing carbon atoms and direct evidence for the formation of molecular hydrogen is reported in some cases. The CO<sub>2</sub> produced during the reaction can be sequestered in situ as clathrate hydrate. The reaction is triggered by the two-photon excitation of the water molecules, leading to the formation of highly reactive OH radicals. Such species are able to induce a partial cleavage of the triple bond in the extremely stable nitrogen molecule.

[1] M. Ceppatelli, R. Bini, V. Schettino, *P. Natl. Acad. Sci. USA*, **106**, 11454-11459 (2009).

[2] M. Ceppatelli, R. Bini, V. Schettino, *J. Phys. Chem. B*, **113**, 14640-14647 (2009).



## Time-resolved spectroscopy of native and mutated *Thermobifida fusca* hemoglobins

S. Abbruzzetti<sup>1</sup>, A. Bonamore<sup>2</sup>, A. Boffi<sup>2</sup>, A. Feis<sup>3</sup>, P. Foggi<sup>4</sup>, C. Gellini<sup>3</sup>, A. Marcelli<sup>5</sup>, P.R. Salvi<sup>3</sup>, C. Viappiani<sup>1</sup>

<sup>1</sup>Department of Physics, University of Parma, Italy

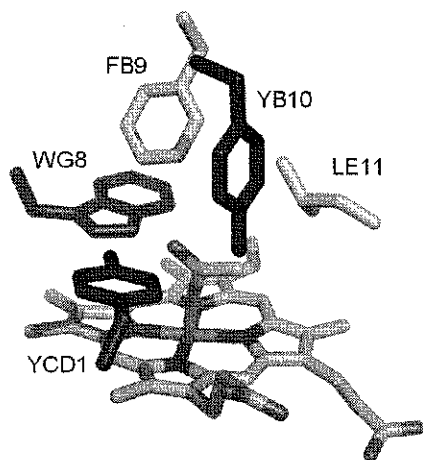
<sup>2</sup>Department of Biochemical Sciences, University of Rome "La Sapienza", Italy

<sup>3</sup>Department of Chemistry "Ugo Schiff", University of Florence, Italy

<sup>4</sup>Department of Chemistry, University of Perugia, Italy

<sup>5</sup>LENS, European Laboratory for Non-linear Spectroscopy, Florence, Italy

*Thermobifida fusca* hemoglobin (TFH) is a prototypical bacterial (class 2) hemoglobin. It has been identified in a thermophilic actinobacterium [1] and overexpressed. The heme cavity structural properties are mainly related to the polarity and H-bonding capability of the "distal" amino acids: tyrosine (B10 in the myoglobin helix notation), tyrosine (CD1), tryptophan (G8).



Single, double and triple phenylalanine (Phe) mutants of these key residues have recently become available. We have applied several techniques of time-resolved optical spectroscopy to study the dynamics following the photolysis of carbon monoxide-bound TFH.

1. Femtosecond transient absorption has shown that CO can rebind from TFH distal cavity in few ns. TrpG8 substitution with the apolar Phe accelerates the recombination, which takes place in hundreds of ps.

2. Laser flash photolysis measurements have allowed to extend the study of the dynamics to the ns and  $\mu$ s range. The yield of the geminate rebinding and the kinetics of recombination from the solvent are both influenced by the single TrpG8  $\rightarrow$  Phe mutation.

Further changes are observed when the three polar amino acids are replaced by Phe. Rate constant distributions have been obtained by the maximum entropy method [2].

3. Photoacoustic measurements have yielded both volume and enthalpy changes [3] following CO photodissociation in the ns -  $\mu$ s range. The thermodynamic parameters for the observed intermediates can be related to those measured by laser flash photolysis.

All the results point to an overwhelming role for TrpG8. This is in agreement with a recent study on a related bacterial hemoglobin from *Bacillus subtilis* [4].

- [1] A. Bonamore, A. Ilari, L. Giangiacomo, A. Bellelli, V. Morea, A. Boffi, FEBS J. 27 (2005) 4189-4201.
- [2] S. Abbruzzetti, S. Bruno, S. Faggiano, E. Grandi, A. Mozzarelli, C. Viappiani, Photochem. Photobiol. Sci. 5 (2006) 1109-1120.
- [3] R.W. Larsen, J. Mikšovská, Coord. Chem. Rev. 254 (2007) 1101-1127.
- [4] A. Feis, A. Lapini, B. Catacchio, S. Brogioni, P. Foggi, E. Chiancone, A. Boffi, G. Smulevich Biochemistry 47(2008) 902-910.

## Tautomerism in pyrimidine derivatives investigated with core level spectroscopy techniques.

B. M. Giuliano<sup>1</sup>, V. Feyer<sup>2</sup>, K.C. Prince<sup>2</sup>, M. Coreno<sup>3</sup>, L. Evangelisti<sup>4</sup>, S. Melandri<sup>4</sup>, W. Caminati<sup>4</sup>

<sup>1</sup>Departamento de Química, Universidade de Coimbra, 3004-535 Coimbra, Portugal

<sup>2</sup>Sincrotrone Trieste, 34149 Basovizza, Italy

<sup>3</sup>CNR-IMIP, 10-00016 Montelibretti, Italy

<sup>4</sup>Dipartimento di Chimica "G. Ciamician", Università di Bologna, 40126 Bologna, Italy

The nucleobases cytosine, thymine and uracil are pyrimidine derivatives. They pair with their complementary purines, guanine and adenine, through hydrogen bonding to form DNA and RNA chains.

In the present communication we report the application of X-ray photoemission spectroscopy (XPS) to the study of the prototypical system 2-hydroxypyrimidine and the related molecules S-methyl-2-thiouracil and 2-thiouracil in the vapor phase (molecular sketches are shown in Fig.1). These systems have been previously studied in laboratory experiments mainly using microwave, infrared and UV photoelectron spectroscopy [1-3], which gave very precise information about the geometry of tautomers and about their relative stabilities. But previous experiments were performed in conditions far from thermal equilibrium and therefore the measured populations of tautomers could not easily be related to equilibrium thermodynamic parameters. XPS is a quantitative technique and the populations ratio of the keto-enol tautomers at the sample temperature can be found experimentally, which is extremely difficult otherwise.

Two different chemical shifts can be determined from our O1s XPS spectrum for the keto and enol tautomers of 4-hydroxypyrimidine and S-methyl-2-thiouracil. For both systems the analysis of the XPS spectra reveals that the relative population of the keto tautomer is 2.3 times higher than that of the hydroxy one. The XPS spectra of 2-thiouracil can instead be interpreted with the presence of a single tautomer, the diketo form, which is calculated to be the most stable one.

In addition, the high resolution valence photoemission and NEXAFS spectra have been measured to gain more information about the electronic structure of the tautomers.

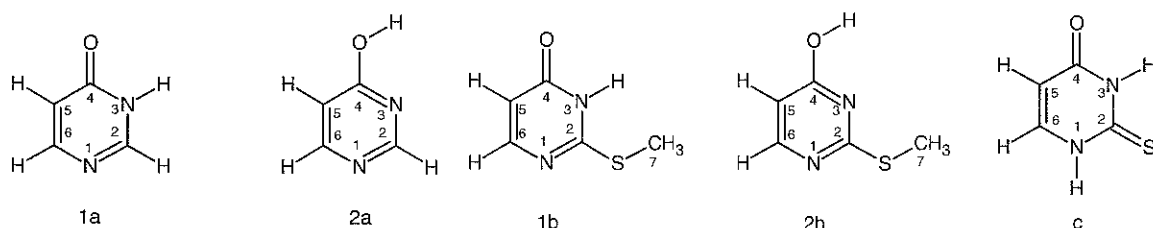


Figure 1. Chemical structures of the a) 4-Hydroxypyrimidine, b) S-methyl-2-thiouracil and c) 2-Thiouracil.

- [1] R. Sanchez, B. M. Giuliano, S. Melandri, L. B. Favero, W. Caminati, J. Am. Chem. Soc. 129 (2007) 6287.  
 [2] A. R. Katritzky, M. Szafran, G. Pfisterguillouzo, J. Chem. Soc. Perkin Trans. 2 (1990), 871.  
 [3] L. Lapinski, M. J. Nowak, J. Fulara, A. Les, L. Adamowicz, J. Phys. Chem. 96 (1992) 6250-6254.



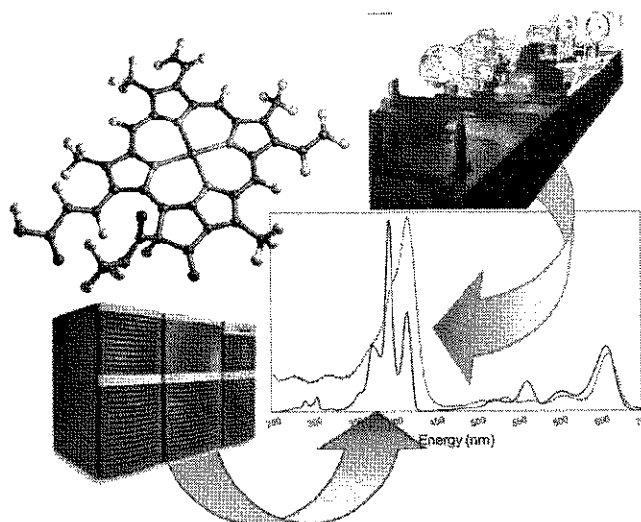
## Computational spectroscopy as a tool to interpret experimental results: from small molecule in the gas phase to large systems in condensed phases.

M. Biczysko<sup>a,b</sup>

<sup>a</sup>*Scuola Normale Superiore, piazza dei Cavalieri 7, 56126 Pisa, Italy*

<sup>b</sup>*Università di Napoli Federico II, Complesso Univ. Monte S. Angelo, via Cintia, 80126 Napoli, Italy*

The subtle interplay of several different effects still makes the interpretation and analysis of experimental spectra in terms of structural and dynamic characteristics a very challenging task. In this context, theoretical studies can be very helpful and this is the reason behind the rapid evolution of computational spectroscopy from a highly specialized research field toward a versatile and widespread tool. However, in the case of electronic spectra (UV-vis, Circular Dichroism, photoelectron, X-ray, etc.), the most popular approach still relies on computation of vertical excitation energies, which are further convoluted to simulate line-shapes. Such a treatment completely neglects the influence of nuclear motions, despite the well recognized notion that proper account of vibrational effects is often mandatory in order to interpret correctly the experimental findings. In this respect, the generation of reliable spectra including the vibronic contributions has become recently feasible even for medium-to-large systems. Here, we present the implementation of an effective procedure rooted into a time-independent model [1,2], integrated in a general-purpose computational chemistry package, offering the possibility to evaluate simply one-photon electronic spectra, using several electronic models [3]. In particular the DFT/N07 scheme [4] coupling a remarkable reliability in the computation of geometric, vibrational and electronic properties with a very favorable scaling with the number of electrons, allows reliable studies of compounds of biological or technological interest. Some specific examples from small molecules in the gas phase to large systems in condensed phases will be discussed to illustrate our recent integrated approach.



- [1] J. Bloino, M. Biczysko, F. Santoro, V. Barone, *J. Chem. Theory Comput.* 6, 1256-1274 (2010)
- [2] V. Barone, J. Bloino, M. Biczysko, F. Santoro, *J. Chem. Theory Comput.* 5, 540-554 (2009)
- [3] A. Pedone, M. Biczysko, V. Barone, *ChemPhysChem*, 11, 1812-1832 (2010)
- [4] V. Barone, J. Bloino, M. Biczysko, *Phys. Chem. Chem. Phys.* 12, 1092-1101 (2010)

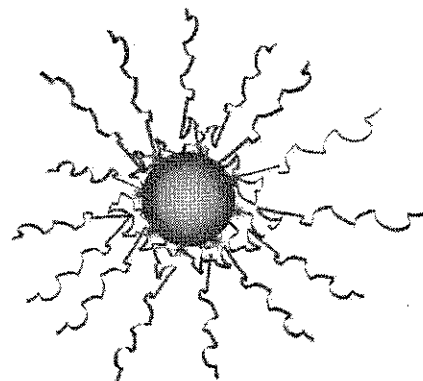
## SERS active gold nanostructures for selective and ultrabright biolabelling: synthesis and quantitative study

V. Amendola<sup>1</sup>, G. Marcolongo<sup>1</sup>, G. Fracasso<sup>2</sup>, M. Colombatti<sup>2</sup> and M. Meneghetti<sup>1</sup>

<sup>1</sup> Department of Chemical Sciences, University of Padova, Via Marzolo, 1 I-35131 Padova, Italy

<sup>2</sup> Department of Pathology-Immunology c/o Policlinico GB Rossi, University of Verona, Piazz.le La Scuro, 10 I-37100, Verona, ITALY

Surface enhanced Raman scattering (SERS) probes based on gold nanoparticles (AuNPs) – organic dyes nanocomposites disclosed new opportunities for multiplexed ultrasensitive biolabelling *in vitro* or *in vivo*. SERS labels also have excellent biocompatibility and can be excited with near infrared laser sources, that match the transparency window of biological tissues. Here we report about the preparation of AuNPs obtained by laser ablation synthesis in solution (LASiS)[1,2] and their functionalization with a series of Raman reporter with different spectral fingerprints. The effective differential Raman scattering cross section of these labels were evaluated using liquid Raman standards and the analysis of the surface plasmon band of AuNPs with the Mie – Gans models.[3] We estimated that few (<10) SERS labels are enough to collect a clear Raman spectrum with a common Raman spectrometer. SERS labels were used for the study of nanoparticles uptake in macrophages[4] in order to quantify the number of nanoparticles phagocytized after different times. The conjugation of SERS labels with antibodies that selectively binds antigens over-expressed by specific types of cancerous cells is under investigation for the antibody – directed selective ultrasensitive detection and imaging of cancer.



[1] V. Amendola, M. Meneghetti, Phys. Chem. Chem. Phys. 2009,

[2] V. Amendola, M. Meneghetti; J. Mater. Chem. 2007, 17, 4705–4710.

[3] V. Amendola, M. Meneghetti, J. Phys. Chem. C 2009, 113, 4277–4285.

[4] V. Amendola, M. Meneghetti, S. Fiameni, G. Fracasso, A. Boscaini, M. Colombatti; Submitted

## Vibrational investigation on the *in vitro* bioactivity of commercial and experimental calcium-silicate cements for root-end endodontic therapy

P. Taddei<sup>1</sup>, E. Modena<sup>1</sup>, A. Tinti<sup>1</sup>, F. Siboni<sup>2</sup>, C. Prati<sup>2</sup>, M. G. Gandolfi<sup>2</sup>

<sup>1</sup>Dipartimento di Biochimica "G. Moruzzi", Sez. di Chimica e Prop. Biochimica, Via Belmeloro 8/2, University of Bologna, 40126 Bologna, Italy

<sup>2</sup>Dipartimento di Scienze Odontostomatologiche, Via S. Vitale 59, University of Bologna, 40126 Bologna, Italy

Portland cements are hydraulic calcium-silicate materials able to set in moist environment. White Portland cements are composed of tricalcium silicate (alite), dicalcium silicate (belite), tricalcium aluminate and calcium sulphate. Grey Portland cements also contain a ferrite phase (aluminoferrite) and other transition metals (Cr and Mn) and metalloids (As).

In the last decade, calcium-silicate hydraulic cements have received great attention in endodontics because able to set in presence of blood and other biological fluids. In the 1990s a first calcium-silicate cement MTA (Mineral Trioxide Aggregate) was developed as root-end filling material.

Recent investigations demonstrated that MTA and calcium-silicate cements are bioactive materials, i.e. they are able to spontaneously form a calcium-phosphate layer when immersed in physiological-like fluids. This bone-like apatite layer can support new tissue formation and the integration in bone tissue and represents an essential requirement for an artificial material to be considered osteoconductive and osteoinductive.

This study was aimed at comparatively investigating the bioactivity of commercial calcium-silicate cements (ProRoot white MTA, Angelus grey MTA, Angelus white MTA, TechBiosealer root end) and an experimental calcium-silicate cement (wTC) upon ageing for different times (from 1 to 28 days), at 37°C, in Dulbecco's Phosphate buffered saline (DPBS). With the exception of wTC, all the cements contained bismuth oxide for radiopacity. ATR/FT-IR and micro-Raman spectroscopy were used to investigate the presence of deposits on the cement surface and the composition changes as a function of storage time (hydration of anhydrite/gypsum and formation of ettringite; hydration of belite/alite and formation of hydrated silicates).

Spectroscopic analyses showed that after one day of ageing all the cements formed an apatite deposit on their surface, as revealed by the appearance of the bands at about 1030, 600 and 560 cm<sup>-1</sup> (IR) and 960 cm<sup>-1</sup> (Raman). The thickness of the deposit was evaluated by the  $I_{960(\text{phosphate})}/I_{990(\text{cement})}$  (Raman) and  $I_{1030(\text{phosphate})}/I_{950(\text{cement})}$  (IR) ratios obtained on the surfaces of the samples. After one day in DPBS, only in Angelus grey MTA the bands of the cement near 830-850 cm<sup>-1</sup> became undetectable due to the high thickness of the superficial apatite deposit suggesting that Angelus grey MTA possesses the highest bioactivity.

At increasing storage times in DPBS (14-28 days), the thickness of the deposit increased as well as its crystallinity and the bands of a B-type carbonated apatite appeared at 1460-1415, 1025, 960, 600-560 cm<sup>-1</sup> (IR) and 1074, 1050, 965, 606-595- 436 cm<sup>-1</sup> (Raman).

All cements produced and released Ca(OH)<sub>2</sub>. Its formation was monitored by the trend of the 3640 cm<sup>-1</sup> IR band and its release was detected by pH measurements.

In conclusion, all calcium-silicate cements resulted bioactive. The higher bioactivity found for Angelus grey MTA must be further investigated considering the presence in its composition of transition metals.





## Molecular aggregation processes in self-assembled micellar systems investigated by Raman scattering and numerical simulation

B. Rossi<sup>1</sup>, G. Cazzolli<sup>1</sup>, G. Viliani<sup>1</sup>, C. M. C. Gambi<sup>2</sup>, S. Marchetti<sup>2</sup>

<sup>1</sup>*Department of Physics, University of Trento, via Sommarie 14, 38123, Povo, Trento, Italy*

<sup>2</sup>*Department of Physics, University of Florence and CNISM, Via G. Sansone 1, 50019, Sesto Fiorentino (Florence), Italy*

Aggregation processes are a topic of current interest in liquid state physics because understanding the interactions involved in the aggregation mechanisms makes it possible to build up new "responsive" materials and to address important challenges in medicine/biology as well as in several industrial-manufacturing processes.

We studied a simple aqueous self-assembled micellar system consisting of an aqueous solution of Sodium Dodecyl Sulphate (SDS) doped with various adhesive sites [1,2], by using Raman scattering and numerical simulation, in order to obtain more precise information on the interactions responsible for the process of aggregation between micelles. The aim is to extend the use of the experimental-numerical approach developed in recent years and successfully applied to the study of molecular complexes [3] to the larger supramolecular systems, as micelles can be considered.

The experimental Raman spectra recorded on monomeric dispersion of SDS are compared with the theoretical Raman intensities computed using quantum chemical computations in order to assign the main vibrational bands of the SDS molecule. Then the experimental Raman spectra recorded on micelles of SDS in water, and on micelles doped with two types of macrocyclic ligands, are compared in order to evidence the differences in intensity and frequency emerging as a consequence of the aggregation process and the action of the ligands [4]. The observed spectral differences are explained in terms of a decrease of the degrees of freedom, in the case of aggregation of pure SDS in water, and considering the different polarizability-modulation mechanisms (BPOL and DID) in the case of SDS-micelles doped with ligands. Our results, in agreement with those obtained by using small-angle neutron scattering techniques, show the reliability of Raman spectroscopy for studying molecular aggregation processes.

[1] P. Baglioni, C.M.C. Gambi, R. Giordano, J. Teixeira, *Physica B* 213 (1995) 597

[2] L. Scaffei, L. Lanzi, C. M. C. Gambi, R. Giordano, P. Baglioni, J. Teixeira, *J. Phys. Chem. B*, 106 (2002) 10771

[3] B. Rossi, P. Verrocchio, G. Viliani, G. Scarduelli, G. Guella, I. Mancini, *J. Chem. Phys.* 125(4) (2006) 044511

[4] A. D'Aprano, A. Lizzio, A.V. Turco Liveri, F. Aliotta, C. Vasi, P. Migliardo *J. Phys. Chem.* 92(15) (1988) 4436



## Surface-enhanced Raman scattering (SERS) from SnO<sub>2</sub> material

E. Fazio<sup>1</sup>, F. Neri<sup>1</sup>, S. Trusso<sup>2</sup>

<sup>1</sup>Dipartimento di Fisica della Materia e Ingegneria Elettronica, Salita Sperone 31, 98166, Messina, Italy  
<sup>2</sup>CNR-Istituto per i Processi Chimico-Fisici Sede di Messina, V.le F. Stagno d'Alcontres 37, Faro Superiore, I-98158, Messina, Italy

Surface Enhanced Raman Scattering (SERS) is a surface sensitive technique that results in the enhancement of Raman scattering by molecules adsorbed on rough metal surfaces. The enhancement factor can be as much as  $10^{14}$ - $10^{15}$ , which allows the technique to be sensitive enough to detect single molecules [1]. SERS exploits an effect whereby chemicals in close proximity to a roughened metal surface (usually gold or silver) have a greatly increased Raman response. It is generally agreed that the SERS effect arises from two mechanisms: an electromagnetic enhancement (EM) and a chemical charge transfer effect. It is widely believed, however, that the long-range EM enhancement mechanism (of the order  $10^4$ - $10^6$ ) plays a much greater role in overall SERS enhancement than the chemical one (of the order  $10^2$ ) [2].

In this work, for the first time, we report about investigations of the SERS effects on SnO<sub>2</sub> in the form of bulk material, nanostructured thin films and colloidal solutions. Raman spectra are characterized by the three Raman scattering peaks at 478, 633, and 776 cm<sup>-1</sup>, assigned to the E<sub>g</sub>, A<sub>1g</sub> and B<sub>2g</sub> modes, typical of rutile SnO<sub>2</sub>. In presence of the silver nanoparticles, in addition to the enhancement intensity of some of the fundamental SnO<sub>2</sub> rutile Raman features, the appearance of two other Raman scattering peaks, at about 300 and 600 cm<sup>-1</sup>, is observed. In particular for the pulsed laser deposited SnO<sub>x</sub> thin films, it is found a dependence of the SERS effects on the films stoichiometry.

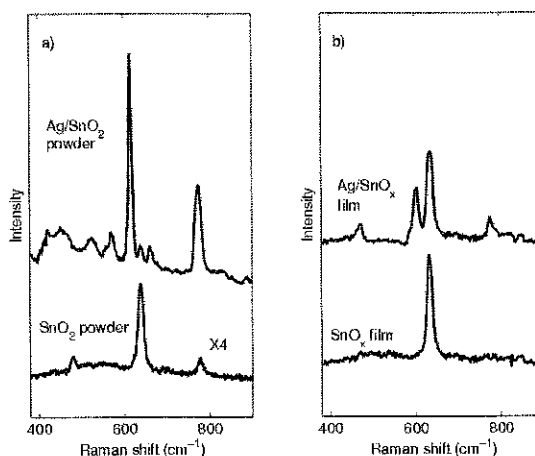


Fig 1: Raman spectra of (a) SnO<sub>2</sub> and Ag-coated SnO<sub>2</sub> powder; (b) PLD grown SnO<sub>x</sub> and Ag-coated SnO<sub>x</sub> thin films.

[1] S. Nie, S.R. Emory Science 275 (1997) 1102-1106

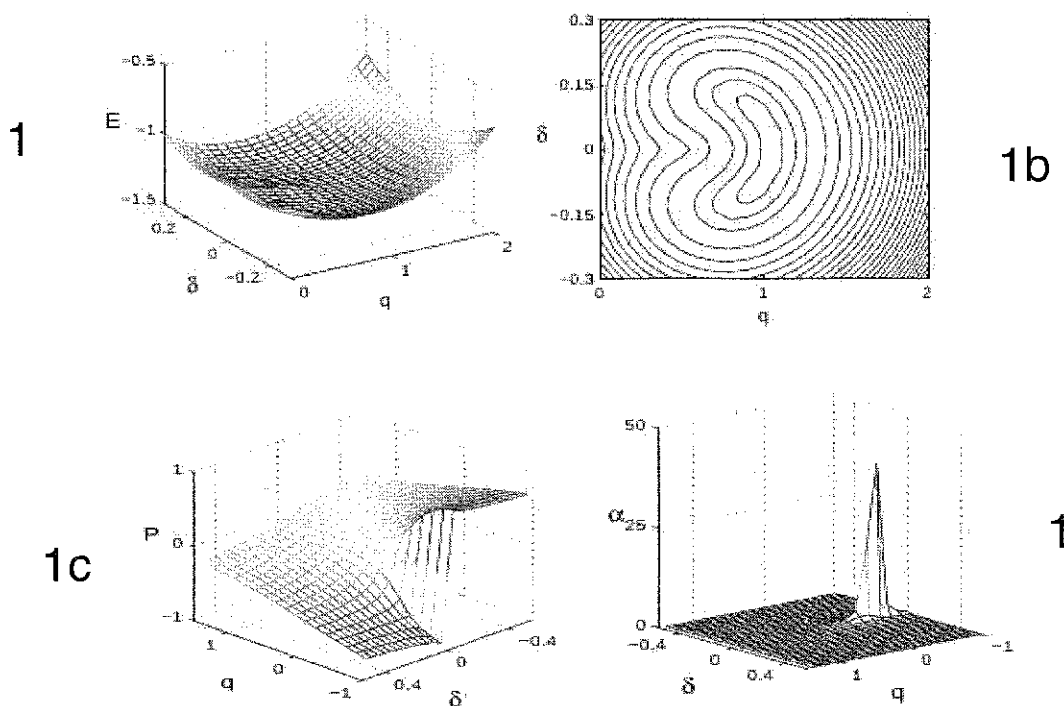
[2] A. Campion, J. E. Ivanecy, C. M. Child, M. Foster, J. Am. Chem. Soc. 117 (1995) 11807-11808

## Electron-phonon entanglement near a ferroelectric phase transition: evidences from low-frequency Raman scattering

G. D'Avino, A. Girlando, M. Masino, A. Painelli

*Dip. Chimica GIAF, Parma University & INSTM-UdR Parma, Parco Area delle Scienze, 43127 Parma, Italy*

The neutral-ionic phase transition in charge-transfer crystal offers an intriguing example of displacive ferroelectric phase transition with intrinsic quantum nature. The entanglement between delocalized electrons in 1D and lattice and molecular phonons is responsible for several unique features, including huge peaks in the dielectric constant, strong infrared intensity of the dimerization mode, and large and narrow diffuse X-ray signals. All these features have been *quantitatively* described by a modified Hubbard model accounting for two zone-center vibrations coupled to the charge-order ( $q$ , Holstein phonon) and to the ferroelectric distortion ( $\delta$ , Peierls phonon). [1] The phonons enter the model as harmonic, but the resulting potential energy surfaces are largely anharmonic in the proximity of the phase transition: this mechanical anharmonicity (fig. 1a, b) results from the interaction with delocalized electrons. [1] The modern theory of polarization ( $P$ ) and polarizability ( $\alpha$ ) is adopted for the calculation of  $q$  and  $\delta$ -dependent  $P$  and  $\alpha$  in Fig. 1c and d, demonstrating a huge electrical anharmonicity. An original implementation of the time-correlation function approach is described here to calculate infrared and Raman spectra fully accounting for anharmonicity. Calculated spectra quantitatively compare with experimental data and shed light on the observed anomalous Raman scattering in the low-frequency region in the close proximity and just below the transition temperature.



[1] L. Del Freato, A. Painelli, Z. Soos, Phys. Rev. Lett. 89 (2002) 027402; G. D'Avino et al. Phys. Rev. Lett. 99 (2007) 156407.

## Enhanced stimulated Raman scattering in silicon nanocrystals embedded in silicon-rich nitride/silicon superlattice structures

M. A. Ferrara<sup>1</sup>, L. Sirleto<sup>1</sup>, I. Rendina<sup>1</sup>, S. N. Basu<sup>2</sup>, J. Warga<sup>3</sup>, R. Li<sup>3</sup>, and L. Dal Negro<sup>3</sup>

<sup>1</sup>National Research Council-Institute for Microelectronics and Microsystems, via P. Castellino 111, I-80131 Napoli, Italy

<sup>2</sup>Division of Materials Science and Engineering, Boston University, 15 Saint Mary's Street, Brookline, Massachusetts 02446, USA

<sup>3</sup>Department of Electrical and Computer Engineering, Boston University, 8 Saint Mary's Street, Boston, Massachusetts 02215-2421, USA

Even if the possibility of light generation and/or amplification in silicon, based on Raman emission has achieved significant results [1,2], limitations inherent to the physics of silicon have been pointed out [3], too. In the last years, in order to try to overcome these limitations, an approach based on stimulated Raman scattering (SRS) in silicon nanostructures has been developed by our group [4].

In this work, we report on the observation of stimulated Raman scattering in amorphous silicon nanocrystals embedded in Si-rich nitride/silicon superlattice structures (SRN/Si-SLs). In particular, we have experimentally demonstrated amplification of Stokes signal at 1540.6 nm using a 1427 nm continuous-wavelength pump laser. In Fig. 1, the maxima of the signal wavelength scans are plotted as a function of the effective pump power both for SRN/Si-SLs and for high resistivity silicon. The maximum SRS gain obtained for SRN/Si-SLs was 0.9 dB/cm. Our data prove a threshold power (defined as the power at which the linear behaviour starts) reduction of about 40% in silicon nanocrystals ( $P_{th} \approx 150$  mW) with respect to silicon ( $P_{th} \approx 250$  mW). As shown in Fig. 1, SRN/Si-SL Raman amplifier exhibits a SRS gain significantly greater than bulk silicon; a preliminary valuation of approximately a fourfold enhancement of the gain coefficient in Raman amplifier based on SRN/Si-SLs with respect to silicon [5] can be obtained.

Our findings indicate that silicon nanocrystals embedded in Si nitride-based superlattice structures show great promise for the fabrication of more efficient Raman lasers compatible with Si technology.

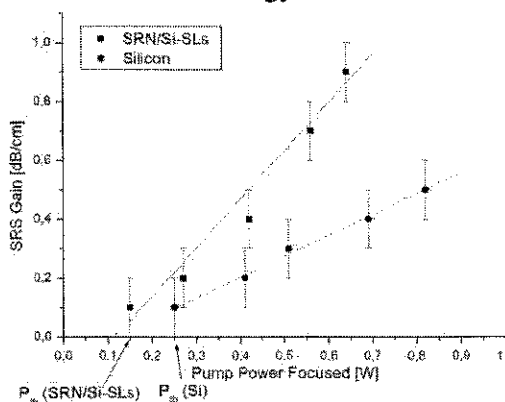


Fig. 1. The SRS-gain is plotted against the effective pump power at the sample surface both for amorphous Si nanoclusters embedded in SRN-Si-SLs and for bulk silicon.

- [1] O. Boyraz and B. Jalali, *Opt. Express* **12**, 5269 (2004).  
 [2] H. Rong, S. Xu, O. Cohen, O. Raday, M. Lee, V. Sih, and M. Paniccia, *Nat. Photonics* **2**, 170 (2008).  
 [3] B. Jalali, V. Raghunathan, D. Dimitropoulos, and O. Boyraz, *IEEE J. Sel. Top. Quantum Electron.* **12**, 412 (2006).  
 [4] L. Sirleto, M. A. Ferrara, I. Rendina, and B. Jalali, *Appl. Phys. Lett.* **88**, 211105 (2006).  
 [5] J. M. Ralston and R. K. Chang, *Phys. Rev. B* **2**, 1858 (1970).

## The dynamics of water in aqueous solutions of biological molecules assessed by broadband depolarized light scattering experiments

M. Paolantoni<sup>1</sup>, L. Comez<sup>2,3</sup>, D. Fioretto<sup>3</sup>, M. E. Gallina<sup>1</sup>, L. Lupi<sup>3</sup>, A. Morresi<sup>1</sup>, S. Perticaroli<sup>1</sup>, P. Sassi<sup>1</sup>, F. Scarponi<sup>3</sup>

<sup>1</sup>Dipartimento di Chimica, Università di Perugia – Via Elce di Sotto, 8, I-06123 Perugia, Italy

<sup>2</sup>IOM-CNR, c/o Dipartimento di Fisica, Università di Perugia – Via Pascoli, I-06123 Perugia, Italy

<sup>3</sup>Dipartimento di Fisica, Università di Perugia – Via Pascoli, I-06123 Perugia, Italy

Depolarized light scattering (DLS) spectra of aqueous solutions of carbohydrates (glucose and trehalose) were measured in a wide frequency range, going from 0.01 to 1000  $\text{cm}^{-1}$ , combining the use of a double monochromator and a multipass Fabry-Perot interferometer [1,2]. The investigated spectral range corresponds to dynamical events which modulate the anisotropic polarizability of the system at temporal scales ranging from fractions of to hundreds of picoseconds [1-3]. The spectral profiles were obtained in a range of temperatures and concentrations and analysed considering the susceptibility formalism.

Evidence is given of the existence of three distinct relaxation processes [1-4]. The slower one (hundreds of picoseconds) is interpreted in terms of the Stokes-Einstein-Debye rotational diffusion of the sugar molecules.

The other relaxation terms, characterized by picosecond relaxation times, relate to the solvent dynamics [4]. From a physical point of view these dynamical events involve molecular rearrangements connected with the rapid hydrogen bond restructuring [3,4]. The fast process (fractions of picoseconds) is attributed to the dynamics of bulk water molecules, scarcely affected by the sugar, while the slow one (few picoseconds) to local rearrangements of hydration water molecules, strongly influenced by the solute. For trehalose it is found that the dynamics of proximal water is 5-6-fold slowed down compared to the bulk and that each sugar molecule basically restricts the motion of 16-18 solvent molecules, these latter being the water molecules directly hydrogen bonded with the solute [4]. These results were discussed in comparison with the findings of other related techniques.

The studied sugars, besides representing an important class of compounds due to the role they play in biological and pharmaceutical processes, may serve as a model to gain important insight into basic hydration properties of more complex systems. In this respect the same experimental approach was lately employed for other biorelevant compounds, such as model peptides and proteins. These results will be also considered.

Overall, broadband DLS experiments were proved useful to improve our knowledge on dynamical properties of complex hydrogen bonding systems in aqueous media.

- [1] D. Fioretto, L. Comez, M. E. Gallina, A. Morresi, L. Palmieri, M. Paolantoni, P. Sassi, F. Scarponi, *Chem. Phys. Lett.* 441 (2007) 232-236
- [2] M. Paolantoni, L. Comez, D. Fioretto, M. E. Gallina, A. Morresi, P. Sassi, F. Scarponi, *J. Raman Spectrosc.* 39 (2008) 238-243
- [3] M. Paolantoni, P. Sassi, A. Morresi, S. Santini, *J. Chem. Phys.* 127 (2007) 024504/1-9
- [4] M. Paolantoni, L. Comez, M. E. Gallina, P. Sassi, F. Scarponi, D. Fioretto, A. Morresi, *J. Phys. Chem. B* 113 (2009) 7874-7878



## The pronounced structural flexibility of the 2/2 hemoglobin of the antarctic cold-adapted *Pseudoalteromonas haloplanktis* TAC125

B. D. Howes<sup>1</sup>, D. Giordano<sup>2</sup>, L. Boechi<sup>3</sup>, M. Fittipaldi<sup>1,4</sup>, D. A. Estrin<sup>3</sup>, M. Coletta<sup>5,6</sup>, G. di Prisco<sup>2</sup>, C. Verde<sup>2</sup>, and G. Smulevich<sup>1,6</sup>

<sup>1</sup>Dipartimento di Chimica, and <sup>4</sup>INSTM, Università di Firenze, Via della Lastruccia 3, I-50019 Sesto Fiorentino (Fi), Italy

<sup>2</sup>Institute of Protein Biochemistry, CNR, Via Pietro Castellino 111, I-80131 Naples, Italy

<sup>3</sup>Departamento de Química Inorgánica, Analítica y Química Física/INQUIMAE-CONICET, Facultad de Ciencias Exactas y Naturales, Universidad de Buenos Aires, Ciudad Universitaria, Pabellón II, Buenos Aires (CI428EHA), Argentina.

<sup>5</sup>Dipartimento di Medicina Sperimentale e Scienze Biochimiche, Università di Roma Tor Vergata, Via Montpellier 1, I-00133 Roma, Italy

<sup>6</sup>Consorzio Interuniversitario di Ricerca in Chimica dei Metalli nei Sistemi Biologici, Via C. Ulpiani 27, I-70126 Bari, Italy

The ability of cold-adapted organisms to survive at permanently low temperatures implies that they have overcome constraints imposed by a permanent cold environment through evolving biochemical and physiological adaptations enabling them to maintain performance and physiological functions at adequate rates in freezing habitats. To gain insight into such modifications the Hb from the cold-adapted bacterium *Pseudoalteromonas haloplanktis* is characterized by resonance Raman, electronic absorption, and electronic paramagnetic resonance spectroscopies, and different computer simulation approaches. The results indicate that *Ph-2/2HbO* has structural features typical of 2/2 Hbs [1] and especially those belonging to Group II. In particular, *Ph-2/2HbO* has Trp in position G8, and positions CD1 and B10 are occupied by Tyr (Figure 1). The ferric state of this protein, unlike other bacterial Hbs, shows an aquo hexa-coordinated high-spin form and multiple hexa-coordinated low-spin forms, where TyrCD1 and TyrB10 are likely coordinating the iron. This is the first example of a 2/2 Hb in which both TyrCD1 and TyrB10 are proposed to be the residues alternatively involved in heme hexa-coordination by endogenous ligands. The various conformers may be distinguished by the strength of the H-bond interactions with the coordinated Tyr ligand and/or disposition of the H-bonding partner. The data highlight pronounced structural flexibility, which may facilitate protein function in a cold habitat.

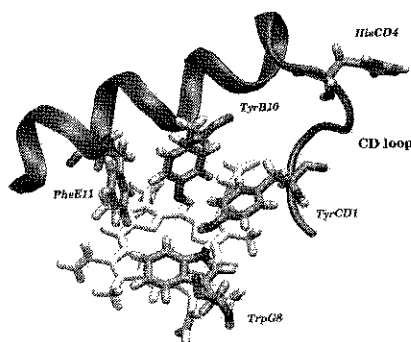


Figure 1. Distal site of the *Ph-2/2HbO* structural model, using HbO from *Bacillus subtilis* as template. The heme group and conserved polar distal residues, namely TyrB10, TyrCD1 and TrpG8, are shown.

[1] Wittenberg J. B., Bolognesi M., Wittenberg B. A., Guertin M., J. Biol. Chem. 277 (2002) 871-874.



## A Raman study of Schiff base protonation in bacteriorhodopsin and related molecular models

M. Tommasini, A. Lucotti, G. Zerbi

*Dipartimento di Chimica, Materiali e Ingegneria Chimica "G. Natta"  
Politecnico di Milano, Piazza Leonardo da Vinci 32,  
20133 Milano, Italy*

The science of the mechanism of vision as well as of the light driven proton pumping in visual membranes has been the centre of a great attention by biochemistry and biophysics. The light-triggered processes go through clearly identified changes of the molecular structure of the retinylidene chromophore which is covalently bonded to the opsin protein by a protonated Schiff base (see Figure 1). In the case of bacteriorhodopsin (bR), at specific molecular steps of the photo-cycle,  $H^+$  are taken up from the cytoplasmic medium and ejected into the extracellular medium, thus acting as a very efficient light-driven proton pump.

For investigating the peculiar molecular structure of the chromophore in bR with Raman spectroscopy, several molecular models have been considered: free retinal, unprotonated Schiff base (SB), Schiff base protonated with HCl (SB-HCl). Raman spectra have been interpreted with the help of Density Functional Theory (DFT) calculations and the Effective Conjugation Coordinate (ECC) theory [1].

In this contribution we explore the molecular origin of the so called "opsin shift", which is defined as the difference between the spectroscopic properties of a molecular model of protonated Schiff base (such as SB-HCl) and the spectroscopic properties of the retinylidene chromophore within the opsin protein. The opsin shift has been matter of many investigations [2], mainly from the point of view of electronic absorption. In this work we focus our attention on the Raman side of the opsin shift. Based on the results from calculations and experiments we conclude that the opsin shift is mainly due to the interplay existing between the  $\pi$  electrons of the retinylidene chromophore and the local environment of the proton attached to the Schiff base nitrogen atom. Simple theoretical molecular models with different counter ions interacting with the Schiff base proton display a remarkable tuning of the Raman spectra which positively compares with experimental trends and allows a sound interpretation of the data within the framework provided by ECC theory. These results pave the way for the application of Raman scattering to visual membranes in the fields of biochemistry and biophysics, even on samples in awkward experimental conditions for which Raman scattering can be still recorded in a reasonably quick and easy way.

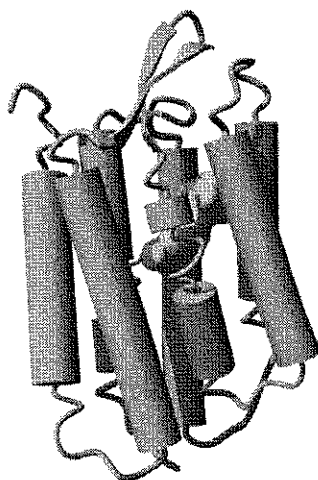


Figure 1. Drawing of the structure of bacteriorhodopsin showing the location of the Schiff base of retinal covalently bonded to the protein chain inside an hydrophobic pocket. Structure taken from the Protein Data Bank, entry 2NTW [3].

[1] C. Castiglioni, M. Gussoni, J.T. Lopez Navarrete, G. Zerbi, *Solid State Commun.* 65 (1988), 625–630; for a review see also C. Castiglioni, M. Tommasini, G. Zerbi, *Phil. Trans. R. Soc. Lond. A* (2004) 362, 2425–2459

[2] A. Altun, S. Yokoyama, K. Morokuma, *Photochemistry and Photobiology* 84 (2008) 845–854 and references therein

[3] J.K. Lanyi, B. Schobert, *J. Mol. Biol.* 365 (2007) 1379–1392.



## The thermal unfolding of lysozyme in solution: the role of the solvent

P. Sassi<sup>1</sup>, G. Onori<sup>2</sup>, A. Giugliarelli<sup>1</sup>, M. Paolantoni<sup>1</sup>, S. Cinelli<sup>2</sup>, A. Morresi<sup>1</sup>

<sup>1</sup> *Dipartimento di Chimica, Università di Perugia, Via Elce di sotto 8, 06123 Perugia, Italy*

<sup>2</sup> *Dipartimento di Fisica, Università di Perugia, Via Pascoli, 06123 Perugia, Italy*

The study of the structural properties of proteins is fundamental in order to access the comprehension of their biological function. For some time, sugars have been recognized as stabilizers of the protein conformation[1-3]; on the contrary, small monohydric alcohols such as methanol, ethanol and propanol show the opposite effect[4-7]. Alcohol and water compete with each other on forming H-bonds on the solvent-exposed surface of the protein molecule but the hydrocarbon functionalities of the alcohol can also attracts the hydrophobic targets and displace water thus leading to conformational consequences. In the present study a the thermal unfolding of lysozyme in D<sub>2</sub>O and D<sub>2</sub>O/CH<sub>3</sub>CH<sub>2</sub>OD solutions is performed by means of FTIR spectroscopy. The detailed investigation of the conformational rearrangement of the protein upon heating is achieved from inspection of the amide bands. The local modification of the folded state of lysozyme in D<sub>2</sub>O solution is observed at a temperature close to physiologic conditions; on the contrary, the analysis of the pre-melting rearrangement of secondary structure in the mixed solvent is not indicative of a conformational transition. The effects of partial and total deuteration on inner amide groups of the macromolecule are also investigated. The kinetics of H/D exchange on these functionalities is followed along the temperatures of the melting process; our results suggest that the complete exposure of inner sites of the molecule to the solvent is transiently achieved by the global unfolding of the polypeptide chain and that the simple two-state model accounts for the unfolding and the exchange process of lysozyme in both environments.

- [1] M. Paolantoni, L. Comez, M.E. Gallina, P. Sassi, F. Scarponi, D. Fioretto, A. Morresi, J. Phys. Chem. B, 113 (2009) 7874
- [2] A. Lerbret, F. Affouard, P. Bordat, A. Hédoux, Y. Guinet, M. Descamps, J. Chem Phys. 131 (2009) 245103
- [3] T.F. O'Connor, P.G. Debenedetti, J.D. Carbeck, J. Am. Chem. Soc., 126 (2004) 11794
- [4] A. Bonincontro, A. De Francesco, M. Matzeu, G. Onori, A. Santucci, Colloids and surfaces B, 10 (1997) 105
- [5] S. Cinelli, G. Onori, A. Santucci, Colloids and surfaces B, 160 (1999) 3
- [6] W. Liu, D. Bratko, J.M. Prausnitz, H.W. Blanch, Biophys. Chem., 107 (2004) 289
- [7] K. Sasahara, K. Nitta, Proteins, 63 (2006) 127





## Ion beam induced defects in graphene: Raman spectroscopy and DFT calculations

G. Compagnini<sup>1</sup>, G. Forte<sup>1</sup>, F. Giannazzo<sup>2</sup>, V. Raineri<sup>2</sup>, A. La Magna<sup>2</sup>, I. Deretzis<sup>2</sup>

<sup>1</sup>*Dipartimento di Scienze Chimiche, Università di Catania, Viale A.Doria 6 Catania 95129, Italy*

<sup>2</sup>*CNR-IMM, Strada VIII, 5, Catania 95121, Italy*

Carbon nanomaterials are becoming day by day much more important for basic science and applied technology. It is possible to obtain in a controlled way structures such as wires, tubes and sheets of arbitrary form and nearly arbitrary extension. In particular graphene, a two-dimensional (2D) sheet of carbon atoms arranged in a honeycomb lattice, attracted recently a huge scientific interest, due to its outstanding transport properties, chemical and mechanical stability and to the scalability of graphene devices to nano-dimensions[1,2].

The study of defects and impurities in single layer and few layers graphene is of crucial importance to understand and predict the behaviour of such material. In fact, the intentional or unintentional presence of those defects strongly affects the electronic transport properties of graphene devices.

On the other hand Raman spectroscopy is considered the most powerful spectroscopic technique to study carbon based materials due to the specific response to any change in carbon hybridization state as well as the introduction of defects or foreign species.

This paper is devoted to compare a number of experimental Raman results, obtained on ion irradiated single and multilayer graphene samples, with theoretical obtained through DFT calculations. In particular we simulate the Raman spectra and discuss the Raman lines associated either with the defects and/or with the existence of spatially confined nano-domains, in such a way to be adopted as their signatures.

[1] K.S.Novoselov, A.K.Geim, S.V.Morozov, D.Jiang, Y.Zhang, S.V.Dubonos *Science* 306 (2004) 666–669

[2] J.H.Chen, C.Jang, S.Xiao, M.Ishigami, M.S.Fuhrer, *Nat.Nanotechnol.* 3 (2008) 206–209

[3] G.Compagnini, F.Giannazzo, S.Songe, V.Raineri, E.Rimini *Carbon* 47 (2009) 3201–3207



## Spectroscopic Analyses on Rock Art Paintings from East Central Ethiopia

C. Lofrumento<sup>1</sup>, M. Ricci<sup>2</sup>, L. Bachechi<sup>3</sup>, D. De Feo<sup>1</sup>, E. M. Castellucci<sup>1,4</sup>

<sup>1</sup>Department of Chemistry, Polo Scientifico e Tecnologico, University of Florence, via della Lastruccia 3, 50019, Sesto Fiorentino (Fi), Italy

<sup>2</sup>Department of Restoration and Conservation of the Architectural Heritage, University of Florence, via Micheli 8, 50121, Florence, Italy

<sup>3</sup>Department of Science of the Antiquity "G. Pasquali", University of Florence, piazza Brunelleschi 3-4, 50121, Florence, Italy

<sup>4</sup>LENS- European Laboratory for Non-Linear Spectroscopy, University of Florence, via Nello Carrara 1, 50019, Sesto-Fiorentino (Fi), Italy

The present research work is aimed at the study of various colored samples from rock art paintings of the Harar region (Eastern Central Ethiopia), found in recently documented sites. The sites are shelters keeping paintings belonging to a stylistic current named Ethiopian-Arabian, spread on the whole territory of the Horn of Africa between the third and the second Millennium BC [1, 2]. The study was carried out in order to characterize the pigments employed in the realization of paintings, as well as to verify the likely presence of organic material, to better evaluate the pictorial execution.

The samples were subjected to different spectroscopic techniques, such as micro-Raman microscopy ( $\mu$ R), Attenuated Total Reflectance (ATR) and Laser Induced Breakdown Spectroscopy (LIBS), which are micro-destructive, furnishing appreciable results by means of a reduced quantity of sample.

$\mu$ R analysis, performed on red, black as well as white paintings, permitted to identify the pigments used for the mural paintings. The pigments found resulted made of material very common in the rock art documented so far [3]: hematite for red, Goethite for yellow, gypsum and calcite for white, whereas amorphous carbon, which has probably a vegetable origin, for black.

The search for organic matter was accomplished by  $\mu$ R, which revealed the presence of beeswax in one sample, and by ATR, that exhibited the same organic material in manifold samples. The origin of beeswax is not univocally defined yet, but it may be utilized as a binder mixed to water, where pigments were dispersed [4]. It may be also applied in a subsequent period to better observe the drawings.

An important result was the baring of the monohydrated calcium oxalate, detected with all the techniques on the totality of the samples, in the form of little crystals dispersed in the surrounding stuff [5]. Its origin could be of biological type [6, 7], or due to the chemical transformation of a natural substance, such as cactus extracts, used as a pictorial binder [8]. In order to furnish an experimental checking to this hypothesis, the inner matter of a cactus leaf was extracted; the gathered stuff contained aggregates of white crystals, identified as whewellite crystals.

[1] P. Červíček, 1978-79 – Rassegna di Studi Etiopici, XXVII (1978-79) 5-12

[2] J. D. Clark, The Prehistoric Culture of the Horn of Africa, London, (1954)

[3] H. G. M. Edwards, Raman Spectr. in Art and Archeology, cap. 5, (2005)

[4] P. Vandenaabeele, B. Wehling, H. Edwards, M. De Reu, G. Van Hooydonk, Anal. Chim. Acta, 407 (2000) 262-274

[5] L. R. Frost, Anal. Chim. Acta, 517 (2004) 207-214

[6] L. Lazzarini, O. Salvadori, Studies in Conservation, 34 (1989) 20-26

[7] P. Adamo, P. Violante, Appl. Clay Science, 16 (2000) 229-256

[8] N. Cole, A. L. Watchman, Rock Art Research, 9 (1992) 27-36



## Combined analysis of structural and spectral observables for heme proteins

M. P. Marzocchi, A. Belshi

*Università di Firenze, Dipartimento di Chimica "Ugo Schiff", Via della Lastruccia, 3-13, 50019 Sesto Fiorentino (Fi), Italy*

A semi-empirical model, based on the quantum theory, which is the extension of a previous empirical relationship for the heme chromophore of several plant peroxidases and some globins [1], is presented.

The approach concerns the analysis of observables such as the frequencies ( $\text{cm}^{-1}$ ) of electronic absorption (Soret and CT1 transitions) and resonance Raman ( $\nu_3$  core-size and  $\nu_{\text{C}=\text{C}}$  vinyl modes) spectra and the Fe-Ligand distances ( $\text{\AA}$ ).

We used functions,  $f(\tau; \delta_{iv})$ , of the torsion angles,  $\tau$ , of the three peripheral substituents,  $i = 2, N, 4$ , for 2-vinyl, proximal imidazole, and 4-vinyl, respectively.

The observed frequency,  $\nu$ , is scaled within two limiting values ( $\nu_{\text{max}} - \nu_0$ ) by the function,  $f(\tau; \delta_{iv})$ . The function, expressed in terms of polar coordinates, is a combination of spherical harmonics (2D  $f(\phi; \delta)$ , and 3D  $f(\theta, \phi; \delta)$ ), as regulated by the phase angle,  $\delta_{iv}$ , a characteristic parameter of the observable. The origin of all the functions is placed at the central Fe atom, therefore the electron-nucleus and atom-atom distances have not been considered as variables.

The FeO, FeN<sub>Im</sub>, and FeN<sub>Core</sub> displacements for each mode are, however, taken as observables involving the functions of the torsion angles,  $\tau$ ,  $f^{2n}(\tau; \delta_{ir})$ , that include the heme-protein interactions. The observed distance,  $r$ , is scaled within two limiting values ( $r_{\text{max}} - r_0$ ) by the function,  $f^{2n}(r; \delta_{ir})$ , being  $n = 1, 3, 6$ .

The  $r(\text{Fe-Ligand})$  distances can be determined with high accuracy (0.01  $\text{\AA}$  resolution) from spectral [2] and structure (Protein Data Bank) data by the ratio  $\nu/r$  (eq.1) once the limiting frequency ( $\nu_{\text{max}}, \nu_0$ ) and distances ( $r_{\text{max}}, r_0$ ) are known.

$$\nu = \nu_0 + (r - r_0) (\nu_{\text{max}} - \nu_0) 1/3 \sum_n 1/2^n f^{2n}(\tau; \delta_{iv}) / (r_{\text{max}} - r_0) 1/3 \sum_n 1/2^n f^{2n}(\tau; \delta_{ir}) \quad (1)$$

If  $\delta_{iv}$  is substituted by  $\delta_{ir}$  a very simple straight line equation (eq.2) is obtained:

$$\nu = \nu_0 + (r - r_0) (\nu_{\text{max}} - \nu_0) / (r_{\text{max}} - r_0) \quad (2)$$

For each observable three straight lines with different slopes for FeO, FeN<sub>Im</sub>, and FeN<sub>Core</sub>, respectively, have been obtained together with the calculated frequencies according eq. 2. The corresponding FeO, FeN<sub>Im</sub>, and FeN<sub>Core</sub> distances are coincident for all the four observables and identical to the data obtained by X-rays, i.e. they are ground state distances.

The excited state distances, deriving from the observed and calculated frequencies according to the  $f^{2n}(\tau; \delta_{iv})$  function, indicate the Fe-ligand displacement vectors involved for each RR mode.

In conclusion, the model also allowed us to determine the axial ligand distances by using  $\nu(\text{Fe-N}_{\text{Im}})$  [2] and  $\nu(\text{Fe-O})$  [3] RR frequencies and only few X-Rays data.

[1] M.P. Marzocchi, G. Smulevich, J. Raman Spectrosc. 34 (2003) 725-736

[2] G. Smulevich, A. Feis, B.D. Howes, Acc. Chem. Res. 38 (2005) 433-440

[3] A. Feis, M.P. Marzocchi, M. Paoli, G. Smulevich, Biochemistry 33 (1994) 4577-4583



## Resonance Raman and UV-vis absorption spectra of *Thermobifida fusca* truncated hemoglobin in its ferric state.

F.P. Nicoletti<sup>1</sup>, E. Droghetti<sup>1</sup>, A. Feis<sup>1</sup>, A. Boffi<sup>2</sup>, G. Smulevich<sup>1</sup>

<sup>1</sup>Dipartimento di Chimica, Università di Firenze, Via della Lastruccia 3, I-50019, Sesto Fiorentino (FI), Italy

<sup>2</sup>Dipartimento di Scienze Biochimiche e Istituto CNR di Biologia Molecolare e Patologia, Università di Roma "La Sapienza", Piazzale Aldo Moro 5, I-00185 Roma, Italy

Truncated hemoglobin (trHb) have been documented in the last 20 years in bacteria, unicellular eukaryotes and plants, and they constitute a distinct phylogenetic group within the hemoglobin (Hb) superfamily [1]. TrHbs are small hemoproteins, typically 20-40 residues shorter than mammalian Hbs, and they exhibit the typical two-over-two  $\alpha$ -helical fold. High affinity for oxygen and sulphide [2,3] and peroxidase activity [4] have been reported for trHbs, but their function is not completely clear. TrHbs are divided into three groups [1] and *Thermobifida fusca* (Tf) belongs to the group II, the most populated of the three, and characterized by the presence in the distal cavity of three residues, TrpG8, TyrB10 and TyrCD1 (Figure 1), providing three potential hydrogen bondings to the sixth coordinated heme axial ligand.

The present study concerns the characterization of the wild-type ferric form, in the presence and in the absence of exogenous ligands such as fluoride, hydroxide and sulphide. The charge transfer band, from  $\pi$  porphyrin orbitals to  $d\pi$  iron orbitals, in the UV-Vis absorption spectra and the Fe-ligand stretching modes in the low-frequency resonance Raman spectra allowed us to understand how the distal residues stabilize the ligand in the sixth position [5]. Moreover, in order to highlight the role of the distal residue(s) for ligand stabilization, we have studied single, double, and triple Phe mutants at positions G8, B10 and CD1. All the results indicate that TrpG8 provides the strongest hydrogen-bonding, whereas TyrCD1 plays an ancillary role.

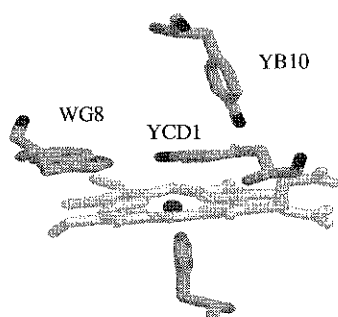


Figure 1. Key residues of the heme cavity from *Thermobifida fusca* [2].

- [1] Wittenberg J. B., Bolognesi M., Wittenberg B. A., Guertin M., J. Biol. Chem. 277 (2002) 871-874.
- [2] Bonamore, A. Ilari, A., Giangiacomo, L., Bellelli, A., Morea, V., Boffi A., Febs J. 272 (2005) 4189-4201.
- [3] Nicoletti F.P., Comandino A., Bonamore A., Boechi L., Boubeta F.M., Feis A., Smulevich G., Boffi A., Biochemistry (2010), in press.
- [4] Torge R., Comandini A., Catacchio B., Bonamore A., Botta B., Boffi, A. J. Mol. Catalysis B: Enzymatic. 61 (2009) 303-308.
- [5] Feis A., Lapini A., Catacchio B., Brogioni S., Foggi P., Chiancone E., Boffi A., Smulevich G., Biochemistry 47 (2008) 902-910.

## Raman spectroscopic study of the effects of ion solvation on liquid phase structure and dynamics of LiI–acetone solutions

F. Palombo<sup>1</sup>, P. Sassi<sup>1</sup>, M. Paolantoni<sup>1</sup>, A. Morresi<sup>1</sup>, and M. G. Giorgini<sup>2</sup>

<sup>1</sup>Department of Chemistry, University of Perugia, Via Elce di sotto 8, 06123, Perugia, Italy

<sup>2</sup>Department of Physical and Inorganic Chemistry, University of Bologna, Viale del Risorgimento 4, 40136, Bologna, Italy

Electrolyte solutions of halide and perchlorate salts, mainly lithium, in non-aqueous solvent have attracted much attention in the past decades due to their employment in electrochemical field. Both ion–solvent and ion–ion interactions may contribute to the structure and dynamics of such systems at an ionic/molecular level, and their specific role depends on the involved species. Acetone is a widely-used solvent with fairly low electron donicity and relative permittivity, and these properties can account for the occurrence of ion aggregates along with single ions in solution. Lithium iodide is moderately soluble in acetone; with its strong -almost covalent- bonds, it is a good candidate to study the modulation of intermolecular (dipolar) interactions in acetone by ion addition.

The vibrational spectroscopic investigation of electrolyte systems, such as LiI–acetone solutions at different concentration, constitutes an important approach to the study of solvation and association processes. Raman and depolarized Rayleigh scattering (DRS) are especially suitable for physicochemical studies in condensed phase allowing information to be obtained on system structure as well as molecular dynamics[1-4]. Low frequency Raman spectra of LiI–acetone solutions will be presented and ion association in this system will be discussed for very low concentrations of the electrolyte.

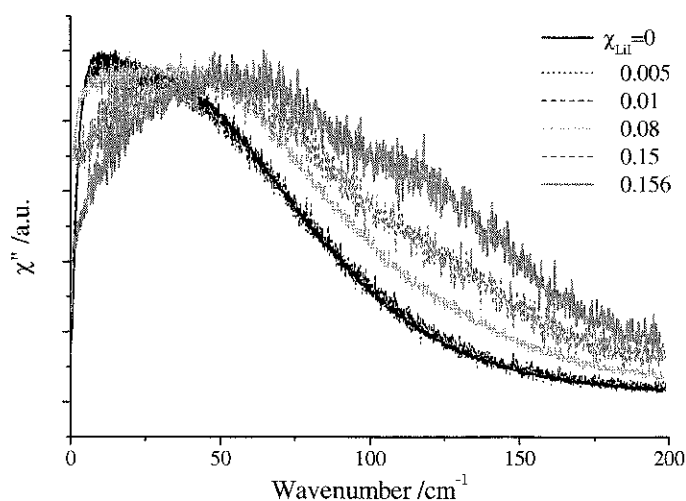


**Figure.** Evolution of the susceptibility representation of the low-frequency DRS spectrum of the LiI–acetone solution as a function of solute mole fraction, in the range  $5 \times 10^{-3}$  to 0.156 (saturated solution). The spectrum of neat acetone is also presented.

- [1] M. Paolantoni, P. Sassi, A. Morresi, S. Santini, *J. Chem. Phys.* 127 (2007) 024504
- [2] M. Paolantoni, L. Comez, D. Fioretto, M.E. Gallina, A. Morresi, P. Sassi, F. Scarponi, *J. Raman Spectrosc.* 39 (2008) 238-243
- [3] P. Sassi, M. Paolantoni, S. Perticaroli, F. Palombo, A. Morresi, *J. Raman Spectrosc.* 40 (2009) 1279-1283
- [4] M. Paolantoni, L. Comez, M. E. Gallina, P. Sassi, F. Scarponi, D. Fioretto, A. Morresi, *J. Phys. Chem. B* 113 (2009) 7874-7878



## Photoelectron imaging on Iodine atoms produced by CF<sub>3</sub>I photodissociation

G. Piani<sup>a</sup>, L. Rubio-Lago<sup>b</sup>, M. Becucci<sup>c</sup>

*LENS – European Laboratory for Non-linear spectroscopy,  
Polo Scientifico e Tecnologico dell'Universita', via Nello Carrara, 1, Sesto Fiorentino (Firenze), Italy*

*<sup>a</sup> now at Laboratoire Francis Perrin, CEA Saclay, France*

*<sup>b</sup> now at Universidad Complutense, Madrid, Spain*

*<sup>c</sup> also at Dipartimento di Chimica, Universita' di Firenze, Italy*

We have recorded photoelectron image from REMPI detection of Iodine atoms produced in CF<sub>3</sub>I photodissociation in order to test the LENS imaging apparatus with respect to electron detection. We have obtained similar results to those already present in the literature, but thanks to the resolution achievable with this apparatus we are able to point out the presence in the photoelectron spectrum of features that were not well resolved, and that are still waiting for a clear interpretation.



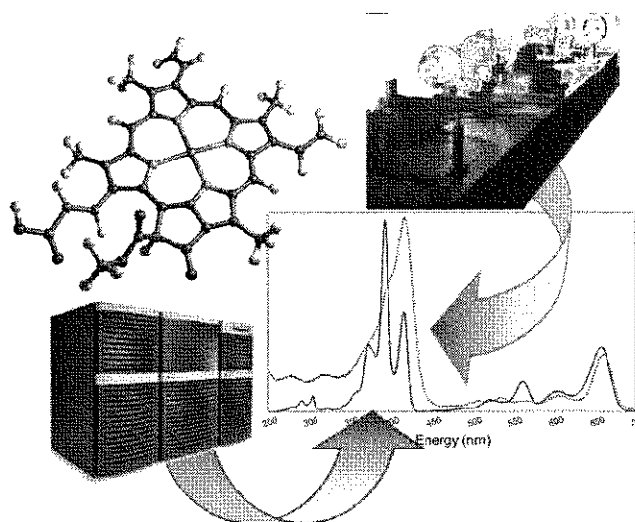
## Computational spectroscopy as a tool to interpret experimental results: from small molecule in the gas phase to large systems in condensed phases.

M. Biczysko<sup>a,b</sup>

<sup>a</sup>*Scuola Normale Superiore, piazza dei Cavalieri 7, 56126 Pisa, Italy*

<sup>b</sup>*Università di Napoli Federico II, Complesso Univ. Monte S. Angelo, via Cintia, 80126 Napoli, Italy*

The subtle interplay of several different effects still makes the interpretation and analysis of experimental spectra in terms of structural and dynamic characteristics a very challenging task. In this context, theoretical studies can be very helpful and this is the reason behind the rapid evolution of computational spectroscopy from a highly specialized research field toward a versatile and widespread tool. However, in the case of electronic spectra (UV-vis, Circular Dichroism, photoelectron, X-ray, etc.), the most popular approach still relies on computation of vertical excitation energies, which are further convoluted to simulate line-shapes. Such a treatment completely neglects the influence of nuclear motions, despite the well recognized notion that proper account of vibrational effects is often mandatory in order to interpret correctly the experimental findings. In this respect, the generation of reliable spectra including the vibronic contributions has become recently feasible even for medium-to-large systems. Here, we present the implementation of an effective procedure rooted into a time-independent model [1,2], integrated in a general-purpose computational chemistry package, offering the possibility to evaluate simply one-photon electronic spectra, using several electronic models [3]. In particular the DFT/N07 scheme [4] coupling a remarkable reliability in the computation of geometric, vibrational and electronic properties with a very favorable scaling with the number of electrons, allows reliable studies of compounds of biological or technological interest. Some specific examples from small molecules in the gas phase to large systems in condensed phases will be discussed to illustrate our recent integrated approach.



- [1] J. Bloino, M. Biczysko, F. Santoro, V. Barone, *J. Chem. Theory Comput.* 6, 1256-1274 (2010)
- [2] V. Barone, J. Bloino, M. Biczysko, F. Santoro, *J. Chem. Theory Comput.* 5, 540-554 (2009)
- [3] A. Pedone, M. Biczysko, V. Barone, *ChemPhysChem*, 11, 1812-1832 (2010)
- [4] V. Barone, J. Bloino, M. Biczysko, *Phys. Chem. Chem. Phys.* 12, 1092-1101 (2010)



## Raman microspectroscopic study of organic inclusions in „watermelon” tourmaline from the Paprok mine (Nuristan, Afganistan)

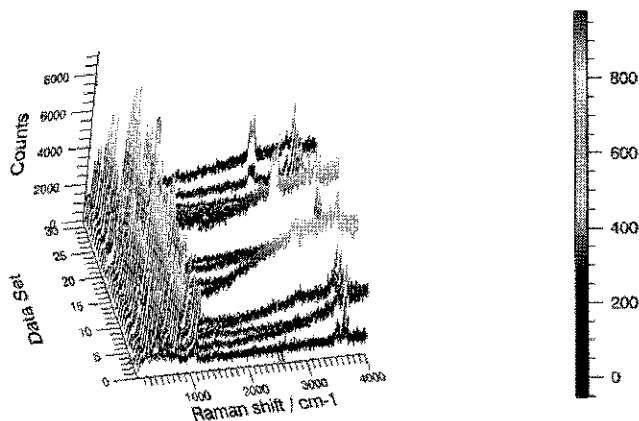
A. Weselucha-Birczyńska<sup>1</sup>, L. Natkaniec-Nowak<sup>2</sup>

<sup>1</sup> Faculty of Chemistry, Jagiellonian University, Ingardena 3, 30-060 Kraków, Poland

<sup>2</sup> Faculty of Geology, Geophysics and Environmental Protection, AGH-University of Science and Technology, al. Mickiewicza 30, 30-059 Kraków, Poland

Only a few articles of Afghan tourmalines were published in the scientific literature in 80th of the last century [1-3]. Some mineralogical description and information about deposits localization appeared later [4,5].

The investigated „watermelon” tourmaline shows characteristic zones of different tourmaline components, differing with colors and chemical content [6]. The Raman microspectroscopic study, were performed with a Renishaw InVia working in confocal mode. Line mapping experiment, from the core of the cross-cut mineral toward the rim, is presented in the Figure. The spectra demonstrate, besides characteristic tourmaline bands [7] at: 223, 731, 1070 3489, 3594 and 3658  $\text{cm}^{-1}$ , also some new bands at: 836, 2855, 2895 and 2928  $\text{cm}^{-1}$ . New bands show up in the spectra of typical, higher background, what signify the concentration of the organic matter as well as liquid hydrocarbons. The Raman spectra are the best markers of the position of the particular zones.



**Acknowledgements:** This work has been supported by the Polish Ministry of Science and Higher Education, Statutory Research.

- [1] A.F. De Lapparent, *Rev. Géogr. Phys. Géol. Dynam.* 14 (1972) 327-344
- [2] G. Fuchs, A. Matura, O. Scherman, *Verh. Geol. Bundesanst. Österr.* 1 (1974) 9-23
- [3] P. Bariand, J.F. Poullen, *Mineral. Rec.* 9 (1978) 301-308
- [4] G.W. Bowersox *Gems & Gemol.* 21 (1985) 192-204
- [5] G.W. Bowersox, B.E. Chamberlin., *Gemstones of Afghanistan*, Geoscience Press, Tucson, Arizona, 1995
- [6] L. Natkaniec-Nowak, M. Dumańska-Słowik, A. Ertl, *N. Jb. Miner. Abh.* 186/2 (2009) 185-193.
- [7] B. Gasharova, B. Mihailova, L. Konstantinov, *Eur. J. Mineral.* 9 (1997) 935-940





## Raman Spectroscopy Investigations of a Chitosan-Clay Nanocomposite

C. Paluszkiwicz<sup>1</sup>, A. Weselucha-Birczyńska<sup>2</sup>, E. Stodolak<sup>3</sup>

<sup>1</sup>AGH – University of Science and Technology, Faculty of Materials Science and Ceramics, Department of Silicates Chemistry, al. Mickiewicza 30, 30-059 Krakow, Poland

<sup>2</sup>Jagiellonian University, Faculty of Chemistry, Department of Chemical Physics, Ingardena 3, 30-060 Krakow, Poland

<sup>3</sup>AGH – University of Science and Technology, Faculty of Materials Science and Ceramics, Department of Biomaterials, al. Mickiewicza 30, 30-059 Krakow

Polymer/clay nanocomposites receive much attention as novel materials originating from the renewable sources. A typical example of a material belonging to this group is chitosane (CS) which is a cationic natural polysaccharide that can be produced by alkaline N-deacetylation of chitine.

In the present work we investigate synthesis and structure of novel polymer/clay nanocomposites based on biodegradable polymer – chitosane (CS).

Commercially available chitosane with deacetylation degree of 75-85% (Sigma-Aldrich) was used in the investigations. Natural montmorillonite MMT-K10 (Sigma-Aldrich) with the grain size of 60 to 80 nm was used as a nanofiller. Nanocomposite samples in the form of thin foils were produced by a casting method.

Organic-inorganic hybrid materials based on chitosane and nanoclay (montmorillonite, MMT) were characterized by vibrational spectroscopy methods (Micro-Raman spectroscopy and FT-Raman spectroscopy) and the scanning electron microscopy (SEM/EDS). It was shown, that small amount of a nanofiller (MMT, 3 wt.%) used to modify the polymer matrix influences the structure of the polymeric chains.

The level of dispersion of the nanofiller particles was investigated using SEM/EDS (FTI Nova NanoSEM). The selected samples were analyzed by means of Micro-Raman spectroscopy and FT-Raman spectroscopy. FT-Raman spectra were obtained using a FTS6000 Bio-Rad spectrometer with Ge detector. The samples were excited with a Nd-YAG laser (1064nm). The MicroRaman spectra were recorded with Renishaw InVia Raman spectrometer coupled with Leica microscope. This coupling permits to work in a confocal mode. The samples were excited with the 785 nm line of the HPNIR laser. In order to determine the exact positions, bandwidths and relative intensities of the bands, the spectra were deconvoluted. A comparative analysis of CS and CS/MMT spectra showed subtle differences in bands related to C-C bonds (c.a. 1560 cm<sup>-1</sup>) and C-N bonds (c.a. 1460 cm<sup>-1</sup>). Decrease of intensity of 1410 cm<sup>-1</sup> band could be the effect of interaction between side groups of chitosane and hydroxyl groups of MMT. This tendency was observed in all Raman shifts independent of the technique (Micro-Raman, FT-Raman).

**Acknowledgments:** This work was financially supported by The Ministry of Science and Higher Education, grant No. N N507 370735.



## Author index

- Abbotto A.....281  
 Abbruzzetti S. .... 356; 373  
 Abramczyk H. .... **13; 91**; 278  
 Adamczyk A. ....46  
 Agaeva G. .... 131; 133  
 Aguiar E. C. ....**258**  
 Airinei A. ....344  
 Akalin E. ....**213**  
 Akkaya Y. .... 124; **137**  
 Akriche S. M. ....268  
 Akyuz S.93; **107**; 124; 131; 133; 137; 213;  
**311**  
 Akyuz T. .... 93; 107; 311  
 Al-Andis N. M. ....156  
 Albelda M. T. ....136  
 Albini A. ....348  
 Albrecht M. ....308  
 Aleksa V. ....283  
 Alenkina I.V. ....88  
 Al-Hokbany N. S. ....268  
 Al-Khamis Kh. M. ....**156**  
 Alloisio M. .... **173**; 207; 269  
 Al-Othman Z. ....156  
 Al-Saadi A.A. ....230  
 Amaral G. A. ....231  
 Amat A. ....**29**  
 Amendola v. ....**376**  
 Anashkin A. ....248  
 Andronie L. ....**108**  
 Andrushchenko V. .... 160; **364**  
 Angelova P. ....186  
 Anglos D. ....**3**  
 Araki T. ....92  
 Aramomi S. ....162  
 Araujo-Andrade A. ....252  
 Ardelean I. ....305  
 Arenas J.F. .... 222; 226; 229  
 Arisan E. D. ....107  
 Arregui A. ....231  
 Astilean S. .... 52; 106; 118; 224; 225  
 Ataç A. ....306  
 Atsbeha T. ....**279**  
 Avadanei M. ....**267**  
 Avaldi L. ....232  
 Aytakin Aydın M. T. .... **168**; 169  
 Baban O. ....193  
 Bachechi L. ....387  
 Baffa C. ....66  
 Bağlayan Ö. ....**169**  
 Bajda T. ....36  
 Bajnóczy É.G. ....154  
 Bakker H. J. ....16  
 Bakulin A. A. ....16; **243**  
 Balarin M. ....190; **195**; 324  
 Balci K. ....107; **124**; 137  
 Balevicius V. ....**283**; **295**; 335  
 Balevicius V. Jr. ....244  
 Balzani V. ....**11**  
 Bañares L. ....231  
 Baraldi C. ....63  
 Baraldi P. ....**42**; **63**  
 Baran A. ....**217**  
 Baranović G. ....57  
 Baranska M. ....217  
 Barboiu V. ....267  
 Barczyński P. ....291; **329**  
 Barlea M. ....179  
 Barone G. ....60; 61  
 Barras A. ....349  
 Barth A. .... 20; **102**; 135; 211; 292; 363  
 Bartoszek M. ....41; 43; 346  
 Basu S. N. ....381  
 Batista de Carvalho L. A. E. ....323  
 Bauman D. ....**184**  
 Baumruk V. .... 72; 84; 103; 119; 132; 143  
 Bayrak C. ....168  
 Bebu A. .... **69**; 96; 215; 310  
 Becker P. ....316  
 Becucci M. ....352; **354**; 391  
 Bednářová L. ....**95**; 103; 119  
 Belić D. S. ....234  
 Bellanato J. ....**141**  
 Belogurova N. ....**77**  
 Belshi A. ....388  
 Ben Altabef A. ....**314**  
 Benassi E. ....99  
 Benedetti L. ....27  
 Berindean C. ....69  
 Berkovsky A. L. ....89  
 Berneschi S. ....174  
 Bertarelli C. ....15  
 Bhaktha S. N. B. ....174  
 Bicanic D. ....**4**  
 Bichara L. C. ....262



## AUTHOR INDEX

- Biczysko M. .... **375; 392**  
 Bidzińska E. .... 298  
 Bielejewska N. .... 184  
 Billes F. .... 160  
 Billinghurst B.E. .... 326  
 Bini R. .... 300; 340; 357; 372  
 Blanc S. .... **28**  
 Blazewicz M. .... 205  
 Błazewicz S. .... 148; 192  
 Blomberg M. .... 20  
 Boca S. .... **106**  
 Boczar M. .... 246; 274  
 Boda Ł. .... 246; 274  
 Boechi L. .... 383  
 Boffi A. .... 356; 373; 389  
 Bogdan M. .... 315  
 Bohaty L. .... 316  
 Bojko B. .... 97; 98  
 Bok J. .... 56  
 Bonamore A. .... 356; 373  
 Bonoldi L. .... 53  
 Bonora S. .... 99  
 Borzęcka-Prokop B. .... 121  
 Bosca M. .... 177  
 Boschiero N. .... 27  
 Boscolo I. .... 354  
 Bouazaoui M. .... 174  
 Bouř P. .... 72; 110; 143; 160; 364  
 Bourhis K. .... 28  
 Bozio R. .... 277  
 Brambilla L. .... 63  
 Brandán S. A. .... **257; 262; 290**  
 Bratu I. .... 214  
 Brehm G. .... 26  
 Breitinger D. K. .... **26**  
 Brożek-Pluska B. .... 91; **278**  
 Brunetti B. G. .... 21  
 Bruździak P. .... **128**  
 Brycki B. .... 101  
 Bryndal I. .... **196; 343**  
 Buljan M. .... 197  
 Buřova T. .... **248**  
 Bussotti L. .... 276; 279  
 Butkus V. .... 244  
 Çalıřır Z. .... 306  
 Caminati W. .... 238; 301; 355; 374  
 Cancio Pastor P. .... 66  
 Candelaresi M. .... 276  
 Canesi E. V. .... 15  
 Canton S.E. .... 154  
 Capoen B. .... 174  
 Capozzi V. .... 65  
 Cardini G. .... 64; 251; 271; 300  
 Carofiglio T. .... 367  
 Cartechini L. .... 29  
 Castellano G. .... 114  
 Castelli F. .... 354  
 Castellucci E.M. .... 25; 31; 352; 370; 387  
 Castiglioni C. .... **15; 249; 261**  
 Castro J.L. .... 222; **226**  
 Cazzoli G. .... 237  
 Cazzolli G. .... 378  
 Čeh M. .... 167  
 Cejkova J. .... 183; 221; 360  
 Çelik B. .... 138  
 Celik S. .... **131; 133**  
 Čeponkus J. .... 70  
 Ceppatelli M. .... 340; **357; 372**  
 Chalifoux W.A. .... 325  
 Chatgialoglu C. .... 71  
 Chelcea R. .... 178; 179  
 Chernev B. .... 150  
 Cheshmedzhieva D. .... 23; 350  
 Chiasera A. .... 197  
 Chiş V. .... 37; 69; 100; 139; 228; **275; 303;**  
     315  
 Chlopek J. .... 202  
 Chojnacki H. .... 298  
 Chowdhry B. Z. .... 73  
 Christensson N. .... 244  
 Chruszcz-Lipska K. .... **331**  
 Ciągka P. .... 278  
 Cialdi S. .... 354  
 Cicchi S. .... 279  
 Cieslarova Z. .... 18  
 Cinelli S. .... 385  
 Cîntă Pînzaru S. .... 80; 96; **284**  
 Citroni M. .... **300; 340**  
 Clupek M. .... 18; 183; 221; 360  
 Coker A. .... 107  
 Coletta M. .... 383  
 Collini E. .... **277; 366**  
 Colombatti M. .... 376  
 Coluccio M. L. .... 358; 371  
 Comelli D. .... 25  
 Comez L. .... 382  
 Compagnini G. .... **386**  
 Contreras C. D. .... 257  
 Copeland G. .... 342  
 Coreno M. .... **236; 355; 374**



## AUTHOR INDEX

- Cornard J. P..... 348; 349  
 Coroiu I..... 179  
 Costa M. L..... 341; 342  
 Coussan S..... 309; 365  
 Cozar I. B..... 37; **100**; 139; 214; 297; 303  
 Cozar O. 54; 100; 108; **139**; 170; 185; 191;  
 214; 228; 305; 315  
 Creaven B. S..... 256  
 Cristini O..... 33; 145; 174  
 Crupi V..... 60; 61; 142  
 Csankó K..... 158  
 Csendes Z..... 194  
 Cubeddu R..... 25  
 Cuda G..... 358; 371  
 Culea E..... 177; 178; 179; 180; 181  
 Culea M..... 54; 177; **214**  
 Cuniberti C..... 173  
 Cyrański M. K..... 339  
 Czakó-Nagy I..... 48  
 D'Antonio P..... 65  
 da Silva J. B. P..... 258  
 Dal Negro L..... 381  
 Dallongeville S..... 32  
 Damm U..... 78  
 Dammer O..... 149  
 Dan V..... 177  
 Daraban L..... 305  
 Darányi M..... 154; 158  
 Darkhalil I. D..... 240  
 Das G..... 358; 371  
 Dascalu C. F..... 40; 152; 359  
 David L. ..69; 80; 100; 139; 214; 215; **303**;  
 310  
 D'Avino G..... 380  
 De Angelis F..... 281; 358; 371  
 De Feo D..... 387  
 de Llanos R..... 8  
 Dēdic R..... 171; 172; 345  
 Deflorian F..... 27  
 Defonsi Lestard M. E..... 314  
 Dega-Szafran Z..... **291**  
 Degtyareva O. V..... 312  
 Dehelean A..... 179; 180  
 Dehelean C..... 80; 96; 284  
 Dei A..... 280; 369  
 del Puerto E..... 8  
 Dellepiane G..... 173; 206; 207; 269; 270  
 Demartin A..... 173  
 Demirci S..... **306**  
 Derek V..... 190  
 Deretzis I..... 386  
 Dhamelincourt M. C..... 32  
 Di Donato E..... 15  
 Di Fabrizio F..... 358; 371  
 Di Foggia M..... **99**; 109  
 Di Lonardo G..... 32  
 Di Prisco G..... 383  
 Dias A. A..... 341; 342  
 Dickman M. H..... 193  
 Dicle I..... 19  
 Dicle Y..... **55**; 144  
 Dienstleder M..... 150  
 Dijanošić A..... **136**  
 Dines T. J..... 73  
 Dittrich B..... 308  
 Dlouhá H..... 95  
 Długoń E..... 188  
 Dobrikov G..... 186  
 Dobrowolski J. Cz..... **339**  
 Doherty B..... **21**  
 Domingo C..... 8  
 Domnisoru D..... 35  
 Dorohoi D. O. 40; 152; 163; 164; **165**; 263;  
 264; 267; 344; 359; 361  
 Doroshenko I..... 295; **335**  
 Droghetti E..... **59**; **87**; 389  
 Dubiel S.M..... 88  
 Duce D..... 206; 270  
 Dulcescu M..... 164; 267  
 Durig J. R..... **240**; 242  
 Dyke J. M..... 342  
 Dyrek K..... 298  
 Dzhagan V. M..... 147  
 Ellmerer M..... 78  
 Engdahl A..... 83  
 Eremina N..... **292**  
 Ernsting N..... 367  
 Eroğlu E..... **290**; **296**  
 Esme A..... **330**  
 Estrin D. A..... 383  
 Ettrich R..... 289  
 Evangelisti L..... 355; 374  
 Fabbri P..... 279  
 Fagnoni M..... 348  
 Fainelli E..... 232  
 Falamas A..... **96**; 284  
 Fanetti S..... **340**  
 Fantacci S..... 29  
 Fausto R..... 252; 332; 333; 334; 336; 338  
 Favero L. B..... 238; 301



## AUTHOR INDEX

|   |                           |                        |                           |
|---|---------------------------|------------------------|---------------------------|
| Fazio E. ....                                     | <b>379</b>                | García-Vela A. ....    | 231                       |
| Fazzi D. ....                                     | 15; 325                   | Gatíal A. ....         | <b>294</b>                |
| Feichtner F. ....                                 | 78                        | Gauger D. R. ....      | 160; 203                  |
| Feis A. ....                                      | <b>356; 373; 389</b>      | Gauss J. ....          | 237                       |
| Felföldi K. ....                                  | 318                       | Gavare M. ....         | 112                       |
| Ferenc W. ....                                    | 116                       | Gdaniec Z. ....        | 283                       |
| Ferrante C. ....                                  | 277; <b>367</b>           | Geiger K. ....         | 79                        |
| Ferrara M. A. ....                                | 381                       | Gellini C. ....        | <b>269; 356; 373</b>      |
| Ferrari G. ....                                   | 354                       | Gentile F. ....        | 358; 371                  |
| Ferrari M. ....                                   | 174; 197                  | Georgieva I. ....      | <b>218; 256</b>           |
| Ferrer E. G. ....                                 | 262                       | Gerasimova M. ....     | 76                        |
| Ferreri C. ....                                   | 71                        | Ghini G. ....          | 279                       |
| Feyer V. ....                                     | 355; 374                  | Ghita A. ....          | 81                        |
| Filip E. ....                                     | <b>164</b>                | Giammarchi M. G. ....  | 354                       |
| Filip S. ....                                     | <b>185</b>                | Giani E. ....          | 66                        |
| Fioretto D. ....                                  | 382                       | Giannazzo F. ....      | 386                       |
| Fittipaldi M. ....                                | 383                       | Giloan M. ....         | <b>224</b>                |
| Flammini R. ....                                  | <b>232</b>                | Giordano D. ....       | 383                       |
| Flegel M. ....                                    | 103                       | Giorgetti E. ....      | 173; 186                  |
| Flego C. ....                                     | 53                        | Giorgini M. G. ....    | 362; <b>368; 390</b>      |
| Focardi C. ....                                   | 59                        | Girlando A. ....       | 380                       |
| Foggi P. <b>276; 279; 280; 281; 356; 369; 373</b> |                           | Giugliarelli A. ....   | 385                       |
| Földi N. ....                                     | 194                       | Giuliano B. M. ....    | 238; <b>332; 355; 374</b> |
| Ford T. A. ....                                   | <b>272</b>                | Goidanich S. ....      | 63                        |
| Forizs E. ....                                    | 215; 310                  | Gojłto E. ....         | 111                       |
| Forte G. ....                                     | 386                       | Gómez-Zavaglia A. .... | <b>252</b>                |
| Fotakis C. ....                                   | 3                         | González M. ....       | 231                       |
| Fracasso G. ....                                  | 376                       | Gosav S. ....          | <b>35; 58</b>             |
| Fraćzek-Szczypta A. ....                          | 148                       | Gotić M. ....          | <b>182</b>                |
| Francia F. ....                                   | 75                        | Grandidier B. ....     | 145; 159                  |
| Freddi G. ....                                    | 62                        | Grdadolnik J. ....     | 68; <b>285</b>            |
| Freire P. T. C. ....                              | <b>122; 199; 200</b>      | Greve T. M. ....       | 83                        |
| Fuentes S. ....                                   | 44                        | Grisanti L. ....       | <b>351</b>                |
| Furić K. ....                                     | 189; 190; 195; 197        | Gróf M. ....           | 294                       |
| Furtmüller P. G. ....                             | 87                        | Grokhovsky V.I. ....   | 22                        |
| Gabudean A. M. ....                               | <b>225</b>                | Grube M. ....          | 104; 112                  |
| Gajewicz M. ....                                  | 155                       | Gulnov D. ....         | 76                        |
| Gajović A. ....                                   | <b>151; 167; 187</b>      | Haber T. ....          | 150                       |
| Galabov B. ....                                   | 350                       | Habinshuti J. ....     | 145                       |
| Gallina M. E. ....                                | 382                       | Hadjieva B. ....       | 350                       |
| Gallone A. ....                                   | 25                        | Haensch T. W. ....     | <b>1</b>                  |
| Gálvez E. ....                                    | 141                       | Hajduch M. ....        | 24                        |
| Gamberini M. C. ....                              | 63                        | Hála J. ....           | 171; <b>172; 345</b>      |
| Gambi C. M. C. ....                               | <b>378</b>                | Handke M. ....         | <b>155; 188</b>           |
| Gamulin O. ....                                   | 190; 195; 197; <b>324</b> | Hanuza J. ....         | 196; 199; 200; 316; 343   |
| Gandolfi M. G. ....                               | 140; 377                  | Hasik M. ....          | 204                       |
| Ganguly A. ....                                   | 240                       | Hauser K. ....         | <b>86</b>                 |
| Garbin E. ....                                    | 367                       | Havlicek V. ....       | <b>24</b>                 |
| García-Espana E. ....                             | 136                       | Heinrich G. ....       | 175                       |
| García-Ramos J. V. ....                           | <b>8; 229</b>             | Heise H.M. ....        | <b>78</b>                 |



## AUTHOR INDEX

- Hemley R. J.....9  
Hendrixson V.....70  
Hense A.....102  
Hermanowicz K.....196  
Hernandez B.....32  
Hesse S.....299  
Hildebrandt P.....7  
Hlaváček J.....103  
Hobza P.....203  
Hofbauerová K..... 84; 95; 132; **289**  
Hofer F.....150  
Holanda R. O.....122  
Holy V.....197  
Horj E..... 54; **80**  
Howes B. D.....**383**  
Hrenar T.....321  
Huang R.....86  
Hudecová J.....143  
Hummelen J. C.....243  
Idrissi A..... 75; 348  
Ilieva S..... **23**; 350  
Iliut M.....**52**  
Illés L.....318  
Inguscio M.....66  
Innocenti F.....261  
Iordache A.....**54**  
Iosin M.....52  
Iriepa I.....141  
Isayeva.....245  
Ishii T.....153  
Itoh K.....**247**  
Ivanda M. .... 189; **190**; 195; 197; 198; 324;  
328  
Ivanković H.....151  
Ivascu C.....**305**  
Iveković D.....187  
Iwata T..... 240; **347**  
Izquierdo I.....8  
Jabłońska J.....91  
Jamróz M. H.....339  
Jankevičius F..... 70; 90  
Jasiewicz B.....**127**  
Jednačák T.....**321**  
Jeleň P.....94  
Joshi P.R.....239  
Jovanovski G.....34  
Juhássová H.....294  
Jurasekova Z.....71  
Kaczor A.....331  
Kalinowska M..... 116; **117**; 210; 219; 220;  
**273**  
Kalnenieks U..... 112  
Kaminskii A. A.....316  
Kaminsky J.....**110**  
Kanazawa H.....153  
Kapica W.....41  
Kapitán J.....143  
Karachevtsev M.V.....286  
Karachevtsev V.A.....**286**  
Karjalainen E. L.....**135**  
Katrusiak A.....291  
Kausteklis J.....283  
Kaveckaitė e.....90  
Kawashima M.....162  
Kecel S.....131; **133**  
Keiderling T. A.....86  
Keresztury G.....**259**  
Kimtys L.....**90**  
Kinali S.....306  
Kinowski C.....33; 145; 174  
Kirsch M.....79  
Kišić A.....321  
Kisiel R.....287  
Kiss J.T.....194; 302; 318  
Koch E.....79  
Kočíšová E.....95; 105; **134**  
Kohoutová J.....289  
Kojima S.....**153**; **162**  
Kokaislova A.....183; 221; 360  
Kokoskova M.....**223**  
Kollipost F.....**299**  
Kotos R.....339  
Koloydenko A.A.....81  
Kondepoti V.R.....78  
Kónya Z.....154; 158  
Kopecký Jr. V..... **84**; 95; 132; 289  
Kordek R.....91  
Kortz U.....193  
Kosović M.....195; 324  
Kostova I.....218  
Kostova K.....186  
Kovalenko S.....367  
Kowalczyk I.....**101**; 313  
Kowalewska A.....155  
Kowczyk M.....220  
Kozanecki M.....67; **287**  
Kožíšek J.....294  
Kozma A.....215; 310  
Kozma G.....158



## AUTHOR INDEX

- Krasnoshchekov S.V.....**245**  
 Kratasyuk V. ....76  
 Krawczyk S.....**146**  
 Krehula.....**208**  
 Krejtschi C. ....86  
 Krim L.....**239**  
 Król M.....36  
 Krsmanović R. ....151  
 Kubáňová M..... 95; 103; **119**  
 Kubelka J. ....110  
 Kucharska E. .... 196; **343**  
 Kuchukova N. ....186  
 Kuckuk R. ....78  
 Kudryasheva N.....77  
 Kuhlmann U.....7  
 Kukovecz Á. .... 154; 158  
 Kumar A.....89  
 Kumar S. .... **211; 363**  
 Kundu S. ....89  
 Kur J.....129  
 Kurek E.....97  
 Kurjane N.....104  
 Kurt M..... 304; 306  
 Kuş N. .... 334; **338**  
 Kwiatek J.W.M. ....94  
 Kwiendacz J.....274  
 L'Abbate N. ....65  
 La Magna A. ....386  
 Laane J. ....**230**  
 Labádi I. ....194  
 Lanús H. E. ....262  
 Lapini A. .... 280; 281; 282; **369**  
 Lapinski L. .... 334; 336  
 Lapouge C..... 348; 349  
 Larionov M.Yu. ....22  
 Larraona-Puy M.....**81**  
 Larsen R. W. ....241  
 Lasalvia M. ....65  
 Lazzaroni S. ....349  
 Leach H.....81  
 Ledesma A. E..... 257; 290  
 Lee J. J. ....299  
 Lees R.M.....**326**  
 Lehene C. ....284  
 Leibl W. ....75  
 Lemr K. ....24  
 Leon Y. ....370  
 Leone M.....120  
 Leontiev V. S. ....286  
 Leopold L. F..... 37; 216  
 Leopold N. .... 37; 69; 100; 139; 228; 284;  
 303; 315  
 Loporatti S. .... 173  
 Lespes G. ....38  
 Lewandowski W. **116; 117; 209; 210; 219;**  
 220; 273; 293  
 Leyton P.....**44**  
 Leyton Y. ....44  
 Li R. ....381  
 Lima M. ....280; **282; 369**  
 Lobello M. ....281  
 Łodziński M.....39; 67  
 Loewenschuss A. ....**235; 337**  
 Lofrumento C.....**370; 387**  
 Longo F.....**60; 61**  
 Longo R. L.....250  
 Lopes S. ....252  
 López-Ramírez M.R. ....222; 226  
 López-Tocón I. ....**229**  
 Lorenc J. ....**317**  
 Lorenzetti G. ....**31**  
 Lubian E.....367  
 Lucaciu C. M. ....159; 297  
 Lucotti A.....**325; 384**  
 Lupi L. ....382  
 Lüttchwager N. O. B. ....**309; 365**  
 Luz-Lima C.....122  
 Macan J.....151  
 Machado N. F. L.....**323**  
 Maciążek-Jurczyk M. ....97; 98  
 Maczka M. .... 196; **199; 200; 316**  
 Mader J.K. ....78  
 Magdas D. A.....170; **191**  
 Mahfouz R. M.....156; **268**  
 Majolino D.....60; 61; 142  
 Makreski P. ....**34; 115**  
 Makulski W. ....**201**  
 Malferrari M. ....75  
 Maloň P.....95; **103; 119**  
 Mančal T.....**244**  
 Mantsch H. H.....**14**  
 Marazzi F. ....42  
 Marcelli A. ....279; 356; 373  
 Marchetti S. ....378  
 Marciuš M.....197  
 Marcolongo G. ....376  
 Mare D. ....303  
 Margheri G.....173; 207  
 Maris A. ....238; **301**  
 Marques M. P. M. ....323



## AUTHOR INDEX

|                        |                         |                    |  |
|------------------------|-------------------------|--------------------|--|
| Marzocchi M. P.        | 388                     | Mrazkova E.        | 203  |
| Masino M.              | 380                     | Mrnka L.           | 18   |
| Matejka P.             | 18; 183; 221; 294; 360  | Mroginski M. A.    | 7  |
| Matejkova K.           | 18                      | Mrozek E.          | 217  |
| Maties V.              | 181                     | Muniz-Miranda F.   | 251; 271                                       |
| Matsuda Y.             | 162                     | Muniz-Miranda M.   | 64; 173; 207; 269                              |
| Mattarelli M.          | 27                      | Muntean C. M.      | 126  |
| Mayer A.               | 302                     | Murgida D. H.      | 7  |
| Mazzaglia A.           | 142                     | Musić S.           | 45; 48; 182; 189; 190; 195; 197; 198; 208; 328 |
| Mazzalai A.            | 353                     | Musso M.           | 368  |
| Mazzola M.             | 197                     | Nalbantova D.      | 350  |
| Mazzoleni P.           | 60; 61                  | Natkaniec-Nowak L. | 393  |
| Meić Z.                | 136                     | Navarra G.         | 120  |
| Melandri S.            | 238; 301; 332; 355; 374 | Nawrocka A.        | 146  |
| Melo F. E. A.          | 122                     | Nedić M.           | 241; 308                                       |
| Mendes Filho J.        | 122; 199; 200           | Negri F.           | 15   |
| Mendes Nuno F.C.       | 265                     | Németh Cs.         | 259  |
| Mendham A. P.          | 73                      | Nemtseva E.        | 76   |
| Meneghetti M.          | 376                     | Neri F.            | 379  |
| Mengon S.              | 27                      | Nevin A.           | 25   |
| Merloni A.             | 238                     | Nguyen T. K. N.    | 28   |
| Mestdagh J. M.         | 233                     | Nicastri A.        | 358; 371                                       |
| Mezzetti A.            | 75; 348; 349            | Nicoletti F. P.    | 389  |
| Michalska A.           | 51                      | Nielsen C.J.       | 235  |
| Mihaylov Tz.           | 218                     | Nielsen O. F.      | 83   |
| Mikac L.               | 189                     | Nieto C. G.        | 262  |
| Mikociak D.            | 192                     | Nocentini M.       | 59   |
| Milani A.              | 15; 249; 261            | Norén K.           | 154  |
| Milata V.              | 294                     | Notingher I.       | 81; 82   |
| Mile G.                | 275                     | Novak P.           | 321  |
| Miliani C.             | 21; 29                  | Nowakowska Z.      | 125  |
| Militello V.           | 120                     | Nunes C. M.        | 333  |
| Miljanić S.            | 136; 321                | Nyczyk A.          | 204  |
| Minh D. T.             | 161                     | Obinger C.         | 87   |
| Mircescu N.            | 228                     | Ocola E.J.         | 230  |
| Mironova-Ulmane N.     | 104; 112                | Ogruc-Ildiz G.     | 307  |
| Misselwitz R.          | 126                     | Oliva E.           | 66   |
| Mitsa V.               | 324                     | Olšina J.          | 244  |
| Mizutani Y.            | 347                     | Olszewski M.       | 129  |
| Modena E.              | 140; 377                | Oltean M.          | 275  |
| Modreanu M.            | 157                     | Ottalu O.          | 290  |
| Mohaček Grošev V.      | 68                      | Oniga O.           | 297  |
| Mojzeš P.              | 56; 95; 105             | Onori G.           | 385  |
| Moldovan C.            | 297                     | Oshtrakh M.I.      | 22; 88; 89                                     |
| Montanari L.           | 53                      | Osmanoğlu Ş.       | 19; 55; 144                                    |
| Montfillette-Dupont N. | 349                     | Osticioli I.       | 25   |
| Morresi A.             | 362; 382; 385; 390      | Otero J.C.         | 222; 226; 229                                  |
| Mosquera Vázquez S.    | 280; 281; 282; 369      | Ottani S.          | 99   |
| Mossberg A. K.         | 102                     | Ottonelli M.       | 206; 270                                       |
| Mozgawa W.             | 36; 46                  |                    |  |





## AUTHOR INDEX

- Ottová P. ....113  
Ozaki Y. ....274  
Ozalpan A. ....107  
Ozel A. E. .... 93; 107; 131; 133  
Ozel M. S. ....93  
Paciaroni A. ....142  
Padilla A. ....260  
Pagliai M. .... 25; 64; 251; 271; 300  
Painelli A. .... 351; 380  
Paipa C. ....44  
Palacký J. ....56  
Palage M. ....315  
Palavan-Unsal N. .... 107; 124  
Pálinkó I. .... 123; 154; 158; 194; 302; 318  
Pallagi A. ....123  
Palombo F. .... 362; 390  
Paluszkiewicz C. .... 94; 192; 202; 204; 205;  
394  
Panikar S. S. ....240  
Panuszko A. ....130  
Paolantoni M. .... 276; 362; 382; 385; 390  
Paraguassu W. .... 199; 200  
Parrinello M. ....10  
Pascut F.C. ....82  
Pascuta P. ....179  
Pasquini M. ....352  
Pastorczyk M. ....287  
Pavlenko A. ....104  
Pazderka T. .... 84; 132  
Pejov L. .... 34; 253  
Péré E. .... 28; 38  
Pereira da Silva K. ....200  
Pérez J. ....260  
Perkins W. ....81  
Perna G. ....65  
Perticaroli S. ....382  
Petersen C. ....16  
Petkova I. ....186  
Petreska J. ....253  
Petruševski G. ....115  
Petruševski V. M. ....320  
Pfleger J. ....149  
Piani G. .... 233; 352; 391  
Piantanida I. ....136  
Piccardo M. .... 206; 270  
Pieczka A. ....39  
Piekut J. ....117  
Pielak K. ....298  
Pietraperzia G. ....352  
Pinho e Melo T. M.V.D. ....333  
Pintea A. ....106  
Pinto R. M. ....341; 342  
Pînzaru S. C. ....108  
Pîrnău A. ....297; 315  
Pisarska J. ....166  
Pisarski W. A. ....166  
Plank H. ....150  
Plevová E. ....47  
Plodínec M. ....167; 187  
Plokhotnichenko A.M. ....286  
Pogorelov V. ....295; 335  
Pohle W. ....160; 203  
Poisson L. ....233  
Pol J. ....24  
Polak J. ....41; 43; 346  
Polakovs M. ....104  
Pop L. ....177  
Poparić G. B. ....234  
Postylyakov O. V. ....266  
Potara M. ....118  
Praisler M. ....35; 58  
Prati C. ....140; 377  
Praus P. ....105  
Prevedelli M. ....354  
Prince K. C. ....236; 355; 374  
Procházka M. .... 134; 149; 223; 227  
Profant V. ....72  
Profire L. ....267  
Prokopec V. ....183; 221; 360  
Prónayová N. ....294  
Protti S. ....348; 349  
Przybył A. K. ....125  
Pshenichnikov M. S. ....16; 243  
Ptak M. ....199; 316  
Pučetaité M. ....70  
Puzzarini C. ....237  
Quartucci G. ....65  
Rada M. ....177; 181  
Rada S. .... 177; 178; 179; 180; 181  
Raineri V. ....386  
Rakowska P. ....129  
Ramos L. A. ....314  
Ramos M. N. ....6; 250; 258  
Raşitoğlu B. ....254  
Refait P. ....212  
Regulska E. ....209; 210; 293  
Reinholds E. ....104  
Rémazeilles C. ....212  
Rendina I. ....381  
Reva I. .... 332; 333; 334; 336; 338



## AUTHOR INDEX

- Řezáčová B. .... 113; **288**  
 Ribeiro-Claro P. .... 265  
 Ricci M. .... 387  
 Ridderbusch O. .... 86  
 Righini G. .... 174  
 Righini G.C. .... 197  
 Righini R. .... 271; 280; 369  
 Rindi A. .... 173; **207**  
 Ristić D. .... 190; 195; **197**  
 Ristić M. .... 45; **48**; 190; 195; 197; 234  
 Ristoiu T. .... 179  
 Ristova M. .... 253  
 Ritz M. .... 47  
 Rode J. E. .... 339  
 Rodríguez J. .... 231  
 Rogojanu A. .... 152; **163**  
 Rogojerov M. .... 259  
 Rossi B. .... **378**  
 Roussel P. .... 174  
 Równicka-Zubik J. .... 97; 98  
 Rozenberg M. .... 235; 337  
 Rubio-Lago L. .... **231**; 391  
 Rudbeck M. .... **20**  
 Rugina D. .... 106  
 Rusu D. .... **193**  
 Rusu M. .... 193  
 Rusu T. .... 177  
 Rusu V. H. .... **250**  
 Rutkis R. .... 112  
 Ryazanova O. .... **176**  
 Rzaigui M. .... 268  
 Šablinskas V. .... **70**; 90; 175; 295; 335  
 Sadlej J. .... 339  
 Sagdinc S. .... 330  
 Salami S. .... 38  
 Salvi P. R. .... 269; 356; 373  
 Salzer R. .... 79  
 Samsonowicz M. .... **209**; **293**  
 Sánchez R. .... 44  
 Sánchez-Cortés S. .... 8; 229  
 Šanda F. .... 244  
 Šarić A. .... **198**  
 Sarzyński J. .... 116  
 Sasiadek W. .... 343  
 Sassi P. .... 362; 382; **385**; 390  
 Satta M. .... 232  
 Sazdov D. .... 320  
 Scarponi F. .... 382  
 Schackert G. .... 79  
 Schettino G. .... **66**  
 Schettino V. .... 25; 64; 251; 271; 300; 357;  
 372  
 Schmitt M. .... **2**  
 Scholes G.D. .... 366  
 Scholz M. .... **345**  
 Sciau Ph. .... 370  
 Scotoni M. .... **353**  
 Sebi A. .... 263  
 Sebők P. .... 123  
 Semionkin V.A. .... 22; 88; 89  
 Şengül A. .... 296  
 Şenyel M. .... 169  
 Sevilla P. .... 8  
 Sezen M. .... 150  
 Sgamellotti A. .... 21; 29  
 Sharma A. .... **334**  
 Siboni F. .... 140; 377  
 Šimáková P. .... **227**  
 Simiti I. V. .... 181  
 Sipiczki M. .... 154; 302  
 Sipos P. .... 123; 154  
 Sirleto L. .... **381**  
 Sissa C. .... 351  
 Sitarz M. .... **39**; **67**; 188  
 Skrycki K. .... 127  
 Slouf M. .... 149  
 Śmiechowski M. .... **111**  
 Smulevich G. .... 59; 87; 383; 389  
 Soep B. .... 233  
 Soica C. .... 80  
 Sołtysiak E. .... 205  
 Šoptrajanov B. .... **253**; **320**  
 Sornosa-Ten A. .... 136  
 Souza-Filho A. G. .... 199; 200  
 Srankó D. .... **154**  
 Stamatovska N. .... 34  
 Stancanelli R. .... 142  
 Stanculescu R. E. .... 163; 263; **264**; **361**  
 Stanescu R. .... 185  
 Stangret J. .... 111; 128; 129; 130  
 Stanila A. .... **216**  
 Stavrov ..... **74**  
 Štefanić G. .... 189; **328**  
 Štefanić I. I. .... 328  
 Steguweit L. .... 26  
 Steiner G. .... **79**; 90; 175  
 Stelling A. .... 79  
 Štěpánek J. .... 105; 113; 134; 288; 289  
 Stepanov ..... 245  
 Stievenard D. .... 145



## AUTHOR INDEX

- Stiufiuc G. ....159  
 Stiufiuc R. ....**159**  
 Stodolak E. .... 94; 394  
 Straka M. ....364  
 Striova J. ....31  
 Strohalm M. ....24  
 Su D. S. .... 151; 187  
 Suhm M. A. .... 241; 299; 308; 309; 365  
 Sułkowska A. .... **97; 98**  
 Sułkowski W. W. .... **41; 43; 97; 98; 346**  
 Sundius T. ....259  
 Sunel V. .... 264; 361  
 Sureau F. ....105  
 Surmacki J. ....91  
 Svanborg C. ....102  
 Svoboda A. .... 171; 345  
 Świdorski G. ....273  
 Świsłocka R. .... 116; **219; 220; 273; 293**  
 Szabó L. ...**37**; 69; 100; 139; 214; 228; 303;  
 315  
 Szafran M. .... 291; **313; 329**  
 Szöllösi Gy. ....302  
 Szostak M. M. ....**298**  
 Szulc A. ....101  
 Taddei P. .... **62; 140; 377**  
 Talu M. ....**85**  
 Tanasi D. ....61  
 Tasheva D. ....23  
 Terenziani F. ....351  
 Terpugov E. L. ....**312**  
 Teslaru T. ....263  
 Thea S. ....206  
 Thomas J. M. ....**5**  
 Tigoianu R. I. ....**344**  
 Timtcheva I. ....**186**  
 Tinti A. .... 109; 120; 140; 377  
 Tobała T. ....327  
 Toderas M. .... **215; 310**  
 Todescato F. ....277  
 Tommasini M. .... 325; **384**  
 Tomsa A. R. ....193  
 Toniolo L. ....63  
 Torii H. ....368  
 Torreggiani A. .... **71; 109; 120**  
 Torrens F. ....**114**  
 Tourón Touceda P. .... **280; 281; 282; 369**  
 Tozzi A. ....66  
 Tran T. V. ....174  
 Trendafilova N. .... 218; **256**  
 Trojsi G. ....42  
 Trusso S. ....379  
 Trzcińska B. ....49  
 Tsukada M. ....62  
 Tudoran L. B. ....106  
 Turpin P. Y. ....105; 288  
 Turrell S. .... **32; 33; 145; 174**  
 Tuttolomondo M. E. ....314  
 Tykwinski R.R. ....325  
 Ugarkovic S. ....115  
 Ulic S. E. ....314  
 Uraz G. ....138  
 Urbonienė V. ....90  
 Uvdal P. ....335  
 Uzluk E. ....85  
 Vachoušek J. ....113  
 Vaculíková L. ....47  
 Valentini G. ....25  
 Valkunas L. ....244  
 van Loosdrecht P. H. M. ....243  
 Varga N. ....194  
 Varga R. A. ....315  
 Varma S. ....81  
 Vauthey E. ....186  
 Vedeanu N. .... **170; 185; 191; 297**  
 Venturoli G. ....75  
 Venuti V. ....**60; 61; 142**  
 Verbanec G. ....321  
 Verde C. ....383  
 Vértes A. ....48  
 Viappiani C. ....356; 373  
 Vidova V. ....24  
 Vieillescazes C. ....28  
 Viliani G. ....378  
 Villa F. ....354  
 Vlckova B. ....**149; 223**  
 Volka K. ....**161**  
 Volny M. ....24  
 Voloshin I. ....176  
 Vukajlović J. ....167  
 Vyklický V. ....**171; 172**  
 Vyskovska M. ....**183; 221; 360**  
 Wandas M. ....196; 343  
 Wang J. ....322  
 Warga J. ....381  
 Waś-Gubała J. ....49; 50  
 Wassermann T. N. ....241; 309; 365  
 Weidinger I. ....7  
 Weissova J. ....18  
 Welfle H. ....126



## AUTHOR INDEX

---

|                             |                                |
|-----------------------------|--------------------------------|
| Weselucha-Birczyńska A..... | 51; 121; 148;<br>327; 393; 394 |
| Westwood N. P. C.....       | 322                            |
| Wieser H. ....              | 364                            |
| Wilhelm P. ....             | 150                            |
| Williams H.....             | 81                             |
| Wójcik M. J.....            | 246; 274                       |
| Wojtulewski S.....          | 273                            |
| Wu L. ....                  | 86                             |
| Wyrzykowski D. ....         | 130                            |
| Xu L.H. ....                | 326                            |
| Xu T. ....                  | 145                            |
| Yakubov A. A. ....          | 319                            |
| Yalçinkaya O. B.....        | 290                            |
| Yaremko A. M. ....          | 147                            |
| Yasui T.....                | 92                             |
| Yukhymchuk V. O. ....       | 147                            |
| Yurtseven H. ....           | 254; 255; 304                  |
| Żądło M.....                | 43; 346                        |
| Žagar K. ....               | 167                            |
| Zamocky M.....              | 87                             |
| Zárate A. ....              | 44                             |
| Zawadzka P.....             | 287                            |
| Zdyb A. ....                | 146                            |
| Zegber I.....               | 7                              |
| Zelinski B. C. ....         | 40; 152; 359                   |
| Želvys A.....               | 70                             |
| Zentz Ch.....               | 288                            |
| Zerbi G.....                | 325; 384                       |
| Zharnikov M. ....           | 12                             |
| Zhou S. X.....              | 242                            |
| Ziabka M.....               | 202                            |
| Žic M. ....                 | 45                             |
| Zięba-Palus J.....          | 49; 50; 51                     |
| Zimmerer C.....             | 175                            |
| Zimmermann B.....           | 17; 57                         |
| Zinczuk J.....              | 257                            |
| Zoladek A. ....             | 81                             |
| Zoppi A.....                | 31                             |
| Zozulya V. ....             | 176                            |

